Isolation and Structure Elucidation of Insecticidal Secondary Metabolites from *Aglaia* species collected in Vietnam

(Isolierung und Struktur-Identifizierung insektizid aktiver Naturstoffe aus *Aglaia*-Arten von Vietnam)

Inaugural-Dissertation
Zur
Erlangung des Doktorgrades der
Mathematisch-Naturwissenschaftlichen Fakultät
der Heinrich-Heine-Universität Düsseldorf

Vorgelegt von

Duong Ngoc Tu

aus Hanoi, Vietnam

Düsseldorf, 2005

Gedruckt mit Genehmigung der Mathematisch-Naturwissenschaftlichen Fakultät der Heinrich-Heine-Universität, Düsseldorf

Eingereicht am : 19.01. 2006

Referent: Prof. Dr. **Peter Proksch**

Koreferent: Dr. **Rainer Ebel**, Juniorprofessor

Erklärung

Hiermit erkläre ich ehrenwörtlich, daß ich die vorliegende Dissertation “Isolierung und Struktur-Identifizierung insektizid aktiver Naturstoffe aus *Aglaia*–Arten von Vietnam´´ selbständig angefertigt und keine anderen als die angegebenen Quellen und Hilfsmittel benutzt habe. Ich habe diese Dissertation in gleicher oder ähnlicher Form in keinem anderen Prüfungsverfahren vorgelegt. Außerdem erkläre ich, daß ich bisher noch keine weiteren akademischen Grade erworben oder zu erwerben versucht habe.

Acknowledgements

First of all, I would like to express my sincere thanks to my "Doktorvater", supervisor, Prof. Dr. **Peter Proksch**, who gave me the great opportunity to be involved in natural product research in his group with unwavering support, continuous encouragement, and direct expert guidance. I am deeply indebted to him for his kindness, generous considerasions, admirable advices, sympathyse and valuable helps to fulfil my work and made my stay in Düsseldorf warmly appreciated.

I would also like to express my special thanks to Dr. **Ru Angelie Edrada Ebel** who took care of me very much from the beginning, helped me in isolation techniques as well as her expert guidance through many NMR courses and NMR spectra interpretation. I myself respect her very much as a very kind teacher, who is always willing to share her knowledge and experiences to others. Her evaluation and patient revision of my thesis are deeply appreciated.

I would also wish to express my great thanks to Dr. **Rainer Ebel** (Juniorprofessor) for his evaluation and expert guidance in structure elucidation of isolated compounds in the dissertation. I personally respect and admire him as the strick teacher, who always works very hard with high spirit and motivating power but very kind, friendly and humorous in life. This influenced me a lot in the brilliant habit and scicentific behaviours in my future career.

I would like to acknowledge the DAAD (Deutscher Akademischer Austauschdienst) for a scholarship grant. Especially I would like to thank Mrs. **Elke Burbach**, my DAAD coordinator, who always kindly help and guide me in every situation in the administration.

I wish to express my special thanks to Prof. Dr. **Duong Anh Tuan** (my Father) and Mrs. **Dong Thi Hong Luyen** (my Mother) at the Department of Chemicals for Plants Protection, Institute of Chemistry, Vietnamese Academy of Sciences and Technology for all of their best advices, brilliant care and important support for me to fulfil my research work.

My special thanks to Dr. **Luu Tham Muu**, who made our collaboration with Prof. Dr. **Peter Proksch**, possible and for his expertise in experimental design under field conditions in Vietnam as well as collection of *Aglaia* materials.

I would also like to express my sincere thanks to Prof. Dr. **Dang Vu Minh** (President of Vietnamese Academy of Sciences and Technology) and Prof. Dr. **Tran Van Sung** (Director of Institute of Chemistry-VAST) for their decision, recommendation and precious advices to send me to study in Germany with continuous support.

I am deeply indebted to Dr. **Victor Wray** (Gesellschaft für Biotechnologische Forschung, Braunschweig), for the measurement of the NMR spectra and his valuable disscusion in structure elucidation of the isolated compounds.

For the administration and extention procedures of my study in Germany, I would also like to thank Prof. Dr. **Nguyen Khoa Son** (Vice-President of Vietnamese Academy of Science and Technology), Dr. **Pham Van Quy** (Vice-President of the VAST) and Mr. **Dau Sy Thai** (Deputy-Director of Department of International Cooperation of the VAST) for their kind help and advise.

I would also like to express my special thanks to Dr. **Luc Van Puyvelde** for his guidance and teaching me precious knowledge in modern instrumentation used in natural product research at the beginning when I was trained at the University of Ghent-Belgium, and his advice in experimental design for my field experiment in this dissertation.

My deep thanks to Prof. Dr. **Phan Tong Son**, Prof. Dr. **Nguyen Van Dau**, and Dr. **Mai Van Tri**, who passed away in 2000 by lung cancer, were my supervisors for my Master and Bachelor thesis, for teaching me precious knowledge of natural products chemistry, and for the letter of recommendation.

My special thanks to Dr. **Gero Eck**, who guided me in the first months of laboratory work. His friendship helped me a lot to accustome to the work environment in the institute as well as to my life in Düsseldorf. Our discussions and his advices to my field experimental design is highly appreciated.

I would like to express my special thanks to my friends and colleages, Dr. **Franka Teuscher**, Mrs. **Sofia Ortlepp**, Dr. **Suwigarn Pedpradab**, Mr. **Arnulf Diesel** and Ms. **Nadine Weber** who helped me very much during my first months of adapting in the institute with many useful advises and lots of nice discussion related to work and life in Düsseldorf. Their friendships together with many fun activities really helped me to warm up my time of stay in Düsseldorf over the very cold winters. This also helps me to understand more about the people and the culture of Germany.

My highly appreciation is to Mr. **Arnulf Diesel** for all his help and kindness both with computer related problems and as an excellent PADI diving instructor. I am thankful also to Ms. **Nadine Weber** for her translation of my German summary.

My special thanks to Ms. **Mareike Thiel**, the institute secretary, for her kindness and all the administrative help, especially for my apartment arrangements.

I am also grateful to our technical assistant staff, Mrs. **Waltraud Schlag**, Mrs. **Katja Friedrich**, Mrs. **Katrin Rohde**, and Mrs. **Katja Raetke** for their kindness and for always providing me with the materials and glassware which I needed in my work.

I wish also to thank Mr. **Nguyen Van Giap,** my colleague at the Department of Chemical for Plants Protection-Institute of Chemistry, for his precious help in arranging and carrying out my field experiments in Vietnam.

I am thankful to Mr. **Pham Anh Thang** (Director of the Tam Dao National Medicinal Garden) and Mrs. **Le Thi Me** (Institute of Plants Protection, Minsitry of Agriculture) for their cooperations in carrying out my field experiments in Vietnam as well as the toxicity experiment of the *Aglaia* extract on mice.

I am grateful to Dr. **Tran Ngoc Ninh** (Institute of Ecological and Natural Resources), BSc. **Nguyen Kim Dao** (Institute of Chemistry) and Dr. **Nguyen Trong Son** (The University of Hue) for the collection and identification of *Aglaia* species from Vietnam.

My deep thanks to all colleagues at the Department of Chemicals for Plants Protection, Institute of Chemistry (VAST) for their kind help and sharing a nice atmosphere of work in the Institute: Mr. **Le Phi Dam**, Dr. **Bui Kim Anh**, Dr. **Le Kim Bien**, Mr. **Phan Tien Dinh**, Mrs. **Nguyen Ngoc Mai**, Mr. **Ho Dac Hung**, Mrs. **Nguyen Hong Quyen**, Mr. **Dao Quoc Huy**, Mrs. **Nguyen Thanh Tra**, Mr. **Tran Van Thuy**, Mr. **Ngo Van Thanh**, Mr. **Ta Hoang Anh**, Mr. **Dong Tuan Minh**, Mr. **Dong Van Hanh**, Mr. **Dong Thanh Kien**, Mrs. **Nguyen Van Nga**, Mrs. **Luu Hong Han**, Mrs. **Do Thu Hien**, Mr. **Nguyen Viet Anh**, and Mr. **Nguyen Thanh Xuan**.

I am thankful to Prof. Dr.**Thomas Jürgen Schmidt** (University of Münster) and Prof. Dr**. Wen Han Lin** (Natural Research laboratory of Natural and Biomimetic Drug, Beijing Medical University) for the nice discussion in the structure elucidation and configuration assignment of the isolated lignan compounds.

I am grateful to Dr. **Claus Paßreiter** for his safety instructions in the Institute and for the friendly atmosphere.

I would also like to extend my sincerest gratitude to all of my colleagues at the Institute of Pharmaceutical Biology and Biotechnology for sharing a nice atmosphere and their kind help: Mrs. **Ine Dewi Indriani Diesel**, Ms. **Clecia Freitas**, Mr. **Mohamed Ashour**, Ms. **Amal Hassan**, Mrs. **Triana Hertiani**, Dr. **Sabrin Ibrahim**, Mr. **Gamal Hussein**, Mr. **Yosi Murti**, Mr. **Yudi Rusman**, Mr. **Edi Wahyu Sri Mulyono**, Mr. **Yasman**, Ms. **Sabine Heiligtag**, Mr. **Frank Riebe**, Mrs. **Sabine Borstel**, Ms. **Julia Jacob**, Mr. **Mirko Bayer**, Ms. **Annika Putz,** Mrs. **Abimbola Sowemimo**, and Mr. **Yao Wang**.

I am thankful to Dr. **Ziyad Baker**, Dr. **Carsten Thoms**, Dr. **Hefni**, Dr. **Gernot Brauers**, Dr. **Mostafa**, Dr. **Hassan Wafaa**, Dr. **Steffan Bärbel**, Dr. **Ehab,** Dr**. Lanre Omobuwayo**, and Dr. **Liu Hong-Bing** for their kind help and friendly discussions on diverse experiences.

I would like to thank Dr. **Claudia Torre** for her help in graphical design in excel, and for her working time together with *Aglaia duppereana*. My special thanks also to Mrs. **Abimbola Sowemimo** for her correction of my English.

I wish to thank to my best friend **Nguyen Truong Son**, for his correction of my English and for a lot of discussions, sharing nice ideas and encouragement. My deep thanks also to Mr. **Dao Vinh Khiem** for his precious help in dissertation formatting.

I wish to thank Prof. Dr. **Walter Frank** (Institute of Inorganic Chemistry) for the X-ray measurement of dasyclamide.

I am deeply appreciate to Mr. **Jürngen Schölzel** and his wife Mrs. **Kazuko** for their hearty sympathy, warm encouragement, spending a lot of free time for playing tennis, sharing delicious cooking and a lot of German training through his excellent creation of International Friends Game, is the best game of learning a foreign language. Specially when it is as difficult as German.

My special respect and gratitude to my grand father **Duong Chieu**, my kongfu master, who always encourages and eagerly wishes for me to reach higher and higher in education with high spirit physical while my grand mother **Giap Thi Ty** is soft person, who is always willing to sacrifice for the family and thinks a lot of me.

My special thanks to my sisters: Mrs. **Duong Hong Anh**, Mrs. **Duong Phuong Thao**, and Ms. **Duong Thuy Duong**, who always encourage and expect me to be a mirror for them!

I would like to express my special thanks to my wife, **Nguyen Thi Lan Anh**, who has been patiently waiting for me with her faithful love, always ready to sacrifice her time to listen and understand. Her sympathy gave me a lot of energy to do my research work. Her continuous encouragement made my time going faster during these days far away from home.

Especially to my lovely son, **Duong Minh Bao Duc**, who was brought into the world during my writing of this dissertation brings me happiness, a lot of joys, hopes, and promotion to finish this work.

At the end, from the all of my heart I wish to express my sincerest thanks to my Forefathers and the Buddha, who always bless and protect me to preserve and to bring into play my **Duong** family´s tradition.

To All of you, Thank you very much!

Duong Ngoc Tu

Düsseldorf, Germany
October 2005

This work is dedicated to my beloved family, who have entrusted earnestly in me their belief and hopes, who always encouraged and unwavering support to my valuable study and life.

Table of Contents

Zusammenfassung

Verschiedene Extrakte von mehreren *Aglaia* Arten Vietnams wurden auf ihre insektizide Wirkung auf Larven der Art *S. littoralis* untersucht. *Aglaia oligophylla*, *Aglaia abbriviata, Aglaia eleagnoidae, Aglaia duppereana* zeigten hierbei die höchste Aktivität. Nach 24 Stunden konnte eine 100% ige Mortalität der Larven auf Grund dieser Rohextrakte (1000ppm) beobachtet werden. Daneben ergaben *A.rothii* eine 80% ige, *A. dasyclada* eine 70% ige, *A. gigantea* eine 60 % ige, *A. pleuroptiris* eine 45% ige und *A. macrocarpa* eine 15% ige Sterblichkeit.

Es konnten mittels einer Bioassay geleiteten Fraktionierung drei Fraktionen (F3,F4,F5) mit starker insektizider Wirkung gefunden werden, die von den Rohextrakten der Art *Aglaia oligophylla* stammten. Die qualitative Analyse der Fraktionen durch HPLC-DAD und HPLC-MS zeigte die Anwesenheit von Rocaglamid – Derivaten und weiteren Verbindungen. Die Fraktionen wurden über Silika aufgetrennt und es konnte ein neues Rocaglamid, **Rocaglamid AY** (Verbindung **8**) isoliert werden. Außerdem wurden drei Lignane, **Pinoresinol** (Verbindung **10**), **4´-O-Methyl-pinoresinol** (Verbindung **11**), and **Eudesmin** (Verbindung **12**), gefunden, die eine interessante Stereochemie aufweisen. Daneben wurden drei bekannte Flavonoide, **4´,5,7-Trimethoxydihydroflavonol** (Verbindung **15**)**, 4´,5,7-Trimethoxyflavonol** (Verbindung **16**) and **4´,5,7-Trimethoxyflavanone** (Verbindung **17**) erhalten. **Lutein** (Verbindung **29**) wurde als Tetratriterpen kristallin aus Fraktion F3 erhalten.

Aus der Rinde von *Aglaia duppereana* wurden fünf bekannte Rocaglamide erhalten, die identisch waren zu to **Rocaglamid A** (Verbindung **1**)**, Rocaglamid I** (Verbindung **2**), **Rocaglamid W** (Verbindung **3**), **Rocaglamid AB** (Verbindung **4**), **Rocaglamid J** (Verbindung **5**) Daneben wurde **Epicatechin** (Verbindung **13**) gefunden.

Die Fraktionierung des Extraktes von Blätter von *Aglaia gigantea* ergab die Verbindungen **Dasyclamid** (Verbindung **20**)**, Grandiamid D** (Verbindung **22**), **Gigantamid A** (Verbindung **25**) und **Foveolin B** (Verbindung **27**). Die Blätter von *Aglaia dasyclada* enthielten **Niloticin** (Verbindung **28**) während aus den Blättern von *Aglaia elaeagnoidea* **Rocaglaol** (Verbindung **6**) and **Scopoletin** (Verbindung **30**) isoliert werden konnten. Aus dem Ethylacetat-Extrakt von *Aglaia abbriviata* wurden **4´,5,7-tri-O-Methyl-kaempferol**, **Odorinol** (Verbindung **24**) in kristalliner Form und **Aglaxiflorin D** (Verbindung **9**), erhalten wohingegen aus den Blättern von *Aglaia oligophylla* **Kaempferol-3-rutinoside** (Verbindung **18**), **Kaempferol-3-*O*-(4-hydroxy-E-cinnamoyl)-(β)-glucopyranosyde** (Verbindung **19**), **Grandiamid B** (Verbindung **21**)**, Gigantamid A** (Verbindung **25**) and **Pyramidatin** (Verbindung **26**) isoliert wurden.

Vorausgegangene Experimente mit dem Rohextrakt von *Aglaia oligophylla* zeigten eine isektizide Wirkung auch unter Feldbedingungen. Diese wurden im Juli 2003 im Tam Dao National Medicinal Garden in Vietnam durchgeführt. Fünf Zubereitungen mit unterschiedlichen Konzentrationen (500 ppm, 1000 ppm, 2000 ppm, 4000 ppm and 6000 ppm) wurden aus den Methanol - Extrakten von *Aglaia oligophylla* hergestellt. Diese erwiesen sich als effektiv gegen eine in Vietnam neu auftretende Raupe (*Brithys crini*), die gravierende Schäden bei *Crinum asiaticum* (Amaryllidaceae) verursachte. Die Wirkung des Extraktes von *Aglaia oligophylla* an *Brithys crini* konnte nicht auf eine Abtötung zurückgeführt werden wie es für toxisch - chemische Insektizide (e.g. Monitor ®) üblich ist, sondern der Extrakt wirkte eher als Repellent. Der Extrakt war außerdem wirksam bei *Macrosinum phoniella*, die *Cynara scolymus* befallen. Hier wirkten die Inhaltsstoffe vernmundlich auf das zentrale Nervensystem der Insekten. 12 Stunden nach Besprühen mit dem Extrakt konnten Blattläuse mit unkontrollierten Bewegungen beobachtet werden, was auf eine Beeinflussung des Nervensystems zurückgeführt wurde. Bei einer Konzentration von 400 ppm kam es zu einer 100% igen Sterblichkeit nach 7 Tagen.

Ein zweites Experiment mit *Aglaia*-Zubereitungen wurde auf einem Kohlfeld in Dong Anh, Hanoi October 2003 durchgeführt. Hier konnte die Wirksamkeit des *Aglaia oligophylla*-Extraktes an *Spodotera litura* gezeigt werden. Dabei war die Wirkung nicht so stark wie die eines chemischen Vertreters (Regent®), dafür hielt die Wirkung aber länger an. In Petrischalen durchgeführte Versuche mit Blättern von *Brassica rapa*, die mit Larven von *S. litura* befallen waren, zeigten die Zubereitungen von *Aglaia* eine 60% (5000ppm) Mortalität der Insekten. Bei 2500ppm von 40% im Vergleich zu 30% bei dem kommerziell erhältlichen Insektizid (Regent®).

Die Letale Dosis (LD_{50}) der *Aglaia*-Zubereitungen wurde mit 4500mg/kg im Mäuseexperiment bei oraler Zufuhr und 2000mg/kg bei Injektion des Extraktes direkt in die Speiseröhre. Die Stabilität der Zubereitung wurde unter Feldbedingungen getestet, wobei auf den Rückstand von Dasyclamid (ein Zimtsäurebisamid, welches in hohen Konzentrationen in den Blättern von *Aglaia gigantea* vorkommt) untersucht wurde, welches außerdem ein Grundbaustein der Rocaglamide ist. Nach 3 Tagen wurden keine Spuren von Dasyclamid mehr in den Blättern der besprühten Pflanzen gefunden.

I. INTRODUCTION

I.1. Significance of the study

Chemical crop protection has a vital role in securing healthy food supplies for a growing global population. We have to stress the point redundantly to protect our agricultural commodities from harmful agrochemicals. Farmers would be unable to make a living producing food and there would not be enough food to feed the human population [From the Welcome Address of Jost Harr, Chairman of the 10th IUPAC Congress on Chemistry of Crop Protection, 2002].

The traditional agricultural community has relied extensively on synthetic insecticides such as organo-chlorines, -phosphates, and dinitro-phenols, etc. However, these broad spectrum chemical pesticides are toxic and often indiscriminantly destroy other beneficial species [Ley *et al*., 1993]. Also as insects evolve or mutate to resist such toxins, higher doses of pesticides are used which in turn increase environmental pollution as well as ecological disturbance. Moreover, a large proportion of crops are still being lost to predatory insects and other pests [Ley *et al.,* 1993]. Toxic chemicals especially affect the quality of the agricultural products and consequently human health.

In order to achieve environmentally friendly plant protection methods, there is an ongoing effort to search for new classes of insecticides. An example of this are the pyrethroids, which account for about one third of the insecticide used worldwide today. Plants have also evolved to have their own chemical defenses against insect attack and have provided science with a rich pool of biologically active compounds in agrochemical research.

Thus, finding new safe insecticidal products for crop protection in the new millennium which reduce pest population should be target-specific (kill the pest but not other organisms), should break down quickly in the environment, have low toxicity to human and other mammals and successfully meet the challenge of feeding a growing world population.

I.2. History of natural products chemistry in insecticide research

Insecticides are agents of chemical or biological origin that control insects, by either killing or otherwise preventing them from engaging in behaviors deemed to be destructive. For this purpose, insecticides have been used for centuries to fight unwanted pests. Insecticide products could be of natural origin or synthetic, which are applied to target pests in a myriad of formulations and delivery systems as sprays, baits, or slow-release diffusion, etc. [Ley *et al.,* 1993; Ware and Whitacre, 2004].

About 10,000 species of more than 1 million species of insects are crop-eating. Among these, approximately 700 species worldwide cause most of the insect damage either in the field or while storage. Insects have existed for at least 250 million years, which is much earlier than Mankind, who has only been there for 3 million years. One of the first techniques used by our primitive ancestors to reduce insect annoyance was hugging smoky fires or spreading mud and dust over their skin to repel ticks and insects bites, a practice comparable to habits of elephants, swine, and water buffalos. Historians could trace the use of pesticides to Homer´s time which is around 1000 B.C., but the earliest record of the use of insecticides belong to the burning of "brimstone" (sulfur) as a fumigant. According to Pliny the Elder (23-79 A.D.) most of the earlier applications of insecticides were recorded in his book of Natural History. Among these, gall was used from a green lizard to protect apples from worms. Later, a variety of materials was also used with doubtful results and these included extracts from pepper and tobacco, soapy water, whitewash, vinegar, turpentine, fish oil, brine, lye and among many others [Ware and Whitacre, 2004].

Insect pest control has gained great importance. There are approximately several thousands of millions US dollars spent per year, which were utilized to do insecticide research in an effort to confront the continuous attack of over half a million different herbivorous insect species [Ley *et al*., 1993]. To date, more than 2000 species of plants have been reported to have insecticidal value, and many more exist, as described below.

I.2.1. Azadirachtin

One of the most successful examples of insecticides of plant origin is azadirachtin, or azadirachtin-containing extracts. This compound affects a broad spectrum of more than 200 species of insects and mites [Donald *et al.,* 1992]. Azadirachtin acts as an insect feeding deterrent and growth regulator. Insects usually cannot molt to their next life stage and dies after the treatment with azadirachtin. Azadirachtin acts also as a repellent when it is applied to a plant and does not produce a quick knockdown to kill directly. Actually, the insects were found often remaining near to the treated plant and possibly dying through starvation [Ley *et al.,* 1993]. Therefore, the mode of action of azadirachtin is hypothesized to disrupt molting by inhibiting either the biosynthesis or metabolism of the juvenile molting hormone, ecdysone. Besides, azadirachtin exhibits low toxicity to mammals and does not cause skin irritation in most formulations [Buss and Park-Brown, 2002].

Chemically, azadirachtin is one of the most complex structure, which belongs to the C-*seco*-limonoid triterpenoid group (see Fig. 1.1) and has been found to occur in neem tree or Indian lilac tree, *Azadirachta indica* A. Juss (Meliaceae) [Ley *et al.,* 1993]. The neem tree has provided a large source of an array of biologically active triterpenoids which have been isolated mainly from the seeds but also from its bark and leaves. Since neem could provide a large source of biologically important compounds, many neem conferences and meetings have been held in the United States and other countries in the world.

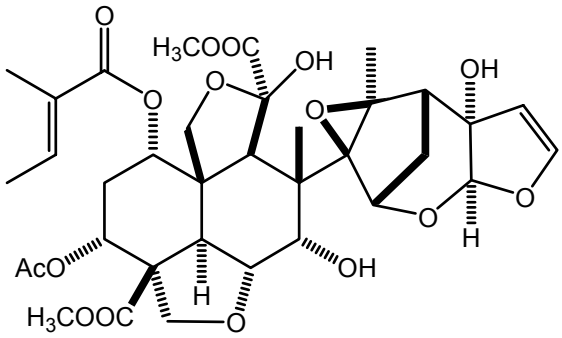

Azadirachtin

Fig. 1.1

Neem, a kind of tree, better known as margosa or Indian lilac and less commonly known as nim, kohomba, verpu, thini, mamba, or sudu, was originally grown in Southern Asia, America, and Australia. In India, neem trees are estimated to account for 14 million plants. If given the right environmental conditions, neem, an evergreen tree, is a fast-growing specie and it could grow up to 25m height. A one single 15 year old neem tree can yield up to 20 kg of fruits, in which about 2 kg of seed kernels could be obtained [Ley *et al.,* 1993]. The leaves are used to protect grain and clothes from insects and its seed oil is used as an insecticide and medicine for the treatment of leprosy, skin diseases, and malaria. *Schistocerca gregaria*, a desert locust, has been recognized over half a century ago and neem leaves act against these insects as antifeedant activity [Ley *et al.,* 1993]. Up to now, many insecticide products from neem including Align, Azatin XL, Margosan-O, Neem-Away, Neemix, Safers BioNeem, and Trilogy are commercially available in many countries around the world, like in the United States or India.

I.2.2. Rotenone

Rotenone and other rotenoids found in the roots of *Derris elliptica* or *Lonchocarpus* (Leguminosae/Fabaceae) are very powerful insecticidal and piscidal (fish poison) agents, interfering with oxidative phosphorylation. Rotenone belongs to flavonoid derivatives (see Fig. 1.2) which inhibits strongly mitochondrial respiration. It also inhibits the conversion of nutrients into energy at cellular level (cellular respiration) that leads insects to stop quickly feeding. Dead insects may occurr several hours to a few days after exposure [Buss and Park-Brown, 2002]. Rotenone is harmless to mammals unless it enters the blood stream, being metabolized rapidly upon ingestion. Rotenone degrades rapidly in air and sunlight thus it provides an excellent biodegradable insecticide. Rotenone is used as such either in pure or powdered plant form or extracts that have been formulated for sprays [Buss and Park-Brown, 2002].

In Malaysia and Indonesia small shrubs of *Derris* plants are cultivated, while *Lonchocarpus* includes shrubs and trees which are imported from Peru and Brazil. Normally, a black resinous extract is supplied to its product as the insecticidal principles. Both *Derris* and *Lonchocarpus* roots contain 3-10% of rotenone and other rotenoids at

lower amounts, e.g. deguelin. The resin may contain approximately 45 % of rotenone and 20 % of deguelin [Dewick, 2003].

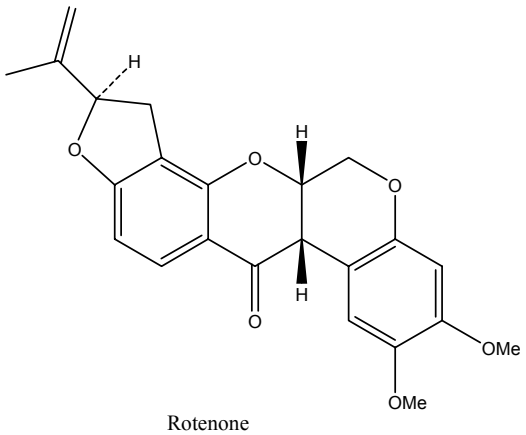

Rotenone

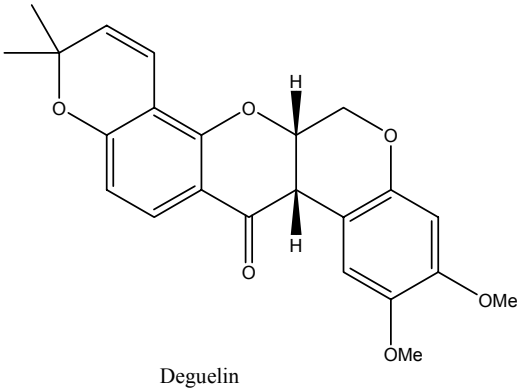

Deguelin

Fig. 1.2

The rotenoids, as insecticides, still be used for modest purposes, and could be useful for their selectivity and rapid biodegradability. Perhaps they could be inactivated too rapidly under the sunlight and the air to compete more effectively with other insecticides such as the modern pyrethrin derivatives. This could be a drawback for the use of rotenoids [Dewick, 2003].

For the last century and a half, rotenone or rotenoids have been used as both stomach and contact insecticides to control leaf-eating caterpillars. Three centuries before that, rotenone was utilized in South America to paralyze fish in order to catch them more easily after they were floating on the surface. Today, rotenone is still used to reclaim the lake for game fishing as well as for rearing shrimp in Asia [Ware and Whitacre, 2004].

Rotenone acts as a respiratory enzyme inhibitor between NAD+ (a coenzyme involved in oxidation and reduction in metabolic pathways) and coenzyme Q (a respiratory enzyme responsible for carrying electrons in some electron transport chains), this can cause respiratory problems in the insect organs [Ware and Whitacre, 2004].

I.2.3. Pyrethrum / Pyrethrins

Pyrethrum is one of the oldest and safest insecticides available. In countries such as Kenya and Ecuador, pyrethrum is extracted from some flowers that come from the specie called *Chrysanthemum*. Pyrethroids have probably become one of the most successful use of a plant product as an insecticide. In other parts of the world it has been used for centuries for the ground, and for dried flowers in the early 19th century as the original anti-louse powder to control body lice in the Napoleonic Wars [Ware and Whitacre, 2004]. Even today, powders of the dried flowers of these plants are sold as insecticides [Duke, 1990].

Pyrethrum destroys insects very quickly causing immediate paralysis, this explains its popularity in fast knockdown household aerosols. By coming into contact with these toxins an immediate knockdown or paralysis will be the outcome, however insects often metabolize themselves and can be recovered to be used as pests once again, unless it is mixed with one of the synergists [Buss and Park-Brown, 2002].

Pyrethrum consists of a mixture of four compounds (see Fig. 1.3): pyrethrins I and II and cinerins I and II, which come from a perennial daisy of the genus *Chrysanthemum*. The biologically active chemicals are esters, which occur in the flower heads. The flowers may contain 0.7-2% of pyrethrins, representing about 25-50% of the extract. A typical pyrethrin extract contains 35 % of pyrethrins I, 32% of pyrethrins II, 10% of cinerins I, 14% of cinerins II, 5% of jasmolin I, and 5% of cinerins II [Dewick, 2003].

Pyrethrins break down so rapidly under the sunlight that why they are of little use outdoors on crops. Therefore they have a short residual, and low mammalian toxicity, making them among the safest insecticides in use. However, a number of synthetic pyrethrin, which are called pyrethroids do not have this instability and are very effective. They have insecticidal activities over a thousand times that of pyrethrin I. Their trade names are Pyrenone or Pyrellin, which are available in dusts, sprays, and aerosol “bombs” of formulation forms [Buss and Park-Brown, 2002; Dewick, 2003].

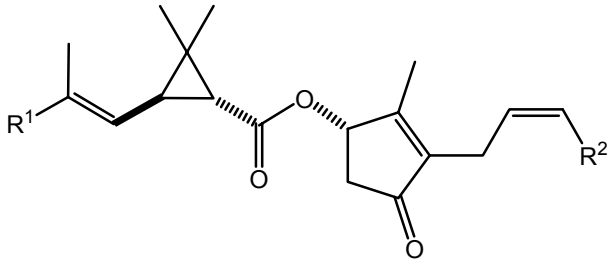

	R^1	R^2
pyrethrin I	CH_3	$CH=CH_2$
pyrethrin II	$COOCH_3$	$CH=CH_2$
cinerin I	CH_3	CH_3
cinerin II	$COOCH_3$	CH_3
jasmolin I	CH_3	CH_2CH_3
jasmolin II	$COOCH_3$	CH_2CH_3

Fig. 1.3

Originally some synthetic pyrethrins used to be called synthetic pyrethroids. Nowadays, pyrethroids are just a better nomenclature. Under the sunlight they are more stable and are more effective when used at the very low concentrations of 0.01 to 0.1 pound per acre against most agricultural insect pests [Ware and Whitacre, 2004].

At lower temperature, pyrethrum and some pyrethroids are more effective as insecticides. The peripheral and central nervous system of the insect are both affected after being treated with pyrethrum. In the earlier stage, pyrethrum activates the nerve cells in order to produce repetitive discharges. This process will eventually paralyse the nerve cells of the insects. Their action on the sodium channel will have a very strong impact on insect nervous system. In addition, in the sodium channel there is a small hole through which sodium ions are permitted to go through the axon and this will cause excitation. These actions will have a direct effect on the insect nerve cord containing ganglia and synapses, as well as in giant nerve fiber axons. Pyrethrin acts as a contact poison which can paralyze the insect victim usually within 90 seconds [Ware and Whitacre, 2004].

I.2.4. Nicotine

Nicotine, a pyrrolidine alkaloid (see Fig. 1.4) has been formulated for agricultural and horticultural uses. It is the main principal active compound from the powdered tobacco leaves *Nicotiana tabacum* and *Nicotiana rustica* (Solanaceae), which has long been used as an insecticide. Nicotine exhibites effectively towards almost types of insect pests, but it is used particularly against aphids and caterpillars, soft bodied insects [Ware and Whitacre, 2004]. The free base is considerably more toxic than salts and soaps. The insecticide product usually is marketed as a 40% liquid concentrate of nicotine sulfate, which is diluted in water and then applied as a spray [Buss and Park-Brown, 2002]. Other *Nicotiana* alkaloids, e.g. anbasine and nornicotine (see Fig. 1.4), also exhibited this insecticidal activity. Nicotine can easily interact with the nicotinic acetylcholine receptors since it is highly toxic to mammals and due to its effect on the nervous system, there is a tight binding observed which is only partially accounted for by the structural similarity between acetylcholine and nicotine [Dewick, 2003].

The insecticide product containing nicotine is more effective when applied during warm weather. Imidacloprid is the first insecticide product from nicotine. It is a systemic insecticide, having good root-systemic characteristics and acts as notable contact and stomachic. Nicotine can be applied in various objects such as a soil, seed, or foliar treatment in cotton, rice cereals, peanuts, potatoes, vegetables, pome fruits, pecans and turf, for the control of sucking insects, soil insects, whiteflies, termites, turf insects and the Colorado potato beetle, with long residual control without effect on mites or nematodes.

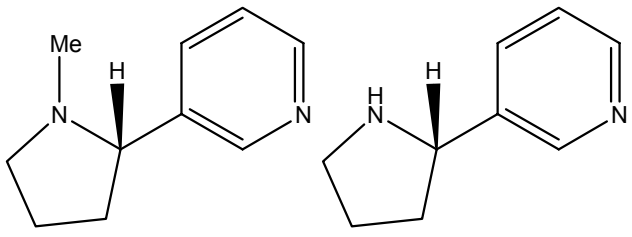

Nicotine Nornicotine

Fig. 1.4

The mode of action of nicotinoids is to act on the central nervous system of insects, causing irreversible blockage of postsynaptic nicotinergic acetylcholine receptors [Ware and Whitacre, 2004].

I.2.5. Ryania

Ryania, an alkaloid belongs to diterpene (see Fig. 1.5) group which was extracted from the stems of a woody South American plant, *Ryania speciosa*. Although Ryania has a slow-acting stomach poison, it can cause insects to stop feeding after ingestion. Ryania is more active when applied in hot weather. It shows moderately in acute or chronic oral toxicity in mammals. Generally it is not harmful to most parasites and predators, unless showing its toxicity to certain predatory mites. The residual activity of Ryania could be lasted for longer time than most of other botanicals. It was used to protect the fruits and vegetable commercially in production to against caterpillars (European corn borer, corn earworm, and others) and thrips. Commercial products are available such as Ryan 50, Ryania dust, Triple Plus, and Veratran D [Buss and Park-Brown, 2002].

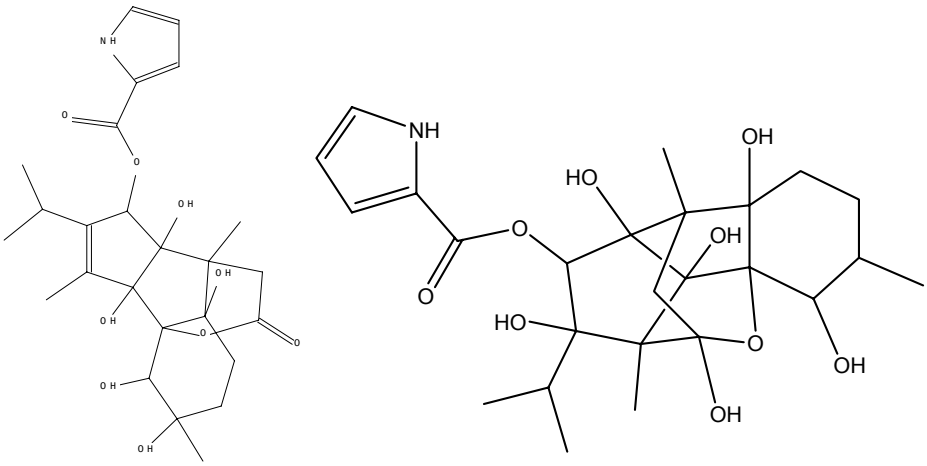

Fig. 1.5

I.2.6. Limonene

Limonene or *d*-limonene is the latest addition to the natural insecticidals. Limonene is a monoterpene (see Fig. 1.6) which belongs to a group often called florals or scented plant chemicals. Limonene is extracted from citrus peel, which exhibits effectivelly against all external pests of pets, including fleas, lice, mites, and ticks, and it is virtually nontoxic to warm-blooded animals. Limonene is the most important insecticidal substance in citrus oil, which constitutes about 98% of the orange peel oil by weight [Buss and Park-Brown, 2002].

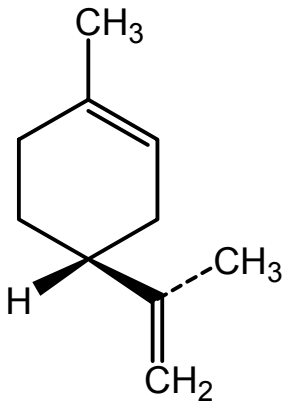

Limonene

Fig. 1.6

The mode of action of limonene is similar to that of pyrethrum. Limonene acts as contact poisons (nerve toxins). It affects the sensory nerves of the peripheral nervous system, but it is not a ChE inhibitor. It may also have some fumigant activity against fleas. Its oral and dermal toxicities are low. Limonene can evaporate readily from treated surfaces therefore it has no residual [Ware and Whitacre, 2004].

I.3. The history of insecticidal activity of rocaglamide derivatives from *Aglaia* sp.

The first remarkable antifeedant report of crude extract from *Aglaia odorata* towards the larvae of the cabbage *Pieris rapae* was published by Chiu *et al.,* in 1985. However, the active principles of *A. odorata* responsible for the strong antifeedant properties of the respective crude extracts against *P. rapae* and against other insects, were identified by Ishibashi [Ishibashi *et al*., 1993] 8 years later. Rocaglamide and three of its congeners are responsible compounds for the activity when using the larvae of the polyphagous noctuid *Peridroma saucia* as experimental insects. Suprisingly, rocaglamide had already previously been isolated by King *et al.,* in 1982 from *A. elliptifolia* [King *et al.,* 1982].

To date, more than fifty naturally occurring rocaglamide derivatives were islolated from different *Aglaia* species collected mainly in Indonesia, China, Thailand, and Vietnam [Proksch *et al.,* 2001].

Rocaglamide and its derivatives were analysed for their insecticidal activity employing *S. littoralis*. Most of different rocaglamide derivatives were usually added at a range of concentrations to artificial diet, which was subsequently offered to newly, hatched larvae in a no choice chronic feeding bioassay. With only a few exceptions all naturally occurring rocaglamide congeners analysed, exhibited strong insecticidal activity towards larvae of *S. littoralis*. The very active rocaglamide compounds exhibited LC_{50} values ranging between 1-2 ppm and are thus comparable with regard to their insecticidal activity to azadirachtin (see Table 1.1) [Nugroho *et al.,* 1999].

Table 1.1: LC_{50} and EC_{50} values of insecticidal rocaglamides derivatives and of azadirachtin towards neonate larvae of *Spodoptera littoralis*

Compounds	LC_{50} (ppm)	EC_{50} (ppm)
Rocaglamide	0.9	0.08
Rocaglamide derivatives	0.8-1.6	0.09-0.52
Azadirachtin	0.9	0.04

The mode of action of rocaglamide compounds is still in discussion. It is difficult to decide whether the mortality of the *S. littoralis* larvae, which was observed in chronic feeding bioassays, is mainly caused by starvation due to feeding deterrency or by a direct toxicity or by a combination of both. When neonate larvae of *S. littoralis* were given the choice between artificial diet treated with rocaglamide and that of the control diet, they avoided the former and showed a clear preference for the latter. The IC_{50} in these experiments varied between 0.2 – 0.25 ppm indicating that rocaglamide and its congeners have strong antifeedant properties [Nugroho *et al.,* 1999]. Rocaglamide also exhibited toxicity when it was injected into the haemolymph of last instar larvae of *S. littoralis*. In these experiments the LC_{50} of rocaglamide varied between 5.6 – 7.5 ppm [Nugroho *et al.,* 1999 and [Proksch *et al.,* 2001]. These experiments prove that rocaglamide and its congeners are active against herbivorous insects as antifeedants but are also toxic to insects. However, the molecular target of rocaglamide and its congeners in insects is still unknown. The insecticidal activity of these compounds can be linked to distinct structural

features such as the OH group at position C-8b that is an indispensable prerequisite for its bioactivity. The structures of rocaglamides known so far are summarized in Table1.2, Fig. 1.7 and Fig. 1.8 [Proksch *et al.,* 2001].

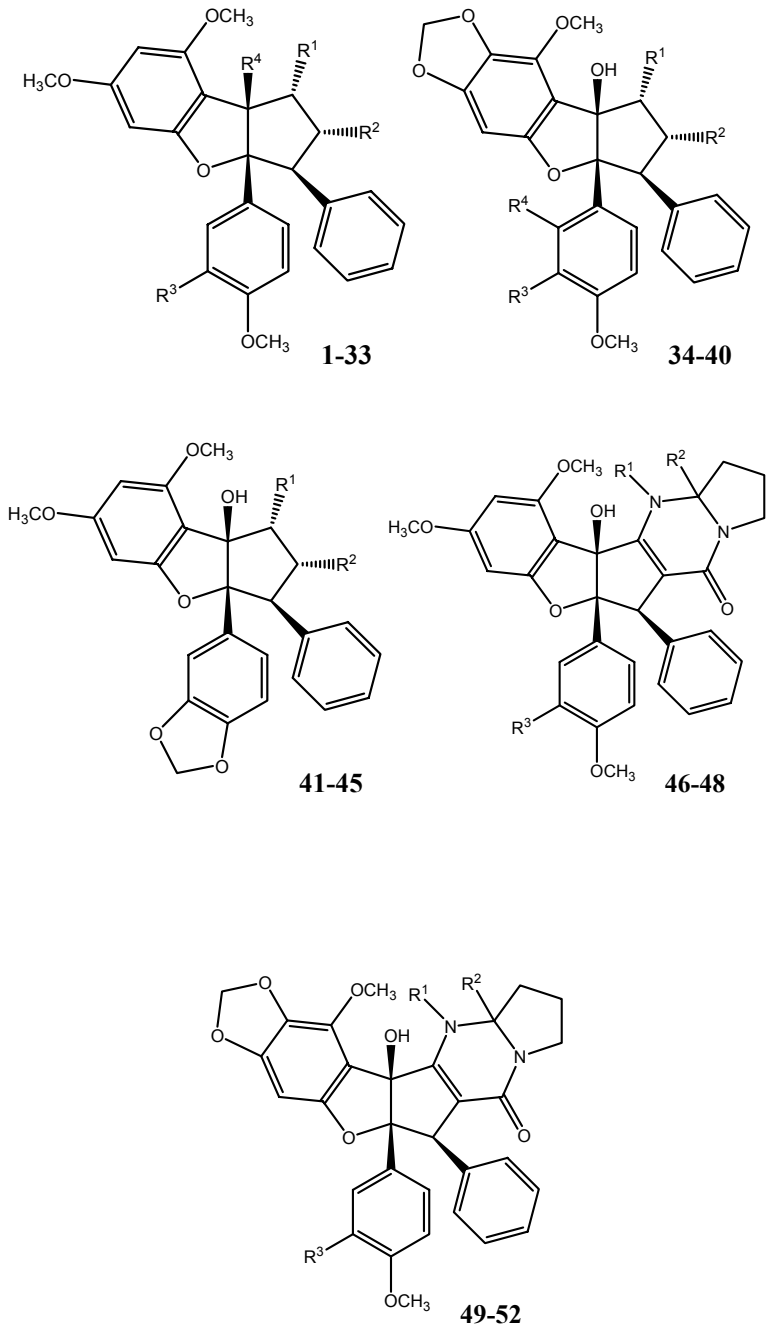

Fig. 1.7

Table 1.2: Rocaglamide derivatives isolated from *Aglaia* species

Com-pound	Trivial name	R^1	R^2	R^3	R^4
1	rocaglamide	OH	$CON(CH_3)_2$	H	OH
2		OH	$CON(CH_3)_2$	OH	OH
3	(aglaroxin E)	OH	$CON(CH_3)_2$	OCH_3	OH
4		$OCOCH_3$	$CON(CH_3)_2$	H	OH
5		$OCOCH_3$	$CON(CH_3)_2$	OH	OH
6		OH	$CON(CH_3)_2$	OH	OC_2H_5
7	desmethyl-rocaglamide	OH	$CONHCH_3$	H	OH
8		OH	$CONHCH_3$	OH	OH
9		$OCOCH_3$	$CONHCH_3$	H	OH
10		$OCOCH_3$	$CONHCH_3$	OH	OH
11		OH	$CONHCH_3$	OH	OC_2H_5
12		OH	$CONH(CH_2)_4OH$	H	OH
13		$OCOCH_3$	$CONH(CH_2)_4OH$	H	OH
14		OH	ring[1]	H	OH
15	didesmethyl-rocaglamide	OH	$CONH_2$	H	OH
16		OH	$CONH_2$	OH	OH
17		$OCOCH_3$	$CONH_2$	H	OH
18	methyrocaglate	OH	$COOCH_3$	H	OH
19		OH	$COOCH_3$	OH	OH
20		OH	$COOCH_3$	OCH_3	OH
21		$OCOCH_3$	$COOCH_3$	H	OH
22		$OCOCH_3$	$COOCH_3$	OH	OH
23		OCHO	$COOCH_3$	H	OH
24		OCHO	$COOCH_3$	OH	OH
25		=NOH	$COOCH_3$	OCH_3	OH
26		OH	$COOCH_3$	H	OCH_3
27	rocagloic acid	OH	COOH	H	OH

28	rocaglaol	OH	H	H	OH
29		OH	H	OCH_3	OH
30		OH	H	sugar[2]	OH
31		OH	H	sugar[3]	OH
32		OH	H	H	OC_2H_5
33		OH	H	H	OCH_3
34	aglaroxin A	OH	$CON(CH_3)_2$	H	H
35	aglaroxin B	OH	$CON(CH_3)_2$	OCH_3	H
36	aglaroxin F	OH	$CON(CH_3)_2$	OCH_3	OH
37	pannellin	OH	$COOCH_3$	H	H
38	pannellin-1-O-acetate	$OCOCH_3$	$COOCH_3$	H	H
39	3‘-methoxy pannellin	OH	$COOCH_3$	OCH_3	H
40		=O	chain[4]	H	H
41		OH	$COOCH_3$	-	-
42		OH	H	-	-
43		=O	H	-	-
44		OCHO	$COOCH_3$	-	-
45		$OCOCH_3$	$COOCH_3$	-	-
46		$\Delta_{9,10}$		H	-
47		$\Delta_{9,10}$		OH	-
48	(aglaroxin D)	H	H	H	-
49	aglaroxin C	$\Delta_{9,10}$		H	-
50	aglaroxin G	$\Delta_{9,10}$		OCH_3	-
51	aglaroxin H	H	H	OCH_3	-
52	aglaroxin I	H	H	H	-

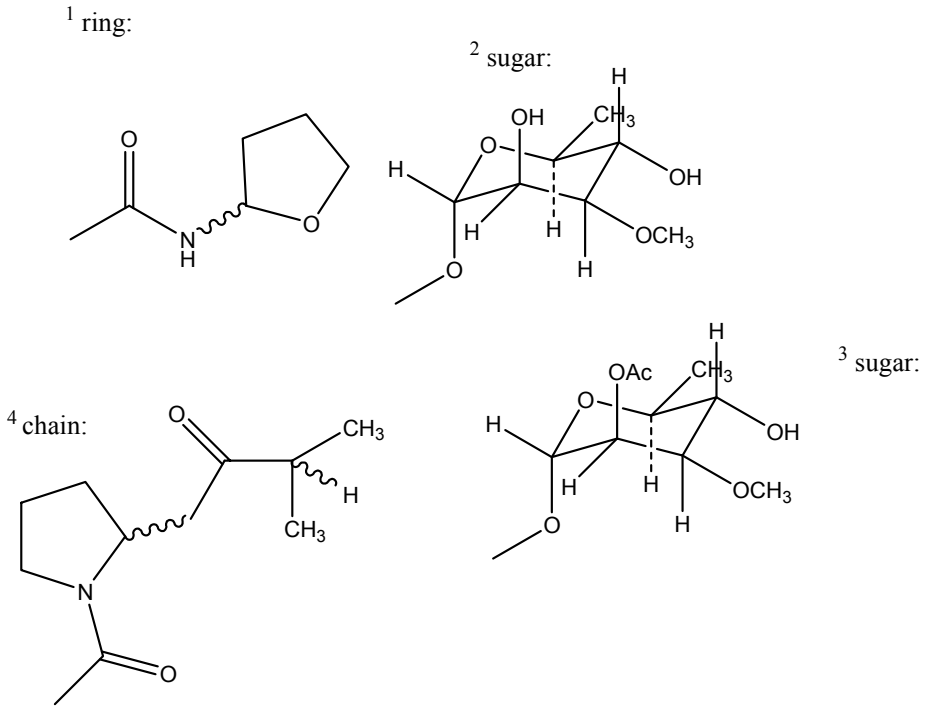

Fig. 1.8

I.4. Aim of the work

I.4.1. The advantages of the natural insecticides

It is obvious that natural products generally have a much shorter half-life in the environment than synthetic pesticides. One advantage of plant insecticides is that many of them are biodegradable. Thus natural insecticides are more environmentally and toxicologically safe and more selective and effective pesticides. Most synthetic chemicals have more relatively long environmental half-lives and more toxicological properties in comparison to natural compounds [Duke, 1990].

In most cases, natural insecticides are less toxic to humans than synthetically derived insecticides. Some of the advantages of botanical insecticides are described below by [Cloyd, 2004].

In general, natural insecticides are quickly degradated under environmental conditions such as sunlight, humidity, and rainfall. Also, they are less persistent and have a short residual life which can reduce their effect on beneficial and nontarget organisms. They are able to kill insects rapidly or stop them from feeding almost immediately after

application. The majority of natural insecticides possesses low mammalian toxicity and is generally nontoxic to humans, mammals, and honeybees. Besides**,** most natural insecticides are generally less harmful to beneficial insects, mites and plants in comparison to those of synthetically-derived insecticides. Thereby, they are selective and minimal impacts on plants [Cloyd, 2004].

It is clear that there is a great potential of using natural products in agriculture for controlling pests with less risk than with synthetic compounds that are toxicologically and environmentally undesirable [Duke, 1990]. Isolation and chemical characterization of the active compounds from plants with strong biological activities could be a major effort compared to new synthetic compounds. Thus, the chemistry of natural compounds has increasingly become the focus of those interested in discovery of new pesticides.

I.4.2. Facing with the problems arising in Vietnam on the field of crops protection

Vietnam is an agricultural land in which agriculture accounts for about 80% of the country's economy. The cultivation of crops and vegetables implies the necessity for protection against herbivorous insects as well as plant pathogens. Up to date, Vietnamese farmers almost always use imported chemical insecticides. These chemical pesticides often decompose very slowly, accumulate in the food chain, decrease quality of agricultural products, pollute the environment, and exhibit a high toxicity towards human beings. This indeed causes serious health problems in Vietnam with many people ending up in the hospital or even dying, recently.

Table 1.3 indicates 898 farmers, who worked with rice, vegetables, tea and grade which were affected with symptoms of pesticide poisoning [Le *et al.,* 2000].

Table.1.3: Percentage of infected farmers with pesticide poisoning in Vietnam

Growers	Number of farmers examined	Number of person harmed by pesticides	Percentage of harmed by farmers
Rice	240	39	16.3
Vegetables	287	53	18.5
Tea	151	27	17.9
Grape	220	45	20.4
Total	**898**	**164**	**18.26**

The data revealed a serious concern that, at least one person per household including 11.5 million households in Vietnam could be a victim of pesticide poisoning. These facts emphasize the urgency to find healthy alternatives for people and environmentally compatible means of plants protection.

According to taxonomists as cited in "An illustrated Flora of Vietnam" [Pham Hoang Ho, 1999] there are about 30 species of *Aglaia* found in Vietnam. They are distributed variously and are easily found from the North to the Middle and Southern Vietnam.

Based on the promising results of the insecticidal potencial of rocaglamide derivatives from *Aglaia* sp. [Nugroho, 1999 and Proksch *et al*., 2001], my study in this disertation is to focus on the isolation of new insecticidal rocaglamide derivatives and other constitutents from *Aglaia* species collected in Vietnam by using different chromatographic techniques like TLC, VLC, LC, MPLC, or semipreparative HPLC. The physical methods such as mass spectrometry, 1D and 2D NMR spectroscopy, X-ray, and Mosher reaction were used for structure elucidation of the isolated compounds;

The second aim is based on the insecticidal screening and bioassay- guided fractionation of the most active extract of *Aglaia* species collected from Vietnam. Bioassays were done under field conditions in Vietnam by formulating Aglaia extracts into liquid spray solution. The main objective is to formulate a new natural insecticide that could be of low cost and constitute an economically efficient substitute for the conventionally commercially available chemical pesticides, which have been a disadvantage to the environment as well as the health of the Vietnamese people.

II. MATERIALS AND METHODS

II.1. Materials

Thirteen different *Aglaia* species were collected from the Northern and the Middle region of Vietnam (see Table 2.1). They were all pre-treated prior to drying in a drying room using dehumidifiers. All the specimens were identified by the botanist (Dr. Tran Ngoc Ninh, BSc. Nguyen Kim Dao, and Dr. Nguyen Trong Son) well kept at the storage department of the Institute of Chemistry, Vietnamese Academy of Sciences and Technology. These samples were ground and extracted with n-hexane, dichloromethane, and methanol or ethanol. The solvent was removed by a vacuum evaporator. Thirty-eight crude extracts were obtained and screened for the insecticidal activity in a chronic feeding assay with larvae of *Spodoptera littoralis* at the Institute of Pharmaceutical Biology and Biotechnology, Heinrich-Heine-University Düsseldorf.

Table 2.1: List of *Aglaia* species collected in Vietnam

N^0	Species (Latin name)	Plant (Vietnamese name)	Part of plant	Place of collection	Time of collecton
1	*Aglaia macrocarpa* (Miq) C.M.Pannel	Goi do	Tg, Lf, Bk	Catba-Haiphong	7/2001
2	*Aglaia oligophylla* Miq	Goi oi	Tg+Bk, Lf	Catba-Haiphong	7/2001
3	*Aglaia gigantea* Pierre	Goi nep, goi tia	Tg, Bk, Lf	Catba-Haiphong	7/2001
4	*Aglaia pleuroptiris* Pierre	Ngau canh	Tg, Lf	Donghy-Haiphong	6/2001
5	*Aglaia elaeagnoidea*		Tg, Lf, Bk	Catba-Haiphong	9/2002
6	*Aglaia aff. poilanei*		Lf+Tg, Bk	Catba-Haiphong	9/2002
7	*Aglaia gigantea*		Lf+Tg, Bk	Catba-Haiphong	9/2002
8	*Aglaia dasyclada*		Tg,Lf	Hue	9/2002
9	*Aglaia roxburghiana*		Tg, Bk, Lf	Hue	9/2002
10	*Aglaia sp. Pierrea*		Lf,Tg, Ft	Hue	9/2002
11	*Aglaia abbriviata*	Ngau rung	Lf	Nghean	6/2003
12	*Aglaia duppereana*	Ngau uop che	Lf	Hanoi	11/2003
13	*Aglaia olygophylla*		Lf	Catba-Haiphong	5/2003
14	*Aglaia roxburghiana*	Ngau	Ft	Phutho	4/2001
15	*Aglaia rothii Syn.Cifadessa baccifera*	*Syn.Melia baccifera*	Lf	Hoabinh	6/2004

Lf = leaf ; Tw = twig; Bk = Bark; Ft= Fruit

II.2. Chemicals used

II.2.1. General laboratory chemicals

Agar-Agar	Merck
Anisaldehyde (4-methoxybenzaldehyde)	Merck
Trichloromethane Deuteri for NMR	Merck
Dichloromethane Deuteri for NMR	Merck
Dimethylsufoxide (DMSO) for NMR	Merck
Pyridine Deuteri for NMR	Merck
Formaldehyde	Merck
L-(+)-Ascorbic acid	Merck
Napagin A	Sigma
Concentrated sulfuric acid	Merck
Trifluroacetic acid (TFA)	Merck
(S)(+)-MTPA and (R)(-)-MPTA	Sigma

II.2.2. Solvents

Acetone
n-Butanol
Dichloromethane
Ethanol
Ethylacetate
n-Hexane
Methanol
Iso-propanol
Chloroform
Acetic acid

Solvents were purchased from the University of Düsseldorf. All solvents were distilled prior to use and spectral grade solvents were used for spectroscopic measurements.

II.2.3. Chromatography

Pre-coated TLC plates (AluO, silica Gel 60 F254, layer thickness 0.2mm)	Merck
Pre-coated TLC plates (Glass, RP-18 F254, layer thickness 0.25mm)	Merck
Silica Gel 60, 0.04-0.063 mm mesh size	Merck
Sephadex LH 20, 25-100 mm mesh size	Merck
Methanol for HPLC , MeOH LiChrosolv HPLC	Merck
Phosphoric acid 0.15%, PH 2.0	Merck
Nonapure water	Barnstead

II.3. Equipment used

Balances	Mettler 200 Mettler AT 250 Mettler PE 1600 Sartorious RC210P
Centrifuge	Kendro D-37520 osterde
Drying ovens	Heraeus T5050
Fraction collector	ISCO Cygnet
Freeze dryer	LYOVAC GT2, Pump TRIVAC D10E
HPLC-Dionex	Pump:Dionex P580A LPG HPLC program:Chromeleon (V.6.3) Detector: Dionex Photodiode Array Detector UVD 340 S Column thermostat: STH 585 Autosampler: ASI-100T
HPLC/MS-Aglient 1100	ThermoFinnigan LCQ Deca
Mill	RETSCH GmbH 5657 HAAN WEST-GERMANY Type:SK1, Nr: 25684
Hot plates - Magnetic stirrer	Variomag Multipoint HP, Camag
PH-Electrode	Inolab Behrotest PH 10-Set
Rotary Evaporator	Büchi Rotavap RE111
Sonicator	Bendelin Sonorex RK 102
HPLC-Semipreparative	Merck
HPLC-Preperative	Varian Model 218,Seri N0.00570 Column: Dynmax 250*21.4 mm (L*ID) S/N 3017 Microsorb 60-8 C18-R00083221C
UV lamp	Camag (254 and 366 nm)
Vacuum desiccator	Savant Speed Vac SPD 11V Savant Refrigerator Vapour Trap RVT400, Pump Savant VLP80
Potter Spray Tower	Standard model from the Agronomics Division of Burkard Scientific
Insects Rearing Chamber	NK System

II.4. Chromatographic Methods

II.4.1. Thin layer chromatography (TLC)

TLC was performed on pre-coated TLC plates with Si gel 60 F_{254} (layer thickness 0.2 mm, E. Merck, Darmstadt, Germany) with either CH_2Cl_2: MeOH (9:1) for semi-polar compounds or n-Hexane: EtOAc (8:2) for non-polar compounds as mobile phase. TLC on reversed phase (RP)-C18 F_{254} (layer thickness 0.2 5 mm, E. Merck, Darmstadt, Germany) was used for polar compounds using the solvent system MeOH:H_2O (95:5, 90:10, or 85:15). The compounds were detected by their UV absorbtion at 254 and 366 nm or by spraying the TLC plates with anisaldehyde reagent followed by heating at 110^0C.

Formular of Anisaldehyde/ H_2SO_4 Spray Reagent (DAB 10)

Anisaldehyde:	5 parts
Glacial Acetic Acid:	100 parts
Methanol:	85 parts

The above ingredients were mixed, to which 5 parts of concentrated H_2SO_4 were added slowly. The reagent was stored in an amber-colored bottle and kept refrigerated until use.

TLC was used to monitor the identity and the qualitative purity of fractions and isolated compounds. It was also ultilised to optimize solvent systems applied for column chromatography in further steps of isolation.

II.4.2. Column chromatography

Crude extracts were subjected to repeated separation through column chromatography using appropriate stationary phases and solvent systems previously determined by TLC. The solvent system used for separation on silica gel was gradient CH_2Cl_2: MeOH, starting with 100% of CH_2Cl_2. For Sephadex columns, the solvent MeOH (100%) was applied.

II.4.3. Vacuum liquid chromatography

Vacuum liquid chromatography (VLC) is a useful method as an initial isolation step for large amounts of sample. The crude extracts were first applied to this chromatographic technique. The apparatus consists of a 500 mL sintered glass Büchner filter funnel with an inner diameter of 12 cm. Fractions were colleceted in

Erlenmeyer flasks. Silica gel 60 was packed to a hard cake at a height of 5 cm under applied vacuum. The samples were dissolved and mixed with such silica gel to form a slurry. The solvent was evaporated and the resulting sample mixture was packed onto the top of the column. Step gradient elution commences with a non polar solvent, i.e. n-hexane, then increasing amouts of a more polar solvent (EtOAc, MeOH) was added.Vacuum was applied to suck each solvent gradient through the column. The column was allowed to run dry between each solvent gradient.

II.4.4. Semi-preparative high pressure liquid chromatography (HPLC)

Semi-preparative HPLC is a technique which is used for isolation of pure compounds from fractions previously cleaned up using conventional column chromatography. The separation column (125 x 4 mm, i.d.) was prefilled with Eurospher C-18 (Knauer, Berlin, Germany) or Dynmax (250 x 21.4 mm, L.ID). The amout of each injection is dependent on the column size. For a smaller column, 3 mg sample was dissolved in 1 mL starting gradient of solvent system and used for one injection. With a big column, samples reaching 20 mg can be injected at once. The gradient solvent system was a mixture of methanol or acetonitrile and nanopure water with or without 0.1% TFA, and the flow rate of 5 mL/min. The eluted substances were collected after detection by an UV-VIS diode array detector.

II.4.5. Analytical high pressure liquid chromatography (HPLC)

In the HPLC an efficient separation is achieved by passing a mobile phase through a column using high pressure pumps. Analytical HPLC was used to identify peaks from raw extracts or fractions, and to evaluate the purity of isolated compounds. The different components in the mixture pass through the column at different rates due to differences in their partitioning behaviour between the mobile liquid phase and the stationary phase. The solvent gradient used started with 10:90 (MeOH: nanopure water (adjusted to pH 2 with phosphoric acid) increasing to 100 % MeOH in 45 minutes. The compounds were detected by an UV-VIS diode array detector.

II.5. Physical chemistry methods for structural elucidation

II.5.1. Mass Spectrometry (MS)

Mass spectrometry (MS) is an analytical method based on the determination of molecular masses of individual species in a sample. In a mass spectrometer a compound is vaporized in vacuum and bombarded with an electron beam of high energy normally, 70 electron-volts (which is more than 1,600 kcal/mol). Since this energy is much greater than the chemical bond energy, fairly drastic things happen when a molecule is subjected to such condition. Mass spectrometers can be classified into several categories based on the mass ionisation techniques used.

II.5.1.1. Electron Ionisation Mass Spectrometry (EI-MS)

Electron ionization is still the most widely used technique for the analysis of volatile molecules. It is considered to be a ``hard ionisation´´ process, which leads to reproducible spectra that can be compared to a library of mass spectra for compound identification. In this technique, ionization occurs in the ion source by collision of the sample molecules with electrons that are emitted from a filament by a thermoionic process [Francis and Annick, 2000]. In EI-MS, the energy for ionization (70 eV) is achieved by accelerating the electrons produced by the filament through a potential drop of 70 V, applied between the filament and the chamber. Ionisation efficiency in EI-MS is in the order of one ion produced for every 10,000 molecules.

II.5.1.2. Fast Atom Bombardment Mass Spectrometry (FAB-MS)

In FAB, a beam of fast atoms (high – energy argon or xenon) is used to induce ionization. The fast atoms are produced by first ionization argon or xenon gas in a cell, accelerating these primary ions formed, then by colliding these ions with slow-moving neutrals of the same gas. In these collisions, the charge of the fast-moving ion is transferred to slow-moving neutral species resulting in a fast neutral atom, which is then directed at the sample. In FAB, the sample is usually dispersed in a non-volatile liqid matrix, such as glycerol or diethanolamine, and deposited at the end of a sample probe that can be inserted into the ion source. The sample on the probe is ionized when bombarded by the fast atom beam. However, ionization of the matrix also occurs, leading to a very large background signal. The technique is thus limited to analysis of small molecules. Fast-moving ions (Cs+ or Ar+) can also be used instead

of fast-moving atoms, the technique is then called Liquid Secondary Ion Mass Spectrometry (LSIMS).

II.5.1.3. Electron Spray Ionisation Mass Spectrometry (HPLC/ESI-MS)

HPLC/ESI-MS was carried out using a ThermoFinningan LCQ-Deca mass spectrometry connected to an UV detector. The samples were dissolved in MeOH and injected to the HPLC/ESI-MS set up. A solution of the sample is then sprayed at atmospheric pressure through a 2-5 kV potential. HPLC was run on a Eurospher C-18 (6 x 2 mm, i.d.) reversed phase column. The mobile phase was H_2O 0.1% Formic acid (A), to which MeOH (B) or ACN (C) was added by a linear gradient: initial, 0% of B; 45 min, 80% of B; 55 min, 100% of B. The flow rate was at 400 µL/min and the absorbance detected at 254 nm. ESI (electrospray ionization) was performed at a capillary temperature of 200^0C and drift voltage of 20eV. Since the molecular ion peak is the most abundant ion in ESI spectra, it is also possible to perform MS/MS experiments. In the MS/MS experiment, the molecular ion from an initial fragment ion corresponds to a certain functional group. Measurements were done at Institute of Pharmaceutical Biology and Biotechnology, University of Heirich-Heine-Düsseldorf.

II.5.2. Nuclear magnetic resonance spectroscopy (NMR)

Nuclear magnetic resonance spectroscopy (NMR) is the one of the most efficient methods for studying molecular structures. An NMR spectrum provides detailed molecular structure, that would be difficult, if not impossible, to obtain by any other methods. NMR measurements were recorded by Dr. Peters at the Institute of Organic Chemistry, Heinrich-Heine-Univeristy Düsseldorf and by Dr. Victor Wray at the Gesellschaft für Biotechnologische Forschung (GBF) in Braunschweig. The ^{1}H NMR and ^{13}C NMR spectra were recorded at 300^0K on Bruker DPX 300, ARX 400, 500 or AVANCE DMX 600 NMR spectrometers. All 1D and 2D spectra were obtained using the standard Bruker software. The sample was dissolved in a deuterated solvent (i.e. CD_3OD, $CDCl_3$, CD_2Cl_2, DMSO), the choice of which is dependent on the solubility of the sample. TMS was used as internal standard reference signal. The observed chemical shifts (δ) were recorded in ppm and the coupling constants (*J*) were recorded in Hz. Several other modern NMR techniques were performed in order to elucidate the structure of isolated compounds, such as; **DEPT** (**D**istortionless **E**nhancement by **P**olarization **T**ransfer) which distinguishes and classifies the carbons as doublets (CH), triplets (CH_2), or quartets (CH_3); **NOE** (**N**uclear **O**verhauser **E**ffect) solved

problems of stereochemical assignments, which could not be solved by analysis of the spin coupling constants; **NOESY** and **ROESY** are two of the most useful techniques as they allow nuclei to correlate through space (distance smaller than 5 Å); **HMQC** (**H**etero **M**ultinuclear **Q**uantum **C**oherence) was used to directly correlate proton and carbon nuclei through one bond and the **HMBC** (**H**etero **M**ultinuclear **B**ond **C**oherence) was utilized to obtained long range correlations of proton and carbon nuclei through two, three, or four bonds.

II.5.3. Optical activity

Optical rotation was determined on a Perkin-Elmer-241 MC polarimeter by measuring the angle of rotation at the wavelength of 546 and 579 nm of mercury vapour lamp at room temperature (25^0C) in a 0.5 mL cuvette with 0.1 dm length. The specific optical rotation was calculated using the formula:

$$[\alpha]_D = \frac{3.199 \times [\alpha]_{579}}{4.199 - \frac{[\alpha]_{579}}{[\alpha]_{546}}}$$

where $[\alpha]_D$ = the specific rotation at the wavelength of the sodium D-line at 589 nm and a temperature of 20^0C. $[\alpha]_{579}$ and $[\alpha]_{546}$ = the optical rotation at wavelengths 579 and 546 nm, respectively, calculated using the formula:

$$[\alpha]_\lambda = \frac{100 \times c}{I \times c}$$

Where α = the measured angle of rotation in degrees, I = the length of the polarimeter tube in dm, c = the concentration of the substance expressed in g/100 mL.

II.5.4. X-ray Crystallography

X-rays, which have an approximate range of wavelengths of 0.1 to 100 Å are usually produced by decelerating rapidly moving electrons very quickly and converting their energy of motion into a quantum of radiation. The wavelength of the emitted radiation will depend on the energy of electrons. To generate X-rays, electrons are accelerated by an electric field and directed against a metal target, which slows them rapidly by multiple collisions. Under the usual conditions most of the electrons are not brought to a full stop by a single collision and a continuum of radiation is formed [George and Lyle, 1968]. Crystals of the compound dasyclamide (compound **20**) were obtained from a 4:1 mixture of hexane and ethyl acetate. A well shaped one, suitable for X-ray study, was selected by means of a polarisation microscope and investigated at ambient

temperature on a Stoe Imaging Plate Diffraction System, using graphite monochromatized Mo Kα radiation (λ = 0.71073 Å). Unit cell parameters were determined by a least-squares refinement on the positions of 6726 reflections, distributed equally in reciprocal space in the range 2.0° < Θ < 25.9°. A monoclinic lattice was found, and space group $P2_1/c$ was uniquely determined by inspection of the systematic extinctions. Crystal data, as well as details of data collection and structure refinement are listed in Table 3.33. For all data Lp corrections were performed. The structure was solved by direct methods [Sheldrick, SHELXS, 1986] and subsequent Fourier-syntheses. Approximate positions of all hydrogen atoms were found *via* different Fourier-syntheses. Refinement by full-matrix least-squares calculations on F^2 [Sheldrick, SHELXS, 1997] converged (shift/esd: 0.000) to the final indicators given in Table 3.34 and Table 3.35. Refined parameters include anisotropic displacement parameters for all the non-hydrogen atoms. The H atoms were treated as riding on their parent carbon and oxygen atoms, respectively, in idealised positions. The orientation of the O-H bond was chosen taking into account the results of Δ*F*-syntheses. Individual isotropic displacement parameters were refined for all the hydrogen atoms with the exception of those of the methyl group that were kept equal to 150% of the equivalent isotropic displacement parameter of the parent carbon atom. Scattering factors, dispersion corrections and absorption coefficients were taken from International Tables for Crystallography (1992, Vol. C, Tables 6.114, 4.268 and 4.2.4.2). Crystallographic data (excluding structure factors) for the structures reported in this paper have been deposited with the Cambridge Crystallographic Data Centre as supplementary publications no. CCDC XXXXXX.

II.5.5. Mosher reaction

Mosher reaction is a method which was applied to differentiate between (*R*) or (*S*) configuration. The method is based on the selective reaction of the compound with either (*R*) (-)-MTPA or (*S*) (+)-MTPA. Compound **22** was divided into two parts, each part , 1 mg, was dissolved in pyridine (0.5 ml) and transferred to an NMR tube. The ^{1}H NMR and ^{1}H-^{1}H COSY of compound **22** were previously measured in pyridine-d_6 before adding 5 µl of (*R*)-MTPA or (*S*)-MTPA reagent to the both parts. The NMR tubes were shaken carefully to mix the samples and the MTPA reagent evenly. The NMR tubes were allowed to stand in room temperature and the reaction monitored by ^{1}H NMR and ^{1}H-^{1}H COSY.

II.6. Bioassays

II.6.1. Insecticidal activity

II.6.1.1. Culture conditions

Spodoptera littoralis (a polyphagous pest insect, Noctuidae, Lepidoptera) is one of the most robust and hazardous insects found in the Mediterranean region and in Africa. It provides a good test model for an insecticidal bioassay on a broad spectrum of natural products. It has a short life cycle of four weeks and is easy to maintain in the laboratory with an artificial diet composed mainly of leguminous beans in agar (see Table 2.2). The larvae of *Spodoptera littoralis* were controlled in the laboratory colony under standardized conditions [Srivastava and Proksch, 1991]. In order to keep *Spodoptera littoralis* continuously alive in laboratory conditions, the maintenance of egg, larvae, pupae, and adult was done as a regular process. Fresh diet was supplied to the larvae, pupae, and adults every two days. Larvae were reared in small plastic boxes depending on their age and kept in a chamber at 28^{o} C. Larvae at their pre-pupal stage were regularly separated (to prevent cannibalism) and set on Vermiculit, a silicated mineral, without food until they reach the pupal stage. The pupae were then stored in a dark humid chamber at 28^{o}C until they develop into their final adult stage. The adults were then transferred to a 10 liter plastic pail, lined with filter paper on which the females could lay their eggs. The adults feed on a saccharose solution and were kept in the incubator at 28^{o}C. The laid eggs were collected every two days and transferred to a dark chamber until the neonate larvae hatch.

II.6.1.2 Artificial diet

Artificial diet for culture maintenance

The formula for artificial diet was prepared in Table 2.2. White beans (600g) were mixed with water (1.6 L) and left overnight. Yeast, Nipagin, Ascorbic acid, Formaldehyde and Gentamycin were added to the mixture and homogenized by using a mixer into a suspension. The agar (40 g) was boiled in water (1 L) and cooled down to ca 50^{o}C, then added into the well-mixed bean suspension. The agar bean mixture was poured into several plastic boxes (20x20x10 cm) and cooled to room temperature to solidify. The ready-to-use agar bean diet was stored in the refrigerator.

Table 2.2: Formula of artificial diet

Ingredients	Amounts
1.White beans (Müller´s Mülhle GmbH)	600 g
2.Hefe/yeast extract (Bella back)	100 g (4 packs)
3. Ascorbic acid / Vitamin C (Caelo)	12 g
4.Nipagin/p-hydroxybenzoic acid ethyl ester (Sigma)	12 g
5.Gentamycin sulphate (Serva)	720 mg
6.Formaldehyde (Merck)	4 ml
7.Agar (Caelo)	40 g

Artificial diet for the chronic feeding assay

The artificial diet for the chronic feeding assay was prepared in the same way as described above leaving out gentamycin and agar. The bean suspension was freeze-dried then ground to powder form and kept in a freezer till ready to use.

The test sample was dissolved in methanol then incorporated to 0.735g of the freezed–dried powder homogenated in a 25 mL-glass beaker, the carrier solvent was allowed to evaporate overnight. For the biological screening studies, concentrations of 5.0 mg, 1.0 mg and 0.5 mg were used for crude extracts, fractions, and pure compounds, respectively. Each sample was then added together with 0.75 mg gentamycin into a water solution (1.41 ml). Then 0.3 g /2.2 ml of boiled agar after cooling down was added to each beaker homogenously and left to solidify at room temperature. In this assay, the neonate larvae (n=20) of *Spodoptera littoralis* were forced to feed on the treated artificial diet, then the larvae were monitored after 7 days of incubation at 28^{o}C in a dark humid chamber. After 7 days, survival of the larvae and weight of the surviving larvae were protocolled. This assay was used to detect growth inhibitory activity by comparison of the larvae weights to those of the control larvae.

$$\textbf{\% larvae weight gain} = \frac{Average\,larval\,weight\,(sample)}{Average\,larval\,weight\,(control)} \text{ x } 100$$

$$\textbf{\% Survival rate} = \frac{No.\,of\,\,surviving\,larval\,\,(sample)}{No.\,of\,\,surviving\,larval\,(control)} \text{ x } 100$$

Normally, an active compound should exhibit insecticidal activity at a range of added doses (26-132 ppm). Potency was determined as effective concentration (EC_{50}) of the

test substance added to the diet necessary to cause a 50% reduction in weight. Lethal concentrations that cause 50% death (LC_{50}) were also determined. From the dose response curves obtained, the ED_{50} and LC_{50} were calculated by probit analysis by Finney [Finney, 1971].

II.6.2. Insecticidal assay in Petri dishes

II.6.2.1. Culture maintenance

Spodoptera litura was collected from the field and reared on leaves of *Brassica rapae* under laboratory conditions in the insect rearing chamber. The second instar larvae were used for the toxicity test. The mass rearing method of *S.litura* employed was introduced by FAO (Food Agriculture Organization).

II.6.2.2. Toxicity assay

Instead of an artificial diet as in the chronic feeding assay, fresh leaves of *Brassica rapae* were applied. Experiments were conducted under the FAO guideline in terms of rearing normal insects for LC_{50} and LD_{50} evaluation [Campbell *et al.,* 1943 and Finney, 1971]. Spraying techniques were carried out with a Potter Spray Tower (see Fig. 2.1) for topical applications. The experiment was done in a 12 cm diameter Petri dish, in which wet filter paper was used to keep the humidity at 80%. The leaves of *Brassica rapae* were cut to a similar size as that of the Petri dish and directly sprayed with different *Aglaia* formulations. Ten *Spodoptera litura* larvae, were placed in each of the respective Petri dishes, and then observed after 72 hours. The test was repeated 5 times.

Efficiency of the *Aglaia* formulation was evaluated by Abbott formula:

$$Ef\,\% = \frac{b - k}{100 - k}$$

b = percentage of dead insects at the treated formulation.

k = percentage of dead insects at the control.

II.6.3. Antimicrobial assay

Gram-positive becteria, *Bacillus subtilis*, gram-negative bacteria, *Escherichia coli,* and *Staphylococcus cerevisae* were applied as test microbes in this study.

Agar diffusion assay: Test samples were dissolved in aliquots of the extraction solvent and applied to sterile filter-paper discs (5 mm diameter, Oxoid Ltd.) to give a

final disc loading concentration of 500 µg for crude extracts and 100µg for pure compounds. The impregnated discs were placed on the agar plates previously seeded with the selected test organisms. As the solvents (methanol or acetone) were required to dissolve compounds, solvent blanks were run against each test organism. The plates were incubated at 37^{o}C for 24 h and antimicrobial activity was recorded as the clear zone of inhibition surrounding the disc at which the diameter was measured in mm. The experiments were carried at the Instititute of Pharmaceutical Biology and Biotechnology, University of Heirich-Heine-Düsseldorf.

II.6.4. Field experiments

II.6.4.1. Semi-field scale experiment

Brassica rapae plants were cultivated in plant-pots during twenty days with light, temperature, of 25^{o}C, and 85% humidity. Ten third-instar larvae (*Spodoptera litura*) were transferred to the plant-pots, kept in meca boxes to avoid escaping of the insects. The solution of *Aglaia* formulations was sprayed directly to the plant-pots (50 ml/m^2) based on the indication of FAO (800L/ha). Both the negative control (water) and the positive control (commercial chemical agent-Regent) were also applied separately for the test. The plant-pots were then kept in rearing chambers (see Fig. 2.2) to control humidity and temperature.The status of *S.litura* and *Brassica rapae* were recorded after 6, 12, 24, 48, 72 hours.

Fig. 2.1 Potter spray tower used to spray *Aglaia* solution

Fig. 2.2 Insecticidal testes were carried out in the rearing chamber

II.6.4.2. Field scale experiment

II.6.4.2.1. Field experiment

Field experiments followed the guideline manuals and protocols for field trials authorized by MARD and Farm Chemical Handbook. *Brassica rapae* was cultivated outdoors for twenty days. Seeding was arranged in different lots, each lot *ca.* 1.5 m^2 containing 100 plants, with 5 replicates. *Spodoptera litura* was maintained in the laboratory and transferred to the lots accountably (50 *S.litura* larvae /1 lot). The transferred insects were left to stabilize with the environment one day outside before spraying. The spray technique was applied mostly underneath the leaf surface where *S.litura* usually attacks. Efficiency of the applied formulations were evaluated by the survival and death rate of insects after 1, 2, 3, 5, and 7 days of the treatment. Efficiency value was calculated by the Abbott formula:

$$\text{Ef} = \frac{C_a - T_a}{C_a} x100$$

Whereas C_a = number of survival insects at control lots and T_a = number of survival insects at treated lots.

II.6.4.2.2. Field experiment in the real condition

Experimental design was completely randomized block designed, repeated five times where the insects appeared naturally in the field conditions. The density of insects was investigated prior to the treatment of *Aglaia* formulations. A chemical product (Regent) was used as positive control. The efficiency was calculated by Henderson-Tilton formula:

$$\text{Ef}\,(\%) = (1- \frac{C_b \times T_a}{T_b \times C_a})$$

Whereas: C_b= Number of larvae on the control before the treatment, C_a= Number of larvae on the control after the treatment, T_b= Number of larvae on treated plot before the treatment,T_a= Number of larvae on treated plot after the treatment.

II.6.5. Toxicity assay of Aglaia formulation

The acute oral toxicity of the *Aglaia* extract was tested on two-month-old white mice with an average weight of 20 - 25 g. At least 5 mice were used at each dose level, all of the same sex. When females were used, they were nulliparous and non-pregnant. The acute oral toxic assay method was carried out by administering different

concentrations of the extract orally, by incorporation of the test sample in the food diet. The second test method involved injecting the *Aglaia* extract directly into the gullet of the mice. The observation period was at least 14 days. However the duration of observation should not be rigidly fixed. The toxic reaction should be determined, the time at which signs of toxicity appears and the time of death, especially if there is a tendency for deaths to be delayed. The number of dead and surviving mice was observed after 1, 3, 5, 7 and 14 days. The death rate of the mouse was revised by Abbott formula and by Finney's probit analysis. The levels of toxicity were classified by the WHO (World Health Organisation) (see Table 2.3).

Table 2. 3: The toxic levels determined by the WHO

Level of Toxicity	**LD_{50} (mg/kg)**
Group 1: very toxic	< 200
Group 2: normal toxic	200-2000
Group 3:low toxicity	>2000
Group 4: very low toxicity	>3000

II.7. Procedure for extraction and isolation of secondary metabolites from *Aglaia* sp

II.7.1. Isolation of secondary metabolites from *Aglaia duppereana*

The ground bark material of *Aglaia dupperreana* (3 kg) was extracted with n-hexane, ethylacetate and methanol successively. The ethylacetate extract (20 g) was chromatographed using vacuum liquid chromatopraphy (VLC), utilizing Silica gel 60 as the solid phase and solvent gradients consisting of n-Hexane: EtOAc: MeOH as the mobile phase. Eight fractions (F1-F8) were obtained. Based on the result of the HPLC analysis, fraction F3 (5.4 g) was selected for further chromatography using another VLC column and was eluted employing a gradient of CH_2Cl_2:MeOH. From this, nine smaller fractions (F3.1-F3.9) were obtained. Fraction F.3.1 (1.29 g) was further fractionated by normal liquid chromatography column (mobile phase, CH_2Cl_2: isopropanol 95:5) and this gave nine fractions (F3.1.1-F3.1.9). Based on the HPLC chromatogram, four fractions (F3.1.4-F3.1.7) (412 mg) were combined and further fractionated by a sephadex LH 20 column and eluted with 100% MeOH. Thirty-six fractions were obtained and based on their TLC and HPLC chromatograms, fractions 1-29, 30-34, and 35-36 were combined together. Compounds **1** (**Rocaglamide A**, 3.9 mg), **2** (**Rocaglamide I**, 3.8), **3** (**Rocaglamide W**, 2.1mg), **4** (**Rocaglamide AB**, 7.2 mg) were obtained from fractions 30-34 by semipreparative HPLC as well as compound **5** (**Rocaglamide J**, 1.9 mg) from fractions 35-36. Compound **13** (**Epicatechin**, 15 mg) was obtained from fraction F.3.6 by chromatography over a Si gel column (mobile phase CH_2Cl_2: MeOH 9:1) (see Scheme.2.1).

Following the same chromatographic methods, compound **7** (**Rocaglamide S**, 1.6 mg), compound **14** (**4´,7-di-O-methyl-naringenin**, 24 mg of crystals) and compound **23** (**Odorine**, 36 mg of crystals) were obtained from the leaves of *Aglaia duppereana* (see Scheme.2.2).

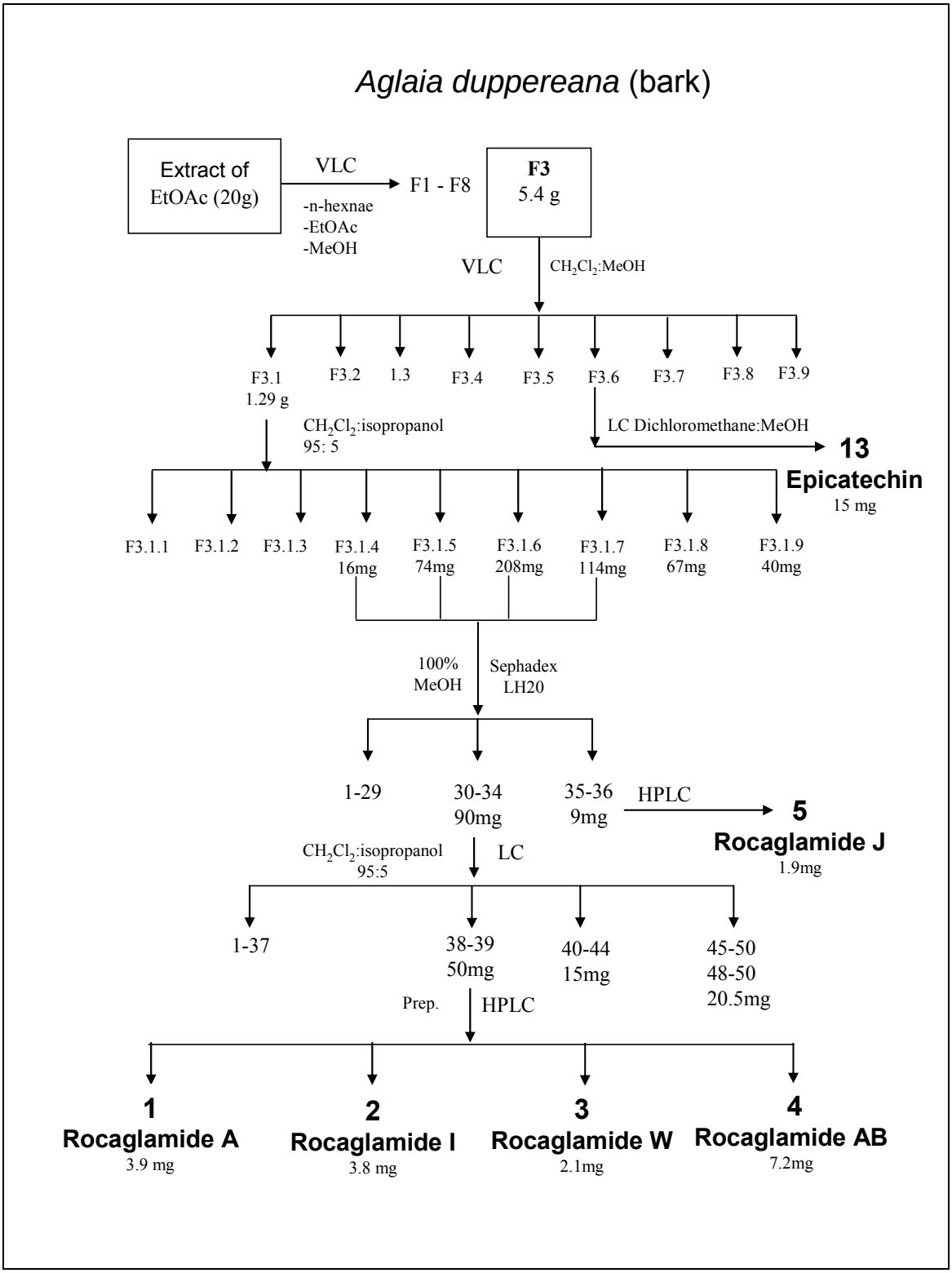

Scheme 2.1: Isolation procedure of compounds from *Aglaia duppereana* (bark)

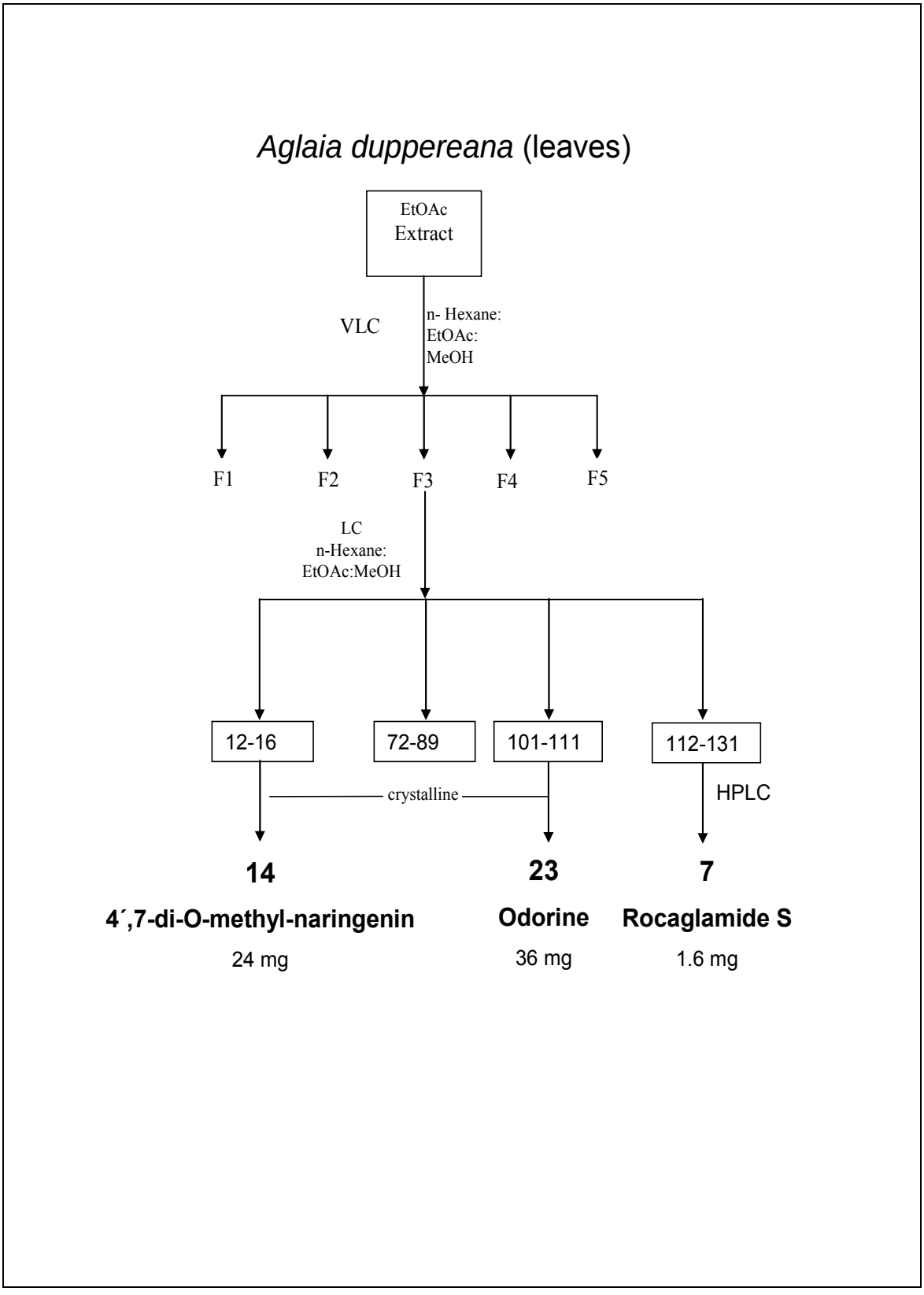

Scheme 2.2: Isolation procedure of compounds from *Aglaia dupperean* (leaves)

II.7.2. Isolation of secondary metabolites from *Aglaia oligophylla*

The dicloromethane extract (3.6 g) of *Aglaia oligophylla* leaves was chromatographed over VLC column packed with Silica gel 60 and seven fractions F1-F7 were obtained. Fraction F3 was further fractionated over a Silica gel column and eighty-eight smaller fractions were obtained. The combined fractions (65-70) were fractionated further by liquid chromatography column over silica gel 60 using CH_2Cl_2:MeOH 8:2 as the mobile phase. Compound **29** (**Lutein**, 11 mg) was obtained as crystalline residue from the semi-polar combined fractions 11-13, while compounds **10** (**Pinoresinol,** 11 mg), **16** (**4´,5,7-Tri-O-methyl-kaempferol,** 15 mg), **17** (**4´,5,7-Tri-O-methyl-naringenin**, 31 mg) were obtained from the more polar fractions 20-25 by further separation using HPLC. The combined polar fractions 17-19 were rechromatographed on a Si 60 Lobar column using EtOAc: MeOH 80:20 as eluent. Combined fractions 25-34 were further separated by preparative TLC. Compound **11** (**4´-O-methyl- pinoresinol,** 19 mg) was obtained as crystallline residue while **8** (**Rocaglamide AY**, 3.3 mg) and **12** (**Eudesmin**, 6.5 mg) were obtained by preparative HPLC. Fraction F4 was chromatographed over Sephadex LH 20 column with MeOH 100%, compound **15** (**4´,5,7-Trimethoxydihydroflavonol,** 21 mg) was obtained as crystalline from the combined fractions (27-29) (see Scheme 2.3).

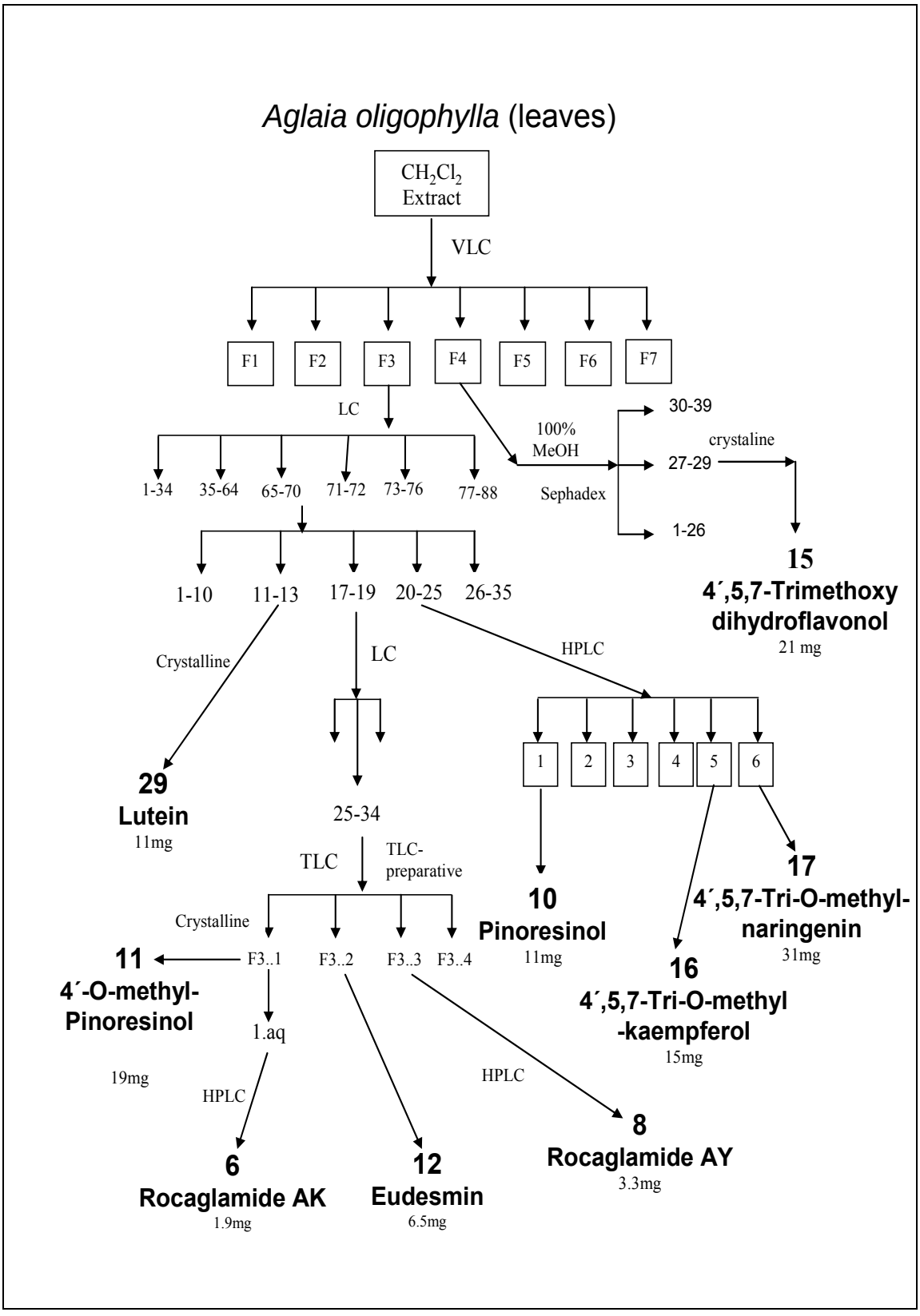

Scheme 2.3: Isolation procedure of compounds from *Aglaia oligophylla* (leaves)

II.7.3. Isolation of secondary metabolites from *Aglaia gigantea*

The dried samples of *Aglaia gigantea* leaves were extracted with n-hexane, dichloromethane and methanol, successivelly. The dichloromethane extract was chromatographed over a Si gel VLC column using a mobile phase with gradients of n-Hexane: EtOAc: MeOH. This yielded nine fractions (F1-F9). Fraction F7 was further chromatographed over Silica gel 60 with gradient elution of EtOAc and MeOH while fraction F8 was further chromatographed using CH_2Cl_2 and MeOH as the mobile phase. The combined fractions F7(789) were further separated by flash chromatography column and this gave 106 fractions. Compound **25** (**Gigantamide A**, 2.5 mg) was obtained by preparative TLC from the combined fractions F7(789)(60-82).

Following the CC of fraction F8, nine other fractions were obtained (F8.1-F8.9). Compound **20** (**Dasyclamide,** 80 mg), was obtained as a crystalline compound by further fractionation of fractions F8(78) and recrystalized in EtOAc:MeOH (75:25), while compound **27** (**Foveolin B**, 10 mg) was obtained over silica gel 60 column. Compound **22** (**Grandiamide D**, 9 mg) was obtained by preparative HPLC from fraction F8(9) (see Scheme 2.4).

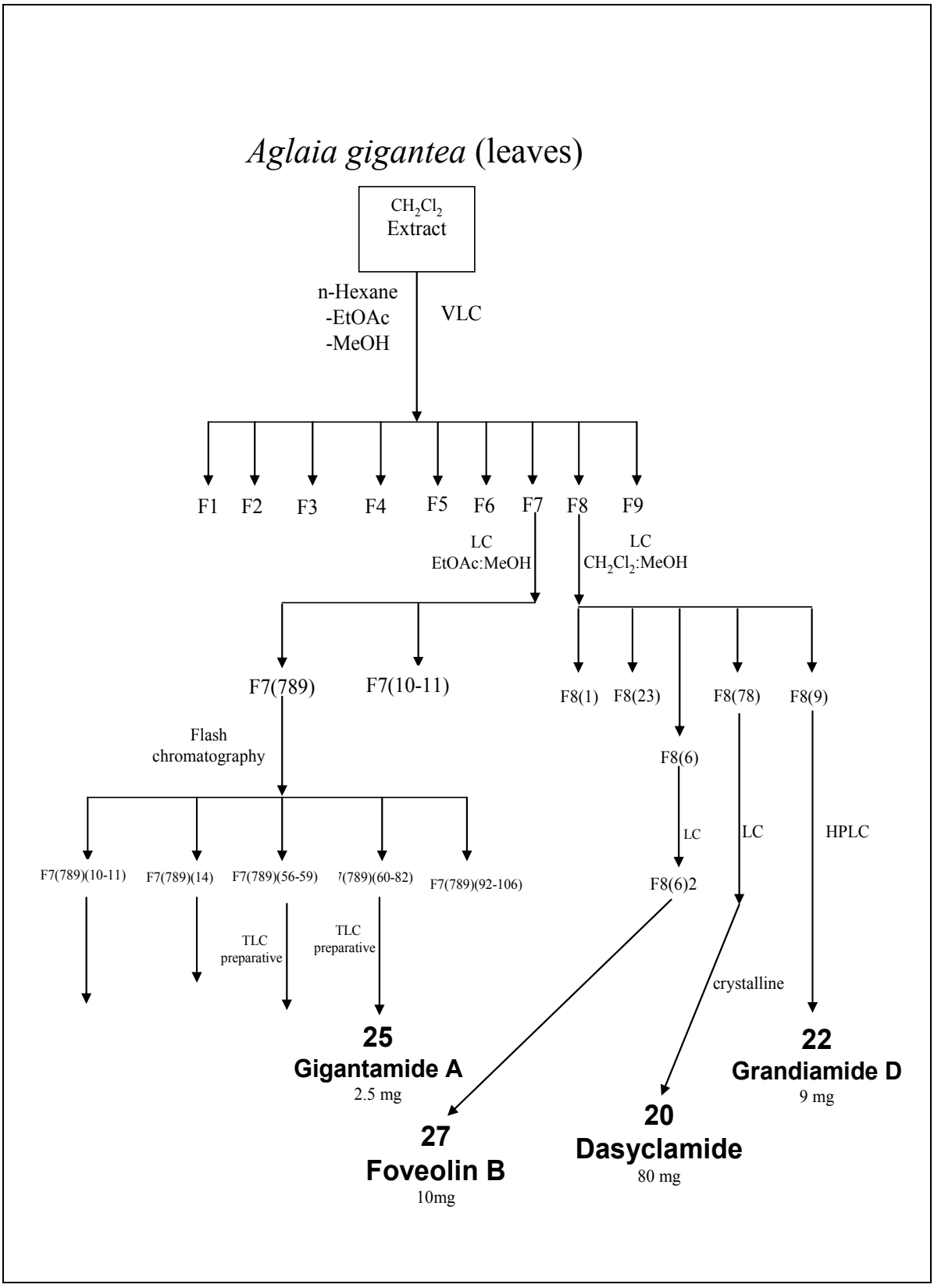

Scheme 2.4: Isolation procedure of compounds from *Aglaia gigantea* (leaves)

II.7.4. Isolation of secondary metabolites from *Aglaia dasyclada*

The dried samples of *Aglaia dasyclada* leaves were ground and extracted with n-hexane, ethylacetate and methanol successively. The ethylacetate extract was chromatographed over a Si gel VLC column utilizing gradient elution of n-Hexane, EtOAc, and MeOH, yielding six fractions (F1-F6). The non-polar fraction F1 was further chromatographed over Silica gel 60 with gradient elution of n:Hexane:EtOAc. Two hundred and twenty seven (227) fractions were obtained. The combined fractions (221-227) were purified by recrystalisazion in n-Hexane:EtOAc (7:3) and yielded compound **28** (**Niloticin**, 200 mg) white needle crystals (see Scheme 2.5).

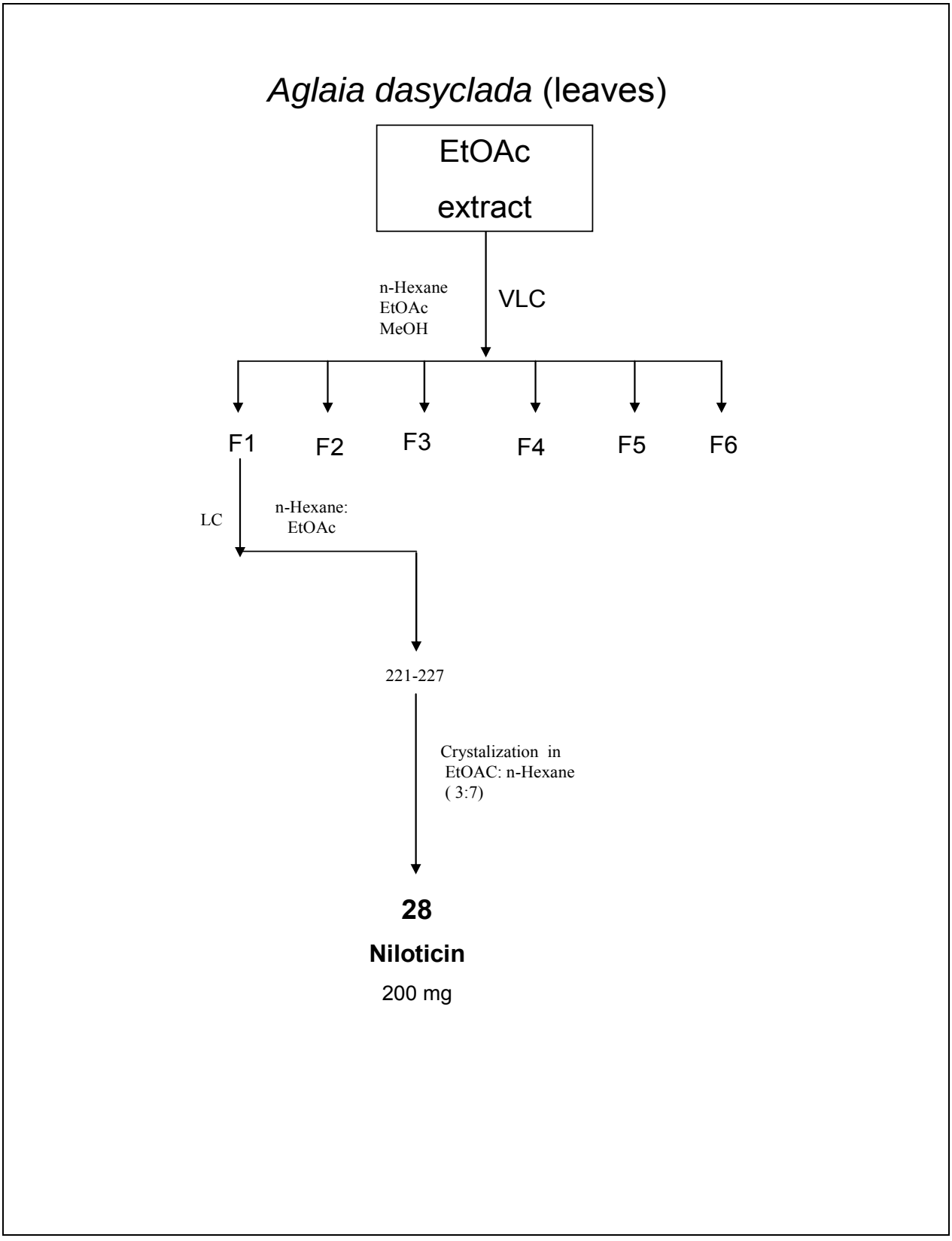

Scheme 2.5: Isolation procedure of compounds from *Aglaia dasyclada* (leaves)

II.7.5. Isolation of secondary metabolites from *Aglaia elaeagnoidea*

The dried samples of *Aglaia elaeagnoidea* bark were extracted with n-hexane, ethylacetate and methanol successively. The ethylacetate extract (8 g) of *Aglaia elaeagnoidea* leaves was chromatographed over VLC column packed with Silica gel 60. Six fractions (F1-F6) were obtained. Fraction F3 was rechromatographed over Sephadex and eluted with 100% MeOH from which twenty fractions were obtained. Based on their HPLC chromatogram, the combined fractions F3(15-17) were further separated by preparative HPLC, yielding compound **6** (**Rocaglamide AK**, 25 mg). Compound **30** (**Scopoletin**, 3 mg) was obtained by repetitive preparative TLC from the combined fractions F3(19-20) (see Scheme 2.6).

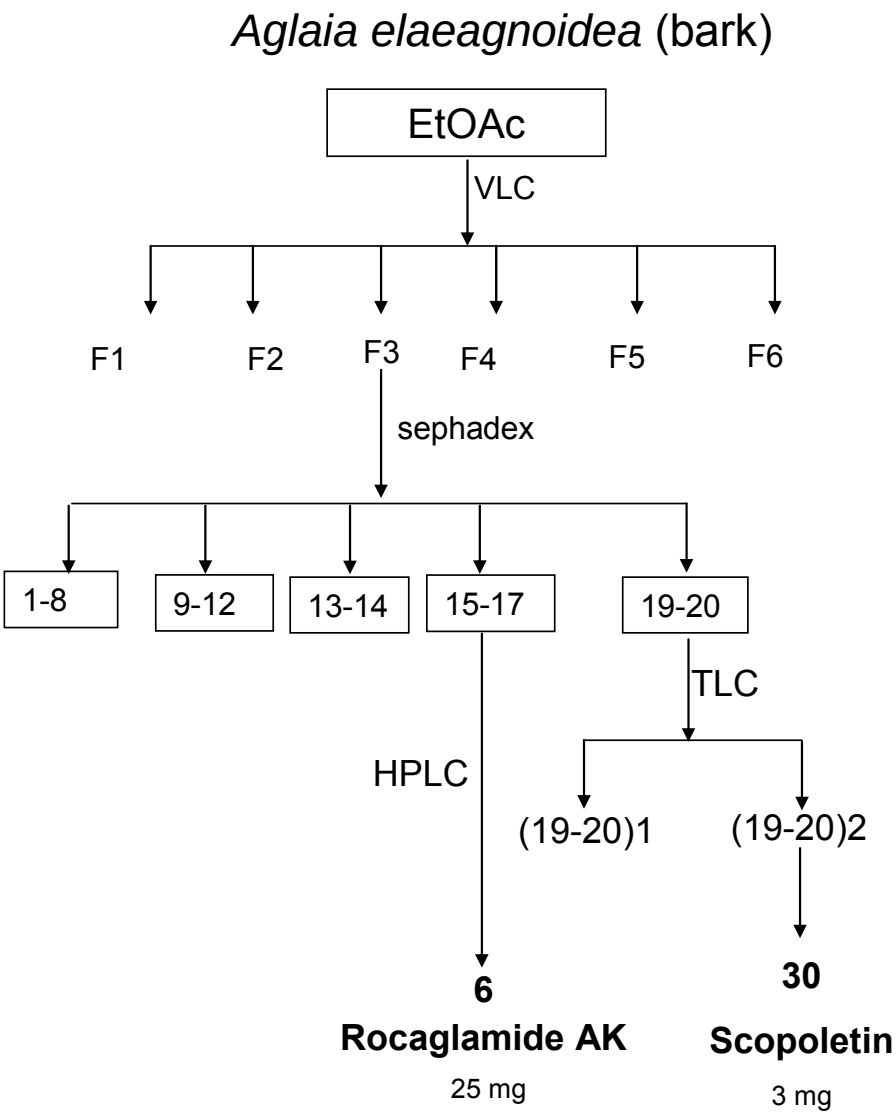

Scheme 2.6: Isolation procedure of compounds from *Aglaia elaeagnoidea* (bark)

II.7.6. Isolation of secondary metabolites from *Aglaia abbriviata*

The dried samples of *Aglaia abbriviata* leaves were extracted with n-hexane, ethylacetate and methanol successively. The ethylacetate extract (11 g) was chromatographed over a VLC column packed with Silica gel 60. Six fractions (F1-F6) were obtained. Fraction F5 was rechromatographed over Sephadex and eluted with 100% MeOH and thirty-nine fractions were obtained. Based on their HPLC chromatograms and TLC, the combined fractions F5(21-23) were recrystalized, yielding compound **16** (**4′,5,7-Tri-O-methyl-kaempferol**, 24 mg) as crystalline compound. Fraction F6 was further separated by preparative TLC, resulting in four fractions (F6.1-F6.4). The fraction F6.1 was rechromatographed over Sephadex LH 20 column using 100% MeOH as mobile phase and yielded eleven fractions. Compound **24** (**Odorinol**, 50 mg) was obtained as crystalline from the fraction F6.1.10. Compound **9** (**Aglaxiflorin D**, 5 mg) was obtained by further separation from fraction F6.1.11 using preparative HPLC (see Scheme 2.7).

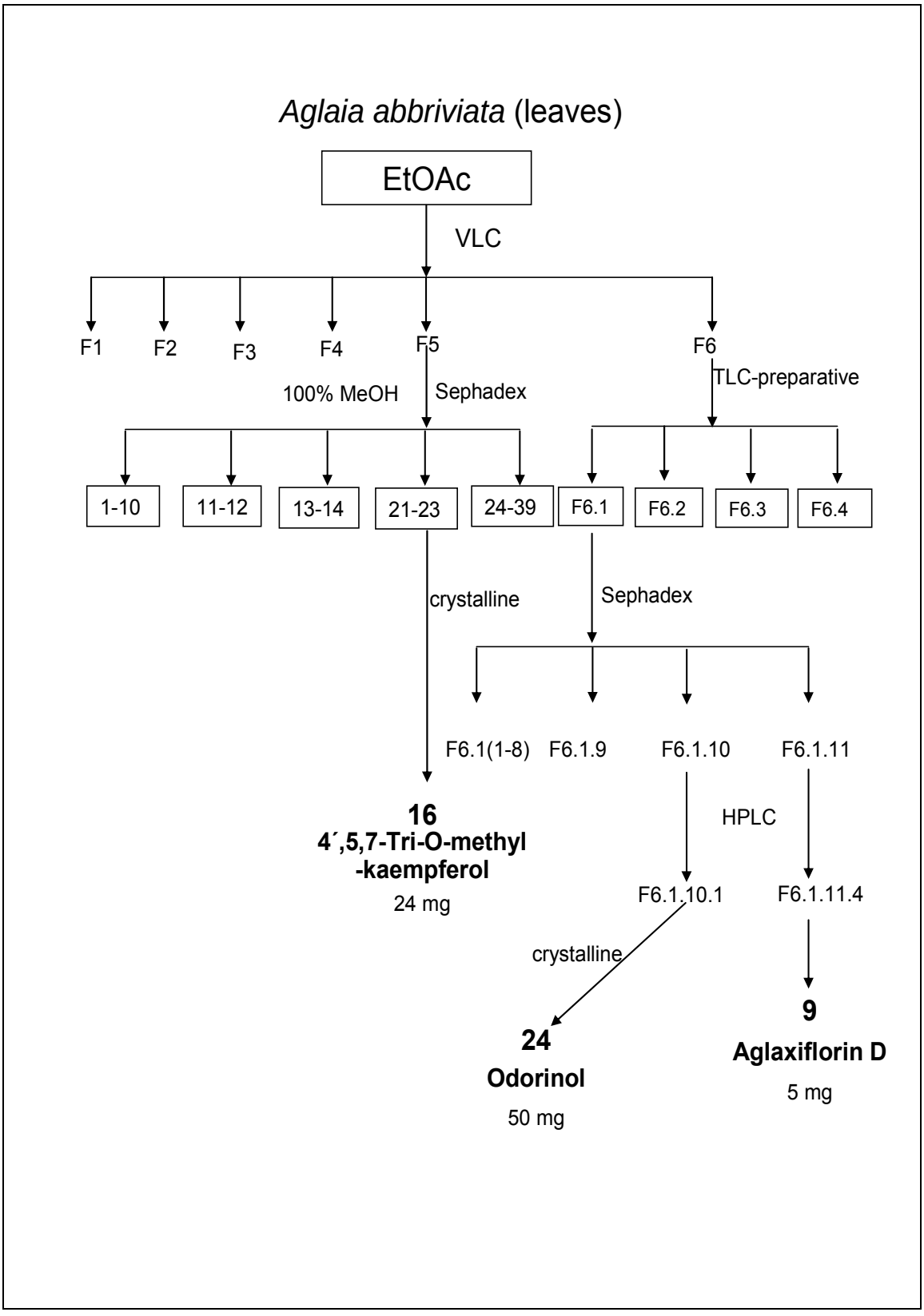

Scheme 2.7: Isolation procedure of compounds from *Aglaia abbriviata* (bark)

II.7.7. Isolation of secondary metabolites from *Aglaia oligophylla* Miq

The dried samples of *Aglaia oligophylla* leaves were extracted using 96% ethanol. The concentrated ethanol extract was partitioned into n-hexane, ethylacetate, and n-butanol. The ethylacetate fraction was taken to dryness and chromatographed over a Silica gel VLC column by gradient elution using n-Hexane, EtOAc, and MeOH as mobile phase and ten fractions were obtained (F1-F10). Fraction F8 was further rechromatographed over a VLC column. This gave four fractions (F8.1-F8.4). The fraction F8.2 was further separated by sephadex LH 20 column, and compound **18** (**Kaempferol 3-rutinoside**, 21 mg) was obtained as crystal residue. Fraction F7 was rechromatographed over Silica gel column, yielding 154 fractions. The combined fractions (125-154) were further separated using a sephadex column, and compound **19** (**Kaempferol 3-*O*-(4-hydroxy-E-cinnamoyl)-(β)-glucopyranosyl**, 14 mg) was obtained as crystals. The combined fractions F7(1-38) was further purified by preparative TLC, resulting to four smaller fractions. Compounds **21** (**Grandiamide B**, 2.5 mg), **25** (**Gigantamide A**, 2.7 mg), and **26** (**Pyramidatine**, 2.3 mg) were obtained by preparative HPLC from these fractions (see Scheme 2.8).

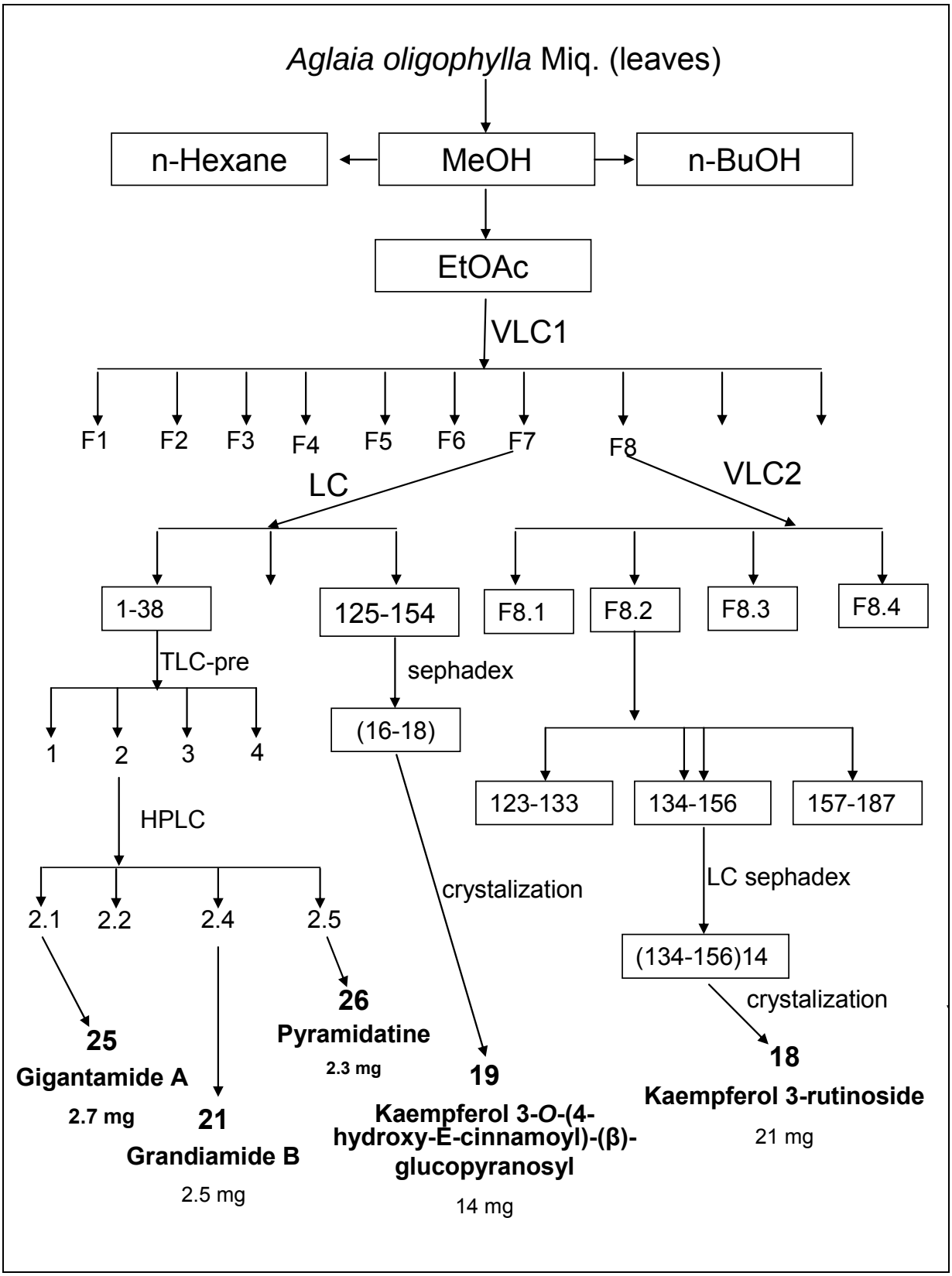

Scheme 2.8: Isolation procedure of compounds from *Aglaia oligophylla* Miq.

II.8. Procedure for extraction of *Aglaia* materials at large scale for field trials

The leaves of *Aglaia oligophylla* and *Aglaia duppereana* were collected in large amounts (50 kg dried material) at Cat Ba-Hai Phong and Hanoi. Fresh material was dried under room condition using a dehumidifier. Dried leaves were weighed, ground, and extracted with 96% ethanol exhaustively stirred and left overnight. The filtered ethanol extract was then concentrated under vacuo (see Scheme 2.9).

Collecting *Aglaia duppereana* and sample treatment of *A. duppereana* and *A. oligophylla* leaves at the Institute of Chemistry (VAST)

Fig. 2.3 Treatment of *Aglaia* materials

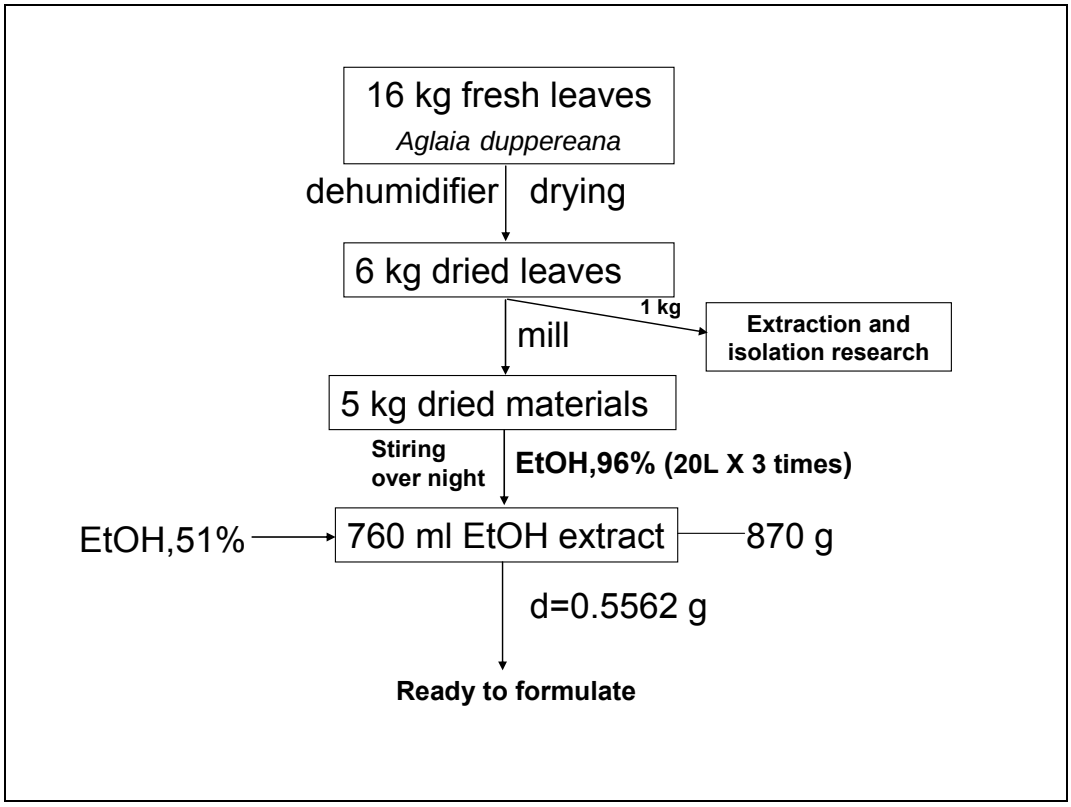

Scheme.2.9: Procedure for extraction of *Aglaia duppereana* for field trial

The equipment used are described below (see Fig. 2.4).

Fig. 2.4 Extraction and evaporation processes

II.9. Procedure for the *Aglaia* formulation process

The dried extract of *Aglaia* does not readily dissolve in water. Thus, a suitable organic solvent such as ethanol was used as a carrier solvent in a diluted concentration for making a water insoluble active extract. In order to eliminate the problem of dissolution, the total ethanol extract was not evaporated to dryness.

In addition, another plant extract (soapberry fruits) which is rich in nonactive saponins, was used as an adjuvant agent for preparing the emulsion of the extract. Neutral soap can also be used as an additional agent to emulsify the extract (see Scheme 2.10). The obtained liquid formulation was stored in the freezer, and was ready for use as a spray after dilution with water.

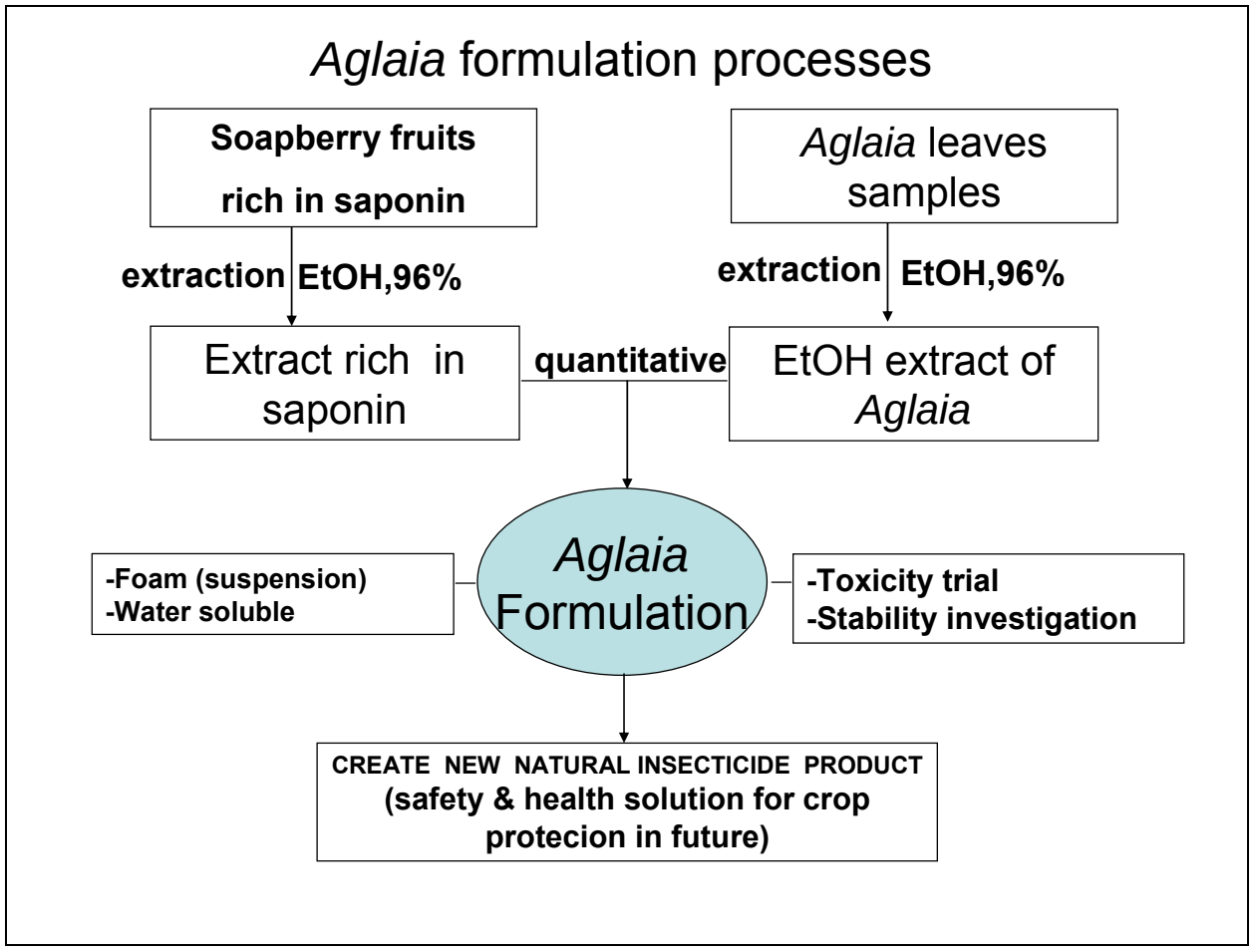

Scheme 2.10: Procedure for processing *Aglaia* formulation

II.10. Procedure for the analysis of the stability of *Aglaia* extract under field conditions

The rocaglamide congeners are responsible for the insecticidal activity of the *Aglaia* extract. However, it is impossible to detect them by HPLC because they occur in very small amounts in the extract. Dasyclamide, was found at high amounts in the leaves of *Aglaia gigantea*, and was reported to be involved as a building block in the biosynthetic pathway of rocaglamide [Nugroho *et al*., 1999]. It is very easily detected from the crude extract by HPLC (see Scheme 2.11). Based on the linear correlation between the concentrations of pure dasyclamide (in µg) and the absorption (in mAU) monitored by HPLC, a secondary order equation, $y = 37.79x$, where y = values of absorption, and x = values of dasyclamide in µg (see Scheme 2.11). The experiments were conducted on white cabbage and red kohlrabi in the Botanical garden of Heiriche-Heine-University Düsseldorf, on July 2004. The plants were cultivated outdoor one and a half month by seeding. After spraying the *Aglaia* emulsion on the cabbage and the kohlrabi, a plastic net was used to cover the plants preventing washing by rain, which could drain the *Aglaia* emulsion from the surface of the cabbage and kohrabi.

The leaves of cabbage and kohlrabi were collected after spraying *Aglaia* emulsion on 0, 1, 3, 5 and 7 days. Small size holes (1.7 cm) were punched out of the leaves. The cut out leaves were cleaned with methanol four times and soaked overnight in methanol. The aqueous methanol extract was filtered, evaporated and its quantitative residue was analyzed by HPLC (see Scheme 2.11).

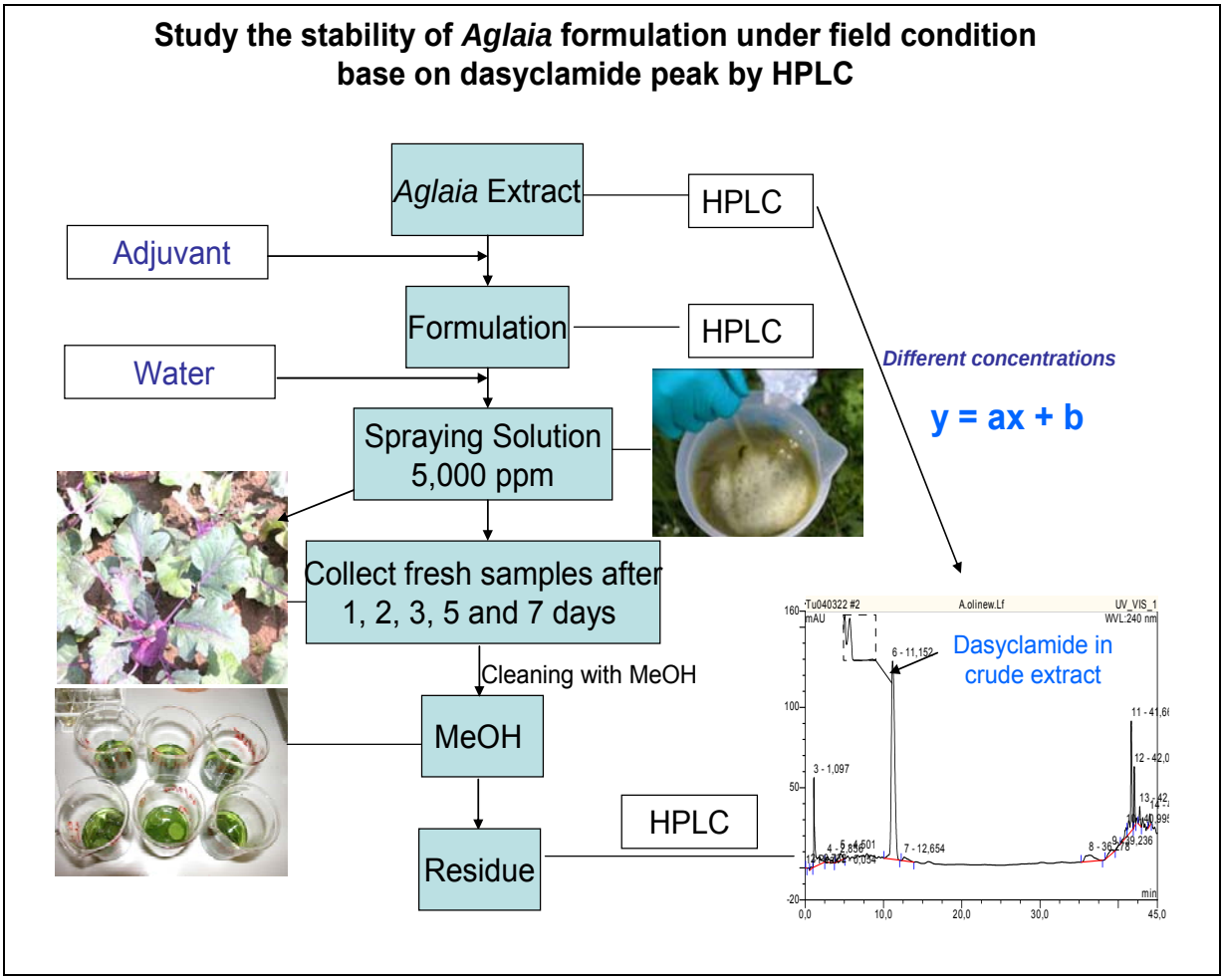

Scheme 2.11: Procedure for analysis the stability of dasyclamide under field condition

III. RESULTS

III.1. Insecticidal screening and bioassay results

III.1.1. Insecticidal screening results

Thirty eight extracts from thirteen different *Aglaia* species collected in Vietnam were screened for insecticidal activity against neonate larvae of *S. littoralis* using an anti-feedant assay. *A. oligophylla*, *A. abbriviata, A. eleagnoidea,* and *A. duppereana* were found to be the most active species (see Table 3.1). Following incorporation into artificial food at a dose concentration of 1000 ppm of the crude organic extract, 100% larval mortality was observed after 24 hours. While *A. rothii* gave 80% mortality, *A. dasyclada* gave 70% mortality, *A. gigantea* caused 60% mortality, *A. pleuroptiris* 45%, and *A. macrocarpa* exhibited 15% mortality rate of the neonates after 7 days.

Table 3.1: Insecticidal activity of Vietnamese *Aglaia* extracts

N_0	Samples	Survival rate [%]*	Growth rate [%]*
1	*A.abbriviata* (Lf) EtOAc	0,0	0,0
2	*A.dasyclada* (Tw) EtOAc	30,0	19,8
3	*A.dasyclada* (Lf) EtOAc	70,0	36,0
4	*A.dasyclada* (Bark) EtOAc	70,0	37,1
5	*A.dasyclada* (Tw) EtOAc	85,0	78,8
6	*A.duppereana* (Lf) n-Hexan	0,0	0,0
7	*A.duppereana* (Lf) Water	35,0	68,2
8	*A.duppereana* (Lf) EtOAc	0,0	0,0
9	*A.duppereana* (Lf) MeOH	0,0	7,4
10	*A.eleagnoidea* (Bark) EtOAc	70,0	0,0
11	*A.eleagnoidea* (Twigs) EtOAc	0,0	0,0
12	*A.eleagnoidae* (Lf) EtOAc	0,0	0,0
13	*A.ff poilanei* (Bark) EtOAc	0,0	259,3
15	*A.ff poilanei* (Lf+Tw) EtOAc	50,0	16,5
16	*A.gigantea* (Bark) EtOAc	80,0	524,1
17	*A.gigantea* (Tw +Lf) EtOAc	90,0	262,0
18	*A.gigantea* (Tw) CH_2Cl_2	55	2,9
19	*A.gigantea* (Lf) EtOH	40,0	29,9
20	*A.gigantea* (Lf) CH_2Cl_2	75,0	18,5
21	*A.gigantea* (Bark) CH_2Cl_2	90	79,0
22	*A.gigantea* (Lf+Tw) EtOAc	90,0	126,7
23	*A.gigantea* (Bark) EtOAc	85,0	76,9
24	*A.macrocarpa* (Bark) CH_2Cl_2	95	132,6
25	*A.macrocarpa* (Tw) CH_2Cl_2	100	83,9
26	*A. macrocarpa* (Lf) CH_2Cl_2	85	31,7
27	*A.oligophyla* (Lf+Tw) CH_2Cl_2	35	0,7
28	*A.oligophylla* (Lf) CH_2Cl_2	0	0,0
29	*A.oloigophylla* (Lf) EtOAc	75,0	38,0
30	*A.oligophylla* (Tw+Bark) CH_2Cl_2	0,0	0,0
31	*A.oloigophylla*.new (Lf) MeOH	100,0	47,6
32	*A.pleuroptiris* (Tw) CH_2Cl_2	85	420,0
33	*A.pleuroptiris* (Lf) CH_2Cl_2	55,0	22,5
34	*A.rothii* (Lf) n-Hex	65,0	17,0
35	*A.rothii* (Lf) CH_2Cl_2	70,0	21,2
36	*A.rothii* (Lf) EtOH	75,0	23,6
37	*A.roxburghiana* (Tw) EtOAc	5,0	1,5
38	*A.roxburghiana* (Tw) EtOH	80,0	49,2

Lf = leaf ;Tw = twig, Bk = Bark

* Relative to the control (100%)

III.1.2. Results of the Bioassay-guided fractionation

Through the results of the insecticidal screening, the most active extracts of *Aglaia* species were further fractionated by VLC and then tested in order to find the major active component. The guided bioassay fractionation insecticidal results are shown in the following tables (see from Table 2.3 to Table 2.9).

Chronic feeding experiments (see Fig. 2.1): Neonate larvae of *S. littoralis* (n=20) were released on diet spiked with concentrations of the analyzed fractions at 200 ppm. After 7 days, survival and weight of the surviving larvae were measured and compared to controls that had been exposed to diet treated with solvent (MeOH) only. From the dose-response cutves LC_{50} and EC_{50} values were calculated by probit analysis.

Table 3.2: Insecticidal bioassay result of fractions from the CH_2Cl_2 extract of *Aglaia oligophylla* (leaves)

Fractions	Survival rate [%]*	Growth rate [%]*
A5F1	70,0	94,3
A5F2	70,0	55,5
A5F3	0,0	0,0
A5F4	0,0	0,0
A5F5	0,0	0,0
A5F6	25,0	3,2
A5F7	0,0	0,0

* Relative to the control (100%)

Table 3.3: Insecticidal bioassay result of fractions from the EtOAc extract of *Aglaia elaeagnoidea* (Bark)

Fractions	Survival rate [%]*	Growth rate [%]*
F1	30,0	82,0
F2	0,0	0,0
F3	0,0	0,0
F4	85,0	114,6

F3: all larvae were dead after 1 day
* Relative to the control (100%)

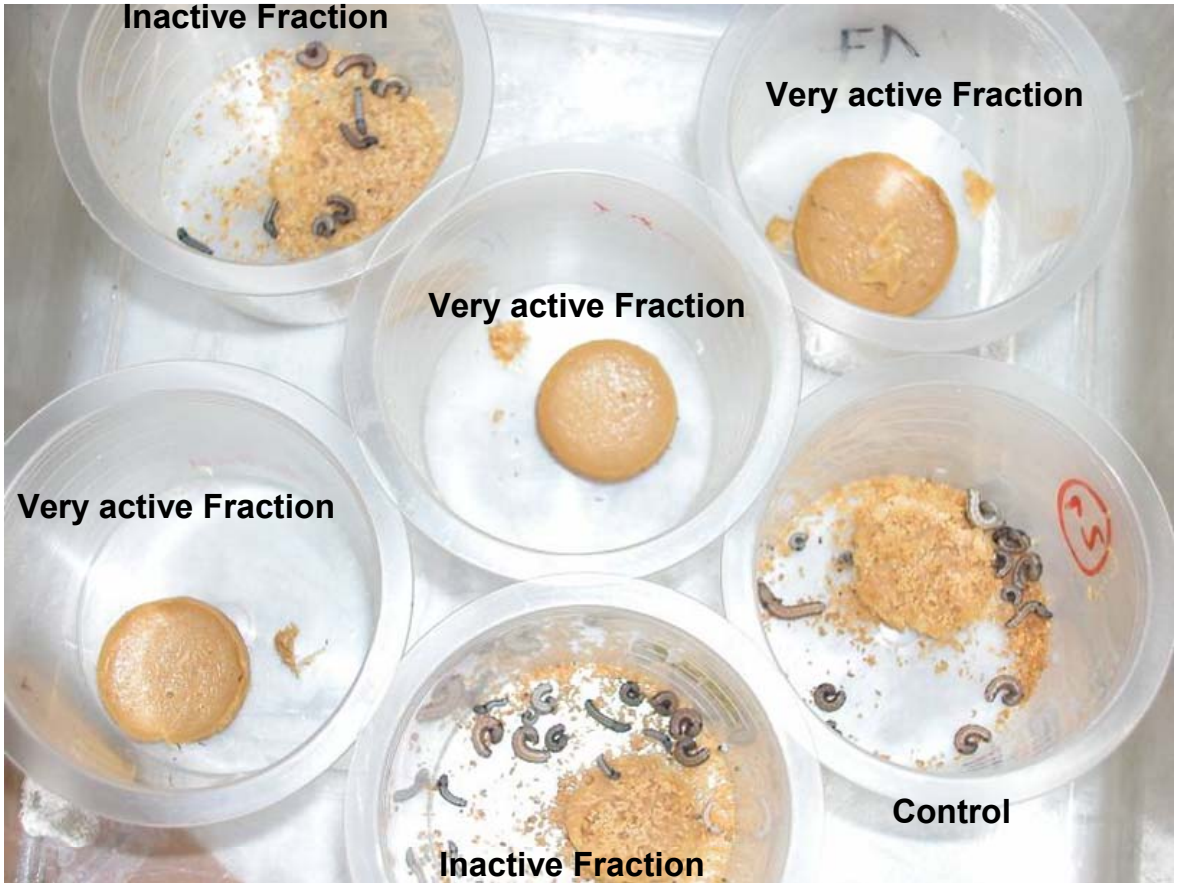

Fig.3.1: Chronic feeding assay with *Spodoptera littoralis*, at HHU-Duesseldorf

Table 3.4: Insecticidal bioassay results of fractions from the EtOAc extract of *Aglaia oligophylla* Miq (leaves)

Fractions	Survival rate [%]*	Growth rate [%]*
F2	85,0	89,8
F3	80,0	49,6
F4	85,0	111,8
F5	30,0	66,2
F6	30,0	52,9
F9	90,0	83,3
F10	0,0	0,0
EtOAc	0	3,5

* Relative to the control (100%)

Table 3.5: Insecticidal bioassay results of fractions from the EtOAc extract of *Aglaia elaeagnoidea* (bark)

Fractions	Survival rate [%]*	Growth rate [%]*
F1	80,0	44,1
F2	75,0	13,3
F4	0,0	0,0
F5	0,0	0,0

* Relative to the control (100%)

Table 3.6: Insecticidal bioassay results of fractions from the EtOAc extract of *Aglaia abbriviata* (leaves)

Fractions	Survival rate [%]*	Growth rate [%]*
F1	75,0	101,4
F2	75,0	16,2
F3	90,0	68,9
F4	45,0	44,9
F5	55,0	5,2
F6	0,0	0,0
F7	55,0	70,3
EtOAc	0,0	0,0

* Relative to the control (100%)

Table 3.7. Insecticidal bioassay results of fractions from F6 of EtOAc extract of *Aglaia abbriviata* (leaves)

Fractions	Survival rate [%]*	Growth rate [%]*
F6(1)	0,0	0,0
F6(1)10	15,0	5,3
F6(1)12	0,0	0,0
F6(2)	85,0	56,0
F6(3)	100,0	19,2
F6(4)	60,0	27,7
F6(5)	85,0	107,3
F6(6)	100,0	98,8
F(6)9	20,0	7,7
EtOAc	0,0	0,0

* Relative to the control (100%)

Table 3.8. Insecticidal bioassay results of fractions from the EtOH extract of *Aglaia duppereana* (leaves collected 2004)

Fractions	Survival rate [%]*	Growth rate [%]*
F1	100,0	6,2
F2	65,0	34,1
F3	95	35,5
F4	55,0	1,3
F5	0,0	0,0
F6	30,0	0,9
F7	0,0	0,0
F8	75,0	28,4
F9	80,0	44,8
F10	90,0	55,0
n-Hexane	30,0	0,5
EtOAc	0,0	0,0
MeOH	15,0	0,9
n-Hex from EtOH	10,0	0,3
EtOAc from EtOH	0,0	0,0

* Relative to the control (100%)

Table.3.9: Insecticidal bioassay results of fractions derived from F6 and F7 of the EtOH extract of *Aglaia duppereana* (leaves)

Fractions	Survival rate [%]*	Growth rate [%]*
F6.I	70,0	3,4
F6.II	100,0	12,9
F6.III	80,0	79,5
F6.IV	75,0	137,4
F6.V	90,0	62,6
F7.I	85,0	104,3
F7.II	80,0	27,5
F7.III	0,0	0,0
F7.IV	0,0	0,0
F7.V	0,0	0,0
F7.VI	0,0	0,0
F7.VII	70	38,9
F7.VIII	95,0	114,2
F7.IX	80,0	181,2
F.7X	90,0	119,1
EtOAC	0,0	0,0
EtOAc from EtOH	0,0	0,0

* Relative to the control (100%)

III.1.3. Other bioassay results

III.1.3.1. Antimicrobial result

Dasyclamide (compound **20**) and 4´,5,7-trimethoxydihydroflavonol (compound **15**) exhibited antimicrobial activity agains *E.coli* at zones of inhibition from 12-14 mm (see Table 3.10).

Table 3.10: Antimicrobial results using Agar Diffusion Assay

Samples	**Zones of inhibition in mm at a loading concentration of 20 µg per disk**		
	E.coli	***B.subtilis***	***S.cereviseae***
Dasyclamide	12	negative	negative
4´,5,7-Trimethoxydihydroflavonol	14	negative	negative
Control	-	-	-
Penicillin	7	12	not-tested
Streptomycin	18	18	not-tested
Gentamycin	14	20	not-tested
Nystatin	not-tested	not-tested	8

III.1.3.2. Preliminary research on the toxicity of *Aglaia* formulations toward mice

The liquid formulation from *Aglaia* extract was tested for acute oral toxic which was carried out by administering different concentrations of the extract orally, after incorporation of the test sample in the food diet. The second test method involved injecting the *Aglaia* extract directly into the gullet of mice.

Table 3.11: LD_{50} (mg/kg) of *Aglaia* formulations on acute oral toxic assay with mouse

***Aglaia* formulations**	**LD_{50} (mg/kg)**
Aglaia formulation (injection)	2000
Aglaia formulation (oral)	4500

Table 3.12: The toxicity levels classified by the WHO

Level of Toxicity	LD_{50} value (mg/kg)
- Group 1: very toxic	< 200
- Group 2: medium toxicity	200 - 2000
- Group 3: low toxicity	>2000 - 3000
- Group 4: very low toxicity	>3000

Based on the classification of the toxicity levels by the WHO, the toxicity value (LD_{50}) of the *Aglaia* extract by administering the extract orally was calculated as 4500 mg/kg, which could be considered to be in the range of a "very low toxicity" level. Besides, the *Aglaia* extract exhibited a medium toxicity level at 2000 mg/kg (see Table 3.11 and Table 3.12) by injecting the *Aglaia* extract directly into the gullet of the mouse.

III.1.3.3. The stability of the *Aglaia* formulation under field conditions

The stability of *Aglaia* formulation was also tested under field conditions. A residual assay was done by using dasyclamide (compound **20**, a cinnamoyl bisamide which was found at high amounts in the leaves of *Aglaia gigantea*, see Fig.3.2), which is structurally a building block for the biosynthesis of rocaglamides. The presence of dasyclamide was analyzed by HPLC coupled to a photo diodearray detector. After 3 days, no trace of dasyclamide was found in the leaves of plants sprayed with the *Aglaia* formulation (see Table 3.13).

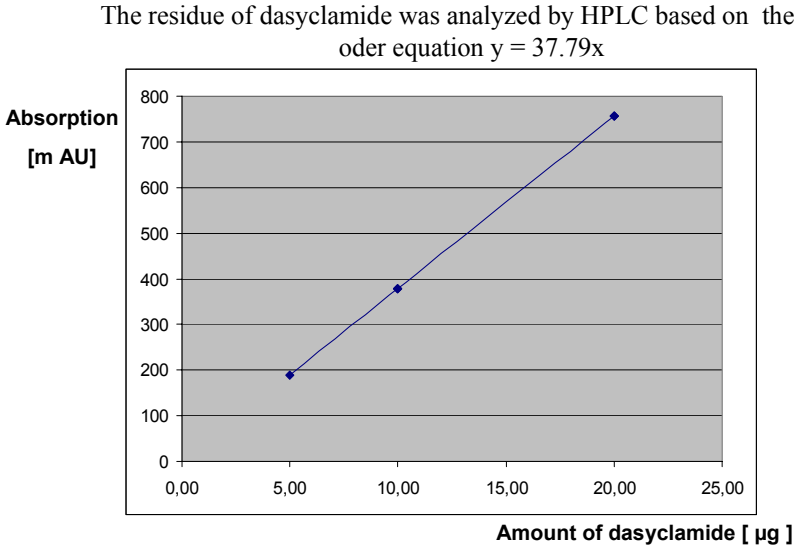

Fig. 3.2

Table 3.13: The analytical result of the stability of dasyclamide under field condistions

Samples	Time	Amount (µg)	Total amount (µg)	Volume (µl MeOH)	mAU	Amount of dasyclamide (µg/20 µl)	Total amount of dasyclamide/leaf (µg/68 cm^2)
After 0 day							
Bc 1	0 day	18.8	71.4	990	28.08	0.74	139.11
Bc 2	0 day	17.8	60.9	990	28.60	0.76	128.71
Bc 3	0 day	20.7	74.8	990	26.28	0.70	125.20
After 1 day							
Bc 1	1 day	11.5	64.1	850	5.15	0.14	33.16
Bc 2	1 day	11.4	57.4	850	7.34	0.19	40.65
Bc 3	1 day	9.4	51.4	850	7.55	0.20	46.47
After 3 days							
Bc 1	3 days	46.9	71.6	700	2.22	0.06	3.20
Bc 2	3 days	36.1	61.0	700	3.74	0.10	5.9
Bc 3	3 days	42.9	68.7	700	4.32	0.11	6.16
After 5 days							
Bc 1	5 days	13.3	80.3	700	-	-	-
Bc 2	5 days	31.7	89.7	700	-	-	-
Bc 3	5 days	35.1	92.4	700	-	-	-
After 7 days							
Bc 1	7 days	13.1	101.9	700	-	-	-
Bc 2	7 days	13.9	91.5	700	-	-	-
Bc 3	7 days	11	74.8	700	-	-	-

Bc=Cabbage

III.2. Structural elucidation of isolated compounds from *Aglaia* sp.

III.2.1. Rocaglamide and its congeners from *Aglaia* sp.

III.2.1.1. Rocaglamide A (1, known compound)

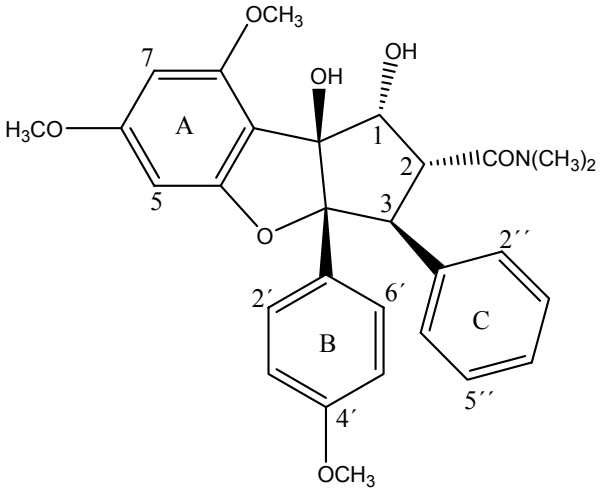

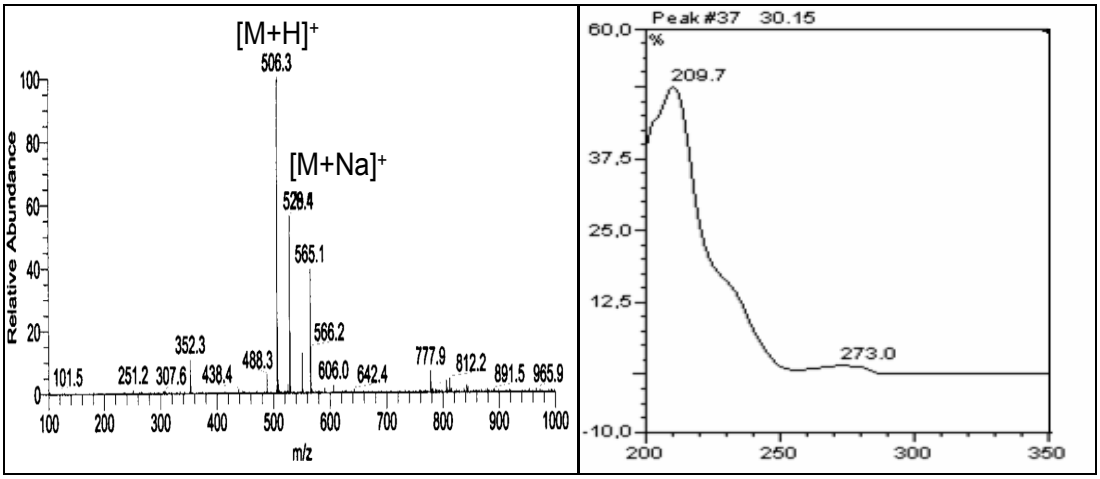

Fig.3.3: ESI-MS and UV spectrum of compound 1

Compound **1** was isolated from the bark of *Aglaia duppereana* as a white amorphous residue, $[\alpha]^{20}_{D}$-90.5 (*c*, 0.25, $CHCl_3$); UV (MeOH) λ_{max} 219.7 and 273.0 nm (see Fig. 3.3). The ESIMS positive mode showed a pseudomolecular ion peak at *m/z* 506.3 $[M+H]^+$, *m/z* 528.4 $[M+Na]^+$(see Fig. 3.3). In conjunction with this molecular weight, the ^{1}H-NMR data were also comparable with those found in the literature for Rocaglamide A. Compound **1** is identical to the known compound Rocaglamide A. Rocaglamide A was first isolated from *Aglaia elliptifolia* by King *et al.,* in 1982 (see Fig.3.4) [King *et al.,* 1982 and B.W.Nugroho *et al.,* 1997]. In the ^{1}H-NMR spectrum

of compound **1** (see Table 3.14 and Fig. 3.5), the presence of three methoxy singlets was observed at δ 3.81 (OC*H*$_3$-8), 3.84 (OC*H*$_3$-6), 3.66 (OC*H*$_3$-4′). Two methine protons for H-5 and H-7 of ring A were observed as *meta* doublets at δ 6.30 and 6.17 with coupling constants of 1.9 Hz as well as two singlets of N-CH_3 groups at 3.34 ppm and 2.86 ppm. The characteristic AA′BB′ resonances for ring B occurred downfield at δ 7.12 and 6.64, which indicated the *para*-type of substitution at ring B, corresponding to H2′/H6′ and H3′/H5′, respectively. The second spin system of the mono-substituted phenyl ring C was observed at δ 6.86 ppm (m, H2′′/H6′′) and at 6.98 ppm (m, H3′′/4′′/5′′). In addition, the appearance of the fourth spin system of the cyclopentane ring was observed at 4.95 ppm (d, 6.9), 4.36 (d, 13.8) and 4.11 (dd, 6.9; 13.8) which indicated the H1-α, H2-α and H3-ß-configuration as well as the *cis*-BC ring junction [Ishibashi *et al.,* 1993]. The ^{1}H NMR data of compound **1** were obtained using the same solvent as used for Rocaglamide A [Nugroho *et al.,* 1997]. Thus, an identical result was obtained without running further spectra such as HMBC and it was concluded that compound **1** was indeed Rocaglamide A.

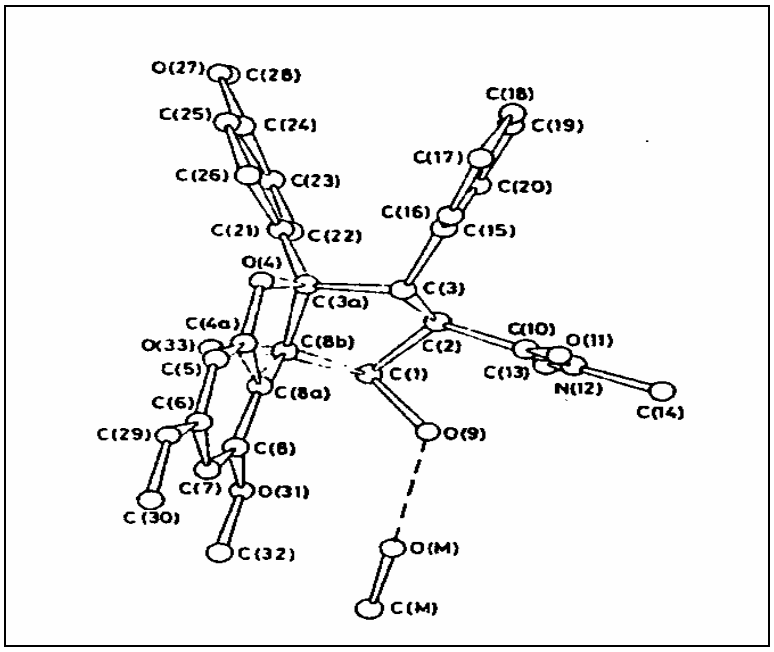

Fig.3.4: Crystal structure of compound 1 [King *et al*., 1982]

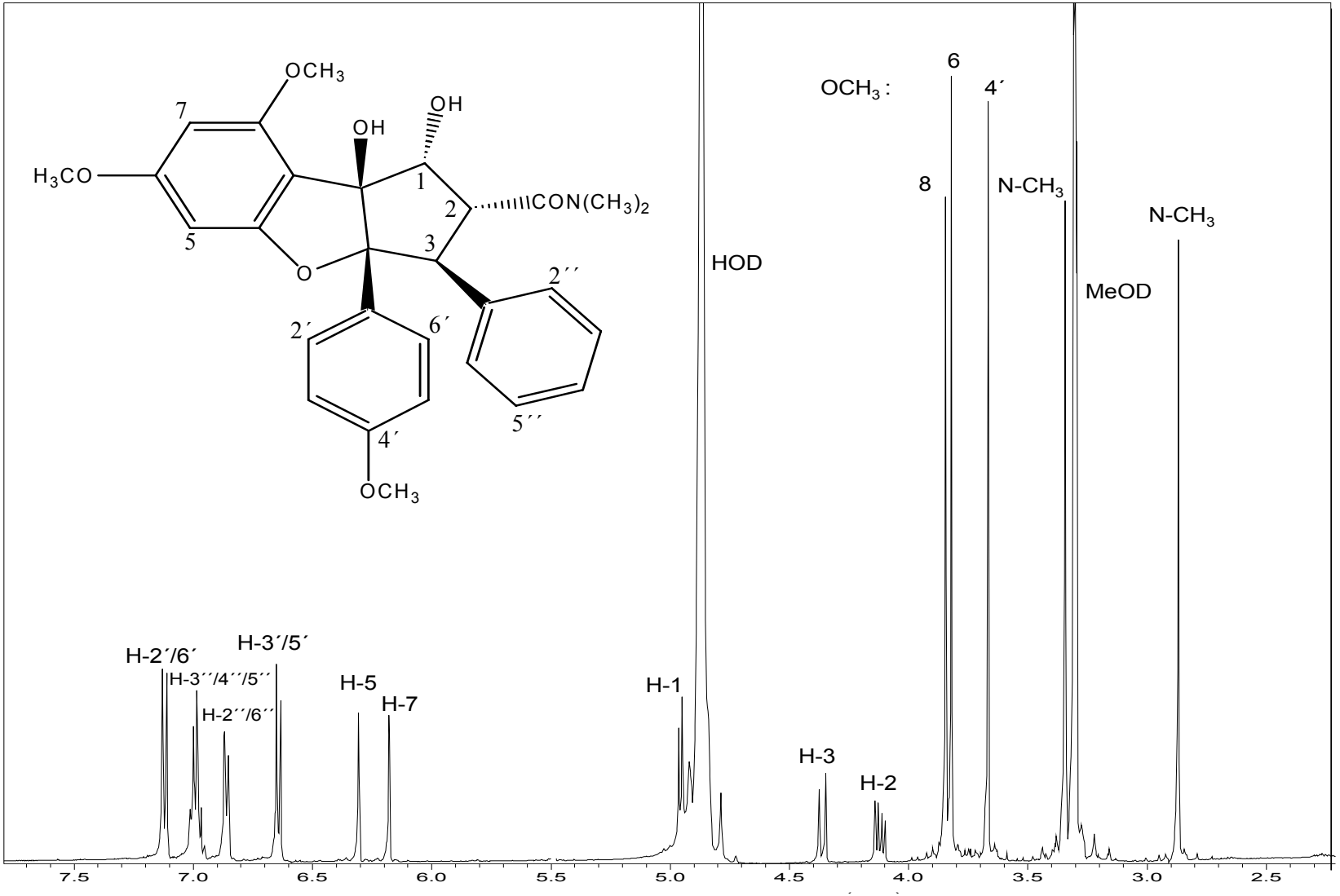

Fig.3.5: ^{1}H NMR of compound 1 in MeOD

Table 3.14: The ^{1}H NMR data of compounds 1, 2, 3, 4, 5, 6 and 7 in MeOD

^{1}H-position	1 Roc A	2 Roc I	3 Roc W	4 Roc AB	5 Roc J	6 Roc AK	7 Roc S
1	4.95(d, 6.9)	6.03 (d, 5.0)	5.99(d, 6.3)	5.95 (m)	5.0(d, 5.7)	4.69(d, 5.5)	
2	4.11(dd, 6.9,13.8)	4.29(dd, 5.0,14.5)	3.94(dd, 5.9,14.5)	4.21(m)	3.96(dd, 5.7,13.9)	α: 2.80(ddd, 6.3,13.5,14.0) β: 2.06(ddd, 1.1,6.2,11.8)	
3	4.36(d, 13.8)	4.29(d, 14.5)	4.19(d, 14.5)	4.21(m)	4.21(d.13.9)	3.89(dd, 13.5,14.0)	4.43 (s)
5	6.30(d, 1.9)	6.26(d, 1.9)	6.26(d, 1.9)	6.18(d, 1.9)	6.27(d, 1.9)	6.28(d, 1.9)	6.28 (d, 1.9)
7	6.17(d, 1.9)	6.11(d, 1.9)	6.12(d, 1.9)	6.03(d, 1.9)	6.15(d, 1.9)	6.17(d, 1.9)	6.12 (d, 1.9)
2′	7.12(d, 8.8)	6.78(d, 1.9)	7.17(d, 8.8)	7.08(d, 8.8)	6.70(d, 1.9)	7.10(d, 8.8)	7.03 (d, 8.8)
3′	6.64(d, 8.8)		6.61(d, 8.8)	6.54(d, 8.8)		6.61(d, 8.8)	6.51 (d, 8.8)
5′	6.64(d, 8.8)	6.62(d, 8.2)	6.61(d, 8.8)	6.54(d, 8.8)	6.64(d, 8.8)	6.61(d, 8.8)	6.51 (d, 8.8)
6′	7.12(d, 8.8)	6.70(d, 6.9)	7.17(d, 8.8)	7.08(d, 8.8)	6.64(d ,8.8)	7.10(d, 8.8)	7.03 (d, 8.8)
2′′	6.86(m)	7.02(m)	6.91(m)	6.80(m)	6.91(m)	7.00(m)	6.82 (m)
3′′	6.98(m)	6.98(m)	7.00(m)	6.92(m)	7.00(m)	7.00(m)	7.01 (m)
4′′	6.98(m)	6.98(m)	7.00(m)	6.92(m)	7.00(m)	7.00(m)	7.01 (m)
5′′	6.98(m)	6.98(m)	7.00(m)	6.92(m)	7.00(m)	7.00(m)	7.01 (m)
6′′	6.86(m)	7.02(m)	6.91(m)	6.80(m)	6.91(m)	7.00(m)	6.82 (m)
OMe-6	3.81(s)	3.81(s)	3.74(s)	3.64(s)	3.81(s)	3.87(s)	3.78 (s)
OMe-8	3.84(s)	3.73(s)	3.81(s)	3.72(s)	3.82(s)	3.85(s)	3.79 (s)
OMe-4′	3.66(s)	3.71(s)	3.65(s)	3.56(s)	3.67(s)	3.81(s)	3.62 (s)
N-Me	3.34(s); 2.86(s)	3.37(s); 2.79(s)	2.57(s)	3.27(s); 2.69(s)			
$OCOCH_3$		1.81(s)	1.84(s)	1.71(s)	3.61(s)		
2′′′							A: 4.11 (m) B: 4.08 (m)
3′′′							A: 3.34 (m) B: 3.28 (m)
4′′′							A: 2.33 (m) B: 2.29 (m)

III.2.1.2. Rocaglamide I (2, known compound)

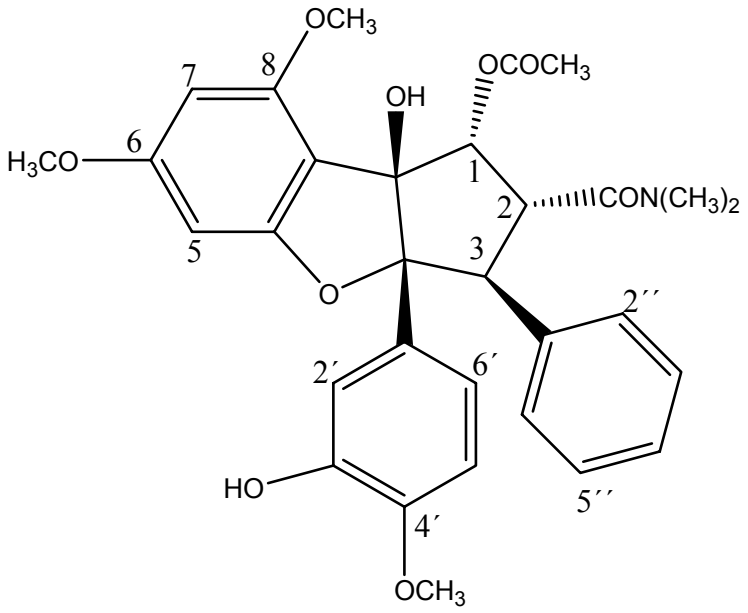

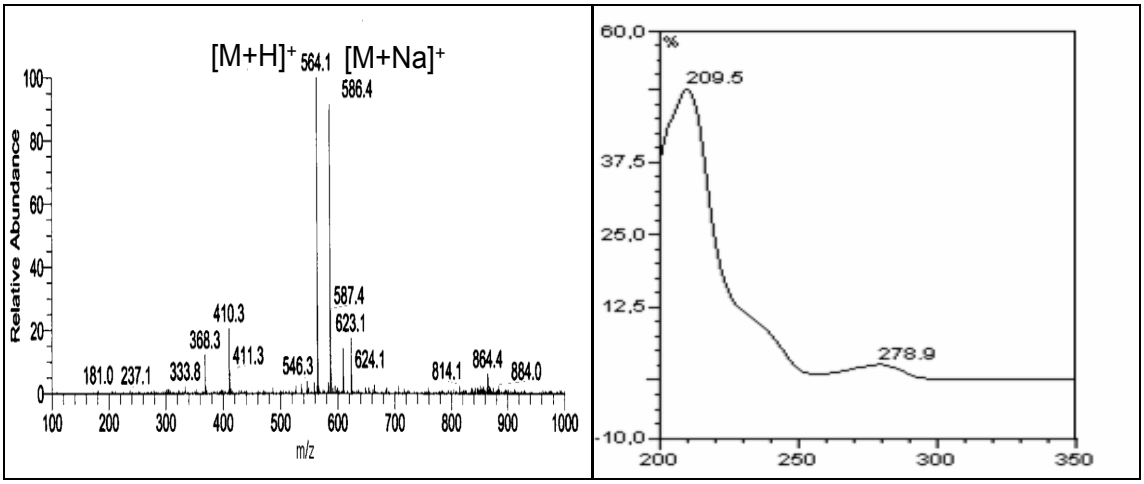

Fig.3.6: ESI-MS and UV spectrum of compound 2

Compound **2** was isolated from the bark of *Aglaia duppereana* as a white amorphous residue; $[\alpha]^{20}_{D}$ -80 (*c*, 0.45, $CHCl_3$); UV (MeOH) λ_{max} 209 nm, 279 nm (see Fig. 3.6). The ESIMS positive mode showed a pseudomolecular ion peak at *m/z* 564.1 $[M+H]^+$, *m/z* 586.4 $[M+Na]^+$ (see Fig. 3.6). In the ^1H NMR spectrum of compound **2**, two methine protons for H-5 and H-7 of ring A were observed as a *meta* doublet with coupling

constants of 1.9 Hz at δ 6.26 and 6.11, respectively. Furthermore, there is an additional methyl signal which occurred upfield at δ 1.81 ppm that indicated the presence of an acetoxy group at C-1. This was in accordance to the downfield shift of H-1 to δ 6.03. Besides, two aliphatic protons, H-2 and H-3, were observed as overlapping peaks at 4.29 ppm. The ^{1}H NMR spectrum of compound **2** implied a hydroxyl-substituent at C-3′ causing a shielding effect on the aromatic protons at ring B in the following order: H-2′>H-6′>H-5′ [Proksch *et al.,* 2001]. Substitution at C-3′, thus, changed the symmetry of ring B and the ^{1}H NMR resonance pattern of the characteristic AA′BB′ system of the *para*-substituted ring B to an ABC system (see Fig. 3.7). This substitution also changed the order of chemical shifts among the three methoxy groups: at δ 3.73 (OC*H*$_3$-8), at 3.81 (OC*H*$_3$-6), and at 3.71 (OC*H*$_3$-4′). Other two singlets of N-CH$_3$ groups occurred at 3.34 ppm and at 2.86 ppm. In comparison with the literature data [Nugroho *et al.,* 1997] and based on the ^{1}H NMR spectrum (see Table 3.14 and Fig. 3.7) compound **2** was identical to Rocaglamide I, which was previously isolated from the twigs of *Aglaia duppereana* collected in Vietnam.

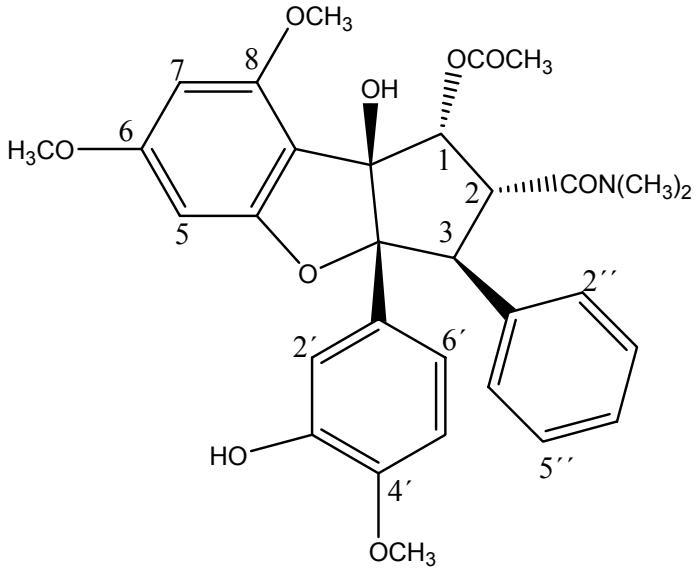

Rocaglamide I

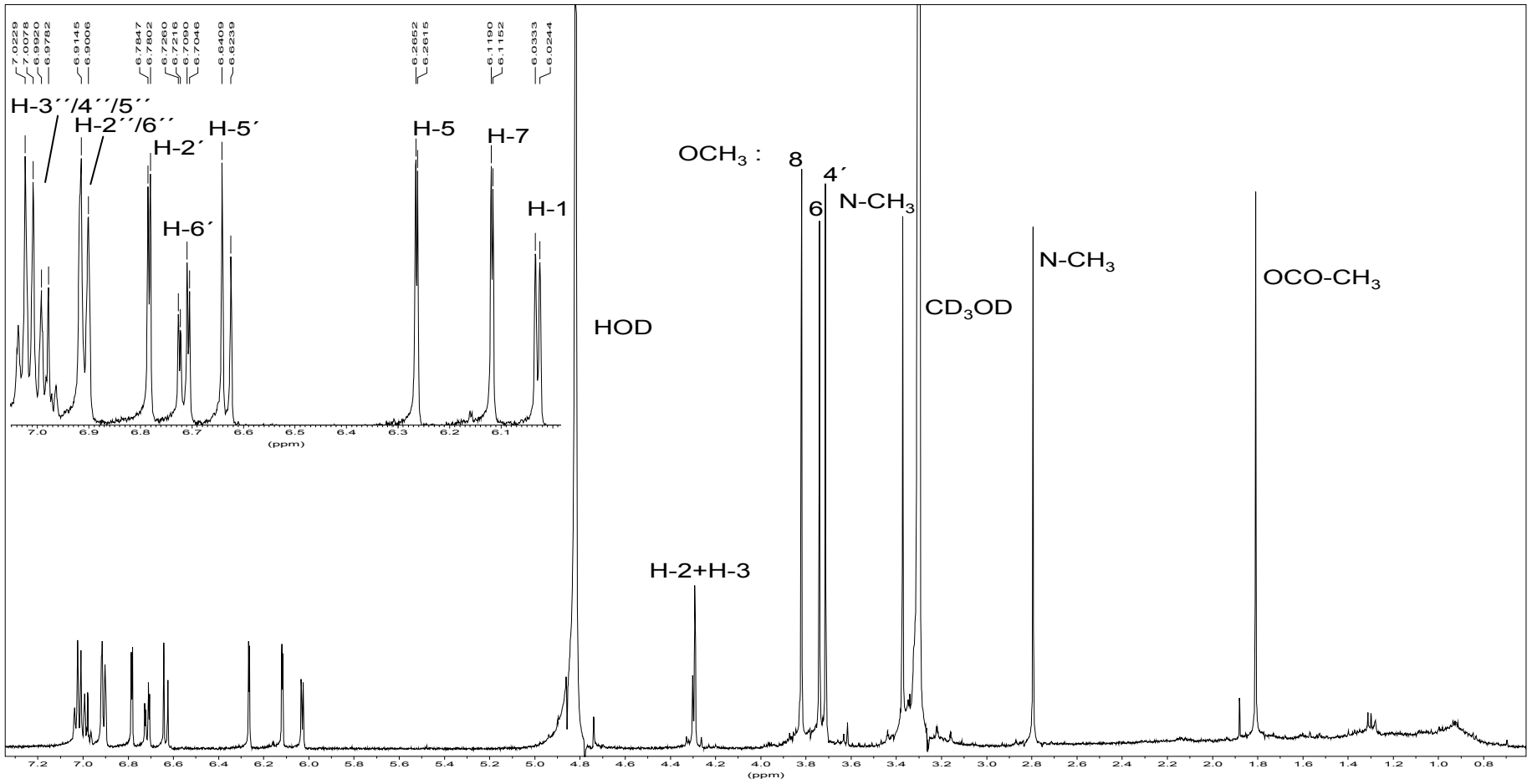

Fig.3.7: ^{1}H NMR of compound 2 in MeOD

III.2.1.3. Rocaglamide W (3, known compound)

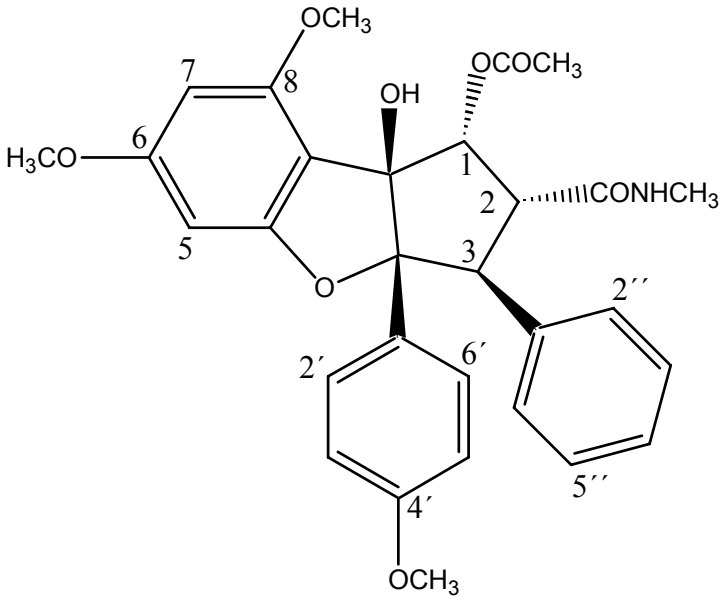

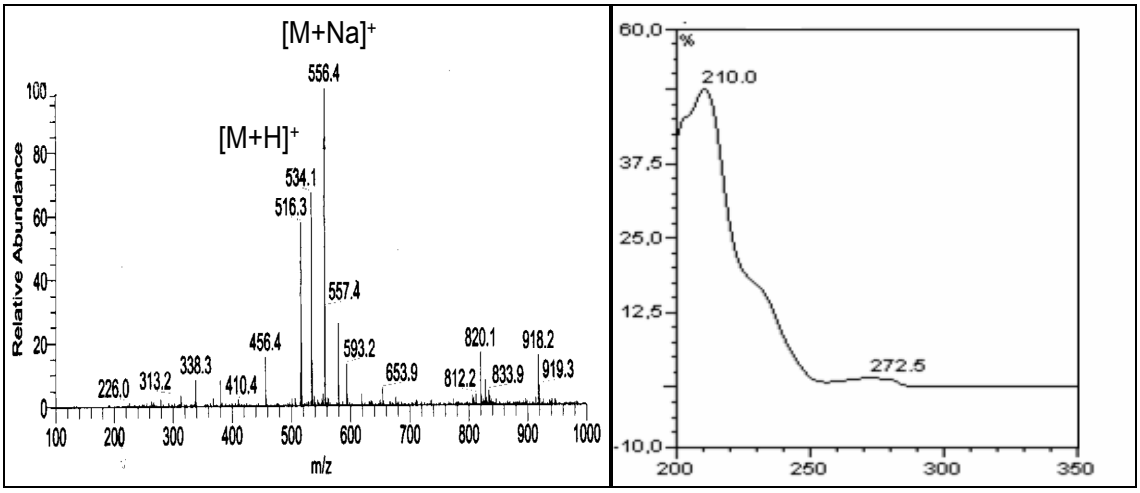

Fig.3.8: ESI-MS and UV spectrum of compound 3

Compound **3** was isolated from the bark of *Aglaia duppereana* as a white amorphous residue; $[\alpha]^{20}_{D}$-55.0 (*c*, 0.45, $CHCl_3$); UV (MeOH) λ_{max} 210 nm, 272.5 nm (see Fig. 3.8). The ESIMS positive mode showed the pseudomolecular ion peak at *m/z* 534.1 $[M+H]^+$, and *m/z* 556.4 $[M+Na]^+$, respectively (see Fig. 3.8). When comparing with the ^{1}H NMR spectrum of compound **1,** the spectrum of compound **3** revealed loss of one N-Me signal at *ca*.3.34 ppm suggesting a $CONHCH_3$ substitution at C-2, instead of a $CON(CH_3)_2$ as in

Rocaglamide I. Two methine protons for H-5 and H-7 of ring A were also observed as a *meta* doublet with coupling constants of 1.9 Hz at δ 6.26 and 6.12, respectively. The characteristic AA´BB´ spin system was again observed at δ 6.61 (d, 8.8) and 7.17 (d, 8.8) typical for a *para*-substituted phenyl ring (ring B). Similar to compound **2**, the acetyl group at C-1 was also observed at δ 1.84 (s). This was in accordance to the downfield shift of H-1 to δ 5.99 (d, 6.3). Other two methine protons resonated at δ 3.94 (dd, 5.9, 14.5) and 4.19 (d, 14.5), corresponding to H-2 and H-3, respectively. The coupling constants of 14.5 Hz imply an axial-axial coupling between H-2 and H-3 while the coupling constant 5.9 Hz corresponds to the axial-equatorial coupling between H-2 and H-1. In comparison with the literature data [Hiort *et al.,* 1999] and based on the ^{1}H NMR spectra (see Table 3.14 and Fig. 3.9) compound **3** was identified as Rocaglamide W, which was previously isolated from the roots of *Aglaia duppereana* collected in Vietnam.

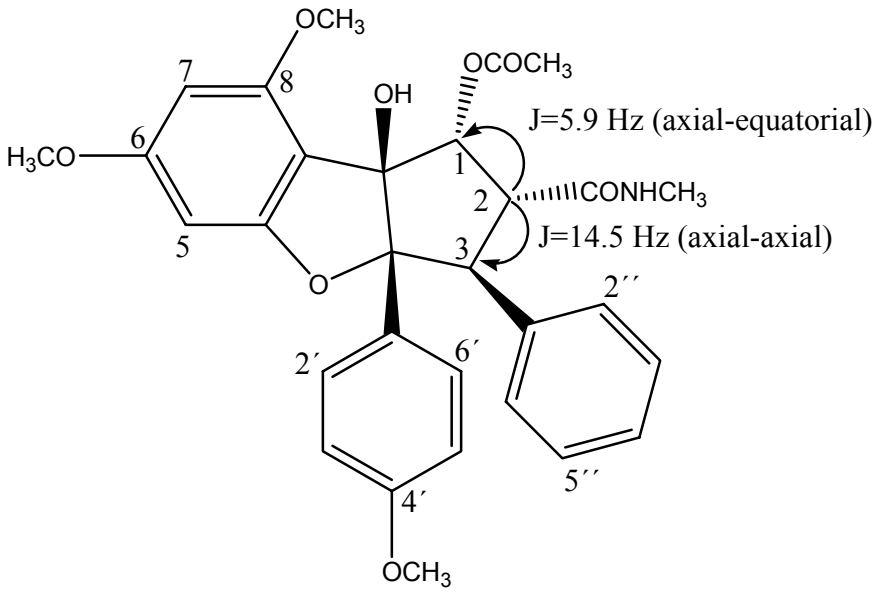

Rocaglamide W

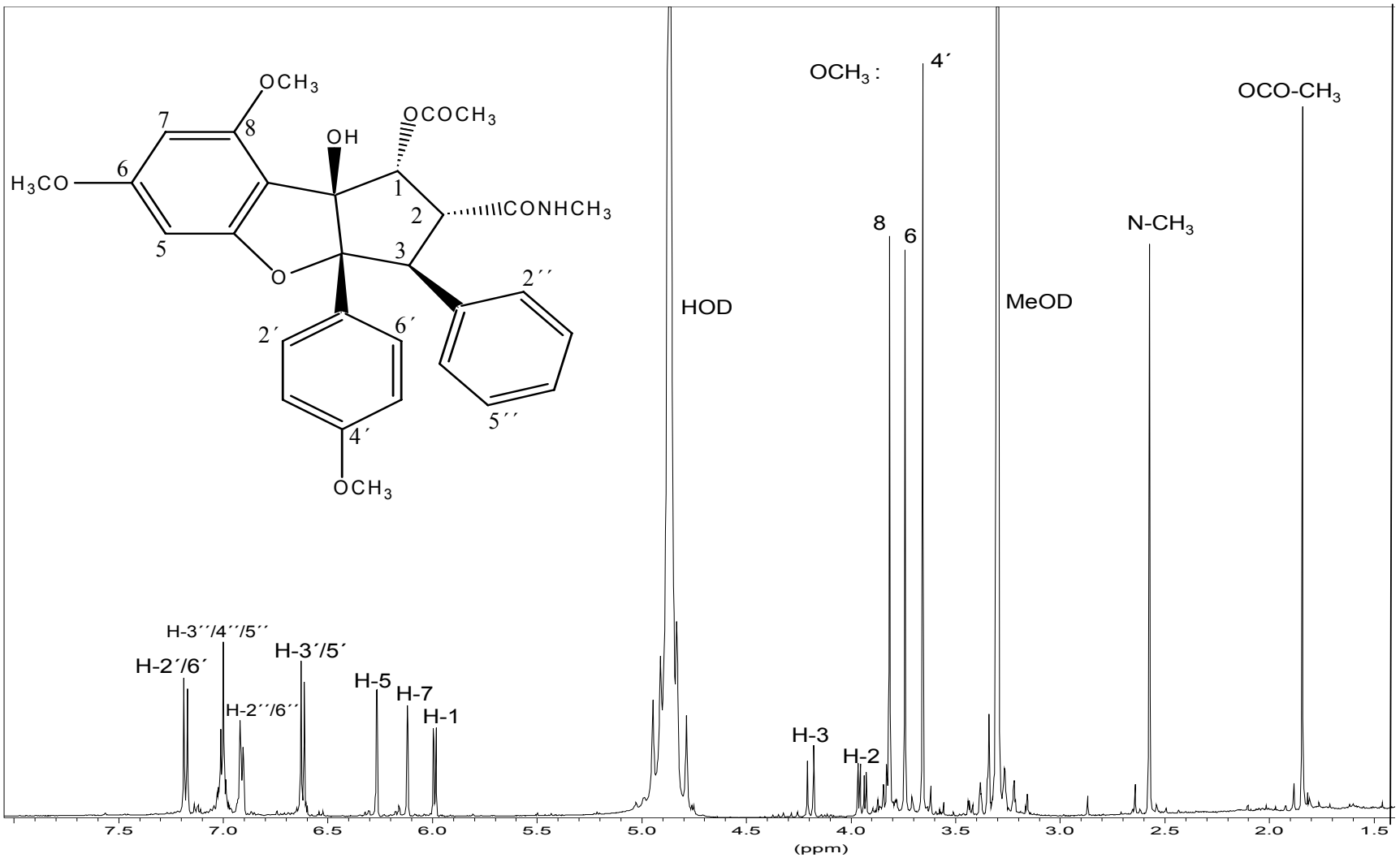

Fig.3.9: ^{1}H NMR of compound 3 in MeOD

III.2.1.4. Rocaglamide AB (4, known compound)

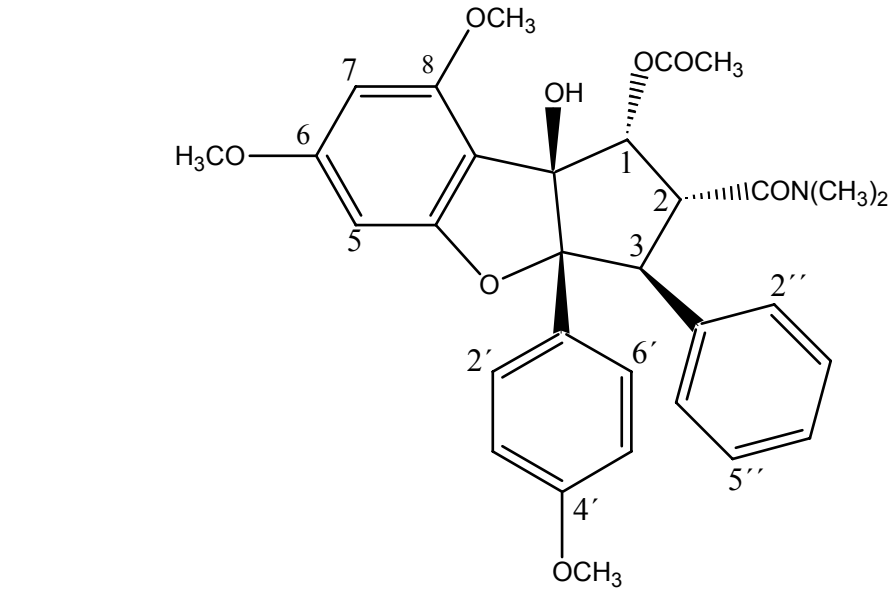

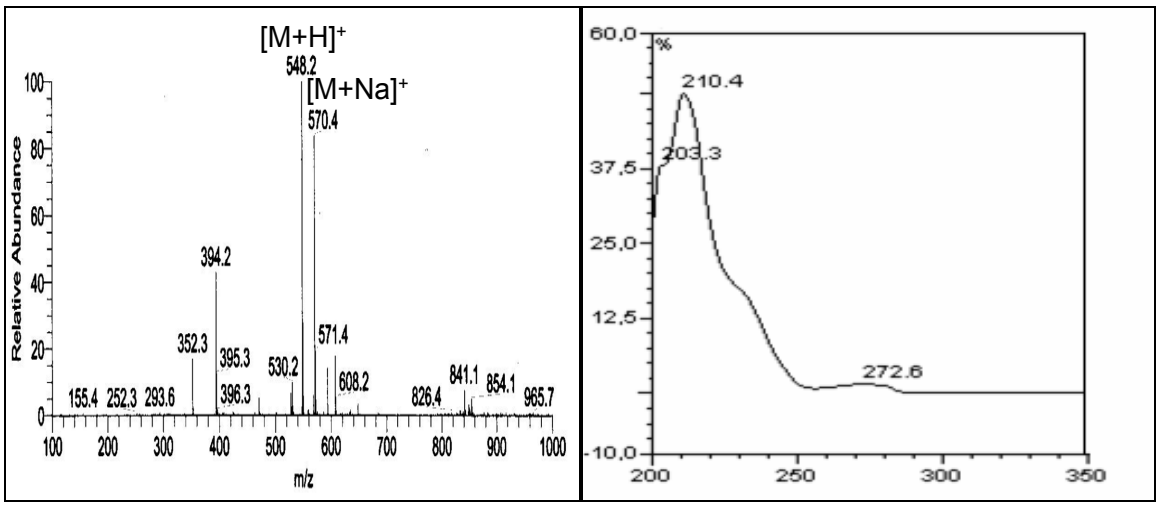

Fig.3.10: ESI-MS and UV spectrum of compound 4

Compound **4** was isolated from the bark of *Aglaia duppereana* as a white amorphous residue; $[\alpha]^{20}_{D}$-110.0 (*c*, 0.45, $CHCl_3$); UV (MeOH) λ_{max} 210.4 and 272.6 nm (see Fig. 3.10). The ESIMS positive mode showed the pseudomolecular ion peak at *m/z* 548.2 $[M+H]^+$, and *m/z* 570.4 $[M+Na]^+$, respectively (see Fig. 3.10). The molecular weight of compound **4** is 14 mass units higher than that of compound **2**. In comparison with the literature data [Hiort *et al.,* 1999] and based on the ^{1}H NMR spectrum (see Table 3.14

and Fig. 3.11) compound **4** was found to be identical to Rocaglamide AB (1-*O*-Acetylrocaglamide) previously isolated from the roots of *Aglaia duppereana* collected in Vietnam. The ^{1}H NMR spectrum of compound **4** revealed a characteristic AA´BB´ spin system of ring B as found in compounds **1** and **3**. Two pairs of protons H-2´/H-6´ and H-3´/H-5´ exhibited signals at δ 7.08 ppm (2H, d, 8.8) and 6.54 ppm (2H, d, 8.8), respectively. In addition, the ^{1}H NMR spectrum also revealed two N-Me singlets at δ 3.27 and 2.69 as found in compound **1**. Besides, the molecular weight of compound **4** is 16 units smaller than that of **2**, which could be attributed for a loss of one hydroxyl group. On the other hand, acetylation at C-1 caused the change of chemical shift of H-1 downfield to 5.95 (m) ppm and overlapping of protons H-2 and H-3 at 4.21 ppm (m) as found in compounds **2** and **3**. The two *meta* doublet protons of H-5 and H-7 of ring A resonated at 6.18 and 6.03 ppm, respectively. The other 5 protons of the mono-substituted ring C were also observed at 6.92 and 6.80 ppm as found in other rocaglamide congeners. The three methoxy singlets were observed at δ 3.64, 3.72 and 3.56, corresponding to OCH_3-6, OCH_3-8 and OCH_3- 4´, respectively as found in the known compounds. Thus, it was concluded that compound **3** was identified as Rocaglamide AB.

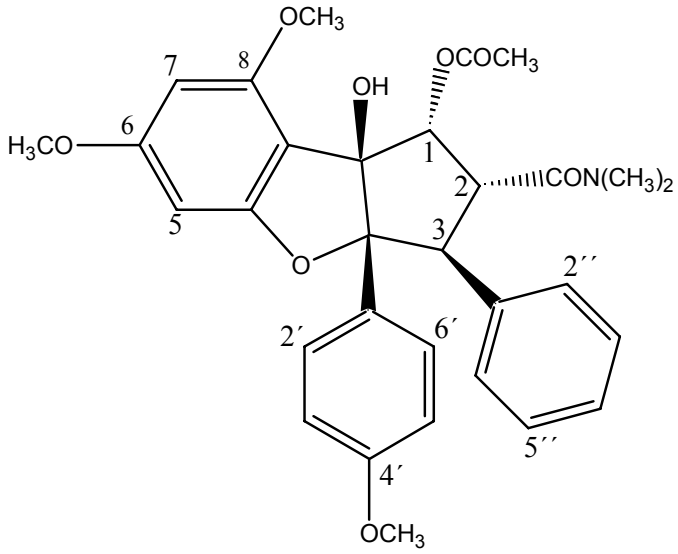

Rocaglamide AB

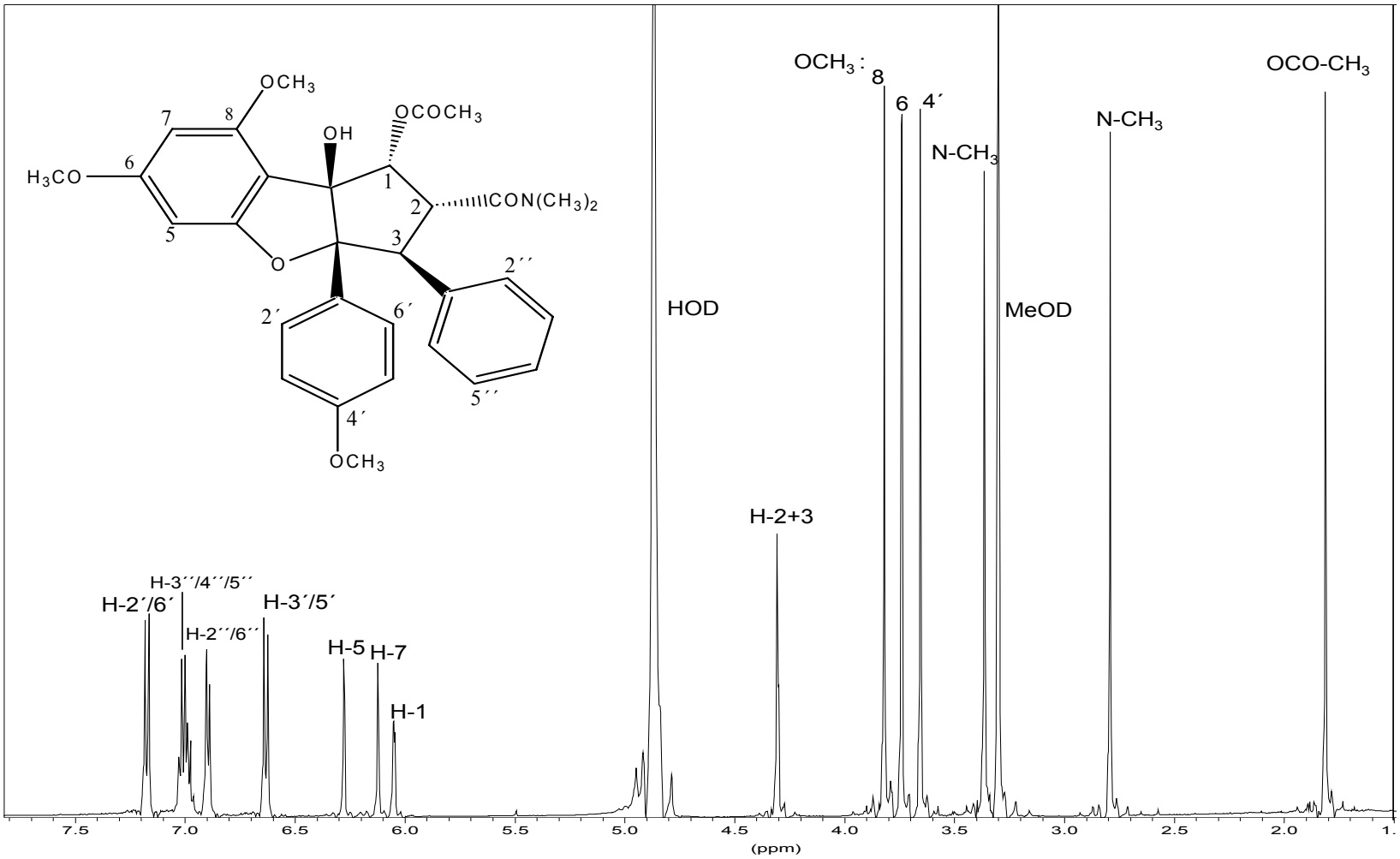

Fig.3.11: ^{1}H NMR of compound 4 in MeOD

III.2.1.5. Rocaglamide J (5, known compound)

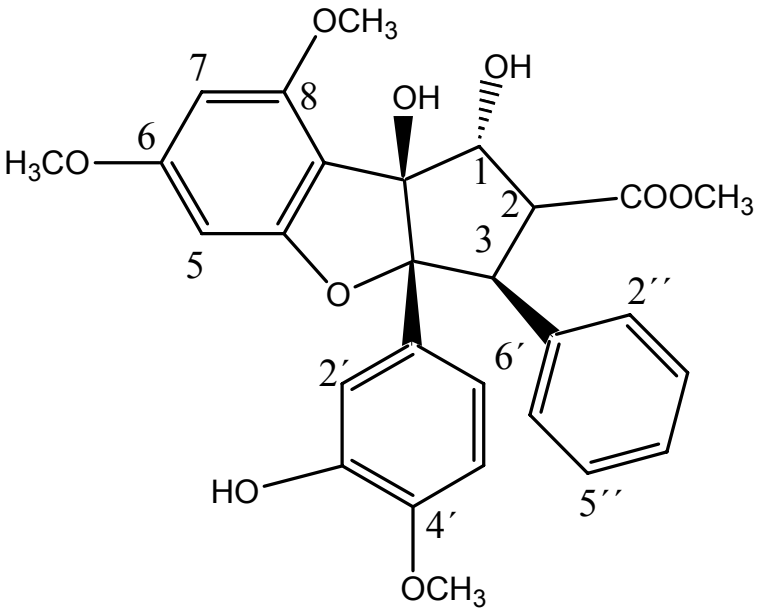

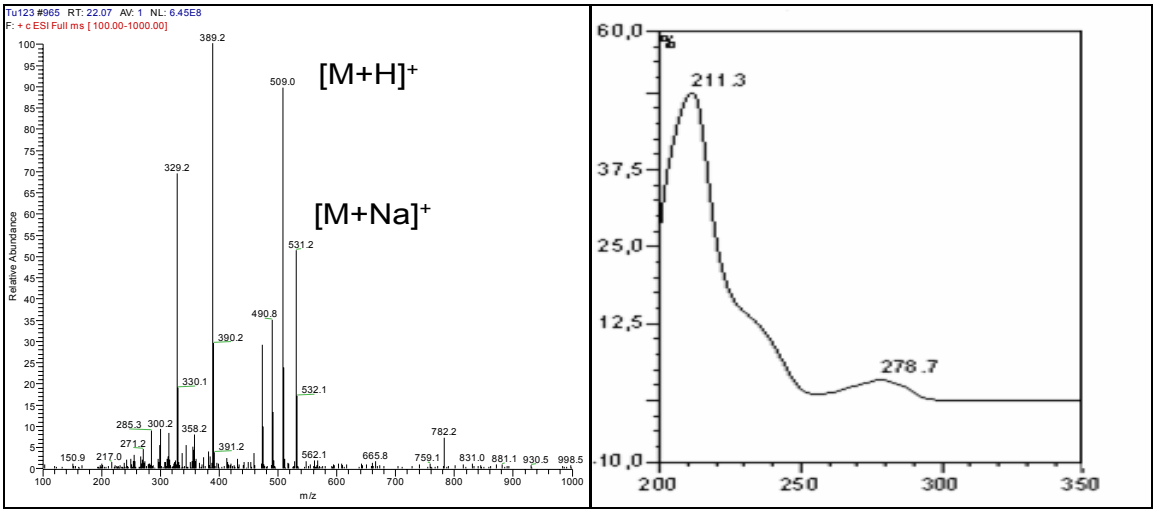

Fig.3.12: ESI-MS and UV spectrum of compound 5

Compound **5** was isolated from the bark of *Aglaia duppereana* as a white amorphous residue; $[\alpha]^{20}_{D}$-41.1 (*c*, 0.22, $CHCl_3$); UV (MeOH) λ_{max} 211.3 nm, 278.7 nm (see Fig. 3.12). The ESIMS positive mode showed the pseudomolecular ion peak at *m/z* 509.0 $[M+H]^+$, and at *m/z* 531.2 $[M+Na]^+$, respectively (see Fig. 3.12).

In the ^{1}H NMR spectrum, the two *meta* protons H-5 and H-7 of ring A resonated at 6.27 ppm (d, 1.9) and at 6.15 ppm (d, 1.9), respectively. The hydroxyl substitutent at C-3′ changed the characteristic AA′BB′ spin system of ring B found for example for rocaglamide to an ABC spin system as found in compound **2**. This substitution, thus, changed the order of chemical shifts among the three methoxy groups: (OC*H*$_3$-6) at 3.81 ppm, (OC*H*$_3$-8) at 3.82 ppm, and (OC*H*$_3$-4′) at 3.67 ppm. The three protons H-1, H-2, and H-3 resonated at 5.0 ppm (d, 5.7), 3.96 (dd, 5.7, 13.9) and 4.21 ppm (d, 13.9), respectively. Furthermore, the methoxy singlet of the acetate moiety at C-2 occurred at 3.61 ppm (s). The five aromatic protons of ring C were observed at δ 6.91-7.00 ppm, as found in other compounds **1**, **2**, **3**, and **4**. In comparison with the literature data [Nugroho *et al.,* 1999] and based on its ^{1}H NMR spectrum (see Table 3.14 and Fig. 3.13), compound **5** was identical to methylrocaglate, or also named Rocaglamide J, which was previously isolated from the roots of *Aglaia duppereana* collected in Vietnam.

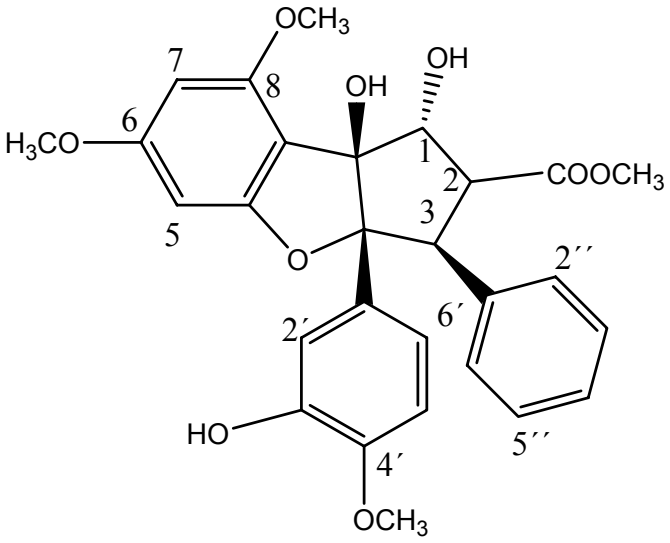

Rocaglamide J

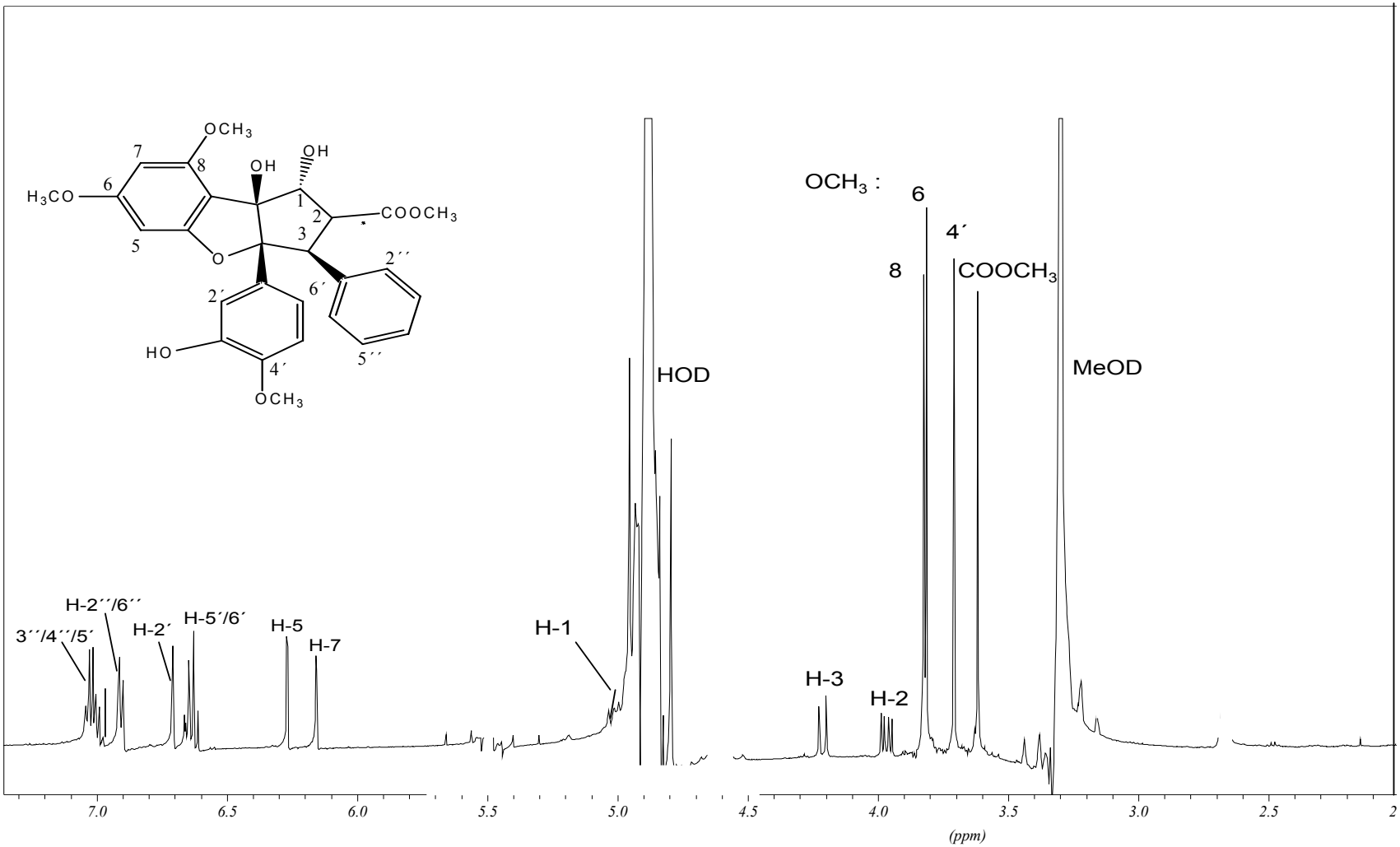

Fig.3.13: ^{1}H NMR of compound 5 in MeOD

III.2.1.6. Rocaglaol (6, known compound)

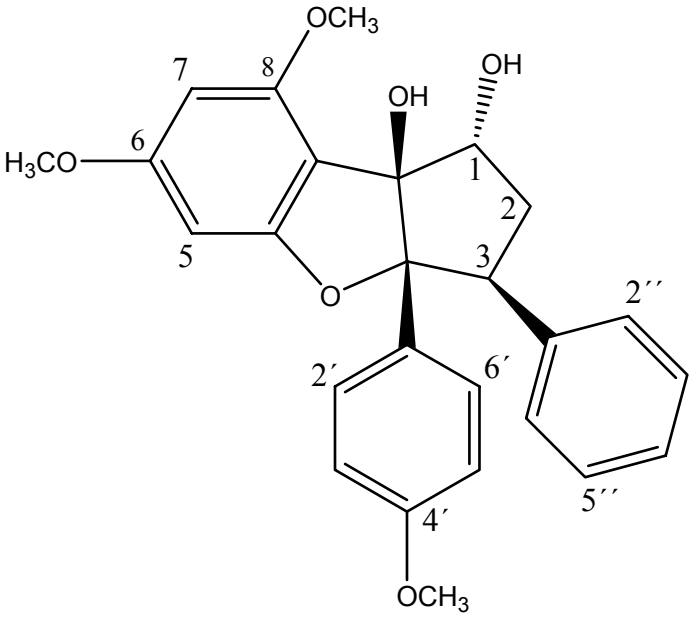

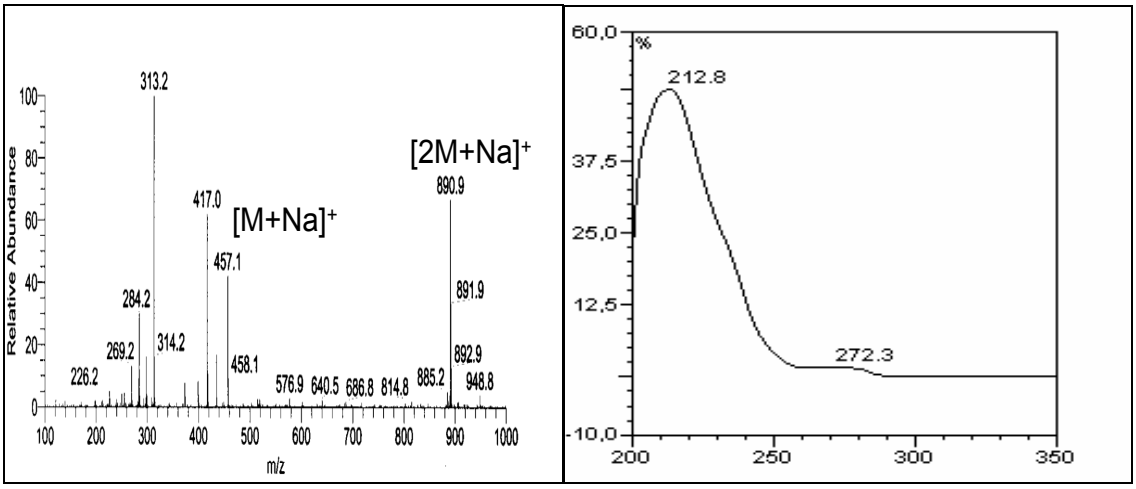

Fig.3.14: ESI-MS and UV spectrum of compound 6

Compound **6** was isolated from both the leaves of *Aglaia oligophylla* and the bark of *Aglaia elaeagnoidea* as a white amorphous residue; $[\alpha]^{20}_{D}$-125 (*c*, 0.48, $CHCl_3$); UV (MeOH) λ_{max} 212.8 nm, 272.3 nm (see Fig. 3.14). The ESIMS positive mode showed the pseudomolecular ion peak at *m/z* 457.1.0 $[M+Na]^+$, and at *m/z* 890.9 $[2M+Na]^+$, respectively (see Fig. 3.14). In the ^{1}H NMR spectrum of compound **6**, two *meta* protons H-5 and H-7 of ring A, resonated at δ 6.28 ppm (d, 1.9), at 6.17 (d, 1.9), the characteristic

AA´BB´ pattern of ring B were observed at δ 7.10 (2H, d, 8.8) and at δ 6.61 (2H, d, 8.8), and the three methoxy singlet at δ 3.87 (OMe-6), at δ 3.85 (OMe-8) and at δ 3.81(OMe-4´), respectively. When compared with Rocaglamide A (**1**), changes were observed for the aliphatic region. The resonance for the methylene protons appeared as a pair of geminally coupled multiplets at δ 2.06 ppm (ddd, 1.1, 6.2, 11.8) and 2.80 ppm (ddd, 6.2, 11.8, 14.0), both of which showed vicinal couplings with the methine signals bearing a phenyl and a hydroxyl group at δ 3.89 ppm and δ 4.69 ppm, respectively. Thus, the methylene signals should be connected between the methines. The methylene signals occurred at δ 2.06 and 2.80, and were assigned as H-2*α* and H-2*β* on the basis of a quite small (1.5 Hz) equatorial-equatorial and a large (14.0 Hz) axial-axial vicinal coupling constant value with H-1*β* and H-3*α*, respectively, following an envelope conformation of the cyclopentane ring [Ishibashi *et al.,* 1993] (see Fig. 3.15). In comparison with the literature data [Ishibashi *et al.,* 1993] and based on its ^{1}H NMR spectrum (see Table 3.14 and Fig. 3.16) compound **6** was identical to Rocaglaol, which was first isolated from the leaves of *Aglaia odorata* collected in Indonesia.

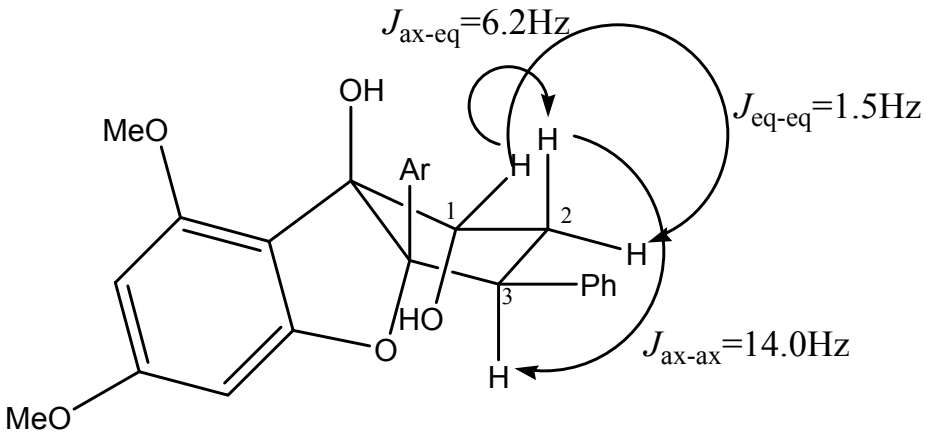

Fig.3.15: Structure of rocaglaol modified from [Ishibashi *et al.,* 1993]

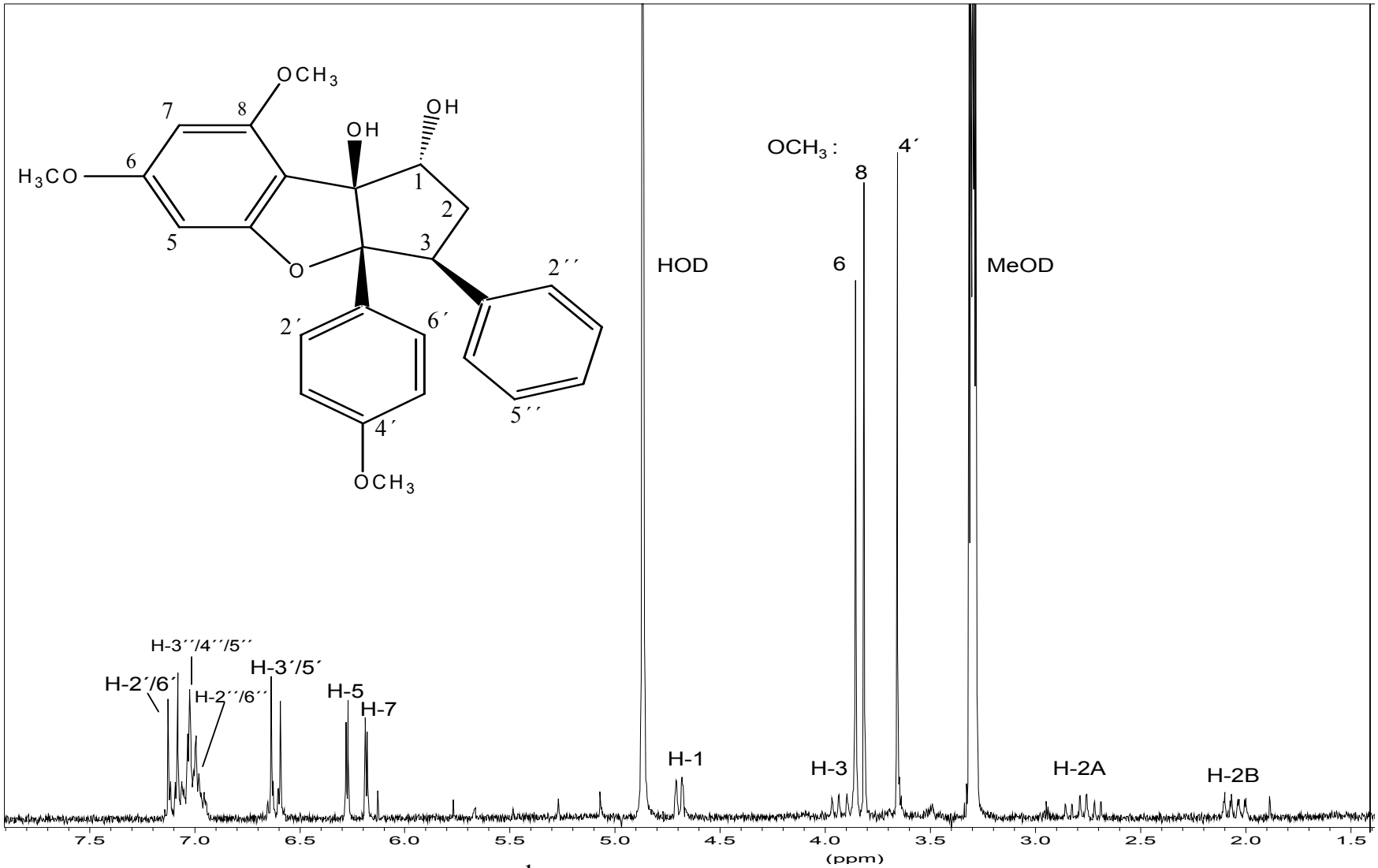

Fig.3.16: ^{1}H NMR of compound 6 in MeOD

III.2.1.7. Rocaglamide S (7, know compound)

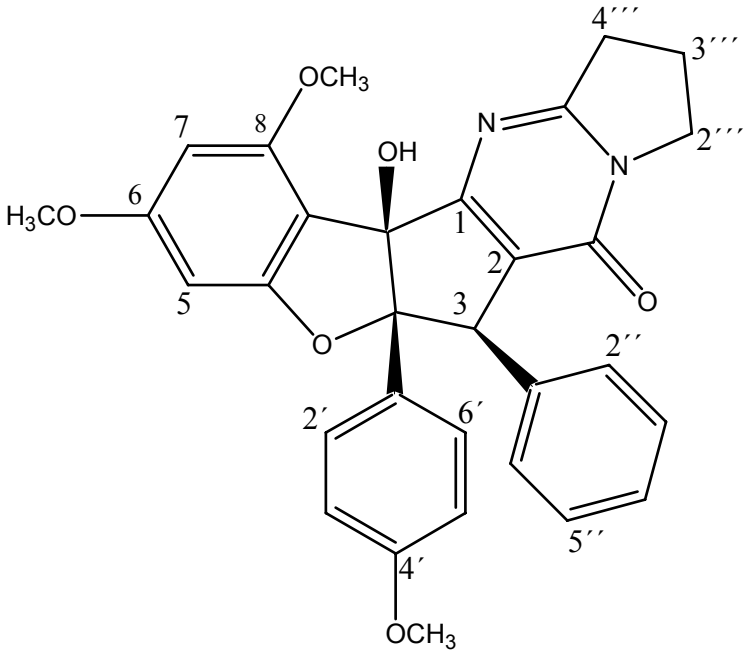

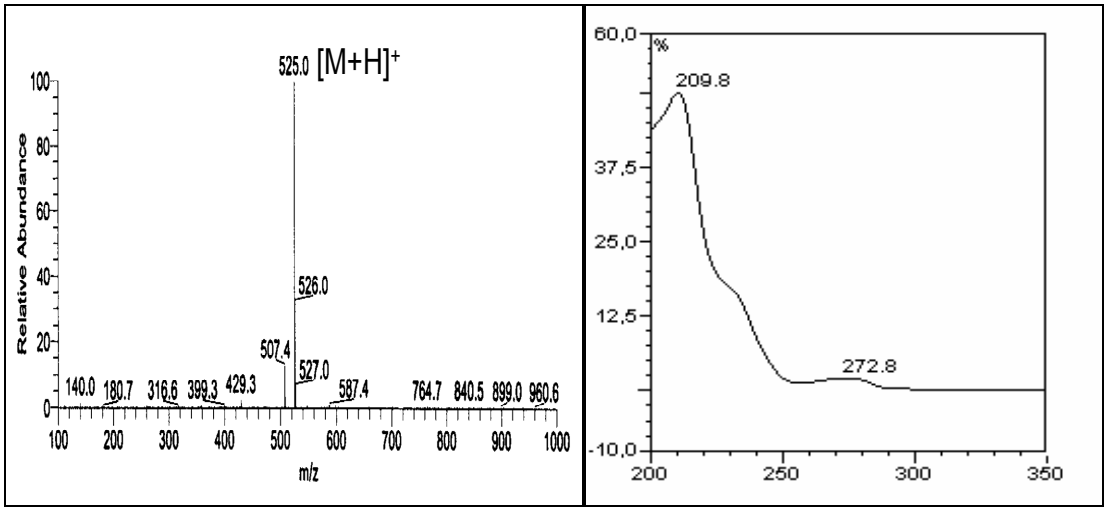

Fig.3.17: ESI-MS and UV spectrum of compound 7

Compound **7** was isolated from the leaves of *Aglaia duppereana* as a white amorphous residue; $[\alpha]^{20}_{D}$-50.5 (*c*, 0.45, $CHCl_3$); UV (MeOH) λ_{max} 209.8 nm, 272.8 nm (see Fig. 3.17). The ESIMS positive mode showed a pseudomolecular ion peak at *m/z* 525.0 $[M+H]^+$ (see Fig. 3.17). The ^1H NMR spectra of **7** revealed an unusual rocaglamide derivative featuring a pyrimidone unit [Kokpol *et al*.1994]. The resonances at δ 4.11 ppm

(H-2´´´-A) and 4.08 ppm (H-2´´´-B); 3.34 ppm (H-3´´´-A) and 3.28 ppm (H-3´´´-B); 2.33 ppm (H-4´´´-A) and 2.29 ppm (H-4´´´-B), were the three methylene groups of the pyrimidone unit. Two *meta* protons H-5 and H-7 of ring A resonated at 6.28 ppm (d, 1.9) and at 6.15 ppm (d, 1.9), respectively. The characteristic AA´BB´ pattern of ring B was again observed at 7.10 ppm (d, 8.8) and 6.61 ppm (d, 8.8). And the proton H-3 appeared as a singlet at 4.43 ppm. In comparison with the literature data [Nugroho *et al.,* 1997] and based on the ^{1}H-NMR spectrum (see Table 3.14 and Fig. 3.18) compound **7** was identical to Rocaglamide S, which was previously isolated from the twigs of *Aglaia duppereana* collected in Vietnam.

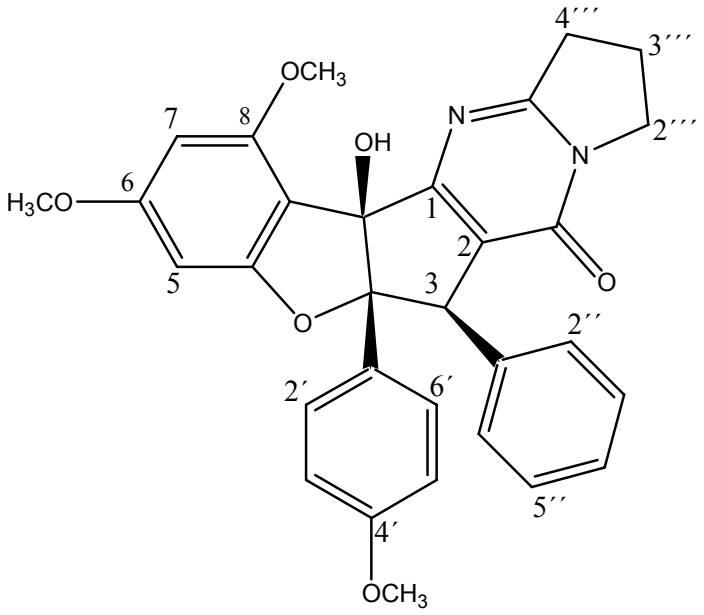

Rocaglamide S

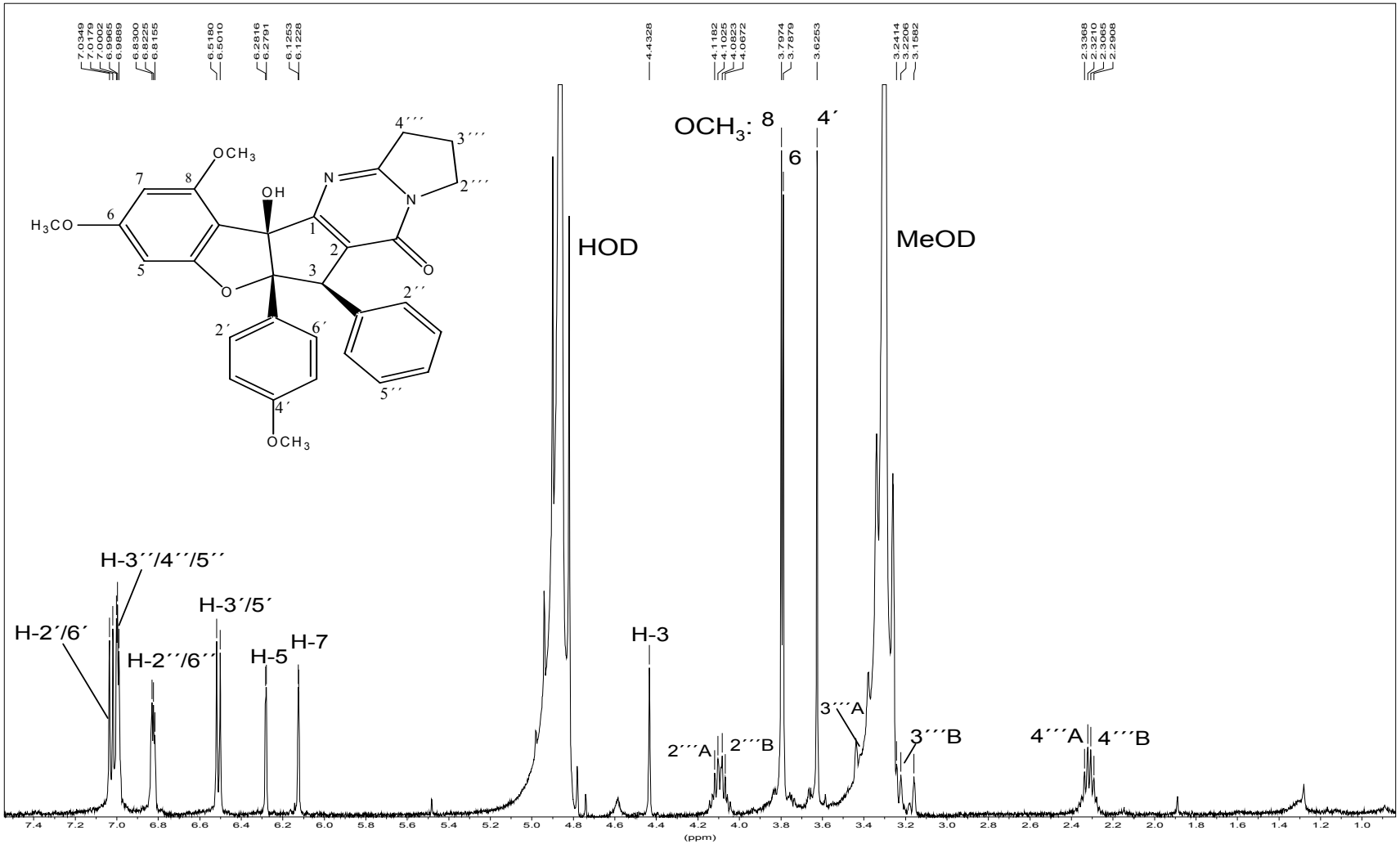

Fig.3.18: ^{1}H NMR of compound 7 in MeOD

III.2.1.8. Rocaglamide AY (8, new compound)

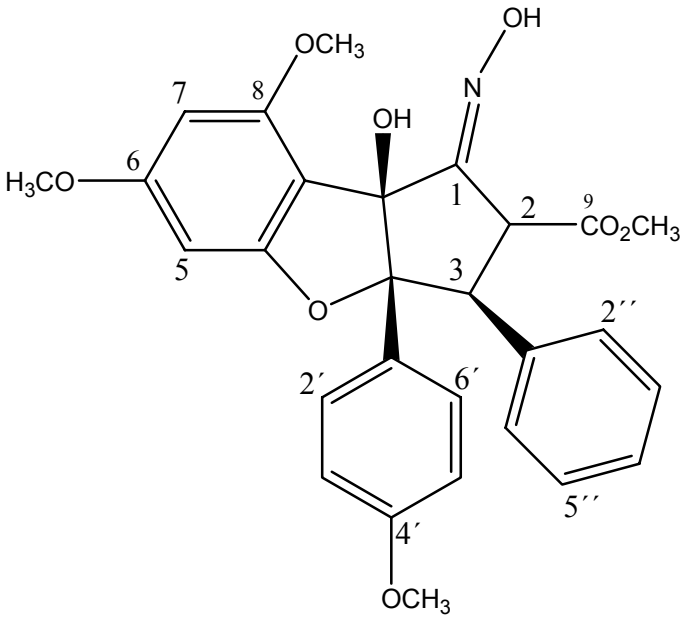

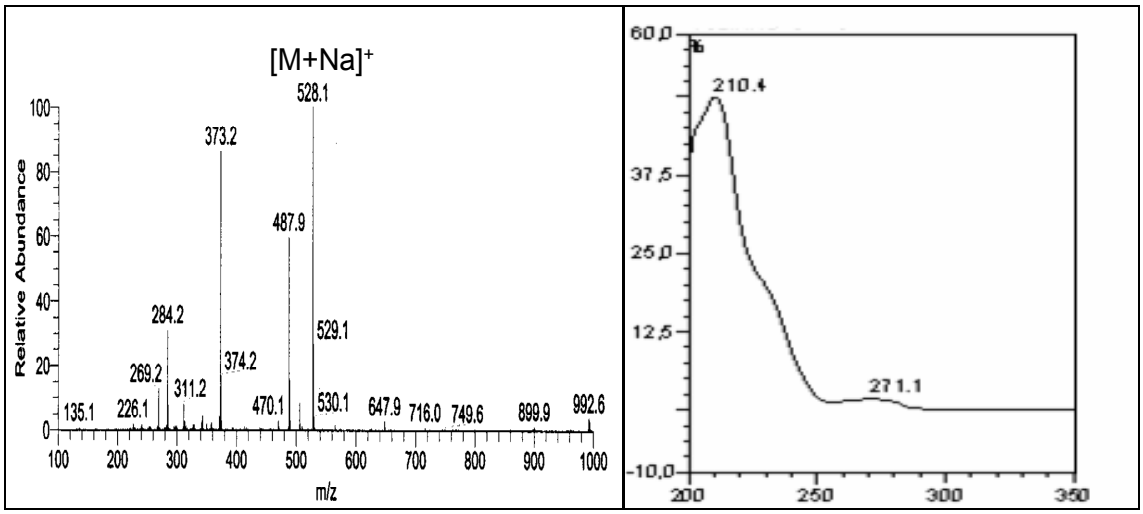

Fig.3.19: ESI-MS and UV spectrum of compound 8

Compound **8** was isolated from the leaves of *Aglaia oligophylla* as a white amorphous residue; $[\alpha]^{20}_{D}$-50.5 (*c*, 0.45, $CHCl_3$); UV (MeOH) λ_{max} 210.4 nm, 271.1nm (see Fig. 3.19). The ESIMS positive mode showed the pseudomolecular ion peak at *m/z* 528.1 $[M+Na]^+$(see Fig. 3.19). The HREIMS also showed the pseudomolecular peak at *m/z* 528.165 $[M+Na]^+$. This exact mass is calculated for the molecular formula $C_{28}H_{27}NO_8$.

The ^{1}H NMR and ^{13}C NMR data are comparable to these of Rocaglamide T. Based on the ^{1}H NMR, ^{1}H-^{1}H COSY, and HMBC spectra (see Table 3.15 and Fig. 3.20, Fig. 3.21, Fig. 3.22) compound **8** was identified as a C-1-oxime congener which caused, as expected, a large downfield shift at C-1 (δ 153.0) compared to the C-1 resonance for methylrocaglate at δ 80.6 ppm. This substitution pattern is also characterized by the deshielding effects on C-2 and C-8b of *ca*. 6 and 23 ppm, respectively. However, no obvious change in the carbon chemical shift was observed for C-3 [Nugroho *et al.,* 1999]. In the ^{1}H NMR spectrum, there is a loss of the H-1 resonance at *ca*. 4.90 ppm and H-2 was observed as a doublet at 3.8 ppm through coupling with H-3 at 3.67 ppm instead of a doublet of a doublet found in methylrocaglate. The correlations between H-2 and H-3 were determined from the ^{1}H-^{1}H COSY spectra (see Fig. 3.21). Furthermore, the HMBC showed the long range correlations of H-2 to C-1´´, C-8 and the carbonyl carbon (C-9) (see Table 3.15, Fig. 3.22 and Fig. 3.23) as well as correlations of H-3 to C-3a, C-1´, C-1´´, C-2´, C-6´ and C-9. From the ^{1}H NMR, the three methoxy groups resonated at δ 3.90 ppm (OMe-C8), 3.84 ppm (OMe-C6) and 3.71 ppm (OMe-C4´), respectively. In comparison to the mass spectrum of rocaglamide T, compound **8** revealed a loss of 30 mass units, which could be attributed to the absence of a methoxy substituent possibly at C-3´. Thus, the characteristic AA´BB´ spin system in ring C of compound **8** was still observed at δ 7.13 (2H, d, 8.8) and at δ 6.71 (2H, d, 8.8) **.** The other 5 protons of ring C resonated at δ 6.99-7.12. The structure of compound **8** was identified as a new rocaglamide derivative, named rocaglamide AY.

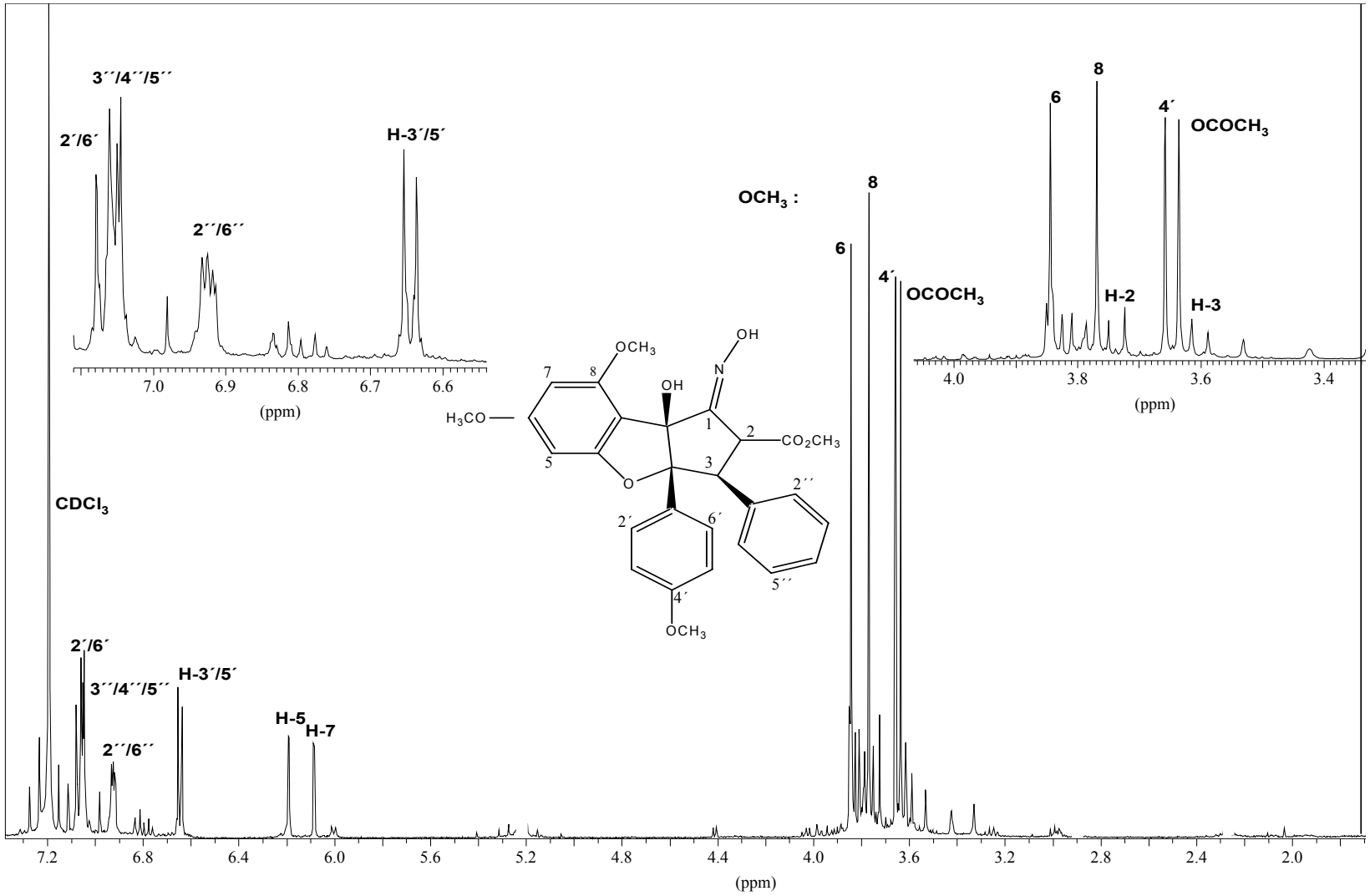

Fig.3.20: ^{1}H NMR of compound 8 in $CDCl_3$

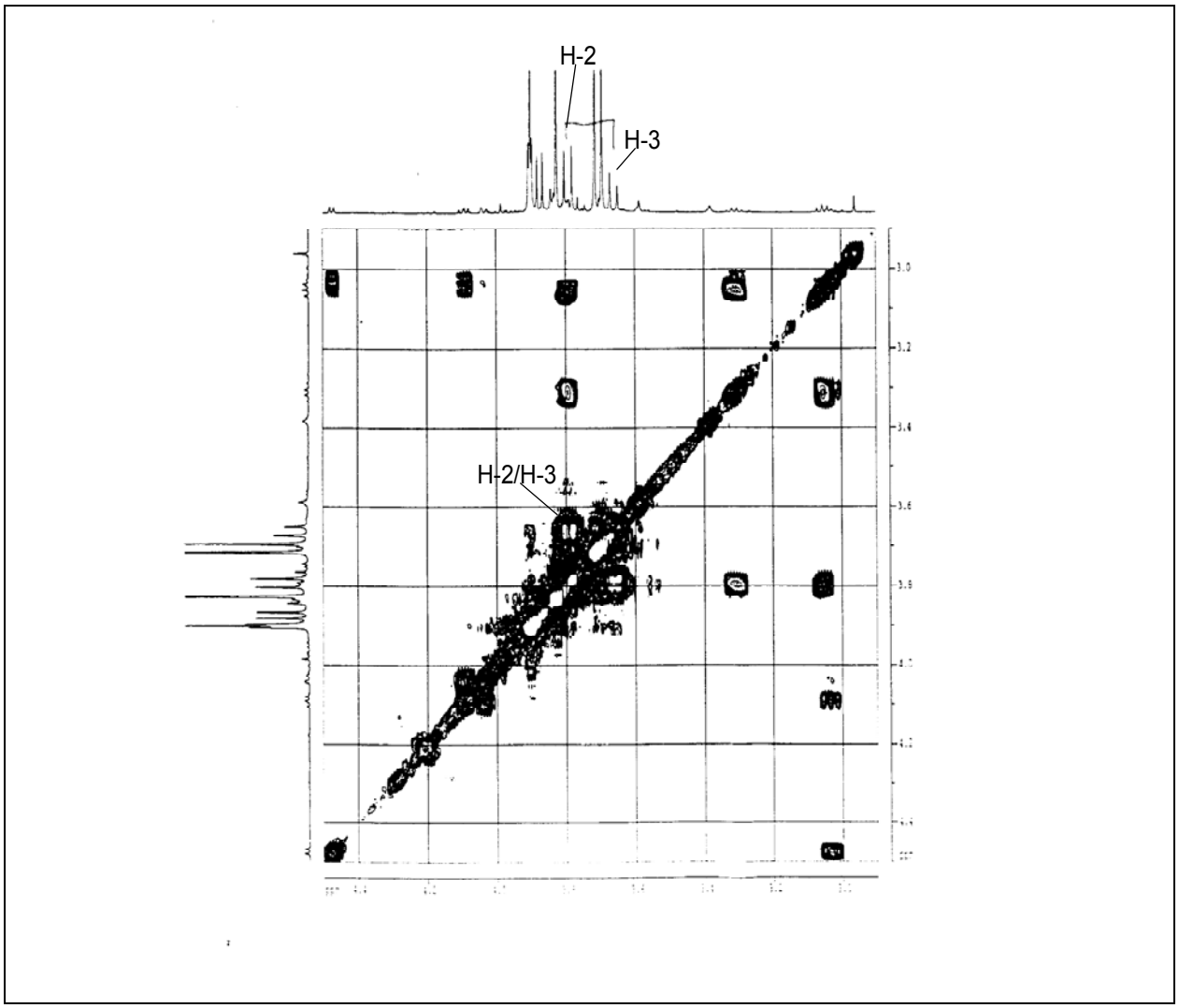

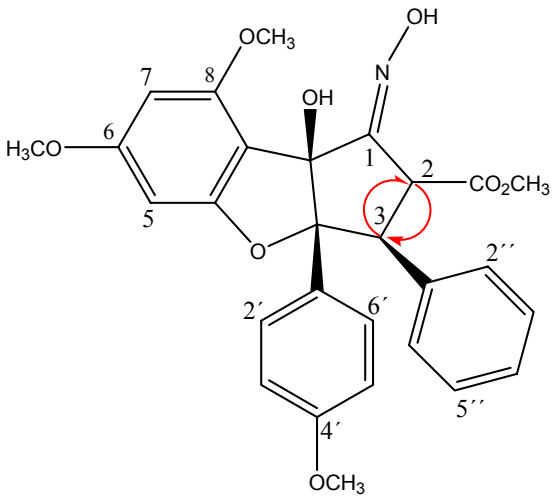

Fig.3.21: ^{1}H-^{1}H COSY correlations of compound 8 in $CDCl_3$

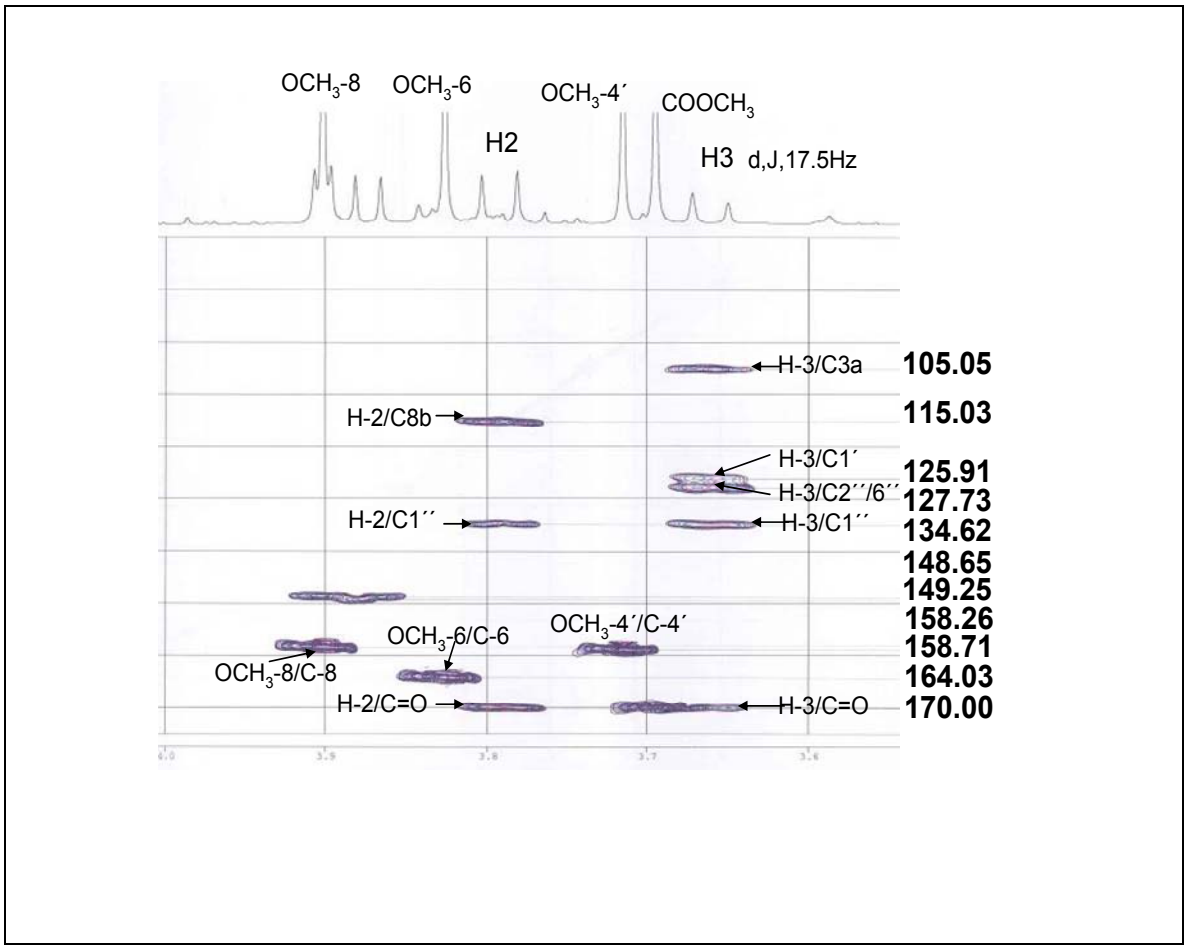

Fig.3.22: HMBC correlations of compound 8 in $CDCl_3$

Table 3.15: ^{1}H NMR, ^{13}C NMR, ^{1}H-^{1}H COSY and HMBC of compound 8 (in $CDCl_3$)

Position	Roc AY δ_C (ppm)	[a]Roc T δ_C (ppm)	Roc AY δ_H (ppm)	HMBC (H→C)	COSY
1	130.0	153.0			
2	57.0	57.1	3.80 (d, 13.5)	1,3,1′′	3
3	57.1	57.2	3.67 (d, 13.5)	2,3a,1′′,9,2′′,6′′	2
3a	105.1	105.7			
4a	160.0	161.3			
5	88.9	89.9	6.26 (d, 1.9)	4a,6,7,8a	
6	164.0	165.3			
7	93.0	93.8	6.15 (d, 1.9)	5,6,8,8a	
8	158.3	160.3			
8a	107.7	110.0			
8b	115.0	117.0			
1′	125.6	128.7			
2′	113.1	113.2	7.13 (d, 8.8)	3a	3′
3′	127.8	149.3	6.71 (d, 8.8)	2′,4′,5′,6′,1′′	2′
4′	158.8	149.5			
5′	126.8	111.5	6.71 (d, 8.8)	4′	6′
6′	125.6	121.4	7.13 (d, 8.8)	3a	5′
1′′	134.8	136.7			
2′′	127.7	129.4	6.99 (m)	5′′	3′′
3′′	127.8	128.7	7.12 (m)	1′′,2′′	2′′,4′′
4′′	127.8	128.0	7.12 (m)		3′′,5′′
5′′	126.8	128.7	7.12 (m)	1′′,2′′	4′′,6′′
6′′	127.7	129.4	6.99 (m)	5′′	5′′
9 (C=O)	170.0	171.7			
C8-OCH_3		56.1	3.90 (s)	8	
C6-OCH_3		56.3	3.84 (s)	6	
C4′-OCH_3		56.3	3.71 (s)	4′	
$COOCH_3$		57.5		9 (C=O)	

[a]: [Nugroho *et al.,* 1999 and Nugroho PhD thesis 1997] (measured in MeOD)

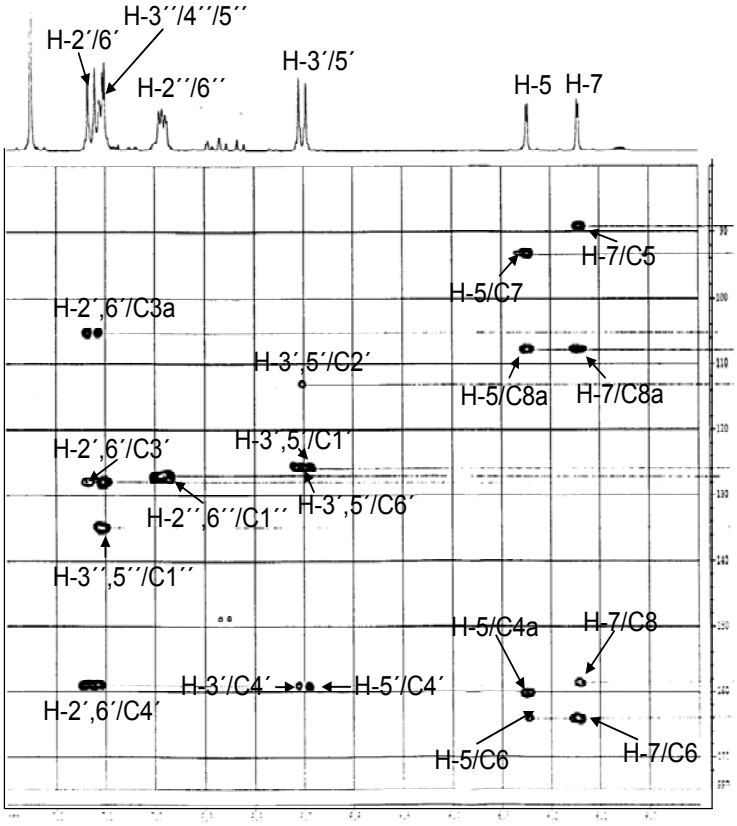

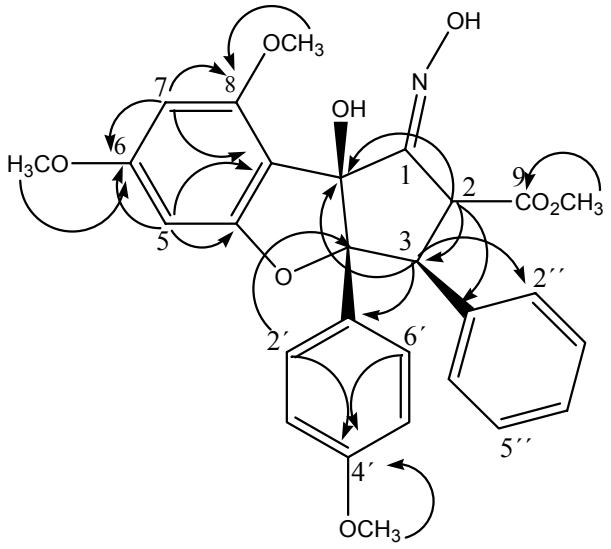

Fig.3.23: HMBC correlations of compound 8 in $CDCl_3$

III.2.2. Aglain derivatives isolated from *Aglaia* sp.

III.2.2.1. Aglaxiflorin D (9, known compound)

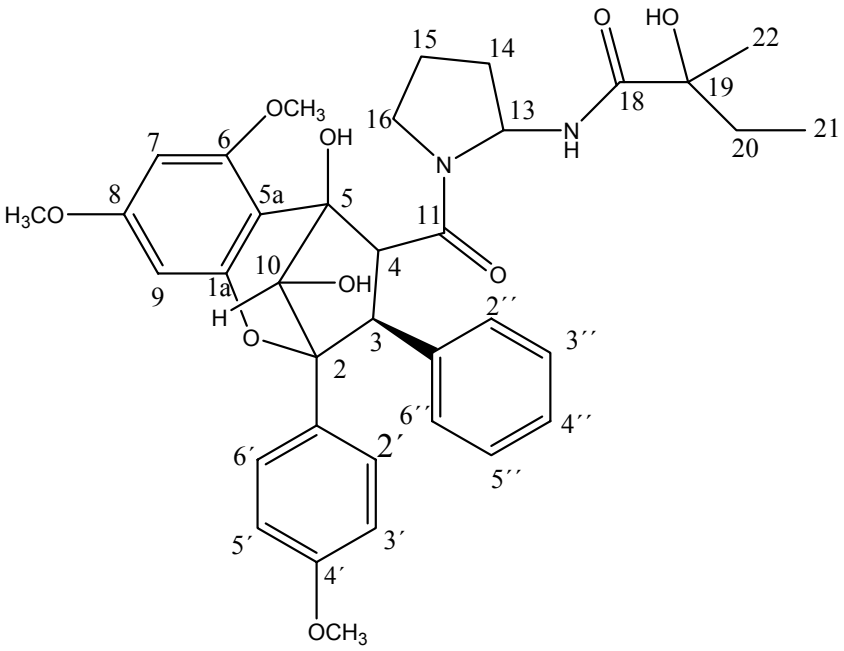

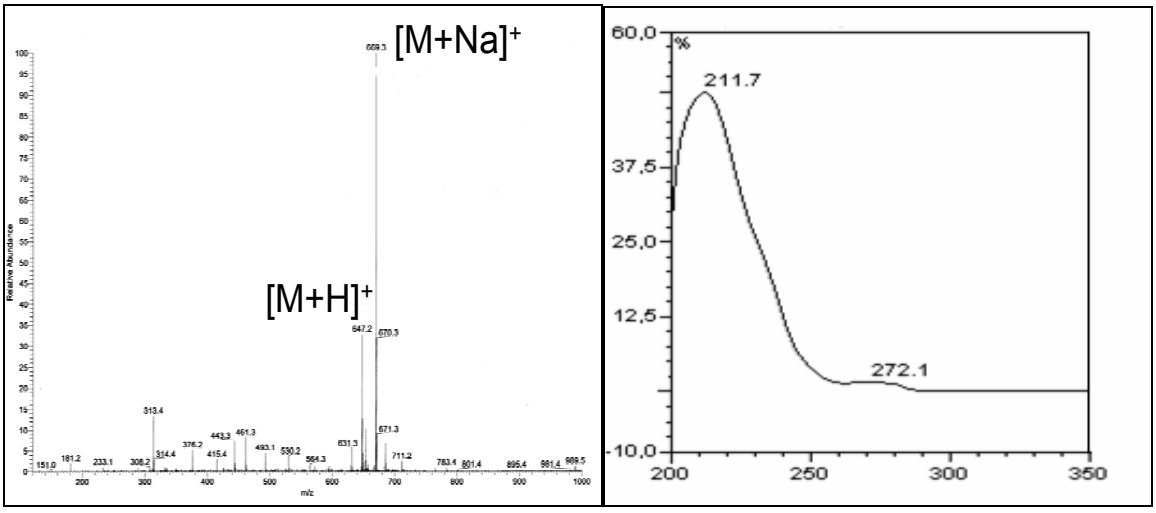

Fig. 3.24: ESI-MS and UV spectrum of compound 9

Compound **9** was obtained as a white amorphous residue from the leaves of *Aglaia abbriviata*, $[\alpha]^{20}_{D}$-50.5 (*c*, 0.45, $CHCl_3$); UV (MeOH) λ_{max} 211.7 nm, 272.1nm (see. 3.24). The EISMS positive mode showed the pseudomolecular ion peak at *m/z* 647.2

$[M+H]^+$, and at *m/z* 669.3 $[M+Na]^+$, respectively (see Fig. 3.24). The ^1H NMR spectrum showed three methoxy groups at δ 3.72 (OCH_3-6), 3.65 (OCH_3-8) and 3.58 (OCH_3-4′). In addition, three aromatic rings similar to those of Rocaglamide A (**1**) were observed, i.e. two *meta* coupled aromatic protons at δ 5.96 ppm (d, 1.9, H-9) and 6.05 ppm (d, 1.9, H-7). The characteristic AA′BB′ system of a *p*-disubstituted benzene ring at δ 6.50 ppm (H3′/H5′, d, 8.8) and 7.31 ppm (H2′/H6′, d, 8.8) and the signals of a monosubstituted benzene ring at δ 6.85 ppm (H3′′/H4′′/H5′′, m) and 7.05 ppm (H2′′/H6′′, m) were likewise detected. The spectrum further exhibited signals at δ 4.22 ppm (d, 9.5) and 4.34 ppm (d, 9.5) typical of H-2 and H-3 in rocaglamide congeners. However, H-10 resonated as a singlet at δ 4.48 ppm, this particular proton signal is indicative of the aglains which differentiate them from the rocaglamide family.

Furthermore, the signals of a 2-methylbutyric amide and a 2-aminopyrrolidine ring reminiscent of the one reported for odorinol were also observed (see Table 3.16), suggesting that part of the odorinol structure could be linked through an amide function to an acid moiety of the rocaglamide type instead of the NMe_2 group [Dumontet *et al.,* 1996]. The odorinol part of the structure was confirmed from its ^1H-^1H COSY spectrum (see Table 3.16 and Fig. 3.25), and was assigned accordingly: δ 0.80 (3H, t, *J*=7.5 Hz, H-21), 1.09 (3H, s), 2.10 (1H, m, H-14A), 1.90 (1H, m, H-14B), 1.85 (1H, m, H-15A), 1.71 (1H,m, H-15B), 3.41 (1H, m, H-16A), 3.19 (1H, m, H-16B). Furthermore, a signal at 6.76 ppm (dd, *J*=4.35 Hz, 11.95 Hz) was assigned to H-13, residing between the two nitrogen atoms of the pyrrimidine ring. Based on the ^1H NMR, ^1H-^1H COSY spectra (see Table 3.16, Fig. 3.25 and Fig. 3.26) compound **9** was identified as aglaxiflorin D, which was previously isolated from the leaves of *Aglaia laxiflora* collected in Taiwan [Xu *et al.,* 2000].

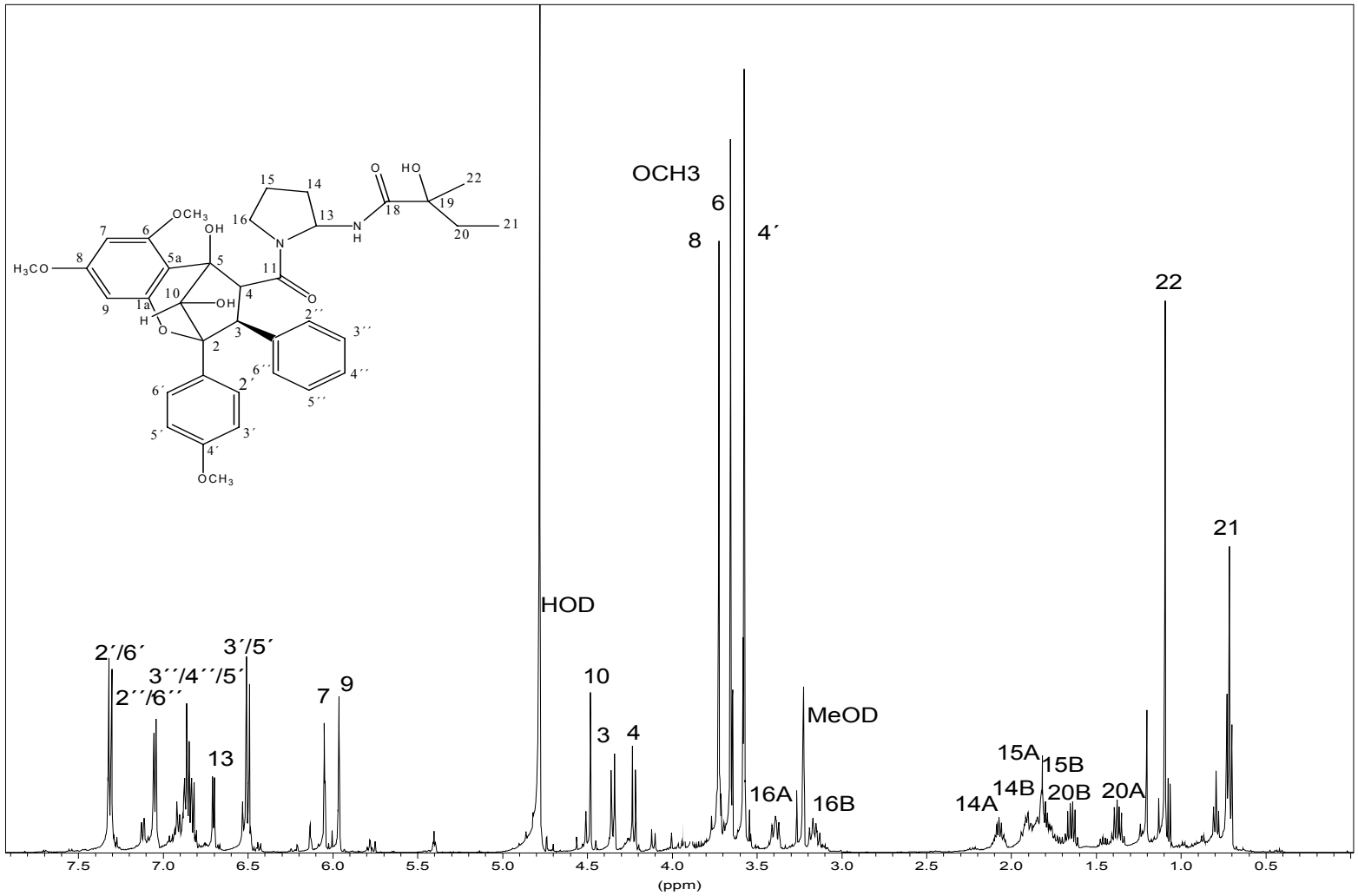

Fig.3.25: ^{1}H NMR of compound 9 in MeOD

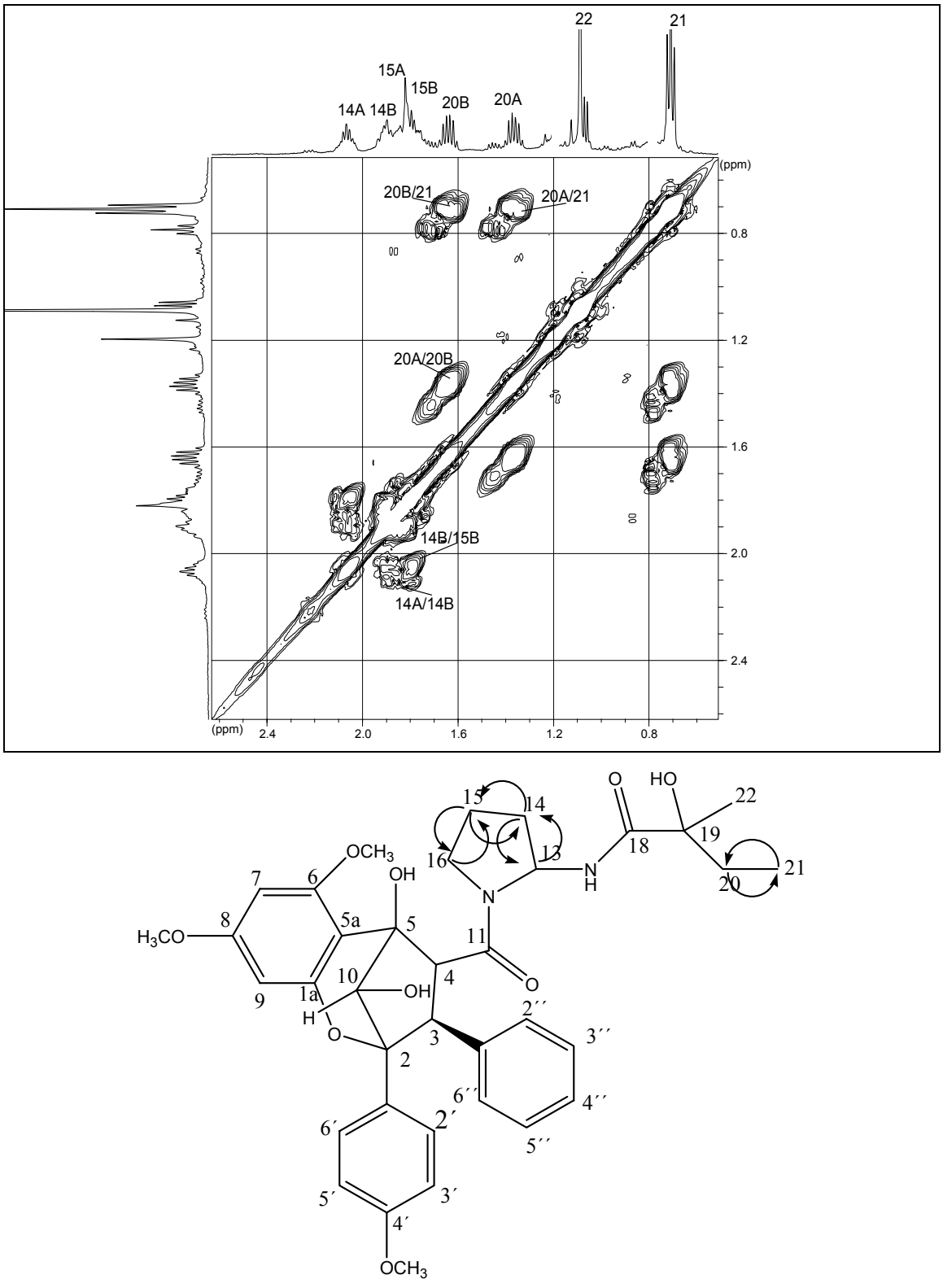

Fig.3.26: ^{1}H-^{1}H COSY correlations of 9 in MeOD (upfield region)

Table 3.16: ^{1}H NMR and ^{1}H-^{1}H COSY of compound 9 (in MeOD)

^{1}H-NMR	**Compound 9**	**[a]Literature**	**COSY**
3	4.34(d, 9.5Hz)	4.56 (d, 9.0)	4
4	4.22 (d, 9.5Hz)	4.04 (d, 9.0)	3
7	6.05(d, 1.9Hz)	6.08 (d, 0.8)	
9	5.96(d,1.9Hz)	6.05 (d, 0.8)	
2′	7.31(d, 8.8Hz)	7.38 (d, 8.4)	3′
3′	6.50(d, 8.8Hz)	6.65 (d, 8.4)	2′
5′	6.50(d, 8.8Hz)	6.65 (d, 8.4)	6′
6′	7.31(d, 8.8Hz)	7.38 (d, 8.4)	5′
2′′	7.05(m)	7.19 (m)	3′′
3′′	6.85(m)	7.00 (m)	2′′,4′′
4′′	6.85(m)	7.00 (m)	3′′,5′′
5′′	6.84(m)	7.00 (m)	4′′,6′′
6′′	7.05(m)	7.19 (m)	5′′
OMe-6	3.72(s)	3.78 (s)	
OMe-8	3.65(s)	3.71 (s)	
OMe-4′	3.58(s)	3.69 (s)	
10	4.48 (s)	4.83 (s)	
13	6.76(m)	6.38 (m)	14
14	B: 1.90 (m) A: 2.10 (m)	B: 1.96 (m) A: 2.05 (m)	13,15
15	B: 1.71 (m) A: 1.85 (m)	B: 1.74 (m) A: 1.91 (m)	14
16	B: 3.19 (m) A: 3.41(m)	B: 3.20 (m) A: 3.61 (m)	
19			
20	A: 1.38(m) B: 1.65(m)	B: 1.42 (m) A: 1.62 (m)	21
21	0.80 (t, 7.5)	0.74 (t, 7.3)	20
22	1.09(s)	1.24 (s)	

[a]Literature:[Xu *et al*., 2000] (measured in MeOD)

III.2.3. Lignan compounds isolated from *Aglaia* sp.

III.2.3.1. (+)-Pinoresinol (10, known compound)

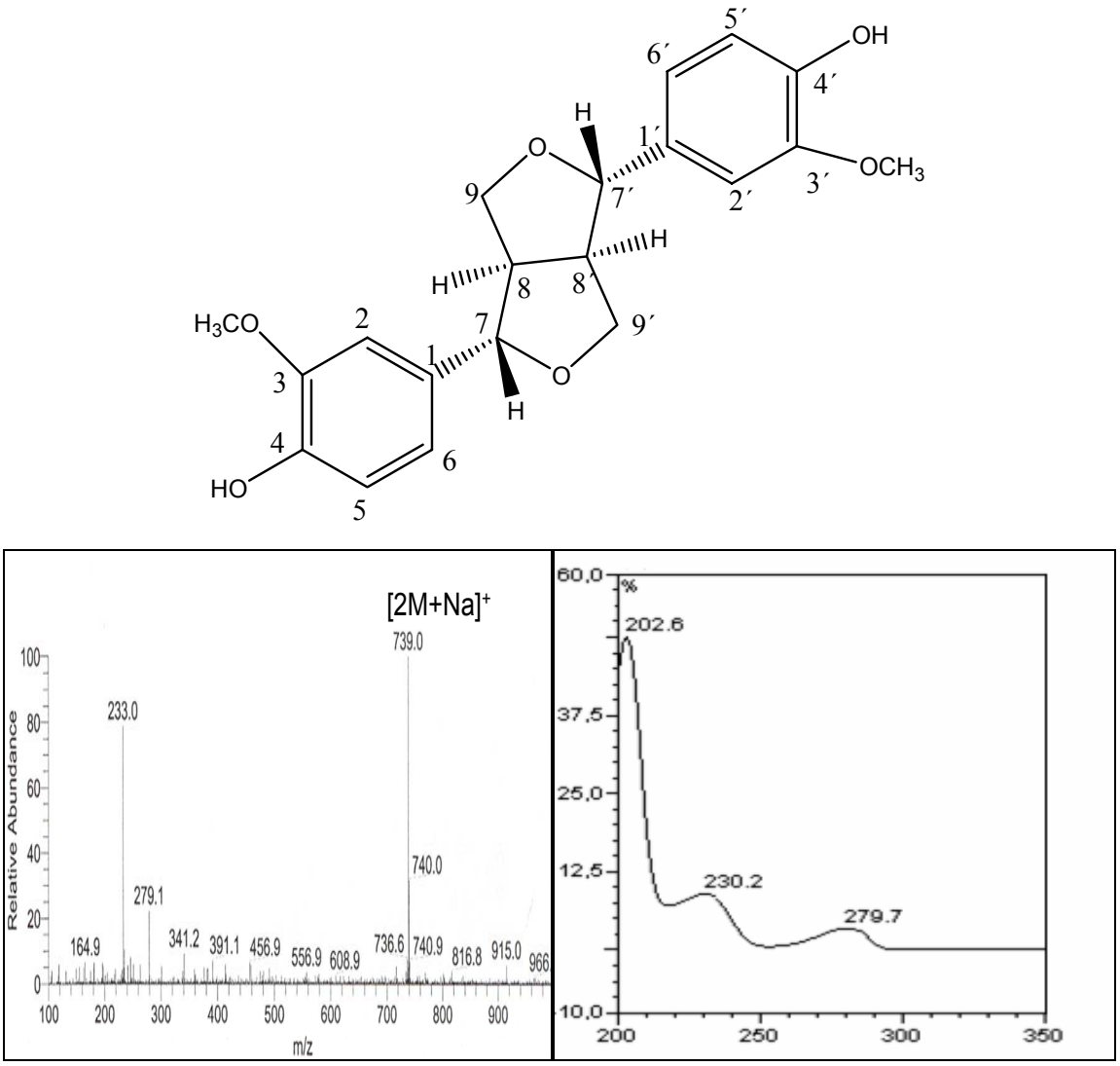

Fig. 3.27: ESI-MS and UV spectrum of compound 10

Compound **10** was obtained as a brown viscous oil from the leaves of *Aglaia oligophylla*, $[\alpha]^{20}_{D}$+95 (*c*, 0.45, acetone); UV (MeOH) λ_{max} 202.0, 230.2, and 279.7 nm (see Fig. 3.27). The positive mode ESI-MS showed a pseudomolecular ion peak at *m/z* 739 $[2M+Na]^+$(see Fig. 3.27) which was compatible with the NMR data. The ^{1}H NMR spectrum (see Fig. 3.28) of compound **10** revealed a symmestric structure which indicated the presence of two overlapping aromatic methoxy groups at δ 3.90 ppm; two sets of six equivalent aromatic

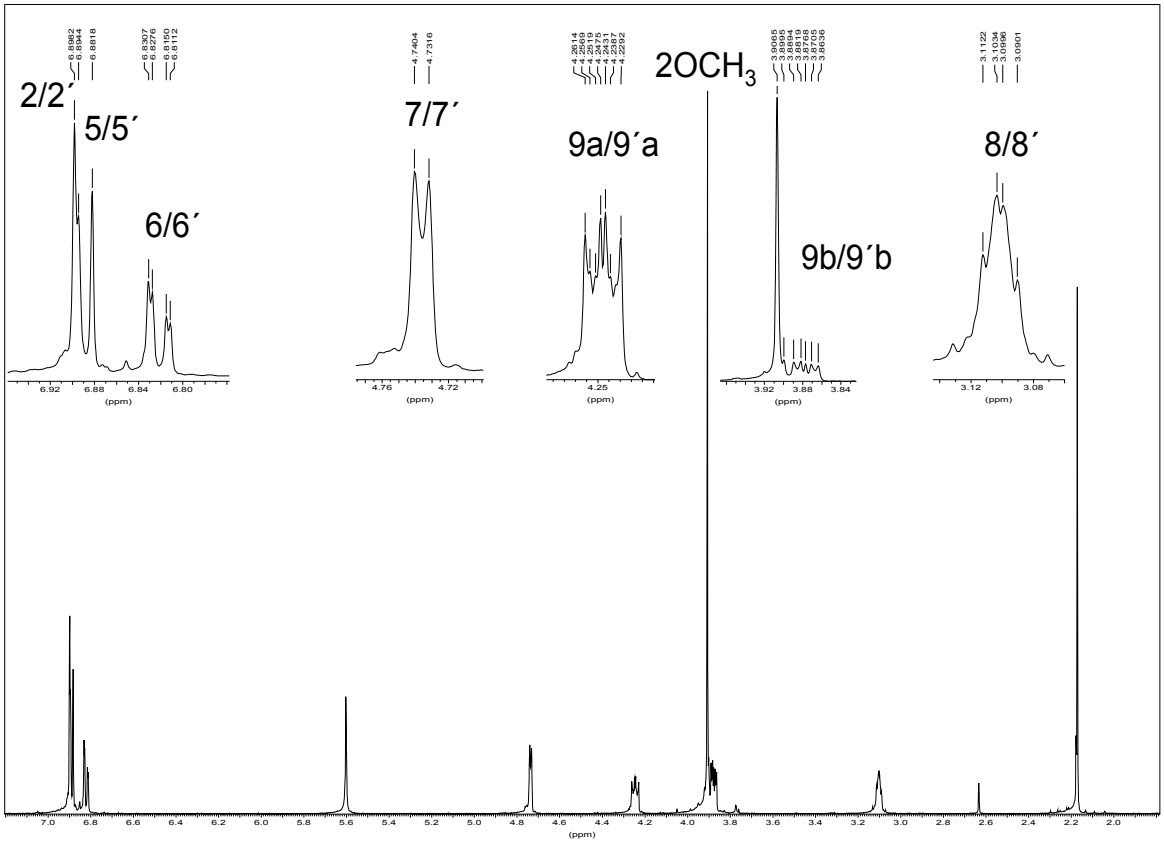

Fig. 3.28: ^{1}H NMR spectrum of compound 10 in $CDCl_3$

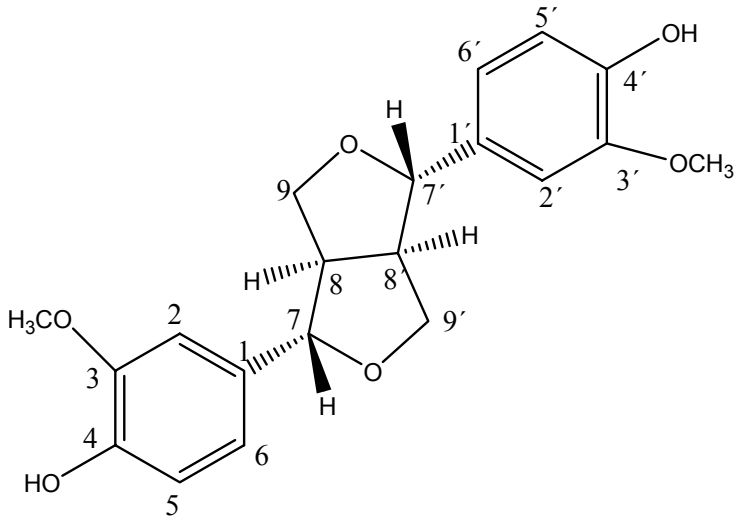

Pinoresinol

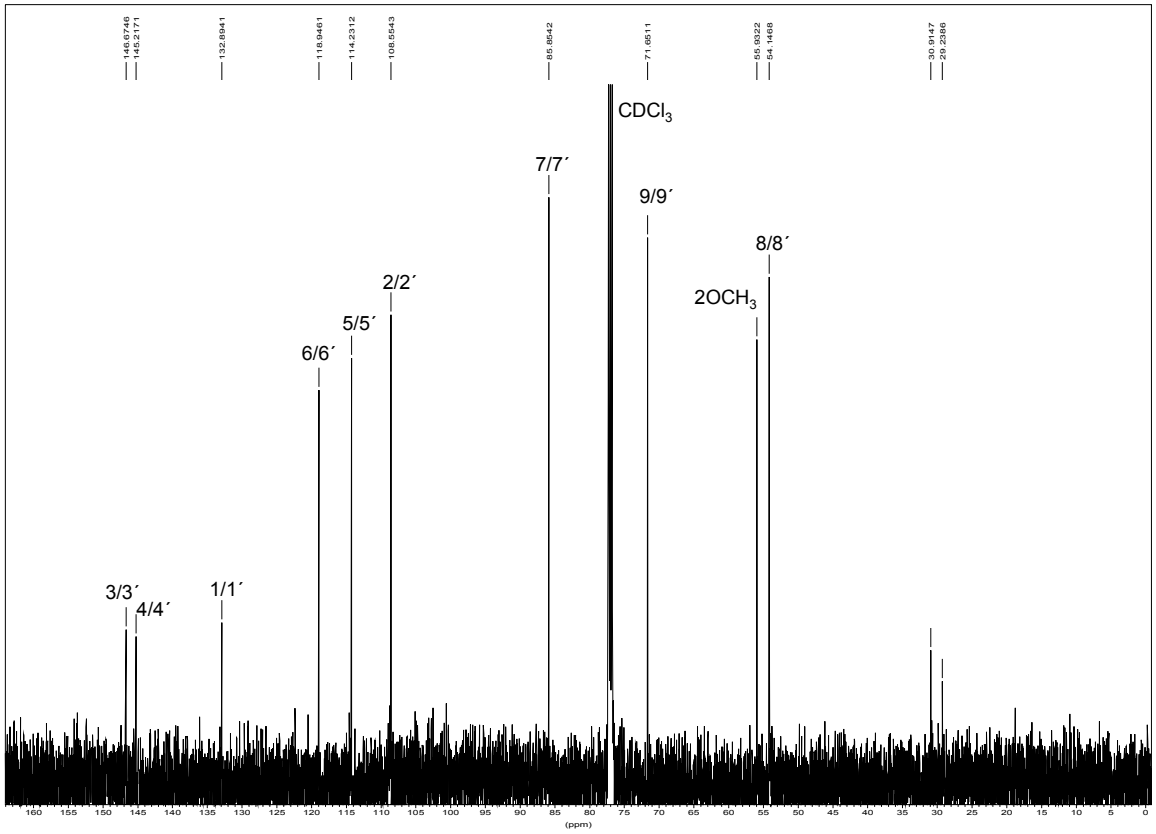

Fig. 3.29: ^{13}C NMR spectrum of compound 10 in $CDCl_3$

protons belonging to an ABC spin system H-2/2′, H-5/5′′′and H-6/6′ at δ 6.89 (d,*J*=1.9Hz), 6.89 (dd, *J*=8.2, 1.9 Hz), and 6.82 (d, *J*=8.2 Hz), respectively. The other eight protons were observed at δ 3.10-4.74 ppm which revealed an epi-diepoxy (bis-tetrahydrofuran ring) system of 7,7′-diaryl-7,9′:7′,9-diepoxy-lignan skeleton [Casabuono and Pomilio, 1994 and Wang *et al.,* 1997]. In addition, two benzylic methine protons for H-7 and H-7′ were observed at δ 4.69 (d, *J*=4.4 Hz), indicating the same *equatorial*-(α)-configuration of the two aryl substituents at C-7 and C-7′ [Roy *et al.,* 2002]. H_2-9 and H_2-9′ were observed at δ 4.19 (dd, *J*=9.5Hz, 7.3 Hz). H-8 and H-8′ were also equivalent and were observed as overlapping signals at 3.10 ppm (see Table 3.17 and Fig. 3.28). Moreover, a broad singlet of overlapping signals of two hydroxyl groups was also observed at δ 5.6 ppm.

Table 3. 17: ^{13}C NMR data of compound 10 in $CDCl_3$ (500 MHz)

C position	Compound 10	[1](+)-pinoresinol
1/1′	132.9	132.9
2/2′	108.5	108.5
3/3′	146.6	146.6
4/4′	145.2	145.2
5/5′	114.2	114.2
6/6′	118.9	118.9
7/7′	85.8	85.8
8/8′	54.1	54.1
9/9′	71.6	71.6
OCH_3-3/3′	55.9	55.9

[1]: [Schmidt, 1994]

The ^{1}H-^{1}H COSY spectrum showed symmetric correlations of eight protons in an epi-diepoxy spin system (see Fig. 3.30). The HMBC spectrum (see Fig. 3.31) revealed the correlations of the hydroxyl group (O*H*-4/4′) at δ 5.60 to C-3/3′ (144.67 ppm), C-4/4′ (145.21 ppm), and C-5/5′ (114.23 ppm), respectively. Two equivalent methoxy groups, OC*H*$_3$-3/3′ resonated at δ 3.90, which exhibited direct correlations with C-3/3′ at δ 144.67. Thus, the chemical shifts of C-3/C-3′ and C-4/C-4′ were distinguished through the HMBC long-range correlations of O*H* with C-3/3′, C-4/C-4′, and C-5/C-5′. Moreover, benzylic protons H-7/7′ correlated with C-1/1′, C-2/2′, and C-8/8′ and confirmed the attachment of the benzyl ring on the furan system. In comparison with the literature data [Fonseca *et al*., 1979; Casabuono *et al.,* 1994; and Schmidt, 1994] and based on the 1D and 2D NMR spectra, as well as $[\alpha]^{20}_D$ value, compound **10** was identical to the symmetrical furofuran-lignan, (+)-pinoresinol.

Table 3.18: ^{1}H NMR data of compound 10, 11, and 12 in $CDCl_3$

Position	Compound 10	Compound 11	Compound 12
2	6.90(d, 1.9)	6.90 (d, 1.9)	6.91 (d, 1.9)
2′	6.90(d, 1.9)	6.90 (d, 1.9)	6.91 (d, 1.9)
5	6.89(d, 8.2)	6.89 (dd, 8.2, 1.9)	6.84 (d, 8.2)
5′	6.89(d, 8.2)	6.89 (dd, 8.2, 1.9)	6.84 (d, 8.2)
6	6.82 (dd, 8.2, 1.9)	6.84 (dd, 8.2, 1.9)	6.88 (dd, 8.2, 1.9)
6′	6.82 (dd, 8.2, 1.9)	6.84 (dd, 8.2, 1.9)	6.88 (dd, 8.2, 1.9)
7	4.74 (d, 4.4)	4.76(d, 7.5)	4.75 (d, 4.4)
7′	4.74 (d, 4.4)	4.74(d, 7.5)	4.75 (d, 4.4)
8	3.10 br dd	3.11 br dd	3.11 br dd
8′	3.10 br dd	3.11 br dd	3.11 br dd
9eq	3.87 m	3.89 m	3.89 m
9ax	4.25 (d, 6.95)	4.26 (d, 6.95)	4.26 (d, 6.95)
9′eq	3.87 m	3.89 m	3.89 m
9′ax	4.23 (d, 6.95)	4.23 (d, 6.95)	4.24 (d, 6.95)
OH-4 OH-4′	5.60 5.60	5.60	
OMe-3 OMe-3′ OMe-4 OMe-4′	3.90 3.90	3.91 3.90 3.87	3.89 3.89 3.87 3.87

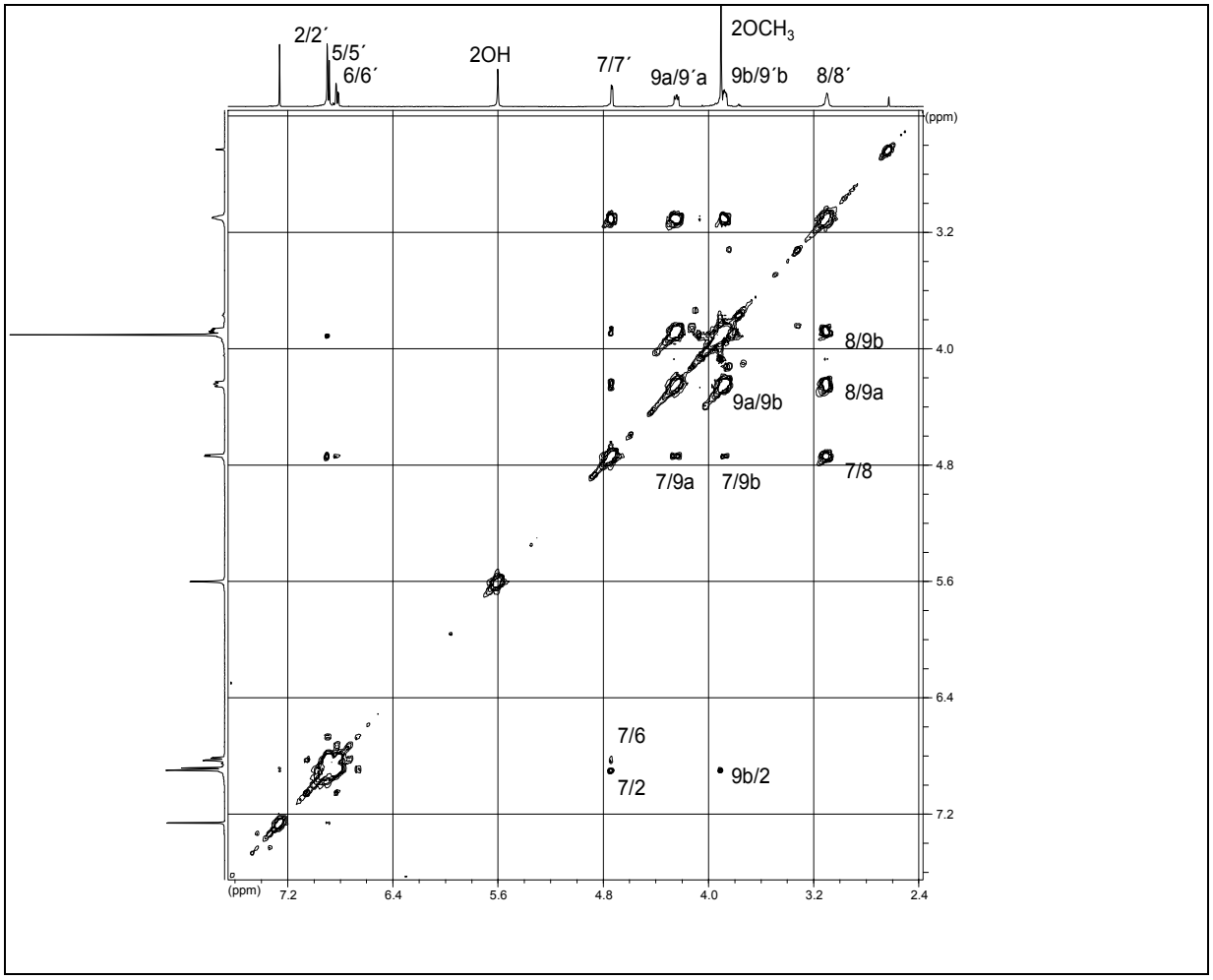

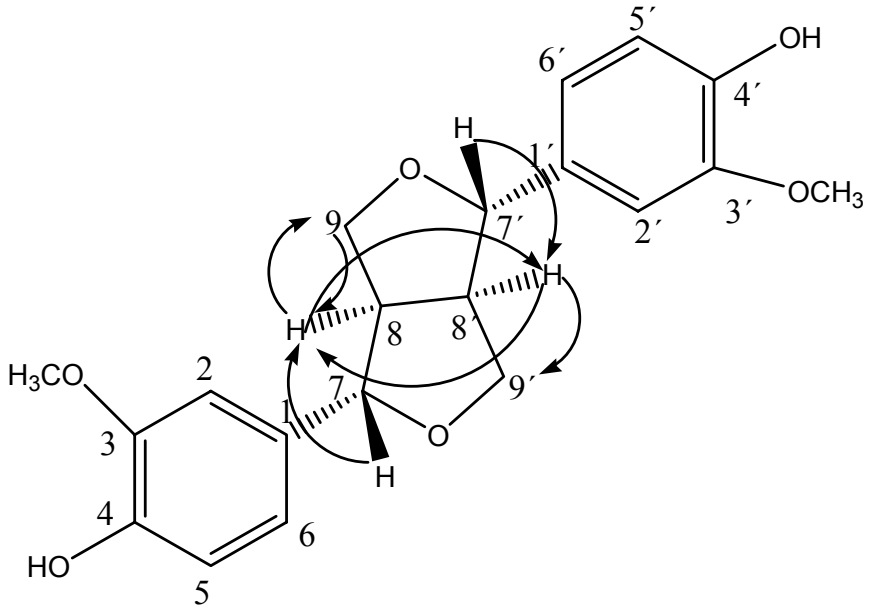

Fig. 3.30: ^{1}H-^{1}H COSY correlations of compound 10 in $CDCl_3$ (500 MHz)

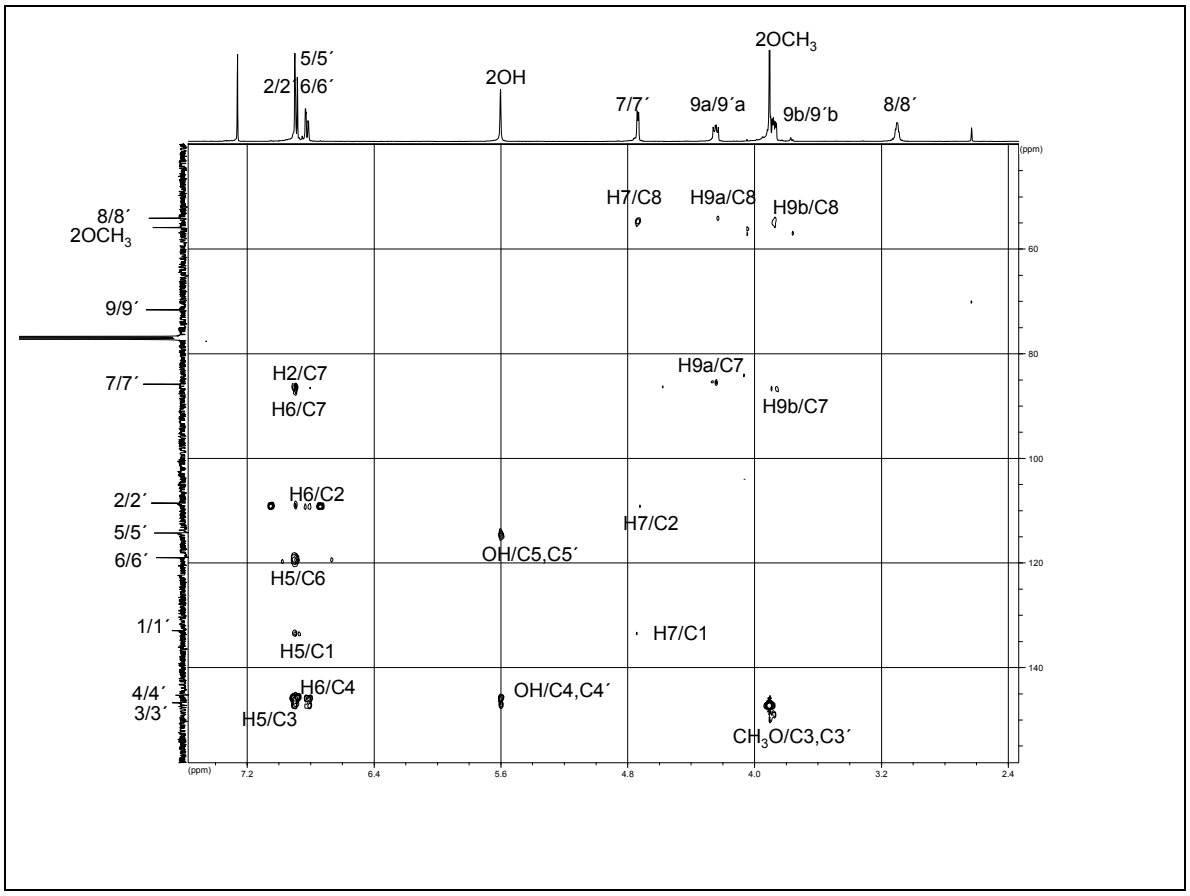

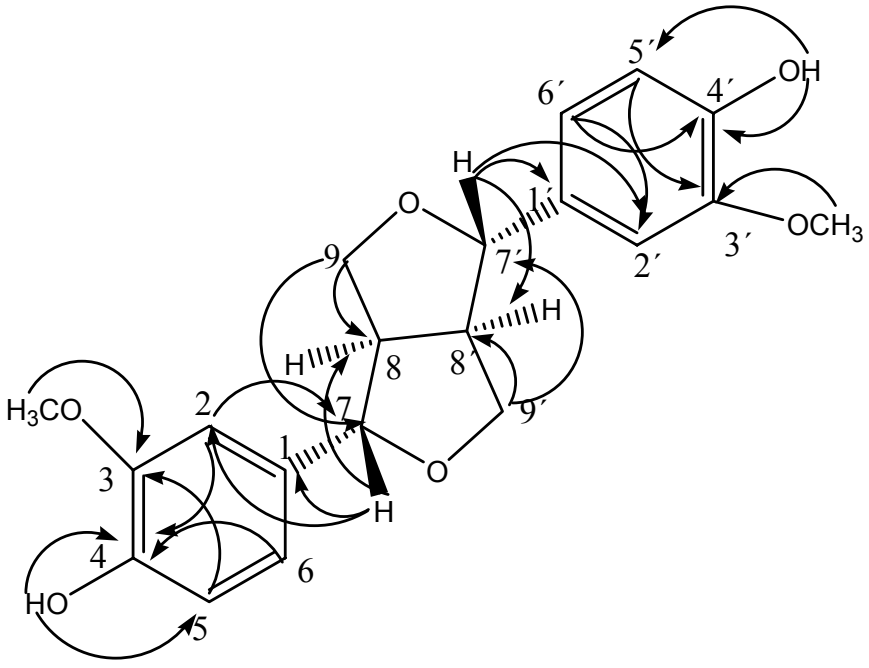

Fig. 3. 31: HMBC correlations of compound 10 in $CDCl_3$

III.2.3.2. (-)-4′-O-methyl-pinoresinol (11, known compound)

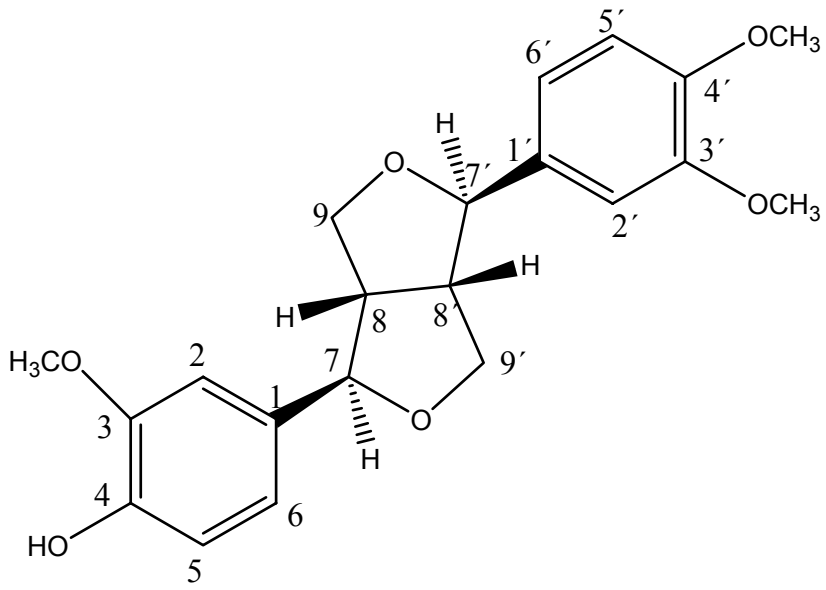

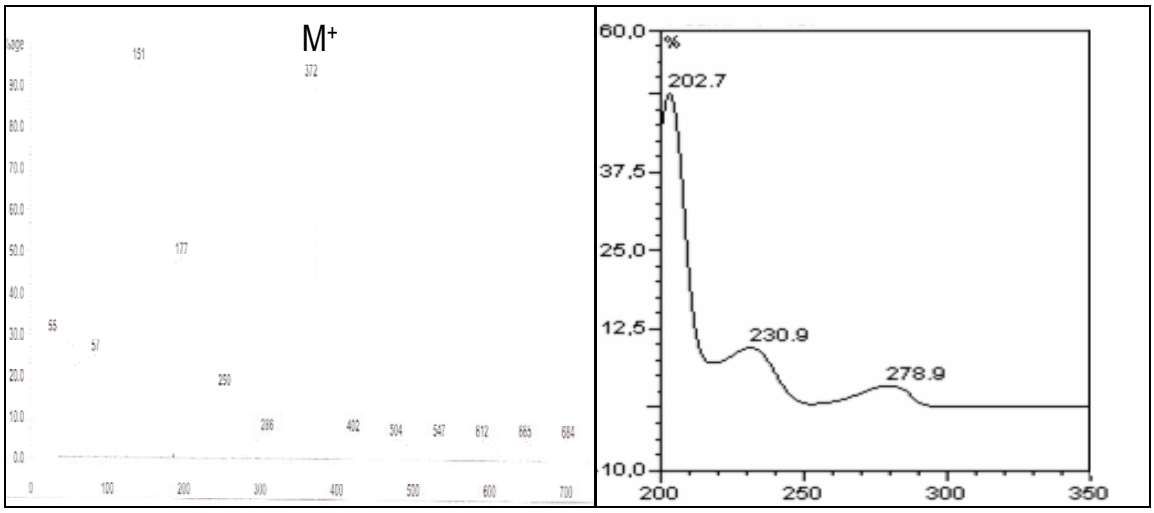

Fig. 3.32: EI-MS and UV spectrum of compound 11

Compound **11** was obtained as a white residue from the leaves of *Aglaia oligophylla*; $[\alpha]^{20}_{D}$ was -116 (*c*, 0.47, acetone); UV (MeOH) λ_{max} 202.7, 230.9, and 278.0 nm (see Fig. 3.2). The EI-MS showed a molecular ion peak at *m/z* 372 M^+(see Fig. 3.2). The ^{1}H NMR spectrum of compound **11** showed similar signals to that of compound **10**. However, the

spectrum of **11** revealed an additional methoxy group, which resonated separately at δ 3.87. Thus, an additional methoxy could be attributed for the methylation of the OH function either at C-4′ or C-4, which explained the 14 mass units difference in molecular weight with that of compound **10**. This methylation changed the symmetrical structure of compound **10** to an asymmetrical form as in compound **11**. Investigation to the ^{1}H NMR spectrum (see Fig. 3.33) of compound **11** displayed three pairs of six aromatic protons, which are not chemically equivalent as observed in compound **10**. Therefore, two benzylic methine protons of H-7 and H-7′ resonated separately as two doublets at δ 4.76 and 4.74 with a coupling constant of 4.4 Hz, indicating the same *equatorial*-(α)-configuration of the two aryl substituents at C-7 and C-7′ [Roy *et al.,* 2002]. The ^{1}H-^{1}H COSY spectrum showed correlations of eight protons in an epi-diepoxy spin system (see Fig. 3.35). The HMBC (see Fig. 3.36) spectrum showed ^{2}J correlation of the hydroxyl group O*H*-4 to C-4 at δ 145.95 which could consequently establish the assigment of C-4 and differentiated it from C-3, C-3′, and C-4′. Carbon C-5 was also distinguished from C-5′ through the HMBC correlation of O*H* group to C-5 at 114.20 ppm. However, in the HMBC spectrum of compound **11**, three methoxy resonances occurred at δ 3.91, 3.90, and 3.87 showed correlations with carbons at δ 146.63 (C-4′), 148.95 (C-3), and 148.42 (C-3′). In comparison with the literature data [Fonseca *et al.,* 1979; Roy *et al.,* 2002 and Rahman *et al.,* 1990] and based on the ^{1}H and ^{13}C NMR data, compound **11** was determined as (-)-4′-O-methyl-pinoresinol.

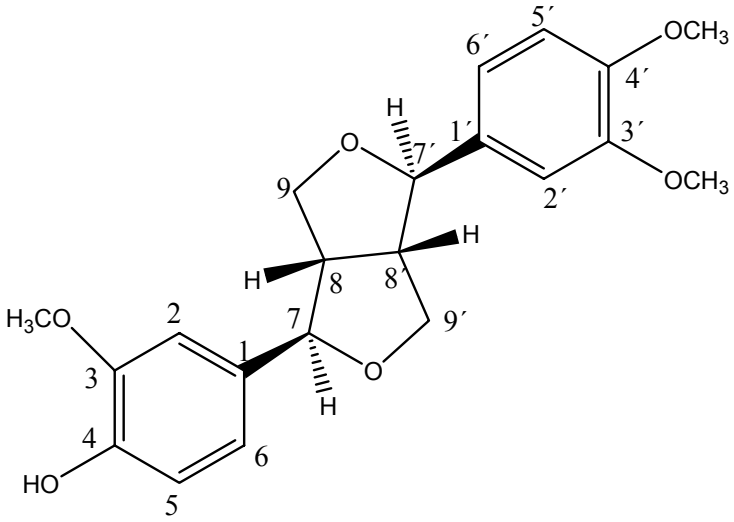

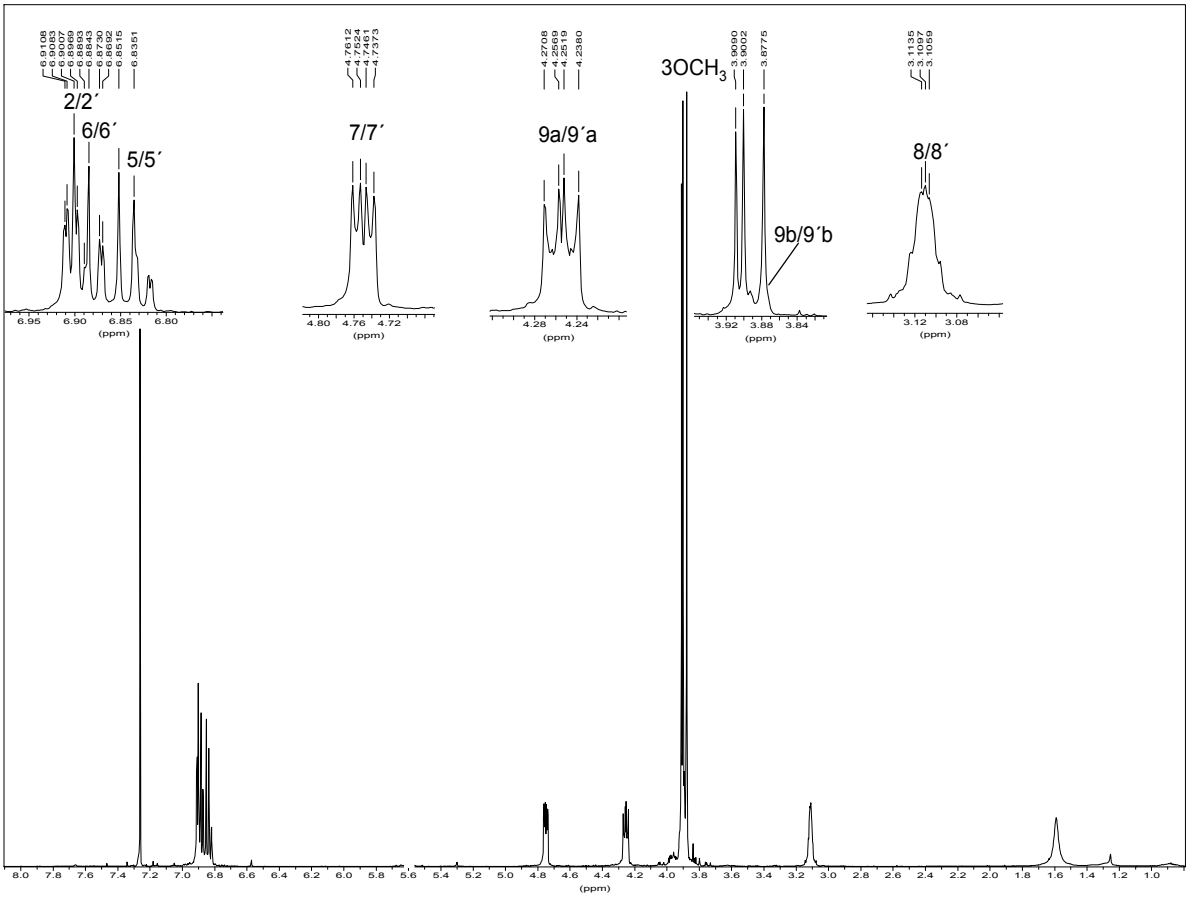

Fig. 3.33: ^{1}H NMR spectrum of compound 11 in $CDCl_3$

Table 3.19: ^{13}C NMR data of compound 11 and the literature in $CDCl_3$

C position	Compound 11	(+)-4´-Methoxy-pinoresinol* Eudesmin form	(-)-phillygenin** Epi-eudesmin form
1	133.4	133.3	132.2
1´	133.4	132.6	131.1
2	108.5	109.0	110.2
2´	109.7	108.4	109.4
3	148.9	148.9	147.4
3´	148.4	148.4	148.4
4	145.9	145.0	145.9
4´	146.6	146.5	147.5
5	110.9	110.8	115.0
5´	114.2	114.1	111.5
6	118.2	118.0	118.5
6´	118.9	118.7	117.4
7	85.8	85.6	86.8
7´	85.7	85.6	81.1
8	54.1	54.0	53.8
8´	54.1	54.0	49.2
9	71.7	71.5	70.2
9´	71.6	71.5	68.7
OCH_3-3	55.9	55.8	55.4
OCH_3-3´	55.9	55.8	55.4
OCH_3-4´	55.9	55.8	55.5

*: [Fonseca *et al.,* 1979], **: [Rahman *et al.,* 1990]

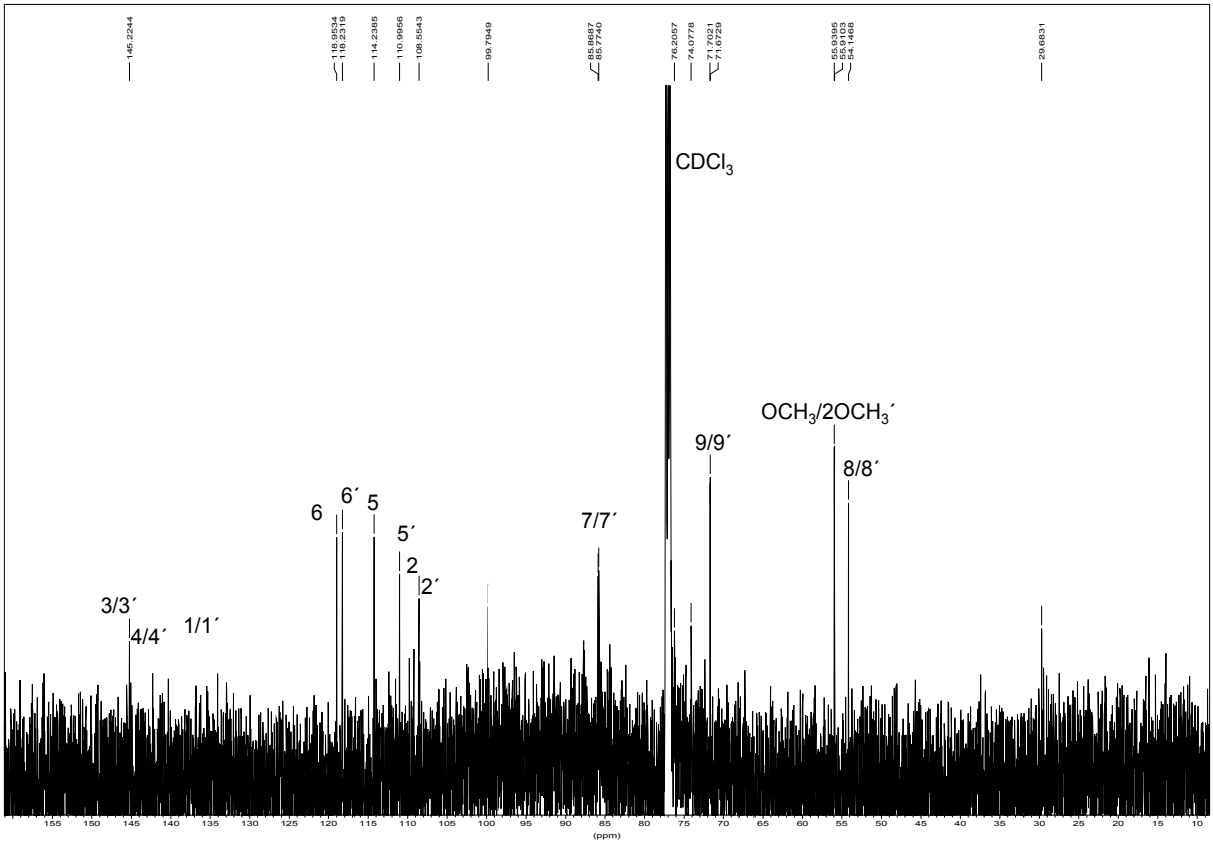

Fig. 3.34: ^{13}C NMR spectrum of compound 11 in $CDCl_3$

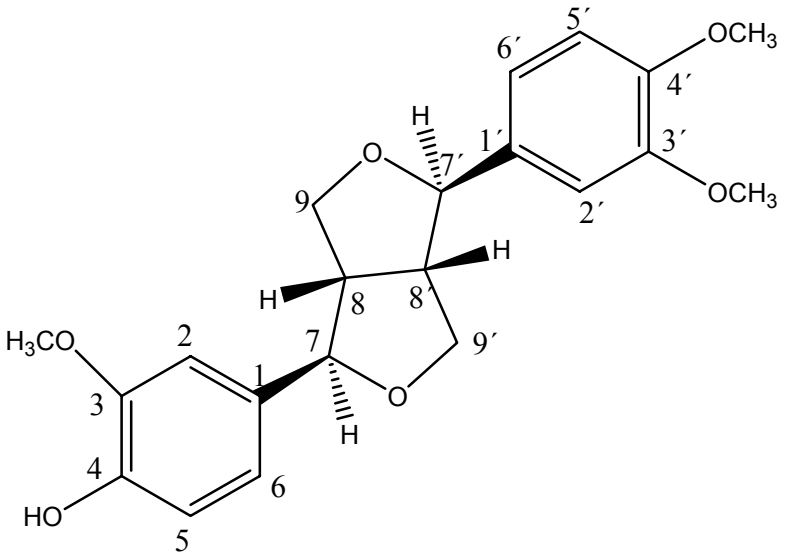

Table 3.20: Comparison ^{13}C NMR data of compound 11 to 10 and 12 in $CDCl_3$

C position	Compound 11	Compound 10	Compound 12
1	133.4	132.8	133.5
1′	133.4	132.8	133.5
2	108.5	108.5	109.2
2′	109.7	108.5	109.2
3	**148.9 (OCH_3)**	**146.6 (OCH_3)**	**149.0 (OCH_3)**
3′	**148.4 (OCH_3)**	**146.6 (OCH_3)**	**149.0 (OCH_3)**
4	**145.9 (OH)**	**145.2 (OH)**	**148.5 (OCH_3)**
4′	**146.6 (OCH_3)**	**145.2 (OH)**	**148.5 (OCH_3)**
5	114.2	114.2	111.0
5′	110.9	114.2	111.0
6	118.2	118.9	118.2
6′	118.9	118.9	118.2

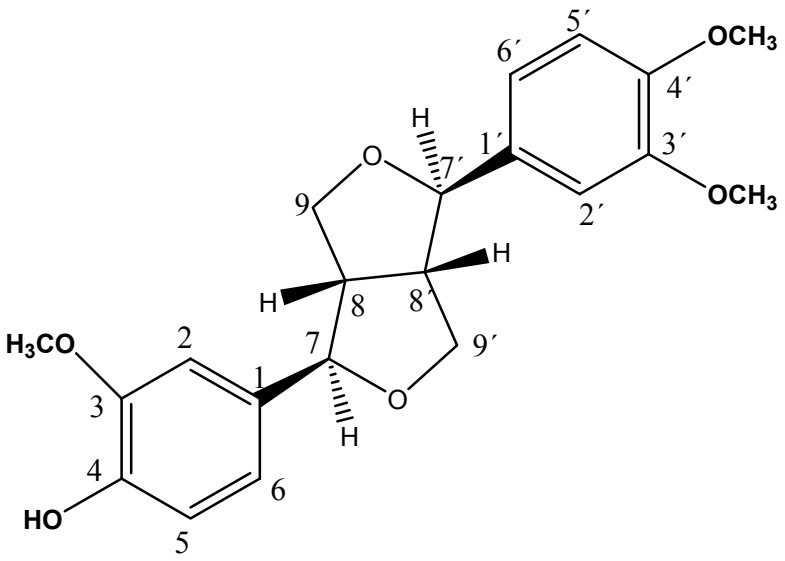

(-)-4′-O-methyl-pinoresinol

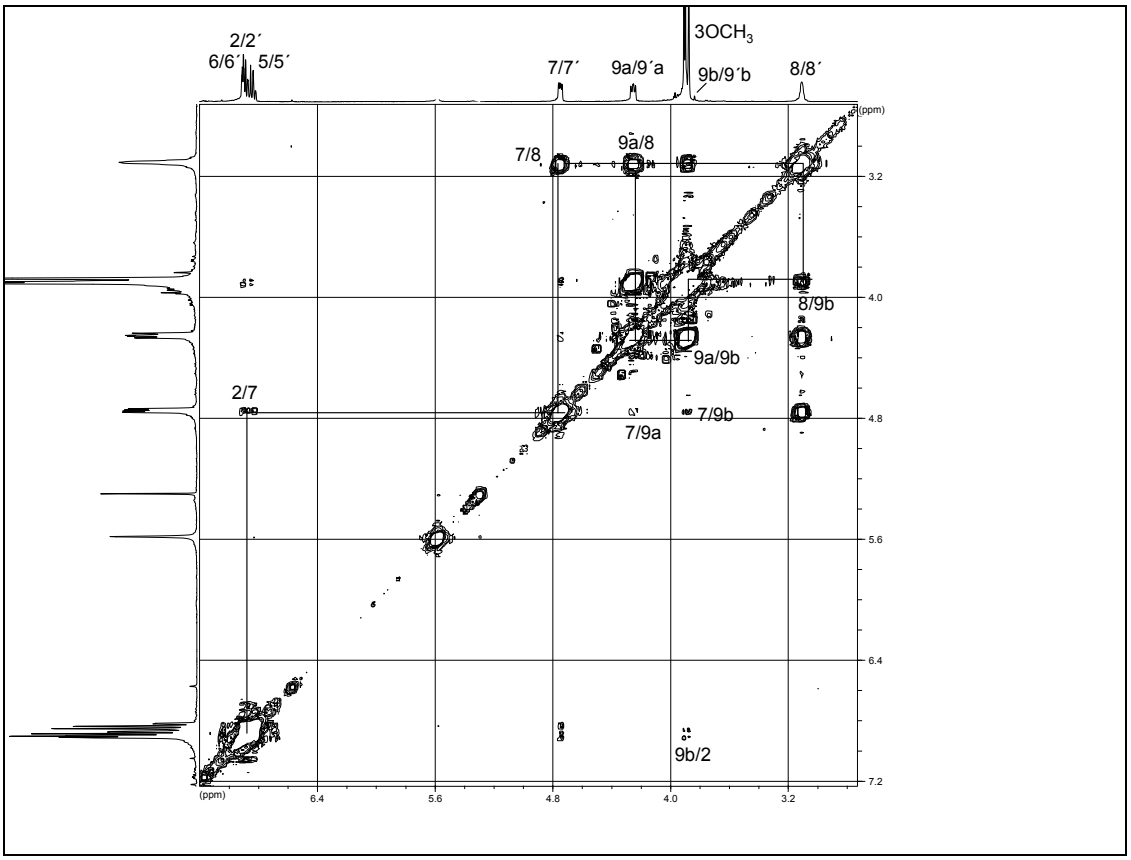

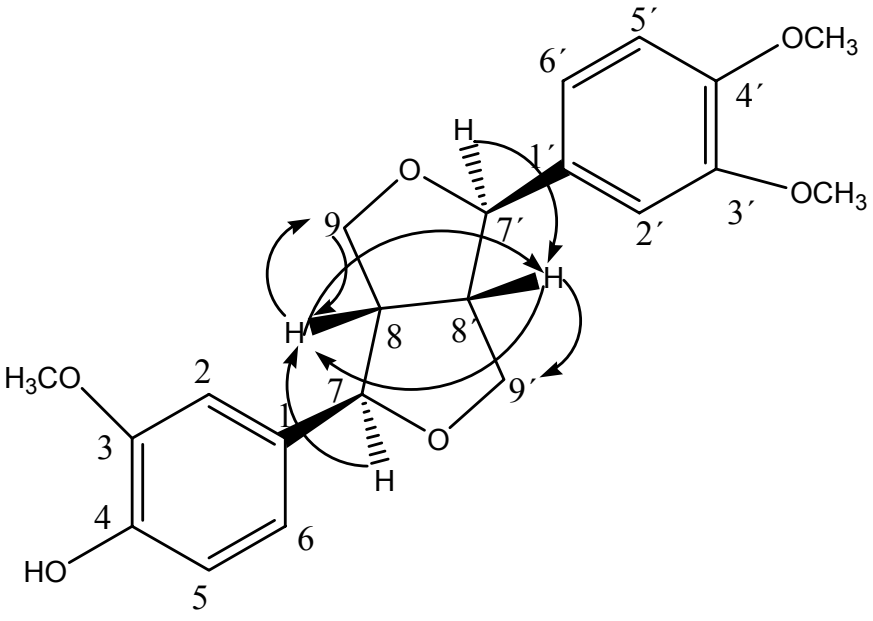

Fig. 3.35: ^{1}H-^{1}H COSY correlations of compound 11 in $CDCl_3$

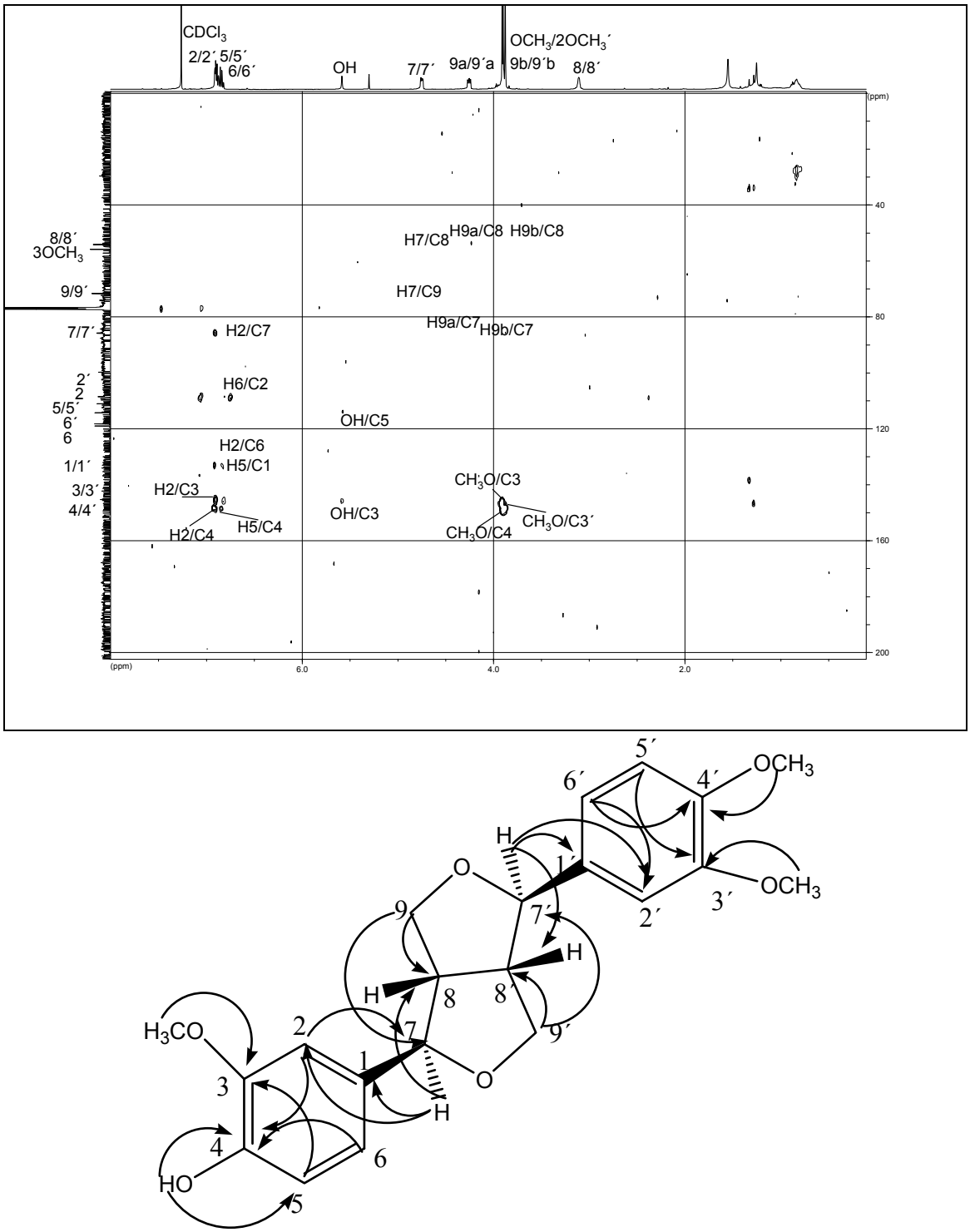

Fig. 3.36: HMBC correlations of compound 11 in $CDCl_3$

III.2.3.3. (-)Eudesmin (12, known compound)

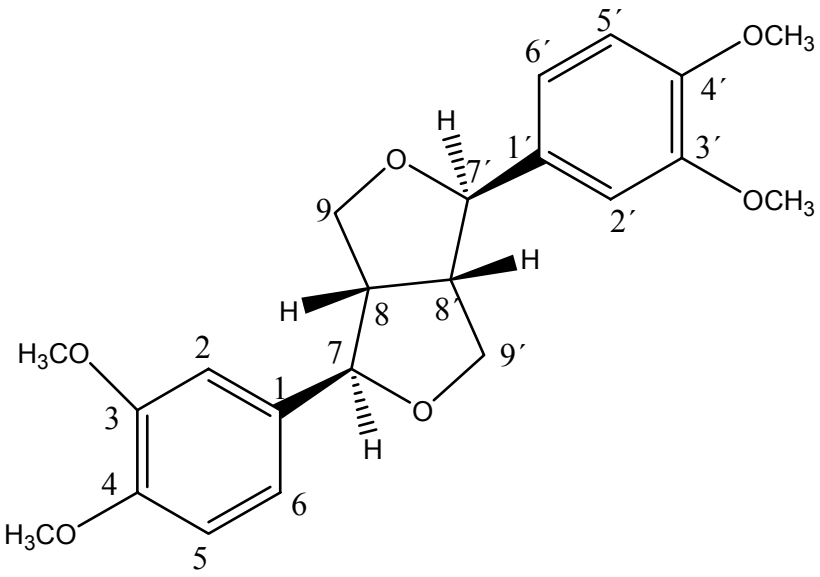

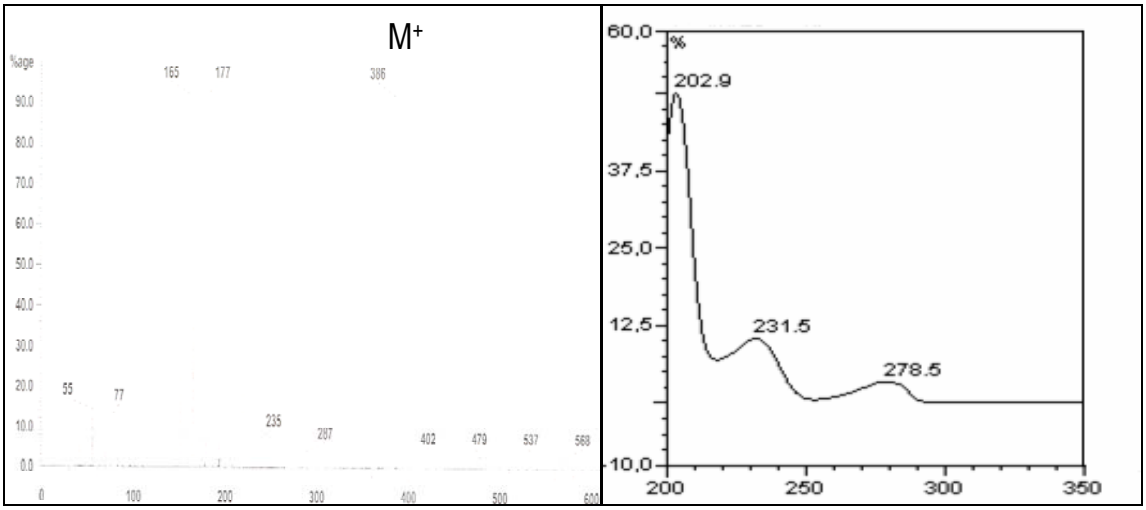

Fig. 3.37: EI-MS and UV spectrum of compound 12

Compound **12** was obtained as white crystalline needles from the leaves of *Aglaia oligophylla*, $^{20}[\alpha]_D$-64 (*c*=0.21, $CHCl_3$), UV(MeOH) λ_{max} 201, 226.3, and 281.2 nm (see Fig. 3.37). The EI-MS showed a molecular ion peak at *m/z* 386 $[M]^+$(see Fig. 3.37). The ^{1}H NMR spectrum (see Fig. 3.38) of compound **12** revealed a symmetrical structure as in

compound **10**. However, the ^{1}H NMR spectrum of compound **12** showed the presence of four methoxy groups, overlapping at δ 3.86 ppm and 3.95 ppm, indicating two pairs of methoxy units, OC*H*$_3$-3/3′ and OC*H*$_3$-4/4′. The molecular weight of compound **12** is 28 mass units larger than that of compound **10**, which could be attributed to the two additional methoxy substituents at C-4 and C-4′. Three pairs of six aromatic protons H-2/2′, H-5/5′ and H-6/6′ resonated at δ 6.84 (d, *J*=1.9 Hz), 6.77 ppm (d, *J*=8.2Hz), and at δ 6.82 (dd, *J*=8.2 Hz, 1.9 Hz), respectively. The two equivalent benzylic methine protons, H-7 and H-7′, resonated at δ 4.69 ppm (d, *J*=4.4 Hz) similarly as found in compound **10**, which indicated the same *equatorial*-(α)-configuration of the two aryl substituents at C-7 and C-7′ [Roy *et al.,* 2002] . Two methylene groups (H-9a, H-9b) and (H-9′a, H-9′b) resonated more upfield at δ 4.19 ppm (dd, *J*=9.5, 7.3 Hz). The ^{1}H-^{1}H COSY confirmed the correlations of eight protons in the epi-diepoxy spin system (see Fig. 3.40). Based on the ^{1}H NMR, ^{13}C NMR (see Fig. 3.39), ^{1}H-^{1}H COSY, HMQC and HMBC (see Fig. 3.41) spectra, compound **12** was identified as (-)-eudesmin [Suginome *et al*., 1995].

Table 3.21: ^{13}C NMR data of compound 12 in $CDCl_3$

C position	Compound 12	Literature[1] (-)-Eudesmin
1/1′	133.5	133.3
2/2′	109.1	109.0
3/3′	149.0	149.0
4/4′	148.5	148.2
5/5′	111.0	110.8
6/6′	118.2	118.2
7/7′	85.7	85.6
8/8′	54.1	54.0
9/9′	71.7	71.5
OCH_3-3/3′	55.9	55.7
OCH_3-4/4′	55.9	55.7

[1]: [Suginome *et al*., 1995]

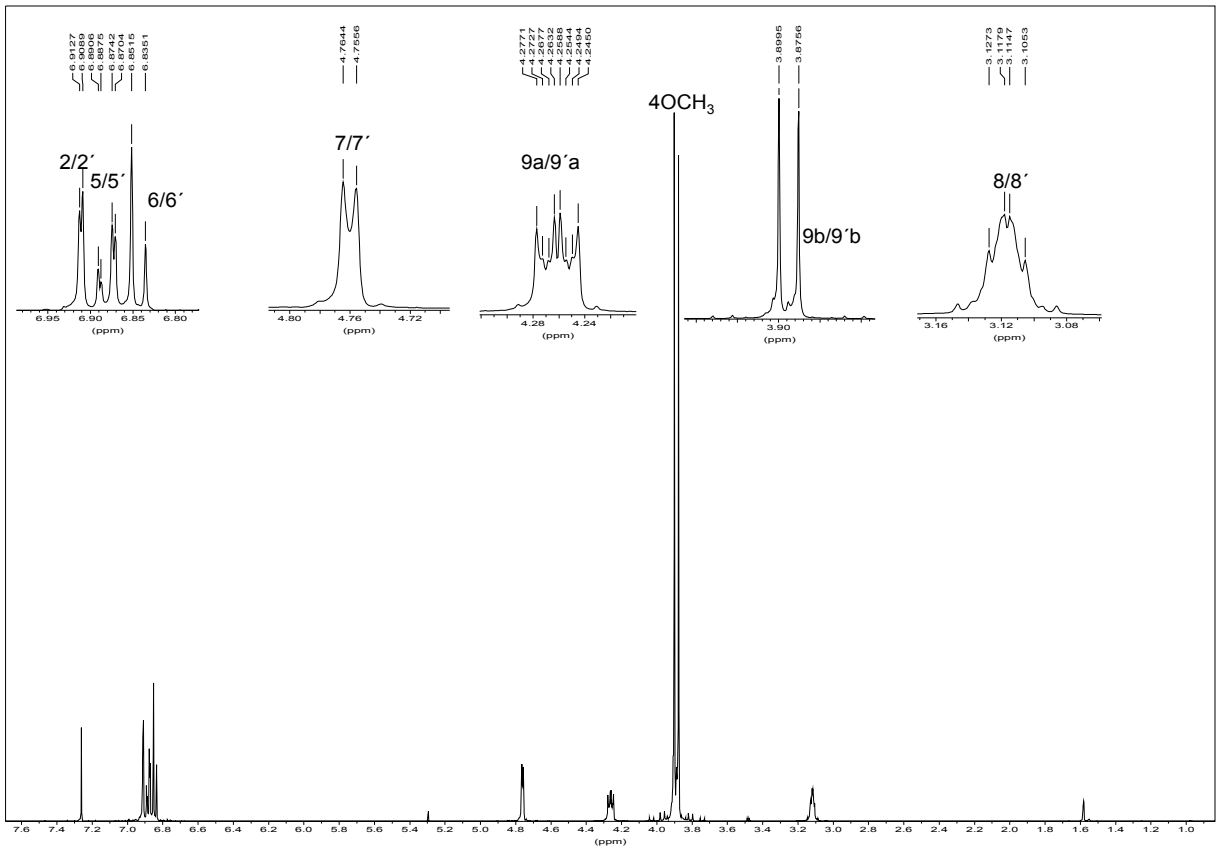

Fig. 3.38: ^{1}H NMR spectrum of 12 in $CDCl_3$

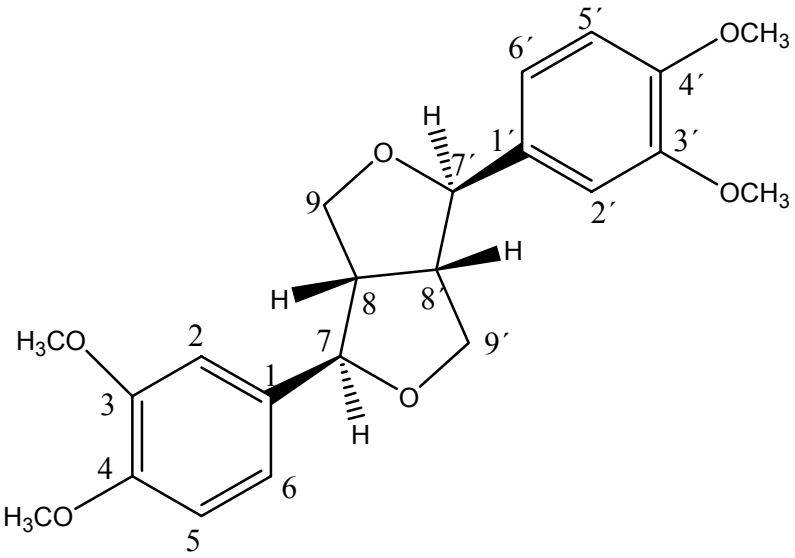

(-)-Eudesmin

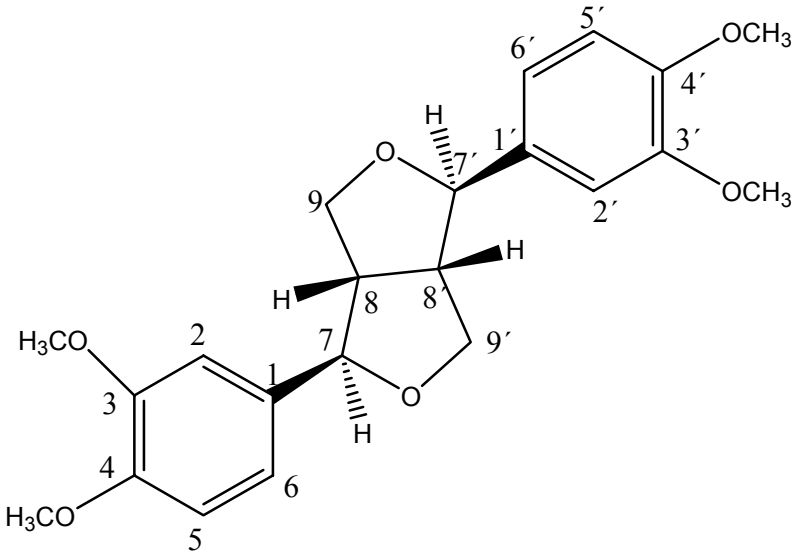

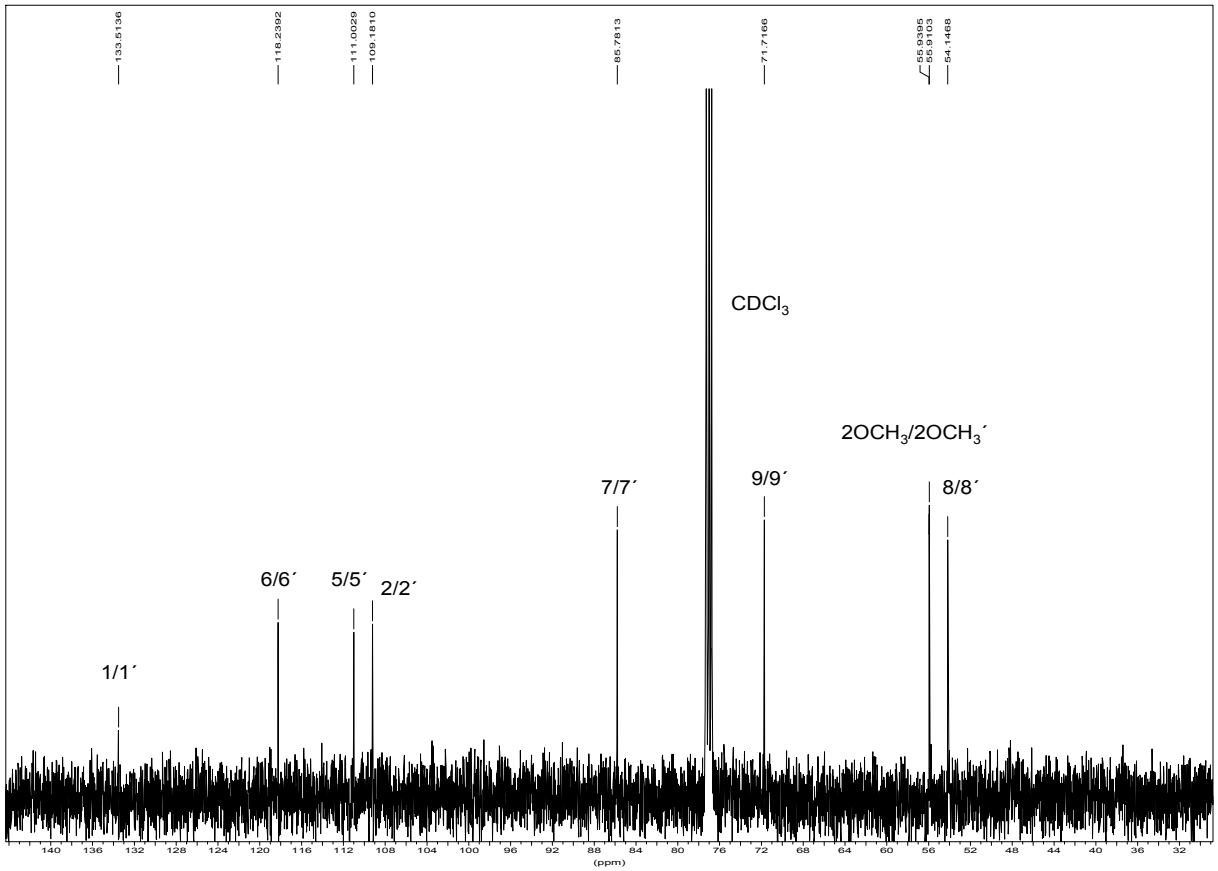

Fig. 3.39: ^{13}C NMR spectrum of 12 in $CDCl_3$

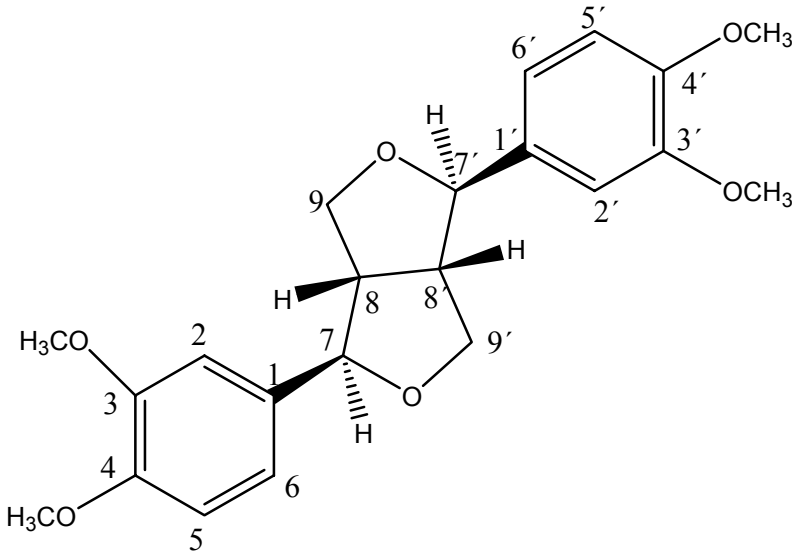

Table 3.22: Comparison of ^{1}H NMR data of eudesmin, dia-eudesmin and epi-pinoresinol

	H-7/7′	H-9a/9a′	H-9b/9b′
*Eudesmin	4.75	4.2-4.4	3.8-4.0
***dia*-Eudesmin	4.90	3.65-4.0	3.3-3.59
*Epi-pinoresinol	4.43-4.85	3.84	3.32-4.12
Compound **10**	4.74	4.24-4.25	3.87
Compound **11**	4.74-4.76	4.23-4.26	3.89
Compound **12**	4.75	4.24-4.26	3.89

Table 3.23: Comparison of ^{13}C NMR data of eudesmin, dia-eudesmin and epi-pinoresinol

	C-7/7′	C-8/′8′	C-9/9′
*Eudesmin	85.75	54.31	71.72
***dia*-Eudesmin	83.96	49.49	68.75
*Epi-pinoresinol	86.88-81.30	53.79-49.29	70.20-68.74
Compound **10**	85.85	54.14	71.65
Compound **11**	85.77-85.86	54.14	71.67-71.70
Compound **12**	85.781	54.146	71.716

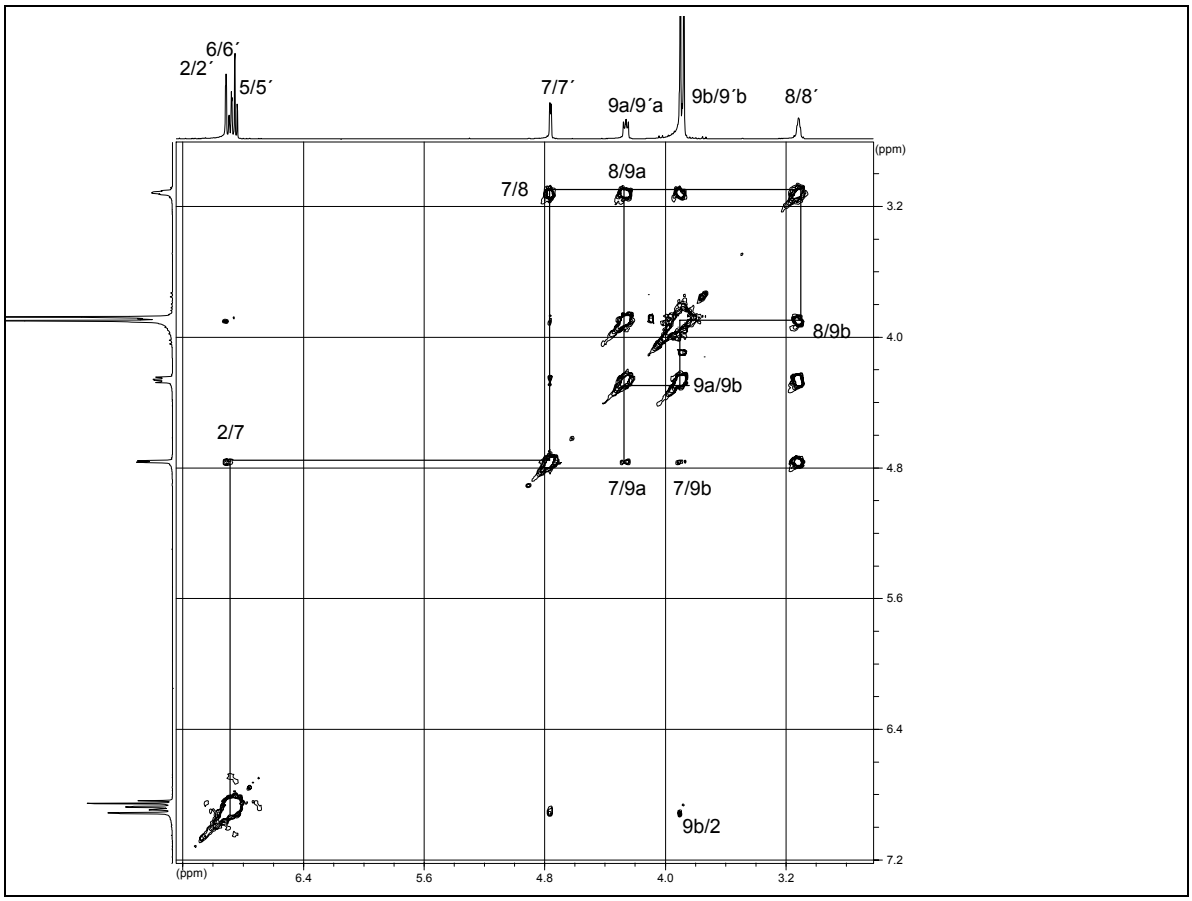

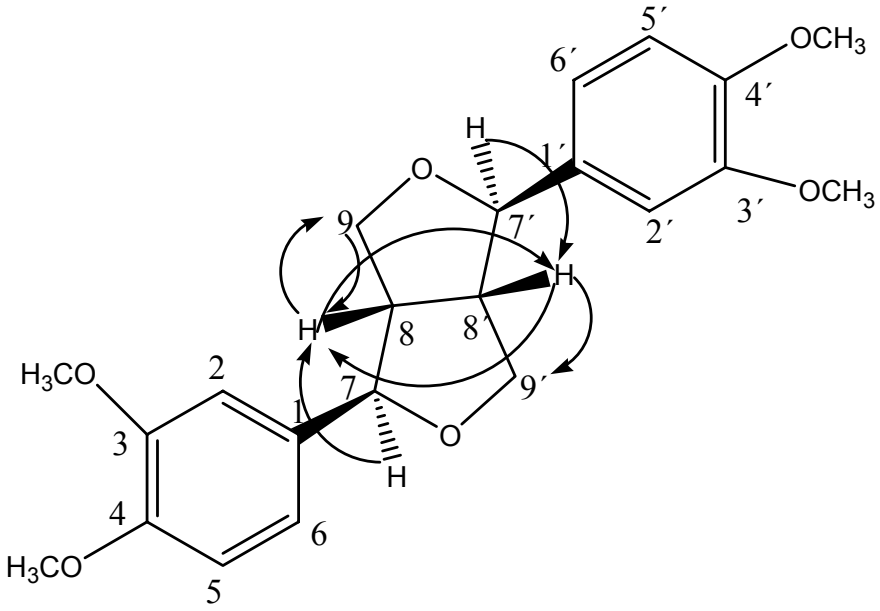

Fig. 3.40: ^{1}H-^{1}H COSY correlations of compound 12 in $CDCl_3$

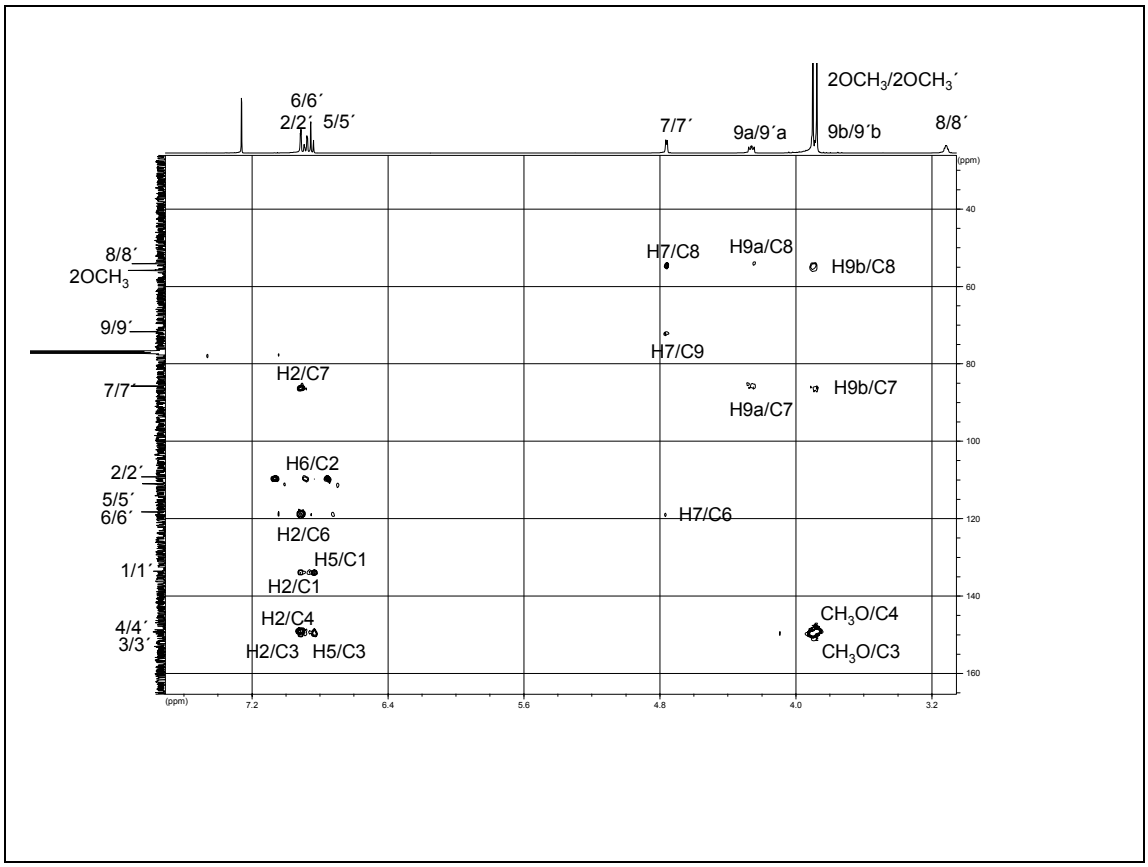

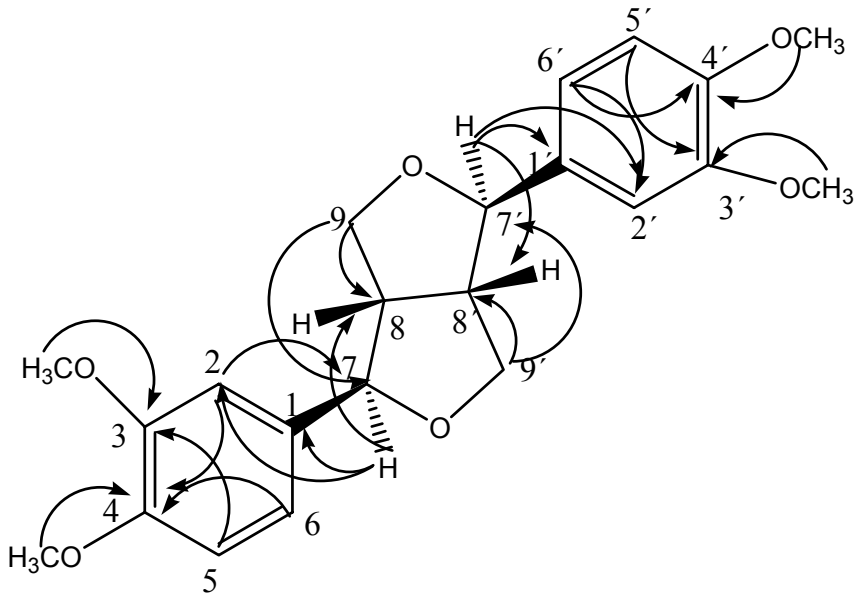

Fig. 3.41: HMBC correlations of compound 12 in $CDCl_3$

III.2.4. Flavonoids and flavonoid glycosides compounds isolated from *Aglaia* sp

III.2.4.1. (-)Epicatechin (13, known compound)

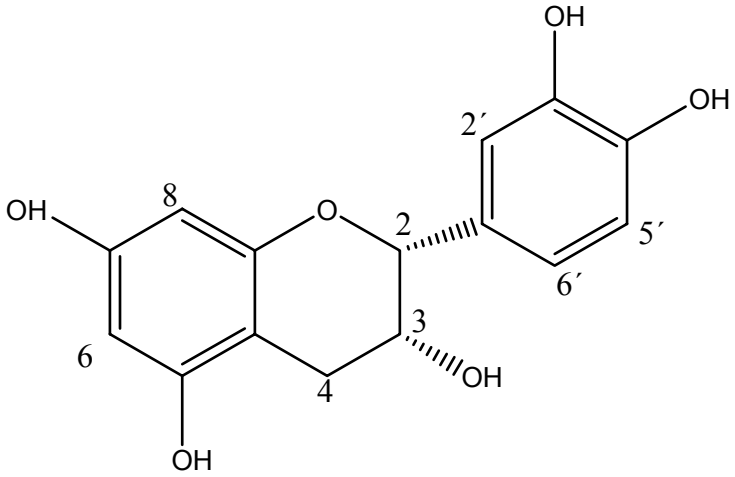

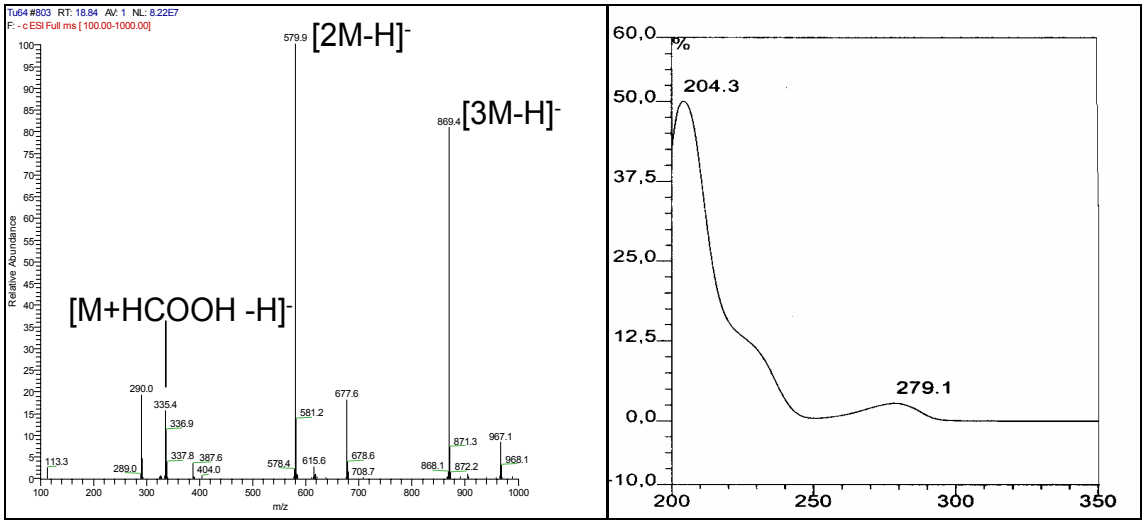

Fig. 3.42: ESI-MS and UV spectrum of compound 13

Compound **13** was isolated from the bark of *Aglaia duppereana* as a red-brown residue (see Fig. 3.42), $[\alpha]^{20}_{D}$-68 (*c*, 0.5, MeOH), UV (MeOH) λ_{max} 204.3, 279.1 nm (see Fig. 3.42). The negative mode ESI-MS showed the pseudomolecular ion peaks at *m/z* 335.4 $[M+HCOOH -H]^-$, at 579.9 $[2M-H]^-$, and 869.4$[3M-H]^-$ (see Fig. 3.42), respectively. The ^{1}H NMR spectrum of compound **13** (see Fig.3.43) revealed two *meta* coupling protons of ring A which resonated at δ 5.93 (d, 2.5) and at 5.91 (d, 2.5), corresponding to H-6 and

H-8. The characteristic ABC pattern of ring B was observed at δ 6.97 (H-2′, d, 1.53), 6.75 (H-5′, d, 8.2), and 6.78 (H-6′, dd, 8.2, 1.9), respectively. Besides, two signals occurred at δ 2.85 (dd, 17.0, 4.4) and 2.65 (dd, 17.0, 2.9) for the methylene protons at C-4. The coupling constant 17.0 Hz indicated the geminal coupling between H-4a and H-4b, while 4.4Hz and 2.9 Hz indicated an axial-equatorial and equatorial-equatorial coupling with H-3, respectively. In addition, H-3 resonated as a multiplet peak at δ 4.16 ppm. H-2 resonated at δ 4.80 as a doublet with a very small coupling constant overlapping with the water peak, which proved the β-position of H-3. Furthermore, the ^{13}C NMR spectrum exhibited 15 carbon signals, in which no carbonyl carbon was observed proving the loss of the carbony group at position C-4 when compared to normal flavonoids. In comparison with the literature data [Shen *et al.,* 1993 and Davis *et al.,* 1996] and based on the assigments shown in Table 3.24, compound **13** was identical to (-)-epicatechin.

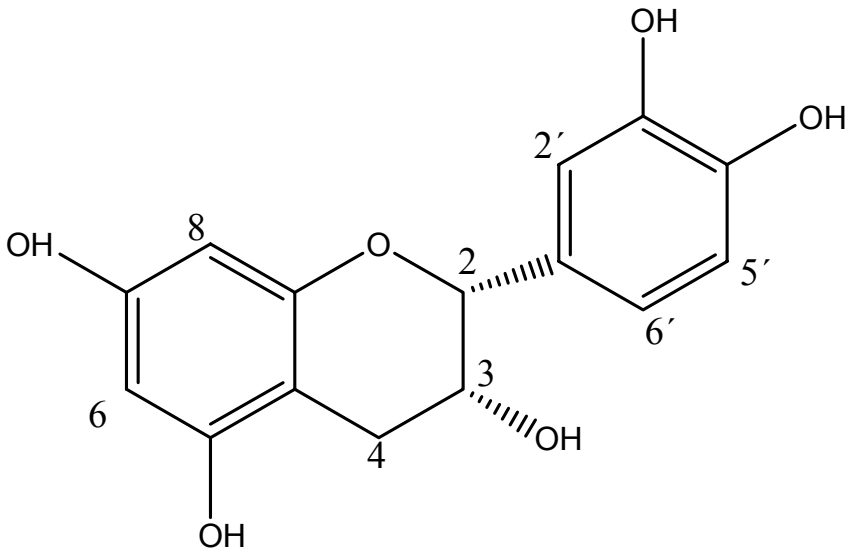

(-)-Epicatechin

Table 3.24 : ^{1}H-NMR and ^{13}C-NMR data of compound 13 in MeOD

Position	δ_H (ppm) compound 13	$^{b}\delta_H$ (ppm) Literature	δ_C (ppm) compound 13	$^{a}\delta_C$ (ppm) Literature
2	4.80(s)	4.88(d, 1.6)	79.8	79.46
3	4.16(m)	4.21 bm	67.4	66.97
4 A B	2.85 (dd, 17.0, 4.4) 2.73 (dd, 17.0, 2.9)	2.87(dd,16.5, 4.6) 2.74(dd, 16.5, 3.2)	29.2	29.01
5			157.9	
6	5.93(d, 2.2)	6.02 (d, 2.3)	96.3	96.22
7			157.6	
8	5.91(d, 2.5)	5.92 (d, 2.3)	95.5	95.75
9			157.3	157.19
10			100.0	99.85
1′			132.2	132.32
2′	6.97(d, 1.5)	7.05 (d, 2.0)	115.8	115.32
3′			145.7	145.42
4′			145.8	145.31
5′	6.75(d, 8.2)	6.69 (d, 8.1)	115.3	115.51
6′	6.78(dd, 8.2, 1.9)	6.84 (dd, 8.1, 2.0)	119.3	119.41

[a] : [Davis *et al.,* 1996] (in Acetone-d_6)

[b]: [Shen *et al.,* 1993] (in $CDCl_3$)

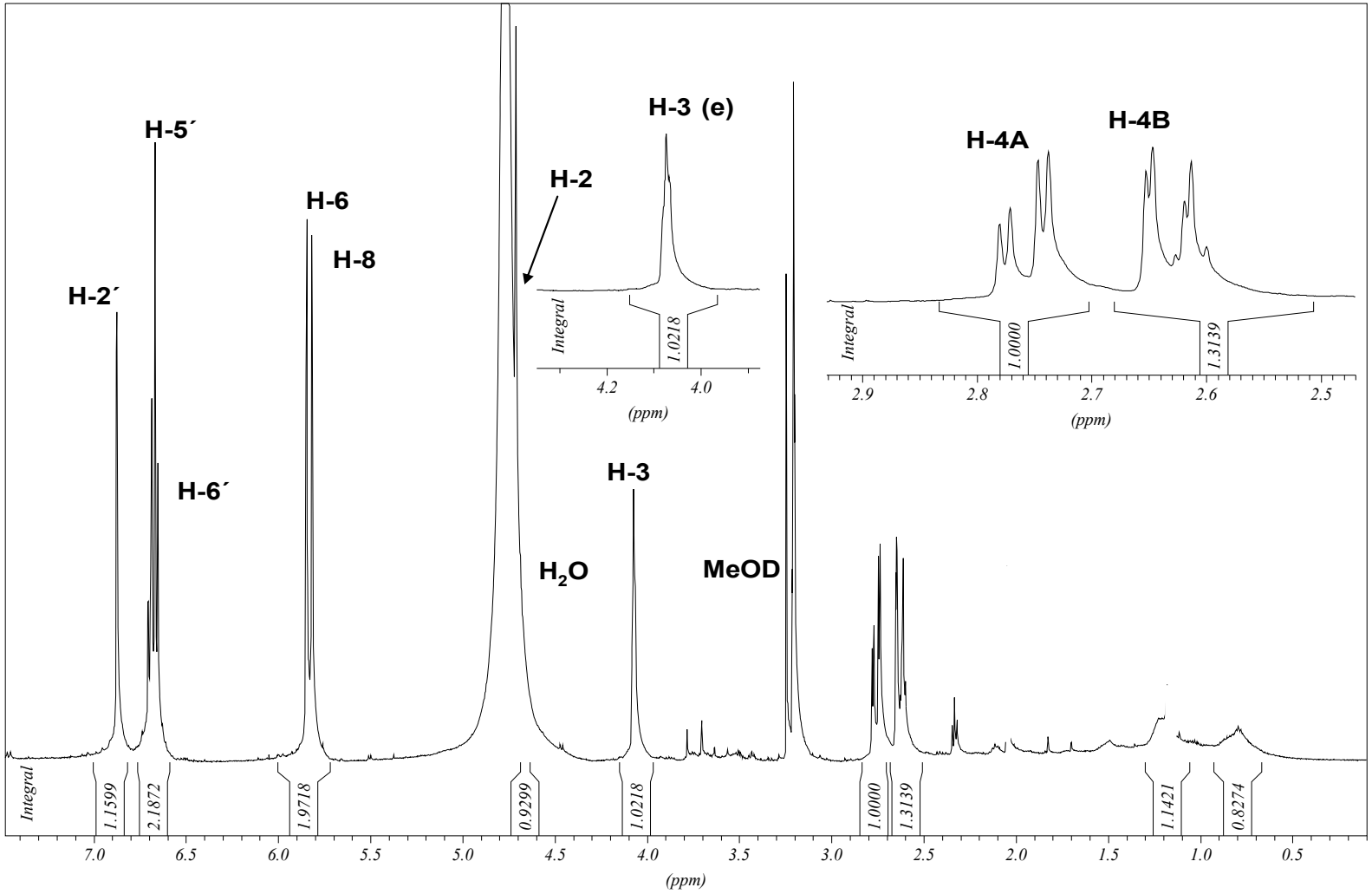

Fig. 3.43: ^{1}H NMR spectrum of compound 13 in MeOD

III.2.4.2. 4´,7-di-O-methyl-naringenin (14, known compound)

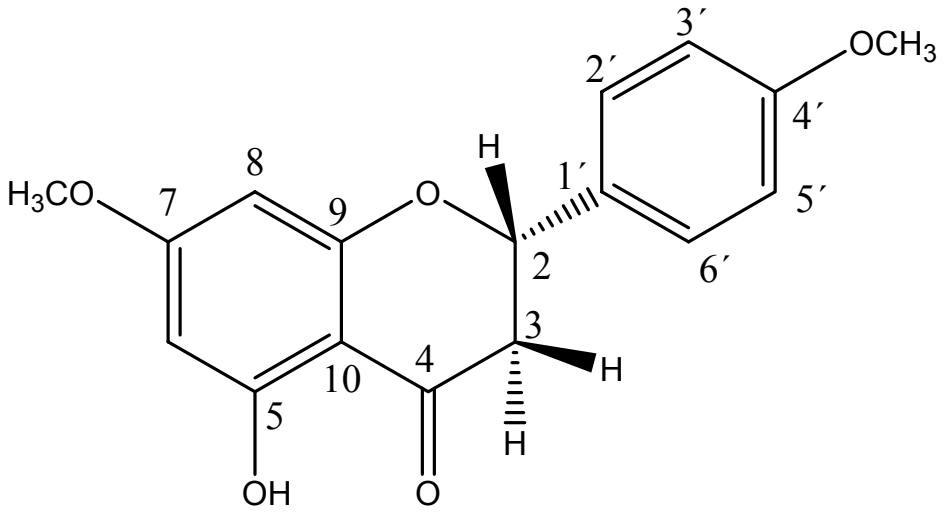

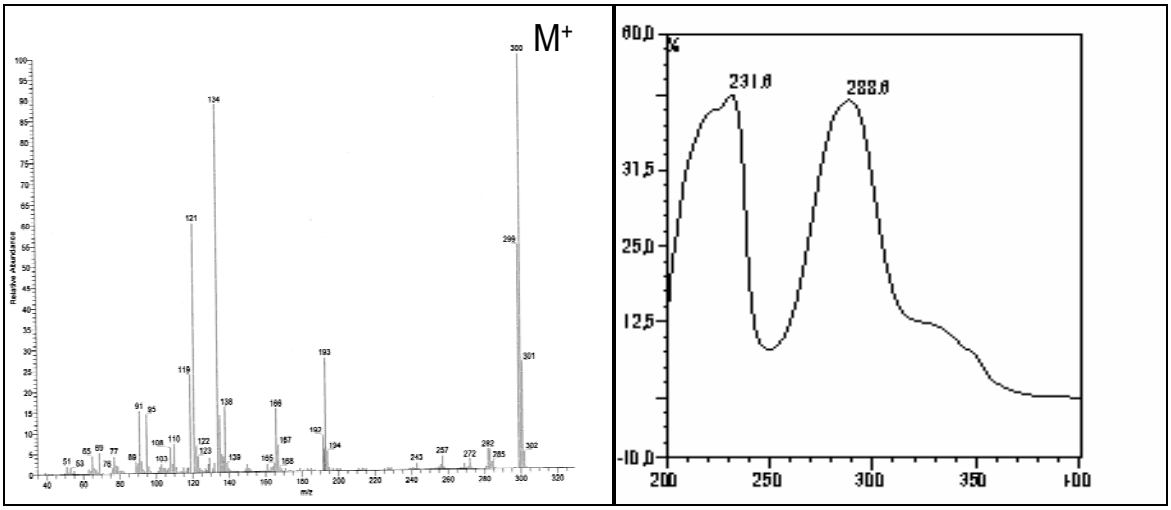

Fig. 3.44: EI-MS and UV spectrum of compound 14

Compound **14** was isolated from the leaves of *Aglaia duppereana* as white crystalline needles (see Scheme 2.2), $[\alpha]^{20}_{D}$-68 (*c*, 0.5, MeOH), UV (MeOH) λ_{max} 231.6, 288.6 nm (see Fig. 3.44). The EI-MS showed a molecular ion peak at *m/z* 300 $[M]^+$ (see Fig. 3.44). The ^{1}H NMR spectrum (see Fig. 3.45), measured in $CDCl_3$, revealed a down field signal at 12.03 ppm, indicating a hydroxyl substitutent at C-5, which was deshielded by the

hydrogen bonding with the carbonyl carbon at C-4. Two *meta*-coupling protons of ring A were also observed at δ 6.07 (H-6, d, 2.2) and 6.04 (H-8, d, 2.2). Besides, the characteristic AA′BB′ partern of ring B occurred at δ 7.38 (d, 8.8) and 6.95 (d, 8.8) corresponding to H-2′/H-6′ and H-3′/H-5′, respectively (see Table 3.25 and Fig. 3.45). Furthermore, a methine proton, H-2, occurred as a double doublet at δ 5.37 with coupling constants of 12.9, and 2.8 Hz, which indicated an axial-axial and an axial-equatorial coupling to H-3A and H-3B, respectively. H-3A and H-3B occurred as two doublets of doublets at 3.10 and 2.97 ppm. The coupling constant 17.0 Hz indicated a geminal coupling of the methylene protons at H-3A and H-3B. The ^{1}H-^{1}H COSY confirmed the correlations of H-2 to H-3A and H-3B, which belong to the spin system of ring C (see Fig. 3.46). Through the HMBC spectrum (see Fig. 3.47), H-2, H-3a, and H-3b exhibited correlations to the carbonyl (C-4) resonance at 196.5 ppm. The two methoxy singlets resonated at δ 3.80 (OCH_3-7) and 3.83 (OCH_3-4′), which showed long-range correlations to C-7 (169.8 ppm) and C-4′ (160.3 ppm). From the HMBC spectrum, all assignments of compound **14** were elucidated as shown in Table 3.25. In comparison with the literature data, compound **14** was identified as the known compound 4′, 7-di-O-methyl-naringenin, which was previously isolated from the leaves and flowers of *Dahlia tenuicaulis* [Jorgen *et al.,* 1975].

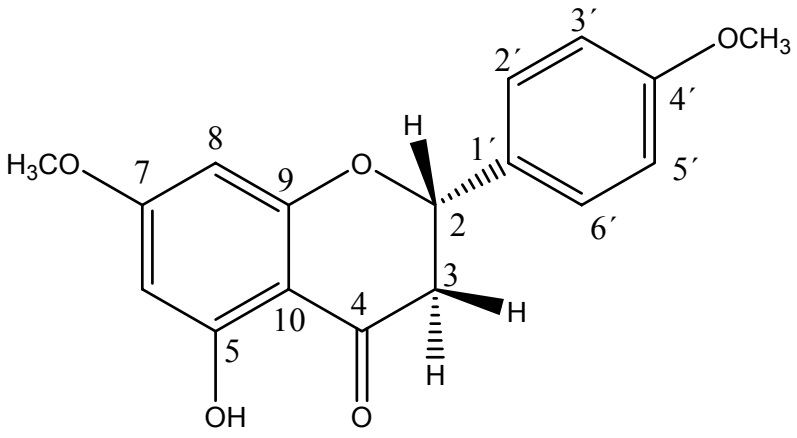

4′, 7-di-O-methyl-naringenin

Table 3.25: ^{1}H NMR,^{1}H-^{1}H COSY and HMBC data of compound 14 (in $CDCl_3$)

Position	^{1}H-NMR, δ (ppm), J (Hz)	COSY	HMBC
2	5.37(dd, 2.8, 12.9)	3	C-1,C-4,C-2′,C-6′
3	A: 3.10(dd, 12.9, 17.0) ax B: 2.79 (dd, 17.0, 2.8) eq	2	C-4,C2′,C-6′
4			
5			
6	6.07(d, 2.2)		C-7, C-8, C-9, C-10
7			
8	6.04(d, 2.2)		C-5, C-6, C-7, C-10
9			
10			
1′			
2′	7.38(d, 8.8)	3′	C-3′, C-4′
3′	6.95(d, 8.8)	2′	C-2′, C-4′
4′			
5′	6.95(d, 8.8)	6′	C-4′,C-6′
6′	7.38(d, 8.8)	5′	C-3′, C-4′, C-5′
OH-5	12.03 (s)		C-5, C-6, C-10
OC*H3*-7	3.80 (s)		C-7
OC*H3*-4′	3.83 (s)		C-4′

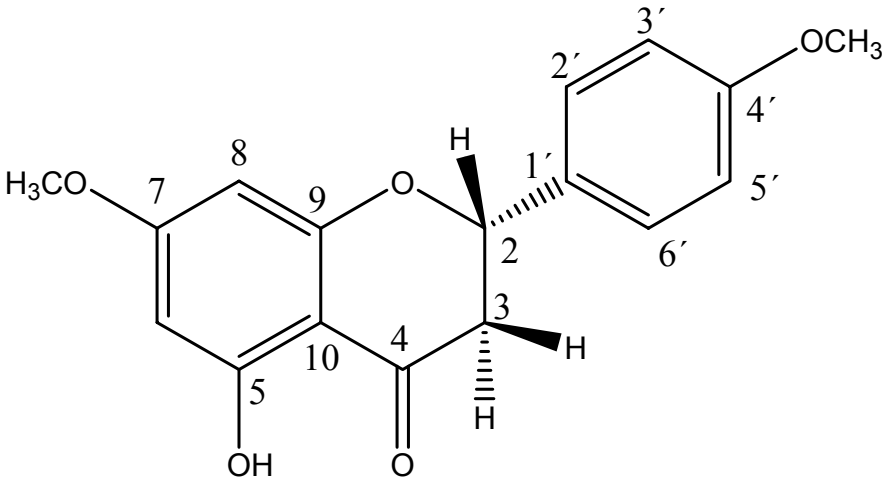

Compound **14**: 4´, 7-di-O-methyl-naringenin

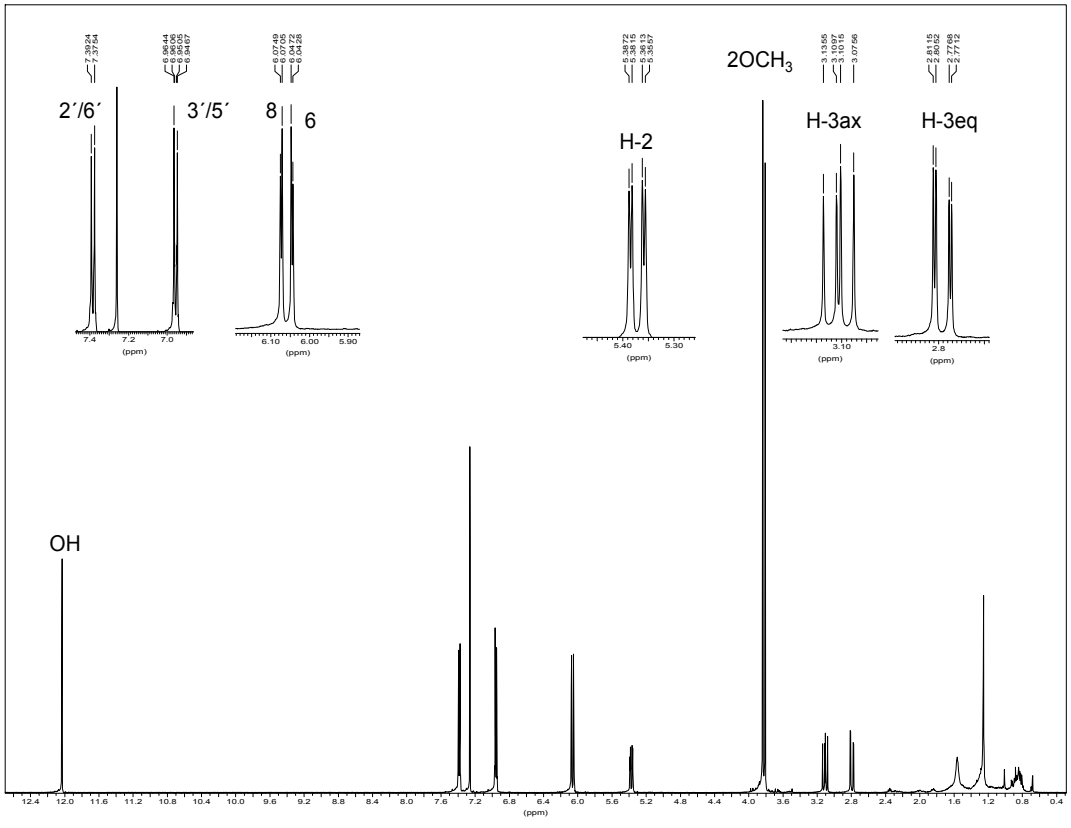

Fig. 3.45: ^{1}H NMR spectrum of compound 14 in $CDCl_3$

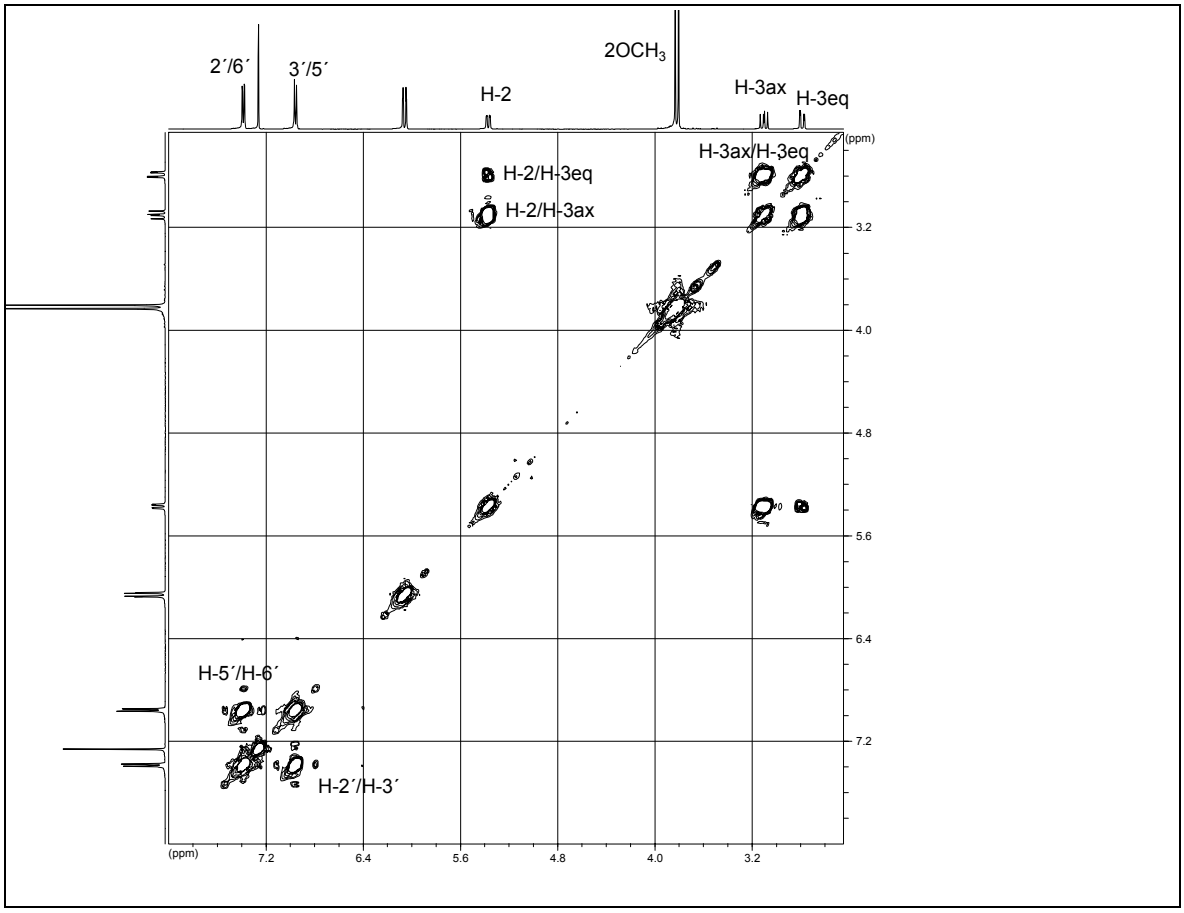

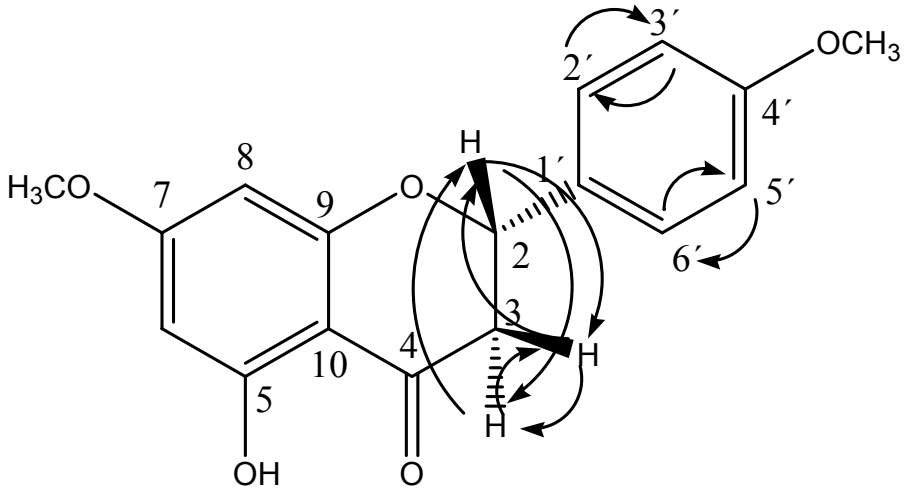

Fig. 3.46: ^{1}H-^{1}H COSY correlations of 14 in $CDCl_3$

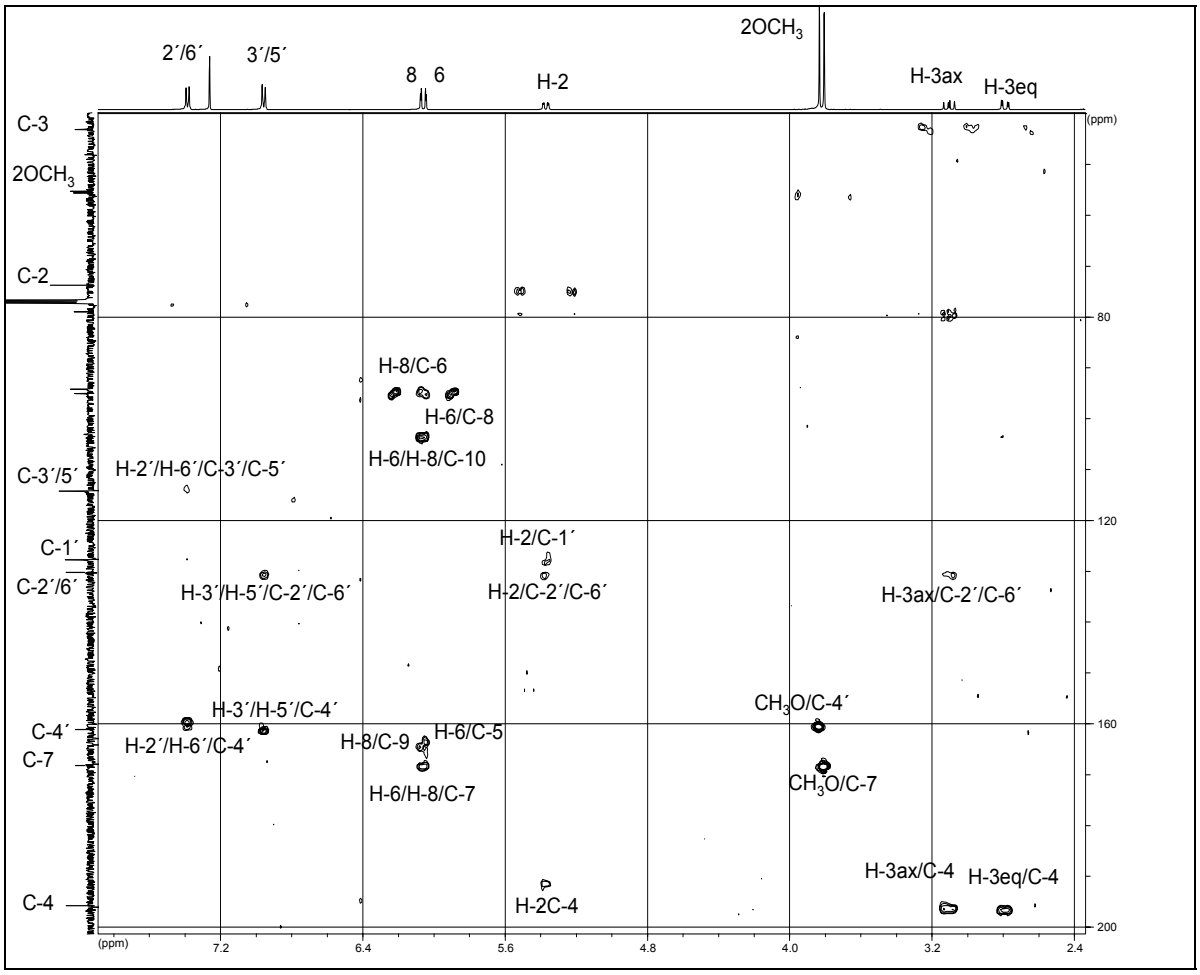

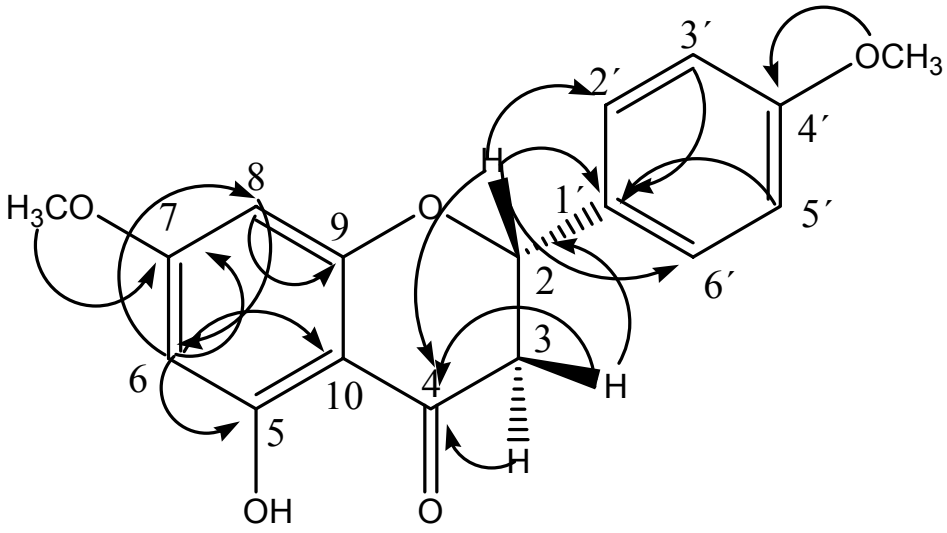

Fig. 3.47: HMBC correlations of 14 in $CDCl_3$

III.2.4.3. 4´,5,7-trimethoxydihydroflavonol (15, known compound)

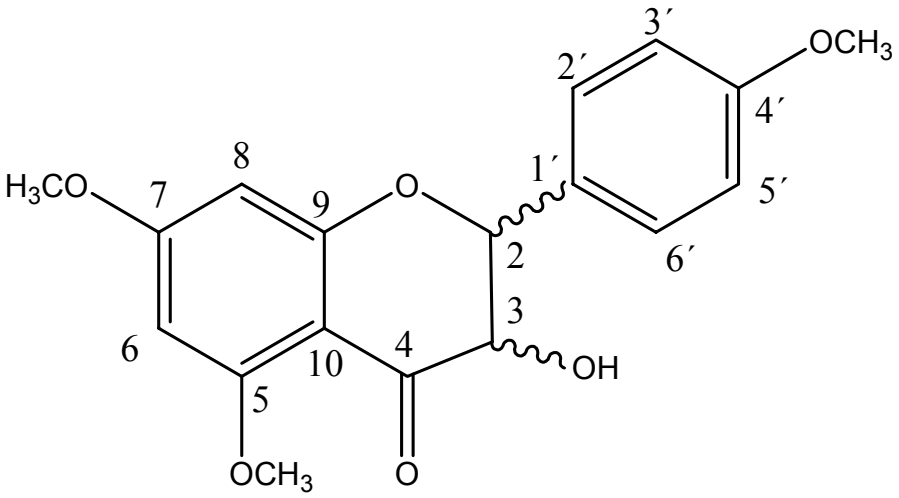

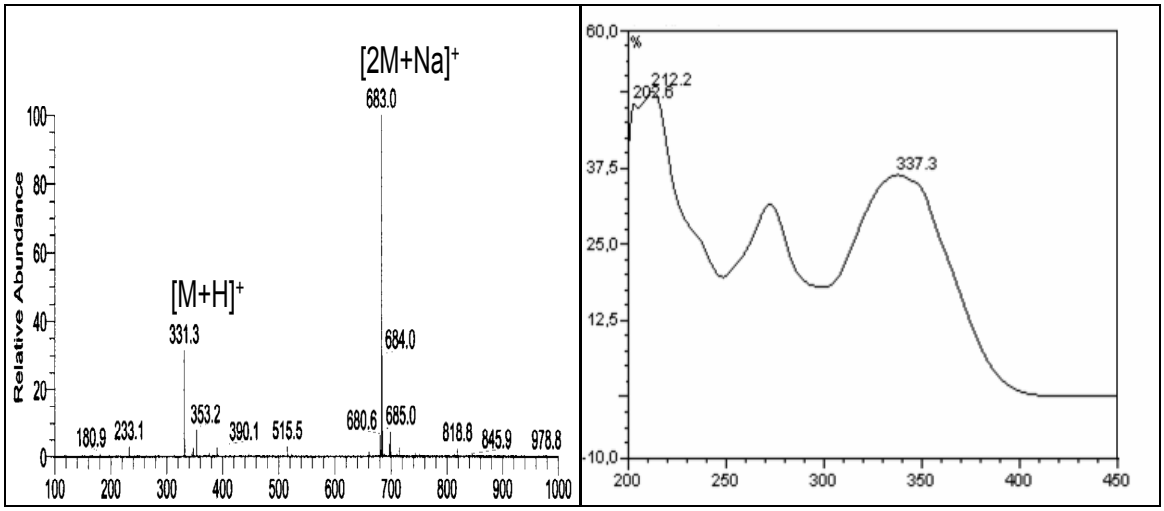

Fig. 3.48: ESI-MS and UV spectrum of compound 15

Compound **15** was isolated from the leaves of *Aglaia oligophylla* as yellow crystalline needles (see Scheme 2.3), $[\alpha]^{20}_{D}$ 0 (*c*, 0.5, MeOH) suggesting compound **15** is a racemic mixture, UV (MeOH) λ_{max} 212.2, 337.3 nm (see Fig. 3.48). The ESI-MS showed the pseudomolecular ion peaks at *m/z* 331.3 $[M+H]^+$, and at *m/z* 683.0 $[2M+Na]^+$ (see Fig. 3.48). In the ^{1}H NMR spectrum (see Fig. 3.49) of compound **15**, two *meta*-protons of ring A resonated at δ 6.12 (d, 2.2), and 6.11 (d, 2.2) corresponding to H-6 and H-8, respectively. The characteristic AA´BB´ pattern of ring B occurred at δ 7.49(2H, d, 8.8) and 6.98 (2H, d,

8.8), indicating two pairs of protons H-2′/H-6′ and H-3′/H-5′, respectively. Moreover, the ^{1}H NMR spectrum showed the presence of three methoxy singlets, which occurred at δ 3.87, 3.88, and 3.91.

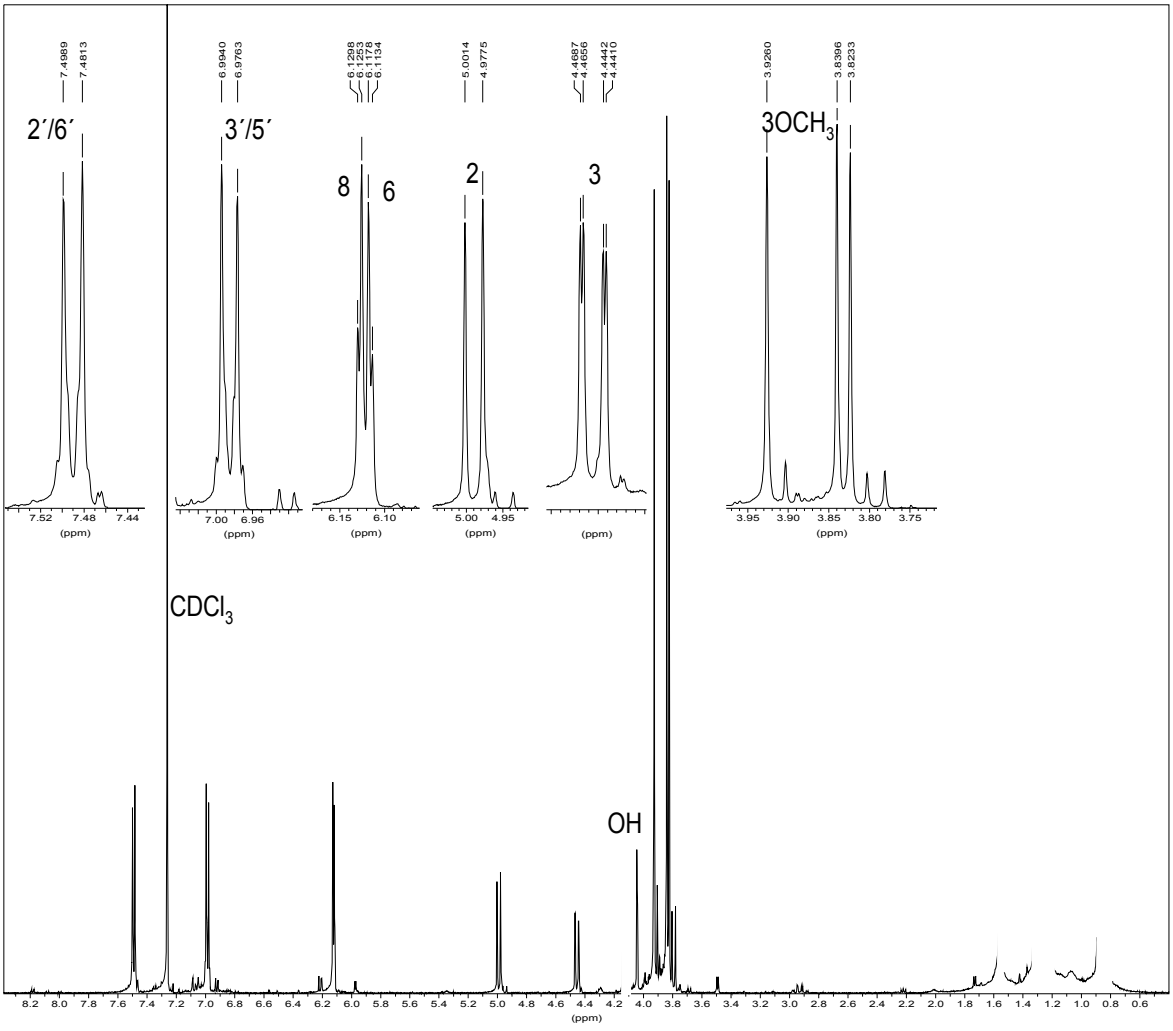

Fig. 3.49: ^{1}H NMR spectrum of 15 in $CDCl_3$

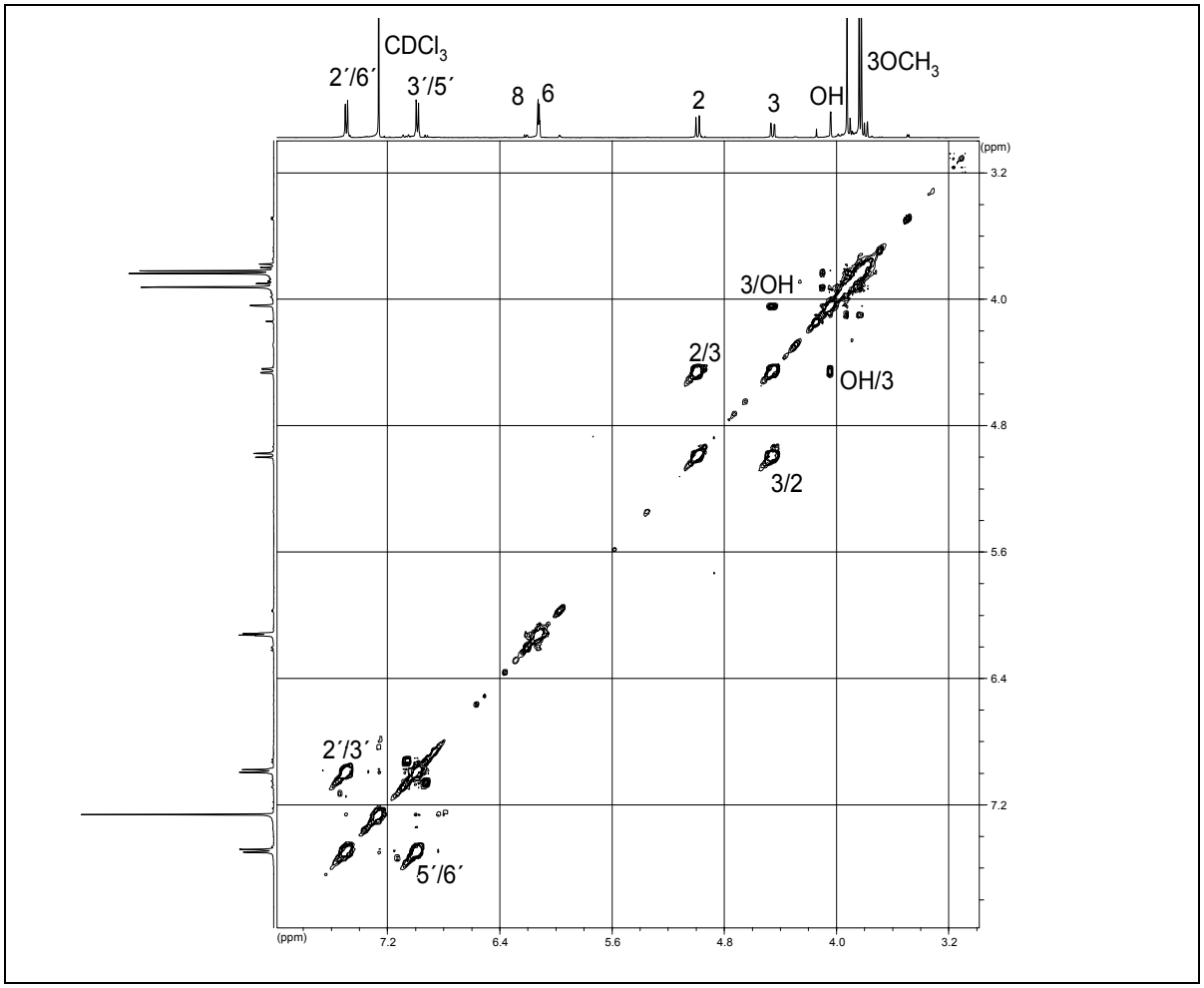

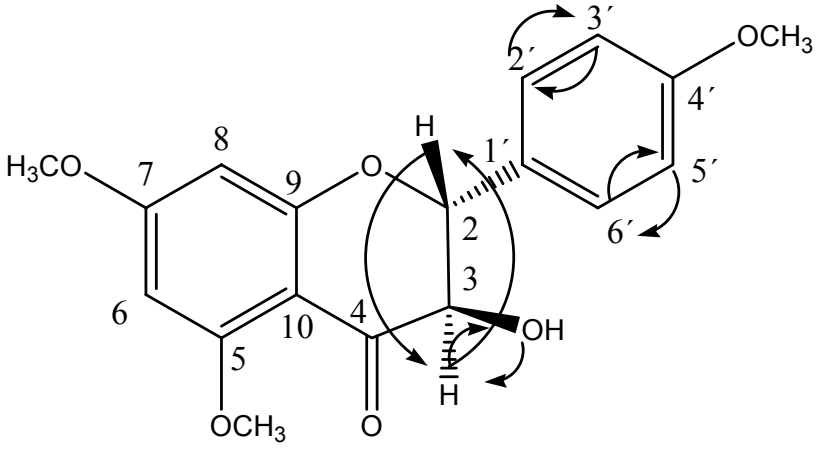

Fig. 3.50: ^{1}H-^{1}H-COSY spectrum of 15

In addition, a methine proton, H-2, of ring C was observed as a doublet at δ 5.00 (d, 11.9). The magnitude of its coupling constant ($J_{2,3}$=11.9 Hz) indicated a *trans*-type of dihydroflavonol [Islam *et al.,* 2000]. H-3 occurred as a double doublet signal at δ 4.45 (dd, 11.9, 1.6), which indicated an additional coupling with the hydroxyl group at C-3. The ^{1}H-^{1}H COSY (see Fig. 3.50) confirmed this spin system through correlations of H-2 to H-3 and H-3 to the OH group (see Table 3.26). In comparison to the literature [Islam *et al.,* 2000], compound **15** was comparable to (*2R*,*3R*)-(+)- 4′,5,7-trimethoxy-dihydro-flavonol, a known compound previously isolated from *Lannea coromandelica* L. (Anacardiaceae) collected in Bangladesh. However, the isolated compound is a racemic mixture.

Table 3.26: ^{1}H NMR,^{1}H-^{1}H COSY data of compound 15

Position	^{1}H-NMR, δ (ppm), J (Hz)	COSY
2	5.00(d, 11.9)	3
3	4.45 (dd, 11.9, 1.6)	2, O*H*
4		
5		
6	6.12 (d,2.2)	
7		
8	6.11(d,2.2)	
9		
10		
1′		
2′	7.49(d, 8.8)	3′
3′	6.98(d, 8.8)	2′
4′		
5′	6.98(d, 8.8)	6′
6′	7.49(d, 8.8)	5′
OH-3	4.04 (d, 1.6)	3
OC*H3*-4′	3.87(s)	
OC*H3*-5	3.88(s)	
OC*H3*-7	3.91(s)	

III.2.4.4. 4′,5,7-Tri-O-methyl-kaempferol (16, known compound)

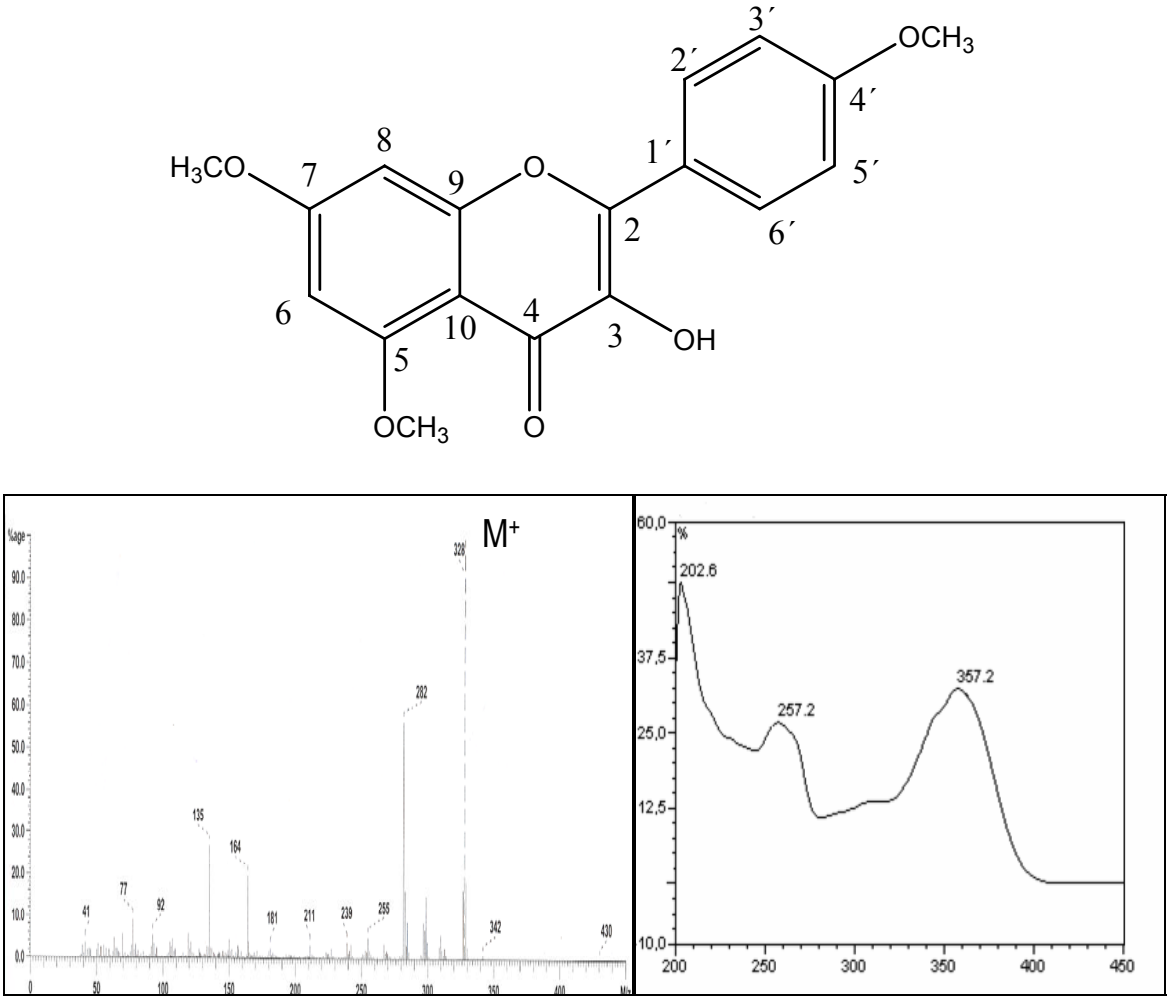

Fig. 3.51: EI-MS and UV spectrum of compound 16

Compound **16** was obtained as yellow crystalline needles from the leaves of *Aglaia oligophylla* and *Aglaia abbriviata* (see Scheme 2.3 and Scheme Fig.2.7), UV (MeOH) λ_{max} 202.6, 257.2 nm, 357.2 nm (see Fig. 3.51). The EI-MS showed a molecular ion peak at *m/z* 328 $[M]^+$ (see Fig. 3.51). The ^{1}H NMR spectrum of compound **16** showed again a characteristic AA′BB′ pattern of ring B at δ 8.17 (d, 8.8) and δ 7.02 (d, 8.8), corresponding to H-2′/H-6′ and H-3′/H-5′ (see Table 3.27 and Fig. 3.52). The resonances of two *meta*-coupling protons of ring A were observed at δ 6.54 (H-6, d, 2.2) and δ 6.34 (H-8, d, 2.2). The ^{1}H-NMR spectrum showed three methoxy singlets resonating at δ 3.97 (OCH_3-4′) and

3.88 (OC*H*$_3$-5), and 3.91 (OC*H*$_3$-7), which correlated with H-3′/H-5′, H-6, and H-8, respectively (see Fig. 3.53) as revealed by the ^{1}H-^{1}H COSY spectrum. Through the HMBC spectrum (see Fig. 3.54), the three methoxy singlets showed correlations with C-4′ (160.51 ppm), C-5 (160.61 ppm) and C-7 (164.28 ppm). Two *meta*-coupling protons of ring A (H-6 and H-8) exhibited long-range correlations to C-4 (171.91 ppm), C-7 (164.28 ppm), C-9 (158.84 ppm), C-5 (160.61 ppm) and C-10 (106.21 ppm). The full assignments of compound **16** are shown in Table 3.27. In comparison with the literature data [Paul *et al.,* 1992], compound **16** was identified as 4′, 5,7-tri-O-methyl-kaempferol.

Table 3.27: ^{1}H NMR,^{13}C NMR, ^{1}H-^{1}H COSY and HMBC data of compound 16 in $CDCl_3$

Position	δ_H NMR	δ_C NMR	COSY	HMBC
2		142.26		
3		137.42		
4		171.91		
5		160.61		
6	6.54(d,2.2)	95.64	OC*H3*-5	C-4,C-5,C-7,C-8,C-10
7		164.28		
8	6.34(d,2.2)	92.38	OC*H3*-7	C-4,C-6,C-7,C-9,C-10
9		158.84		
10		106.21		
1′		123.55		
2′	8.17(d, 8.8)	113.98	H-3′	C-3′,C-4′
3′	7.02(d, 8.8)	128.86	H-2′	C-2′,C-4′
4′		160.51		
5′	7.02(d, 8.8)	128.86	H-6′	C-4′,C-6′
6′	8.17(d, 8.8)	113.98	H-5′	C-3′,C-4′,C-5′
OC*H3*-4′	3.97 (s)	56.37	H-3′,H-5′	C-4′
OC*H3*-5	3.88 (s)	55.36	H-6	C-5
OC*H3*-7	3.91 (s)	55.78	H-8	C-7

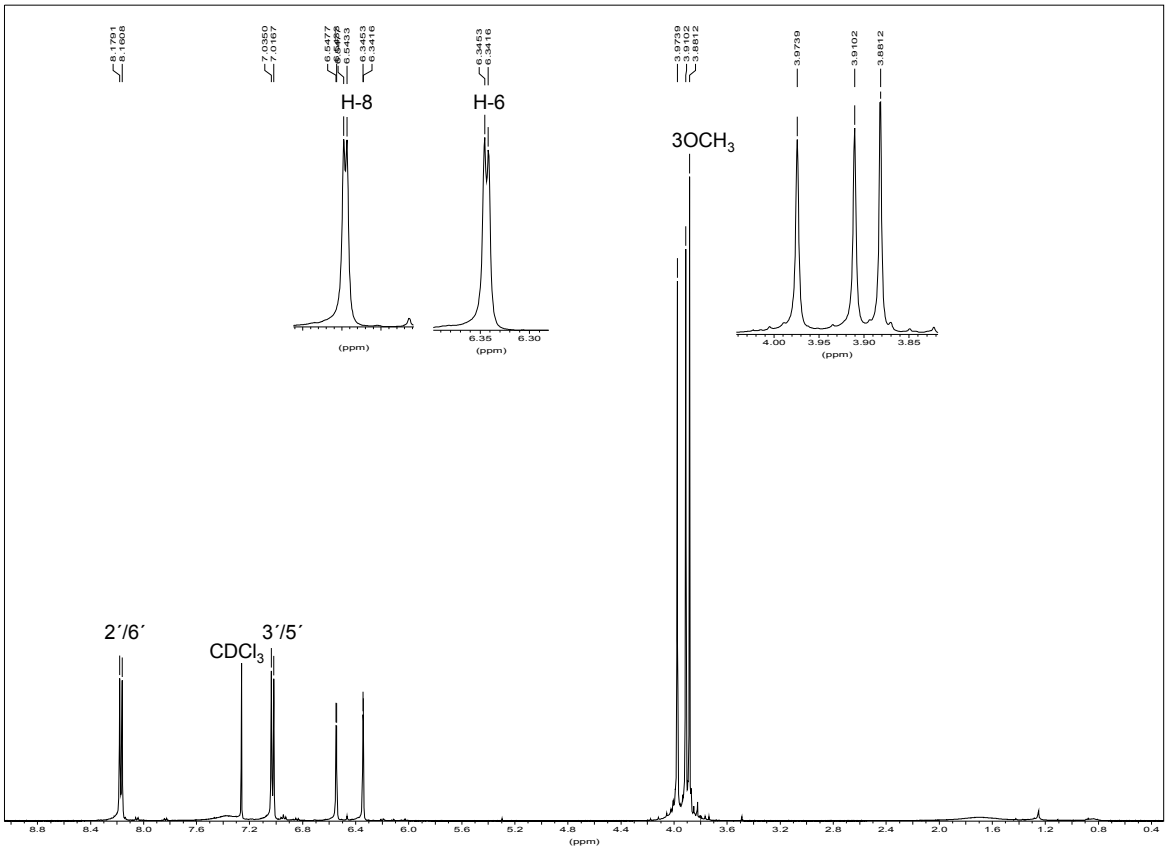

Fig. 3.52: ^{1}H NMR spectrum of 16 in $CDCl_3$

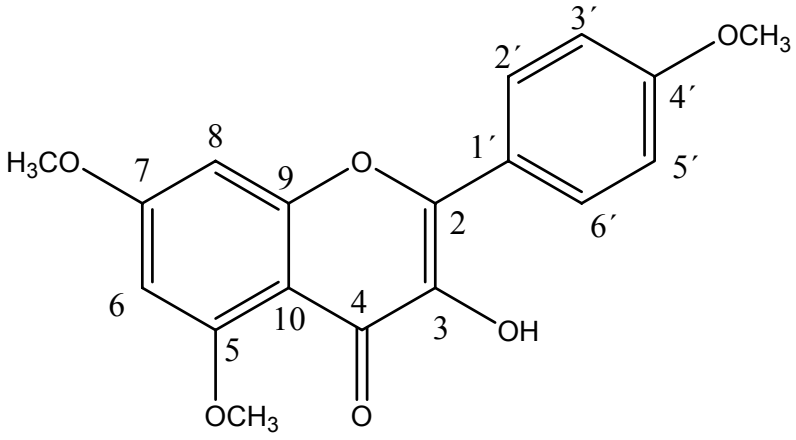

4′, 5,7-tri-O-methyl-kaempferol

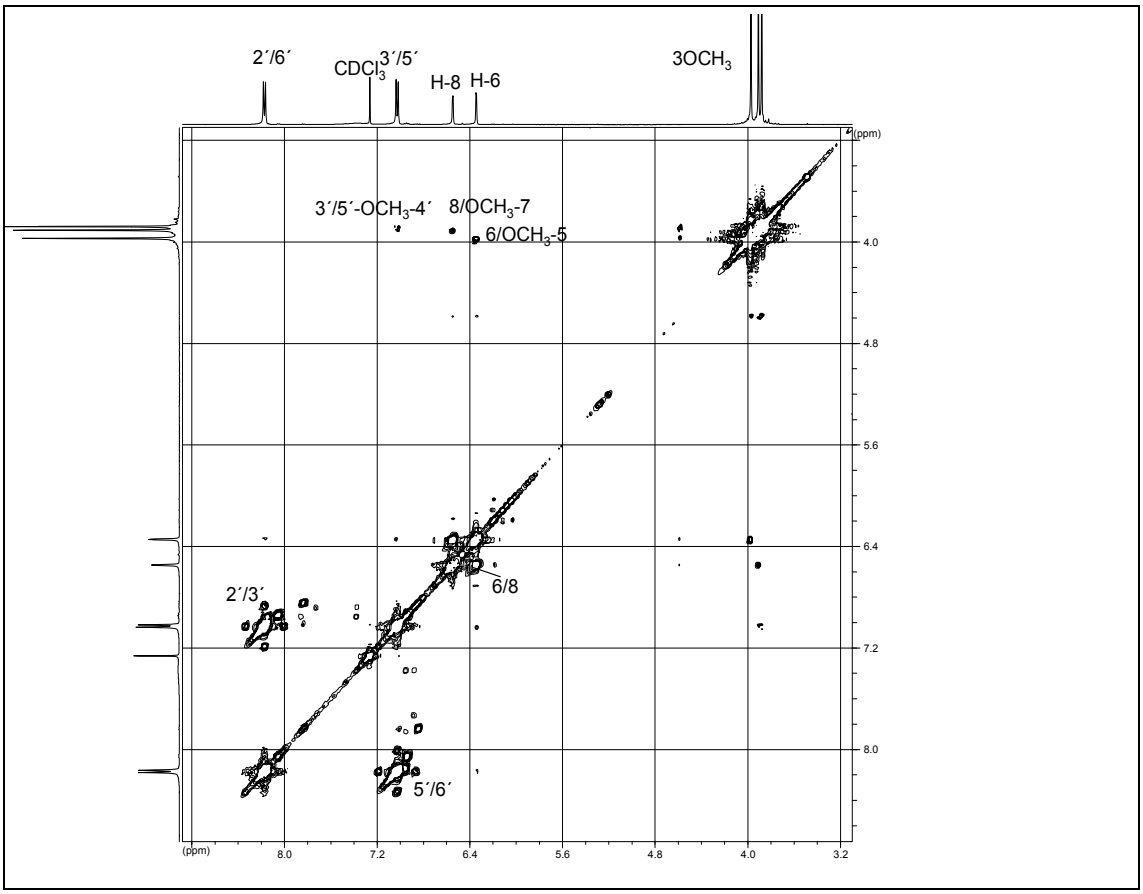

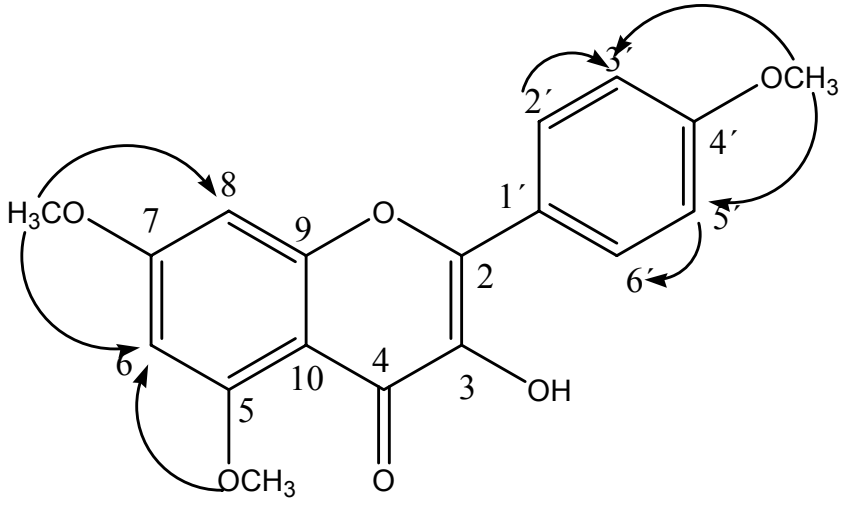

Fig. 3.53: ^{1}H-^{1}H-COSY correlations of compound 16 in $CDCl_3$

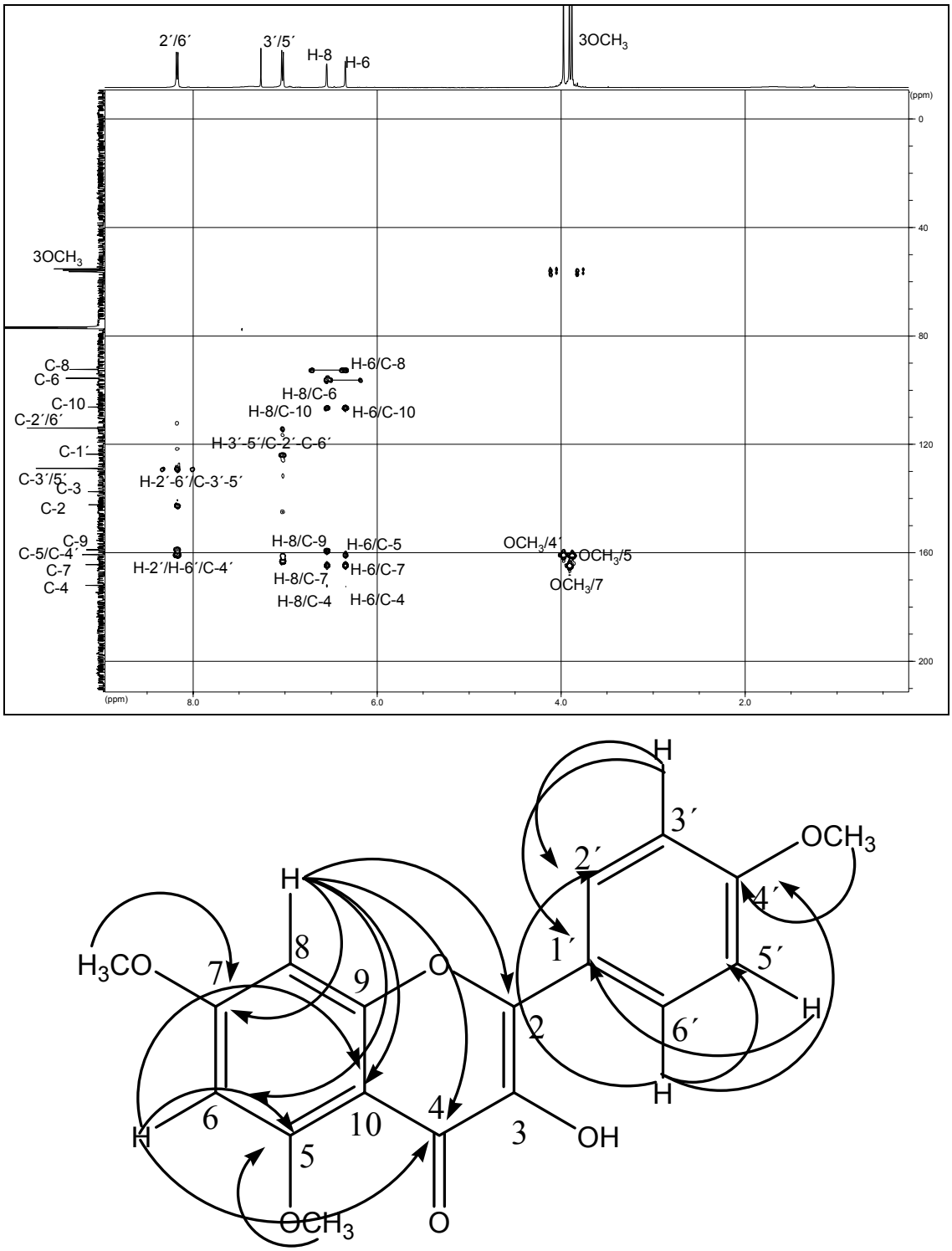

Fig. 3.54: HMBC correlations of compound 16 in $CDCl_3$

III.2.4.5. 4´,5,7-Tri-O-methyl-naringenin (17, known compound)

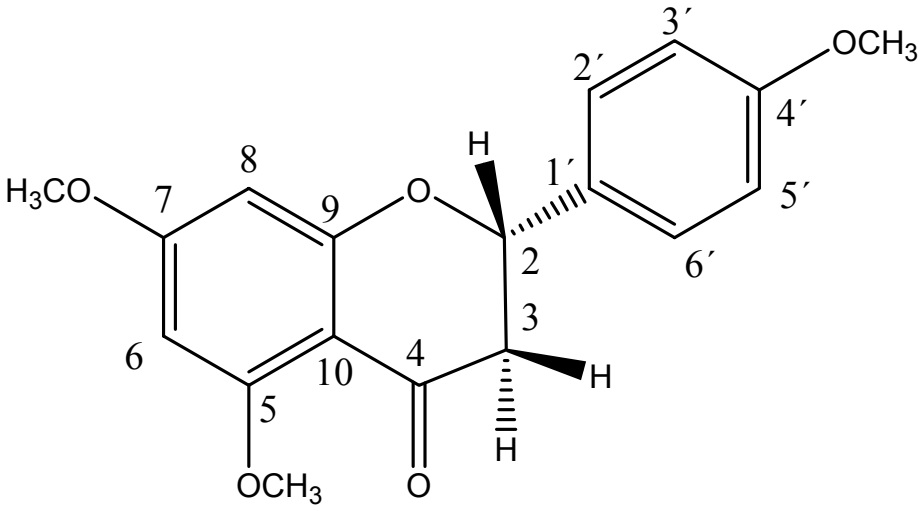

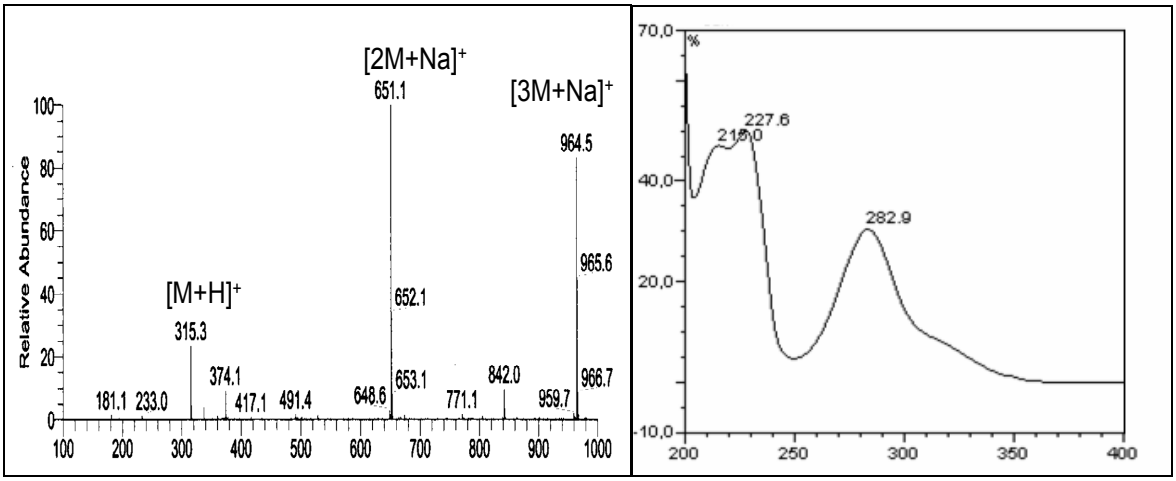

Fig. 3.55: ESI-MS and UV spectrum of compound 17

Compound **17** was isolated from the leaves of *Aglaia oligophylla* as a white amorphous residue (see Scheme 2.3), $[\alpha]^{20}_{D}$-30 (*c*, 0.5, MeOH), UV (MeOH) λ_{max} 210.0, 227.6, and 282.9 nm (see Fig. 3.55). The ESI-MS positive mode showed the pseudomolecular ion peaks at *m/z* 315.3 $[M+H]^+$, and at *m/z* 651.1 $[2M+Na]^+$ (see Fig. 3.55).

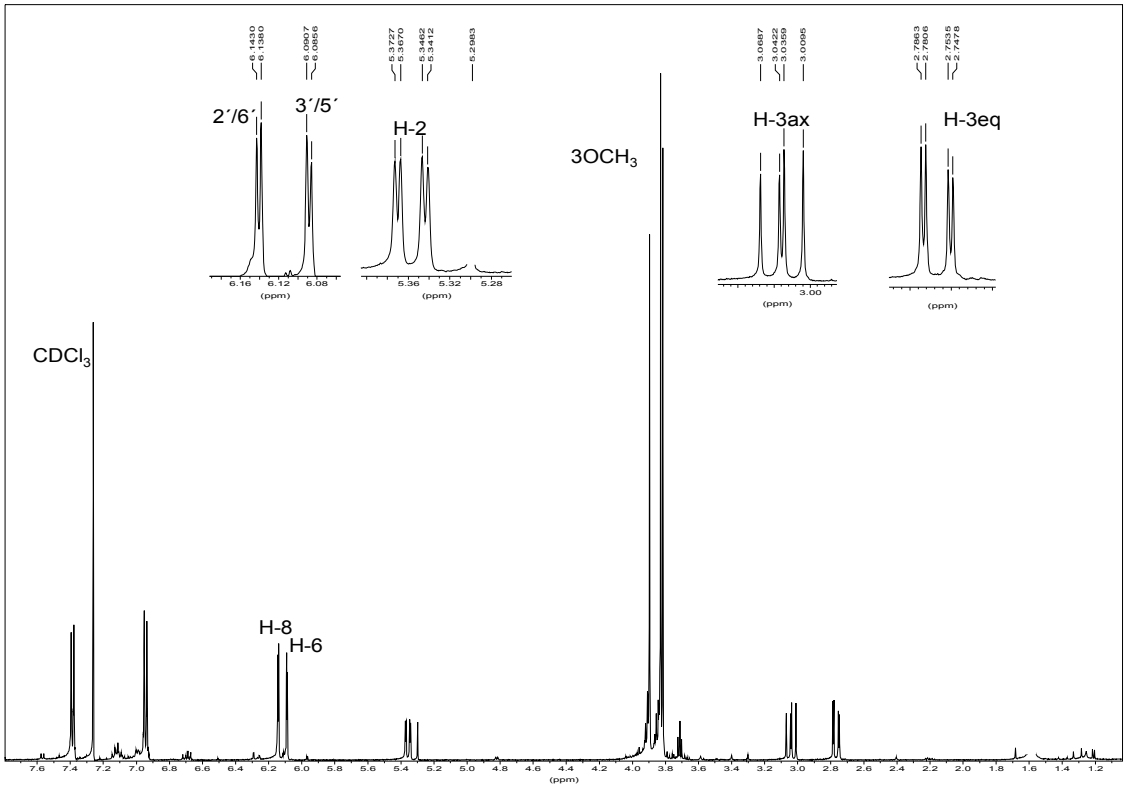

Fig. 3.56: ^{1}H NMR spectrum of 17 in $CDCl_3$

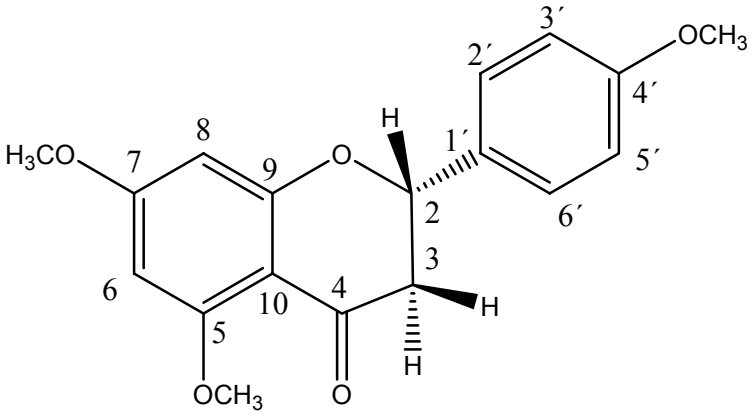

The ^{1}H NMR spectrum (see Table 3.28 and Fig. 3.56) of compound **17** exhibited the characteristic AA′BB′ pattern of ring B, which occurred at δ 7.39(2H, d, 8.8) and 6.95 (2H, d, 8.8) indicating two pairs of protons situated at C-2′/C-6′ and at C-3′/C-5′. Two *meta*-coupling protons of ring A resonated at δ 6.14 (d, 2.2), and 6.08 (d, 2.2), corresponding to H-6 and H-8, respectively. Moreover, the ^{1}H NMR spectrum showed the presence of three methoxy singlets, which occurred at δ 3.89, 3.80, and 3.82.

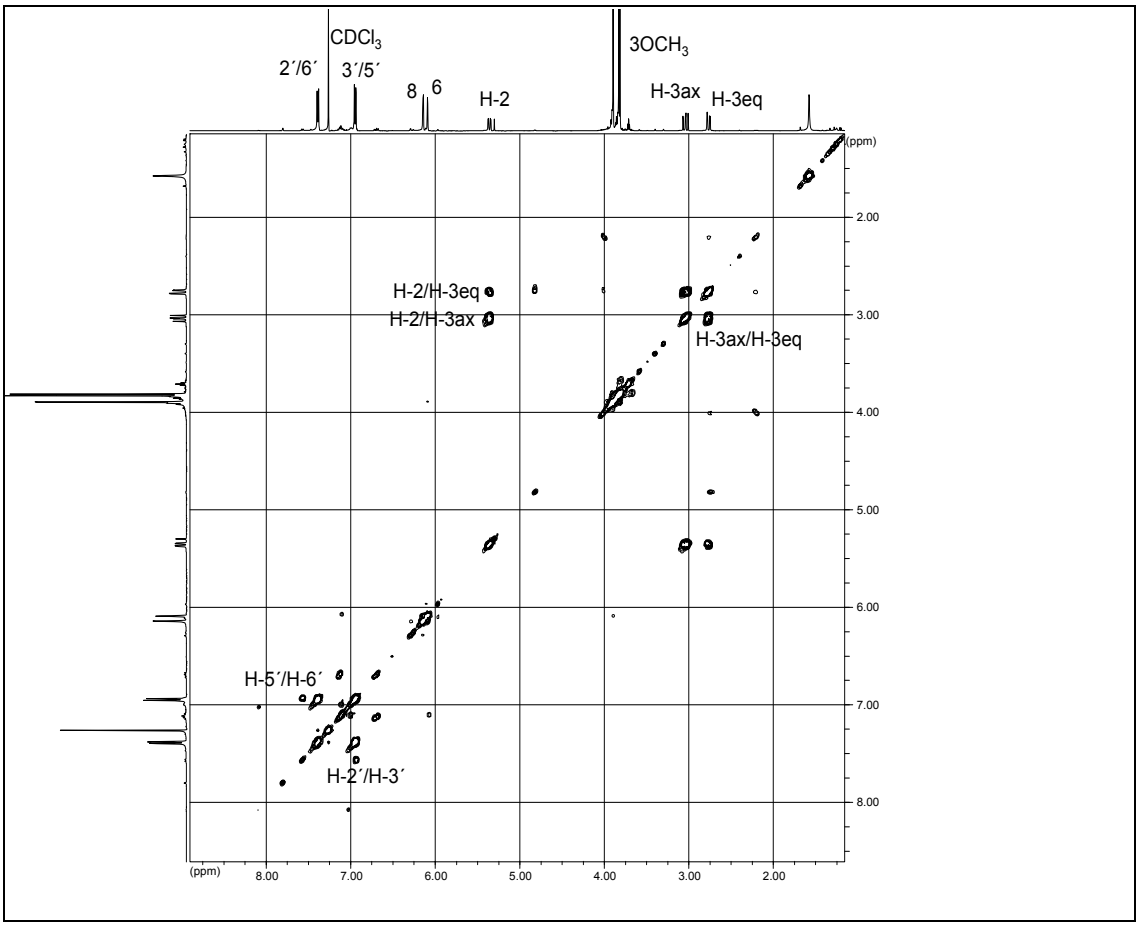

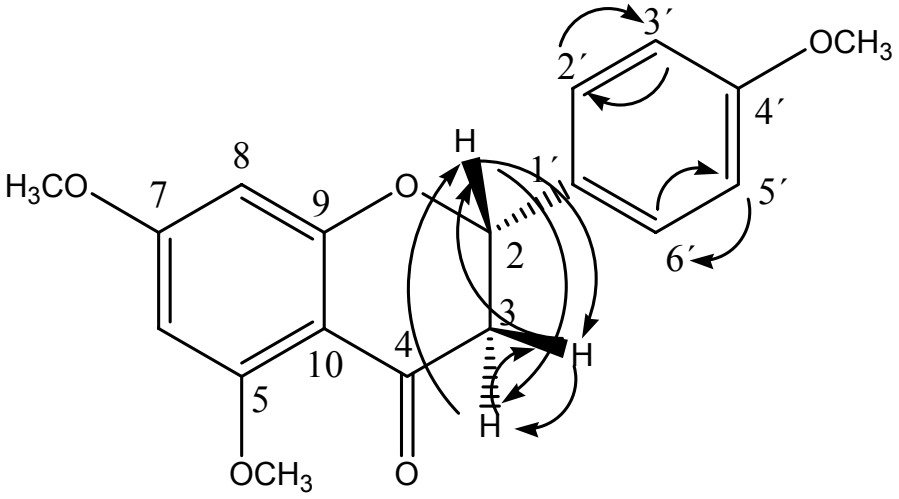

Fig. 3.57: ^{1}H-^{1}H-COSY correlations of compound 17 in $CDCl_3$

In addition, a methine proton, H-2, of ring C was observed as a doublet of a doublet at δ 5.37 (dd, 2.9, 13.3). The magnitude of the coupling constant 13.3 Hz indicated an axial-axial, while the value of 2.9 Hz revealed an axial-equatorial coupling of H-3A and H-3B which occurred as two doublets of doublets at 3.04 and 2.77 ppm as found in dihydroflavanone. The ^{1}H-^{1}H COSY (see Fig. 3.57) confirmed this spin system through correlations of H-2 to H-3A and H-3B (see Table 3.28). In comparison with the literature data [Jorgen *et al.,* 1975], compound **17** was identified as 4′,5,7-tri-O-methyl-naringenin (or 4′,5,7-trimethoxy-flavanone) which was previously isolated from the leaves and flowers of *Dahlia tenuicaulis* collected in Denmark.

Table 3.28: ^{1}H NMR,^{1}H-^{1}H COSY data of compound 17

Position	^{1}H-NMR, δ (ppm), J (Hz)	COSY
2	5.37(dd, 2.9, 13.3)	3
3	A: 3.04 (dd, 13.3, 16.4) B: 2.77 (dd, 2.9, 16.4)	2
4		
5		
6	6.14 (d, 2.2)	
7		
8	6.08(d, 2.2)	
9		
10		
1′		
2′	7.39(d, 8.8)	3′
3′	6.95(d, 8.8)	2′
4′		
5′	6.95(d, 8.8)	6′
6′	7.39(d, 8.8)	5′
OC*H3*-4′	3.89(s)	
OC*H3*-5	3.81(s)	
OC*H3*-7	3.81(s)	

III.2.4.6. Kaempferol-3-rutinoside (18, known compound)

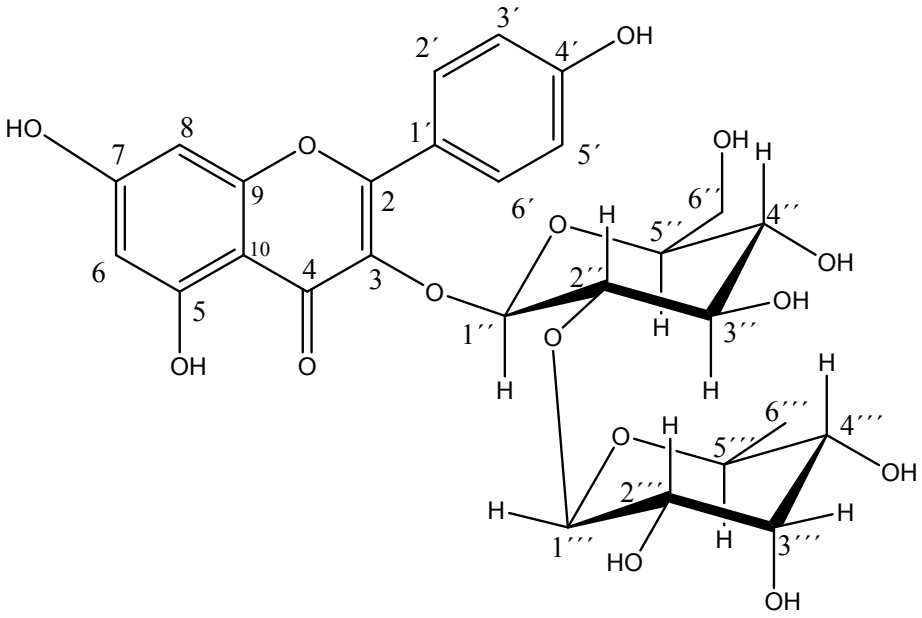

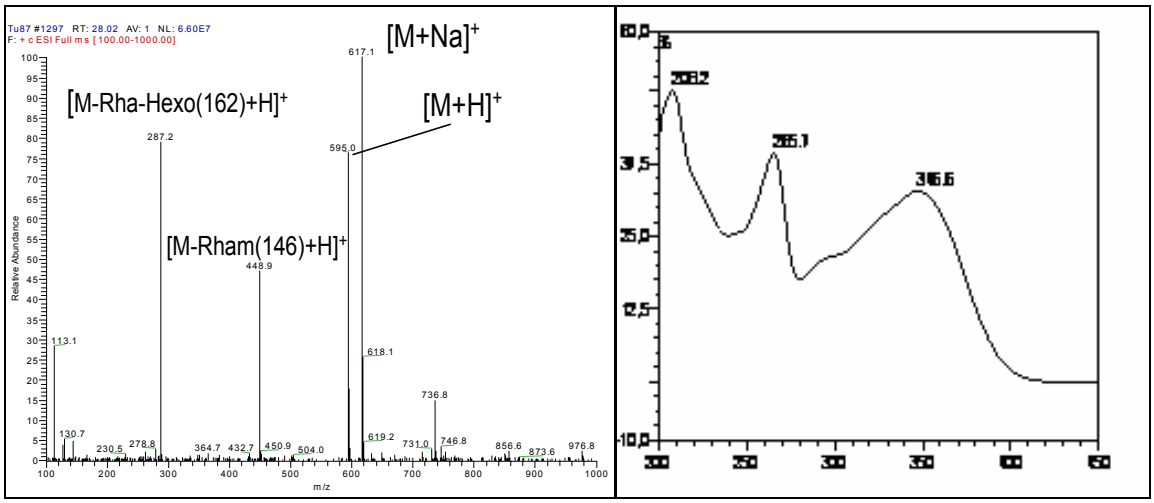

Fig. 3.58: ESI-MS and UV spectrum of compound 18

Compound **18** was isolated from the leaves of *Aglaia oligophylla* Miq as yellow crystalline needles (see Scheme 2.8), $[\alpha]^{20}_{D}$-20 (*c*, 0.5, MeOH), UV (MeOH) λ_{max} 202.4, 265.6, and 348.7 nm (see Fig. 3.58). The ESI-MS showed the pseudomolecular ion peaks at *m/z* 617.1 $[M+Na]^+$, and at *m/z* 595.0 $[M+H]^+$, respectively (see Fig. 3.58). The fragment ion peaks occurred at *m/z* 448.9 $[M+H-146]^+$, indicating the loss of a terminal rhamnosyl unit (-142),

and *m/z* 278.2 $[M+H-146-162]^+$, which was assigned to the additional loss of a primary hexosyl moiety (-162). Fragment at m/z 287 corresponds to kaempferol and this observation was supported by the ^{1}H NMR data. The characteristic AA´BB´ pattern of ring B was again observed at δ 7.98 (d, 8.8) and 6.81 (d, 8.8) for H-2´/H-6´ and H-3´/H-5´, respectively. Two *meta*-protons of ring A resonated at δ 6.33 (d, 2.2), 6.13 (d, 2.2) for H-6 and H-8, respectively. The ^{1}H NMR revealed a methyl signal which occurred as a doublet at 1.02 ppm (*J*=6.3 Hz), which is typical for a rhamnose moiety. Two anomeric protons resonated at δ 5.02 (1H, d, 6.9) and at δ 4.41 (1H, d, 1.9), which were assigned to the two sugar units, α-glucopyranosyl (Glu), and α-rhamnopyranosyl (Rha) (see ^{1}H-^{1}H-COSY, Fig. 3.60). The HMBC spectrum showed correlations between Glu-H-1´´ (*δ* 5.02) and kaemp ferol C-3 (*δ* 132.5), and between Glu H-2´´ (δ 3.42) and Rham C-1´´´ (*δ* 101.9), Rham H-6´´´/C-4´´´/C-5´´´ (*δ* 1.04/69.8/72.3), which further established the connectivities between gluco and of the 2 sugar units to the flavonoid. In comparison to the literature data [Rikke *et al.,* 1999] compound **18** was established as kaempferol-3-*O*-β-D[2-O-α-rhamnopyranosyl]- glucopyranoside which was previously isolated from *Tulipa gesneriana* cultivated in Poland.

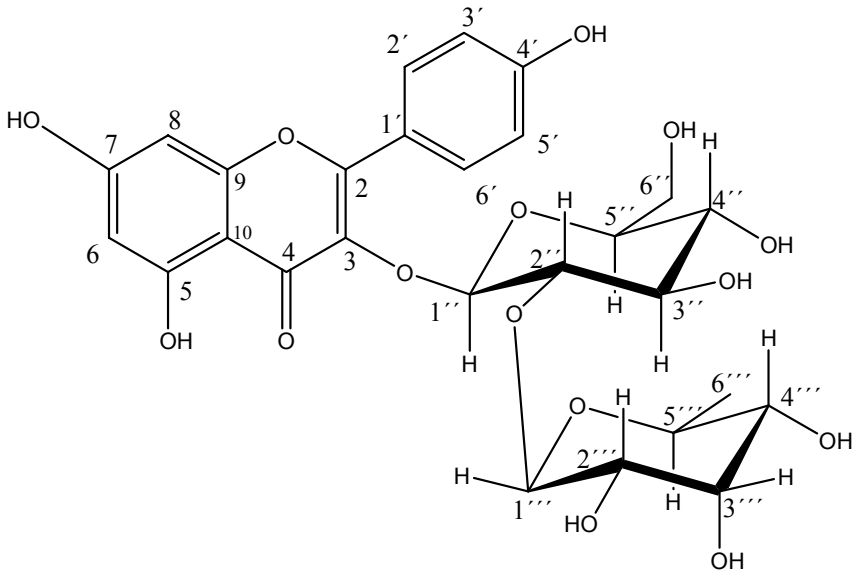

Kaempferol-3-*O*-β-D[2-O-α-rhamnopyranosyl]- glucopyranoside

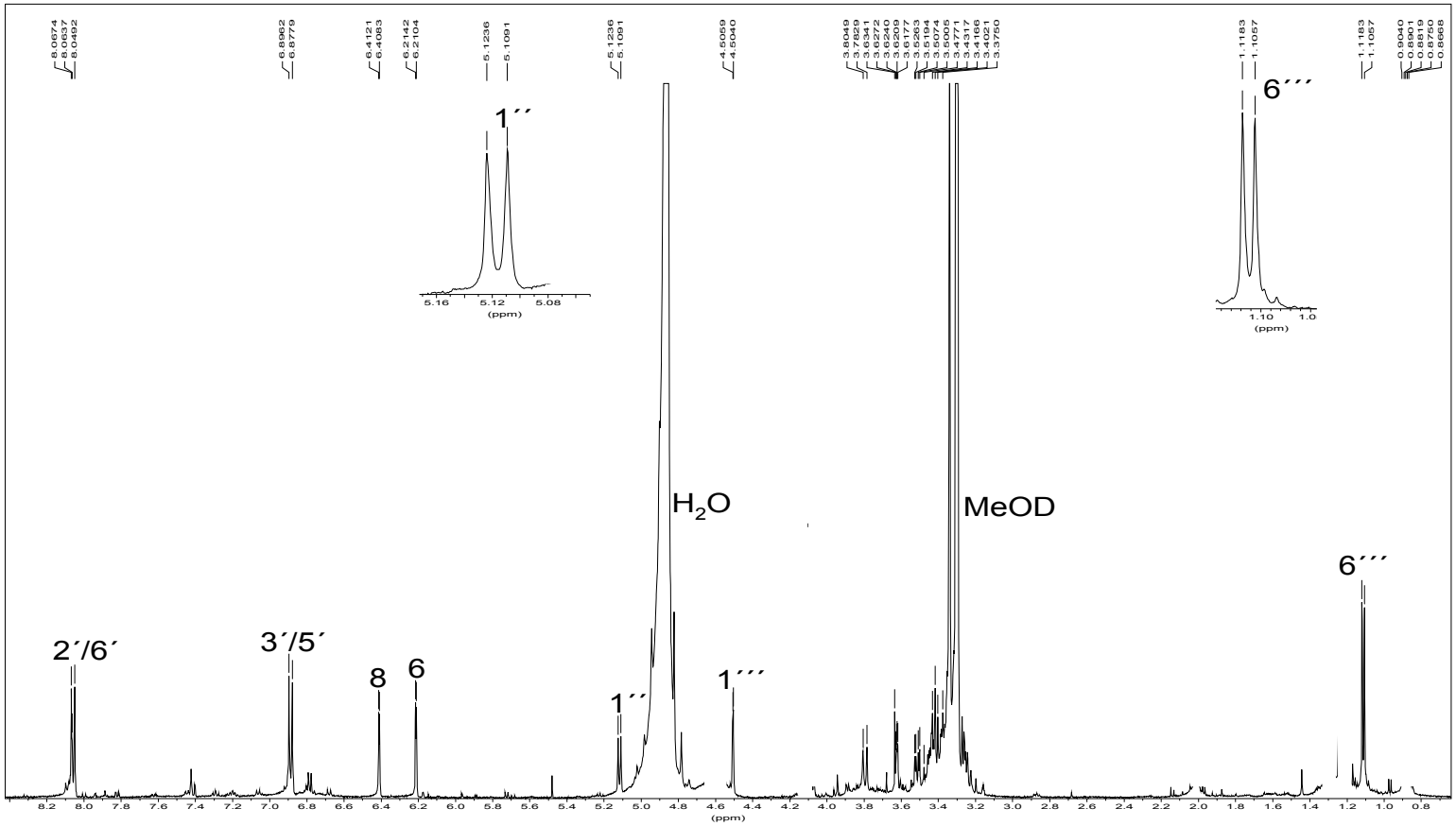

Fig. 3.59: ^{1}H NMR spectrum of compound 18 in MeOD

Table 3.29: ^{1}H NMR and COSY data of compound 18 (in MeOD)

Position	δ_H(ppm), *J* (Hz)	*δ_H(ppm),*J* Hz)	[a]δ_C(ppm)	COSY
aglycon				
2			156.8	
3			133.5	
4			177.9	
5			161.8	
6	6.33 (d, 2.2)	6.33 (d, 2.2)	99.4	
7			164.5	
8	6.13(d, 2.2)	6.13(d, 2.2)	94.7	
9			156.9	
10			104.8	
1′			121.7	
2′	7.98(d, 8.8)	7.98(d, 8.8)	131.5	3′
3′	6.81(d, 8.8)	6.81(d, 8.8)	115.8	2′
4′			160.6	
5′	6.81(d, 8.8)	6.81(d, 8.8)	115.7	6′
6′	7.98(d, 8.8)	7.98(d, 8.8)	131.4	5′
glucose				
1′′	5.02 (d, 6.9)	5.65(d, 7.8)	98.9	2′′
2′′	3.35 (t, 9.0)	3.42 (t, 9.0)	78.0	1′′, 3′′
3′′		3.37 (t, 9.0)	77.8	2′′, 4′′
4′′		3.08 (t, 9.0)	71.2	3′′, 5′′
5′′		3.07 (m)	77.5	4′′, 6′′
6′′ A: B:		3.27 (m) 3.53 (m)	61.4	5′′
rhamnose				
1′′′	4.41 (d, 1.9)	5.07 (bs)	101.0	2′′′
2′′′	3.53(dd, 1.9, 3.2)	3.72(dd, 4.2,9.6)	70.5	1′′′, 3′′′
3′′′	3.69(dd, 1.3,10.1)	3.46(dd, 3.0,9.6)	70.8	2′′′, 4′′′
4′′′		3.12(t, 9.0)	72.2	3′′′, 5′′′
5′′′	4.08 (ddd, 6.3)	3.71(m)	68.9	4′′′, 6′′′
6′′′	1.04 (d, 6.3)	0.76(d, 6.0)	17.7	5′′′

*: Literature [Rikke *et al.,* 1999], in DMSO

[a]: ^{13}C data extract from HMBC

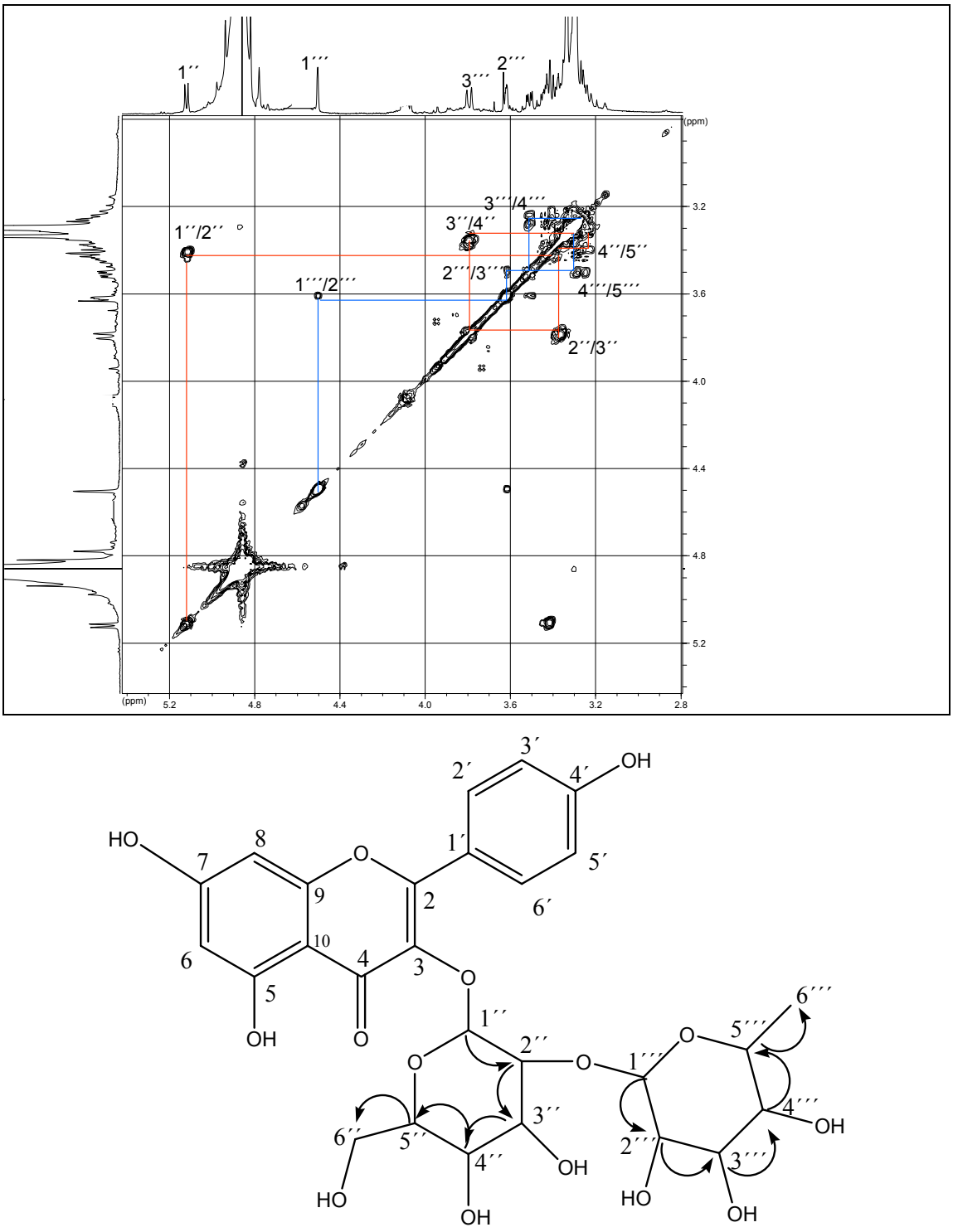

Fig. 3.60: ^{1}H-^{1}H-COSY correlations of compound 18 in MeOD

III.2.4.7. Kaempferol 3-O-(4-hydroxy-E-cinnamoyl)-(β)-glucopyranosyl (19, known compound)

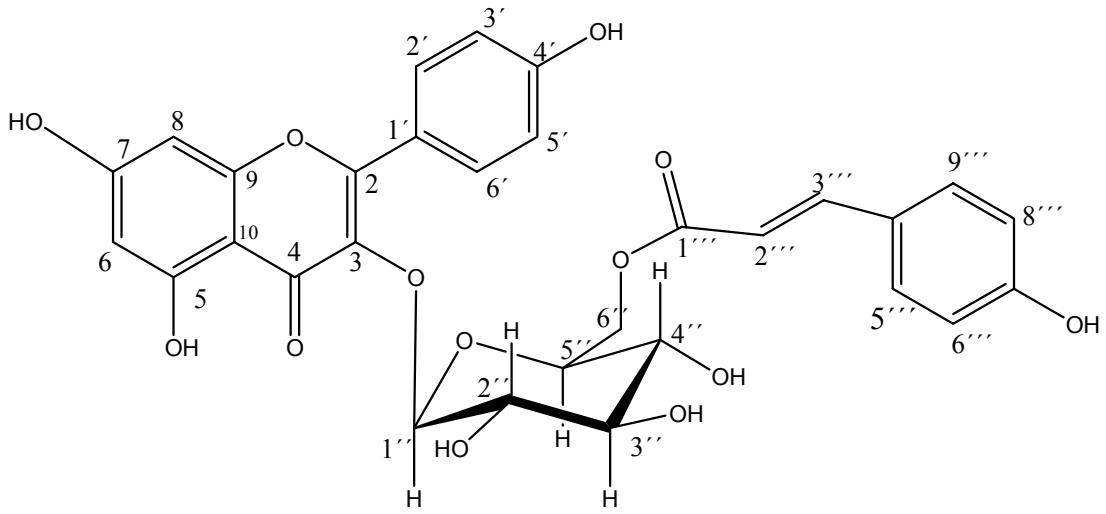

Fig. 3.61: ESI-MS and UV spectrum of compound 19

Compound **19** was isolated from the leaves of *Aglaia oligophylla* Miq as yellow crystalline needles (see Scheme 2.8), $[\alpha]^{20}_{D}$-25 (*c*, 0.5, MeOH), UV (MeOH) λ_{max} 205.7, 266.6, and 313.5 nm (see Fig. 3.61). The ESI-MS positive mode showed the pseudomolecular ion peaks at *m/z* 617.1 $[M+Na]^+$, and at *m/z* 594.9 $[M+H]^+$, respectively (see Fig. 3.61). The fragment ion peaks occurred at *m/z* 309.0 $[M+Na-308]^+$, and at *m/z* 278.2 $[M+H-308]^+$.

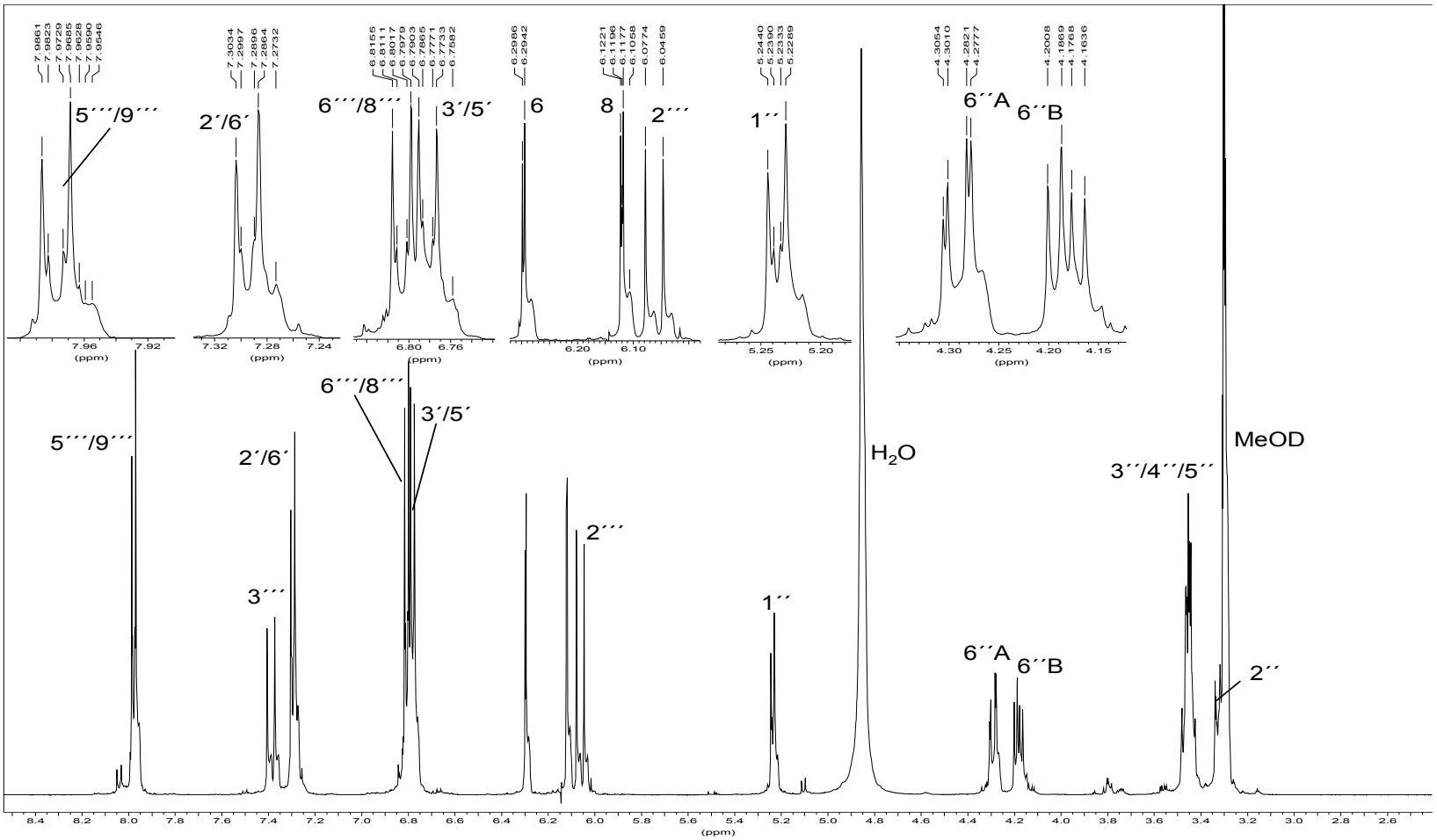

Fig. 3.62: ^{1}H NMR spectrum of compound 19 in MeOD

The ^{1}H NMR spectrum of compound **19** revealed the presence of a cinnamoyl moiety, as explained by the 146 mass unit fragment. The olefinic protons revealed a typical *trans*-configuration with the coupling constant of 15.7 Hz, which resonated at δ 7.38 and at δ 6.05. The characteristic AA´BB´ pattern of the cinnamoyl moiety, which occurred at δ 7.98 (2H, d, 8.8) and at δ 6.79 (2H, d, 8.8), indicated the *para*-substitution pattern. Besides, the characteristic AA´BB´ pattern of ring B was also observed as found in compound **18** at δ 7.29 (2H, d, 8.8) and at δ 6.78 (2H, d, 8.8) (see Fig. 3.62). The presence of two *meta*-protons of ring A at δ 6.29 (d, 2.2) and at δ 6.11 (d, 2.2), indicated protons H-6 and H-8, respectively. Moreover, the ^{1}H NMR spectrum of compound **19** revealed an anomeric proton (H-1´´) signal at δ 5.23 (d, 7.5). The spin system of this glucose was shown in the ^{1}H-^{1}H COSY spectrum (see Fig. 3.63). The connectivity of the monsaccharide unit with the flavonoid and cinnamoyl moiety was established on the basis of HMBC correlations (see Fig. 3.64 and Fig. 3.65). The anomeric proton H-1´´ with the chemical shift (δ 5.23 ppm) correlates with C-3 (δ 134.5 ppm). Besides, this anomeric proton H-1´´ also correlates with C-5´´ (δ 74.9 ppm). In particular the lower field shifts of H-6´´A and H-6´´B (δ 4.29, 4.18 ppm) showed direct correlation with C-6´´ (δ 63.3 ppm) and C-1´´´ (δ 167.6) while only H-6´´B correlates with C-3´´(δ 74.8 ppm) through a W long-range correlation. Compound **19** was determined to be kaempferol 3-*O*-(4-hydroxy-*E*-cinnamoyl)-(β)-glucopyranosyl.

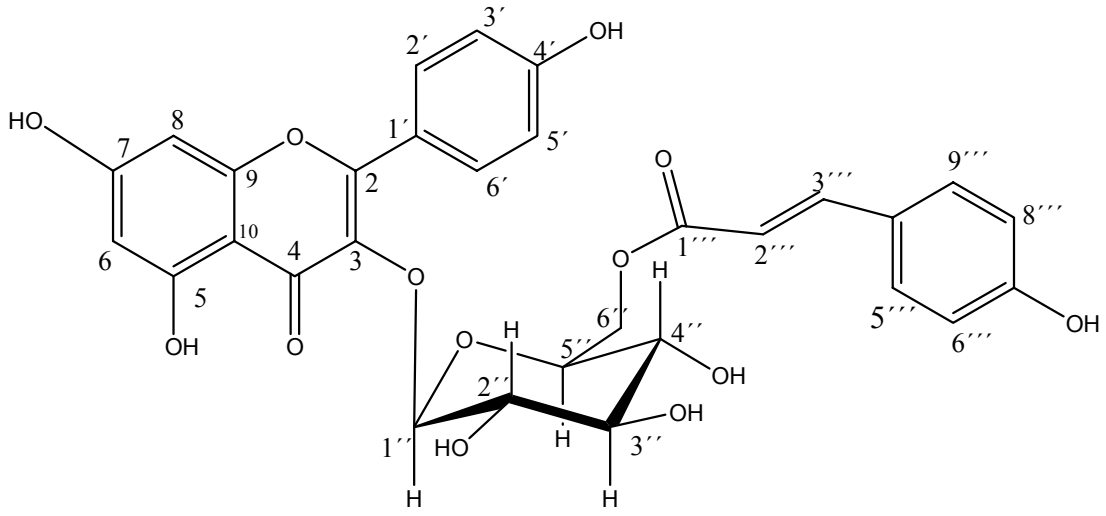

Kaempferol 3-*O*-(4-hydroxy-*E*-cinnamoyl)-(β)-glucopyranosyl

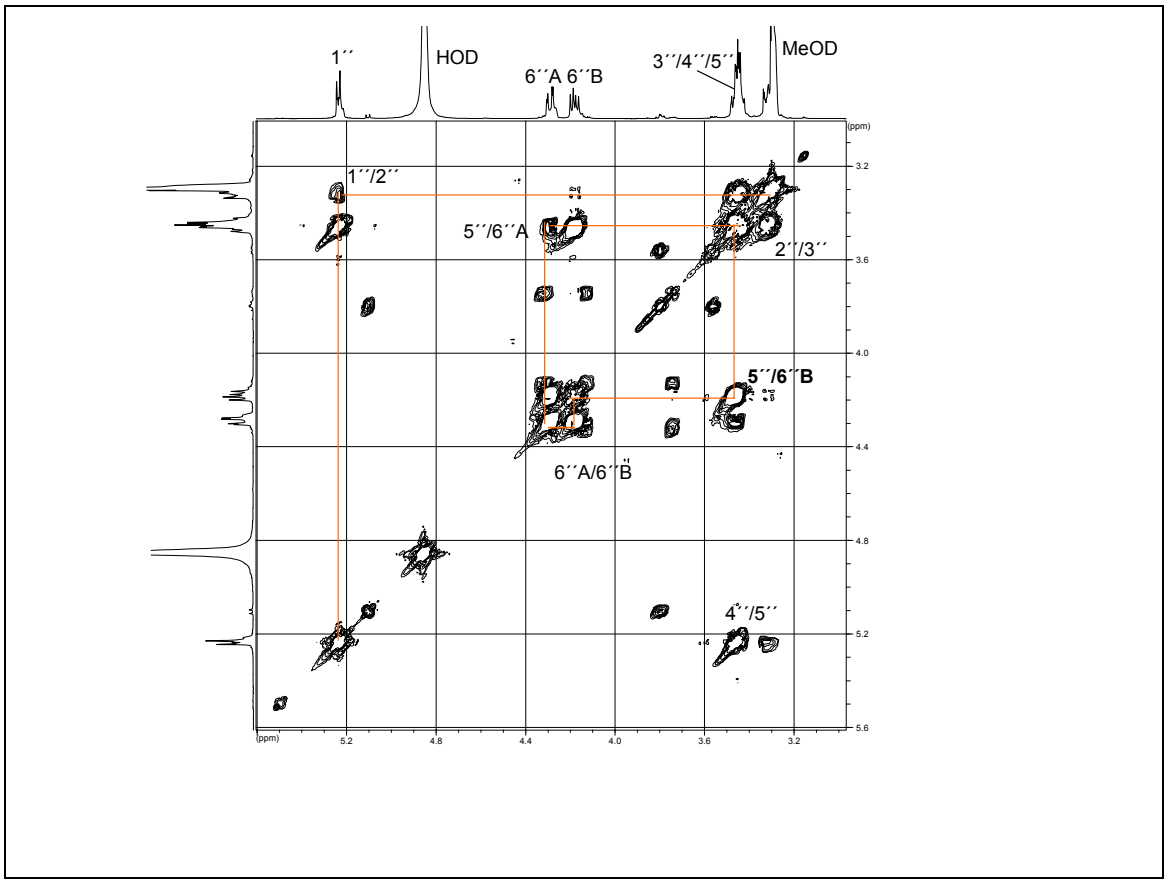

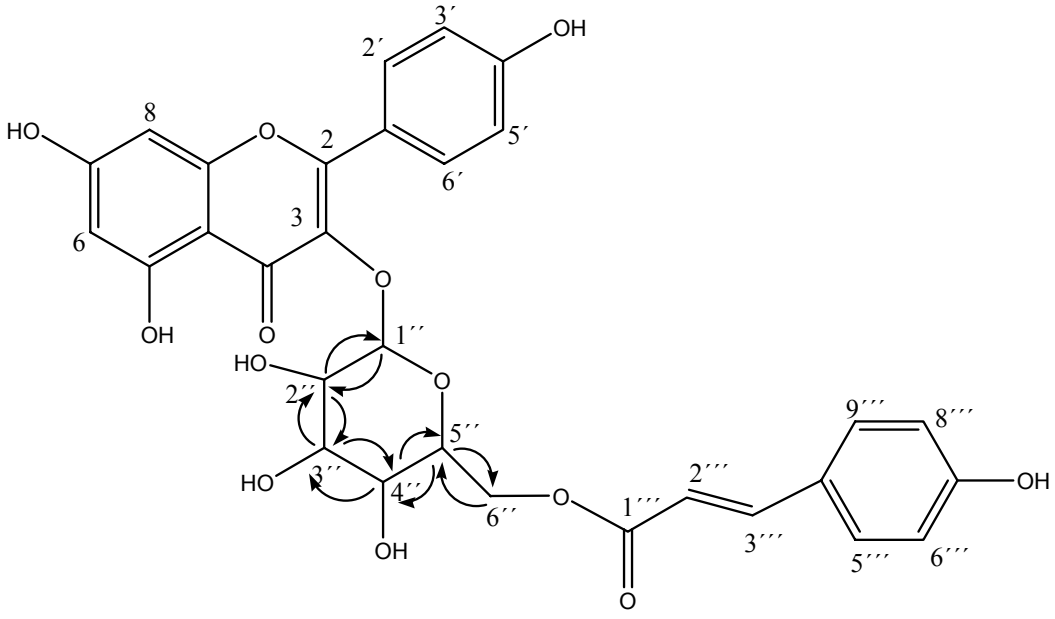

Fig. 3.63: ^{1}H-^{1}H-COSY correlations of sugar moiety of compound 19 in MeOD

Table 3.30: ^{1}H NMR and COSY data of compound 19 in MeOD

Position	δ_H(ppm), *J* (Hz)	*δ_C(ppm)	COSY
aglycon			
2			
3			
4			
5			
6	6.29 (d,2.2)		
7			
8	6.11(d,2.2)		
9			
10			
1′			
2′	7.29(d, 8.8)		3′
3′	6.78(d, 8.8)		2′
4′			
5′	6.78(d, 8.8)		6′
6′	7.29(d, 8.8)		5′
glucose			
1′′	5.23 (d, 7.5)		2′′
2′′			1′′, 3′′
3′′			2′′, 4′′
4′′			3′′, 5′′
5′′			4′′, 6′′
6′′ A B	4.29(dd, 7.0, 12.0) 4.18(dd, 6.6, 12.0)		5′′
7′′′-hydrxy-cinnamoyl			
1′′′			
2′′′	6.05 (d, 15.7)		
3′′′	7.38 (d, 15.7)		
4′′′			
5′′′	7.98 (d, 8.8)		
6′′′	6.79 (d, 8.8)		
7′′′			
8′′′	6.79 (d, 8.8)		
9′′′	7.98 (d, 8.8)		

*:^{13}C NMR data was extracted from HMBC

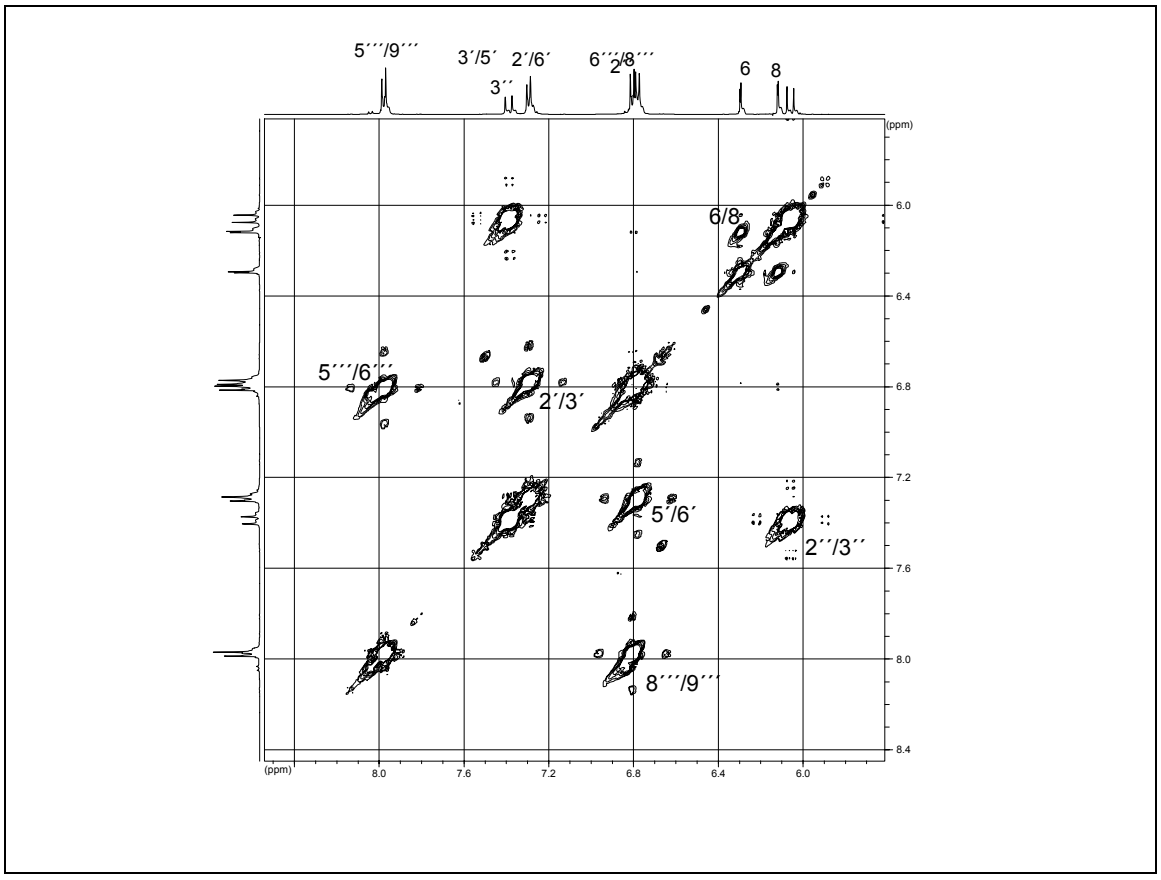

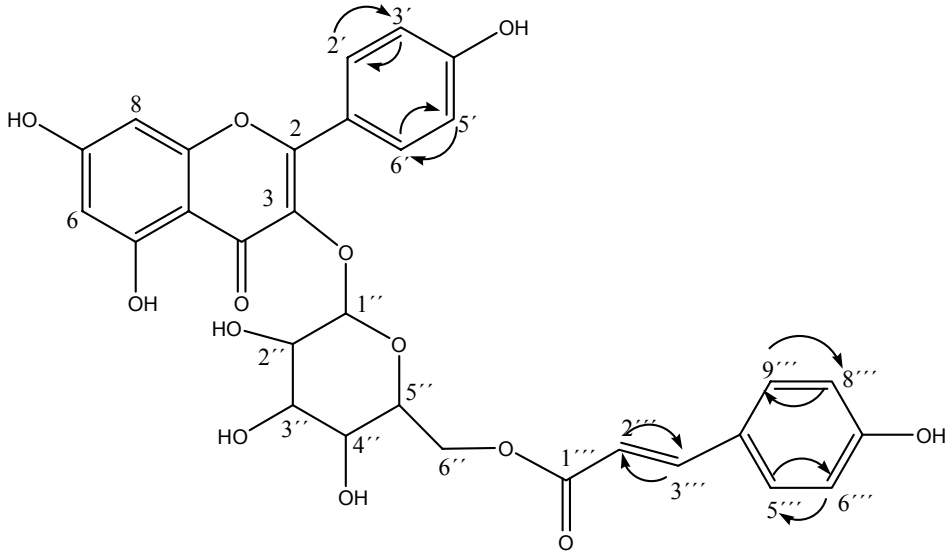

Fig. 3.64: ^{1}H-^{1}H COSY correlations of compound 19 in MeOD (at lowfield)

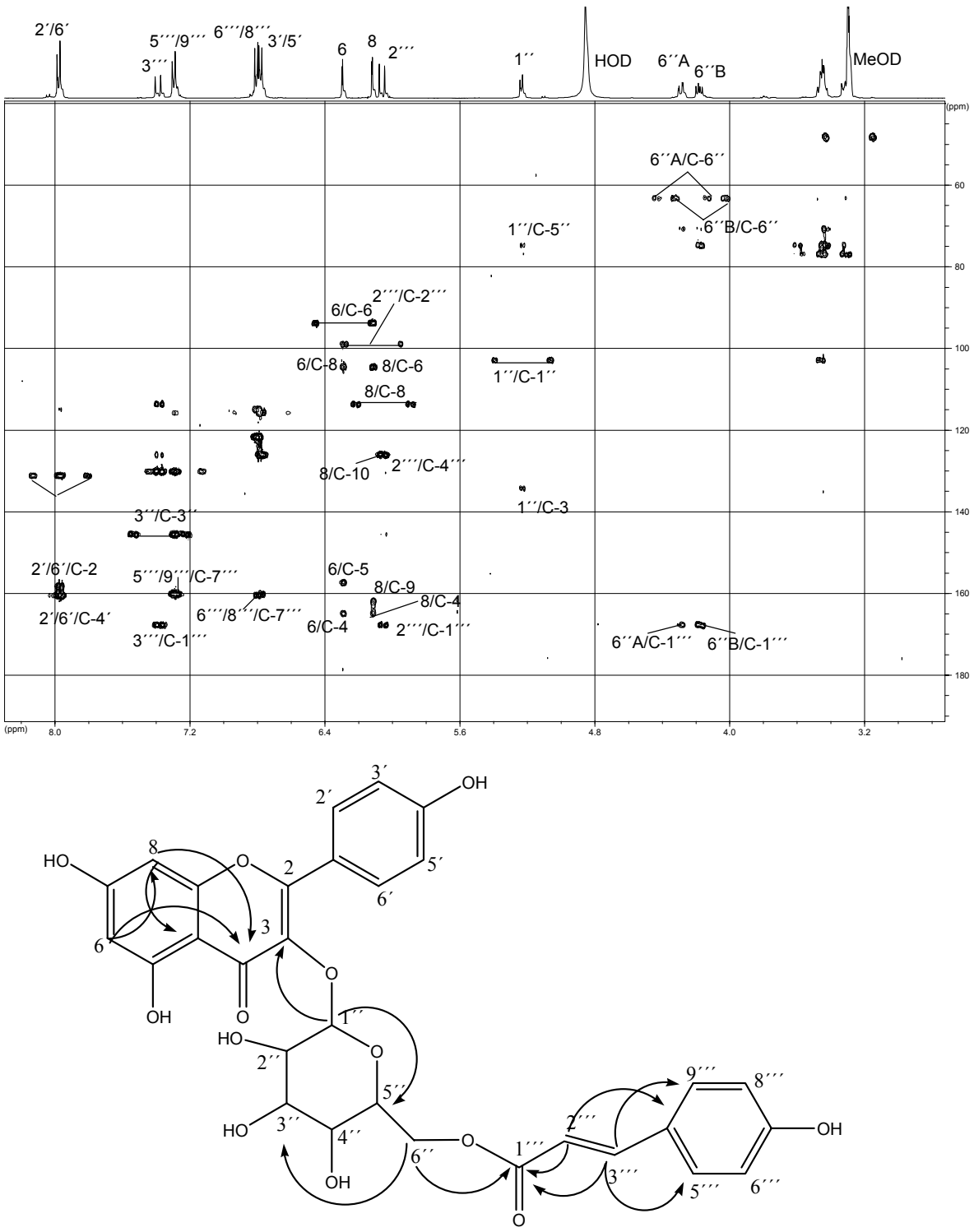

Fig. 3.65: HMBC correlations of compound 19 in MeOD

III.2.5. Cinnamoyl bisamide derivatives from *Aglaia* sp.

III.2.5.1. Dasyclamide (20, known compound)

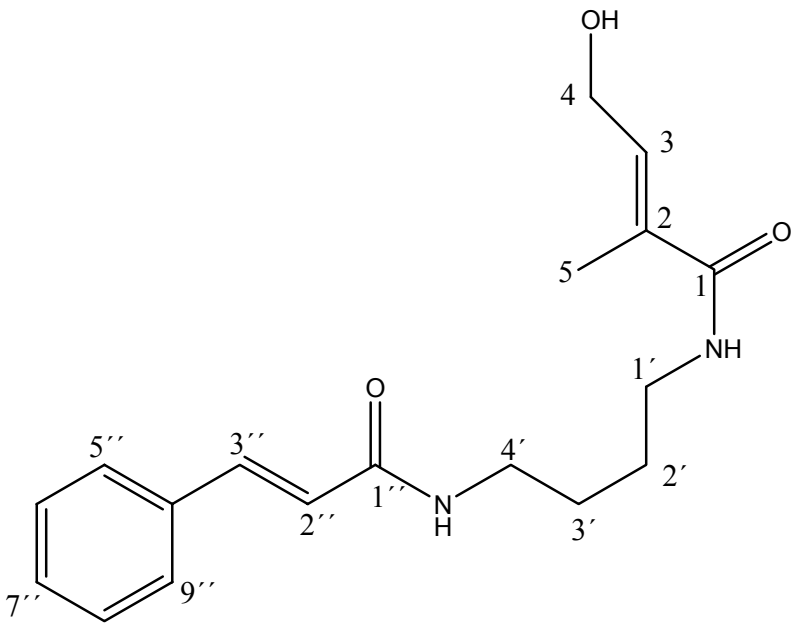

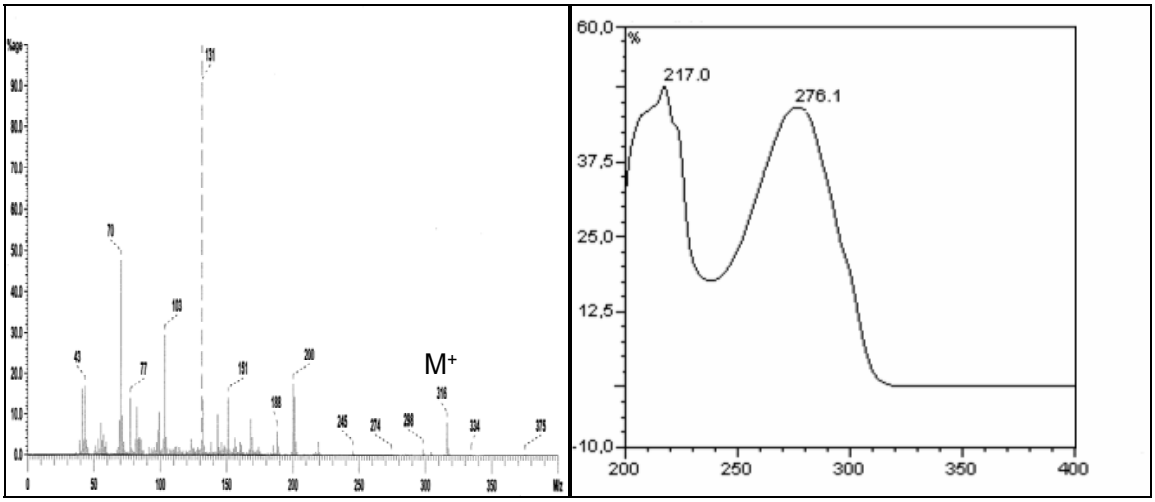

Fig. 3.66: EI-MS and UV spectrum of compound 20

Compound **20** was obtained as white crystalline needles from the leaves of *Aglaia gigantea*; UV (MeOH) λ_{max} 217.0 and 276.1 nm (see Fig. 3.66). The positive ESI-MS showed the pseudomolecular ion peaks at *m/z* 317.3 $[M+H]^+$, 339.3 $[M+Na]^+$, and at 655.3 $[2M+Na]^+$, respectively (see Fig. 3.66).

The negative mode ESI-MS showed pseudomolecular peaks at *m/z* 315.9 $[M-H]^-$, 361.8 $[M+HCOOH]^-$, 677.9 $[2M+HCOOH-H]^-$. The EI-MS showed a molecular ion peak at *m/z* 316 $[M]^+$ (see Fig. 3.66). This molecular weight is in accordance with the 1D and 2D NMR data. The presence of a cinnamoyl moiety was indicated by the appearance of ion peaks at *m/z* 131 $[PhCH=CHCO]^+$ and 103 $[PhCH=CH]^+$ (see Fig. 3.66). In addition, compound **20** posseses a putrescine group, with amide linkages to two carboxylic acids. ^{1}H NMR spectrum of compound **20** is similar to that of grandiamide B (**21**) [Rechard Detterbeck *et al* 2002]. The only difference in the ^{1}H NMR (in MeOD) spectrum of compound **20** from that of grandiamide B is the absence of a methyl signal as found in the tiglic acid moiety [Chaidir *et al* 2001]. The molecular ion peak of compound **20** is 16 mass units larger than that of grandiamide B, and the presence of a methylene signal at 4.22 ppm (dd,*J*=6.3Hz; 0.9Hz) indicated that C-4 of the tiglic acid moiety was substituted by a hydroxyl group in compound **20**. The presence of a putrescine group [δ1.59 - 1.61, 4H, m, -HN(CH_2)($\underline{CH_2}$)$_2$(CH_2)NH- and 3.20 – 3.24 , 4H, m,-HN($\underline{CH_2}$)(CH_2)$_2$($\underline{CH_2}$)NH-] was shown in the ^{1}H NMR (in MeOD) spectrum (see Fig. 3.67). These four methylene signals were also confirmed by the DEPT spectrum (see Fig. 3.69) and their assignments were elucidated by ^{1}H-^{1}H COSY (see Fig. 3.70). The ^{13}C NMR spectrum of dasyclamide revealed the presence of 18 carbons (see Table 3.32 and Fig. 3.68), which included two amide carbonyl carbons resonating at 172.0 (C-1´´) and 168.6 ppm (C-1) (see Table 3.32). Furthermore, in its ^{1}H NMR spectrum in DMSO two amino protons (NH) appeared at 7.82 ppm (t,*J*=5.7 Hz) and 8.15 ppm (t,*J*=5.7 Hz).The proton signal of H-3 appeared as a triplet of a quatet at 6.34 ppm (tq, *J*=1.6Hz; 6.0 Hz). Two proton doublets, H-2´´ and H-3´´ resonated at 6.60 and 7.40 ppm with a coupling constant of 15.7 Hz which indicated a *trans*-configuration at the double bond. Through the ^{1}H-^{1}H COSY (see Fig. 3.70), HMQC (see Fig.3.71), and HMBC (see Fig. 3.72) spectra, all signals of compound **20** were completely assigned as those of dasyclamide, a known compound which was isolated from the leaves of *Aglaia dasyclada* obtained from China [Chaidir *et al* 2001]. Dasyclamide was also determined by X-ray crystallography (see Fig. 3.73). All crystal structure data of dasyclamide are shown in Table 3.33, Table 3.34 and Table 3.35.

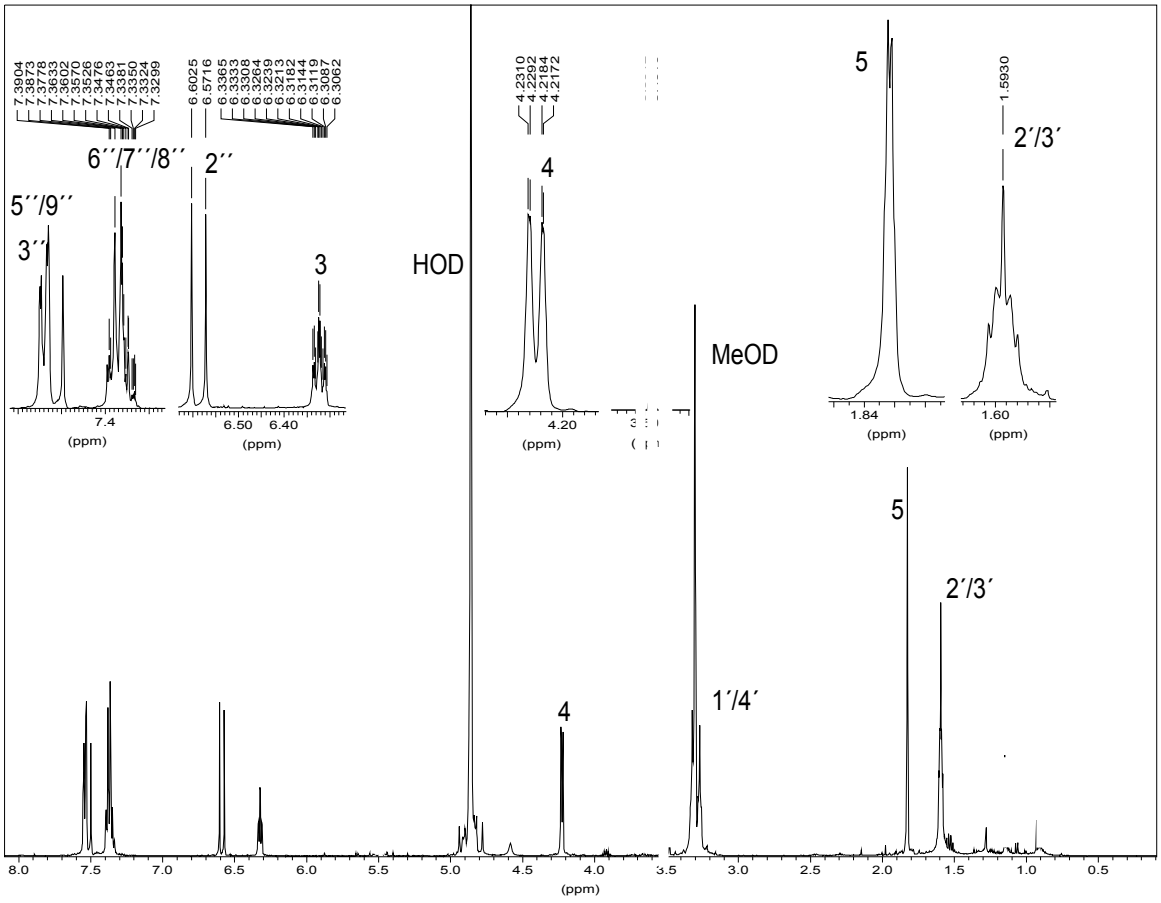

Fig. 3.67:[13]H NMR of compound 20 in MeOD

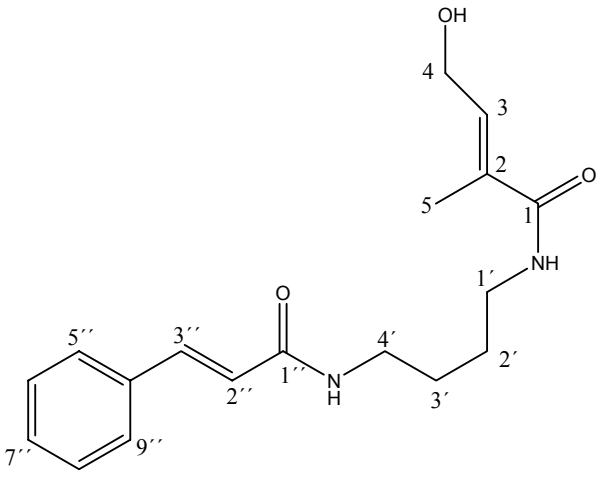

Dasyclamide

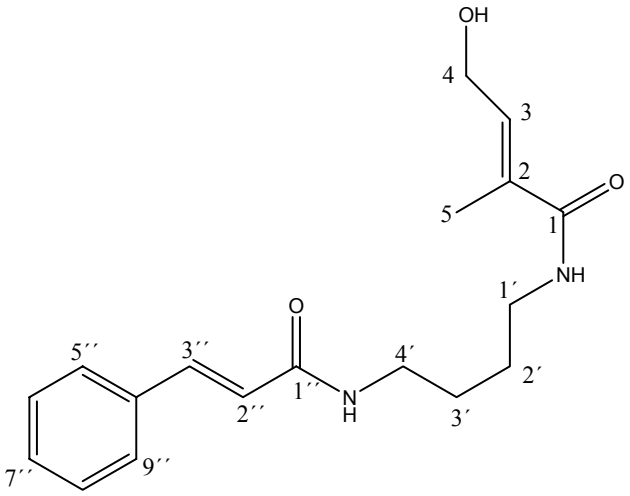

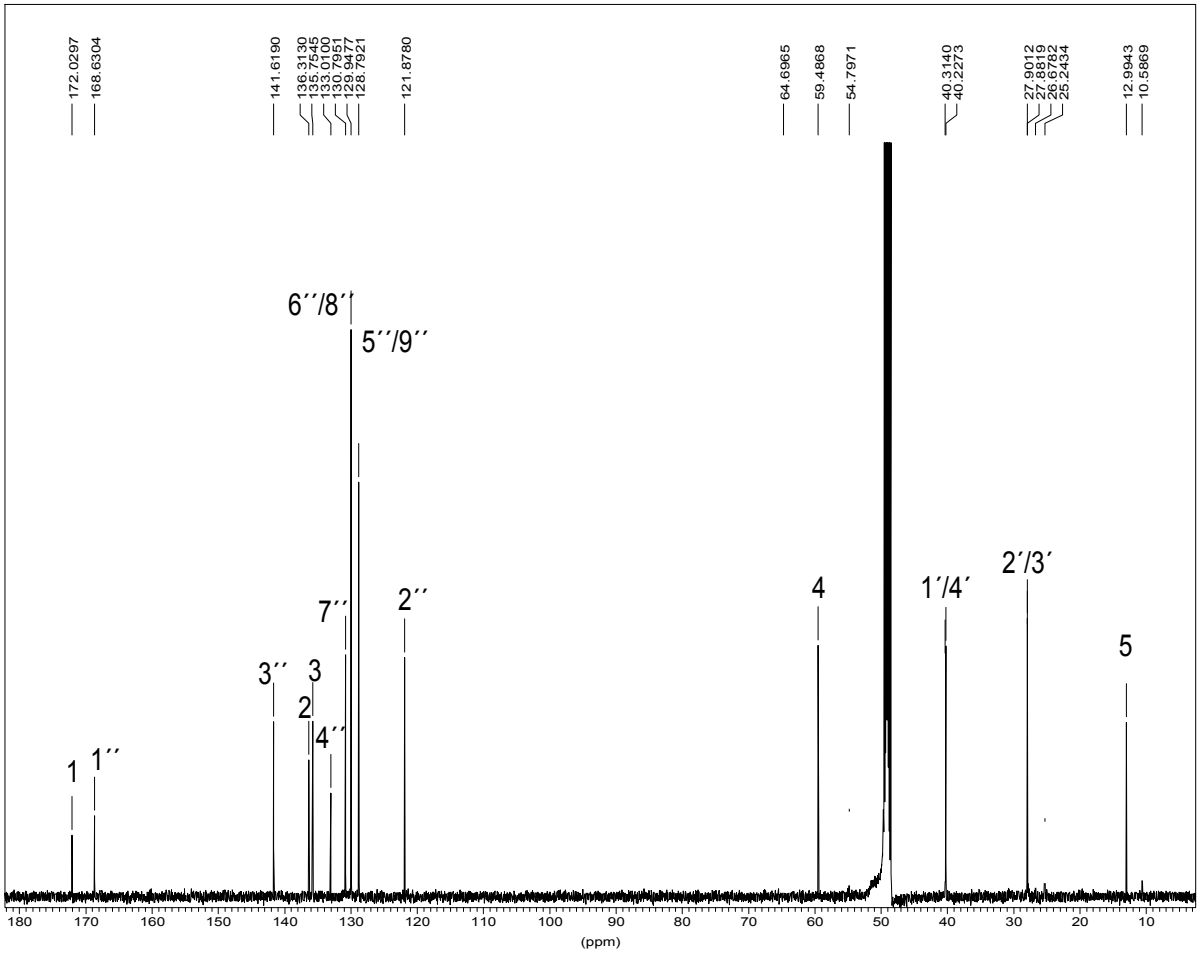

Fig. 3.68: ^{13}C NMR of compound 20 in MeOD

Table 3.31: ^{1}H NRM data of compounds 20, 21, 22, 23, 24 and 25 (in MeOD)

^{1}H position	20	21	22	23	24	25
2				2.25 m		
3	6.33 (*qt*, 1.2,5.7)	6.30(*dq*,6.9, 1.1)	4.40 (*dd*,3.8, 6.3)	A: 1.58 m B: 1.30 m	A: 1.80 m B: 1.71 m	6.62(*dq*, 1.6, 3.2)
4	4.22(*dd*,6.3,0.9)	1.65(*dd*,6.9, 1.1)	A:3.55(*dd*,11.4, 4.4) B:3.40 (*dd*, 11.4, 6.9)	0.70 t	0.78 t	5.33 (*d*, 3.1)
5	1.82(*dt*)	1.73 (*t*, 1.0)	A: 5.69 B: 5.52 exomethylen	1.10(*d*,16.9)	1.30s	1.75(*dt*,1.3, 1.9)
1´	3.30 m	3.30 m	3.30 m			3.53 (*m*,2H)
2´	1.60 m	1.49 m	1.51 m	6.12(*dd*,4.4,11.9)	6.03(*dd*,2.2, 6.9)	1.67 m
3´	1.60 m	1.49 m	1.51 m	A: 2.20m B: 2.15 m	A: 2.25 m B: 1.86 m	1.60 m
4´	3.30 m	3.30 m	3.30 m	A: 2.1 m B: 1.1.95 m	A: 2.0 m B: 1.90 m	3.30 m
5´				A: 3.70 m B: 3.48 m	A: 3.65 m B: 3.45 m	
2´´	6.58 (*d*, 15.7)	6.58(*d*, 15.7)	6.49(*d*, 15.7)	7.05(*d*, 15.5)	6.93(*d*, 15.5)	6.58 (*d*, 15.7)
3´´	7.39 (*d*, 15.7)	7.53 (*d*, 15.7)	7.40(*d*, 15.7)	7.55(*d*, 15.5)	7.50(*d*, 15.5)	7.53 (*d*, 15.7)
5´´/9´´	7.49 m	7.54 m	7.44 m	7.58 m	7.50 m	7.55 m
6´´/8´´	7.36 m	7.37 m	7.27 m	7.37 m	7.30 m	7.36 m
7´´	7.37 m	7.52 m	7.44 m	7.54 m	7.48 m	7.54 m

Table 3.32: ^{13}C NMR data of compounds 20, 22 & 25 (in MeOD)

Position ^{13}C	20	22*	25*
1	172.0 s	170.0	170.9 s
2	133.0 s	145.5	130.2 s
3	136.1 d	72.5	137.5 d
4	59.4 t	65.5	82.4 d
5	13.4 q	123.2	11.3 q
1′	40.3 t	39.1 t	39.4 t
2′	28.3 t	26.8 t	25.5 t
3′	28.3 t	26.8 t	27.4 t
4′	40.7 t	39.1 t	39.0 t
1′′	168.6 s	168.0	167.2 s
2′′	121.8 d	121.0	120.6 d
3′′	141.6 d	140.8	141.9 d
4′′	136.3 s	135.7	138.4 s
5′′/9′′	128.7 d	129.0	128.2 d
6′′/8′′	130.7 d	129.8	129.2 d
7′′	130.7 d	129.8	130.2 d

*: obtained from the HMBC spectrum

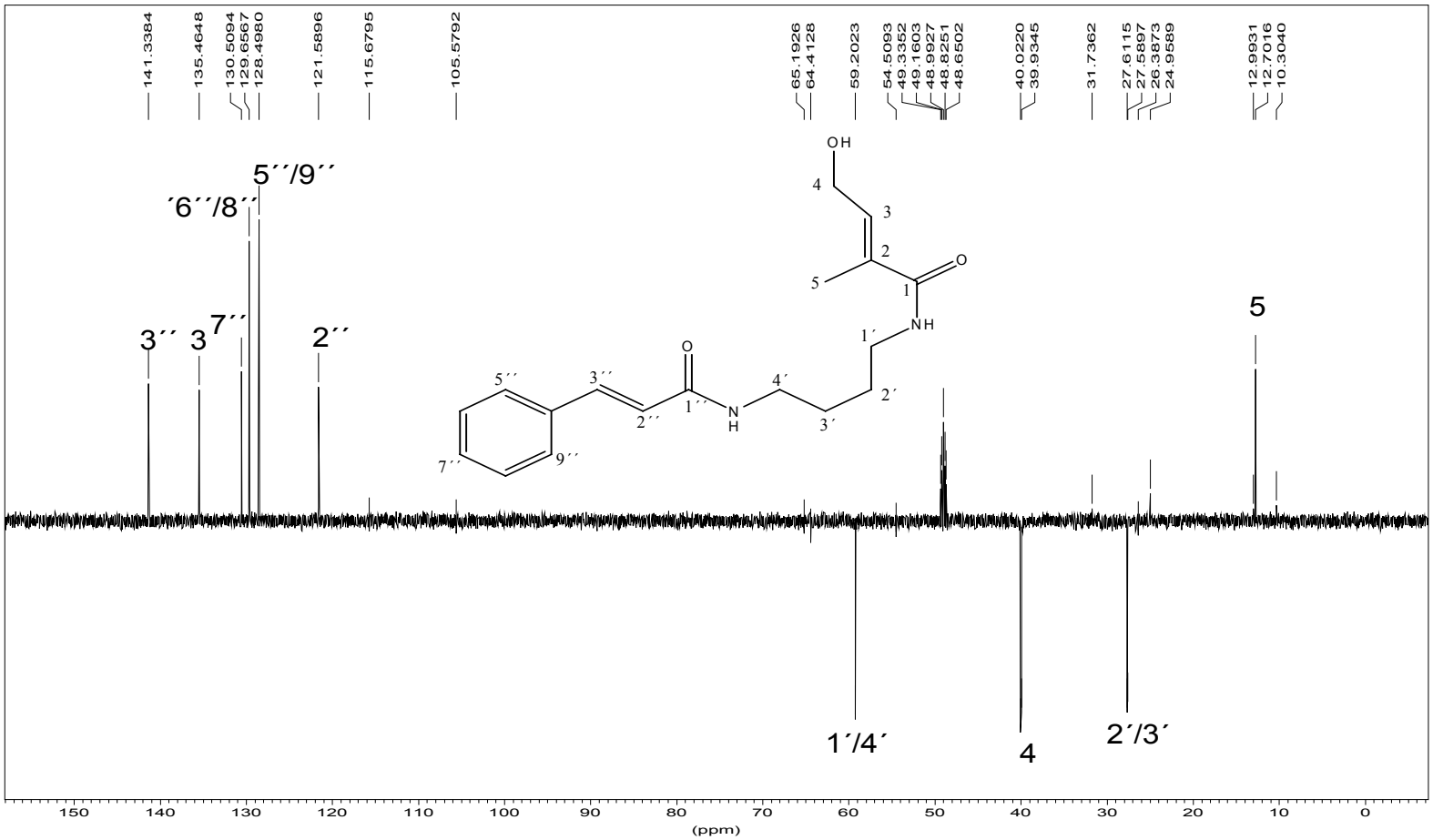

Fig. 3.69: DEPT spectrum of compound 20 in MeOD

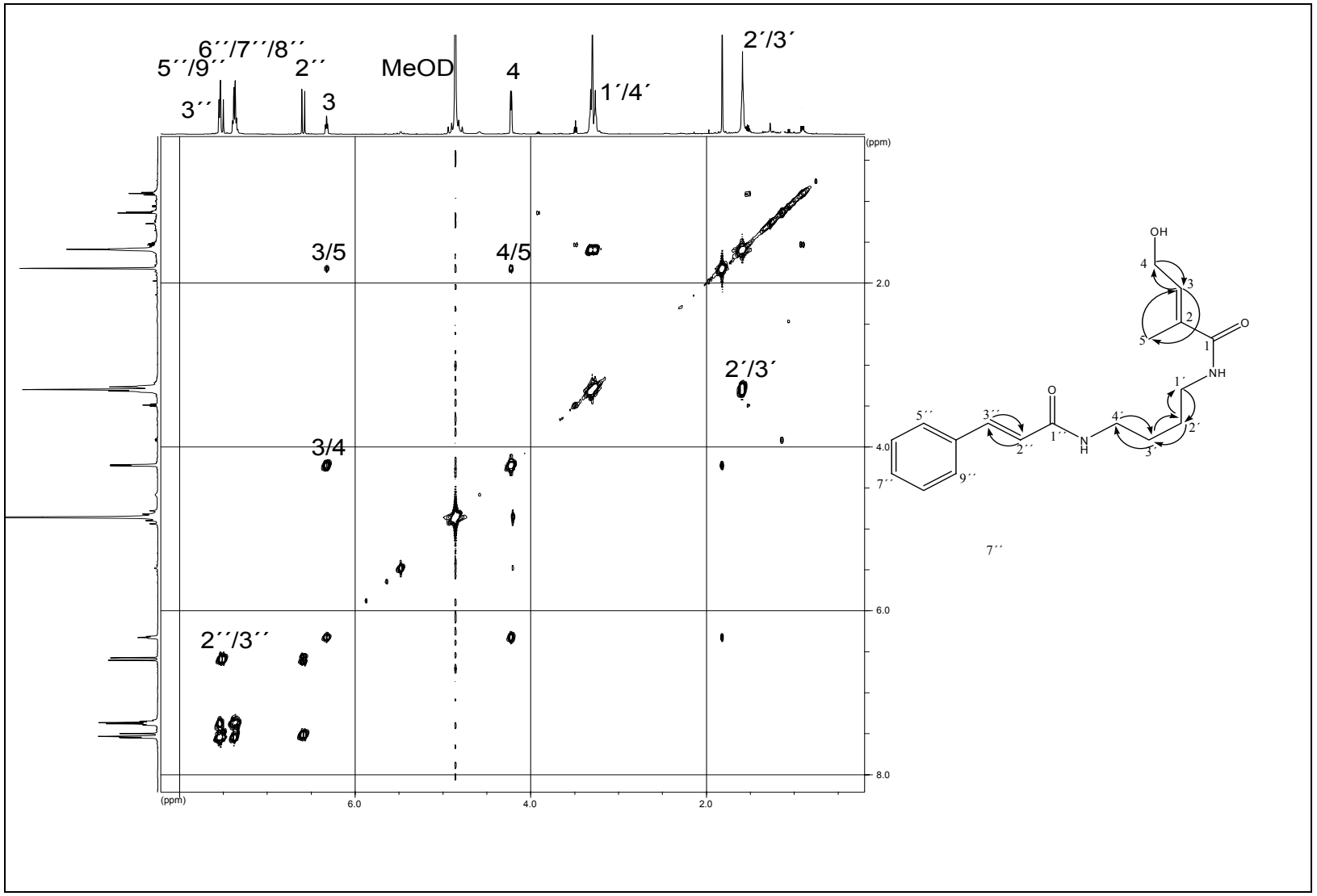

Fig. 3.70: COSY correlations of compound 20 in MeOD

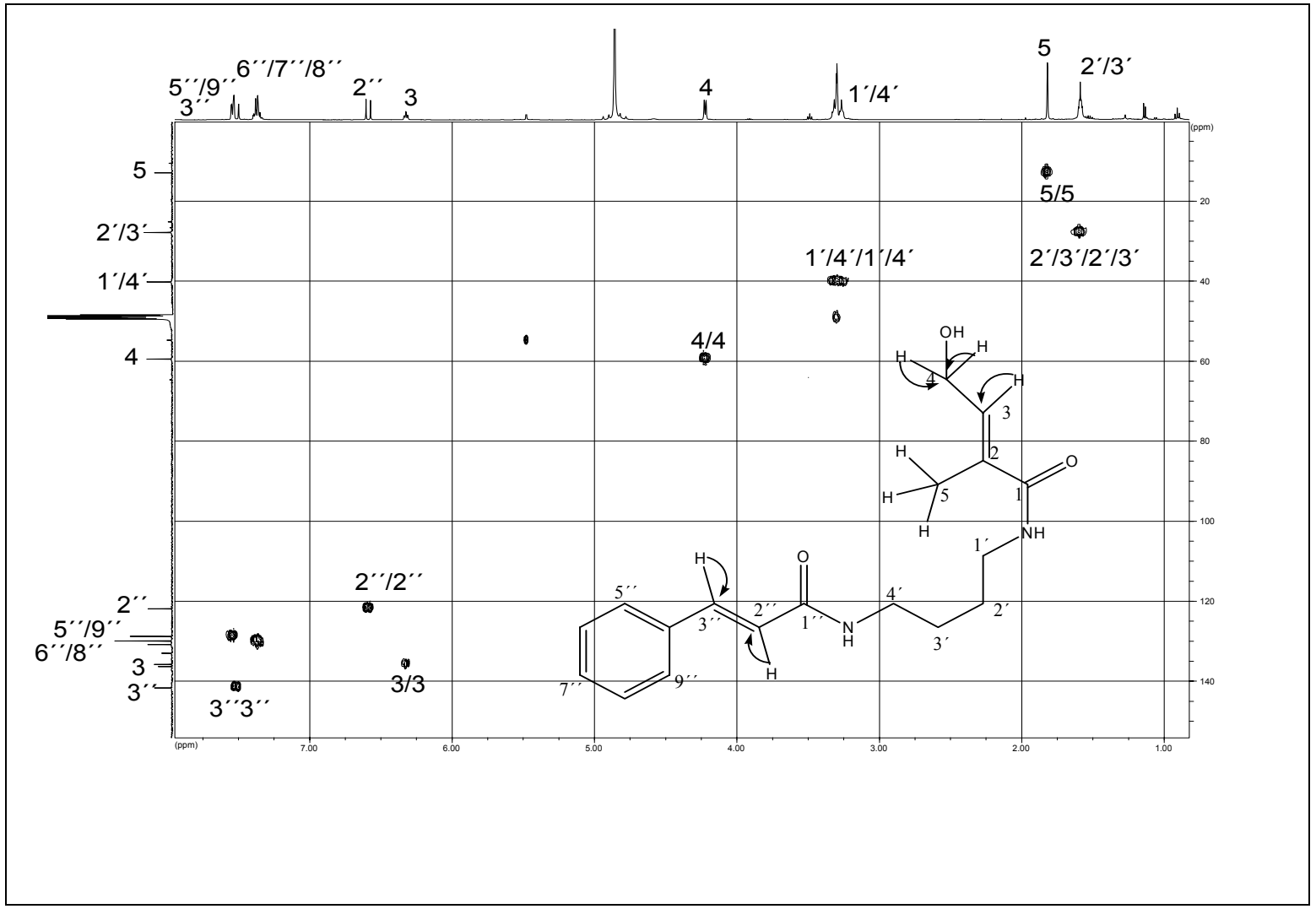

Fig. 3.71: Important direct HMQC correlations of compound 20 in MeOD

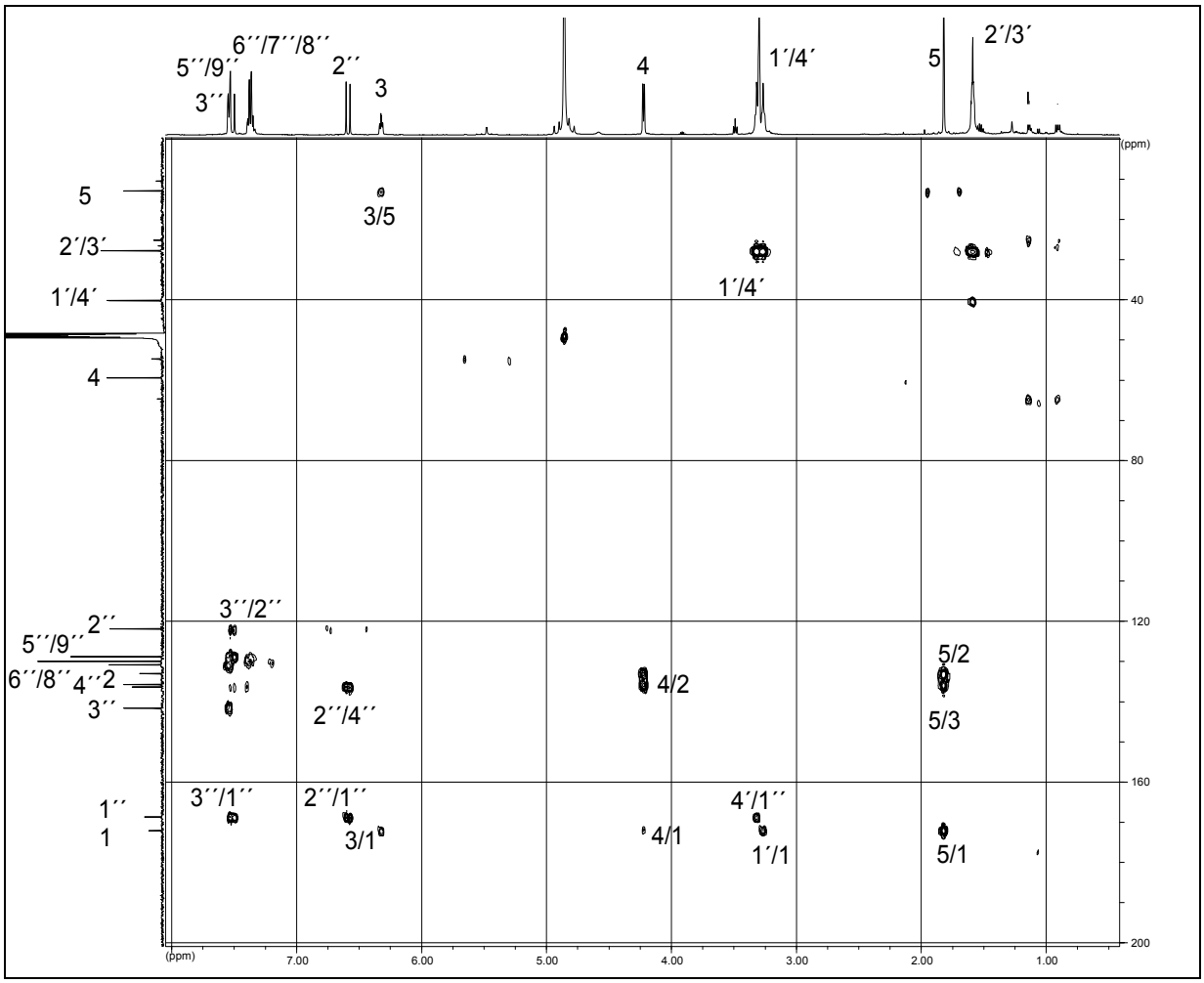

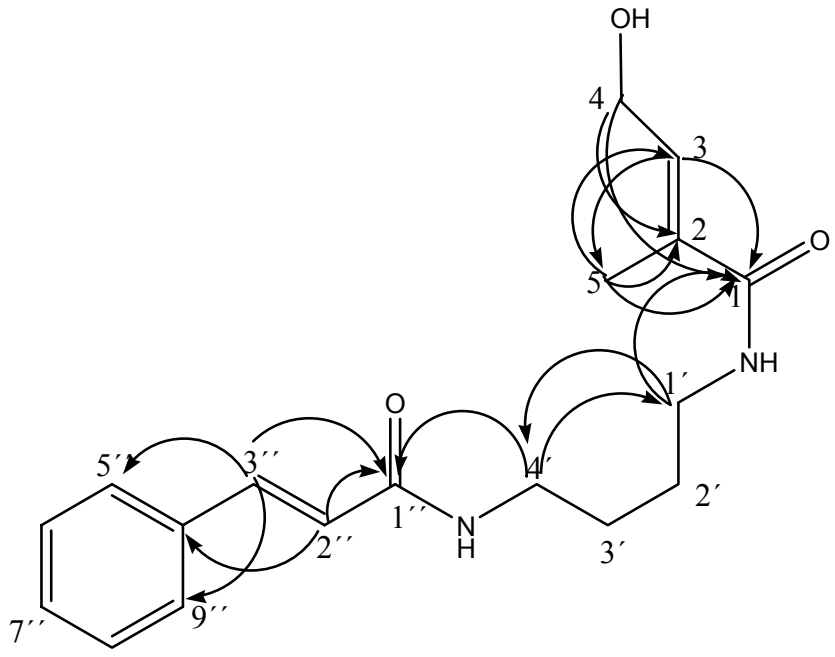

Fig. 3.72: HMBC correlations of compound 20 in MeOD

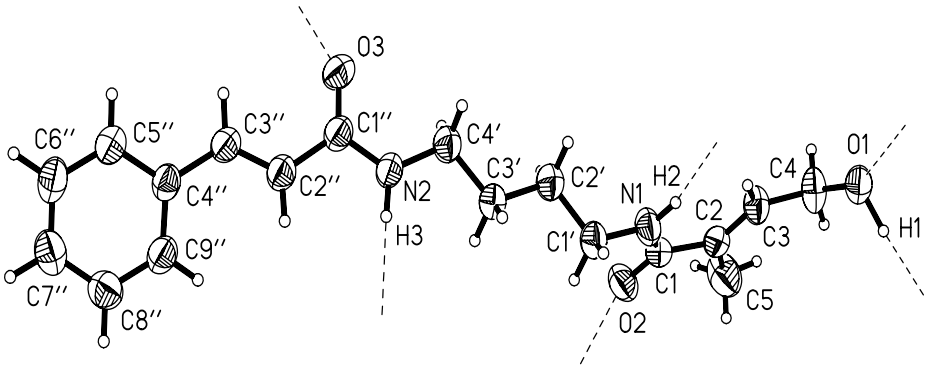

Fig. 3.73: X-ray structure of Dasyclamide

Table 3.33: Crystal data, X-ray measurements and structure determination summary for compound 20

Empirical Formula	$C_{18}H_{24}N_2O_3$
Formular weight	316.39
Crystal colour; habit	colourless, prism
Crystal size (mm^3)	0.4×0.3×0.15
Crystal system	monoclinic
Space group	$P2_1/c$
Unit cell dimensions	a = 7.7089(4) Å
	b = 16.8036(12) Å
	c = 13.2584(8) Å
	β = 100.454(7) °
Volume ($Å^3$)	1688.95(18)
Z	4
Density (calc.; $g \cdot cm^{-3}$)	1.244
Temperature (K)	291(2)
Diffractometer	STOE IPDS
Wavelength (Å)	Mo-K_α, λ = 0.71073
Absorption coefficient (mm^{-1})	0.085
F(000)	680
Data collection mode	φ-scans
θ Range (°)	$1.98 \leq \theta \leq 25.00$
Index ranges	$-9 \leq h \leq 9$; $-19 \leq k \leq 19$;
	$-15 \leq l \leq 15$
Reflections collected/unique	21836/2828 (R_{int} = 0.041)

Observed reflections [$I > 2\sigma(I)$]	1691
Data/parameters	2828/248
Goodness of fit on F^2	1.002
Final R indices [$I > 2\sigma(I)$]	$R_1 = 0.035$; $wR_2 = 0.060$
R indices (all data)	$R_1 = 0.059$; $wR_2 = 0.062$
Largest diff. peak/hole (e·Å^{-3})	0.274/–0.136

Table 3.34: Selected bond lengths (in Å) and angles (in °) for 20

O1-C4	1.411(2)	O1-C4-C3	112.25(17)
O2-C1	1.233(2)	C4-C3-C2	128.0(2)
O3-C1''	1.2344(18)	C3-C2-C1	122.66(18)
N1-C1	1.332(2)	C3-C2-C5	122.88(17)
N1-C1'	1.455(2)	C1-C2-C5	114.45(16)
N2-C1''	1.3276(19)	C2-C1-O2	119.99(18)
N2-C4'	1.452(2)	O2-C1-N1	121.69(17)
C1-C2	1.503(2)	C2-C1-N1	118.32(17)
C2-C3	1.310(2)	C1-N1-C1'	123.30(17)
C2-C5	1.496(3)	N1-C1'-C2'	115.13(15)
C3-C4	1.493(2)	C1'-C2'-C3'	110.64(15)
C1''-C2''	1.478(2)	C3'-C4'-N2	109.85(14)
C2''-C3''	1.316(2)	C4'-N2-C1''	123.15(15)
C3''-C4''	1.465(2)	N2-C1''-C2''	114.98(16)
C4''-C5''	1.385(2)	C1''-C2''-C3''	124.33(18)
C5''-C6''	1.379(2)	C2''-C3''-C4''	126.59(17)
C6''-C7''	1.362(2)	C3''-C4''-C5''	120.10(17)
C7''-C8''	1.373(2)	C3''-C4''-C9''	122.34(16)
C8''-C9''	1.377(2)	C4''-C5''-C6''	120.93(19)
		C5''-C6''-C7''	120.2(2)
		C6''-C7''-C8''	120.3(2)
		C7''-C8''-C9''	119.4(2)
		C8''-C9''-C4''	121.64(18)
		C9''-C4''-C5''	117.55(17)
		C3'-C2'-C4'	114.32(15)
		O3-C1''-N2	121.76(16)
		O3-C1''-C2''	123.23(15)

Table 3.35: The hydrogen bond geometries (in Å and °) for 20

D–H···A	D–H	H···A	angle	D···A
O1–H1···O3*a*	1.09	1.56	174.9	2.6471(17)
N1–H2···O1*b*	0.91	2.04	160.8	2.919(2)
N2–H3···O2*c*	0.92	1.97	175.8	2.8898(19)

Symmetry transformations used to generate equivalent atoms:

a x+1, y, z+1 ; *b* –x+2, -y+1, -z+1 ; *c* x,-y+3/2, z-1/2

III.2.5.2. Grandiamide B (21, known compound)

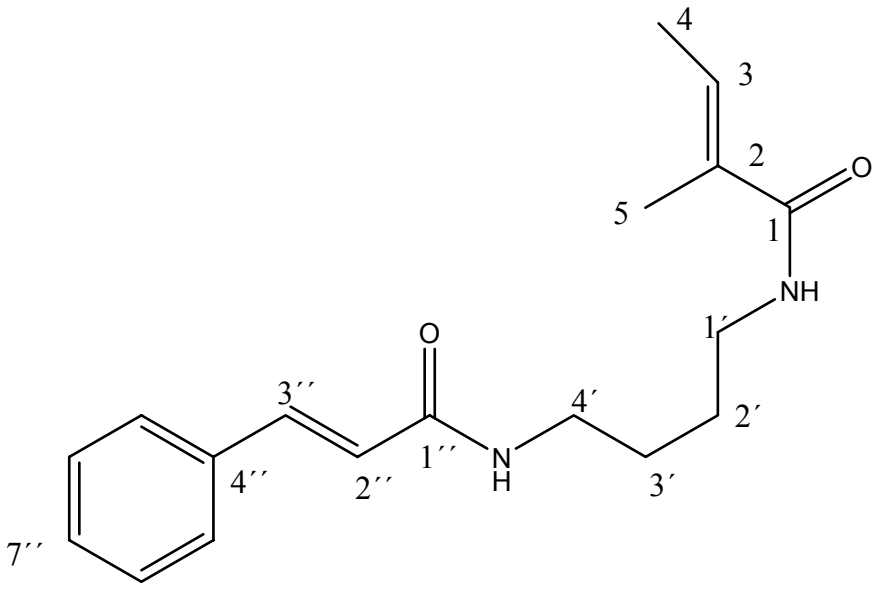

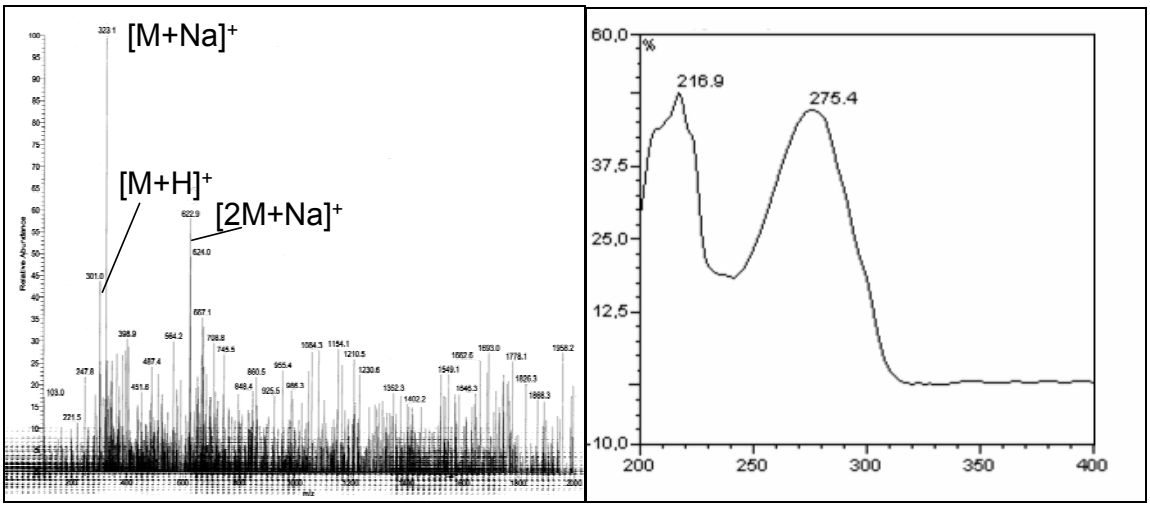

Fig. 3.74: ESI-MS and UV spectrum of compound 21

Compound **21** was isolated from the leaves of *Aglaia gigantea* as a white amorphous residue, $[\alpha]_D^{20}$ + 10 (*c*, 0.25, MeOH); UV (MeOH) λ_{max} 216.0 and 275.4 nm (see Fig. 3.74). The ESI-MS (see Fig. 3.74) showed pseudomolecular ion peaks at *m/z* 301.2 $[M+H]^+$, *m/z* 623.1 $[2M+Na]^+$ which are compatible to its NMR data. Comparison between ^{1}H NMR spectrum of compound **21** (see Fig. 3.75) to that of compound **20**, showed a difference in the upfield region by the presence of a methyl group at δ 1.65 ppm (3H,*dd*, 1.1, 6.9) while the oxygened methylene signal at δ 4.22 ppm (2H, *dd*, 0.9, 6.3) was absent.

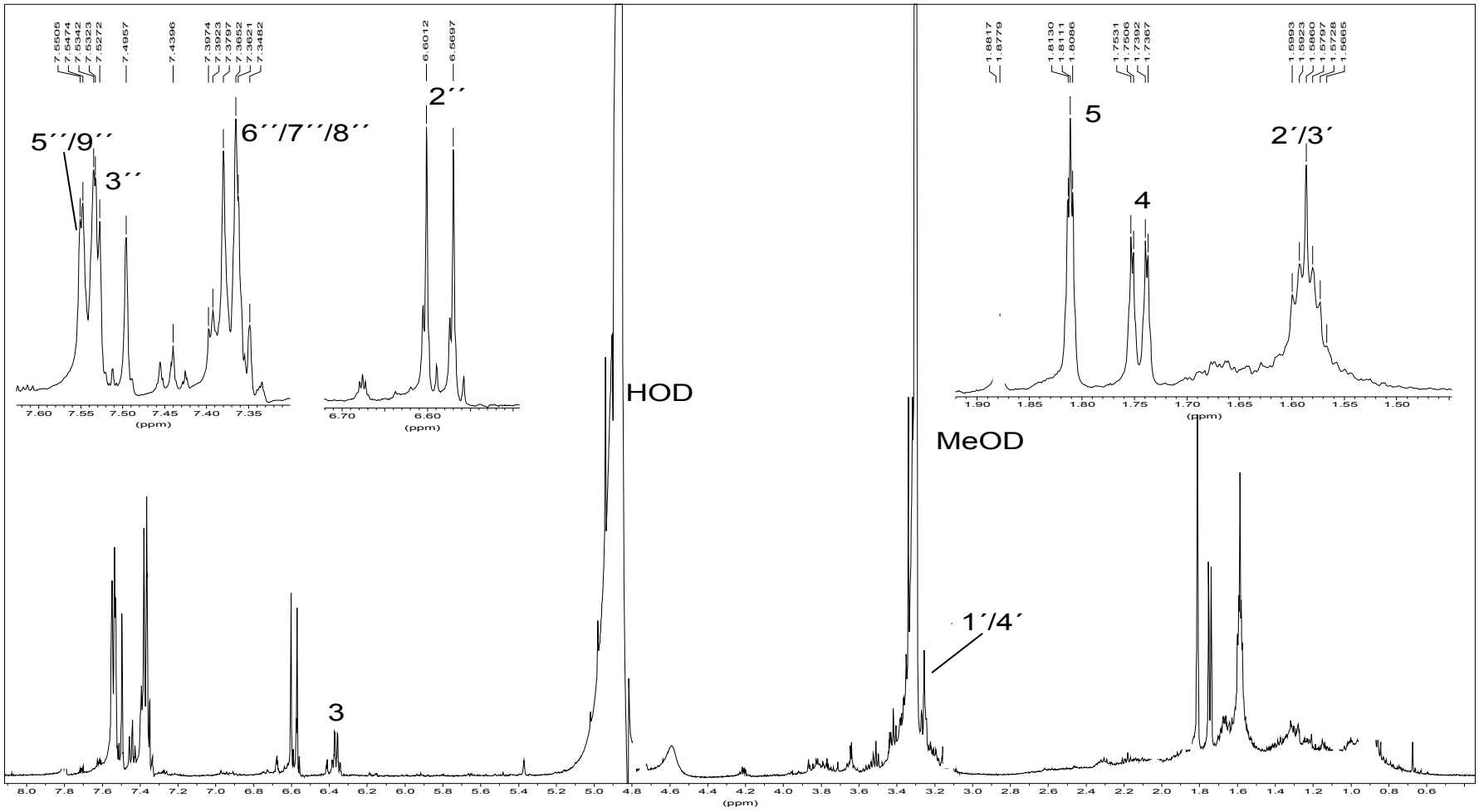

Fig. 3.75: ^{1}H NMR of compound 21 in MeOD

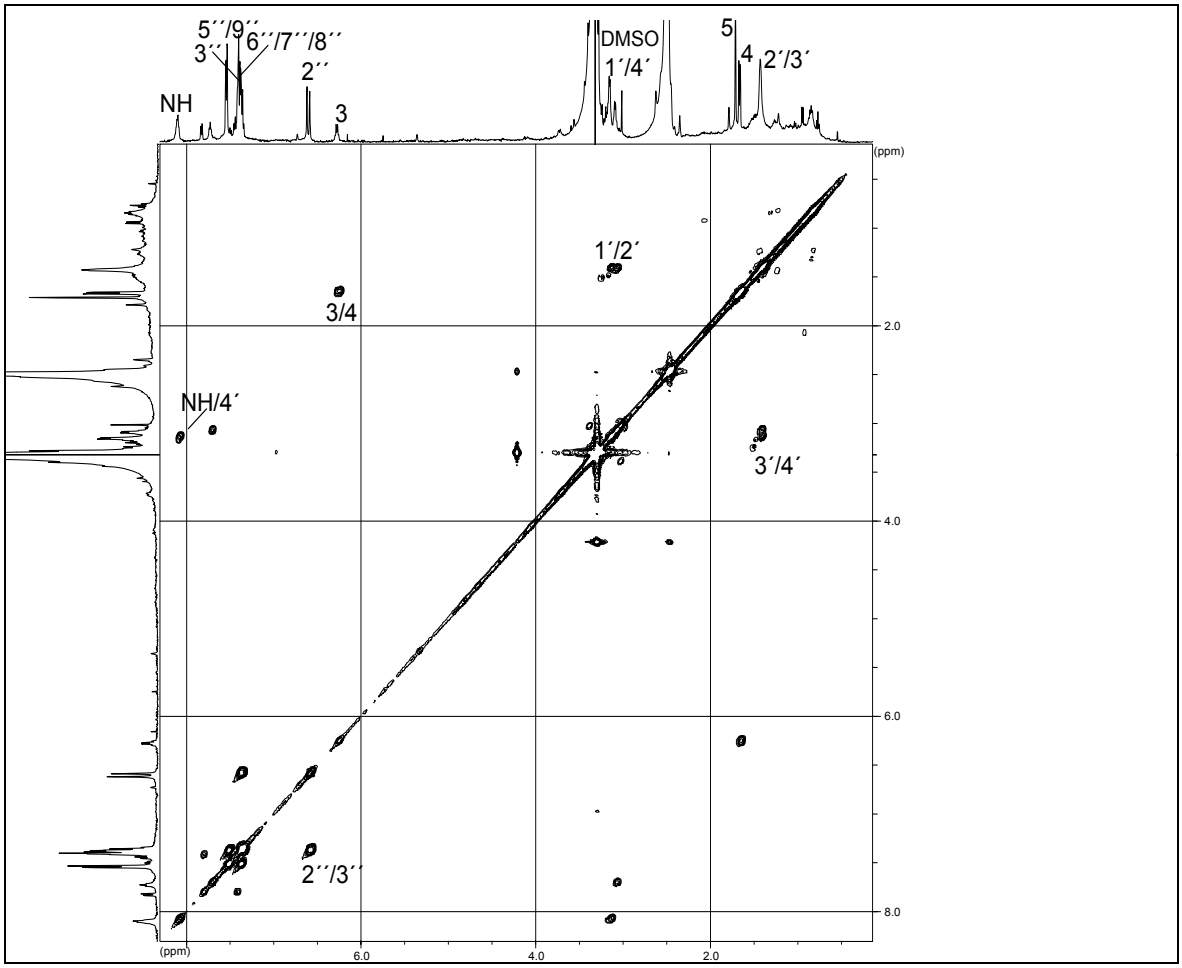

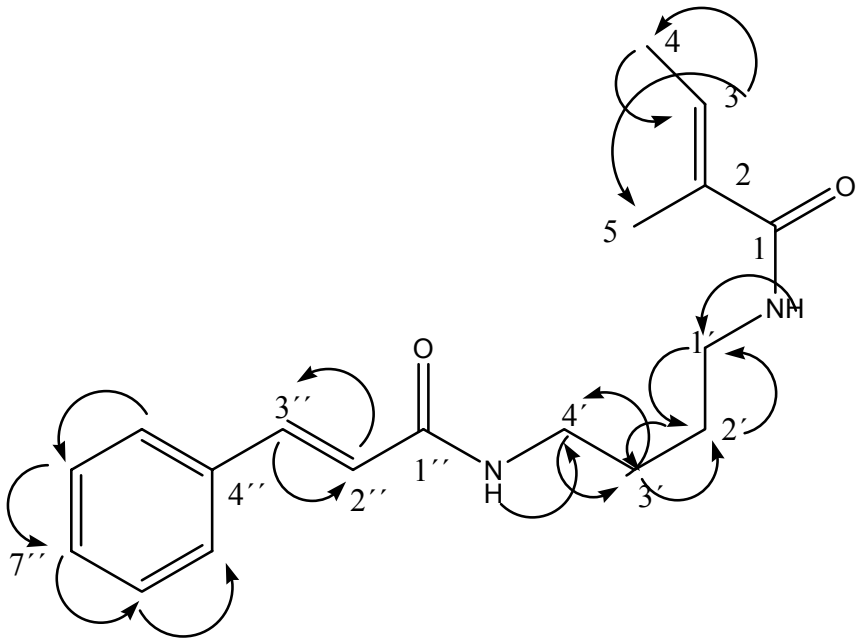

Fig. 3.76: ^{1}H-^{1}H COSY correlations of compound 21 in DMSO

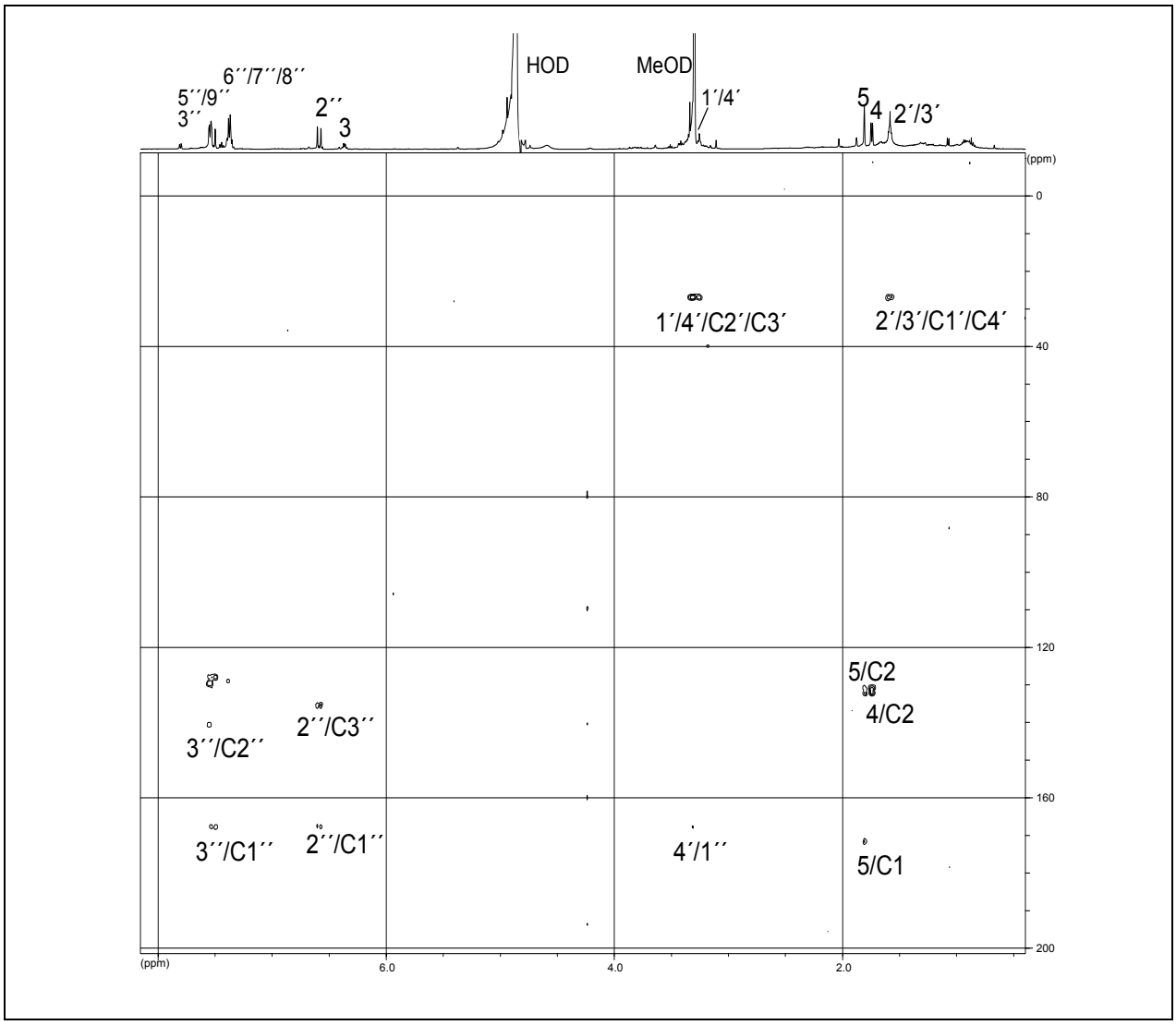

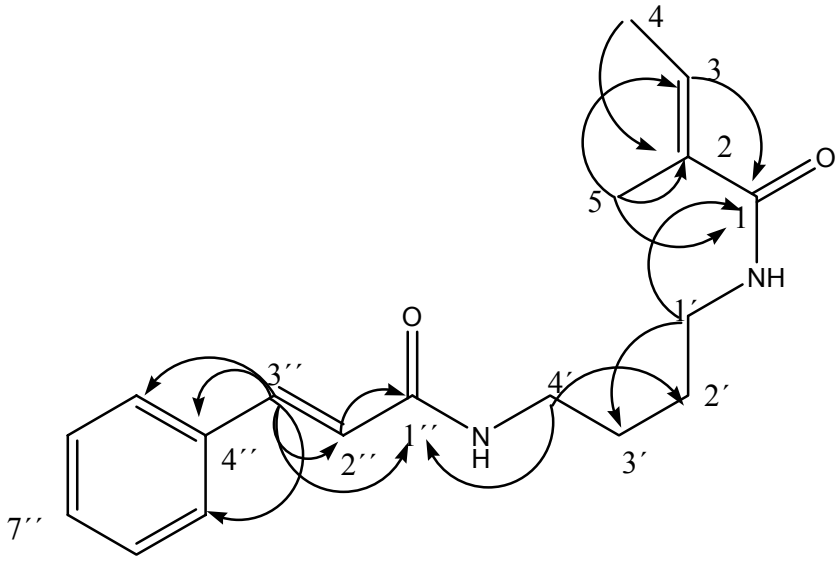

Fig. 3.77: HMBC correlations of compound 21 in MeOD

The molecular weight of compound **21** is 16 mass units smaller than that of compound **20** which could suggest a loss of a hydroxyl group at C-4. The typical *trans*-configuration of H-2´´ and H-3´´ resonating as a doublets at 6.58 ppm (*J*=15.7) and 7.53 ppm (*J*=15.7) was retained for compound **21**. H-3 appeared as a doublet of a quartet at 6.30 ppm. The monosubstituted aromatic ring was identified by the chemical shift value at δ 7.54 (*m*, 2H), 7.37 (*m*, 2H), and 7.52 (*m*, 1H), which represent protons H-5´´/ H-9´´, H-6´´/H-8´´ and H-7´´, respectively (see Table 3.31). Furthermore, the putrescine group was also observed through the ^{1}H-^{1}H COSY spectrum (see Fig. 3.76).

From its HMBC spectrum (see Fig.3.77), both the methyl signal CH_3-5 (δ 1.73) and the methylene protons H-1´ (δ 3.30) showed correlations to the carbonyl carbon C-1 at 171.3 ppm, which proved the connection of the putrescine moiety to the (Z)-2-methylbut-2-enamide chain, while the other methylene protons H_2-4´ exhibited correlations to the carbonyl carbon C-1´´ at 168.7 ppm, to prove the connection of the other side of the putrescine to the cinnamoyl moiety, respectively. Both *trans*-olefinic doubles of H-2´´ (δ 6.85) and H-3´´ (δ 7.53) correlated to the carbonyl carbon C-1´´ at δ 168.7 which also showed the presence of the cinnamoyl moiety. In comparison with the literature [Brader *et al.,* 1998 and Detterbeck *et al.,* 2002] and based on the ^{1}H-NMR, ^{13}C-NMR and 2D-NMR data, compound **21** was identical to grandiamide B, which was isolated from *Aglaia grandis* from Taiwan.

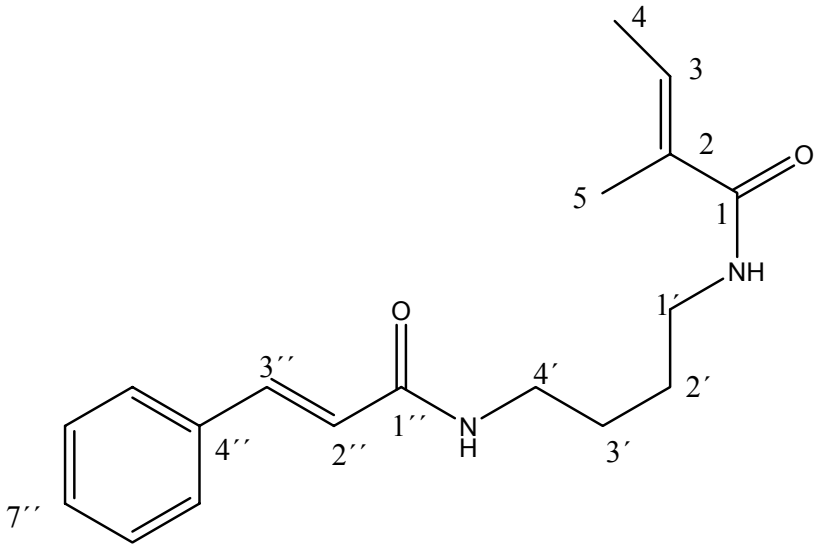

Grandiamide B

III.2.5.3. Grandiamide D (22, new compound)

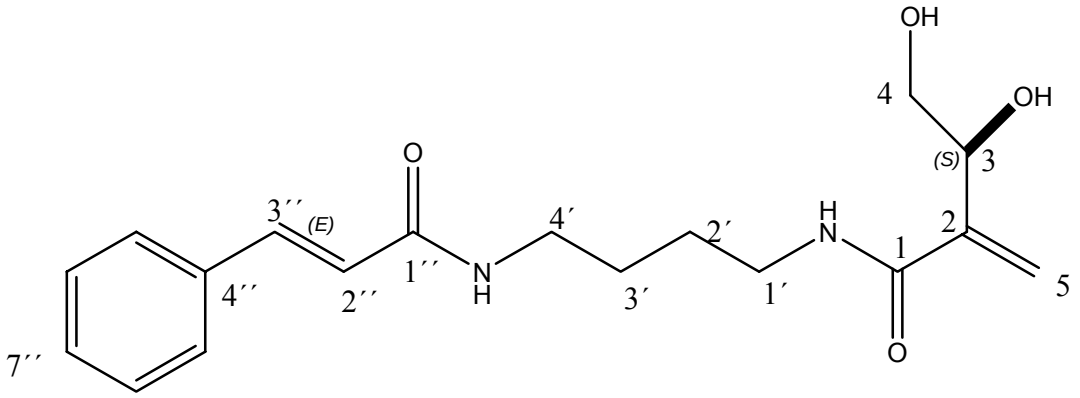

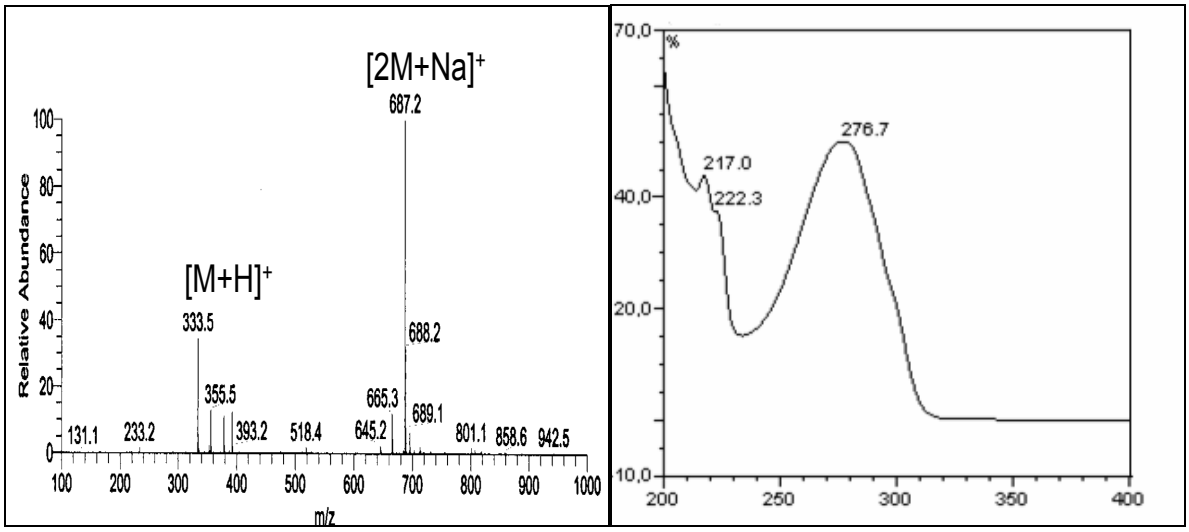

Fig. 3.78: ESI-MS and UV spectrum of compound 22

Compound **22** was isolated as a white amorphous residue from the leaves of *Aglaia gigantea*, $[\alpha]_D^{20}$ + 2 (*c*, 0.47, MeOH); UV (MeOH) λ_{max} 217.0, 222.3, and 275.4 nm (see Fig. 3.78). The positive mode ESI-MS showed pseudomolecular ion peaks at *m/z* 687.2 $[2M+Na]^+$, 355.5 $[M+Na]^+$, and 333.5 $[M+H]^+$ (see Fig. 3.78). The negative mode ESI-MS showed pseudomolecular ion peaks at *m/z* 709.6 $[2M+HCOOH-H]^-$, 377.5 $[M+HCOOH]^-$, and 331.8 $[M-H]^-$. The HREIMS also showed pseudomolecular ion peak at *m/z* 355.163 $[M+Na]^+$, and at *m/z* 333.182 $[M+H]^+$. This molecular weight is compatible with the molecular formula $C_{18}H_{24}N_2O_4$ as determined by HRESIMS. Compound **22** is quite similar to grandiamide C which was isolated as a white amorphous residue from *Aglaia grandis* [Brader *et al.,* 1998]. The structure of grandiamide C was proved by synthesis [Detterbeck *et al.,* 2002]. The molecular weight of compound 22 is 16 mass units larger than that of grandiamide C, which

could be proved by the loss of a hydroxyl group. In the ^{1}H NMR, the monosubstituted aromatic ring system was identified by the chemical shift value at δ 7.44 (*m*, 2H); 7.27 (*m*, 2H) and 7.29 (*m*, 1H), which corresponded to H-5′′/ H-9′′, H-6′′/ H-8′′ and H-7′′, respectively. The *trans*-configuration of protons H-2′′ and H-3′′ was determined from the ^{1}H NMR spectrum (see Fig. 3.79) as indicated by the signal at 6.58 ppm (d, *J*=15.7 Hz) and 7.37 ppm (d, *J*=15.7 Hz). Both protons H-2′′ and H-3′′ revealed their correlations with C-1′′ at 168.0 ppm through the long-range HMBC spectrum (see Table 3. 36 and Fig.3.80) proved for the presence of the cinnamoyl moiety. The *exo*-methylene group was identified by two broad singlets at 5.69 ppm and 5.52 ppm, representing H-5A and H-5B. From the HMBC spectrum (see Fig.3.80) these two protons showed their strong correlations with C-1 at 170.0 ppm, C-2 at 145.5 ppm and C-3 at 71.5 ppm. To compare with dasyclamide, the H-3 of compound **22** was shifted upfield to 4.4 ppm (dd, *J*=3.8Hz; 6.3Hz) due to a hydroxyl substituent at C-3, which replaced the quartet of a triplet at 6.34 ppm (qt, *J*= 1.2Hz, 5.7 Hz), indicating the loss of the double bond between C-3 and C-2 as found in dasyclamide (see Fig. 3.80). In addition, the signal of H-4a was observed at 3.55 ppm (dd,*J*=11.4Hz, 4.4 Hz), and H-4b at 3.40 ppm (dd, *J*=11.4 Hz, 6.9 Hz). Furthermore, its HMBC spectrum showed correlations of H-3 to C-2 and C-4 observed at 149.5 ppm and 65.5 ppm, respectively. H-4a and H-4b were confirmed by their correlations to C-2 at 149.5 ppm. The multiplicities of H-4′ and H-1′ were difficult to identify from the ^{1}H NMR spectrum because their resonances were overlapping with the methanol peak at 3.30 ppm. However, their HMBC correlations proved the structure. The correlations of H-4′ to C-1′′ at 168.0 ppm and H-1′ to C-1 at 170.0 ppm, proved for an open-chained structure of the putrescine moiety. The other proton signals for H-2′ and H-3′ overlapped at 1.51 ppm. From its HMBC spectrum, correlations were observed between H-1′ to C-3′ at 26.8 ppm and H-4′ to C-2′ at 26.8 ppm as well as the correlations of H-2′ with C-4′ and H-3′ with C-1′ at 39.1 ppm, which proved for the presence of the putrescine moiety. Compound **22** was completely elucidated as a new derivative and is the open-chained putrescine-bisamide derivative, which was named grandiamide D.

Table 3.36: ^{1}H NMR, ^{13}C NMR, COSY and HMBC of compound 22 (in MeOD)

Position	δ_H (ppm), *J* (Hz) **22**	δ_C (ppm)	COSY	HMBC
1		170.0		
2		145.5		
3	4.4 (*dd*, 3.79, 6.31)	72.5	4A, 4B	2,4
4	A: 3.55 (*dd*, 11.3, 4.4) B: 3.40 (*dd*, 11.3, 6.9)	65.5		2,3 2,3
5	A: 5.69 B: 5.52 exomethylen	123.2		1,2,3 1,2,3
1′	3.30 m	39.1 t		1
2′	1.51 m	26.8 t		
3′	1.51 m	26.8 t		
4′	3.30 m	39.1 t		1′′
1′′		168.0		
2′′	6.49(*d*, 15.7)	121.0	3′′	1′′, 4′′
3′′	7.40 (*d*, 15.7)	140.8	2′′	1′′, 4′′, 5′′,9′′
4′′		135.7		
5′′/9′′	7.44 m	129.0		
6′′/8′′	7.27 m	129.8		
7′′	7.44 m	129.8		

The absolute configuration of compound **22** at the stereocenter C-3 was determined via Mosher ester derivatization method (see Table 3.37, Fig. 3.81 and Fig. 3.82). It is evident that proton H-3 with $\Delta\delta < 0$ is located on the left side of the MTPA plane, while H-4A, H-4B and H-5A, H-5B with $\Delta\delta > 0$ are on the right side [Ikuko *et al.,* 1991]. Based on the relative priorities of the four substituents by Ingold and Prelog rule, the chiral center (C-3) must be viewed from the side opposite the lowest priority group (-H), substituent groups with the highest priority (-OMTPA), the secondary priority (-C=CH_2) and the third priority (-CH_2OH). The turn was counter-clockwise and then the chiral center was classified to follow the ***S*** configuration.

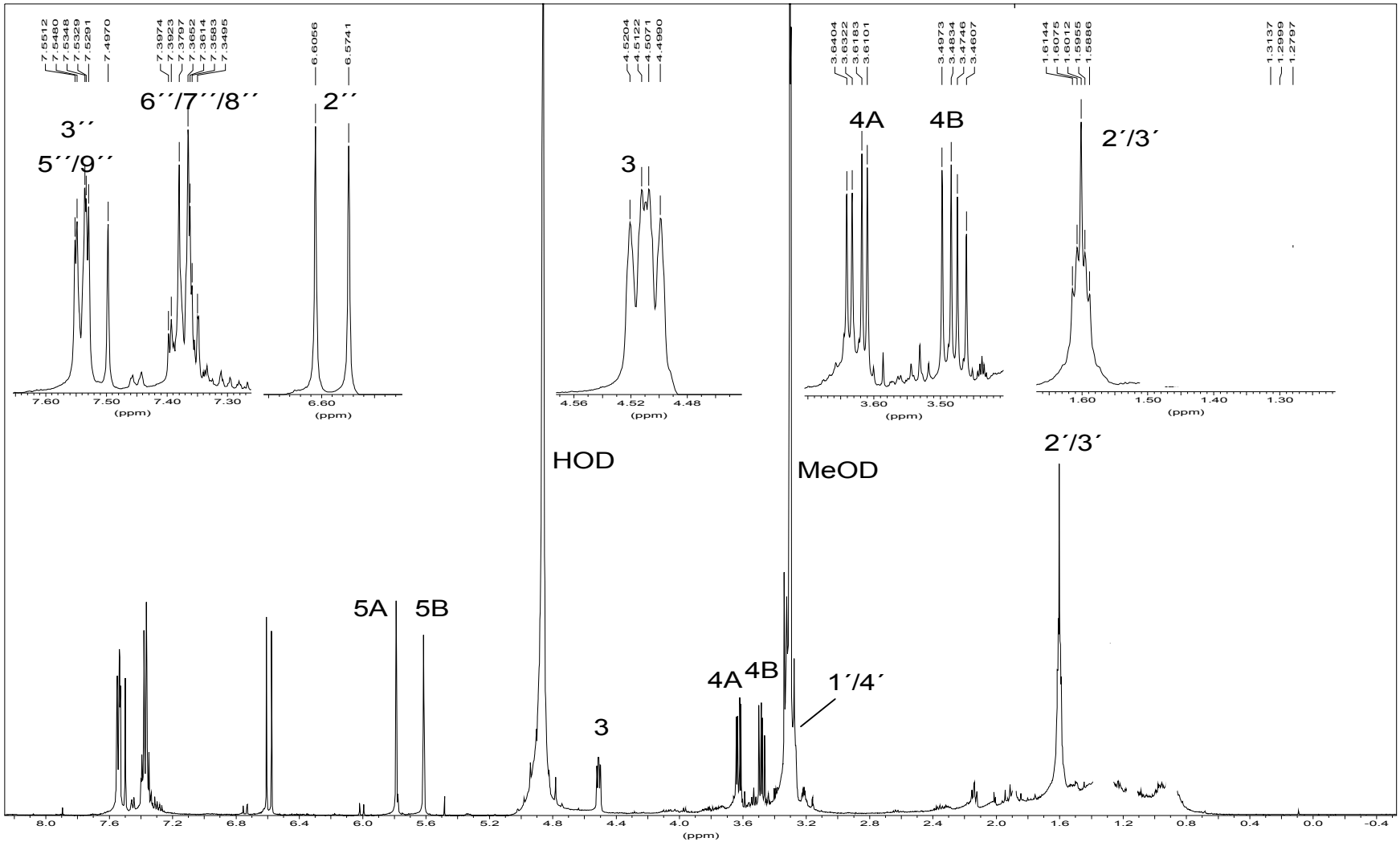

Fig. 3.79: ^{1}H NMR of compound 22 in MeOD

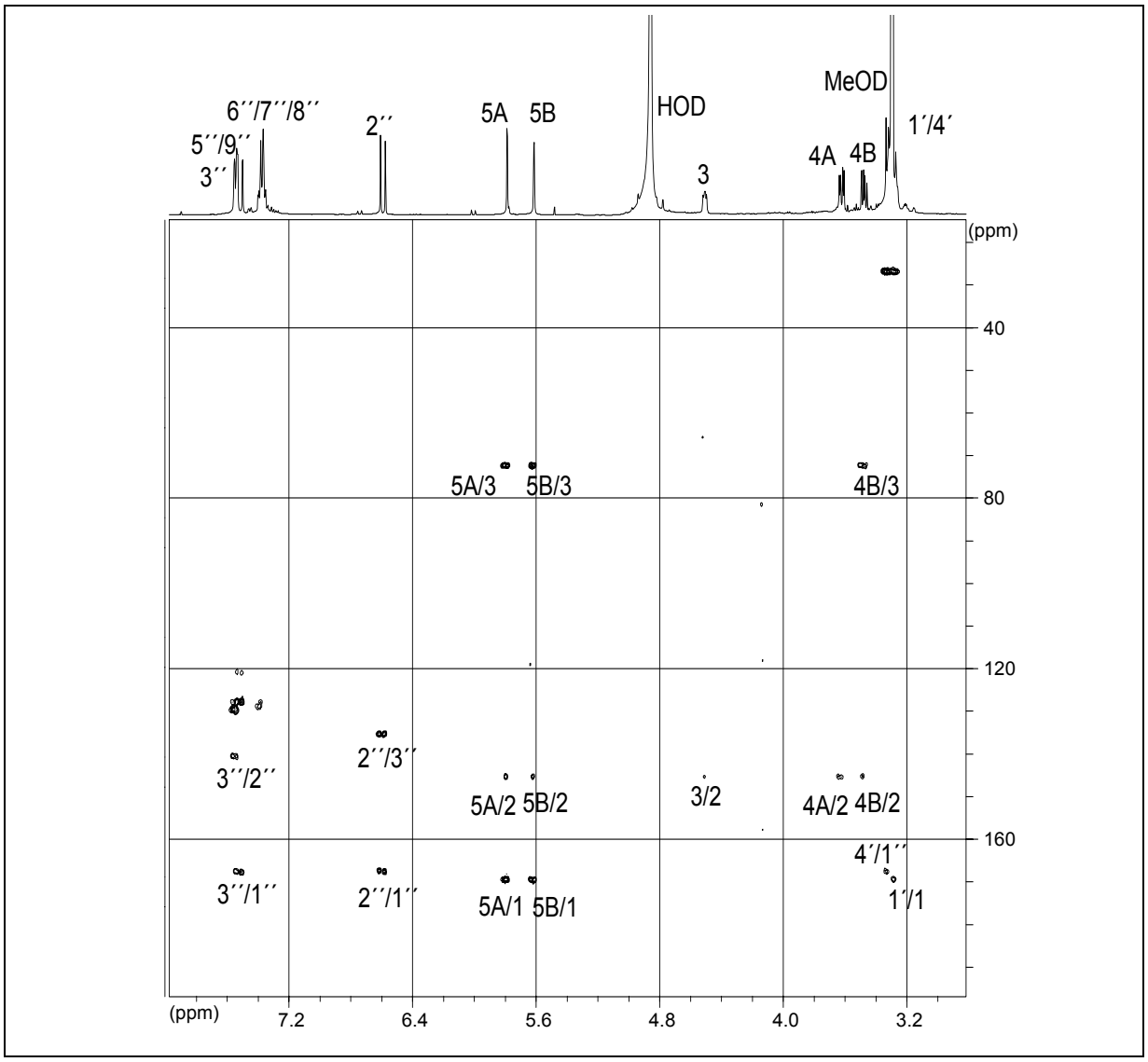

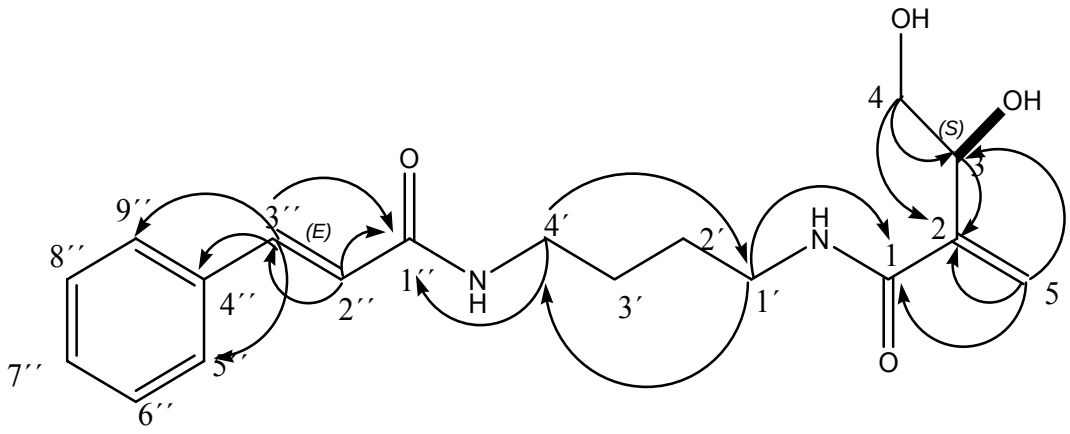

Fig. 3.80: HMBC correlations of compound 22 in MeOD

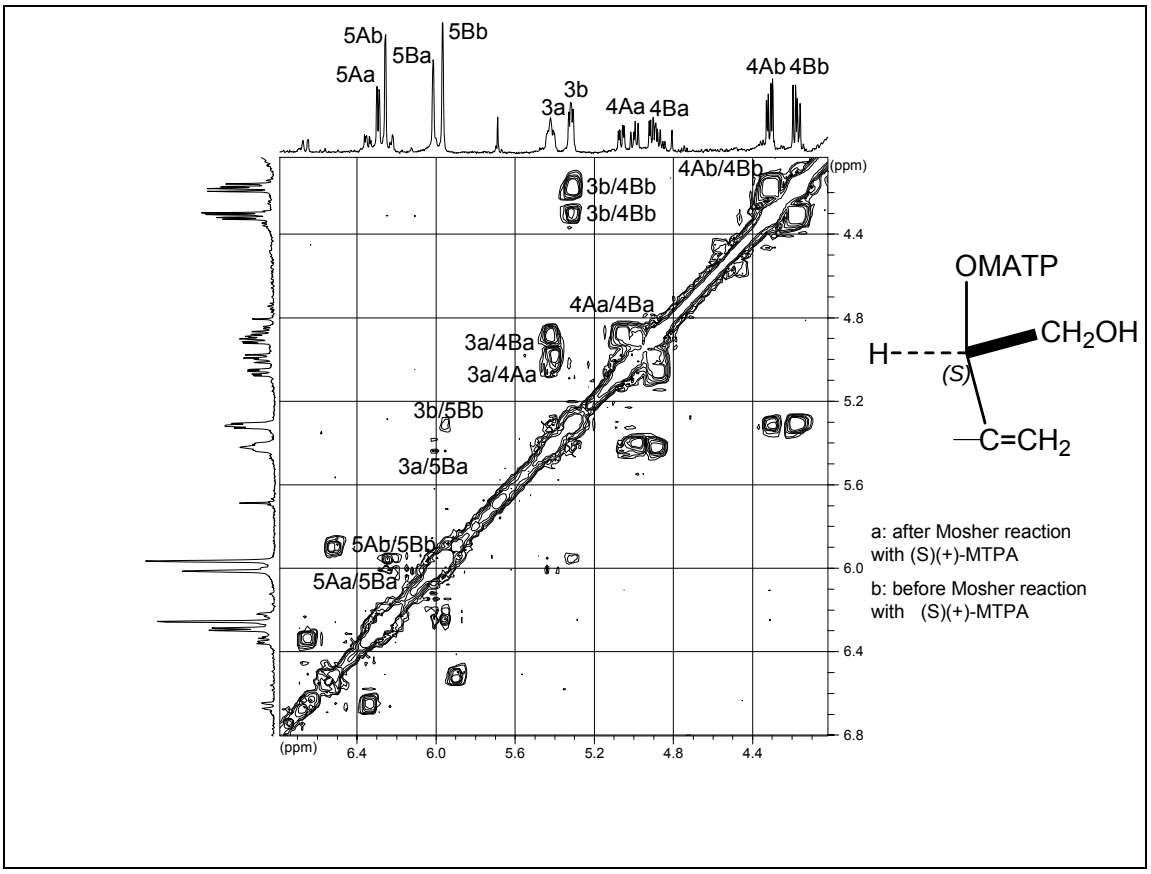

Fig. 3.81: ^{1}H-^{1}H COSY of 22 after Mosher reaction with (*S*)(+)-MTPA (in Pyridne-d_6)

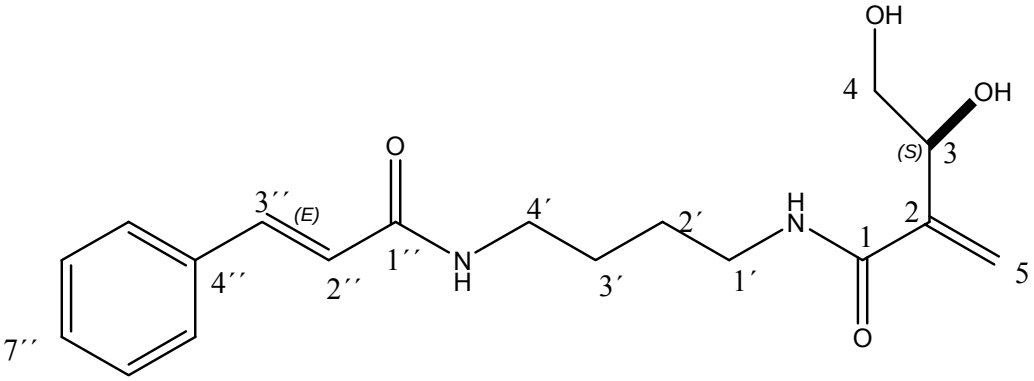

Table 3.37: ^{1}H NMR results of Mosher analysis of compound 22 in pyridine d-*6*

^{1}H-Position	(in pyridine-d$_6$)	(*S*)(+)-MTPA ester	(*R*)(+)MTPA ester	Δ_{S-R}
3	5.3193	5.4152	5.4164	-0.0012
4A	4.3220	5.0493	5.0433	+0.0006
4B	4.1827	4.8970	4.8964	+0.0006
5A	6.2541	6.2862	6.2750	+0.0112
5B	5.9660	6.0139	6.0065	+0.0074

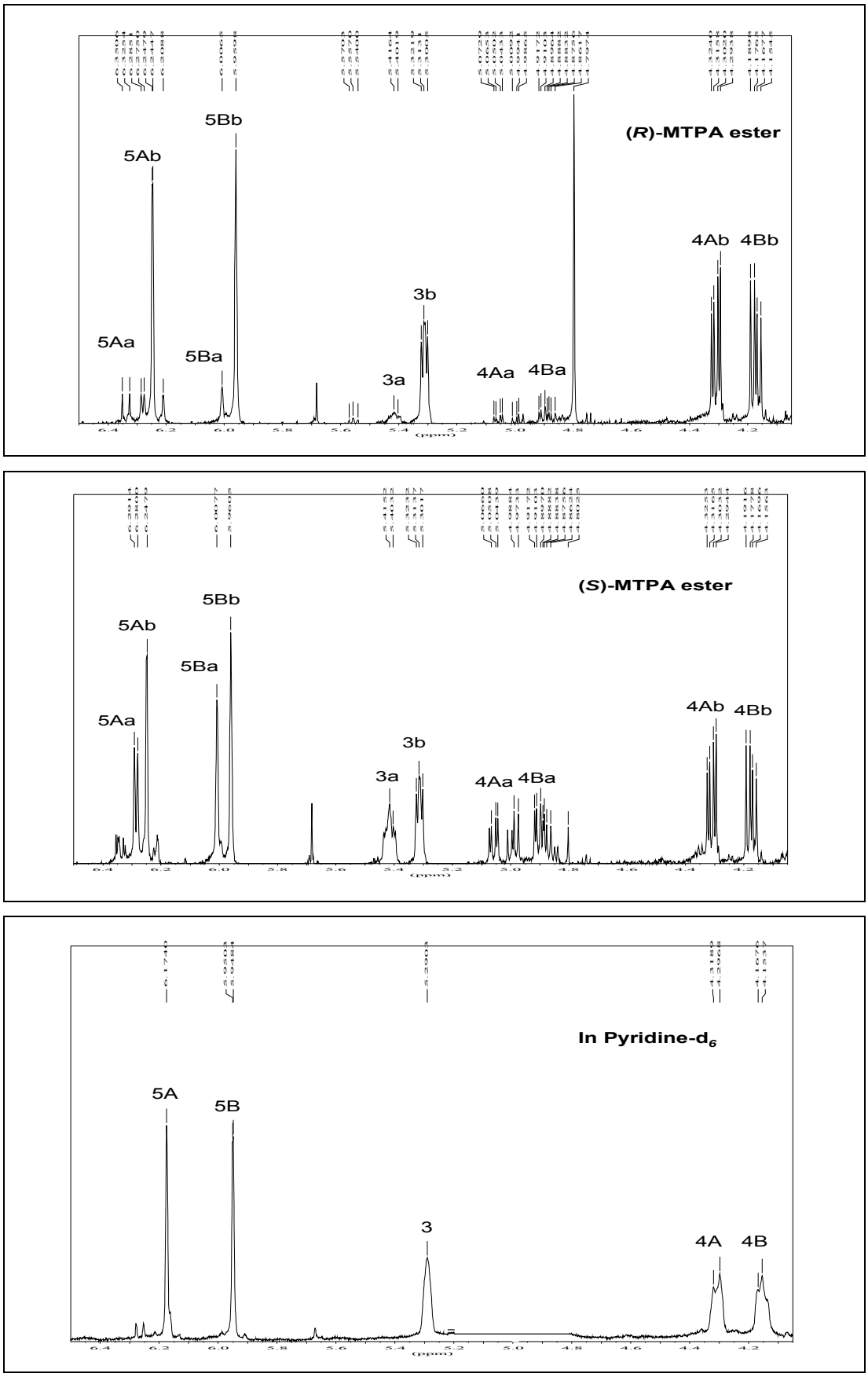

Fig. 3.82: ^{1}H NMR spectra of 22 in (*R*)-MTPA (top), (*S*)-MTPA (middle) esters and in Pyridine-d_6 (bottom)

III.2.5.4. Odorine (23, known compound)

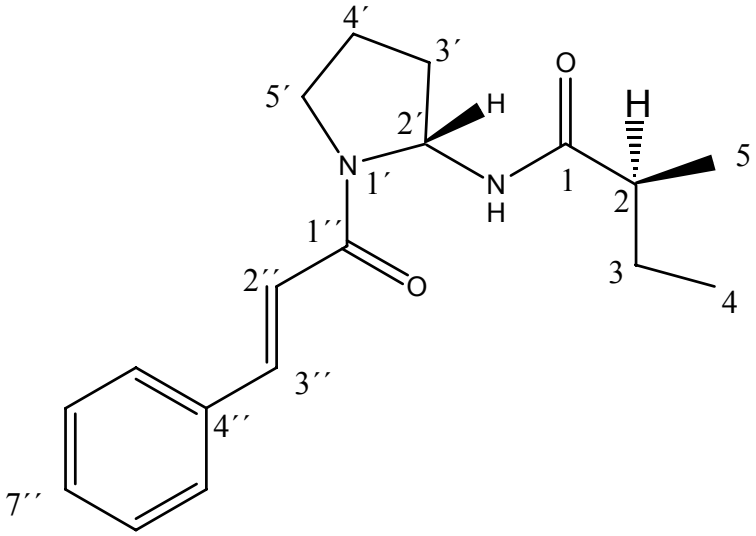

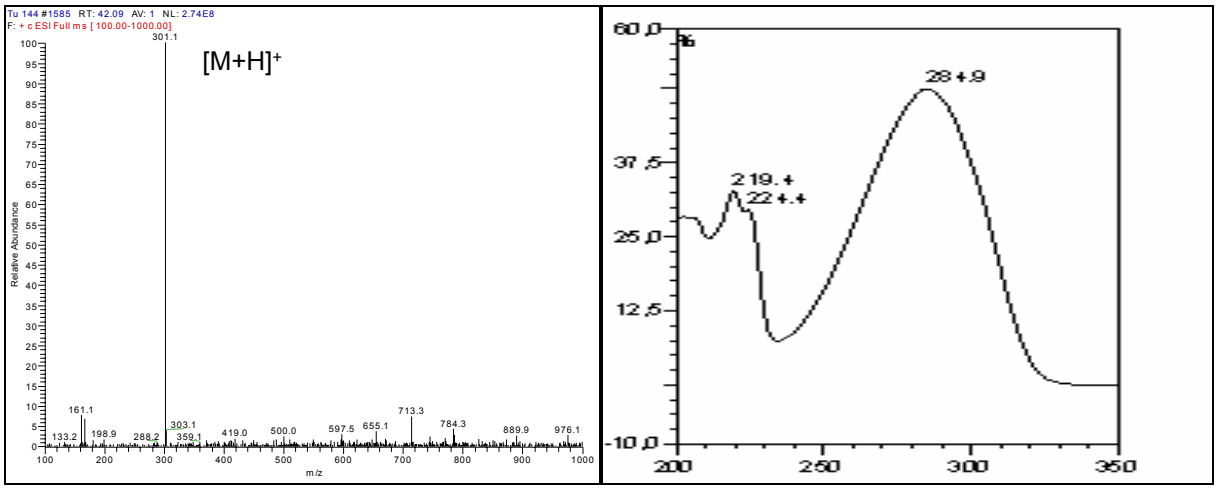

Fig. 3.83: ESI-MS of and UV spectrum of compound 23

Compound **23** was isolated from the leaves of *Aglaia duppereana* as white needles crystalline; $[\alpha]^{20}_{D}$- 35 (*c*, 0.5, $CHCl_3$); UV (MeOH) λ_{max} 219.0, 224.4, and 284.8 nm (see Fig. 3.83). The positive mode of ESI-MS showed a pseudomolecular ion peak at *m/z* 301.0 $[M+H]^+$ (see Fig. 3.83). In the ^{1}H NMR spectrum (see Fig. 3.83), the characteristic lowfield signals appeared at 7.05 ppm (1H, d, *J*=15.7 Hz), 7.55 ppm (1H, d, *J*=15.7 Hz), corresponding for the *trans*-conjugated double bond of H-2′′ and H-3′′, δ 7.37 -7.58 ppm (5H, m). The ^{1}H-^{1}H COSY spectrum yielded the following assignments: δ 0.70 (3H, t, *J*=7.7 Hz, H-4), 1.10 (3H, d, *J*=16.9Hz, H-5), 1.58 (1H, m, H-3A), 1.30 (1H, m, H-3B), 2.25 (1H, m, H-2), 2.20(1H,m, H-3′A), 2.15 (1H, m, H-3′B), 2.1 (1H, m, H-4′A), 1.95 (1H, m, H-4′B), 3.70 (1H, m, H-5′a), 3.48 (1H, m, H-5′b). Furthermore, a signal at 6.12 ppm (dd, *J*=4.35 Hz, 11.95 Hz) was assigned for proton H-2′, residing between the two nitrogen atoms of the pyrimidine

ring. Thus, the chemical shift of C-2′ appeared more downfield at 63.97 ppm (see Table 3.38 and Fig. 3.85) compared to that of 28.3 ppm in compound **20** or at 26.8 ppm from that of compound **22**. The spin system of a pyrimidine ring was shown by ^{1}H-^{1}H COSY spectrum (see Fig. 3.86). Besides, the HMBC spectrum (see Fig. 3.87) exhibited correlations of H-2′ to C-1, C-1′′, C-3′,C-4′ and C-5′ to prove the cyclization of the putrescine moiety. The triplet signal of the methyl H-4 at δ 0.7 ppm revealed strong correlations with C-3 (see Fig. 3.87) and showed the W-HMBC long-range correlations with C-2. This methyl signal could be differentiated from the other H_3-5 methyl signal, which occurred as a doublet. Also, a second doublet signal for the H_3-5 methyl was observed at 1.1 ppm and correlations with C-1, C-2 and C-3. In comparison with the literature data, compound **23** was identical to odorine, which was previously isolated from the leaves of *Aglaia odorata* collected in Thailand [Shiengthong *et al.,* 1979], and later from the leaves and twigs of *Aglaia odorata* from Taiwan [Hayashi *et al.,* 1982].

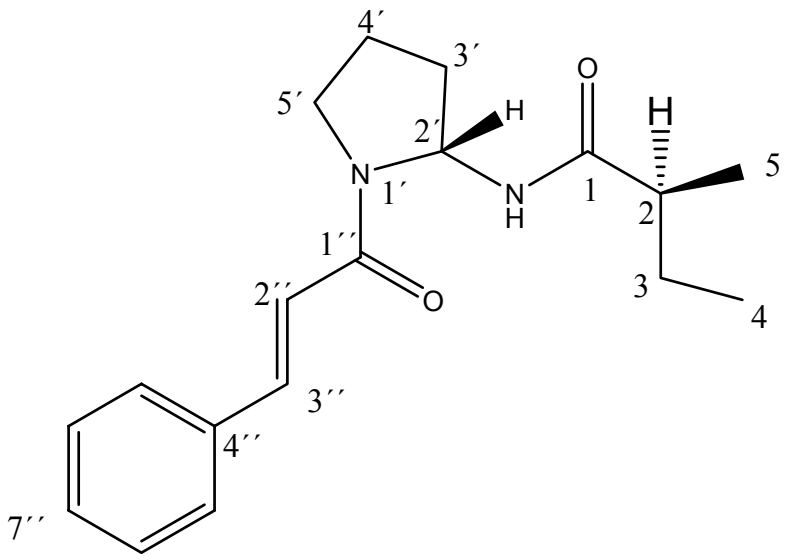

Odorine

Table 3.38: ^{1}H NRM, ^{13}C NMR, ^{1}H-^{1}H COSY and HMBC of compound 23 (in MeOD)

Position	^{1}H-NMR	^{13}C-NMR	COSY	HMBC
1		178.3 (s)		
2	2.25 m	43.6 (d)	3A, 3B, 5	1,3,4,5
3	A: 1.58 m B: 1.30 m	28.2 (t)	2,4	1,2,4,5
4	0.70 t	12.3 (q)	3A, 3B	2,3
5	1.10(d, 16.9)	17.9 (q)	2	1,2,3
1′				
2′	6.12 (dd, 4.35, 11.95)	63.9 (d)	3′	1,3′, 4′, 1′′
3′	A: 2.20m B: 2.15 m	35.0 (t)	2′, 4′	2′, 4′, 5′
4′	A: 2.1 m B: 1.1.95 m	22.5 (t)	3′, 5 ′	2′, 3′, 5′
5′	A: 3.70 m B: 3.48 m	47.2 (t)	4′	3′, 4′
1′′		167.6 (s)		
2′′	7.05 (d, 15.5)	143.8 (d)	3′′	1′′, 3′′, 4′′
3′′	7.55 (d, 15.5)	119.6 (d)	2′′	1′′, 2′′, 4′′, 5′′, 9′′
4′′		136.2 (s)		
5′′/9′′	7.58 m	129.3 (d)	6′′, 8′′	3′′, 4′′, 6′′, 7′′
6′′/8′′	7.37 m	129.9 (d)	5′′, 7′′, 9′′	4′′, 5′′, 7′′, 9′′
7′′	7.54 m	131.1 (d)	6′′, 8′′	5′′, 6′′, 8′′, 9′′

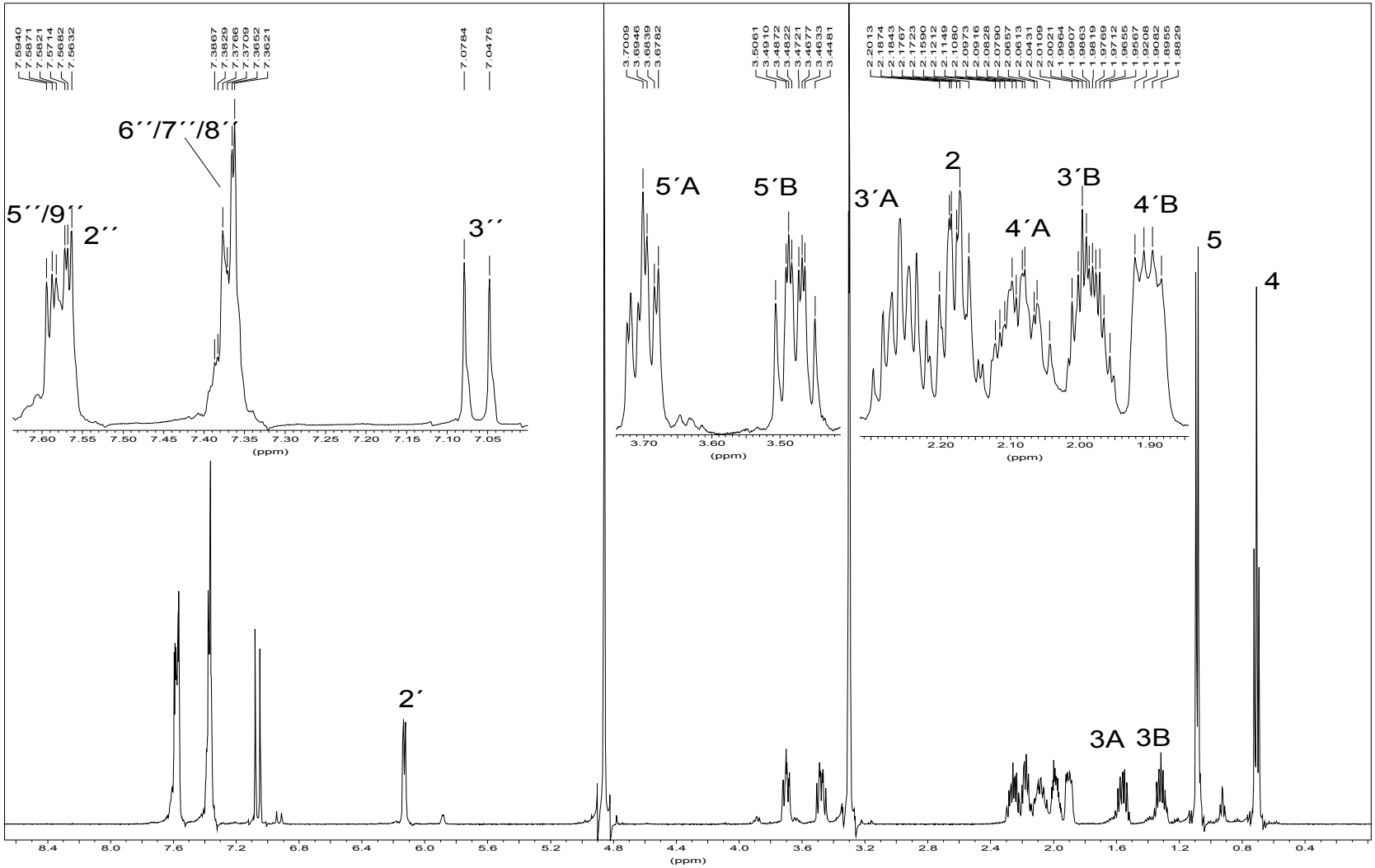

Fig. 3.84: ^{1}H NMR spectrum of compound 23 in MeOD

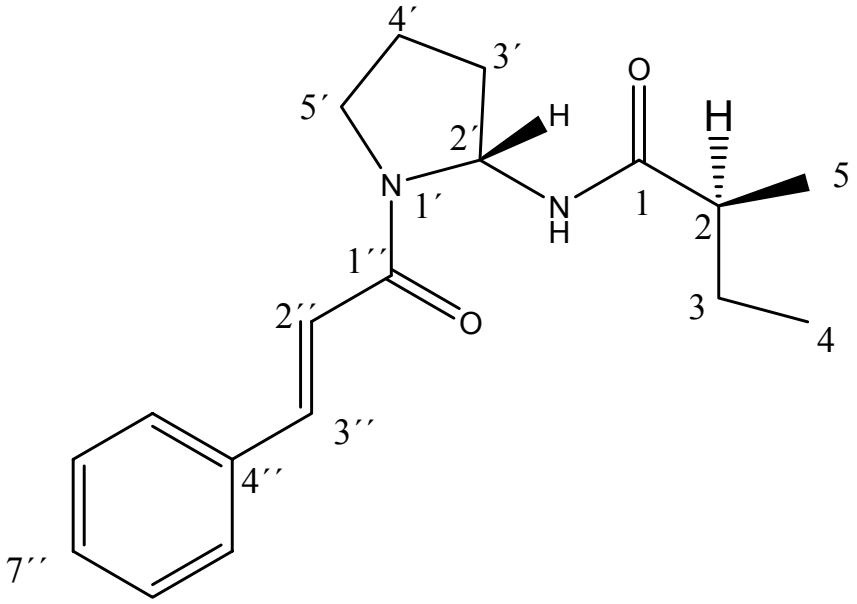

Compound **23**: **Odorine**

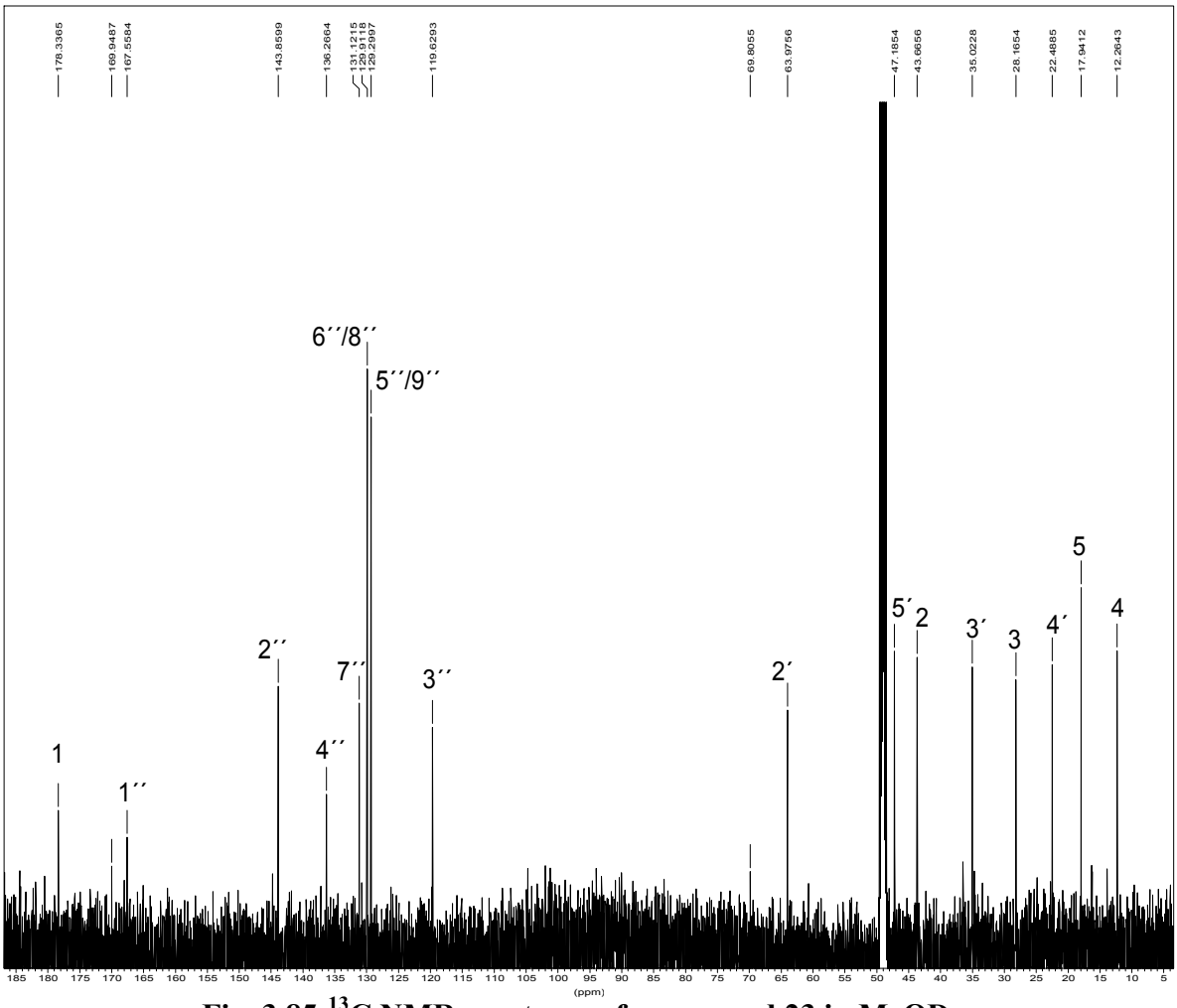

Fig. 3.85: ^{13}C NMR spectrum of compound 23 in MeOD

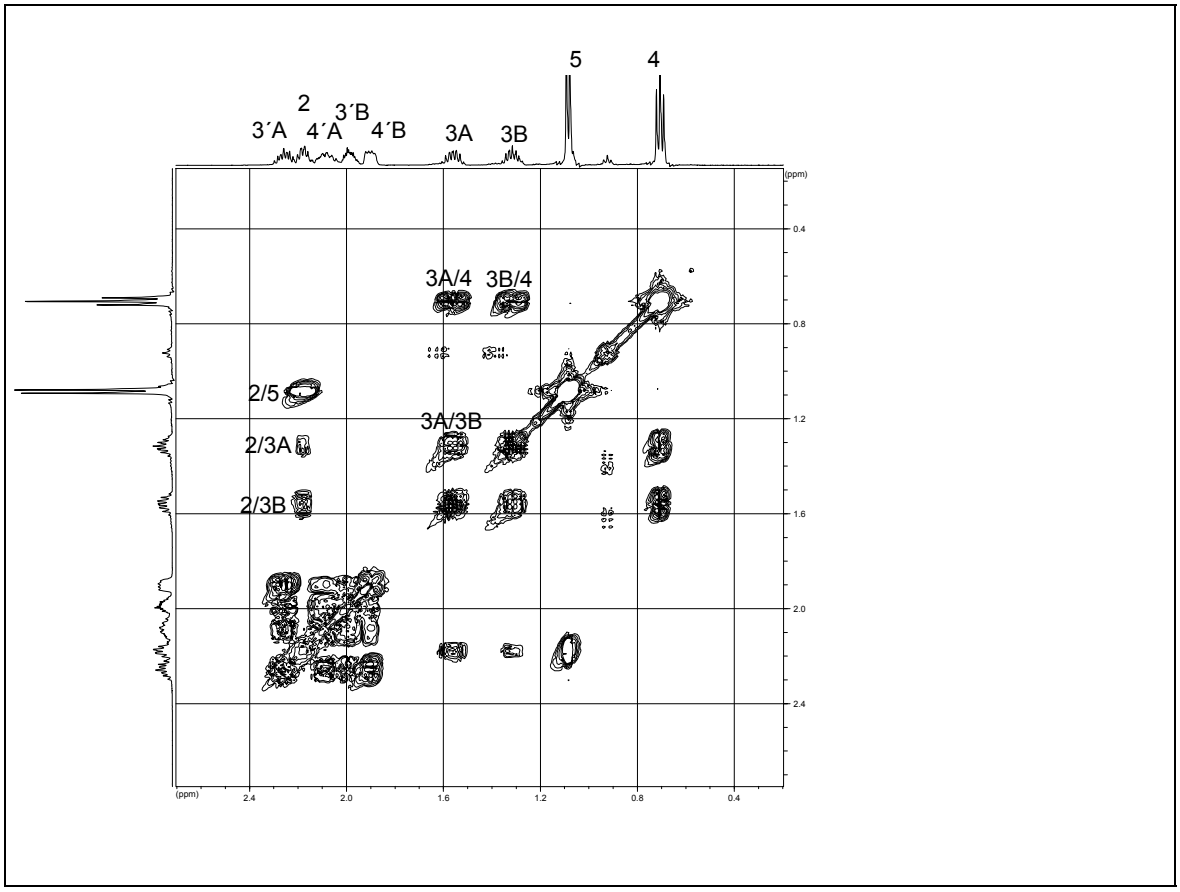

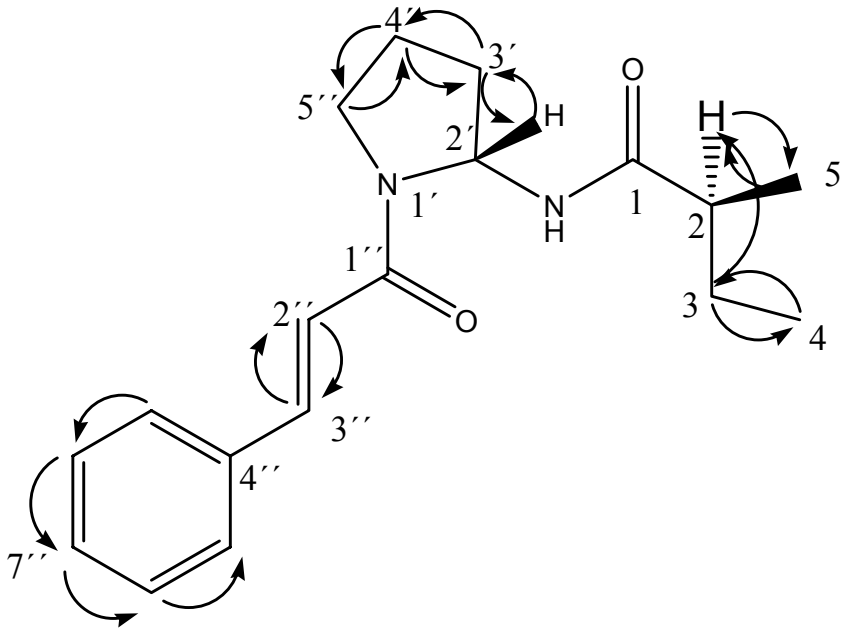

Fig. 3.86: ^{1}H-^{1}H COSY correlations of 23 in MeOD

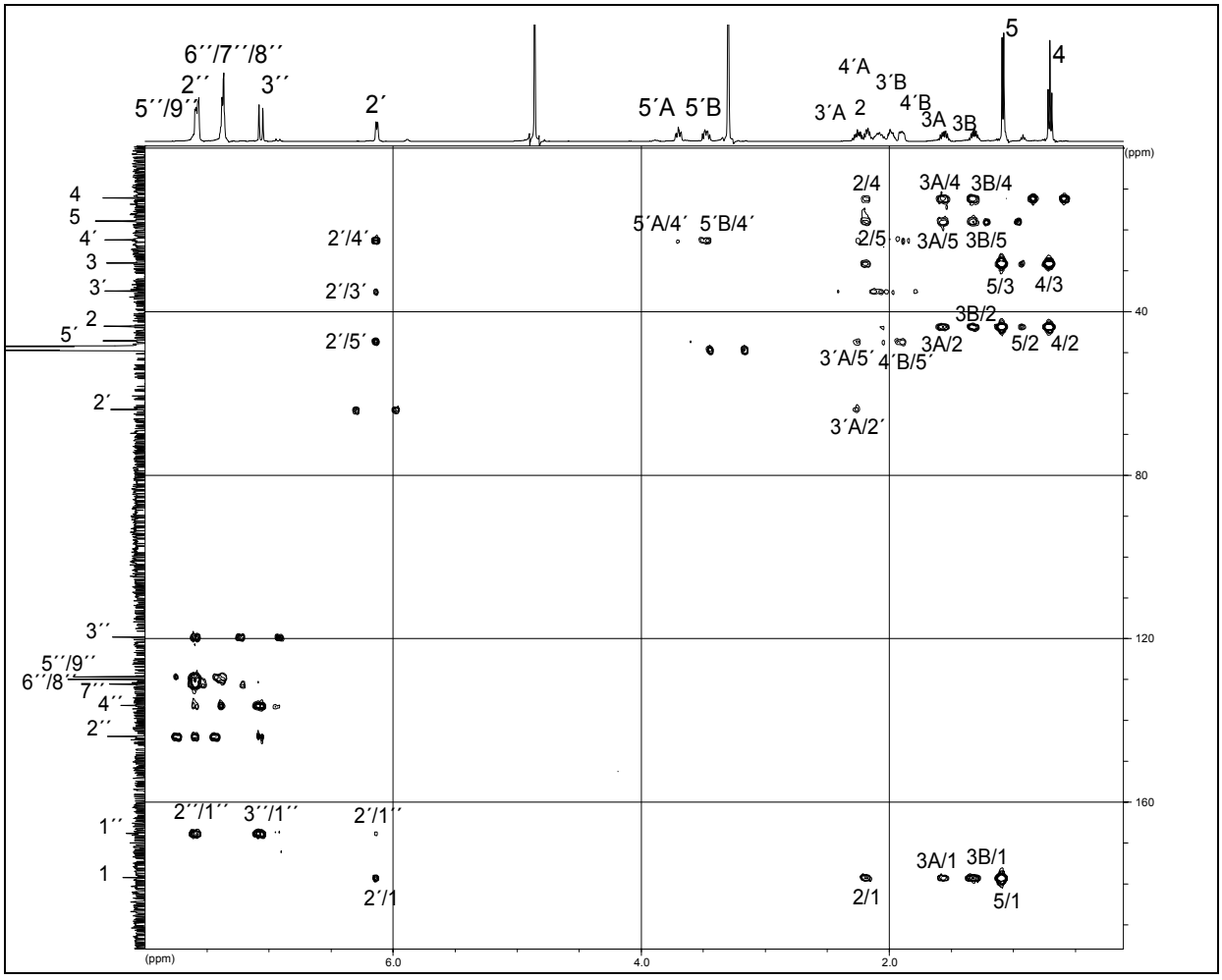

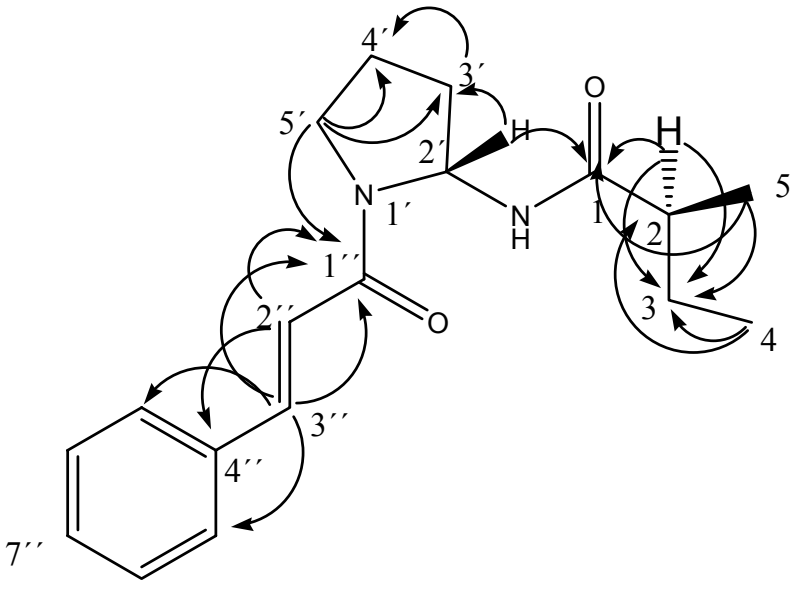

Fig. 3.87: HMBC correlations of compound 23 in MeOD

III.2.5.5.Odorinol (24, known compound)

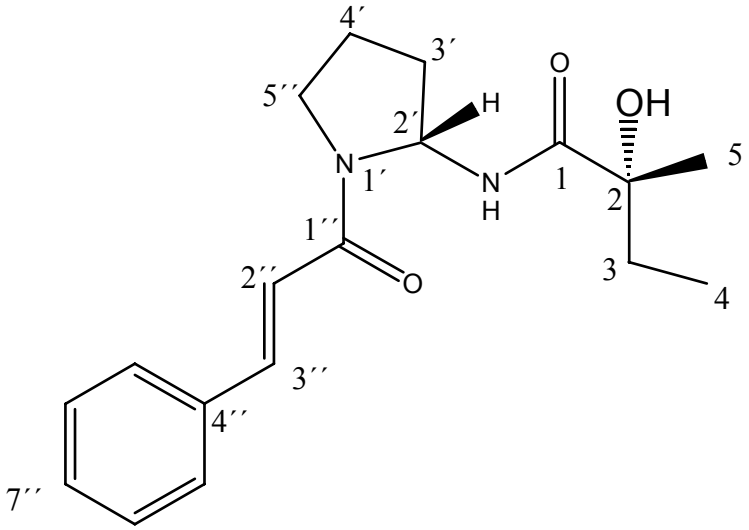

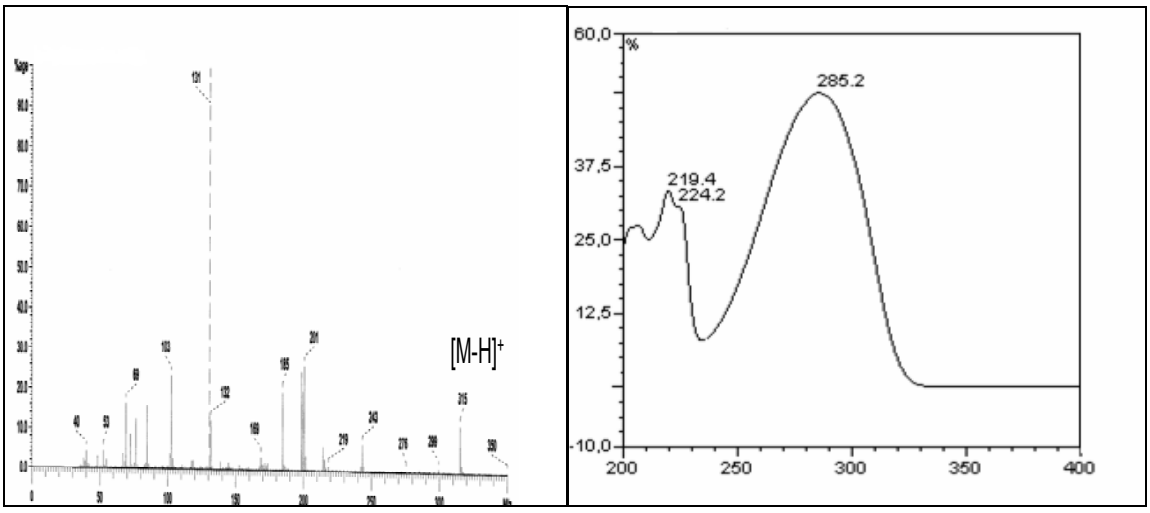

Fig. 3.88: EI-MS spectrum and UV spectrum of compound 24

Compound **24** was isolated from the leaves of *Aglaia duppereana* as white needles; $[\alpha]^{20}_{D}$-20 (*c*, 0.5, $CHCl_3$); UV (MeOH) λ_{max} 219.4, 224.2, and 285.2 nm (see Fig 3.88). The ESI-MS showed a pseudomolecular ion peak at *m/z* 315.0 $[M-H]^+$ (see Fig 3.88).

The presence of a cinnamoyl moiety was indicated by the appearance of mass peaks at *m/z* 131 $[PhCH=CHCO]^+$ and 103 $[PhCH=CH]^+$ .The molecular weight of compound **24** is 16 mass units larger than that of compound **23** due to a hydroxyl substitution at C-2. In the ^1H NMR spectrum (see Fig. 3.89), the hydroxyl substituent at C-2 was evident by the absence of a signal for H-2 at δ 2.25 ppm.

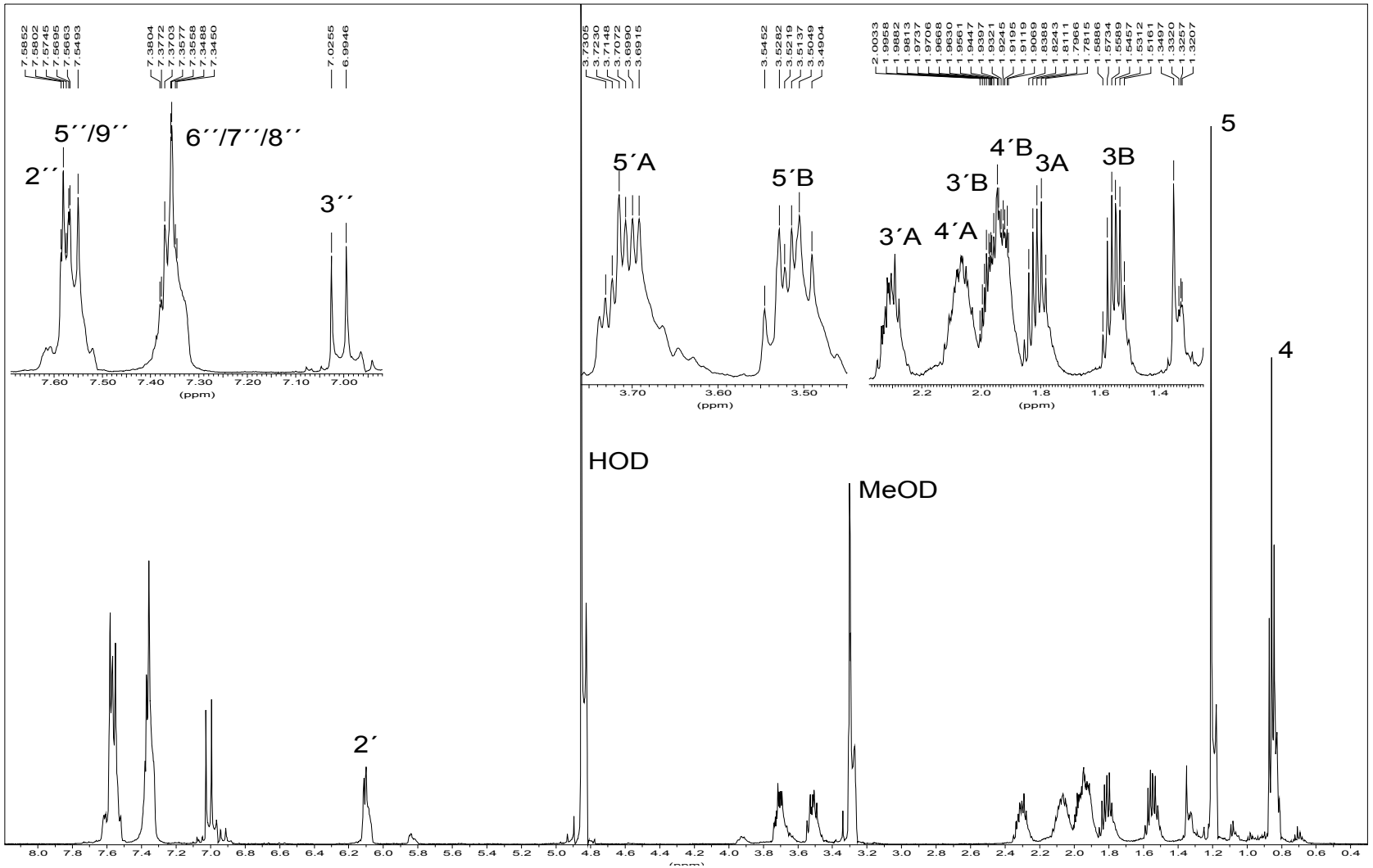

Fig. 3.89: ^{1}H NMR spectrum of compound 24 in MeOD

Thus, the H_3-5 methyl group was observed as a singlet instead of a doublet, as found in compound **23**. In addition, the ^{13}C NMR spectrum (see Fig. 3.90) revealed chemical shift of C-2 was shifted to 76.2 ppm due to a hydroxyl substituent. Furthermore, the methyl singlet signal of H_3-5 revealed strong correlations with C-1, C-2, C-3 and C-4 in the HMBC spectrum (see Fig. 3.92), which proved its position at C-2. H-2′ appeared at 6.15 ppm (dd, 1.6, 3.2) and HMBC long-range correlations with C-1, C-1′′,C-3′,C-4′,C-5′ were also observed to show cyclization of the putrescine moiety in comparison to that of an open chain in dasyclamide (**20**), or grandiamide B (**21**). The rest of the structure is similar to that of compound **23** as revealed by its ^1H NMR, ^1H-^1H COSY (see Fig. 3.91) and ^{13}C NMR data (see Table 3.31). Compound **24** was identical to odorinol, which was previously isolated from the leaves of *Aglaia odorata* collected in Thailand and Taiwan [Shiengthong *et al.,* 1979 and Hayashi *et al.,* 1982, respectively].

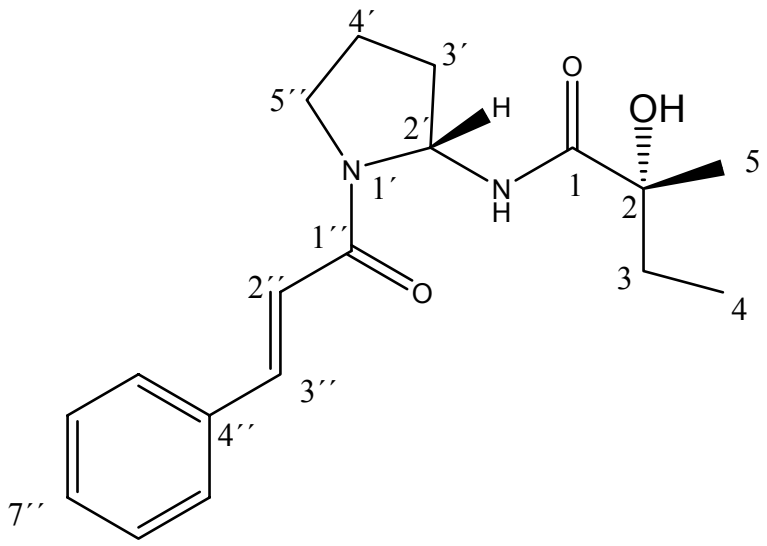

Odorinol

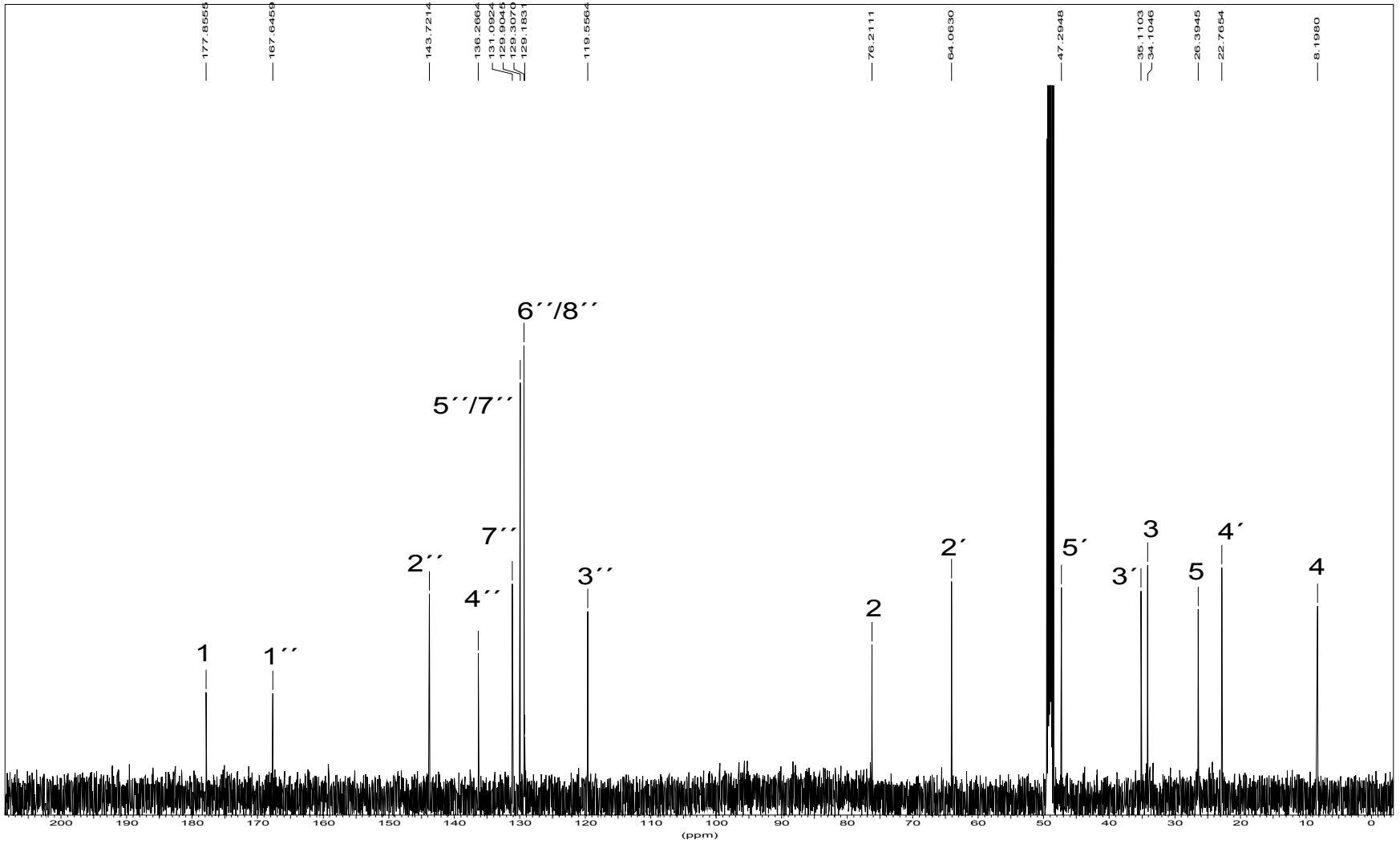

Fig. 3.90: ^{13}C NMR spectrum of compound 24 in MeOD

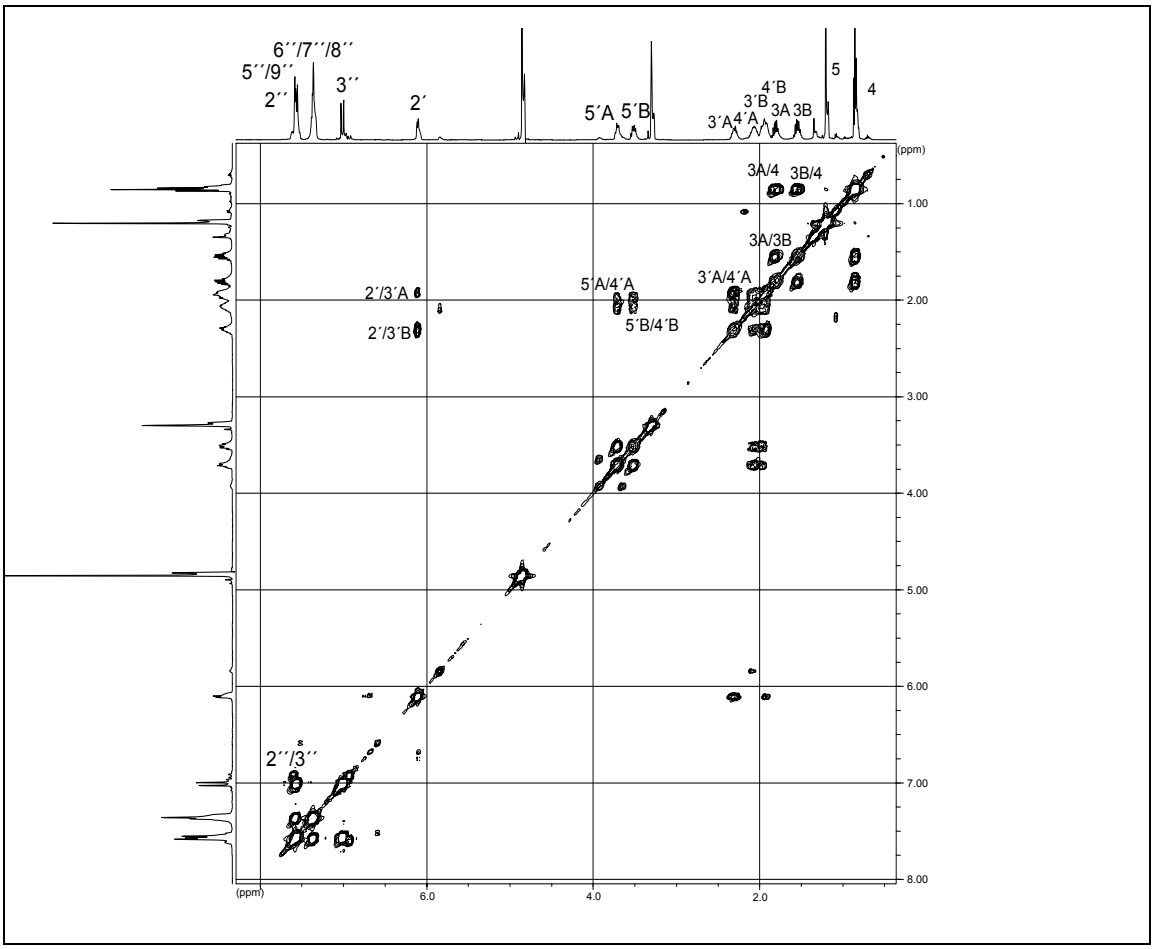

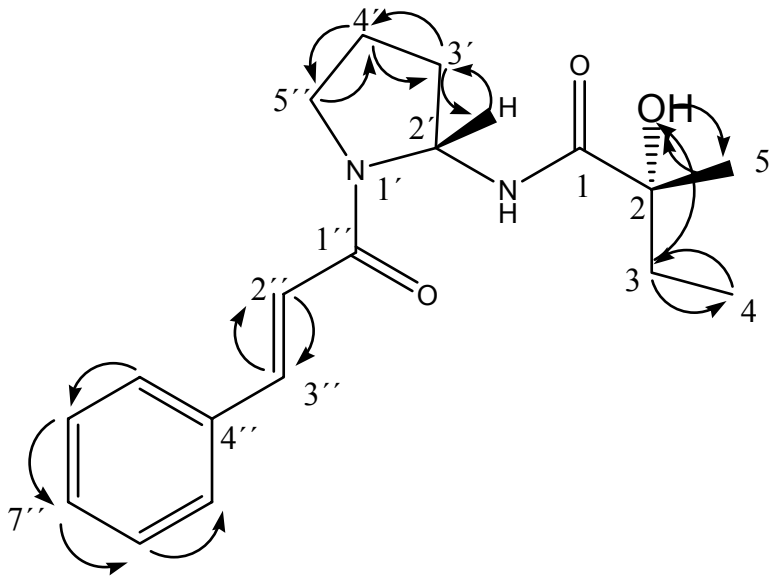

Fig. 3.91: ^{1}H-^{1}H COSY correlations of compound 24 in MeOD

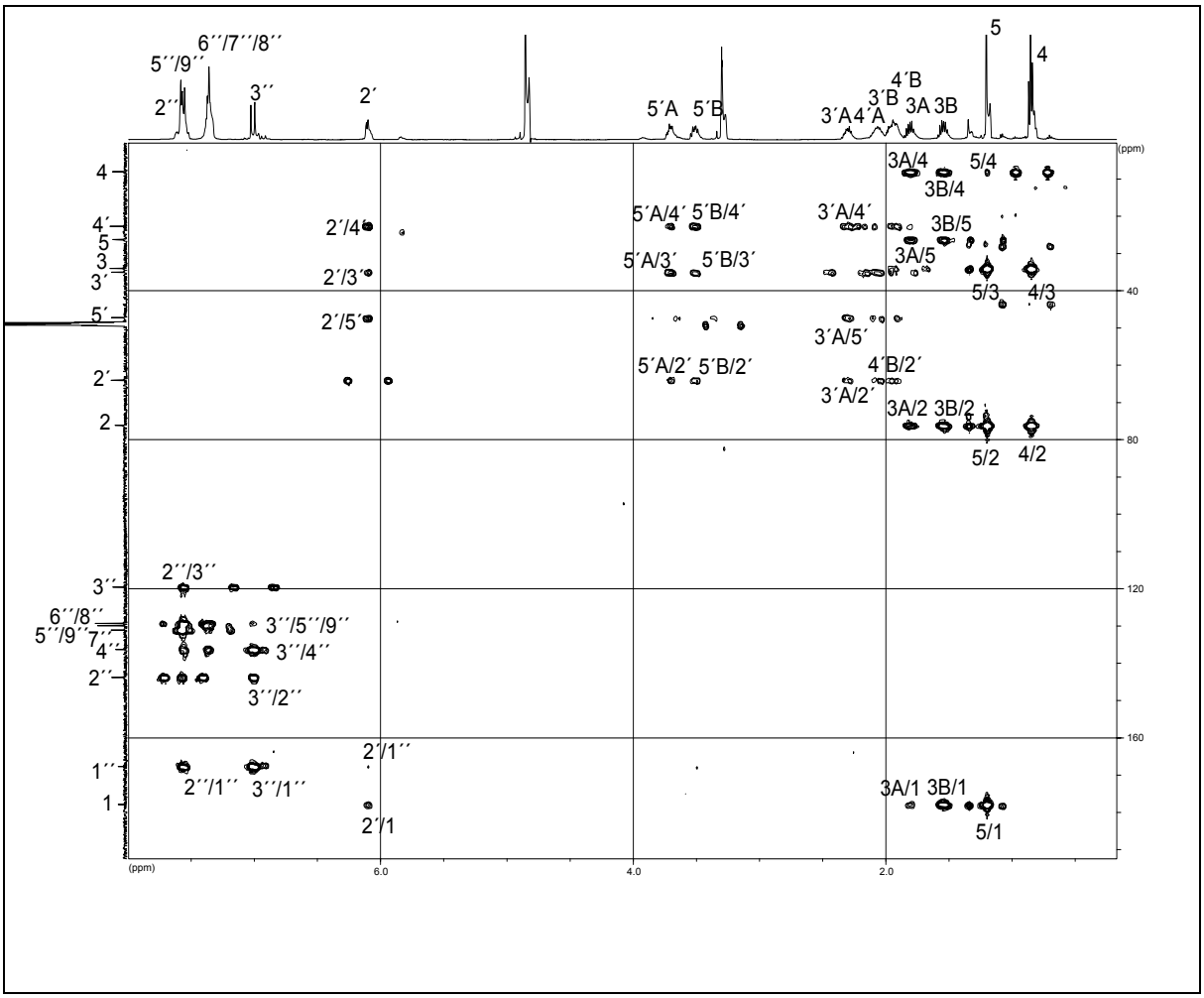

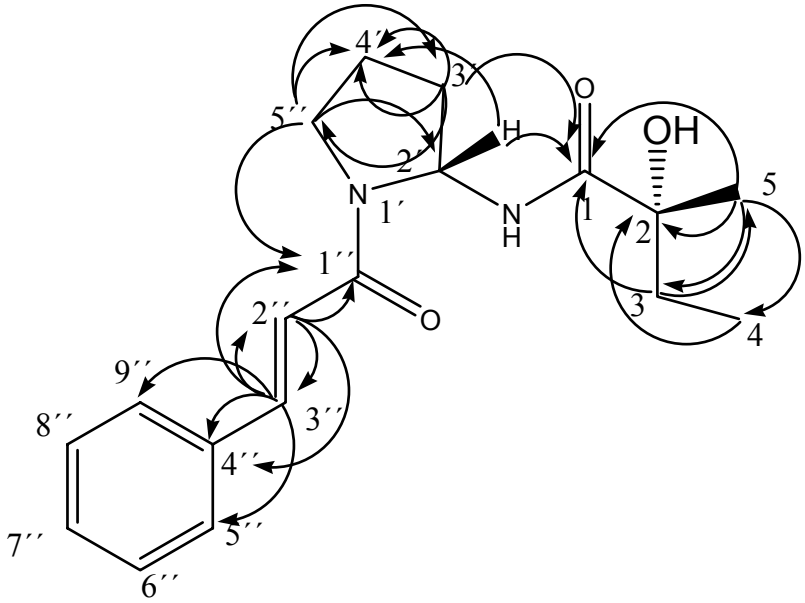

Fig. 3.92: HMBC correlations of compound 24 in MeOD

III.2.5.6. Gigantamide A (25, new compound)

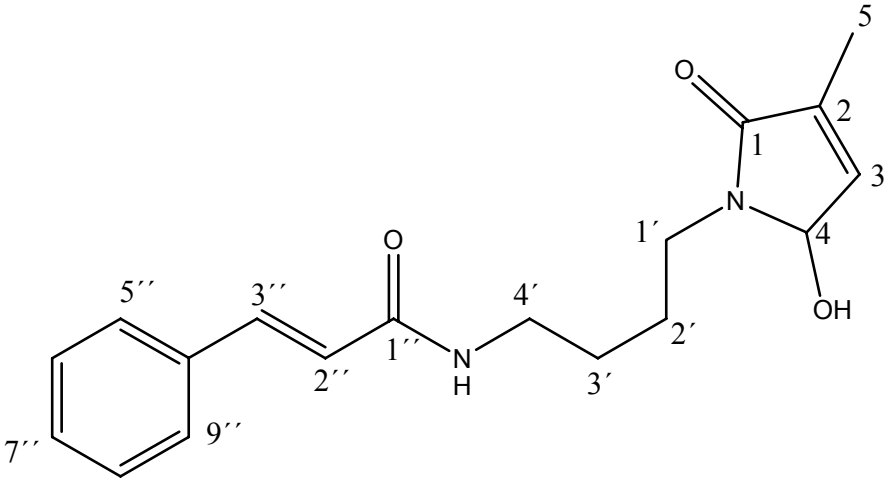

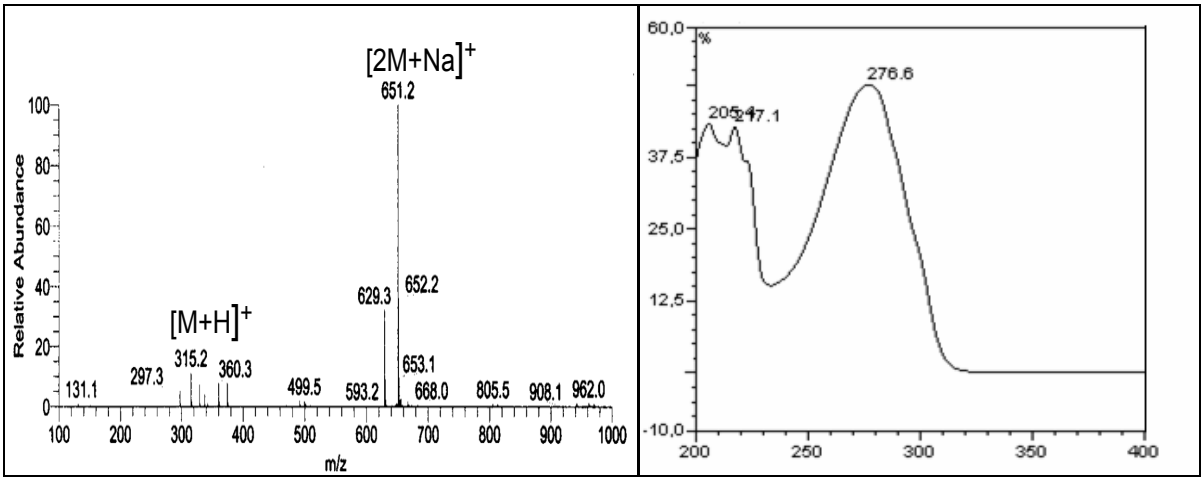

Fig. 3.93: EIS-MS spectrum and UV spectrum of compound 25

Compound **25** was isolated as a white amorphous residue from the leaves of *Aglaia gigantea*, $[\alpha]^{20}_{D}$-10 (*c*, 0.3, $CHCl_3$); UV (MeOH) λ_{max} 219.4, 224.2, and 285.2 nm (see Fig 3.93).The positive mode ESI-MS showed pseudomolecular ion peaks at *m/z* 315.2 $[M+H]^+$, *m/z* 629.3 $[2M+H]^+$, *m/z* 651.2 $[2M+Na]^+$ (see Fig 3.93). The negative mode ESI-MS showed peudomolecular ion peaks at *m/z* 313.8 $[M-H]^-$, *m/z* 359.4 $[M+HCOOH-H]^-$, and *m/z* 672.8 $[2M+HCOOH-H]^-$. The HREIMS also showed a pseudomolecular ion peak at *m/z* 337.151 $[M+Na]^+$, and the molecular weight is compatible with the molecular formula $C_{18}H_{22}N_2O_3$ as determined by HRMS. The ^{1}H NMR spectrum of compound **25** showed similar signals to dasyclamide. Mono-substituted aromatic ring system resonances appeared at δ 7.55 ppm -7.36 ppm (5H, *m*), the typical *trans*-configuration of proton H-2´´ and H-3´´ at 6.58 ppm (*d*, 15.7) and at 7.53 ppm (*d*, 15.7) were also present, and four methylene groups of the putrescine moiety at C-1´, C-2´, C-3´ and C-4´ were also observed. However, H-4 in compound **25** was

detected more downfield at δ 5.34 (d, *J*=6.9Hz), due to a hydroxyl substitutent at C-4 and the residing nitrogen atom of the pyrrolidinone ring. The chemical shift of H-3, in the pyrrolidinone ring, was also shifted to lower field at δ 6.62 (d,q, *J*=1.6Hz; 6.9 Hz) in comparison to that of dasyclamide, which is an open chain. H-3 was identified as a coupling of homoallylic spin system occurred at δ 6.62 (dq, 1.6, 3.2). Therefore, in the ^{13}C NMR spectrum (see Fig. 3.95), C-4 in compound **25** was shifted more down field at δ 82.4 (*d*), due to the presence of an hydroxyl group at C-4 and the residing nitrogen atom of the pyrrolidinone ring, compared to that of dasyclamide (**20**) at δ 60.0 (*t*). The carbonyl group at position C-1 was also 2 ppm shifted upfield to 170.9 ppm due to the effect of the pyrrolidinone ring, when compared to dasyclamide, which is an open chain. The ^{1}H NMR spectrum (in DMSO) of compound **25** showed a broad triplet at 8.10 ppm (t, *J*=5.4 Hz) corresponding to an amino group NH, which coupled with two neighbouring methylene protons of H-4′A and H-4′B (see Table 3.39 and Fig. 3.94). The hydroxy group at C-4 was also observed at δ 6.10 (d, *J*=7.5Hz). Through ^{1}H-^{1}H COSY (see Fig. 3.98), the homoallylic correlation of H-3 (^{4}J) to H_3-5 methyl was observed as well as the correlation between H-4 and H-3 in the pyrrolidinone ring system. The (^{3}J) correlation of H-4 to hydroxyl group (OH) was also observed in the COSY spectrum. Furthermore, the amino proton (NH) showed correlations to the methylene protons (H-4′A and H-4′B), which proved an open chain of the putrescine moiety. The correlation between H-2′′ and H-3′′ doublets belonging to the typical *trans*-olefinlic protons, was also observed clearly through the COSY spectrum. In the HMBC spectrum (see Fig. 3.97), H-5′′/H-9′′ signals at 7.51 ppm exhibited correlations with C-1′′ at 167.2 ppm proving for the presence of the cinnamoyl moiety.

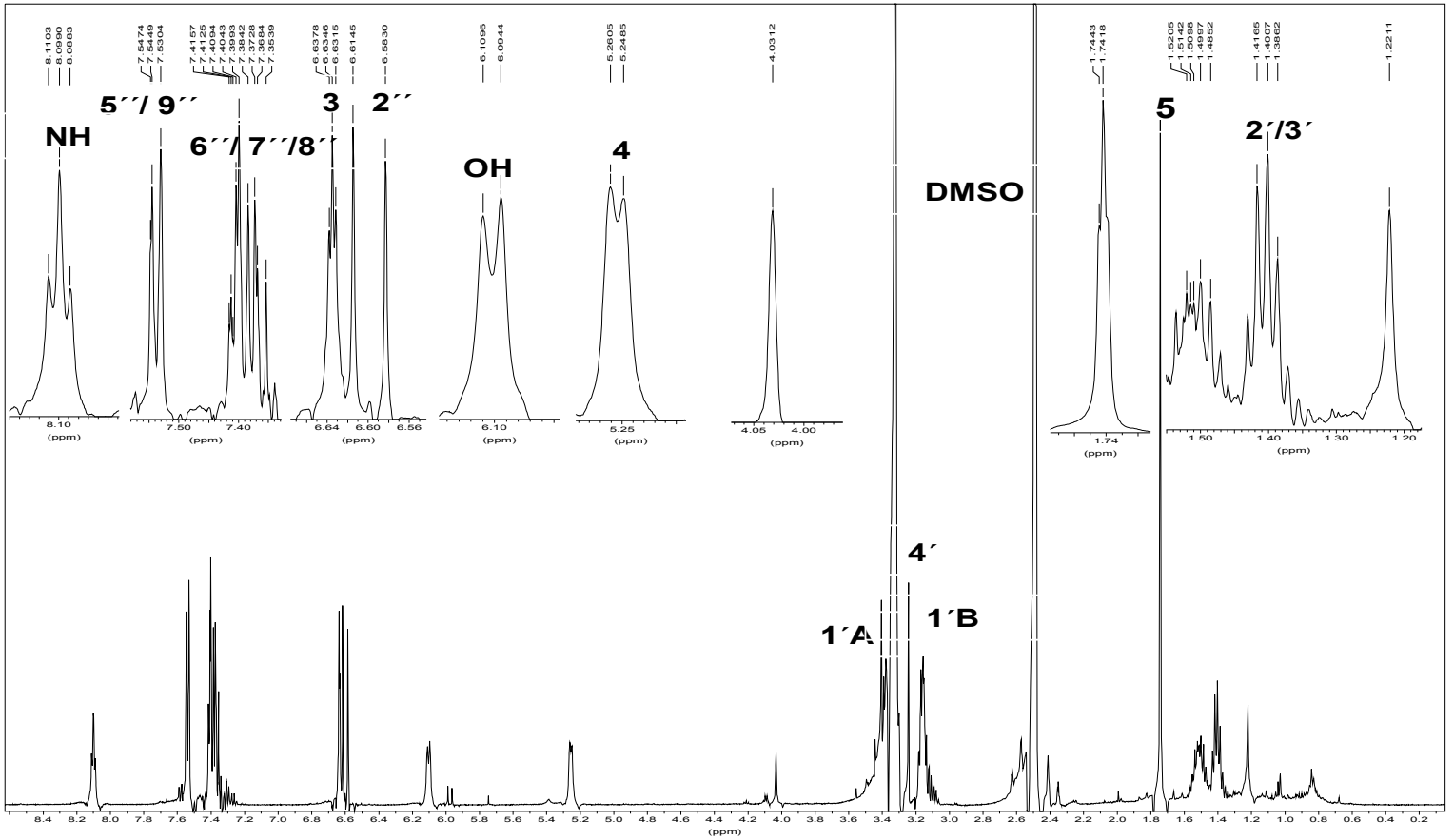

Fig. 3.94: ^{1}H NMR spectrum of compound 25 in DMSO

Besides, H-3′′ occurred at 7.63 ppm (d, *J*=15.7Hz) and H-2′′ at 6.41ppm (d, *J*=15.7Hz) also showing correlations to the carbonyl (C-1′′) at 167.2 ppm, which again proved the presence of the cinnamoyl moiety. H-3 resonated at δ 6.62 (dq, *J*=1.6Hz, 6.9Hz) and showed correlations with the carbonyl (C-1) at 170.9 ppm, which showed the occurrence of the pyrrolidinone ring . Furthermore, H_3-5 methyl signal at 1.89 ppm also showed its correlation with C-1 at 170.9 ppm, C-2 at 130.2 ppm and C-3 at 137.5 ppm, respectively. Compound **25** was identified as a new cinnamoyl bisamide, isolated from the leaves of *Aglaia gigantea* collected from Vietnam. Compound 25 was named gigantamide A. The absolute stereochemistry at C-4 was not determined due to the very small amount of the compound isolated.

Table 3.39: ^{1}H NMR and ^{13}C NMR data of compound 25 in MeOD

Position ^{13}C	**δ_H (ppm), *J* (Hz)**	**δ_C (ppm)[a]**
1		170.9 s
2		130.2 s
3	6.62(*dq*,1.6, 3.2)	137.5 d
4	5.33 (*d*, 3.1)	82.4 d
5	1.75(*dt*,1.3, 1.9)	11.3 q
1′	3.53 (*m*,2H)	39.4 t
2′	1.67 m	25.5 t
3′	1.60 m	27.4 t
4′	3.30 m	39.0 t
1′′		167.2 s
2′′	6.58 (*d*,15.7)	120.6 d
3′′	7.53 (*d*,15.7)	141.9 d
4′′		138.4 s
5′′/9′′	7.55 m	128.2 d
6′′/8′′	7.36 m	129.2 d
7′′	7.54 m	130.2 d

[a]: obtained from the HMBC spectrum

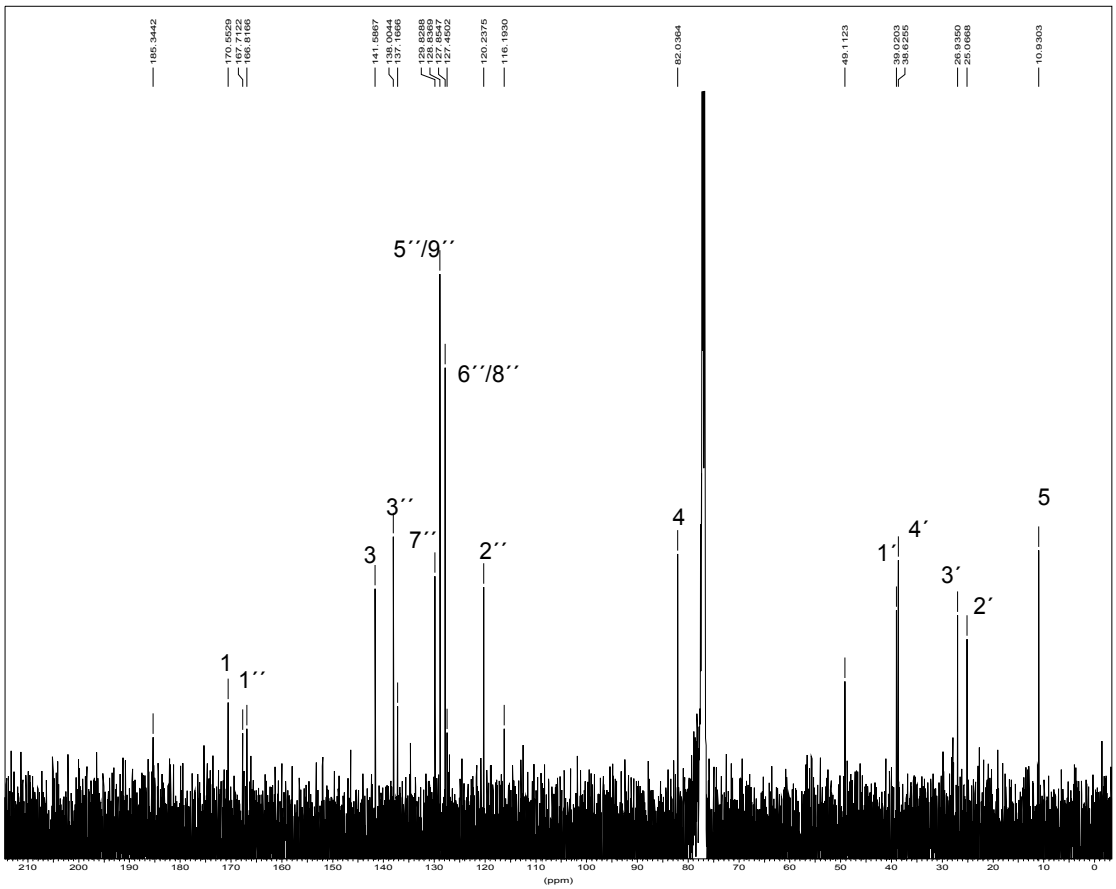

Fig. 3.95: ^{13}C NMR spectrum of 25 in $CDCl_3$

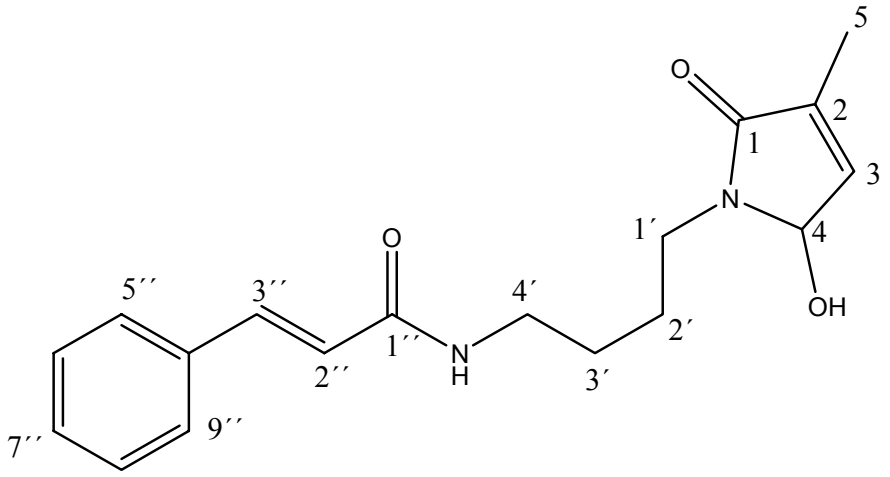

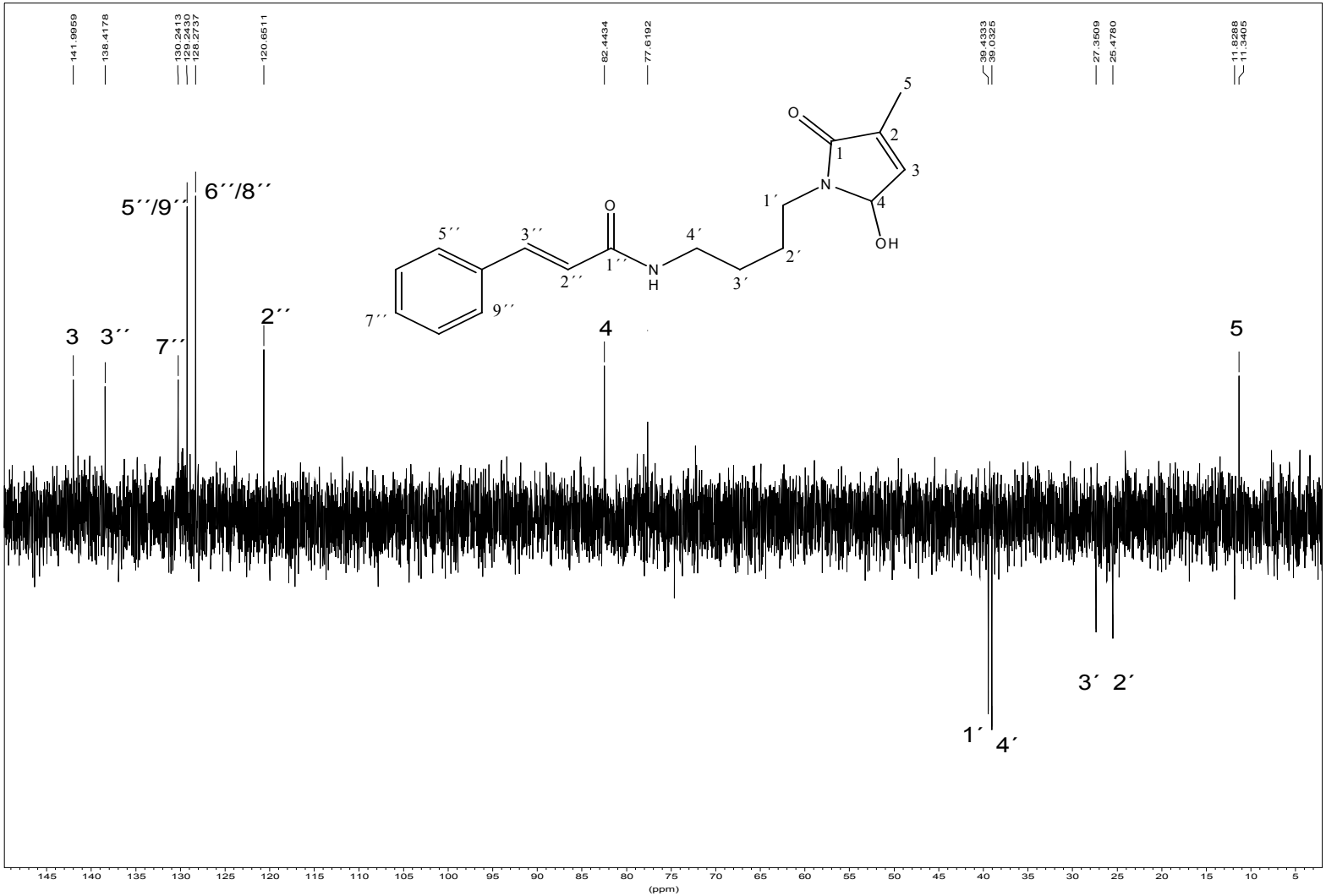

Fig. 3.96: DEPT spectrum of compound 25

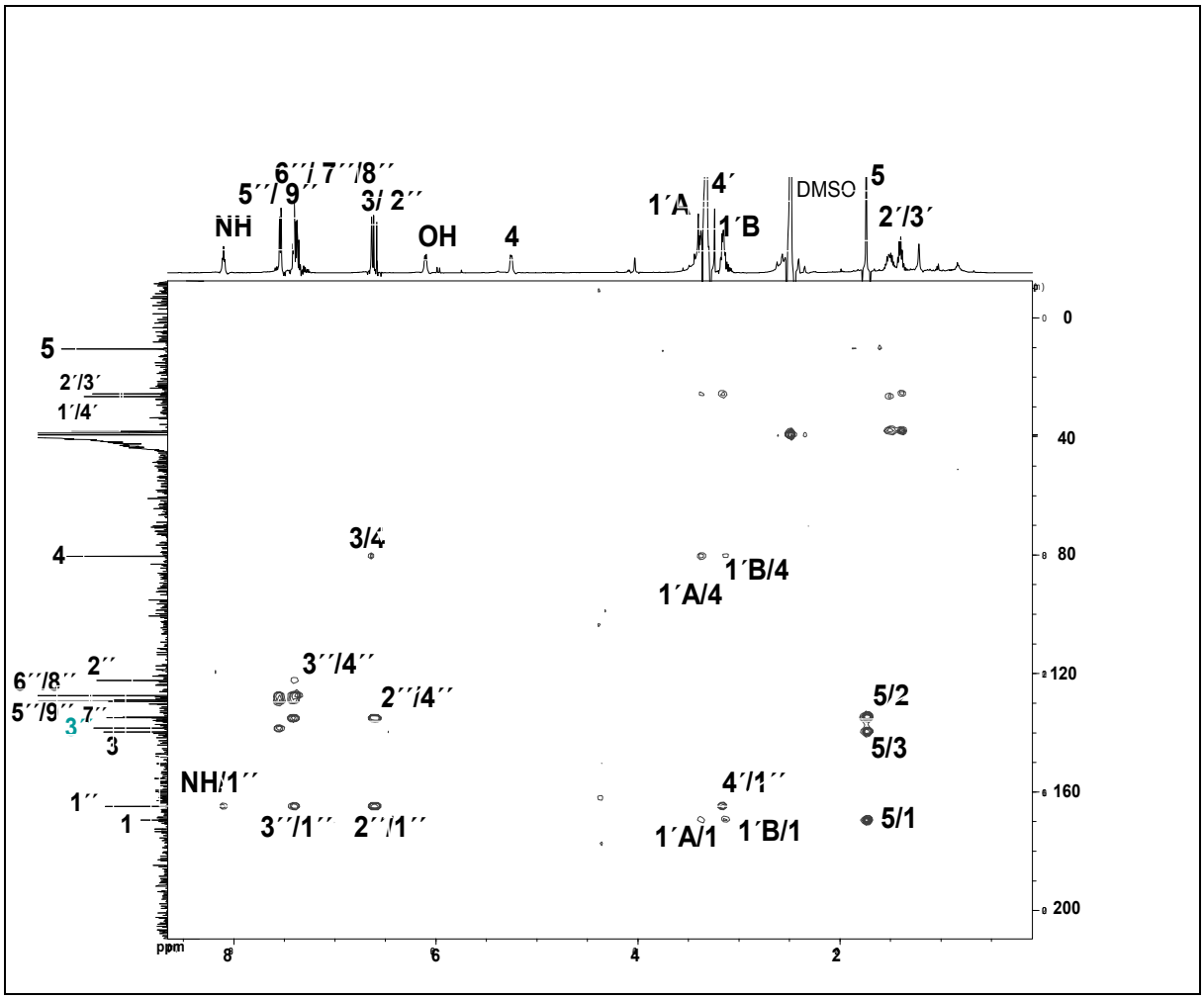

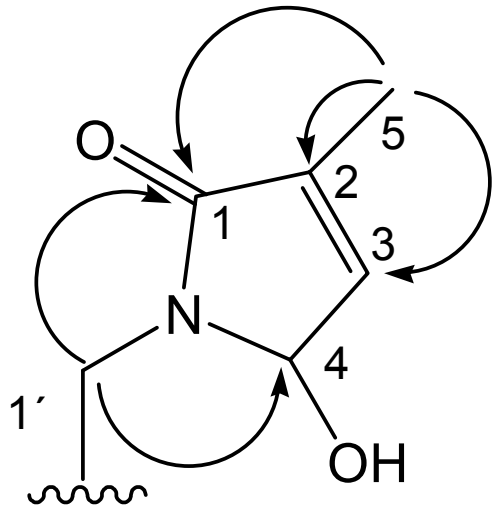

Fig. 3.97: HMBC correlations of compound 25 in DMSO

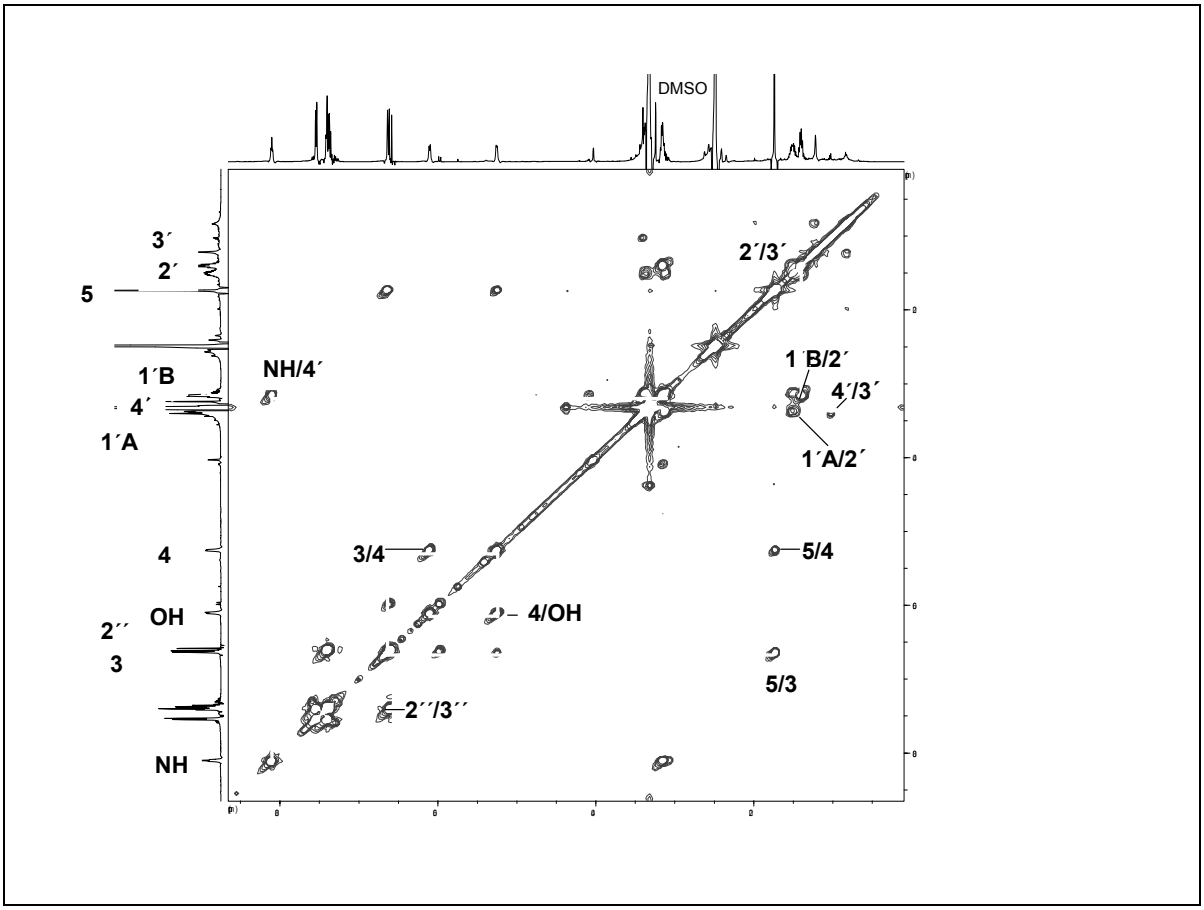

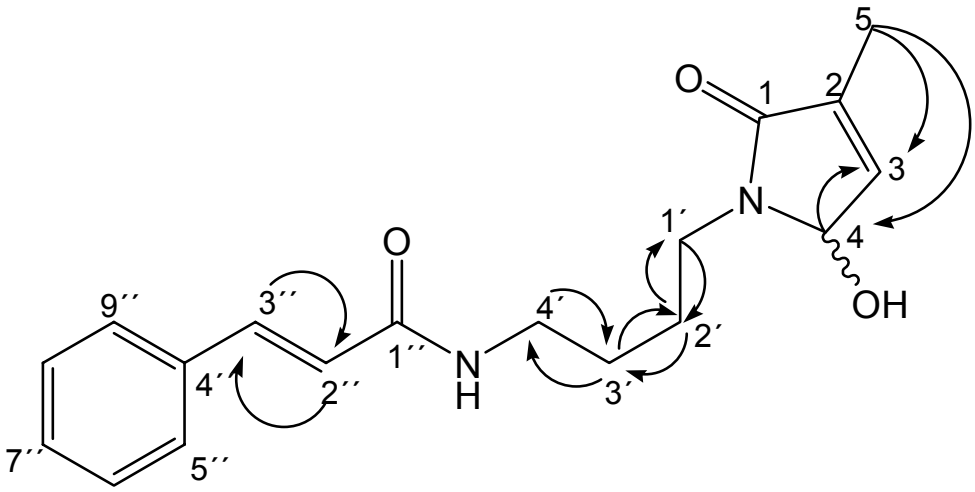

Fig. 3.98: ^{1}H-^{1}H COSY correlations of compound 25 in DMSO

III.2.5.7. Pyramidatine (26, known compound)

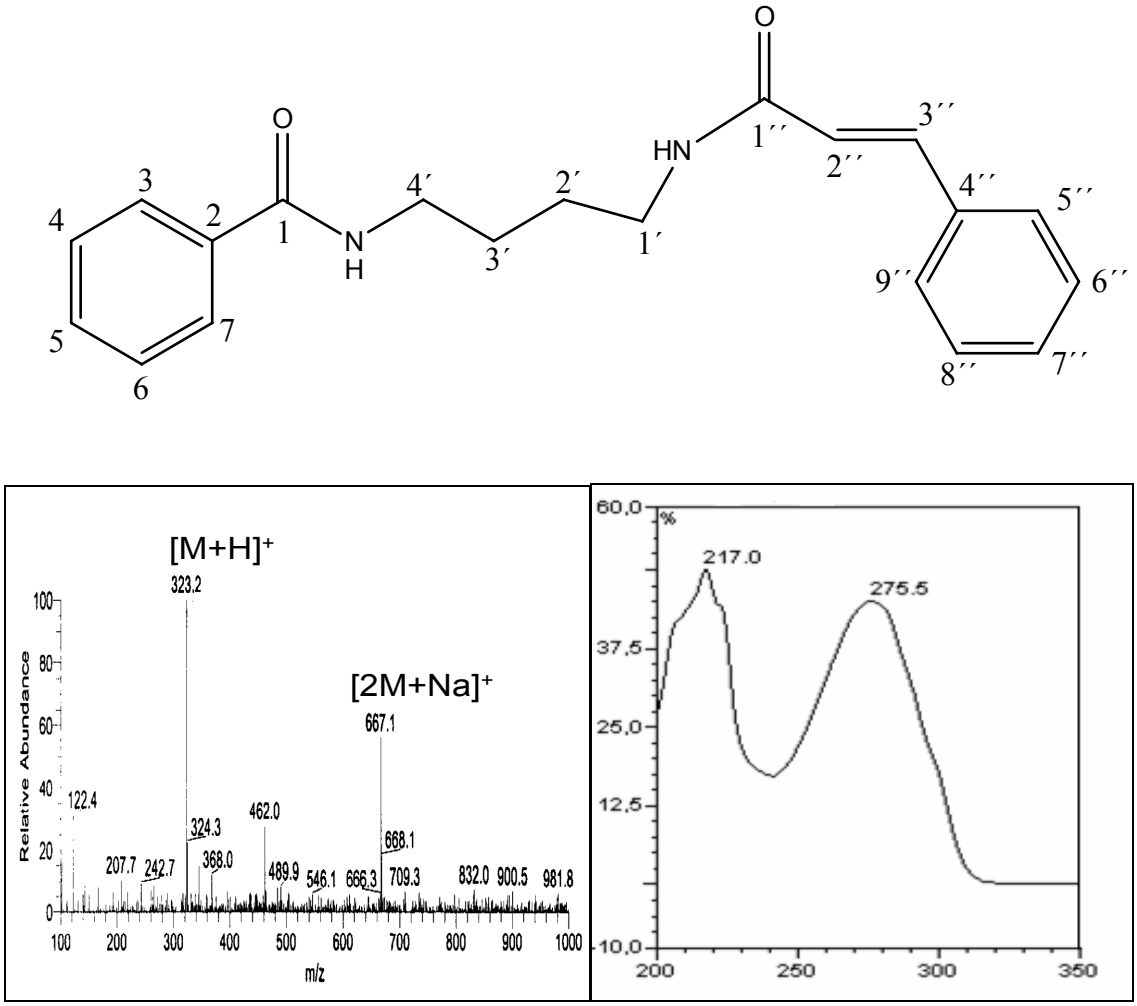

Fig. 3.99: ESI-MS and UV spectrum of compound 26

Compound **26** was isolated from the leaves of *Aglaia oligophylla* as a white amorphous residue; $[\alpha]^{20}_{D}$-125 (*c*, 0.48, $CHCl_3$); UV (MeOH) λ_{max} 217.0 and 276.5 nm (see Fig. 3.99). The positive mode of ESI-MS showed the pseudomolecular ion peak at *m/z* 323.2 $[M+H]^+$, and *m/z* 667.1 $[2M+Na]^+$, respectively (see Fig. 3.99). The occurrence of a cinnamoyl moiety was suggested by the ion at *m/z* 131 in the EI-MS spectrum. The *trans* stereochemistry was again confirmed by a pair of doublets (*J*= 17.5 Hz) at δ 6.58 ppm (H-2´´) and 7.39 ppm (H-3´´) in the ^{1}H NMR spectrum (see Fig. 3.100). The ^{1}H-^{1}H COSY spectrum (see Fig. 3.101) showed the correlations of the methylene protons at δ 3.35 and 1.69 of the putrescine moiety and ten aromatic protons of the two phenyl rings which occurred in the region at 7.34-7.77 ppm (see Fig. 3.102). In comparison with the literature [Saifah *et al.,* 1993] and based on the spectra data (see Table 3.40), compound **26** was identified as a known compound, pyramidatine, which was previously isolated from *Aglaia pyramidata* collected in Thailand.

Table 3.40: ^{1}H NRM data of compound 26 (in MeOD)

^{1}H position	δ_H (ppm), *J* (Hz)	Literature*
3/7	7.79 (dd, 8.2, 1.9)	7.84 (dd, 8.3, 1.6)
4/6	7.44 (dd, 8.2, 8.2)	7.44 (dd, 8.3, 8.3)
5	7.52 (m)	7.48 (m)
1′	3.25 (dd, 11.9, 6.7)	3.21 (dd, 12.5, 6.6)
2′	1.55-1.61 (m)	1.43-1.58 (m)
3′	1.62-1.68 (m)	1.50-1.64(m)
4′	3.40 (dd, 11.9, 6.7)	3.28 (dd, 12.5, 6.6)
2′′	6.59 (d, 15.7)	6.63 (d, 15.8)
3′′	7.51 (d, 15.7)	7.42 (d, 15.8)
5′′/9′′	7.54 (dd, 8.2, 1.9)	7.54 (dd, 8.0, 1.6)
6′′/8′′	7.37 (dd, 8.2, 1.9)	7.39 (dd, 8.0, 1.6)
7′′	7.34 (m)	7.35 (m)

*:[Saifah *et al.,* 1993]

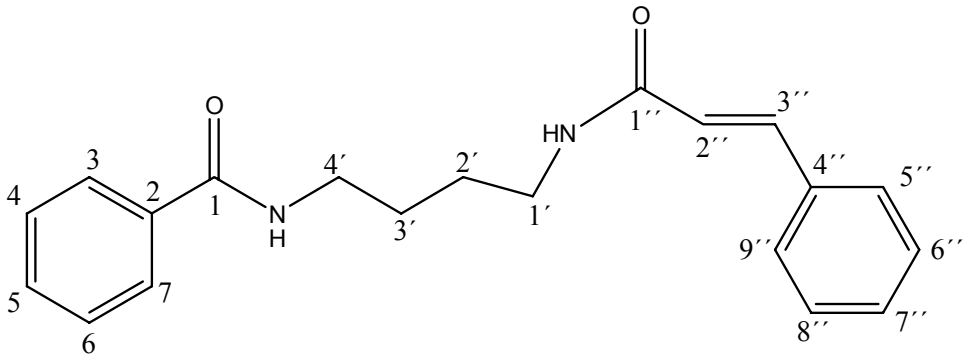

Pyramidatine

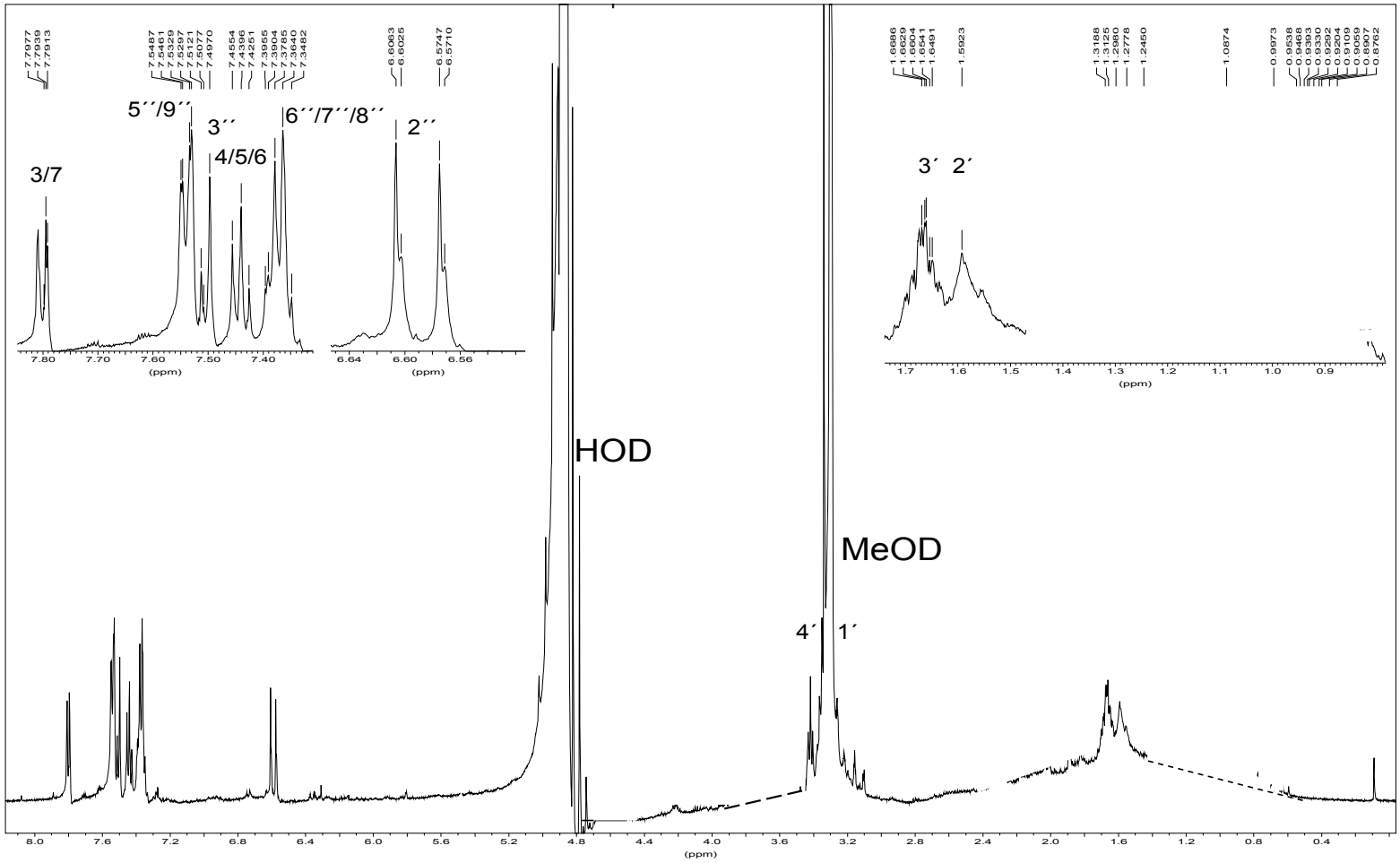

Fig. 3.100: ^{1}H NMR spectrum of compound 26 in MeOD

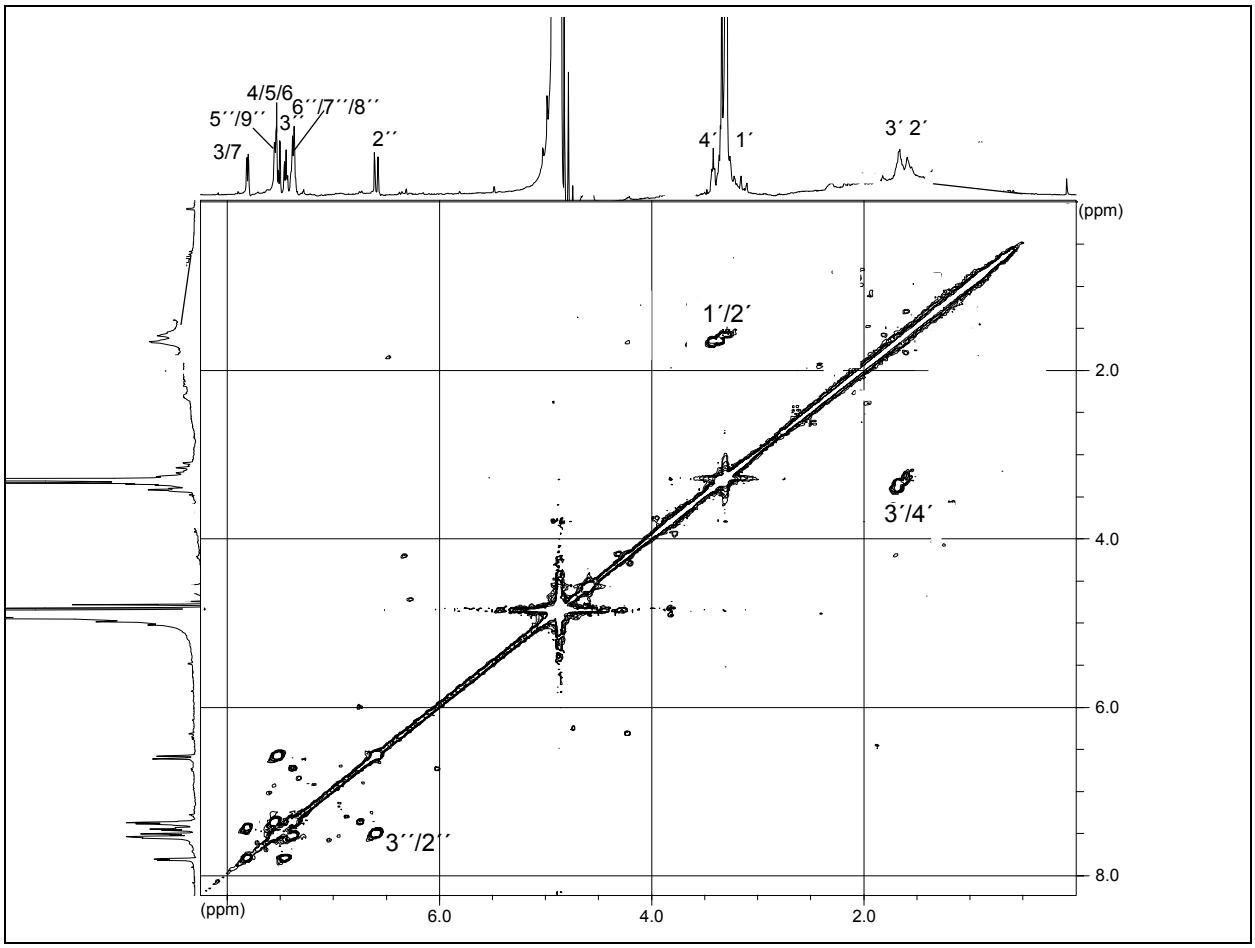

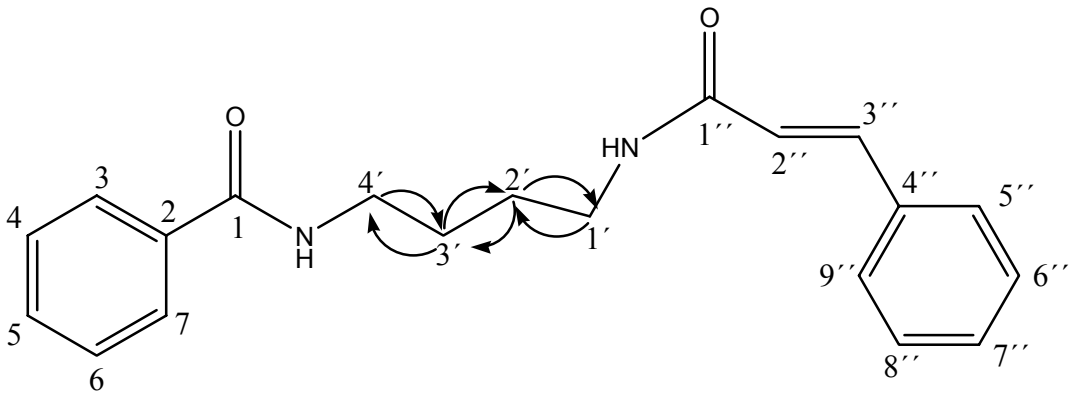

Fig. 3.101: ^{1}H-^{1}H-COSY correlations of compound 26 in MeOD (at highfield)

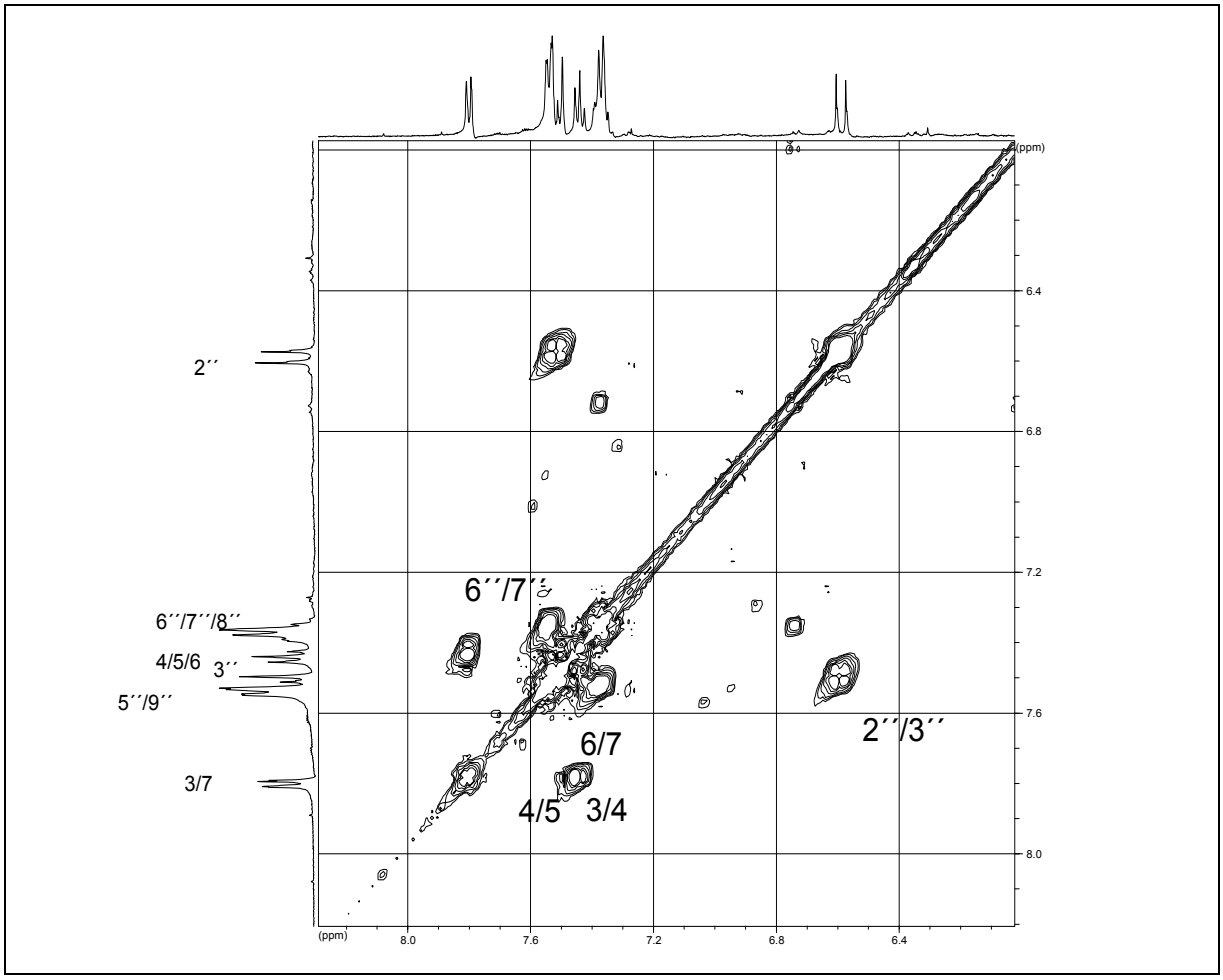

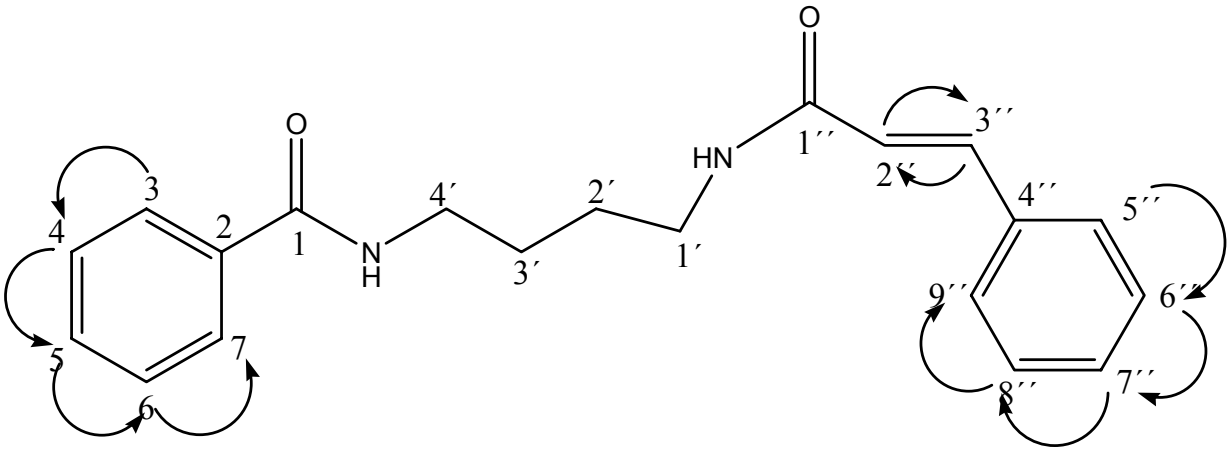

Fig. 3.102: ^{1}H-^{1}H-COSY correlations of compound 26 in MeOD (at lowfield)

III.2.6. Terpenoid compounds from *Aglaia* sp.

III.2.6.1. Triterpenoids from *Aglaia* sp.

III.2.6.1.1. Foveolin B (27, known compound)

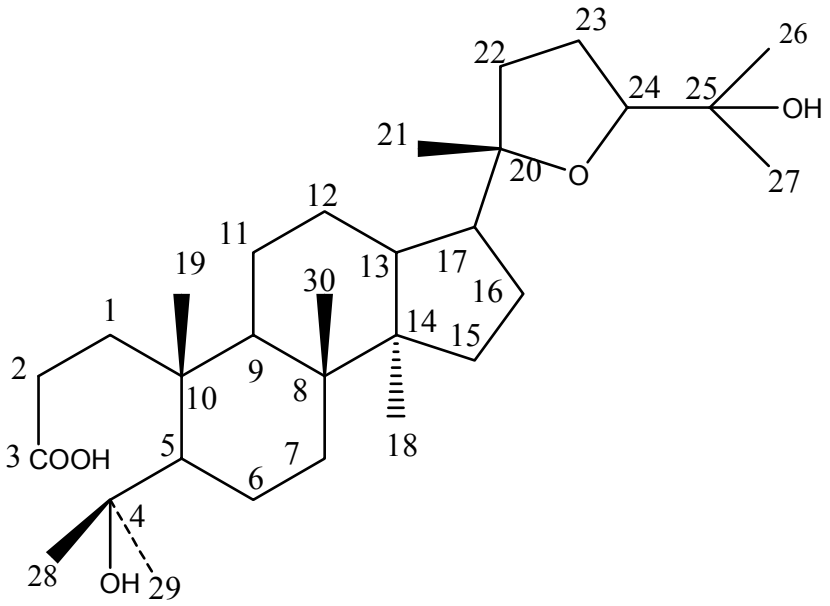

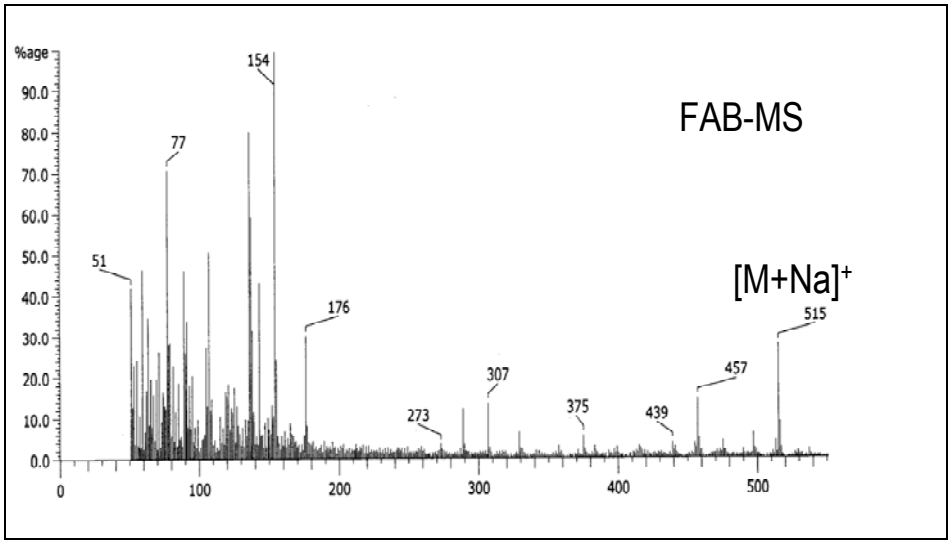

Fig. 3.103: FAB-MS spectrum of compound 27

Compound **27** was isolated from the leaves of *Aglaia gigantea* as a white amorphous residue; $[\alpha]^{20}_{D}$+25 (*c*, 0.5, $CHCl_3$). The FAB-MS showed a pseudomolecular ion peak at *m/z* 515 $[M+Na]^+$ (see Fig. 3.103). The ^{1}H NMR spectrum (see Fig. 3.104) of compound **27** exhibited the signal of eight tertiary methyls between 0.85 and 1.30 ppm and of an oxymethine at δ 3.72 (dd, 7.5, 7.5). Besides, the ^{13}C NMR spectrum (see Fig. 3.105) exhibited 30 signals including

that of a carbonyl resonance at δ 178.8 attributed for a carboxylic acid residue of a triterpenoid. The DEPT spectrum (see Fig. 3.106) revealed eight methyl singlets, nine methylenes and five methine carbons, suggesting eight remaining quaternary carbons.

In the HMBC spectrum (see Fig. 3.108), all methyl singlets showed their correlations with their neighboring carbons and unequivocally defined their positions along with the other substituents, as shown in Table 3.41. The long-range correlations of the methyl proton signal at δ 1.12 (H_3-21) with the quaternary carbon signal at δ_{C-20} 86.3 as well as the correlations of δ 1.19 (H_3-26) and δ 1.07 (H_3-27) with the methine carbon signal at δ_{C-24} 83.2 identified the oxygen linkage between C-20 and C-24 of the epoxy ring (see HMBC spectrum, Fig. 3.110). In addition, the placement of another oxygenated substituent at C-25 was supported by the long-range correlations of CH_3-26 and CH_3-27 with the quaternary carbon at δ_{C-25} 71.5. Similarly, the placement of the other oxygenated substituent at C-4 was also supported by the long-range correlations of CH_3-28 at δ 1.29 and CH_3-27 at δ 1.24 with the quaternary carbon at δ_{C-4} 76.4. Moreover, CH_3-18 (δ 0.84) correlates with C-8, C-13, C-14, and C-15, while CH_3-19 (δ 0.99) correlated with C-1, C-5, C-9, and C-10; H_3-21 (δ 1.12) correlated with C-17, C-20, and C-22; CH_3-26 (δ 1.19) correlated with C-24, C-25, C-27; CH_3-27 correlated with C-24, C-25, C-26; CH_3-28 (δ 1.29) correlated with C-4, C-5, C-29; while CH_3-29 (δ 1.24) correlated with C-4, C-5, and C-28, and H_3-30 (δ 0.96) correlated with C-7, C-8, C-9 and C-14. The ^{1}H NMR spectrum revealed a typical oxymethine at δ 3.72 (dd, 7.5, 7.5) of H-24 in 20*S*, 24*R*-epoxy-25-hydroxydammaranes [Roux *et al* 1998] (see Table 3.41 and Fig. 3.104). The typical oxymethine (H-24) was confirmed by its long-range correlations to C-22, C-23, C-25, C-26 and C-27 through the HMBC spectrum (see Fig. 3.109).

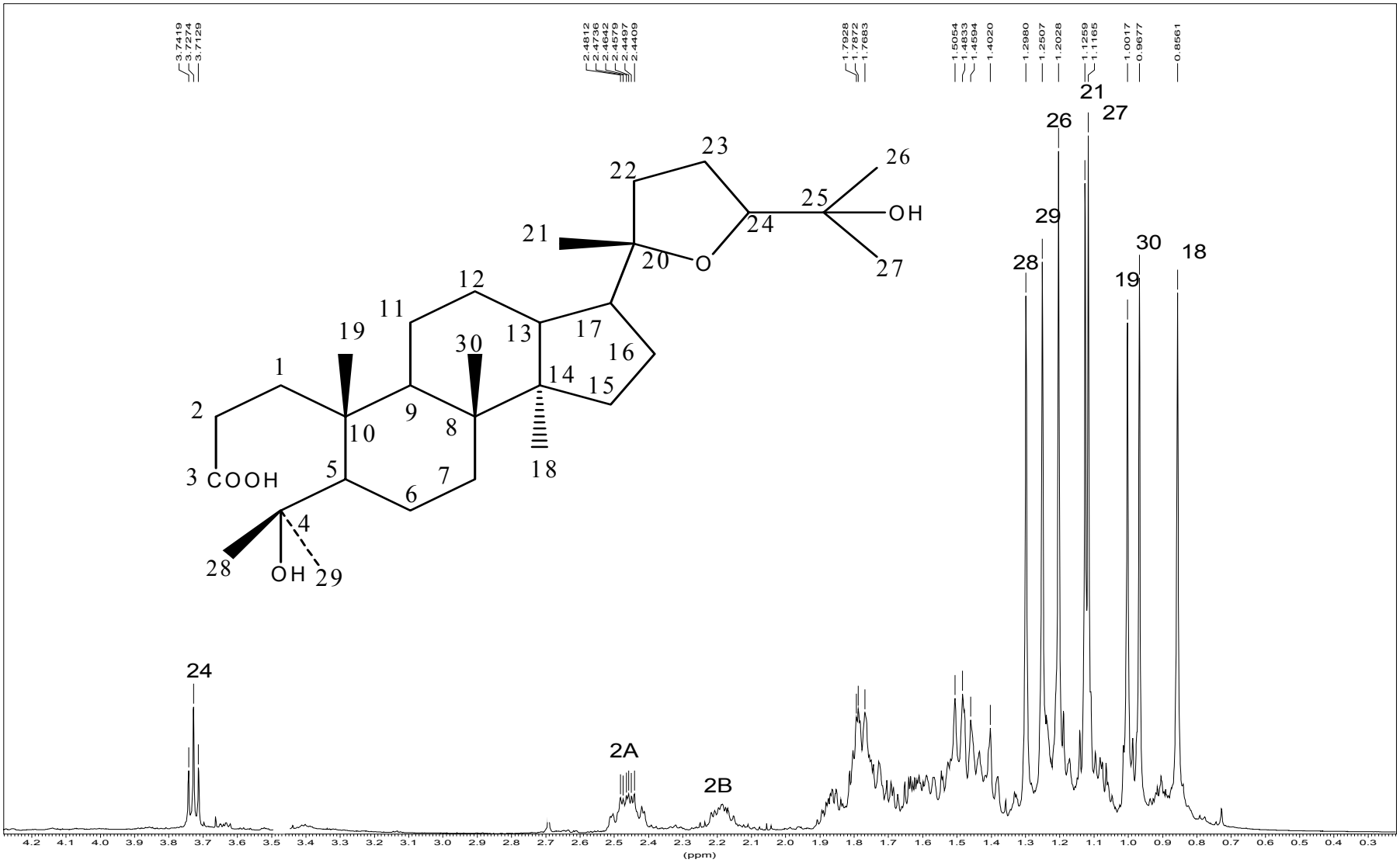

Fig. 3.104: ^{1}H NMR spectrum of 27 in $CDCl_3$

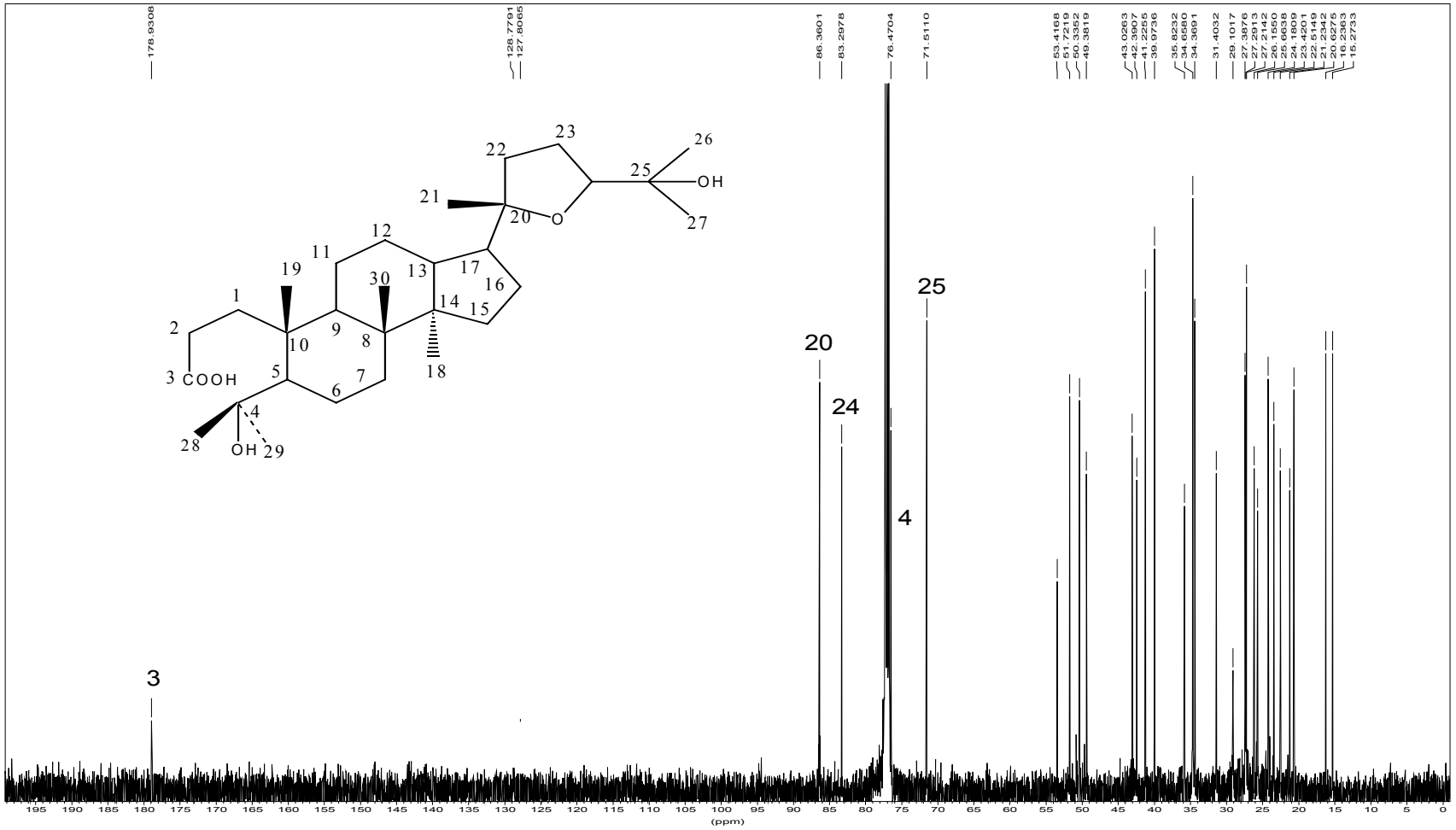

Fig. 3.105: ^{13}C NMR spectrum of 27 in $CDCl_3$

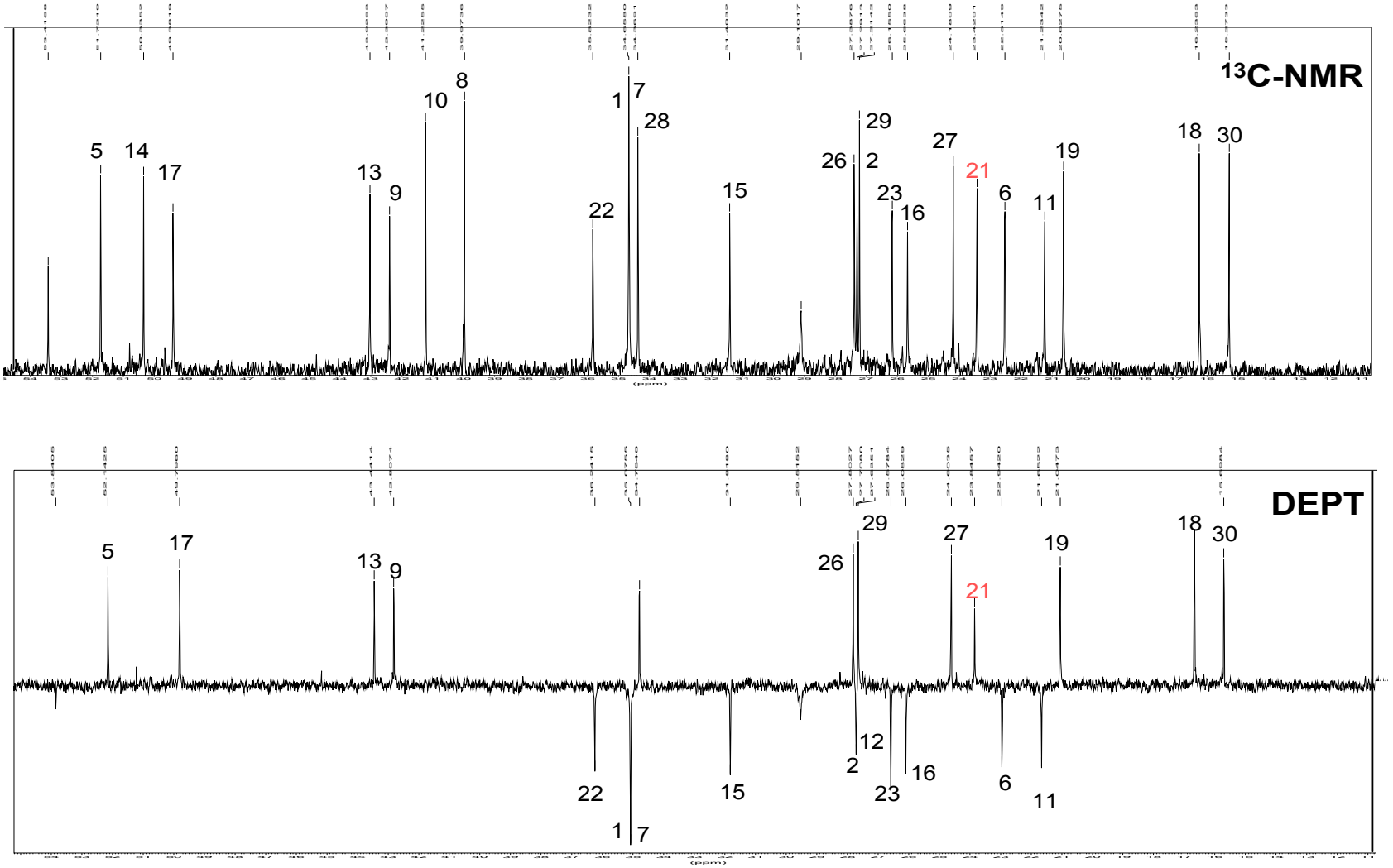

Fig. 3.106: ^{13}C NMR (above) and DEPT (below) spectrum of 27

The HMQC (see Fig. 3.107) showed direct correlations of methyl protons to their methyl carbons. However, the resonances of these methyl signals were also observed as pairs of symmetric cross peaks in the HMBC. In comparison with the literature data [Roux *et al.,* 1998] and based on the 1D and 2D NMR spectra, compound **27** was identified as foveolin B.

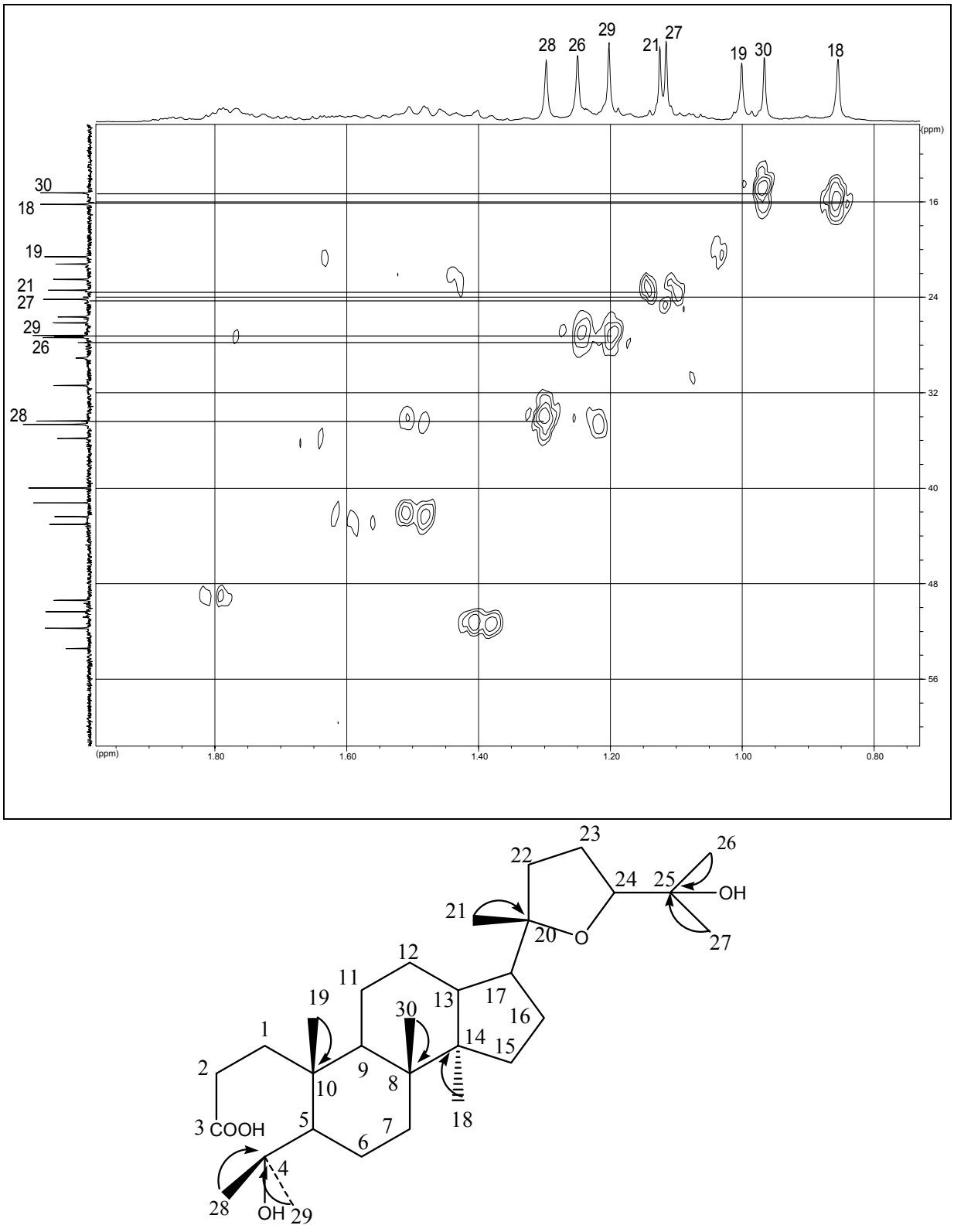

Fig. 3.107: Direct HMQC correations of methyl groups of compound 27 in $CDCl_3$

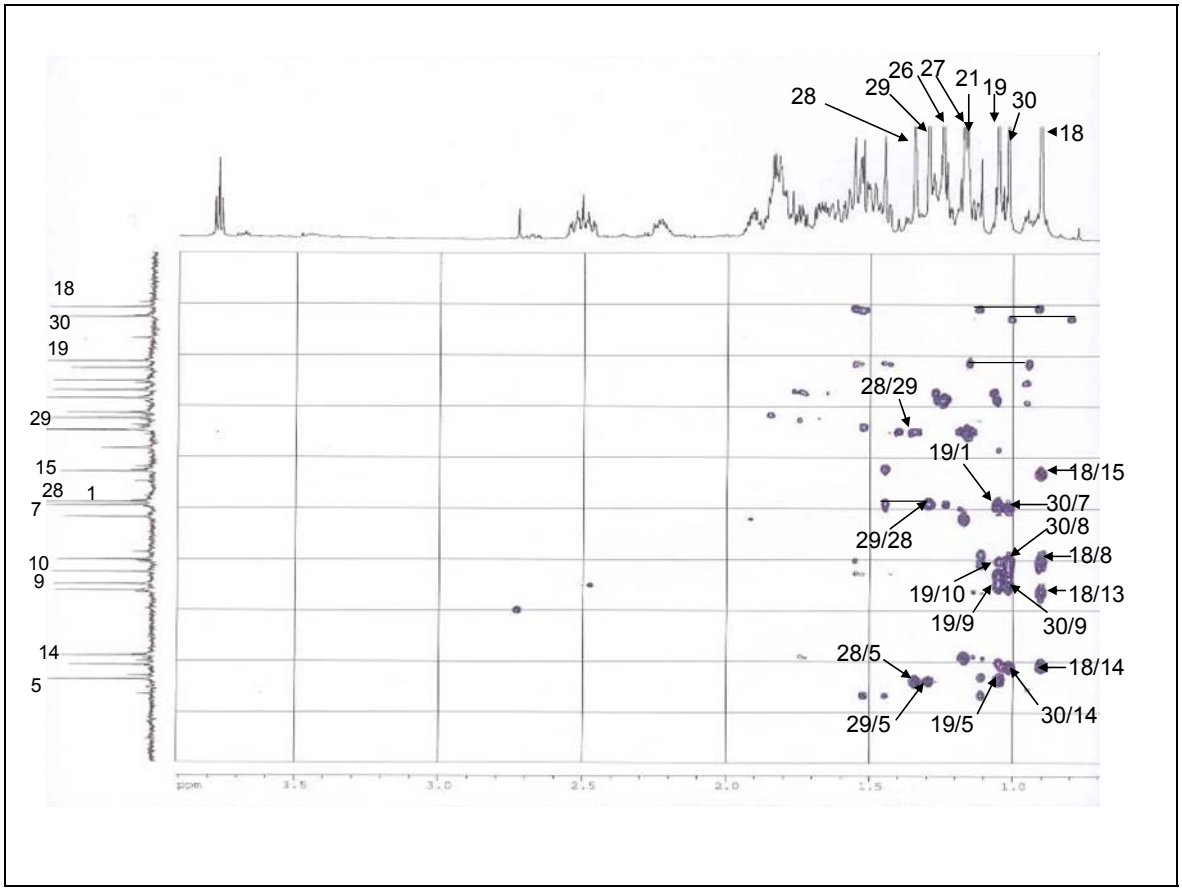

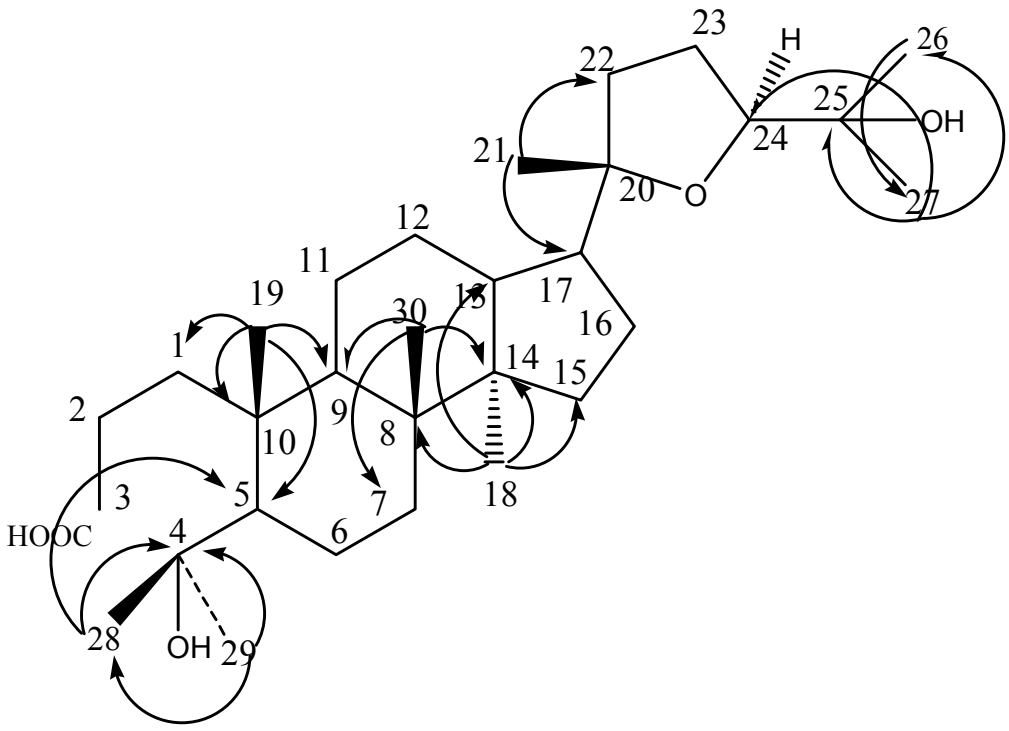

Fig. 3.108: HMBC spectrum of compound 27 in $CDCl_3$ (at highfield)

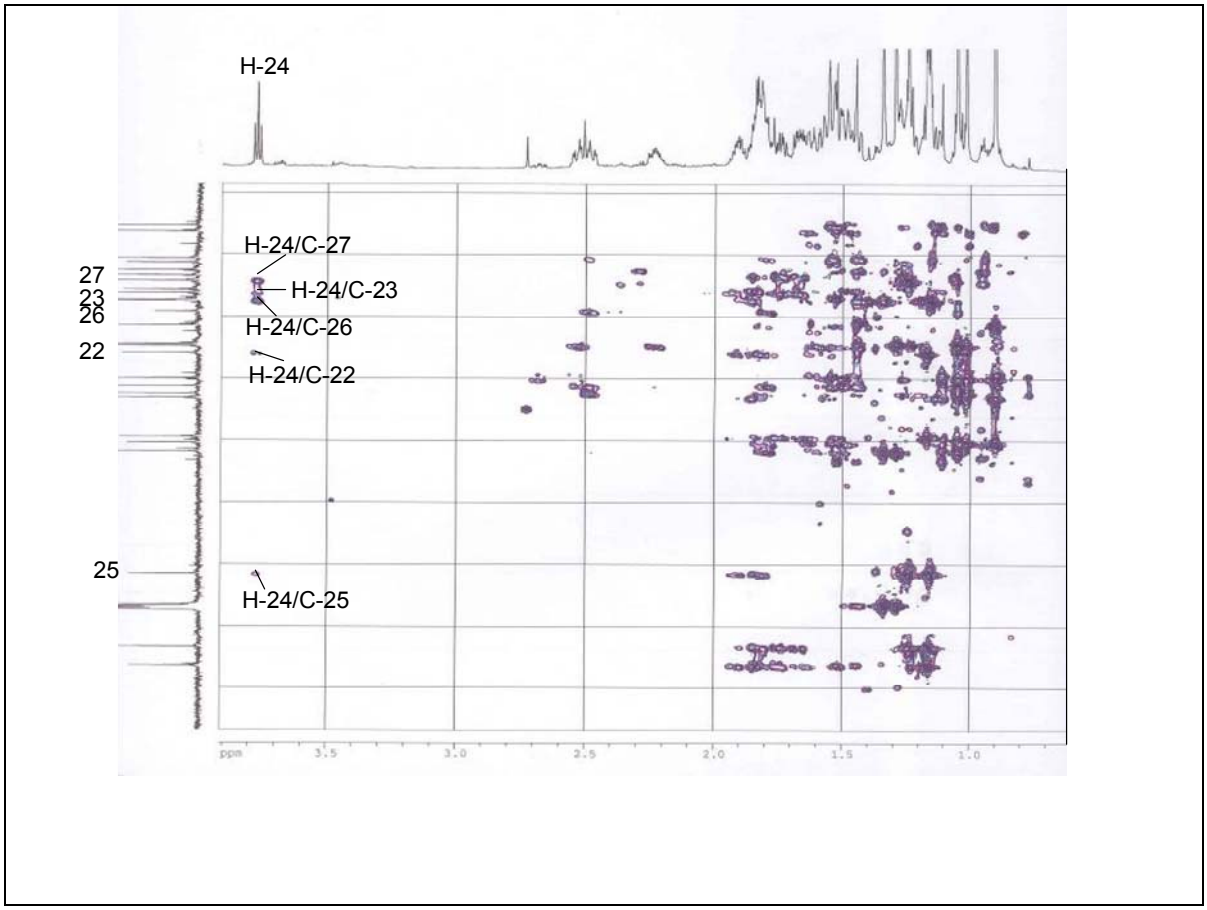

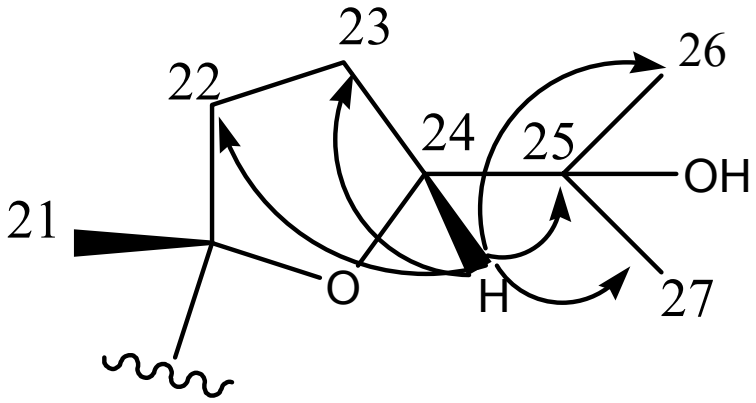

Fig. 3.109: HMBC correlations of oxymethine in the epoxy of compound 27

Table 3.41: ^{1}H NMR, ^{13}C NMR, and HMBC of compound 27 in $CDCl_3$

Position	^{13}C, δ	^{13}C, δ *Literature in $CDCl_3$	^{1}H, δ *Literature in $CDCl_3$	^{1}H, δ	HMBC
1	35.0	34.9			19
2	27.5	27.8	2.18 2.44	2.18 2.45	
3	178.8	179.7			
4	76.4	76.8			
5	52.2	53.3			19,28,29
6	22.5	22.7			
7	34.6	34.9			
8	39.9	40.2			30,18
9	43.3	42.5			19,30
10	41.2	41.5			
11	21.2	21.4			
12	27.5	27.2			
13	43.0	43.2			
14	50.3	50.4			30,18
15	31.4	31.3			18
16	25.6	26.0			
17	49.8	51.9			21
18	16.2	16.1	0.84 s	0.85 s	13,14,7,8
19	20.6	20.7	0.99 s	1.01 s	9,1,10,5
20	86.3	86.6			
21	22.52	22.0	1.12 s	1.12 s	20,17,22
22	36.3	37.5			21,17,23,24
23	26.0	26.0			
24	83.2	84.5	3.73 dd (7.7)	3.72 dd (7.5)	25,26,27
25	71.5	71.6			24,26,27
26	27.6	27.8	1.19 s	1.20 s	27,25,24
27	24.1	24.5	1.09 s	1.11 s	26,25,24
28	34.3	34.6	1.29 s	1.30 s	4,5,29
29	27.6	27.4	1.24 s	1.25 s	4,5,28
30	15.27	15.5	0.96 s	0.96 s	9,14,8,15

*: [Roux *et al.,* 1998]

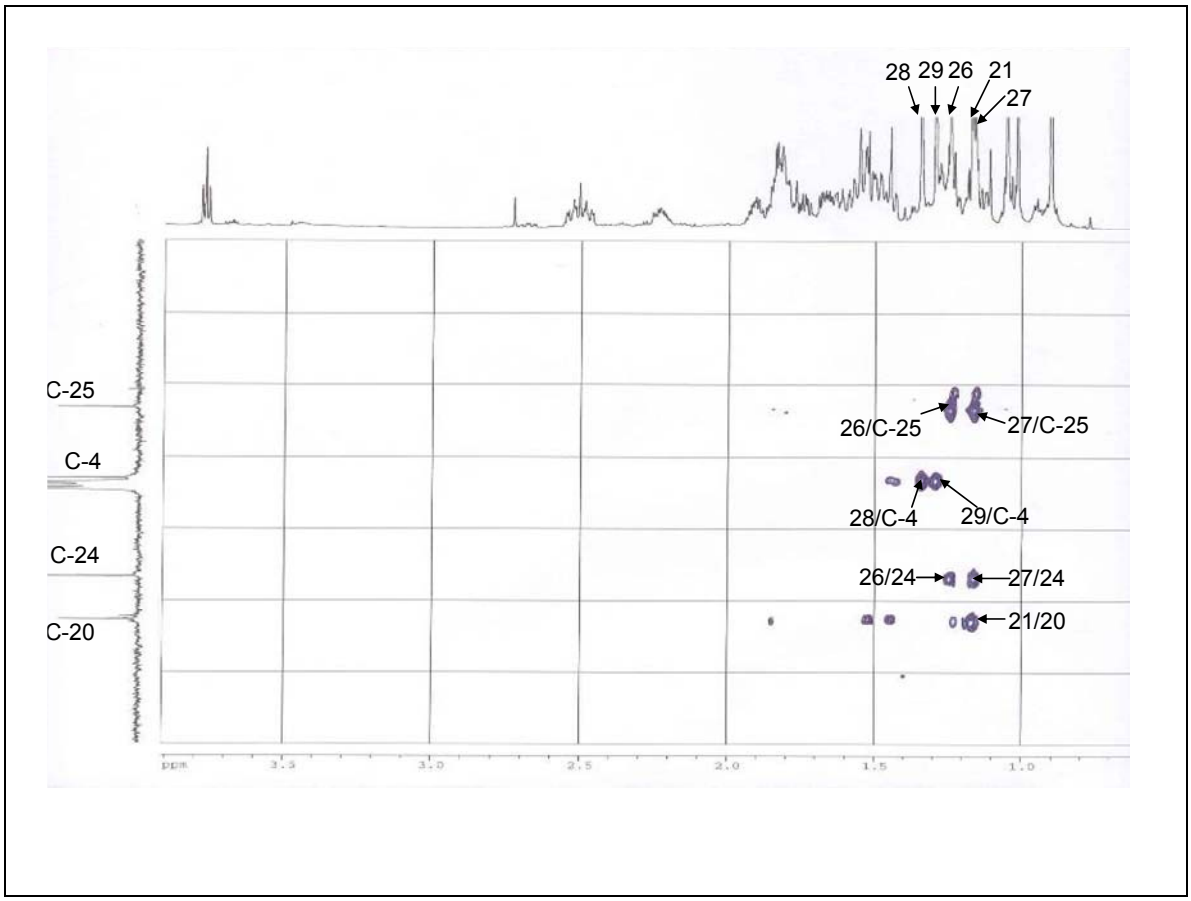

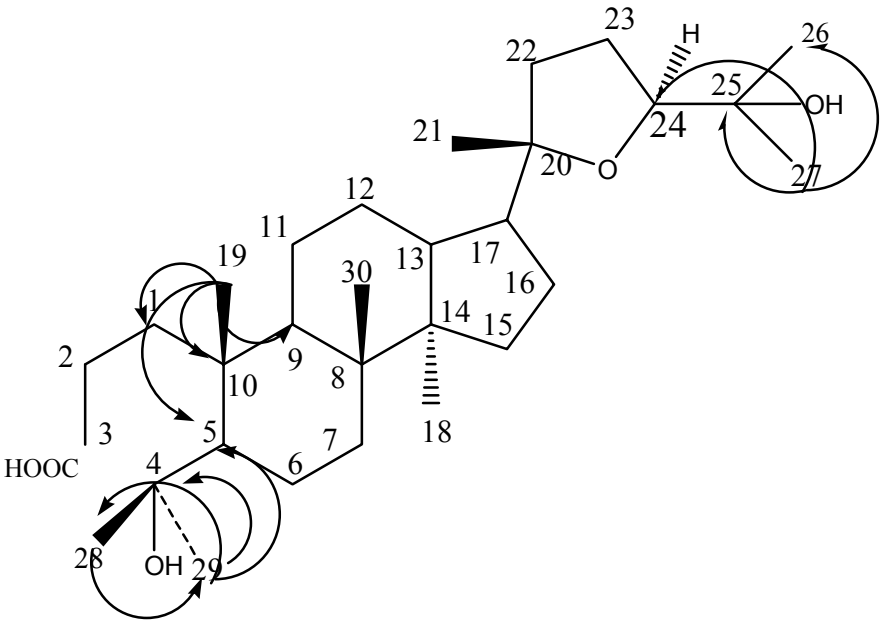

Fig. 3.310: HMBC correlations of methyl groups of compound 27 in $CDCl_3$

III.2.6.1.2. Niloticin (28, known compound)

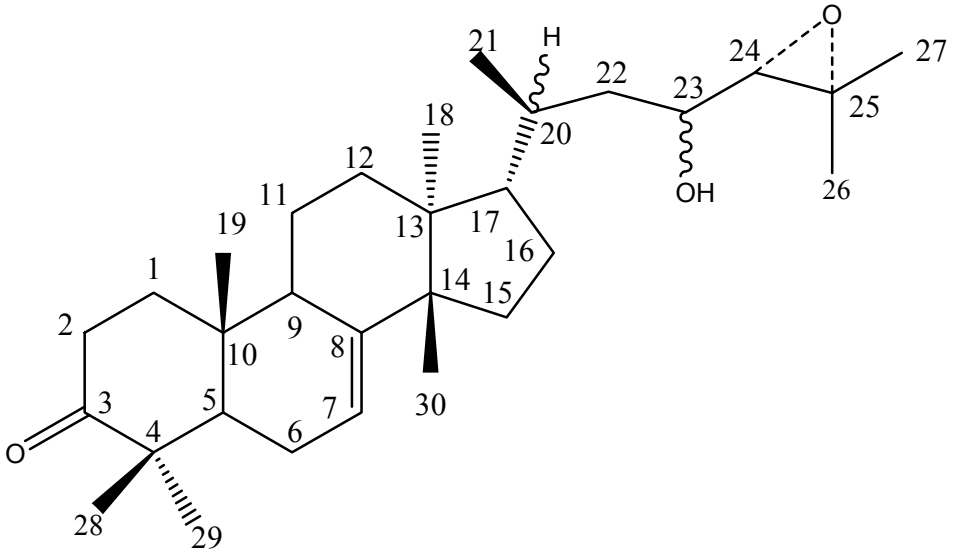

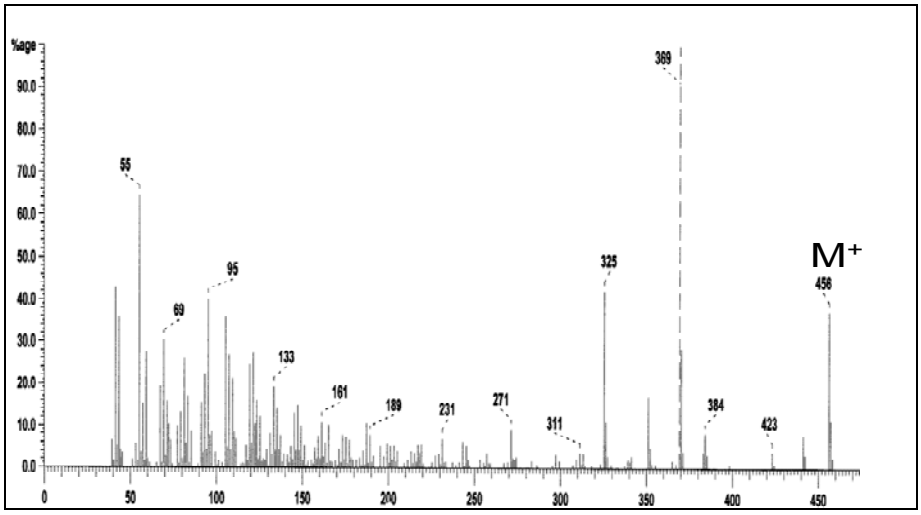

Fig. 3.111: EI-MS spectrum of compound 28

Compound **28** was isolated as white crystalline needles from the leaves of *Aglaia dasyclada*, $[\alpha]^{20}_{D}$-25 (*c*, 0.1, $CHCl_3$). The EI-MS showed a molecular ion peak at *m/z* 456 $[M]^+$ (see Fig. 3.111). The ^{13}C NMR and DEPT spectra (see Table 3.42 and Fig. 3.113) revealed 30 carbons including six tertiary methyls, one secondary methyl, eight methylene groups, and eight methine groups, and suggesting seven quaternary carbons. The presence of two olefinic carbons at δ_C 146.1 (s, C-8) and δ_C 118.1 (dd, C-7), and a ketonic carbonyl δ_C 216.9 (C-3), was characteristic for the tricucallane-7-ene system [Luo *et al.,* 2000].

In the HMBC spectrum (see Fig. 3.114), all methyl singlets showed their correlations with their neighboring carbons and unequivocally defined their positions along with the other

substituents, as shown in Table 3.42. The long-range correlations of the methyl proton signals at δ 1.31 (H_3-26) and δ 1.32 (H_3-27) with the quaternary carbon signal at δ_{C-25} 60.6 and the methine carbon signal at δ_{C-24} 68.8 identified the oxygen linkage between C-24 and C-25 of the epoxy ring. These two methyl groups, CH_3-26 and CH_3-27 were also identified as geminal pairs of carbons through their correlations with C-24 (at δ 68.8), C-25 (60.6), and with each other as well. The presence of an epoxide ring was also confirmed through the correlations in the COSY and HMBC spectra (see Fig. 3.115). A signal occurred at δ 2.70 (d, 8.2) in the ^{1}H NMR spectrum (see Fig. 3.112), and was assigned to methine proton H-24, while H-23 which appeared more down field at δ 3.59 (dd) corresponded to the epoxide ring. From the ^{13}C NMR data, the chemical shifts of C-23 at δ 69.6, C-24 at δ 68.8, and C-25 at δ 60.6 accordingly suggested the occurrence of oxygen bearing carbons. Thus, an epoxide linkage was attributed between C-24 and C-25 [Itokawa *et al.,* 1992]. The keto function at C-3 was supported by the long-range correlations of CH_3-28 at δ 1.04 and CH_3-29 at δ 1.11 with the quaternary carbon at δ_{C-4} 47.9 and the carbonyl carbon at δ_{C-3} 216.9. These two methyl groups, CH_3-28 and CH_3-29, showed correlations with C-4 at δ 47.9 and suggested a geminal orientation. The olefinic methine proton signal for H-7 at δ 5.33, which exhibited correlations with C-8 at δ 146.1 and C-14 at δ 51.6 similar to the methyl group CH_3-30 proved the double bond to be situated between C-7 and C-8. Furthermore, H_3-30 and H_3-18 showed the same correlations to C-13 and C-14 at δ 43.9 and 51.6, respectively. The methyl doublet for CH_3-21 occurred at δ 0.95 (J=5.7 Hz) and showed correlations with C-17, C-20 and C-22 at δ 53.6, 33.9, and 41.0, respectively. In comparison with the literature data [Gray *et al.,* 1998] and based on the 1D and 2D spectra, compound **28** was identified as Niloticin.

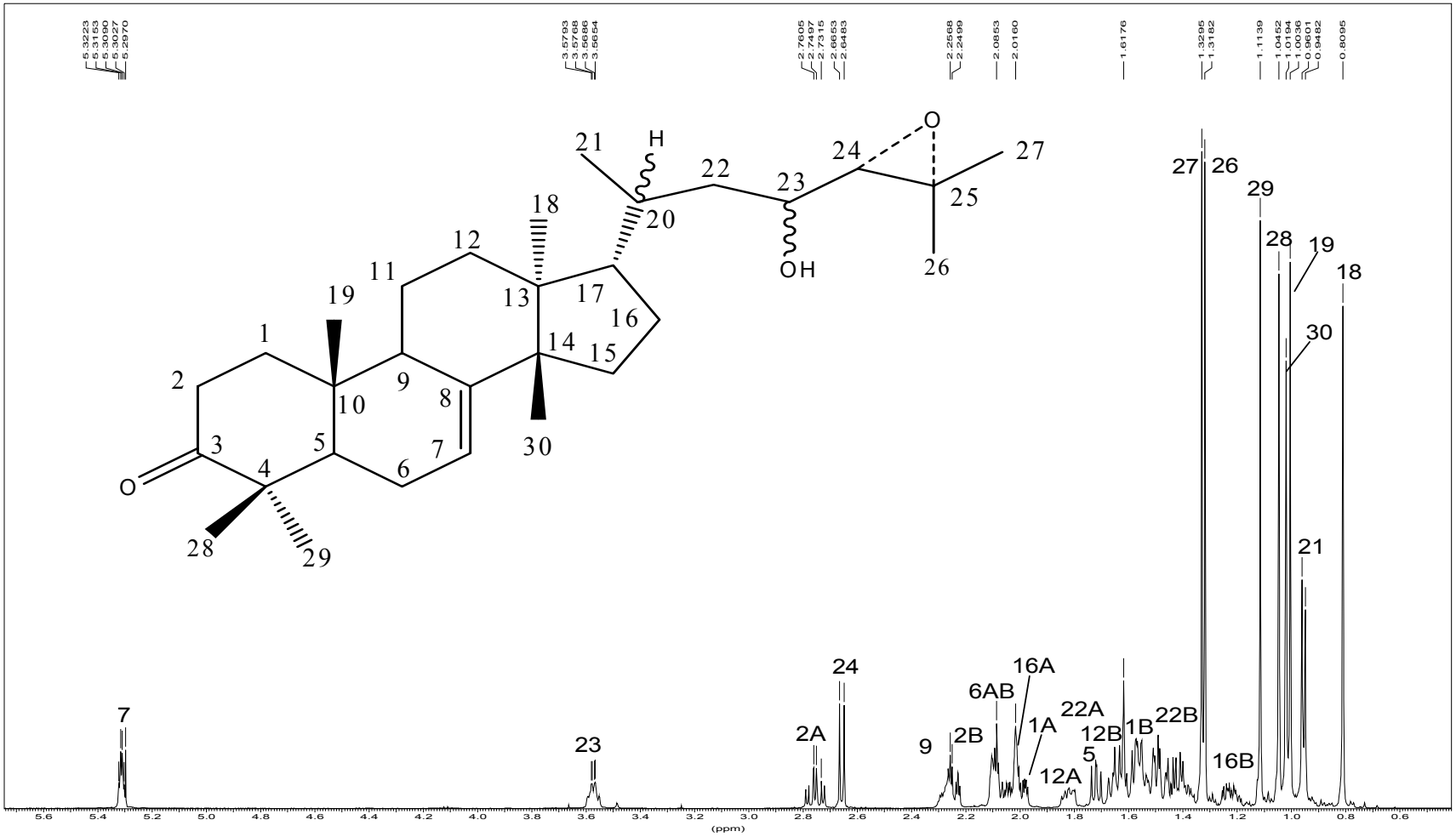

Fig. 3.112: ^{1}H NMR spectrum of compound 28 in $CDCl_3$

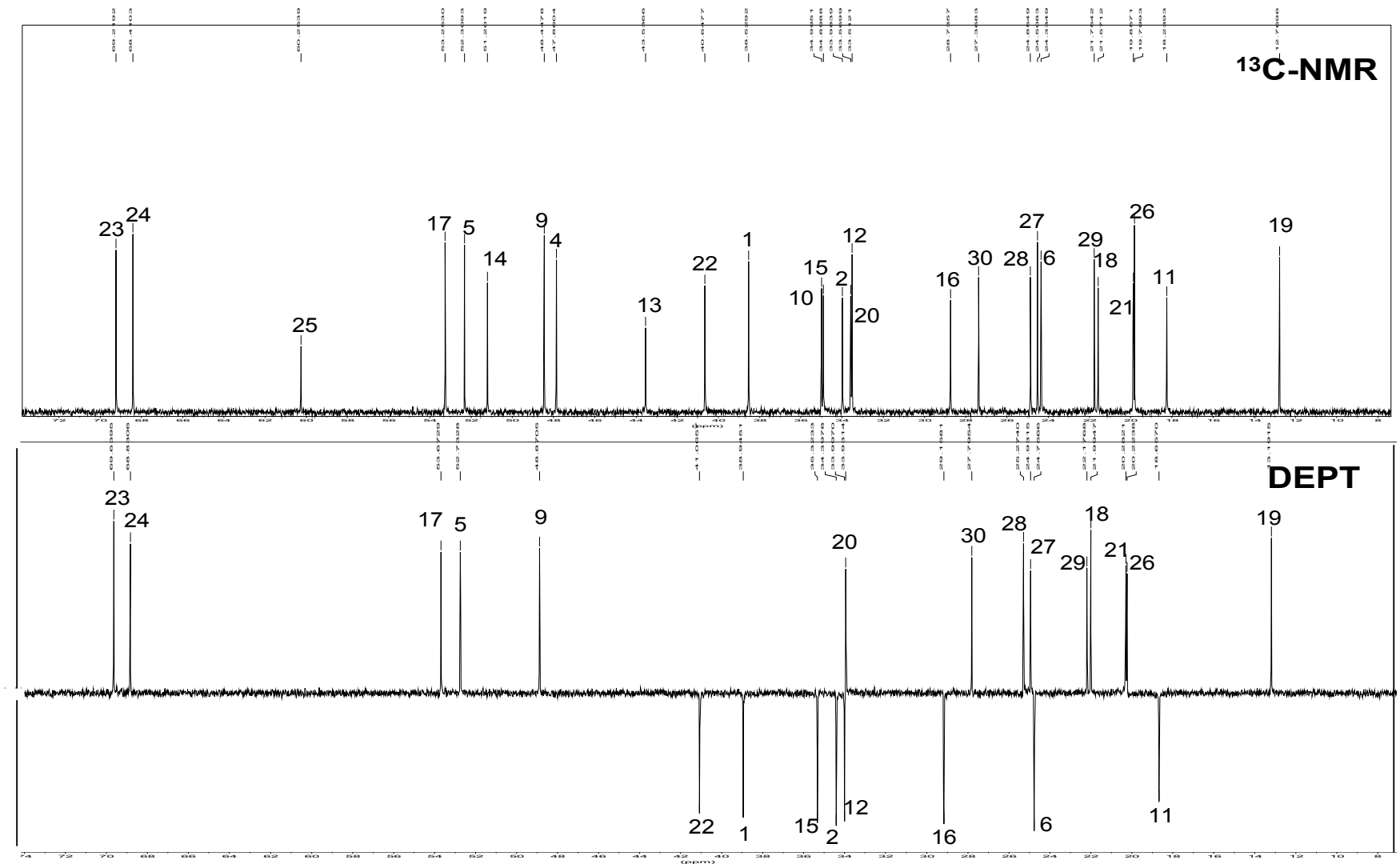

Fig. 3.313: ^{13}C NMR (above) and DEPT (below) spectra of compound 28 in $CDCl_3$

Table 3.42: ^{1}H NMR , ^{13}C NMR and HMBC data of compound 28 in $CDCl_3$

Position	^{13}C, δ	^{13}C, δ *Literature in $CDCl_3$	^{1}H, δ	HMBC
1	38.5	38.6	A: 1.99 m B: 1.45 m	2,3,5,10
2	34.9	34.9	A: 2.78 ddd(5.7;14.5;20.0) B: 2.22 m	1,3,10
3	216.9	216.8		
4	47.9	47.9		
5	52.3	52.3	1.73 m	3,4,6,19,28,29
6	24.4	24.3	A: 2.20 m B: 2.20 m	
7	118.1	118.3	5.33 t	
8	146.1	145.7		30,18
9	48.8	48.5	2.28 m	19,30
10	35.4	35.0		
11	18.6	18.3	A: 1.61 m B: 1.61 m	
12	33.9	34.0	A: 1.86 m B: 1.66 m	
13	43.9	43.6		
14	51.6	51.2		30,18
15	33.9	33.7	A: 1.48 m B: 1.48 m	18
16	29.1	28.8	A: 2.10 m B: 1.30 m	
17	53.6	53.3	1.59 m	21
18	21.9	21.8	0.80 s	12,13,14,17
19	13.1	12.8	1.00 s	1,5,9,10
20	33.9	33.6	1.43 m	
21	20.2	19.8	0.95 d (5.7)	17,20,22
22	41.0	40.7	A: 1.68 m B: 1.44 m	17,21,23,24
23	69.6	69.3	3.59 m	
24	68.8	68.2	2.70 d (8.2)	23,25,26,27
25	60.6	60.2		24,26,27
26	20.2	19.8	1.31 s	24,25,27
27	24.9	24.9	1.32 s	24,25,26
28	24.7	24.6	1.04 s	3,4,5,29
29	22.1	21.6	1.11 s	3,4,5,28
30	27.7	27.4	1.01 s	8,13,14,15

* : [Gray *et al.,* 1998]

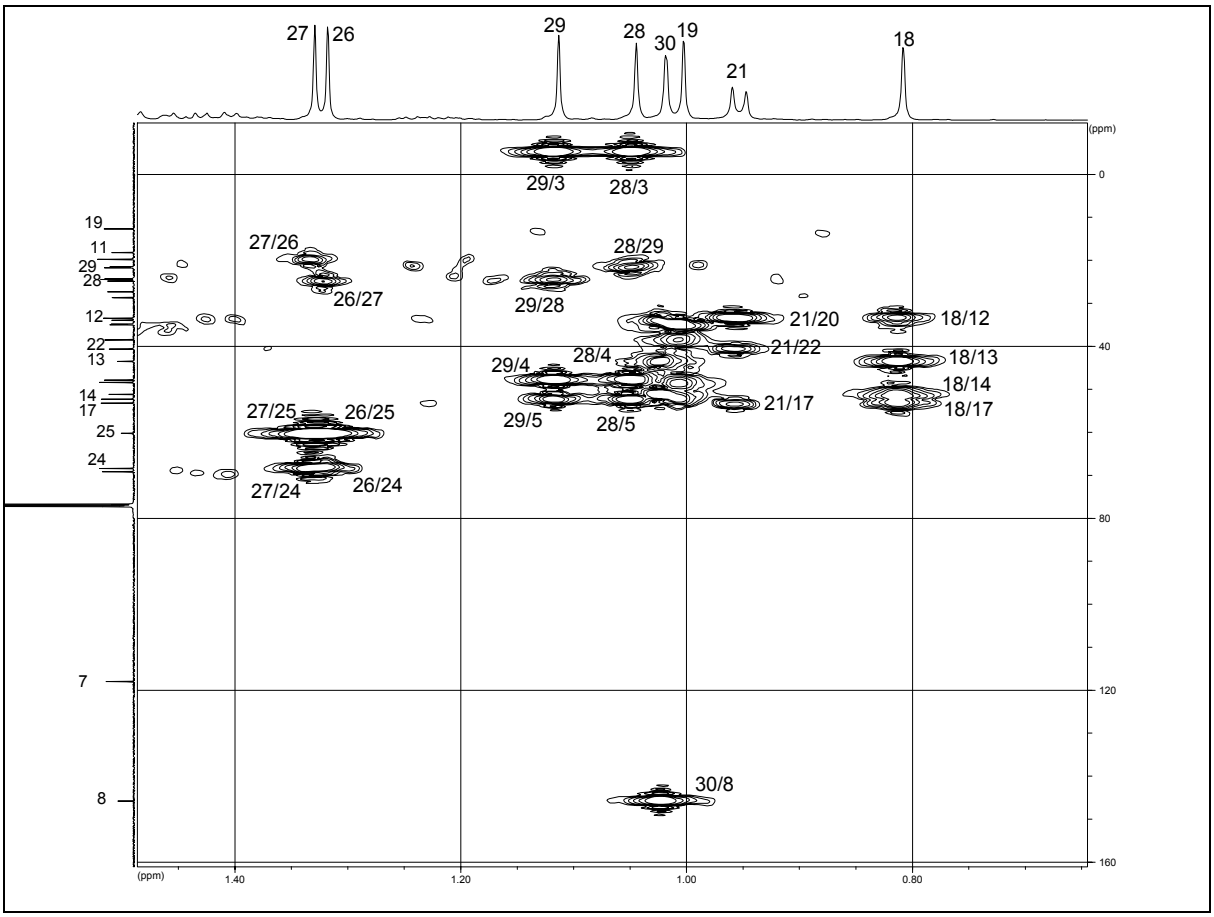

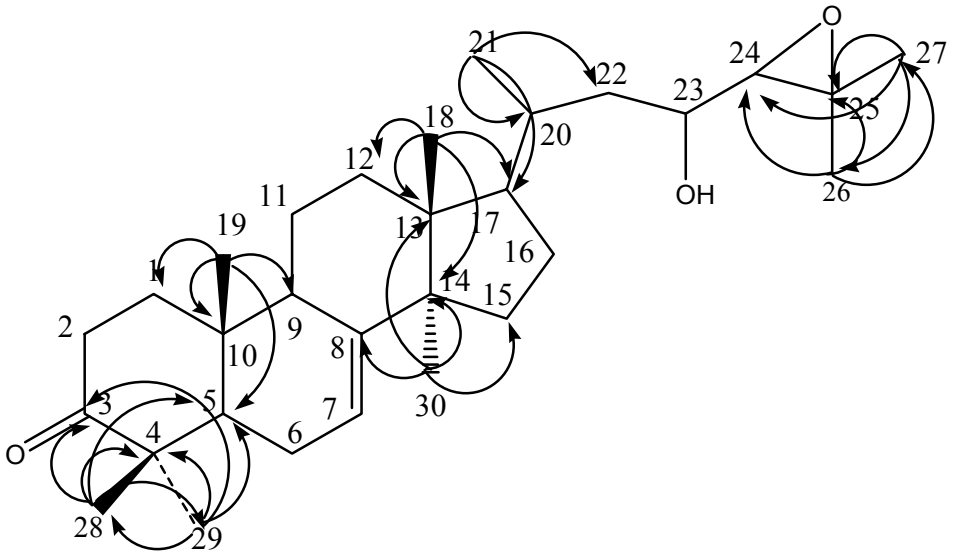

Fig. 3.114: HMBC correlations of methyl groups of compound 28 in $CDCl_3$

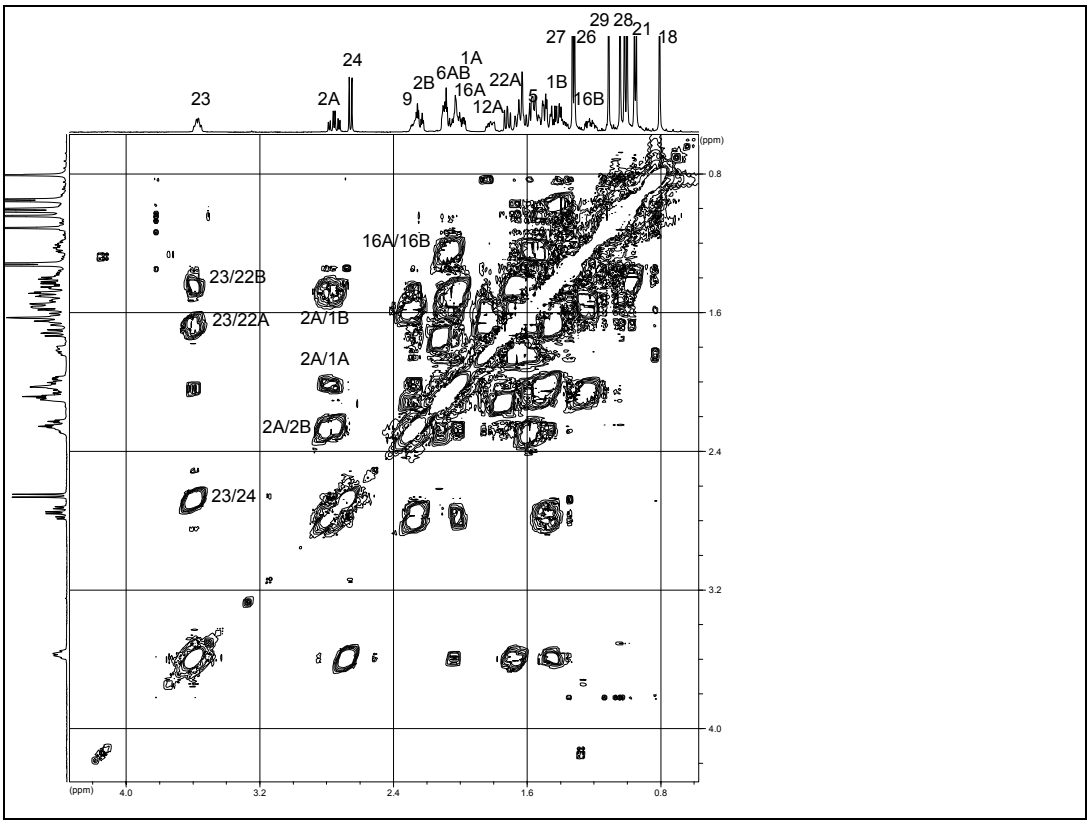

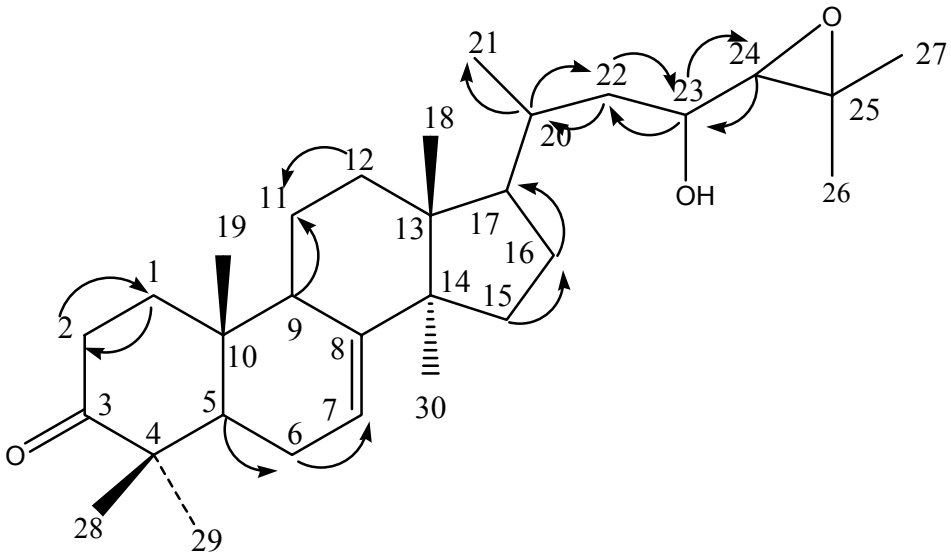

Fig. 3.115: ^{1}H-^{1}H COSY correlations of compound 28 in $CDCl_3$

III.2.6.2. Tetraterpenoids

III.2.6.2.1. Lutein (29, known compound)

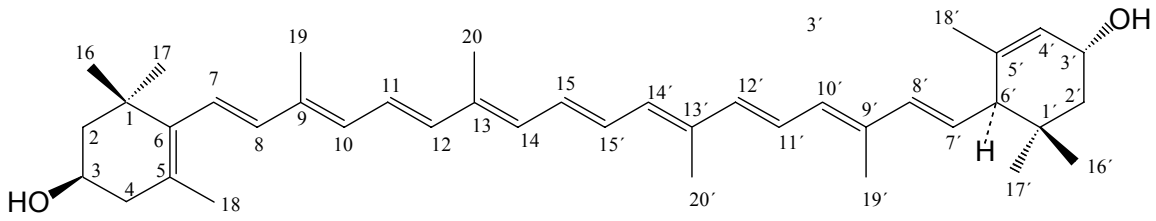

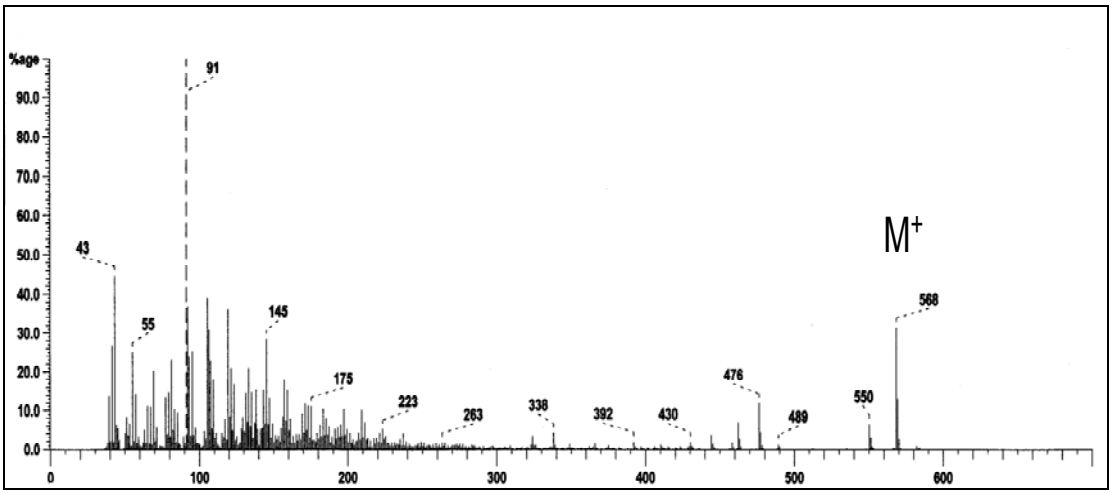

Fig. 3.116: EI-MS spectrum of compound 29

Compound **29** was isolated from the leaves of *Aglaia oligophylla* as a coppery crystalline residue in MeOH, $[\alpha]^{20}_{D}$+155 (*c*, 0.5, $CHCl_3$).The EI-MS showed an ion molecular peak at *m/z* 456 $[M]^+$ (see Fig. 3.116). Compound **29** has λ_{max} 420, 444, and 472 nm (MeOH), which is characteristic for a long chain system containing conjugated double bonds as found in plant carotenoid pigments. The ^{1}H NMR spectrum (see Fig. 3.117) showed ten methyl singlets, fourteen olefinic protons, which are typical for tetraterpenoids. The coupling constants of 14.8 -16.8 Hz indicated the *trans*-configuration of the double bonds. The chemical shifts of methyl groups, C*H*$_3$-16, C*H*$_3$-17, C*H*$_3$-16′, and C*H*$_3$-17′ resonated more upfield at δ 1.07, 1.07, 1.00, and 0.84 in comparison to the olefinic methyl groups, C*H*$_3$-18, C*H*$_3$-19, C*H*$_3$-20, C*H*$_3$-18′, C*H*$_3$-19′, and C*H*$_3$-20′ which occurred more downfield at δ 1.73, 1.97, 1.96, 1.62, 1.90, and 1.96, respectively.

In comparison with the literature data [Deli *et al.,* 1998] showed in Table 3.43, compound **29** was identical to lutein ((3R,3′R,6′R)-β,ε-carotene-3,3′-diol) [Baranyai *et al.,* 1981].

Table 3.43: ^{1}H NMR data of compound 29 in $CDCl_3$

C	δ_H (ppm) *J* (Hz) of 29	*δ_H (ppm) *J* (Hz) in $CDCl_3$	C	δ_H (ppm) *J* (Hz) of 29	*δ_H (ppm) *J* (Hz) in $CDCl_3$
1			1′		
2	1.38(dd, 11.9; 6.9)	1.48 (dd, 12.1; 6.9)	2′	1.83 (dd, 11.9; 6.9)	1.84 (dd, 11.9; 6.9)
3	4.02	4.0 m	3′	4.27 m	4.25 m
4	2.07 (dd, 16.8; 9.2) ax 2.43(ddd, 16.8; 9.2; 1.6)eq	2.05 (dd, 16.8; 9.2) 2.39 (ddd, 16.8; 9.2; 1.6)	4′	5.55 m	5.57 m
5			5′		
6			6′		
7	6.13 (d, 16.3)	6.11(d, 16.3)	7′	5.47 (dd, 15.1; 9.8)	5.43 (dd, 15.1; 9.8)
8	6.13 (d, 16.3)	6.14 (d, 16.3)	8′	6.16 (d, 16.3)	6.14 (d, 16.3)
9			9′		
10	6.17 (d, 11.4)	6.16 (d, 11.4)	10′	6.17 (d, 11.4)	6.14 (d, 11.4)
11	6.62(dd, 11.4; 14.8)	6.64 (dd, 11.4; 14.8)	11′	6.60 (dd, 11.4; 14.8)	6.60 (dd, 11.4; 14.8)
12	6.37(d, 15.2)	6.36 (d, 15.2)	12′	6.36 (d, 15.2)	6.36 (d, 15.2)
13			13′		
14	6.25 (d, 15.2)	6.25 (d, 15.2)	14′	6.25(15.2)	6.24 (15.2)
15	6.63 (dd, 11.4; 14.8)	6.63 (dd, 11.4; 14.8)	15′	6.63 (dd, 11.4; 14.8)	6.63(dd, 11.4; 14.8)
16	1.07 s	1.07 s	16′	0.99 s	1.00 s
17	1.07 s	1.07 s	17′	0.84 s	0.85 s
18	1.73 s	1.74 s	18′	1.62 s	1.63 s
19	1.97 s	1.97 s	19′	1.90 s	1.91 s
20	1.96 s	1.96 s	20′	1.96 s	1.96 s

*: [Deli *et al.,* 1998]

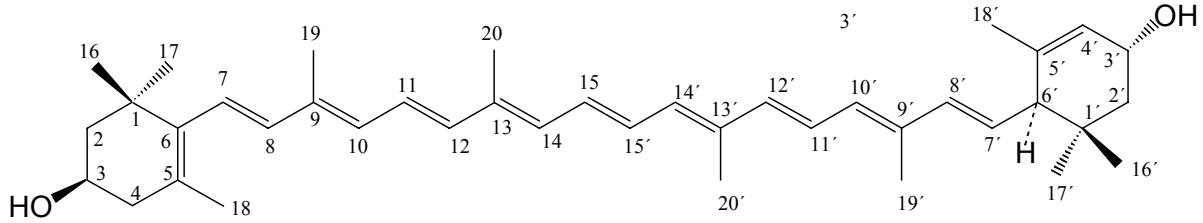

Lutein

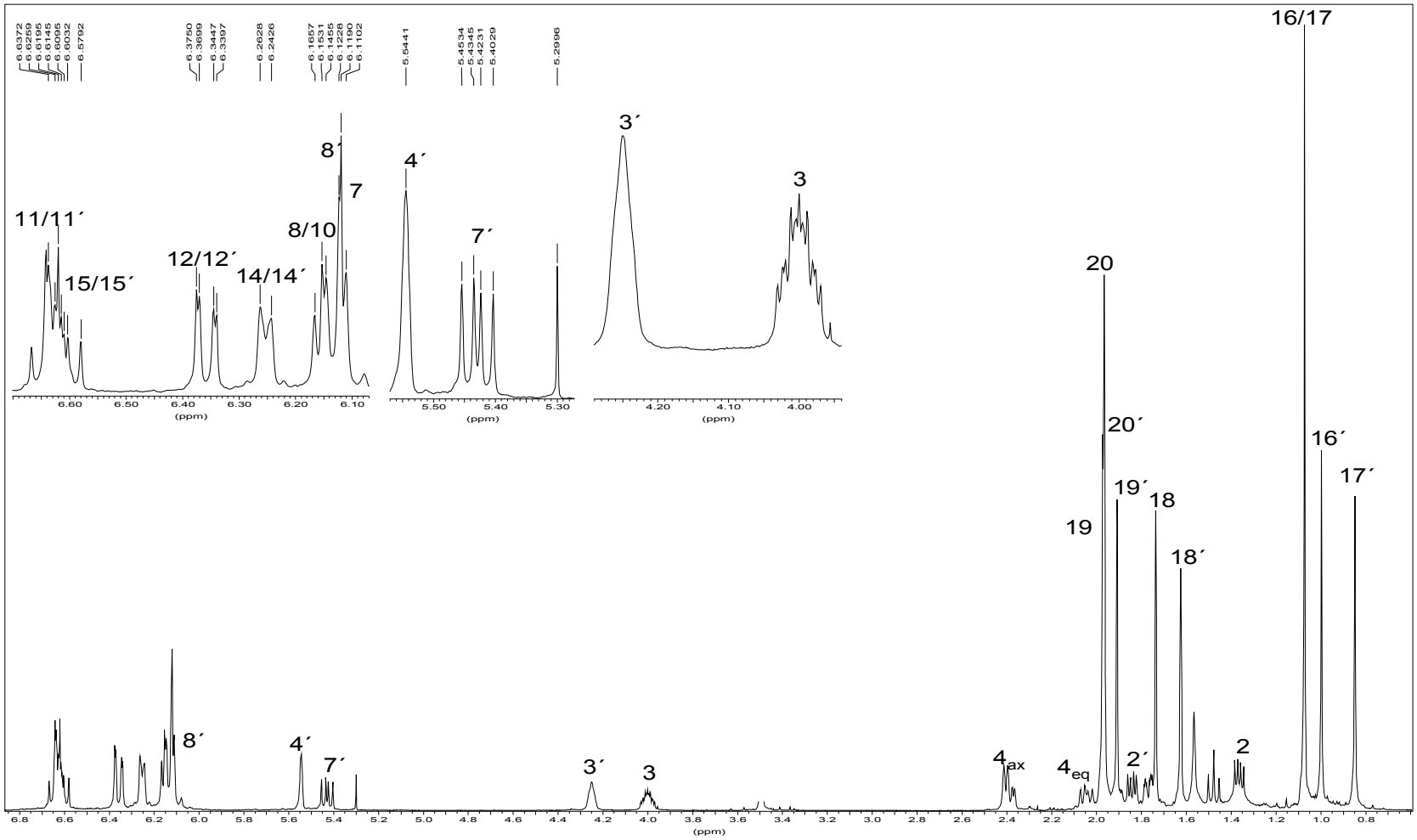

Fig. 3.117: ^{1}H NRM spectrum of compound 29 in $CDCl_3$

III.2.7. Cumarine from *Aglaia* sp.

III.2.7.1 Scopolectin (30, known compound)

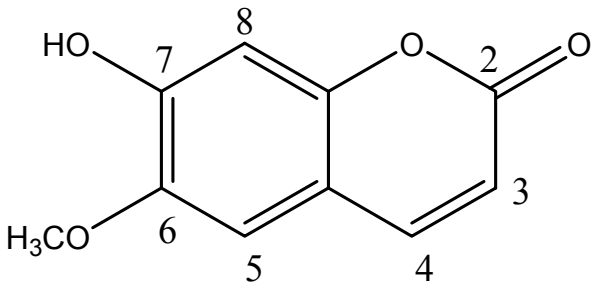

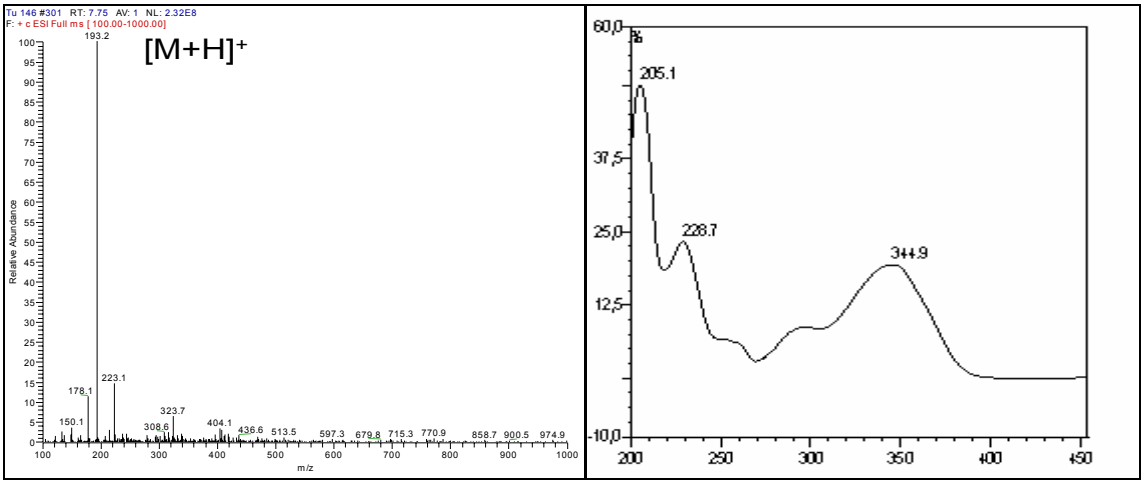

Fig. 3.118: ESI-MS and UV spectrum of compound 30

Compound **30** was isolated from the bark of *Aglaia elaeagnoidea* as a dark brown amorphous residue. Compound **30** shows absorbances at λ_{max} 205.1, 227.7, and 344.9 nm (see Fig. 3.118). Compound **30** expressed flourescence on TLC plate at 366 nm, which is typical for a cumarin. The ESI-MS showed a pseudomolecular ion peak at *m/z* 193.2 $[M+H]^+$ (see Fig. 3.118). The ^1H NMR spectrum (see Fig. 3.119) revealed two singlets at δ 7.11 ppm and 6.76 ppm corresponding to two aromatic protons H-5 and H-8 of ring A, respectively. The typical *cis*-coupling of H-3 and H-4 at δ 7.85 (*J*=9.5Hz) and 6.19 (*J*=9.5Hz) was observed. Moreover, a methoxy signal occurred at δ 3.85 ppm, which is indicative for a methylated substituent at C-6. In comparison with the literature data (see Table 3.44) [Pouchert and Behnke, 1993] compound **30** was identified as scopoletin (7-hydroxy-6-methoxycumarin).

Table 3.44: ^{1}H NMR data of compound 30 in MeOD

Position	δ_H (*J* Hz)
3	6.19 (d, 9.5)
4	7.85(d, 9.5)
5	7.11 (s)
6-OCH3	3.81
7-OH	
8	6.76 (s)

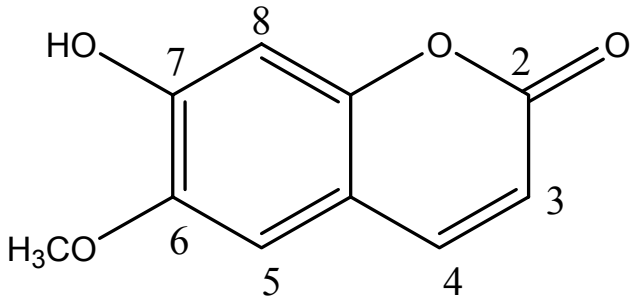

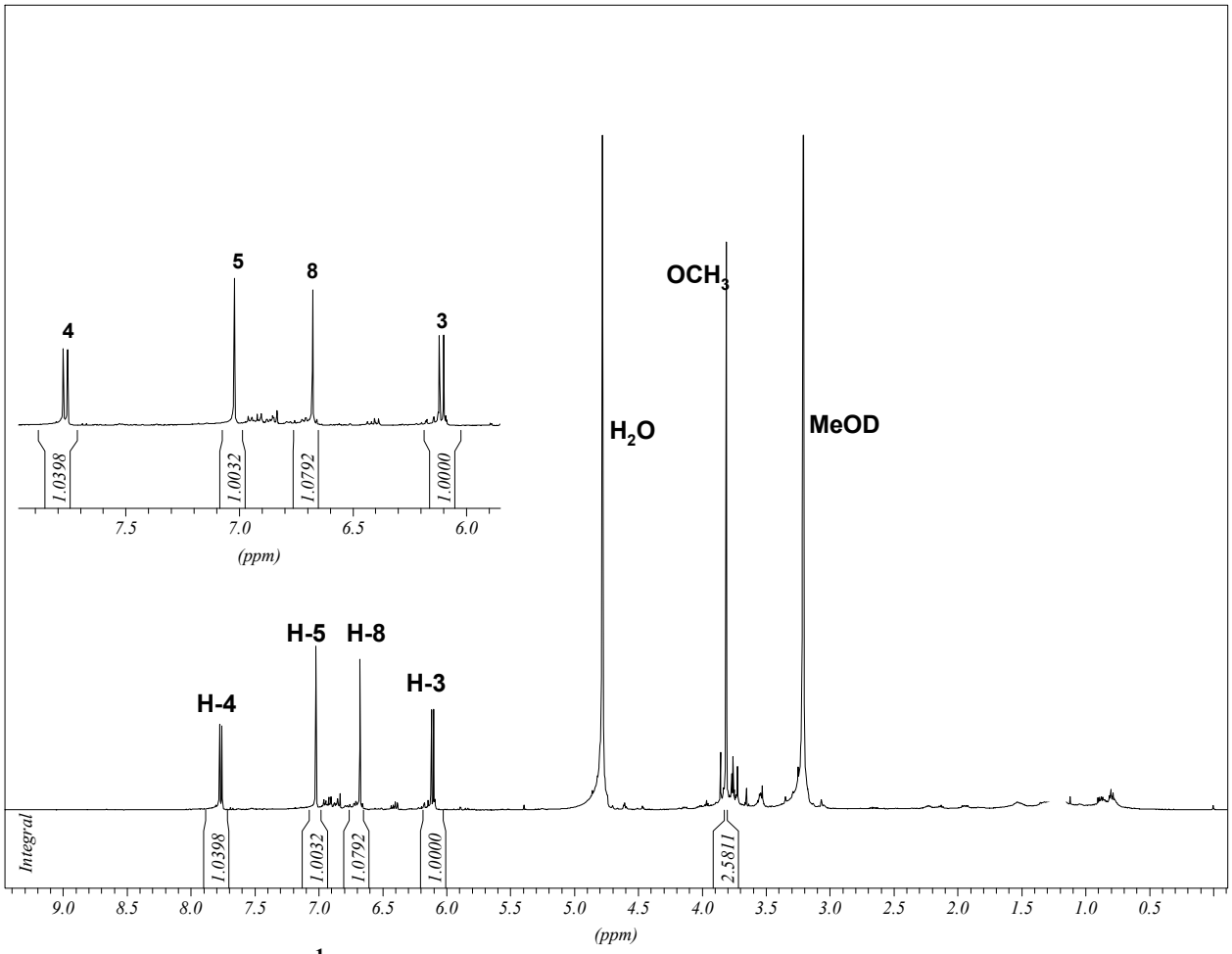

Fig. 3.119: ^{1}H NMR spectrum of compound 30 in MeOD

III.3. Field experimental results

III.3.1. Efficiency of *Aglaia oligophylla* extract towards *Brithys crini* feeding on *Crinum asiaticum* (Amaryllidaceae)

Five different *Aglaia* formulations containing different concentrations of methanolic extract of *Aglaia oligophylla* (500 ppm, 1000 ppm, 2000 ppm, 4000 ppm and 6000 ppm) were proven effective against a new species of pest caterpillar in Vietnam (related to *Brithys crini*, Lepidoptera), which seriously damaged the medicinal plant *Crinum asiaticum* (Amaryllidaceae, see Fig. 3.120). The experiments were conducted at the Tam Dao National Medicinal Garden, in Vietnam on July 2003. The *Aglaia oligophylla* extract on *Brithys crini* does not directly kill the caterpillar as compared to most of the very toxic chemical insecticides (e.g. Monitor ®), but it acts rather as a repellent by driving the insects away from the sprayed plants (see Fig. 3.121 and Fig. 3.122).

Fig. 3.120: Status of *Crinum asiaticum* before treatment with *Aglaia*

After 6, 12, and 24 hours following treatment with the *Aglaia* formulation, the behaviour of *Brithys* catterpillars was observed. The catterpillars reduced their feeding and crept to the base of treated plants moving to nearby grass plantation or on the ground (see Fig. 3.121). After two days, dead young caterpillars were found. After three days, weak and dead insects were also found on the grass (see Fig. 3.121) as well as on the ground. The efficiency of *Aglaia* formulations (see Table 3.45 and Fig. 3.123) was evaluated by the **Henderson-Tilton** formula as follows:

$$\text{Efficiency} = (1 - T_A / C_A \times C_B / T_B) \times 100\%.$$

Where: C_B: number of surviving insects on control plants before the test,
C_A: number of surviving insects on control plants after the test,
T_B: number of surviving insects on treated plants before the test,
T_A: number of surviving insects on treated plants after the test.

Fig. 3.121: Repellent effect observed after 48 hours

Table 3.45: Efficiency of *Aglaia oligophylla* formulation towards *Brithys* sp. feeding on *Crinum asiaticum* at Tam Dao National Medicinal Garden, Vietnam July 2003

***Aglaia* formulations**	Differences in number of insects before and after the test / Efficiency [%]						
	before spraying	***after 1 day***	***after 2 days***	***after 3 days***	***after 4 days***	***after 7 days***	***status of plants and insects at the end of the experiment***
500 ppm	28	28 (0%)	22 (16.8%)	20 (24.3%)	20 (24.3%)	0	plant dead, insects move away, young insects die
2000 ppm	34	26 (25.6%)	21 (34.6%)	17 (47%)	17 (47%)	0	plant dead, insects move away and die
4000 ppm	19	8 (57.9%)	6 (68.4%)	5 73.6%	4 (77.7%)	4 (77.7%)	plant grown in good condition, insects move away and die
6000 ppm	34	19 (51.2%)	6 (84%)	4 (88.8%)	2 (93.7%)	0 (100%)	plant grown in good condition insects move away and die
Control	36	35	34	34	34	34	plant almost completely consumed, insects are in good condition,start moving to other plants

Field experiments were conducted on *Crinum asiaticum* at the Tam Dao National Medicinal Garden, Vietnam July 2003

Fig. 3.122: Weak or dead insects observed after 2 to 5 days

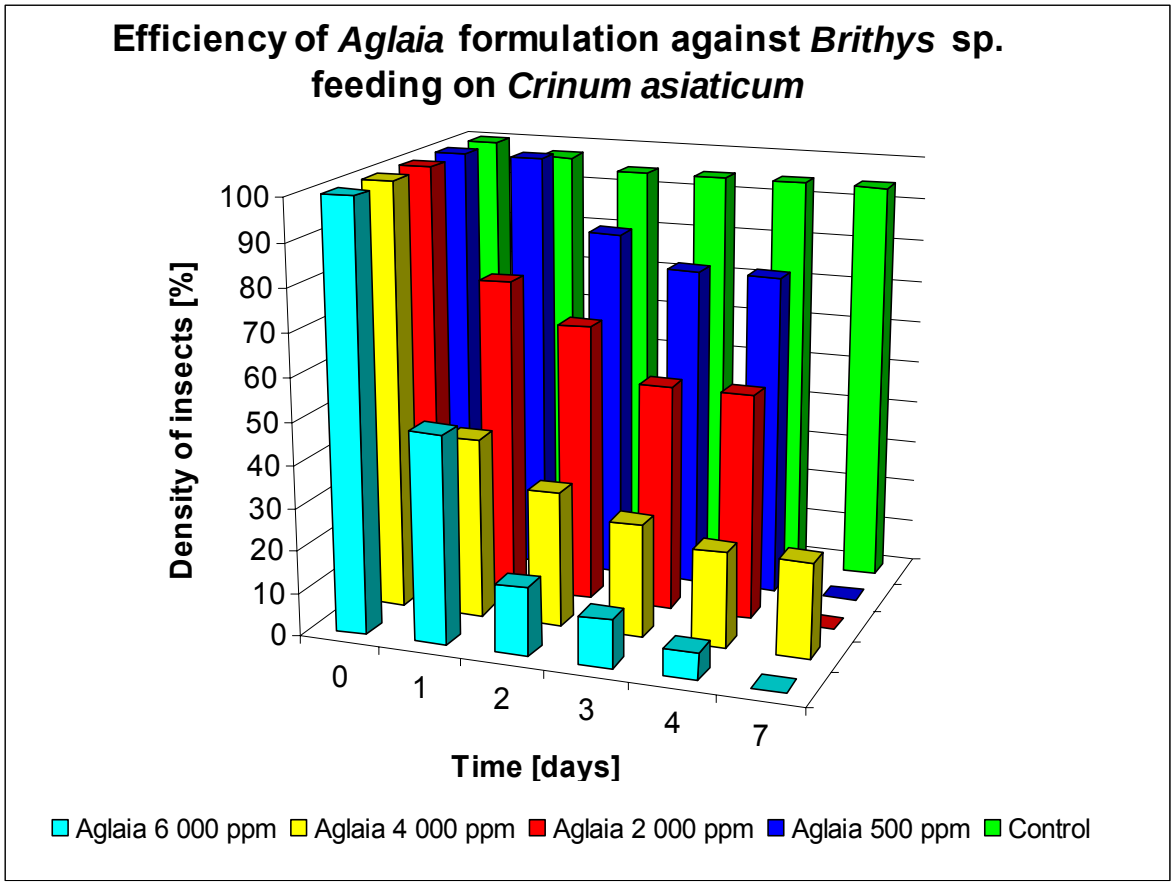

Fig. 3.123: Efficiency of *Aglaia* formulation against *Brithys* sp.

***Aglaia* 500 ppm** ***Aglaia* 6000 ppm**

Fig. 3.124: Status of *Crinum asiaticum* after 7 days of treatment with *Aglaia* formulations

III.3.2. Efficiency of *Aglaia oligphylla* extract against *Macrosiphum phoniella* feeding on artichoke plants (*Cynara scolymus*, Asteraceae)

The second experiment on the efficiency of the *Aglaia* formulation was conducted on artichoke plants in the Tam Dao National Medicinal Garden. Aphids of *Macrosinum phoniella* occurred at high density reaching up to 300 aphids per plant (see Fig. 3.125). Three different concentrations of the *Aglaia* formulation (500, 2000, and 4000 ppm) were sprayed on the artichoke plants.

After 12 hours of spraying, at concentration of 4000 ppm, the central nervous system of the aphids was observed to be affected which led to their uncontrolled movements followed by death after 7 days. Thus, the *Aglaia oligophylla* formulation is effective against *Macrosiphum phoniella* feeding on *Cynara scolymus* by apparently acting on the central nervous system of the insects (see Fig. 3.126).

Fig. 3.125: *Macrosiphum phoniella* feeding on artichoke plants in high density

Field experiments were conducted on artichoke plants at the Tam Dao National Medicinal Garden, Vietnam July 2003

Fig. 3.126: Efficiency of *Aglaia* formulations against aphids after 7 days of treatment

III.3.3. Efficiency of *Aglaia* formulation towards *Spodoptera litura*

III.3.3.1. Field experiment of *Aglaia* formulations against *S. litura* feeding on cabbages and kohlrabi (Dong Anh, Vietnam October 2003)

Two different *Aglaia* formulations were prepared from extracts of *Aglaia oligophylla* and *Aglaia abbriviata* and sprayed on cabbages and kohlrabi infected with *Spodoptera litura* (see Fig. 3.128).

Fig. 3.127: Cabbage field at Dong Anh

Experiment was conducted at a cabbage (see Fig. 3.127) and kohlrabi field at Dong Anh, Hanoi in October 2003. The formulations from extracts of *Aglaia oligophylla* and *Aglaia abbriviata* were also effective against *Spodotera litura* encountered in a vegetable field in a suburban community of Hanoi (see Fig. 3.129 and Fig. 3.130). The effect of *Aglaia* extract on *Spodoptera litura* (see Fig. 3.131) was not strong as that of the chemical product (Regent ®) at the beginning of the experiment but the effects of *Aglaia* extract lasted longer (see Table 3.46).

Fig. 3.128: Status of cabbages in the field before treatment with *Aglaia* formulation

Table 3.46: The efficiency of *Aglaia* formulation against *S.litura* feeding on cabbages

Formulation	Differences (average) of *Spodotera litura* before and after the treatment / Efficiency [%]			
	before spraying	***After 1 day***	***After 3 days***	***After 8 days***
Aglaia oligophylla 5,000 ppm	33.2	29.0 (12.56%)	23.3 (54.20%)	18.2 (60.56%)
Aglaia abbriviata 5,000 ppm	57.3	52.6 (8.25%)	37.7 (56.90%)	10.7 (86.50%)
Chemical product (Regent ®)	7.2	0.8 (88.88%)	1.6 (85.51%)	5.8 (42.04%)
Control	26.3	26.3	40.4	36.6

Field experiment was conducted at a cabbage and kohlrabi at Dong Anh, suburb of Hanoi in October 2003

Fig. 3.129: Status of cabbage after 15 days of treatment with *Aglaia*, Chemical-Regent and the Control

Fig. 3.130: Status of kohlrabi after 7 days of treatment with *Aglaia*, Chemical-Regent and the Control

Field experiment result of *Aglaia* formulations against *S. litura* feeding on cabbages and kohlrabi at Dong Anh, Vietnam October 2003

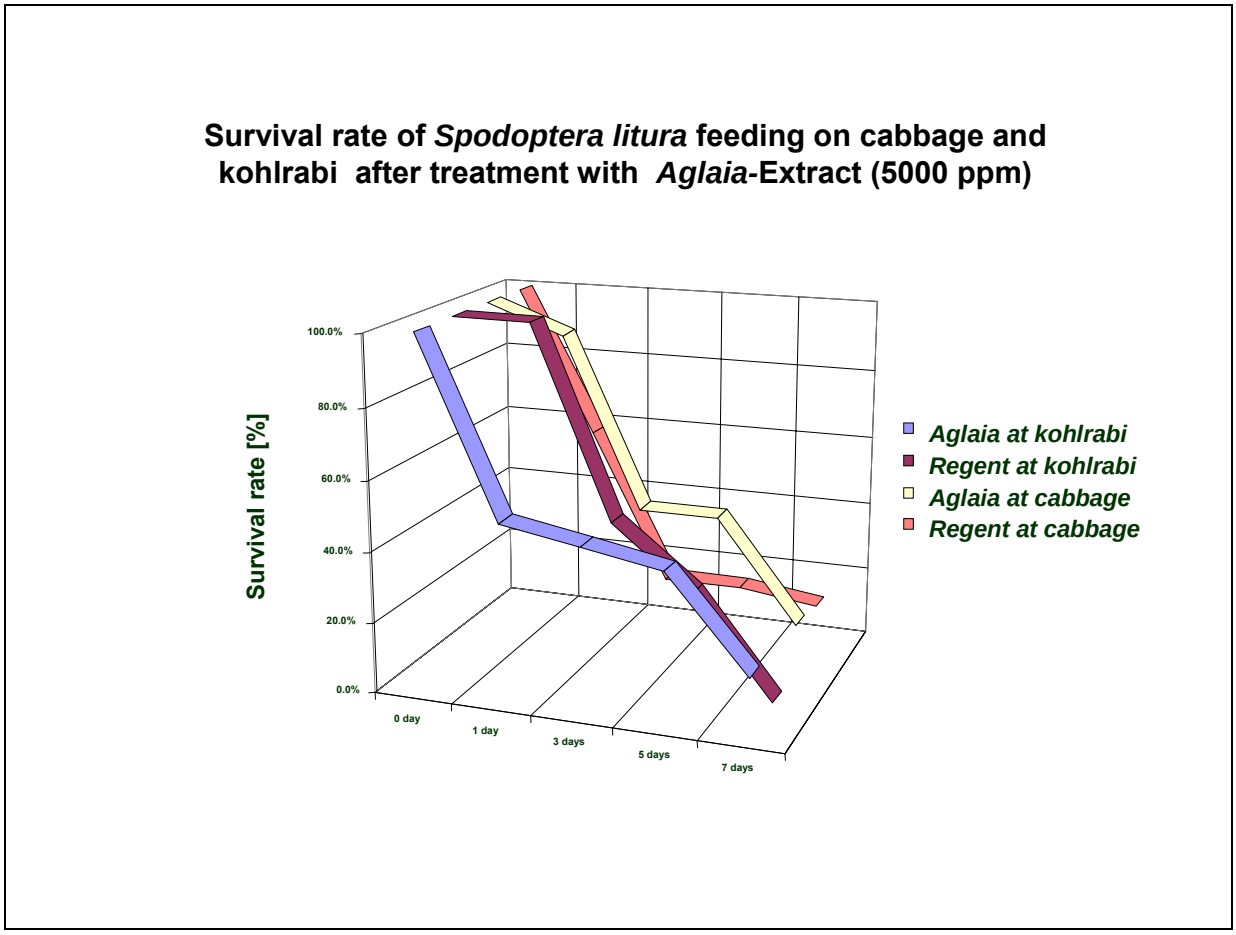

Fig. 3.131: Efficiency of *Aglaia* extract against *S.litura* feeding on Kohlrabi and cabbage

III.4.3. Insecticidal activity result of *Aglaia* formulations on Petri dish

The experiments were conducted in the Institute of Plant Protection, Ministry of Agriculture of Vietnam, on September 2004, as described in part II (see Fig. 3.132). After 6 hours of treatment with the *Aglaia* formulations, the insects seemed to move slowly and ate very little of the treated leaves compared to those in the control dishes. After 12 hours, the insects started eating but moved slowly till 24 hours. After 24 hours, the insects were found dead at the *Aglaia* IV (5 000 ppm) treatment as well as in the treatment with the chemical agent (Regent ®). However, the bodies of the dead insects were dry and hard unlike the wet bodies observed for the insects treated with Regent ®. There was no observed change in weight and appearances of insects after 48 hours in the *Aglaia* treatment. The insects ate less. After 72 hours, 60% of the insect population died at 5 000 ppm and 40% at 2500 ppm in the *Aglaia* formulations, while 30 % death was observed with the chemical agent (Regent ®) (see Table 3.47). At the end of the experiment, the insects could not molt to their next life stage and died.

Table 3.47: Percentage of dead insects at 72 hours after treatment with *Aglaia* formulations

Formulations	Concentration	Percentage of dead insects after treatment (%)				
		Death(%) after 6 hours	***Death(%) after 12 hours***	***Death(%) after 24 hours***	***Death(%) after 48 hours***	***Death(%) after 72 hours***
Aglaia I	1 250 ppm	0.0	0.0	0.0	16.0	26
Aglaia II	2 500 ppm	0.0	0.0	0.0	14.0	40
Aglaia III	3 750 ppm	0.0	0.0	0.0	16.0	34
Aglaia IV	5 000 ppm	0.0	0.0	2.0	34.0	60
Saponin-C		0.0	0.0	0.0	4.0	18
Regent 800WG	0,05	0.0	0.0	2.0	16.0	30
Control	water	0.0	0.0	0.0	0.0	4

The experiments were conducted on Petri dishes at the Institute of Plant Protection, Ministry of Agriculture of Vietnam, September 2004

Result of insecticidal testes in Petri dishes after 72 hours of treatment

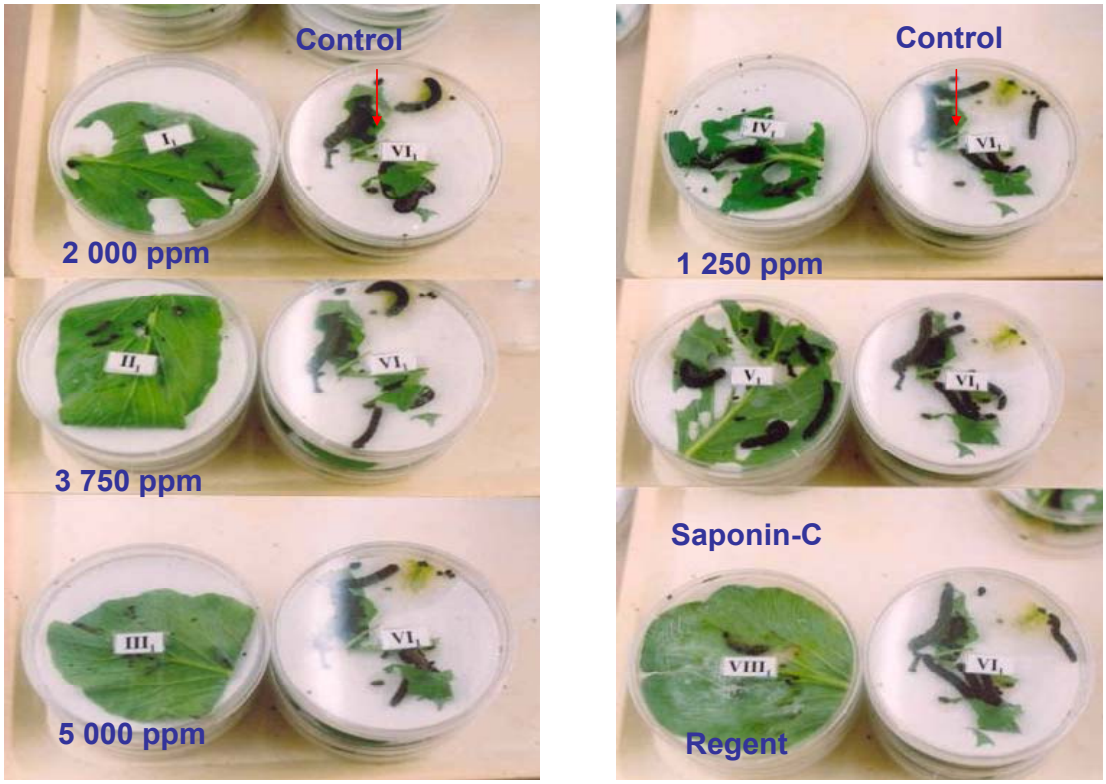

Fig. 3.132: Insecticidal results of *Aglaia* formulations on Petri dish experiment

The efficiency of *Aglaia* formulations was evaluated by the Abbot formula, and the results are given in Table 3.48. The efficiency of the *Aglaia* formulation at 5 000 ppm was 58.33% while that of regent was 37.50%.

Table 3.48: Mortality and Efficiency of *Aglaia* formulations (%) after 72 hours

Formulation	Concentration	Mortality and Efficiency of *Aglaia* formulations (%) after 72 hours				
		6 h	***12 h***	***24 h***	***48 h***	***72 h***
Aglaia I	1 250 ppm	0.0	0.0	0.0	16.0	22.92
Aglaia II	2 500 ppm	0.0	0.0	0.0	14.0	37.50
Aglaia III	3 750 ppm	0.0	0.0	0.0	16.0	31.25
Aglaia IV	5 000 ppm	0.0	0.0	2.0	34.0	58.33
Saponin-C		0.0	0.0	0.0	4.0	18.75
Regent-800WG	0,05	0.0	0.0	2.0	16.0	27.08
Control	water	0.0	0.0	0.0	0.0	-

III.4.4. Semi-field experiment result of *Aglaia* formulations on plant-pots

Ten third-instar larvae (*Spodoptera litura*) were transferred to the plant-pots of *Brassica rapa*. The different concentrations of *Aglaia* formulations were sprayed directly to the plant-pots (50 ml/m^2) (see Fig. 3.133). The experiment was kept in meca boxes to avoid escaping of the insects, and conducted in rearing chamber at the Institute of Plant Protection. Unfortunately, all the leaves of *Brassica rapa* were damaged by *Spodoptera litura* after 24 hours, as well as those treated with Regent ® (see Fig. 3.134).

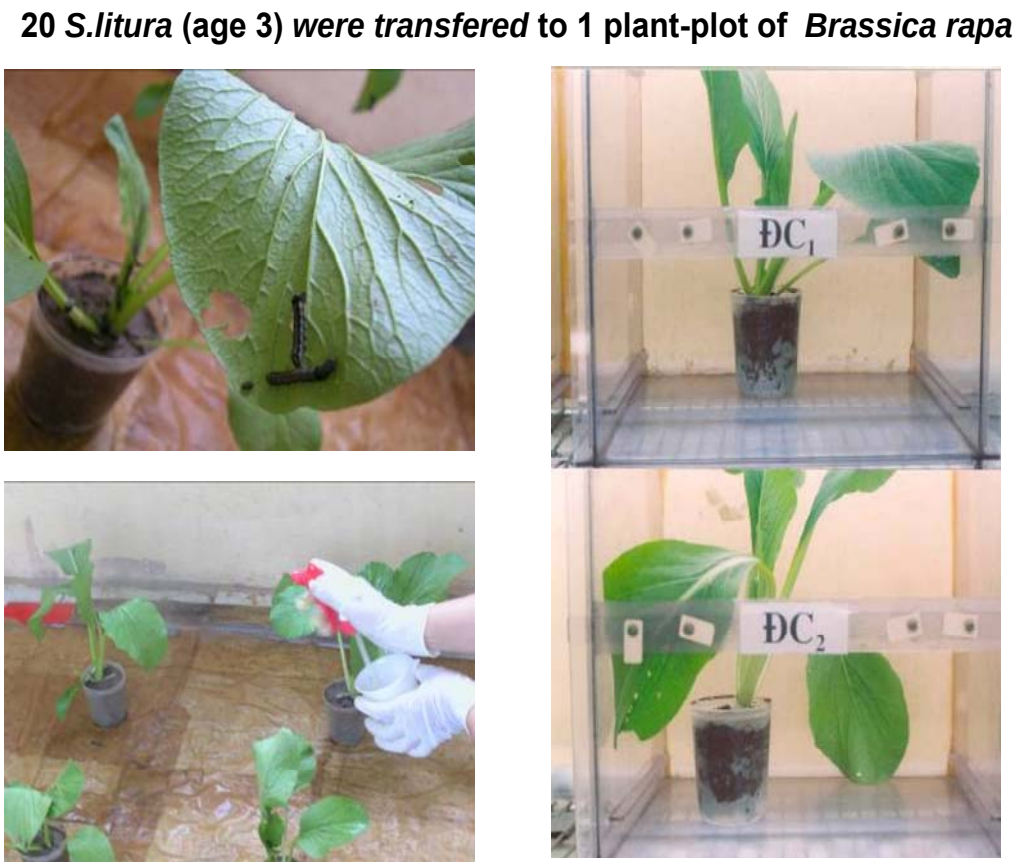

Fig. 3.133: Semi-field experiment on plant-pots of *Brassica rapa*

Semi-field experiment was conducted on plant-pots of *Brassica rapa* at at the Institute of Plant Protection, Ministry of Agriculture of Vietnam, September 2004

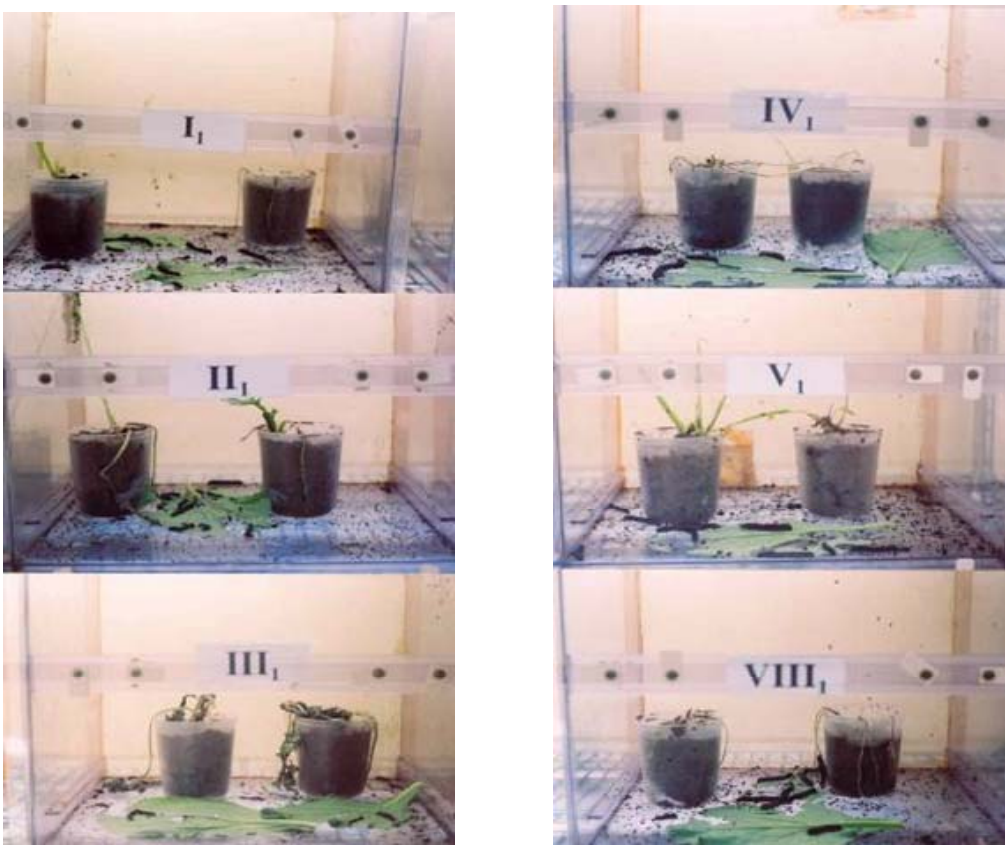

Fig. 3.134: Status of *Brassica rapa* on plant-pots after 36 hours of the treament

III.4.5. Efficiency of *Aglaia* formulation against *S.litura* on *Brassica rapa* in garden set-up

Spodoptera litura was maintained in the laboratory and transferred to lots (50 *S.litura* /1 lot) of *Brassica rapa* which was cultivated outdoors by seeding. The experiment was conducted in different lots at the garden of the Institute of Plants Protection, each lot *ca.* 1.5 m^2 contained 100 plants, with 5 replicates. The transferred insects were left to stabilize with the enviroment for one day outdoor before spraying with *Aglaia* formulation (see Fig. 3.135). The spray technique was applied mostly underneath the leaf surface where *S.litura* usually attacks, following the instruction of FAO. The chemical agent, Sherpa 25 EC was used as a positive control.

After 1 day of treatment, the density of *S.litura* was reduced from 250 to 160 (see Table 3.49 and Table 3.50) and was continuously reduced until the 5th day.

Experiment of *Aglaia* formulation was conducted on *Brassica rapa* in garden set-up at the Institute of Plant Protection, Ministry of Agriculture, Vietnam October 2004

Fig. 3.135: Insects were transfered from the laboratory to *Brassica rapa* in the garden

Efficiency of *Aglaia* formulation was 30.43% after 1 day and 35.9% after 2 to 4 days until the 5th day when it was decreased to 30.71%. The efficiency of Sherpa was 54.35% after 1 day and increased to 68.67% after 7 days (see Table 3.51 and Fig. 3.136).

Table 3.49: Density of *S.litura* after the treatment with *Aglaia* formulation

Formulation	**Dose L/ha**	**Before**	**Differences in density of *S.litura* after the treament**				
			After 1 day	***After 2 days***	***After 3 days***	***After 5 days***	***After 7 days***
Aglaia	5 000 ppm	250	160	140	125	105	88
Sherpa 25 EC	0.1L	250	105	70	65	50	40
Control		250	230	210	195	158	127

Table 3.50: Survival rate of *S. litura* after the treatment with *Aglaia* formulation, Sherpa and water (Institute of Plant Protection 22/9/2004)

Formulation	Concentration	Repeat 1		Repeat 2		Repeat 3		Repeat 4		Repeat 5		Avarage	
		survival	death	survival	death	survival	death	survival	death	survival	death	survival	death
After 1 day													
Aglaia	5000 ppm	31	19	29	21	23	17	35	15	32	8	160	90
Sherpa		19	31	21	29	24	26	23	27	18	32	105	145
Control	water	44	6	48	2	41	9	49	1	48	2	230	20
After 2 days													
Aglaia	5000 ppm	27	4	25	4	31	2	29	6	28	4	140	20
Sherpa		8	11	21	0	15	9	16	7	12	6	70	35
Control	water	41	3	43	5	39	2	43	6	44	4	210	20
After 3 days													
Aglaia	5000 ppm	26	1	21	4	27	4	23	6	28	0	125	15
Sherpa		7	1	19	2	14	1	15	1	12	0	65	5
Control	water	39	2	41	2	37	2	42	1	36	8	195	15
After 5 days													
Aglaia	5000 ppm	16	10	18	3	24	3	19	4	28	0	105	20
Sherpa		5	2	15	4	10	4	13	2	7	5	50	15
Control	water	31	8	34	7	29	8	31	11	33	3	158	37
After 7 days													
Aglaia	5000 ppm	11	5	14	4	19	5	17	2	27	1	88	17
Sherpa		5	0	11	4	7	3	11	2	6	1	40	10
Control	water	23	8	29	5	20	9	25	6	30	3	127	31

Table 3.51: Efficiency of *Aglaia* formulation against *S.litura*

Formulation	Dose L/ha	Efficiency of *Aglaia* formulation (%) after 7 days of the treament				
		1 day	***2 days***	***3 days***	***5 days***	***7 days***
Aglaia	5000 ppm	30.43	33.33	35.90	33.54	30.71
Sherpa 25 EC	0.5 Liter	54.35	66.67	67.50	67.66	68.50

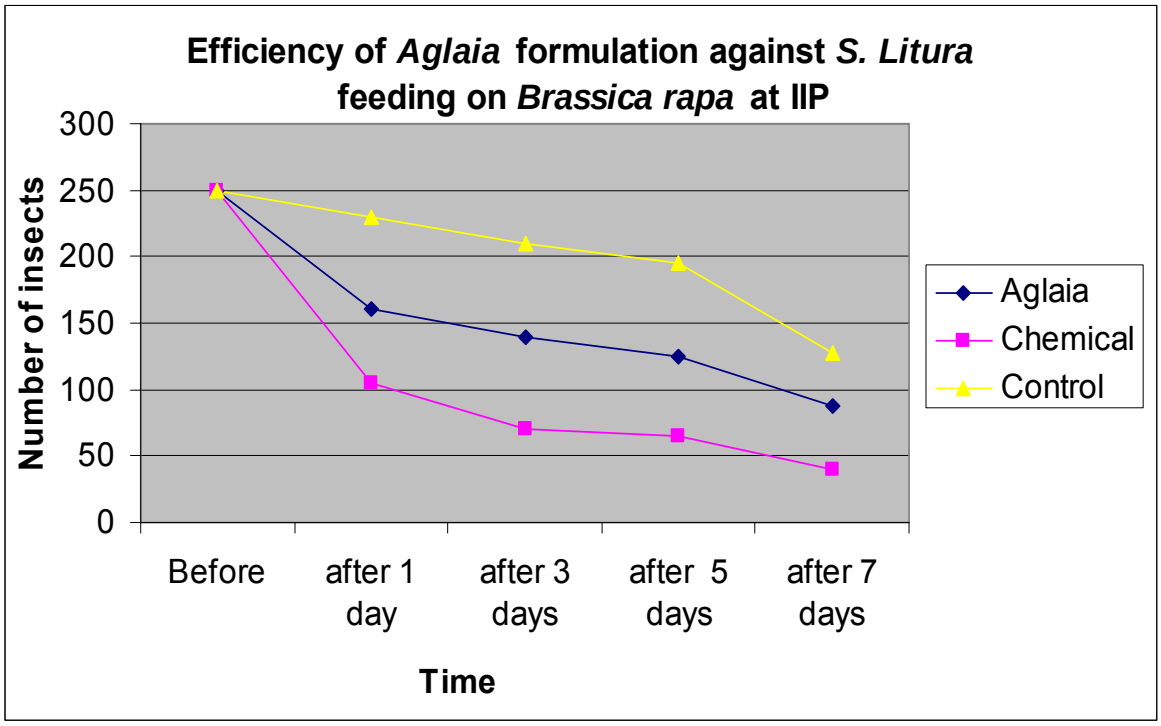

Fig. 3.136: Efficiency of *Aglaia* formulation towards *S.litura* on *Brassica rapa* in garden

III.4.6. Efficiency of *Aglaia* formulation against *Plutella xylostella* L.

The experiments were conducted on *Plutella xylostella* insects found on leaves of *Brassica rapa* using the spray and dip methods. Twenty *P. xylostella* were placed in one Petri dish. This was replicated five times. The spray method was carried out by spraying the *Aglaia* solution to the leaves directly using the Potter tower. The dip method was done by dipping the leaves into the *Aglaia* solution for five seconds. The *Aglaia* formulation exhibited strongest activity against *P.xylstella* after 5 days by the dip method (52.52%) when compared to the spray method (24.24%) (see Table 3.52 and Fig. 3.137)

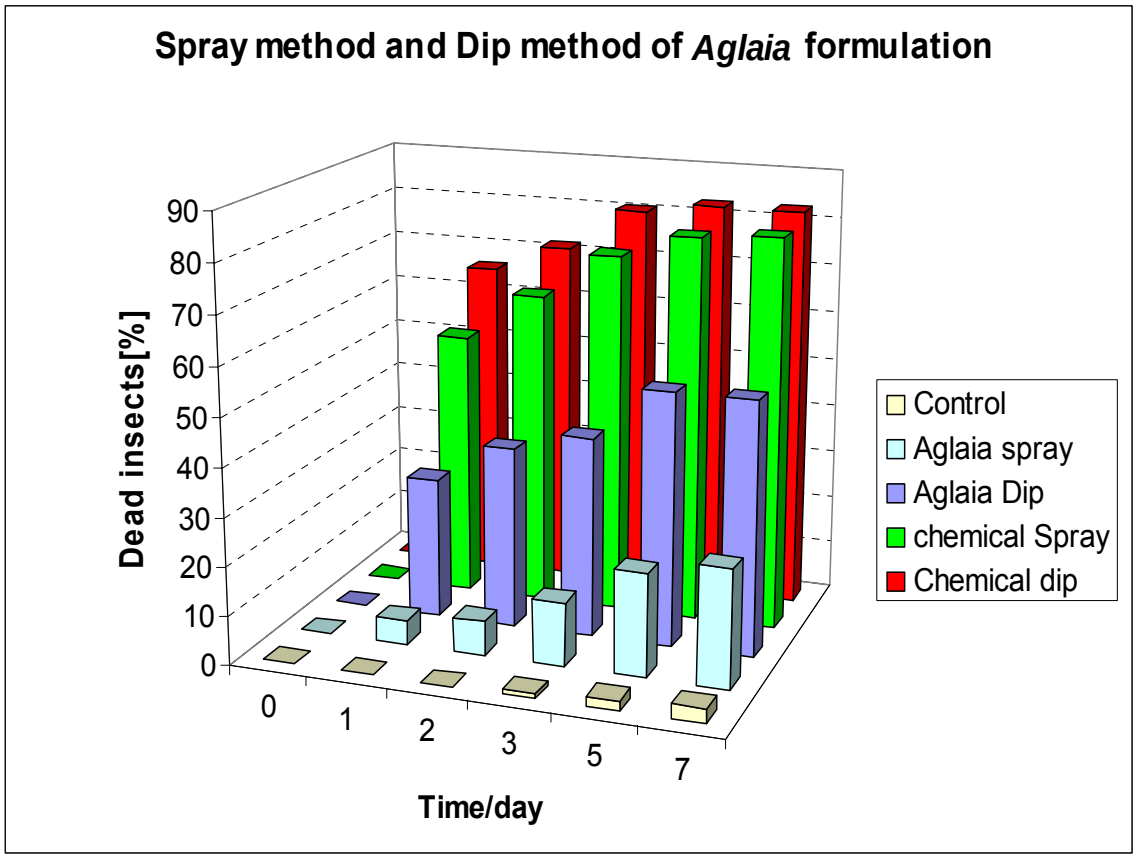

Fig. 3.137: Efficiency of *Aglaia* formulation against towards *P.xylostella*

Table 3.52: Survival rate of (*Plutella xylostella*) after the treatment with *Aglaia* formulation, Sherpa and water (control)
(Institute of Plants Protection 12/10/2004)

Formula	Concentration	Repeat 1		Repeat 2		Repeat 3		Repeat 4		Repeat 5		Average	
		survival	death	survival	death	survival	death	survival	death	survival	death	survival	death
After 1 day													
Aglaia	5000 (ppm)	19	1	20	0	18	2	19	1	19	1	95	5
Sherpa		11	9	10	10	9	11	8	12	7	13	45	55
Control	water	20	0	20	0	20	0	20	0	20	0	100	0
After 2 days													
Aglaia	5000	18	1	19	1	18	0	19	0	19	0	93	7
Sherpa		9	2	9	11	7	2	7	1	6	1	38	62
Control	water	20	0	20	0	20	0	20	0	20	0	100	0
After 3 days													
Aglaia	5000	17	1	18	1	18	0	17	2	17	2	86	14
Sherpa		7	2	8	1	5	2	6	1	5	1	31	69
Control	water	20	0	19	1	20	0	20	0	20	0	99	1
After 5 days													
Aglaia	5000	15	2	16	2	17	1	15	2	16	1	78	22
Sherpa		6	1	7	1	5	0	6	0	4	1	28	70
Control	water	20	0	19	0	20	0	20	0	20	0	99	0
After 7 days													
Aglaia	5000	15	0	16	0	15	2	14	1	16	0	75	25
Sherpa		6	0	7	0	5	0	6	0	2	2	26	74
Control	water	20	0	19	0	20	0	20	0	20	0	99	0

IV. DISCUSSION

IV.1. Rocaglamides and its congeners from *Aglaia* sp.

IV.1.1. Biogenesis of rocaglamides and bioactivity

Aglains are structurally similar groups of compounds to rocaglamides, which are also found in *Aglaia* species. However, aglains have been shown to be devoid of insecticidal activity against *S.littoralis* [Nugroho *et al*., 1999]. Rocaglamides and aglains have been hypothesized to originate biosynthetically from common structurally related precursors that include cinnamic acid amides and flavonoids [Proksch *et al*., 2001](see Fig. 4.1).

Rocaglamides showed antiproliferative activity against human cancer cell lines. During in *vitro* testes, rocaglamides exhibited IC_{50} values of 1.0 ng/ml against the human carcinoma cell line KB and an IC_{50} of 2.1 ng/ml against P388 cells, respectively [Proksch *et al.,* 2001]. The mode of action of rocaglamide and derivatives was suggested to be cytostatic rather than cytotoxic. This hypothesis provided the first information about the possible mode of action of these natural products [Proksch *et al*., 2001].

Besides, rocaglamide derivatives also exhibited potent immunosuppressive activity and inhibit cytokine gene expression at the transcriptional level. A very low dose (50 nM) of rocaglamides could completely inhibit IL-4 and IFN-γ production and suppress 60-86% of IL-2 and the proinflammatory cytokine TNF-α production. This strong inhibitor of effect of rocaglamide may explain the effect of the crude extracts in treatment of inflammatory skin disease and allergic asthma in traditional medicine, e.g., in Vietnam [Proksch *et al.,* 2005].

Thus, rocaglamides and its congeners could be developed into the direction of cytostatic agents against human cancer cells. Their apoptosis promoting effects in resistant acute T cell leukemia cells make them interesting candidates for therapeutic agents especially in the field of cancer [Proksch *et al*., 2001].

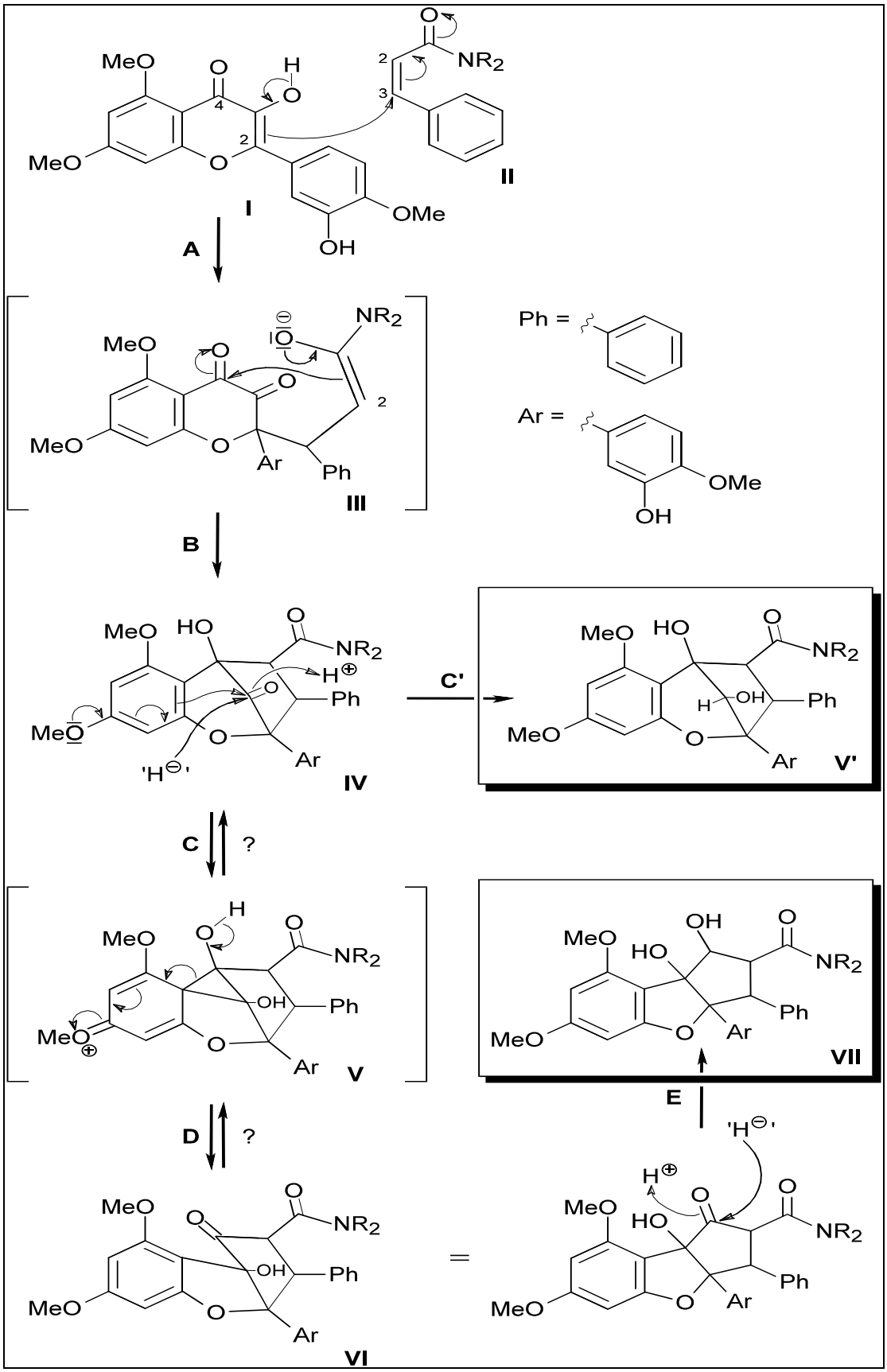

Fig. 4.1. Proposed joint biosynthetic origin of aglain derivatives V′ and rocaglamide derivatives VII [Nugroho *et al.*, 1999].

IV.1.2. MS fragmentations of rocaglamides

Analysis from the spectra of rocaglamide and its derivatives revealed characteristic pairs of fragments at *m/z* 300 and 313 dependent on the substitution pattern. The ions *m/z* 300 and 313 depict the plausible fragmentation of rocaglamide and its congeners under EI conditions (see Fig.4.2) Moreover, the fragmentation patterns in the range *m/z* 300 - 343 proved to be indicative of the type of substitution at ring B and C-8b of the furan ring [Proksch *et al*., 2001]. For example, the presence of a hydroxyl substituent at C-3' shifted the characteristic pair of fragments at *m/z* 300 and 313 (as in rocaglamide A, compound **1**) to *m/z* 316 and 329 while a methoxyl substituent at the same position gave rise to fragments at *m/z* 330 and 343 in the EI mass spectrum of the respective derivative. [Nugroho *et al*., 1997, Chaidir *et al.*, 1999 and Proksch *et al.*, 2001].

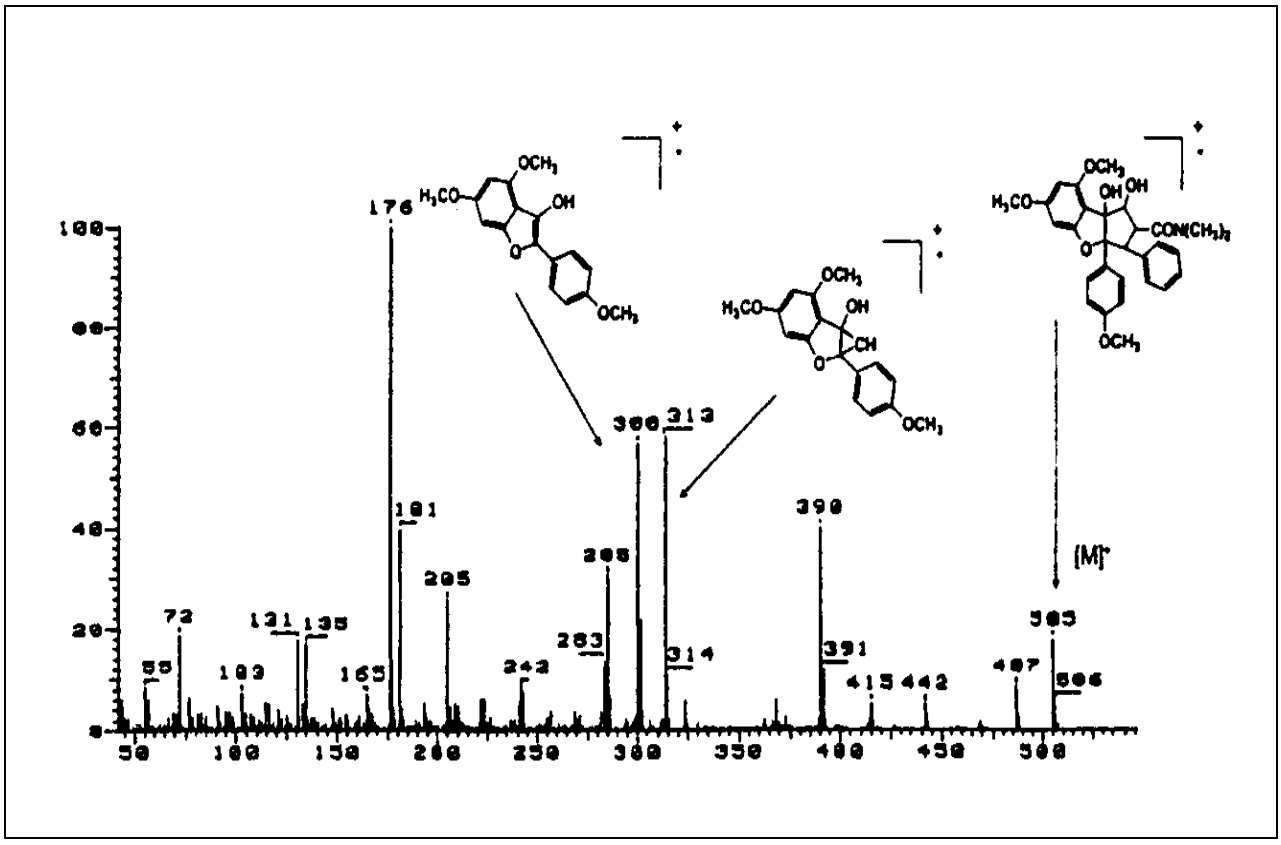

Fig. 4.2. Plausible structures for fragment ions *m/z* 300 and *m/z* 313 of Rocaglamide A (1) under EI-MS [Nugroho *et al.*, 1999]

IV.2. Lignan compounds from *Aglaia* sp.

IV.2.1. Biogenesis of lignans in plants

(+)-Pinoresinol (**10**), (-)-4′-O-methyl-pinoresinol (**11**), and (-)-eudesmin (**12**) belong to the resinol linkage lignans, which were first reported from *Aglaia* species. In nature, pinoresinol was reported mostly in (+) form. In this case, it was the same in A*glaia*, pinoresinol (**10**) was determined in its (+) form, while, both derivatives 4′-methyl-pinoresinol (**11**) and eudesmin (**12**) were found from the same fraction of *Aglaia oligophylla*, existing in the (-) form. Therefore, it could be hypothesized that pinoresinol existed as a racemic mixture in A*glaia*, but only the (-)-form of pinoresinol was involved in the systhesis of (-)-4′-methyl-pinoresinol and (-)-eudesmin (see Fig. 4.3). In plant, biosynthesis pathway of lignan compounds was described by Dewick as shown see Fig. 4.4.

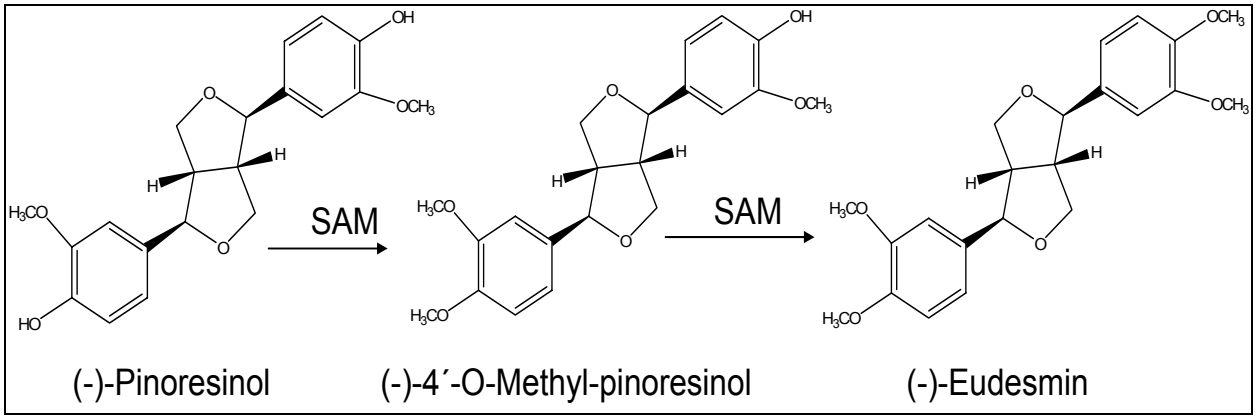

Fig. 4.3: Biosynthesis of pinoresinol derivatives in *Aglaia*

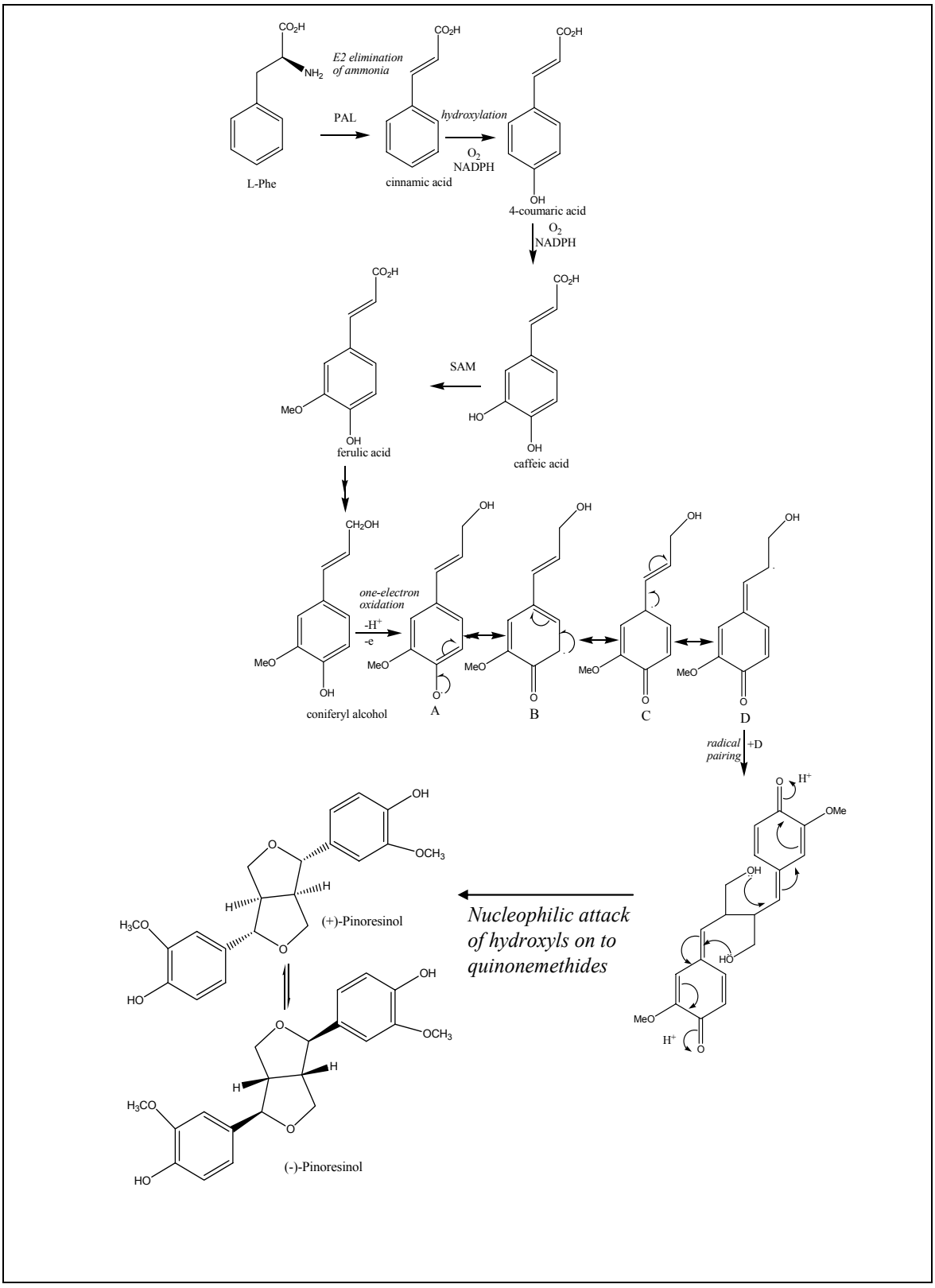

Fig. 4.4. Biosynthesic origin of lignans in plant [Dewick, 2003]

IV.2.2. MS fragments of pinoresinol and its derivatives

Analysis of MS spectra of eudesmin gave the following plausible fragments (see Fig. 4.5).

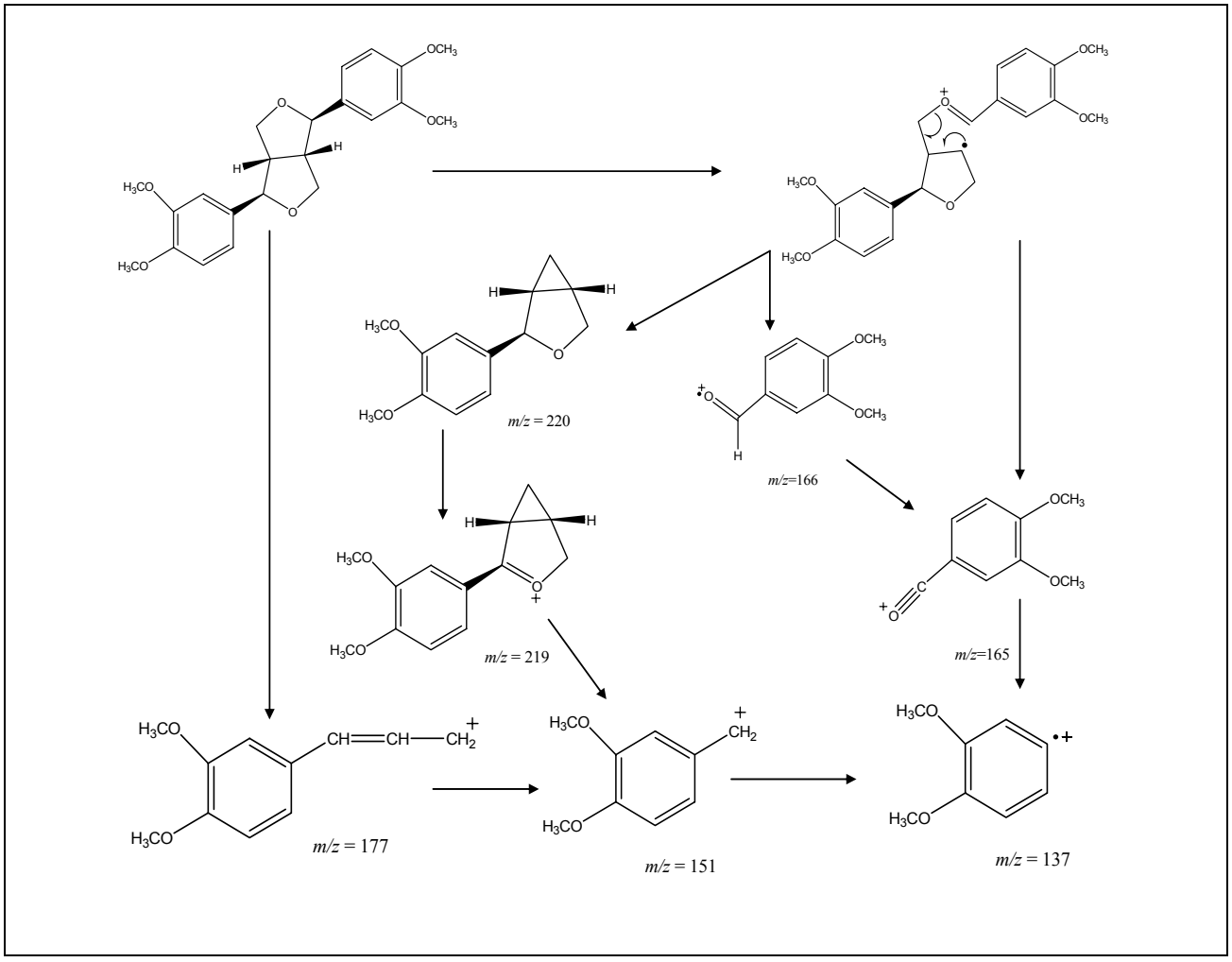

Fig. 4.5: Plausible fragments of compound 12 under EI-MS modified from Schmidt 1994

IV.2.3. Configuration assignment of furofuran-lignans by employing NMR data

Furofuran –lignans exist in three forms of conformers, namely eudesmin, dia-eudesmin, and epi-eudesmin (see Fig. 4.6) [Roy *et al.,* 2002]. Differentiating the stereoisomers by ^{1}H NMR could be a problem. The first problem is deciding whether the benzylic protons are axial or equatorial and the second problem is to determine which aryl group is linked to which benzylic hydrogen atom [Pelter *et al.,* 1976].

With regard to the first problem, two methods have been used to assign the stereochemistry of the benzylic protons. One is based on the coupling constants of the benzylic protons as shown in Table 4.1. This method indicates clearly the differences between eudesmin from its epi-

eudesmin form as based on the coupling constants of of 4.0-4.5 Hz and 6.9-7.5 Hz, respectively. Therefore, the benzylic protons at C-7 and C-7′ are readily distinguished as two doublets with different coupling constants.

However, the di-equatorial (eudesmin) and di-axial (dia-eudesmin) series are more analogous to each other than either to that of the epi-series. Moreover, the coupling constants in the di-equatorial and di-axial series are so similar that the stereochemistry could not be deduced from these NMR informations. The epi-series shows that one of the benzylic protons is at high field, and this feature is found in all of the known epi-compounds. That is an important and diagnostic characteristic of the epi-compounds and that like the 9′-axial protons it is a result of a direct anisotropic field effect of an axial aryl group in the 7′ position. In the epi-conformers, the benzylic proton is held closer to the axial aryl group in the opposite ring as found in phillygenin [Rahman *et al.,* 1990 and Pelter *et al*., 1976]. Besides, in the di-equatorial series both of the aryl protons are of course equatorial while in the di-axial series there are no axial benzylic protons to be influenced. This indicates that in the epi-compounds the high field proton is the axial proton and this directly solves the problem of assigning the stereochemistry at C-7 and C-7′. Thus, based on the coupling constants of the benzylic protons at C-7 and C-7′, the stereochemistry of isolated compound **10**, compound **11**, and compound **12** from *Aglaia oligophylla* were solved relatively as di-equatorial which belongs to the eudesmin form.

The second method for assigning the stereochemistry of these furofuran-lignans was also proposed by Pelter (1976) and was based upon an examination of molecular models [Pelter *et al.,* 1976]. This method showed that an axial aryl group is held very close indeed to the axial proton of the methylene group of the opposite ring, i.e. an axial C-7′ aryl group would affect H-9′(axial), and an axial C-7 aryl group would affect H-9 (axial). In every case the high field benzylic proton is axial, which was shifted upfield [Pelter *et al*., 1976].

In order to solve the second problem, ^{13}C NMR spectra were also used to decide which aryl group is adjacent to each of the benzylic proton [Pelter *et al*., 1976]. C-1 and C-1′ are sensitive both to the substituents on the aromatic ring and also to the stereochemistry at the neighbouring benzylic position. Table 4.2 shows clearly that proton atoms of equatorial and axial are distinct from each other in position of C-7/C-7′, C-8/C-8′ and C-9/C-9′. Based on

the chemical shift values of carbons at positions C-7/C-7′, C-8/C-8′ and C-9/C-9′, the stereochemistry of compound **10** and compound **12** are identical as conformers of eudesmin.

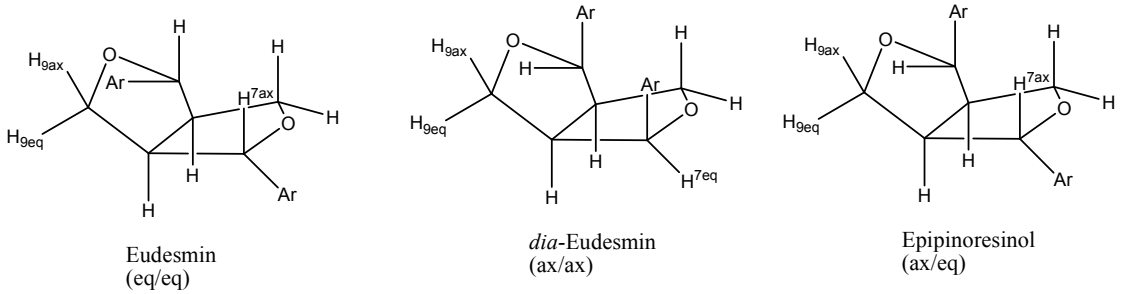

Fig. 4.6: Three conformers of furofuran-lignans

Table 4.1: Comparison of *J* values of eudesmin, dia-eudesmin, and epi-eudesmin conformers at H-7/H-8 and H-7′/H-8′

Furofuran-Lignan	***J* (Hz) H-7/H-8**	***J* (Hz) H-7′/-H8′**
Eudesmin[1]	4.4 (cis)	4.4(cis)
dia-Eudesmin[2]	5.1(cis)	5.1(cis)
Epipinoresinol[3]	5.3(cis)	7.2(trans)
(-)-pinoresinol[4]	5.0 (cis)	5.0 (cis)
Pinoresinol monomer ether acetate[5]	4.0 (cis)	3.5 (cis)
(-)-phillygenin[3]	5.5 (cis)	7.2 (trans)
(+)-epimembrine[6]	5.0 (cis)	7.2 (trans)
(+)-epieudesmin[6]	5.5 (cis)	7.0 (trans)
(+)-epigmagnolin A[6]	5.5 (cis)	7.2 (trans)
(+)-membrine[6]	7.0 (trans)	7.0 (trans)
Compound **10**	4.4 (cis)	4.4 (cis)
Compound **11**	4.1 (cis)	4.4 (cis)
Compound **12**	4.4 (cis)	4.4 (cis)

[1]: Sugiome *et al.,* 1995, [2]: Pelter et al., 1976, [3]: Rahman *et al.,* 1990, [4]: Casabuono *et al.,* 1994, [5]: Fonseca *et al*., 1979, [6]: Estrada-Reyes *et a*l., 2002

Table 4.2: Comparison of NMR data of eudesmin, dia-eudesmin and epipinoresinol

	$^{1}H_{\delta}$ H-7/7′	$^{1}H_{\delta}$ H-9a/9a′	$^{1}H_{\delta}$ H-9b/9b′	$^{13}C_{\delta}$ C-7/7′	$^{13}C_{\delta}$ C-8/′8′	$^{13}C_{\delta}$ C-9/9′
*Eudesmin	4.75	4.2-4.4	3.8-4.0	85.75	54.31	71.72
***dia*-Eudesmin	4.90	3.65-4.0	3.3-3.59	83.96	49.49	68.75
***Epi-pinoresinol	4.43-4.85	3.84	3.32-4.12	86.88-81.30	53.79 49.29	70.20-68.74
Compound **10**	4.74	4.24-4.25	3.87	85.85	54.14	71.65
Compound **11**	4.74-4.76	4.23-4.26	3.89	85.77-85.86	54.14	71.67-71.70
Compound **12**	4.75	4.24-4.26	3.89	85.781	54.146	71.716

*[Suginome *et al.,* 1995], **[Smithd, 1994], ***[Casabuono *et al.,* 1994].

In compound **11**, the NMR data values of carbons at positions C-7/C-7′, C-8/C-8′ and C-9/C-9′ were different from those of (-)-phellygenin (epi- form, see Fig. 4.7) [Rahman et al., 1990] or in comparison to that of epiaschatin [Pelter *et al.,* 1977] existing as *cis*- and *trans*-configuration at H-7 and H-7′, respectively (see Fig. 4.7). Moreover, compound **11** does not belong to the epi-form as (-)-phillygenin, due to coupling constant of H-7 and H-7′ was not identical. The ^{13}C NMR data were neither identical when compared to (-)-phillygenin (see Table 4.2) [Rahman *et al.,* 1990].

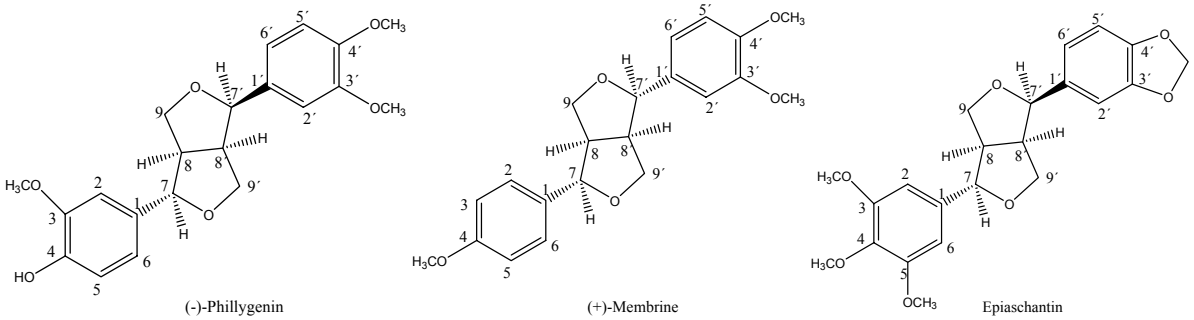

Fig. 4.7

IV.3. Flavonoid congeners from *Aglaia* sp.

IV.3.1. Biosynthesis of flavonoids

Flavonoids are found in fern and higher plants, where they occur both in the free state and as glycosides [Gunnar Samuelson, 2004]. They are products from a cinnamoyl-CoA starter unit. They usually contain a chain extension using three molecules of malonyl-CoA (see Fig. 4.8 and Fig. 4.9). This initially results in a polyketide, which depending on the nature of the responsible enzyme, folds in two different ways. These allow aldol or Claisen-like reactions to occur, generating aromatic rings [Dewick, 2003]. Enzymes chalcone synthase couples a cinnamoyl-CoA unit with three malonyl-CoA units giving chalcones.

Flavonoids contribute to plant colours, e.g. yellows from chalcones and flavonols, and reds, blues, and violets from anthocyanidins. This is also a growing belief that some flavonoids are particularly beneficial, acting as antioxidants and giving protection against certain cancer forms and cardiovascular disease. The polyphenolic nature of this group of compounds enables them to scavenge injurious free radicals such as hydroxyl and superoxide radicals.

An example is Quercetin which is almost always present in substantial amounts in plant tissues, and is also a powerful antioxidant, chelating metals, scavenging free radicals, and is also to prevent the oxidation of low density lipoproteins [Dewick, 2003].

Flavonoid compounds were also isolated from *Aglaia* species that were used in this study. They were all obtained by chromatography over a Sephadex LH-20 column using 100% of MeOH as eluent. The fractions were collected in tubes and left overnight in the fumehood for slow evaporation. The crystals appeared on the tube wall within 12 to 24 hours. Through TLC and HPLC the identity of the flavonoids was checked prior to pooling fractions containing the same flavonoids. These fractions were concentrated and flavonoid crystals were obtained.
(-)-Epicatechin (compound **13**) was found widespread in plants, present in red wine and green tea. Its activity was reported as anti-inflammatory agent and it showed hepatotropic activity [Chapman & Hall-CRC, DNP,Version 13.2, December 2004].

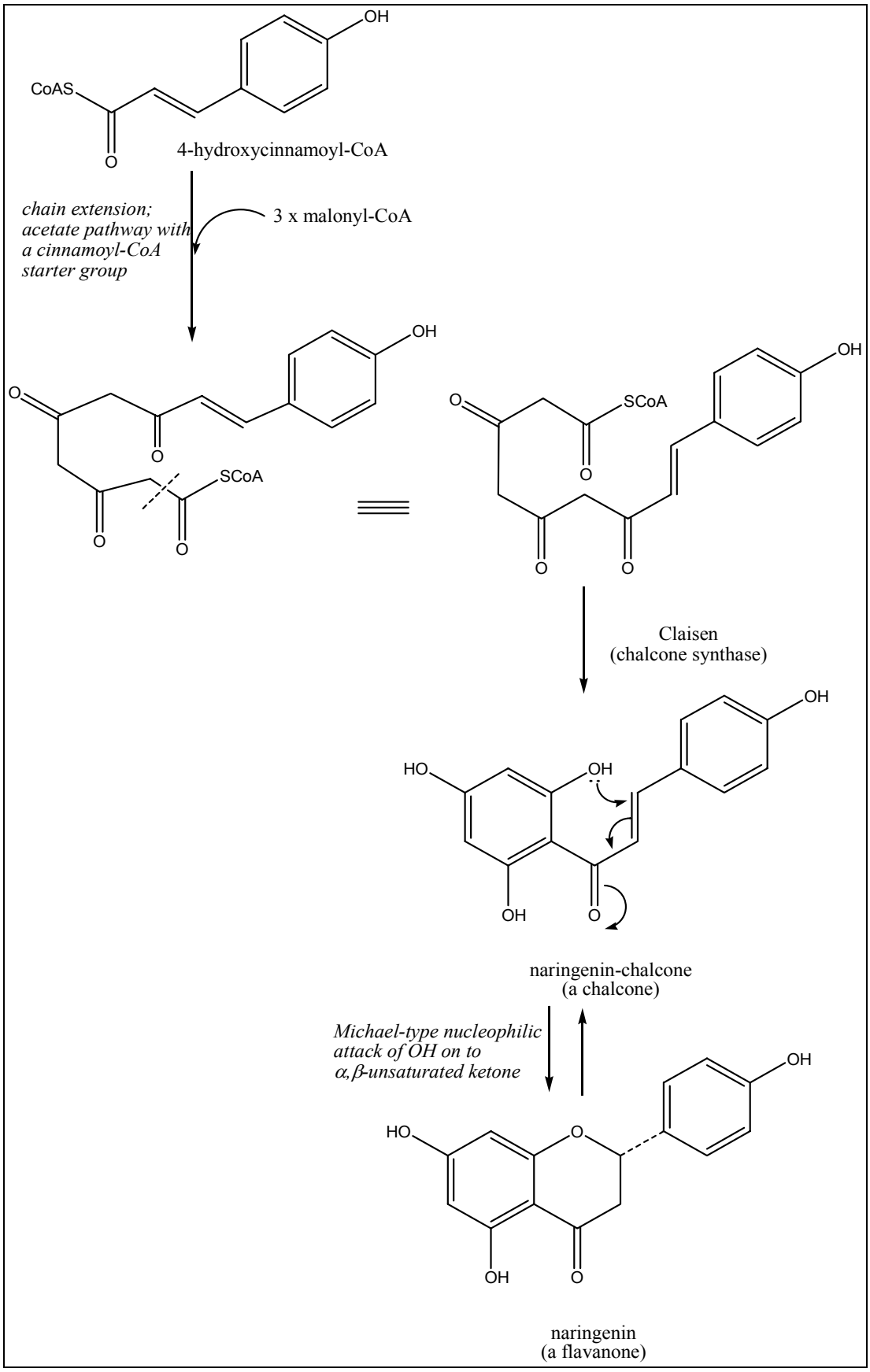

Fig. 4.8: Biosynthesis of flavonoids from plants [Dewick, 2003]

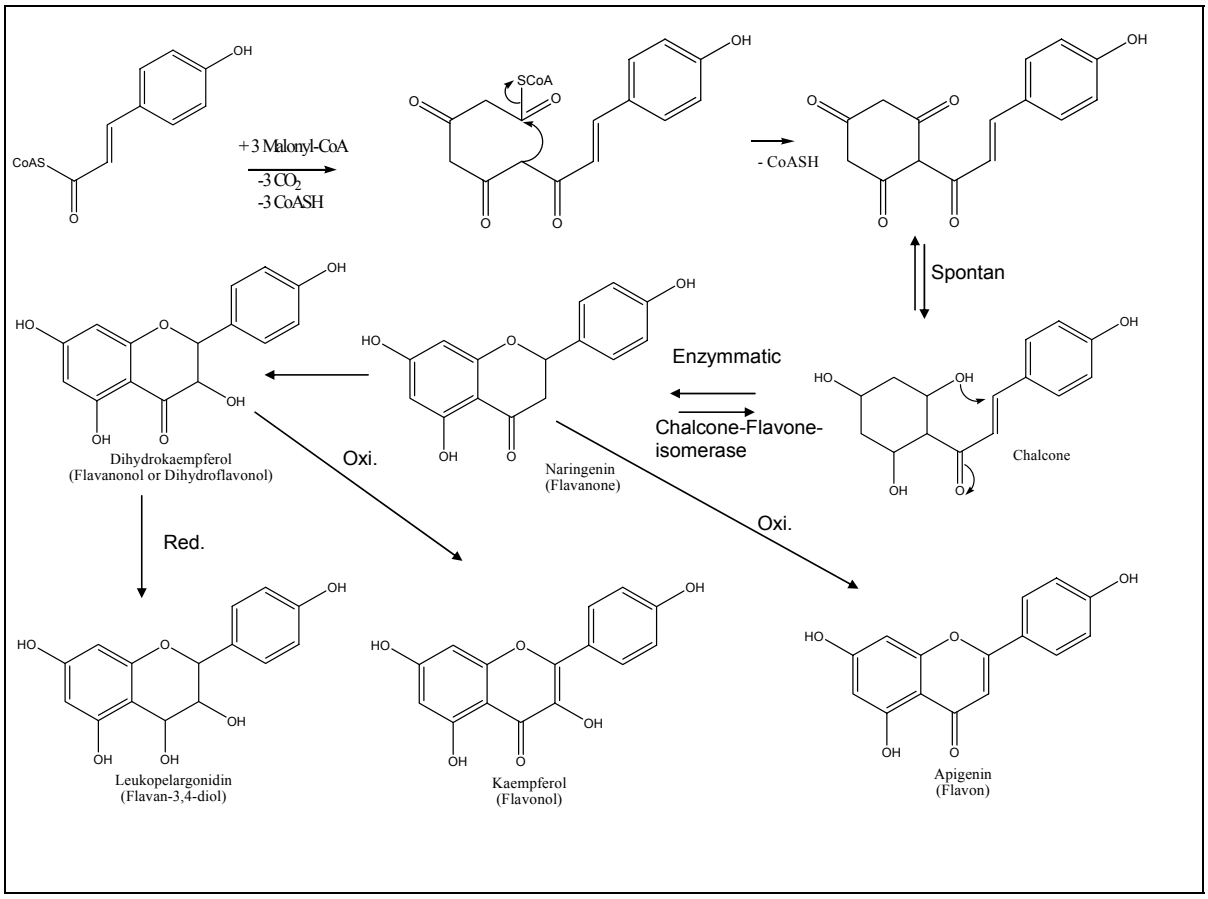

Fig. 4.9: Biosynthesis of flavonoids from plants [Dewick, 2003]

IV.3.2. MS fragmentation of flavonoids by EI

MS fragmentation of flavonoids by EI was described by Markham and Kingston *et al.,*1978 was shown in Fig. 4.10 and Fig. 4.11.

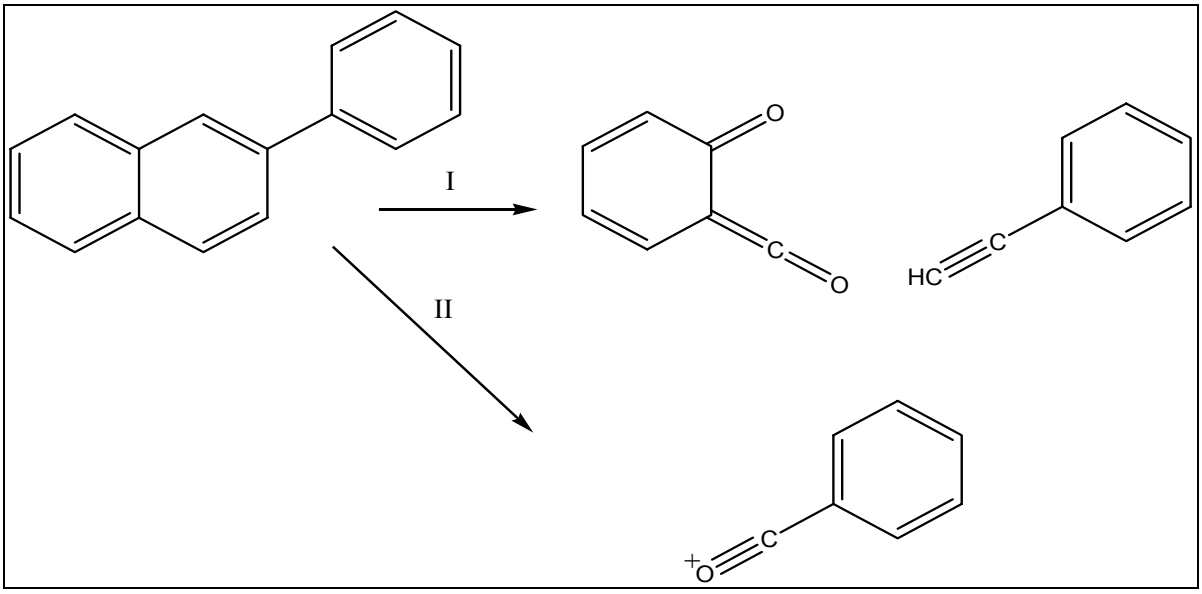

Fig. 4.10: Plausible fragments of flavonoids [Markham, 1978]

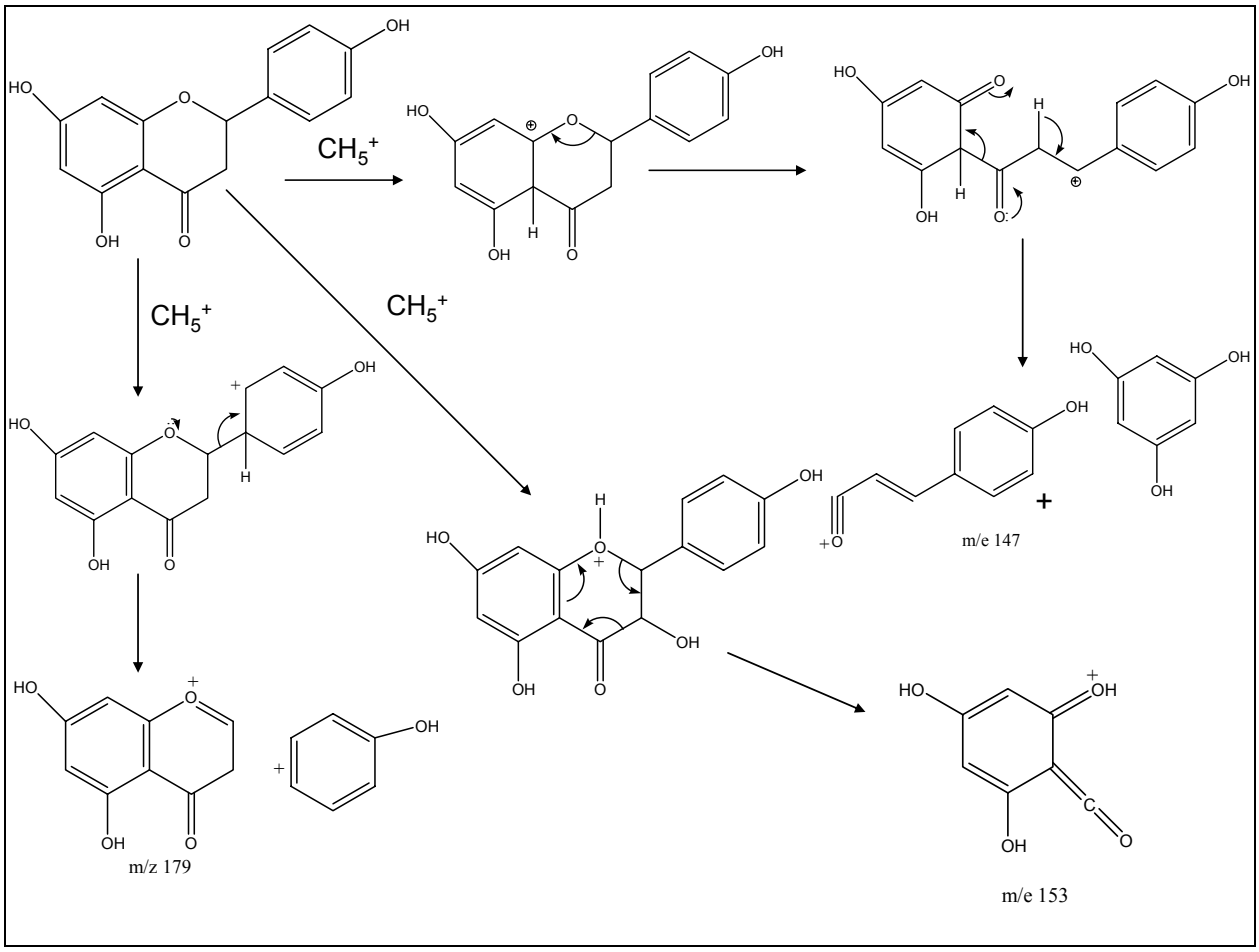

Fig. 4.11: MS fragmentation of flavonoids as modified by Kingston *et al.*, 1973

IV.4. Cinnamoyl bisamide derivatives from *Aglaia* sp.

Dasyclamide (compound **20**) was found in high amounts in *Aglaia oligophylla* leaves collected in Vietnam. Compound **20** was previously isolated from *Aglaia dasyclada* and *Aglaia rubiginosa*. It was inactive when tested against *S.littoralis*. However, dasyclamide exhibited moderate antimicrobial activity against *E.coli*.

Grandiamide D (compound **22**) is a new natural product, which was isolated from the leaves of *Aglaia gigantea* collected in Vietnam. The absolute configuration of compound **22** at the stereocenter C-3 was determined via Mosher ester derivatization method. The result of analysis is shown in Table 3.37 and Fig. 3.81.

It is evident that proton H-3 with $\Delta\delta < 0$ is located on the left side of the MTPA plane, while H-4A, H-4B and H-5A, H-5B with $\Delta\delta > 0$ are on the right side of the molecule [Ikuko *et al.,* 1991]. Based on the relative priorities of the four substituents by Ingold and Prelog rule, the chiral center (C-3) must be viewed from the side opposite the lowest priority group (-H),

substituent groups with the highest priority (-OMTPA), the secondary priority (-C=CH_2) and the third priority (-CH_2OH). The turn was counter-clockwise and then the chiral center was classified to follow the ***S*** configuration.

Odorine (compound **23**) and odorinol (compound **24**) were isolated and structurally elucidated by Shiengthong *et al.,* 1979 from *Aglaia odorata*, a Thai medicinal plant. In 1982, Hayashi *et al* reported on the antileukemic activity of odorinol (**24**) in the in vivo *P*-388 system. This interesting result prompted other groups in which Saifah *et al.,* 1993, eleven years later, reported again these compounds together with another derivative known as pyramidatine (compound **26**) from *Aglaia pyramidata,* which posses a potential to reverse drug resistance in cultured cells [Saifah *et al.,* 1993]. Both compounds, odorine and odorinol, exhibited remarkably both the inhibition of the initiation and promotion stages in a two-stage skin carcinogenesis [Inada *et al.,* 2001]. Pyramidatine (compound **26**) was previously isolated from *Aglaia pyramidata* and *Haplophyllum latifolium.*

The structures of odorine and odorinol possess an unusal bisamide moiety with both nitrogen atoms attached to a chiral centre. The MS fragmentation of odorine and odorinol are shown in Fig. 4.12. The major mass-spectral fragmentation of the molecule consists of successive losses of mass units of 101 and 68 from the molecular ion to give the cinnamoyl cation, which then undergoes the normal mass-spectral decomposition. As a common fragmentation pattern, the simple cleavage of the molecular ion to give an ion with m/z 85 was observed. This ion subsequently loses carbon monoxide to yield an ion at m/z 57, and it is possible to conclude that the second carbonyl is attached to the butane chain [Shiengthong *et al.,* 1979].

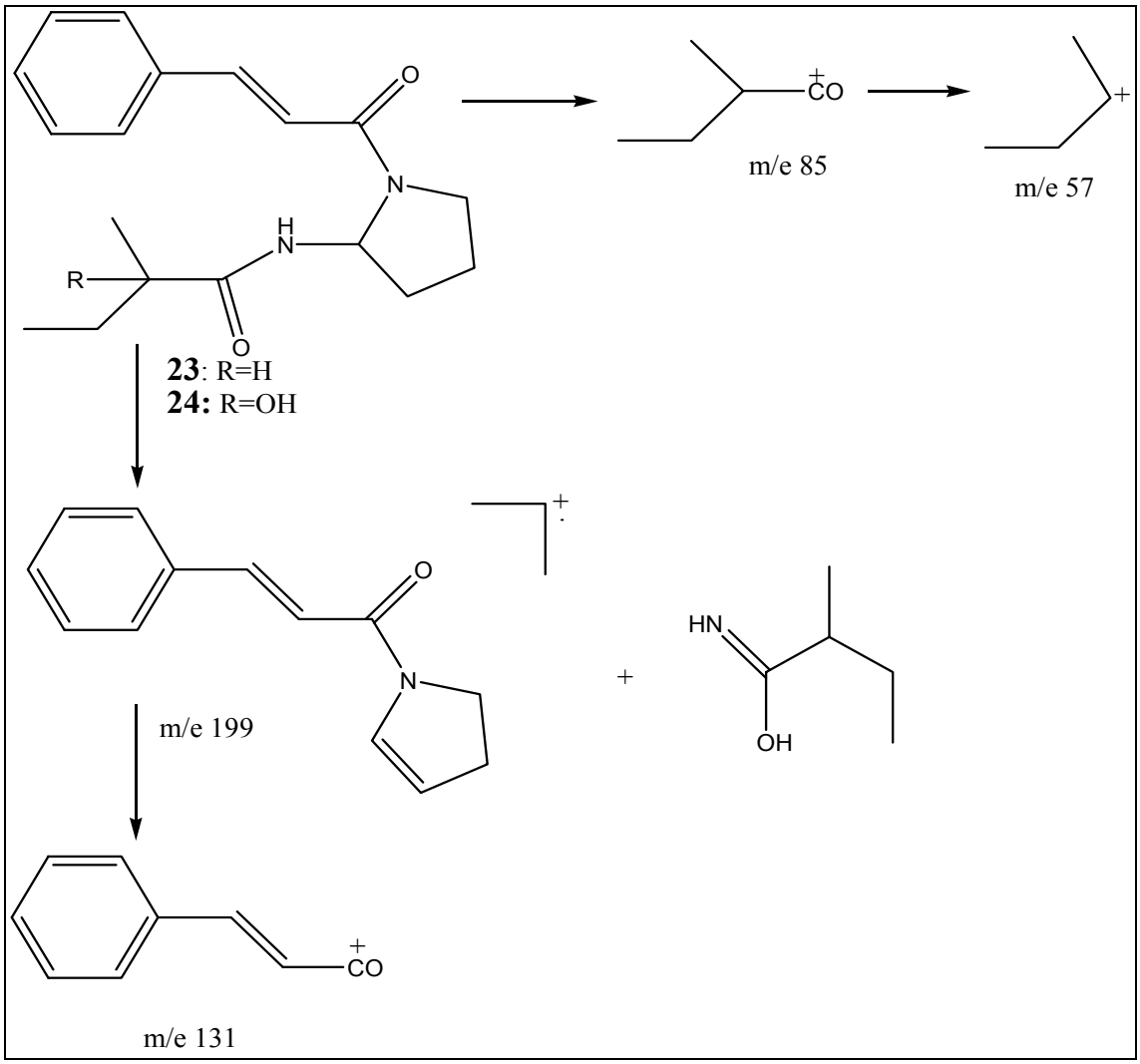

Fig. 4.12: Pausible MS fragmentation pattern of compounds 23 and 24 [Shiengthong *et al.,* 1979]

IV.5. Terpenoid compounds from *Aglaia* sp. collected in Vietnam

IV.5.1. Biosynthetic pathway of triterpenoids

Triterpenes are formed by two molecules of farnesyl PP (pyrophosphate) which are joined tail to tail to yield the hydrocarbon **squalene**, which was originally isolated from the liver oil of sharks (*Squalus* sp.). Cyclization of squalene is via the intermediate **squalene-2,3-oxide**, produced in a reaction, which is catalysed by flavoprotein requiring O_2 and NADPH cofactors [Dewick, 2003] (see Fig. 4.13).

Niloticin (compound **28**) was previously reported from *Turraea nilotica, Phellodendron chinense*, and *Eurycoma longifolia* [Gray *et al.,* 1988, Mulholland *et al.,* 1987 and Itokawa *et al.,* 1992]. Niloticin showed moderate cytotoxic activity against P388 and KB cells at 1.5 and 8.3 (IC_{50} μg/ml), respectively [Itokawa *et al.,* 1992].

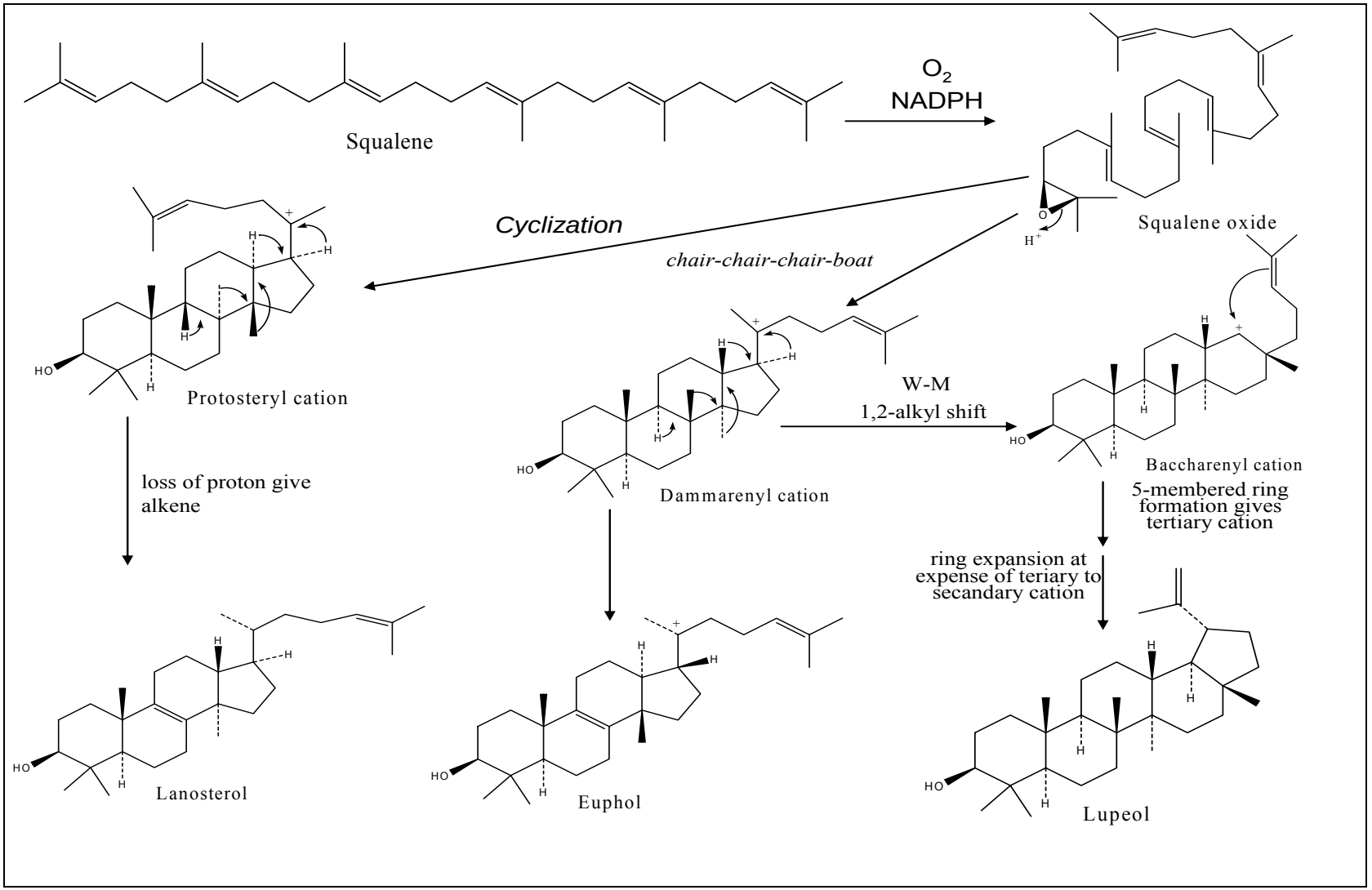

Fig. 4.13: Biosynthetic pathway of triterpenes [Dewick, 2003]

IV.5.2. Biosynthetic pathway of lutein

The tetraterpenes are represented by only one group of compounds known as the carotenoids. Although these compounds play a role in photosynthesis, they are also found in non-photosynthetic plant tissues, in fungi and bacteria. The tetraterpene skeleton involes tail-to-tail coupling of two molecules of geranylgeranyl diphosphate (GGPP) in a sequence essentially analogous to that seen for squalene and triterpenes is cyclized. γ –Carotene (a precursor of β-carotene) and δ-carotene (a precursor of α-carotene) illustrate carotenoids where only one end of the chain has become cyclized. Oxygenated carotenoids (termed xanthophylls) are also widely distributed, and the biosynthetic origins of the oxygenated rings found in lutein (compound **29**) are shown in Fig. 4.14 [Dewick, 2003].

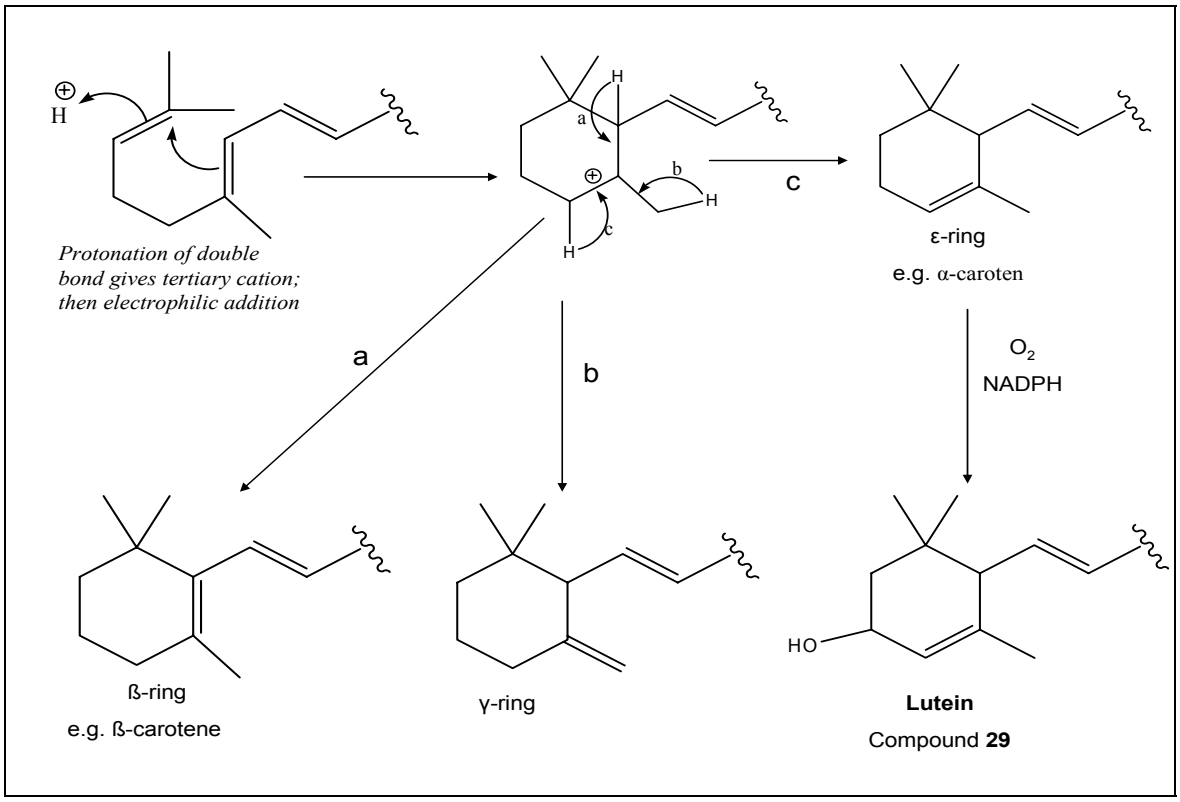

Fig. 4.14: Biosynthesis of lutein [Dewick, 2003]

Lutein (compound **29**) is a tetraterpene which in this study, for the first time, has been isolated from *Aglaia*. Lutein has been described in *Mimosa invasiva*, *Cosmos caudatus,* and *Porphyra* spp. Lutein is a pigment from egg yolk and leaves found in all higher plants and also in microorganisms e.g. *Staphylococcus aureus*. It exhibits antioxidant activity. Lutein showed also antitumour, antimutagenic and a wide range of antimicrobial activity. It is potentially useful in treating vascular degeneration and is used as a drug for the eye [Chapman and Hall/CRC, 2004].

IV.6. Coumarins from *Aglaia* sp.

IV.6.1. Biosynthetic pathway of scopoletin

The hydroxylation of cinnamic acid *ortho* to side-chain is a crucial step in the formation of a group of cinnamic acid lactone derivatives called coumarins. Hydroxylation of cinnamic acid or 4-coumaric acid can occur *ortho* to the side chain (see Fig. 4.15).
This is followed by the change in configuration in the side-chain of the two 2-hydroxy cinnamic acids from the *trans* (*E*) to the less stable *cis* (*Z*) form.

Chemical lactonizations can occur on treatment with acid. The trans-cis isomerization and lactonization are enzyme-mediated in nature, and light is not needed for coumarin biosynthesis. Hence, cinnamic acid and 4-coumaric acid give rise to the coumarins and umbelliferone. Coumarins with additional oxygen substituents (e.g. aesculetin and scopoletin) appear to be derived by modification of umbelliferone, rather than by a general cinnamic acid to coumarin pathway [Dewick, 2003].

Scopoletin occurs widely in the plant world, for example, in *Gelsemium sempervirens*, *Atropa belladonna*, *Convolvulus scammonia*, *Ipomoea orizabensis*, *Prunus serotina*, *Fabiana imbricata* and also *Diospyros spp*., *Peucedanum spp*., *Heracleum spp*., *Skimmia spp*. Scopoletin also occurs in the Chinese crude drug Toki (from *Angelica acutiloba*). It exhibits antispasmodic agent, antiinflammatory, eicosanoid release inhibitor [Dewick, 2003 and Chapman and Hall/CRC, 2004].

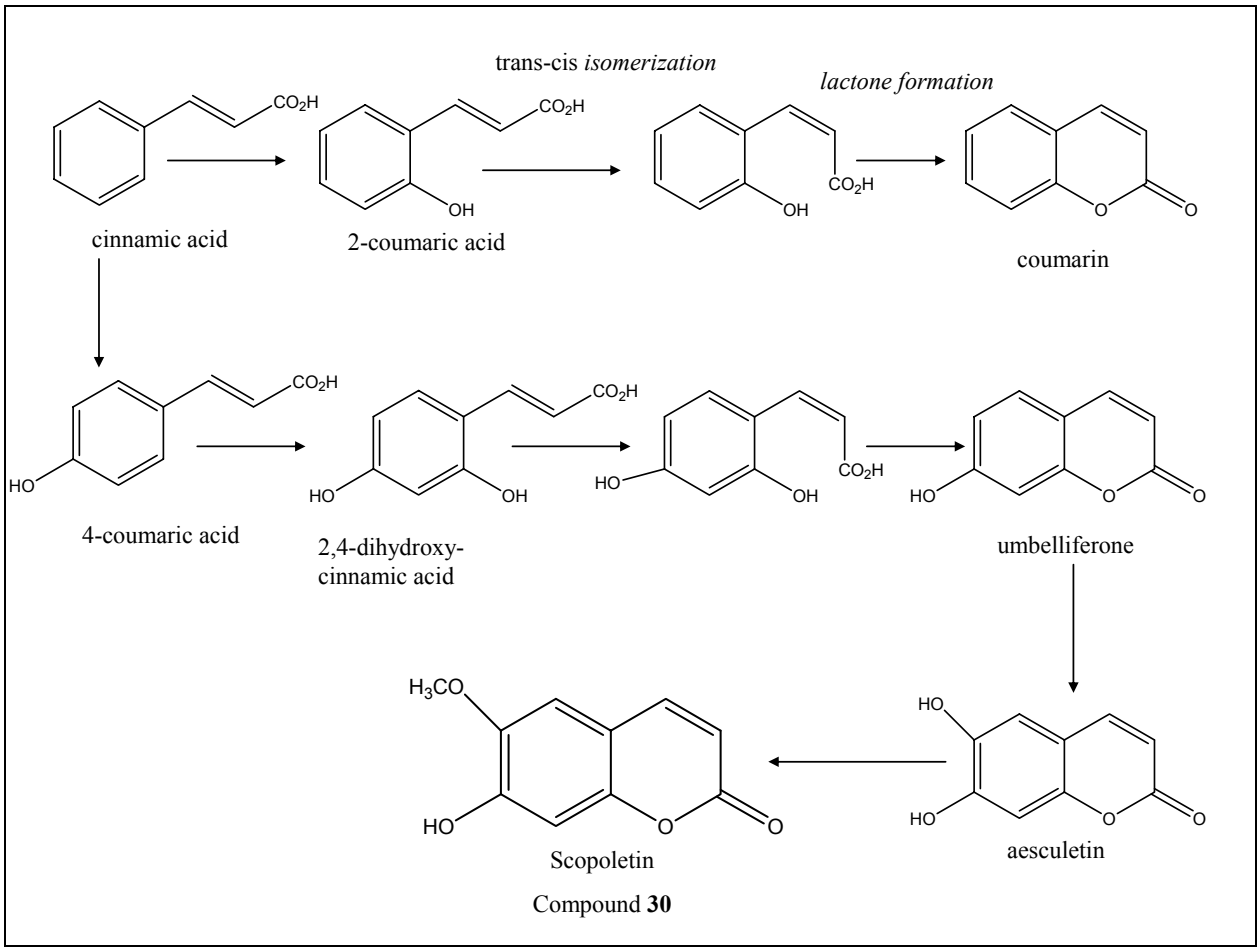

Fig. 4.15: Biosynthesis of scopoletin in plants [Dewick, 2003]

IV.7. Field experiments with *Aglaia* formulations

The first field experiment of *Aglaia* formulation was conducted in this study on *Crinum asiaticum* (Amaryllidaceae), where *Brithys crini* (Lepidoptera, Nuctuidae) are feeding on and seriously damaging the medicinal plant at the Tao Dao national medicinal garden, Vietnam July 2003. The methanolic extract of *Aglaia oligophylla* was formulated to a liquid spray. Its effects do not consist in directly killing the larvae of *Brithys crini* as compared to most of the very toxic forbidden chemical insecticides (e.g.Monitor®), but it acts rather as a repellent in driving the insects away from the sprayed plants. At concentrations of 4000 and 6000 ppm of applied *Aglaia formulations*, treated plants were grown in good condition while insects moved away and died.

When plants were treated with lower concentrations of 500 and 2000 ppm, the effects were not strong enough to protect the plants from being attacked and destroyed by the insects. With these treatments, all plants were dead after 7 days.

Aglaia formulation from the extract of *A.oligophylla* leaves was also effective against the aphids *Macrosinum phoniella* feeding on artichoke (*Cynara scolymus*). The experiment was also conducted in Tam Dao national medicinal garden, Vietnam July 2003.

The application of *Aglaia* formulations on aphids was observed to probably affect their central nervous system which leads to their uncontrolled movements and is followed by death of after 7 days.

The second field experiment was conducted on cabbages and kohlrabis against *Spodoptera litura* at Dong Anh, October 2003. In this experiment, two 5000 ppm-formulations of *Aglaia* were formulated from extracts of *A.oligophylla* and *A.abbriviata*. Both formulations exhibited effectivity against *Spodoptera litura* which were feeding on cabbages and kohlrabis and were comparable to the commercial chemical product Regent®. Interestingly, the efficiency of *Aglaia* formulations exhibited slow activity at the beginning but lasted longer in contradiction to the chemical product (see Table 3.46, Fig. 3.129 and Fig. 3.130).

The third semi-field experiment was conducted on *Brassica rapa* at the Institute of Plant Protection, Ministry of Agriculture of Vietnam, September 2004.

Efficiency of *Aglaia* formulation was 30.43% after 1 day, and continued to 35.9% after 3 to 4 days until the fifth day, it was down to 30.71%. Meanwhile, the chemical control Sherpa®, exhibited an efficiency of 54.35% after 1 day which increased until the fifth day to 68.67%. After 5 days, the differences in density of *Spodoptera litura* were all reduced by the *Aglaia* formulation, the chemical, and as well as in the control (see Table 3.51 and Fig. 3.136).

However, at the end of the experiment, black spots occurred on the surface of the leaves of *Brassica rapa* treated with *Aglaia* formulation. The colour of the leaves changed from dark-green to yellow then silver-white. This was caused by the chlorophyll present in the *Aglaia* leaves extract. This factor could be eliminated by removing the chlorophyll from the extract by partition extraction with n-hexane.

Moreover, *Aglaia* formulations also exhibited strong effects to *Spodoptera litura* and *Plutella xylostella* L. in the Petri dish experiment. However, the dip method (dipping the leaves into *Aglaia* solution) exhibited stronger activity at 52.5% compared to the spray method (24.2%, spraying *Aglaia* solution by using Potter tower). *Aglaia* formulation changed the physical characteristics of the leaves of *Brassica rapa* after the treatment. The field experiments have shown that the *Aglaia* formulation is effective toward a broader spectum of pests and could have a broader utilty in crop protection.

The stability of *Aglaia* extract under field conditions

Since rocaglamides are present in the extract in very minute amounts, dasyclamide was used as an internal standard to test the stability of the extract under field conditions. Dasyclamide is a building unit in the biosynthetic pathway of rocaglamide, and was found at high amounts in the leaves of *Aglaia gigantea*. Thus, dasyclamide was used to

analyze the stability of *Aglaia* extract and to assay residual traces of the extract under field conditions.

By HPLC, it was concluded that after 3 days, there are no traces of dasyclamide found on treated leaves of cabbages. This experiment is very important to show lower pest exposure on the extract residue. By shorter residual contact, this strategy could reduce the selection pressure on the pest insect for resistance extending the insecticide lifespan and being less harmful for human beings, the end consumer of the vegetable products that land in the market.

The toxicity test of *Aglaia* formulation on mice

The toxicity test of the *Aglaia* formulation was conducted on two months old white mice with an average weight of 20 - 25 g. The acute oral toxicity assay method was carried out by orally administering different concentrations of the extract, by incorporation of the test sample in the food diet. The second test method involved injecting the *Aglaia* extract directly into the gullet of the mice. The observation period was at least 14 days. The death rate of the mice was analyzed by Abbott formula and by Finney's probit analysis. The levels of toxicity were classified by the WHO (World Health Organisation) (see Table 3.3). The toxicity value (LD_{50}) of the *Aglaia* extract by incorporation with the food diet was calculated as 4500 mg/kg, which could be considered to be in the range of a "very low toxic" level. The liquid formulation of the *Aglaia* extract, which was injected directly into the gullet of mice, exhibited a medium toxicity level at 2000 mg/kg (see Table 3.2). The low toxicity of *Aglaia* formulation is a great advantage over commercially available insecticides. *Aglaia* formulation is a potential non-toxic agrochemical and is recommended to be utilized as a bio-insecticide in crop protection.

V. SUMMARY

Thirty-eight extracts from thirteen different *Aglaia* species collected in Vietnam were screened for insecticidal activity against neonate larvae of *S. littoralis* using an anti-feedant assay. *Aglaia oligophylla*, *Aglaia abbriviata, Aglaia eleagnoidae, Aglaia duppereana* were found to be most active species. At a dose concentration of 1000 ppm of the crude organic extract (following incorporation into artificial food), 100% larval mortality was observed after 24 hours. While *A.rothii* gave 80% morality, *A*. *dasyclada* gave 70% mortality, *A. gigantea* caused 60 % mortality, *A*. *pleuroptiris* 45% and *A. macrocarpa* 15% mortality of the larvae. Following a bioassay-guided fractionation of all active crude extracts of *Aglaia oligophylla,* three fractions (F3,F4,F5) were found to exhibite very strong insecticidal activity at a concentration of 200 ppm each. Qualitative analysis of these fractions through HPLC-DAD and HPLC-MS showed the presence of rocaglamide congeners as well as of other natural products. Fraction F3, F4, and F5 were further fractionated over a Silica gel column and these gave a new rocaglamide derivative, **Rocaglamide AY** (compound **8**). From these fractions, three lignans with interesting stereochemistry were also obtained which included **pinoresinol** (compound **10**), **4´-O-methyl-pinoresinol** (compound **11**), and **eudesmin** (compound **12**). Three other flavonoids were also obtained and were identical to known compounds : **4´,5,7-trimethoxydihydroflavonol** (compound **15**)**, 4´,5,7-trimethoxy-kaempferol** (compound **16**) and **4´,5,7-trimethoxyflavanone** (compound **17**). **Lutein** (compound **29**), being a tetratriterpene was also obtained as a crystal from fraction F3.

From the bark of *Aglaia duppereana*, five known rocaglamide derivatives were isolated which were identified as **rocaglamide A** (compound **1**)**, rocaglamide I** (compound **2**), **rocaglamide W** (compound **3**), **rocaglamide AB** (compound **4**), **rocaglamide J** (compound **5**) and **epicatechin** (compound **13**).

The fractionation of the extract from the leaves of *Aglaia gigantea* yielded **dasyclamide** (compound **20**)**, grandiamide D** (compound **22**), **gigantamide A** (compound **25**) and **foveolin B** (compound **27**). **Niloticin** (compound **28**) was obtained from the leaves of *Aglaia dasyclada*, while **rocaglaol** (compound **6**) and **scopoletin** (compound **30**) were

isolated from the leaves of *Aglaia elaeagnoidea*. The ethylacetate extract of *Aglaia abbriviata* gave **4´,5,7-tri-O-methyl-kaempferol**, **odorinol** (compound **24**) in crystalline form and **aglaxiflorin D** (compound **9**). **Kaempferol-3-rutinoside** (compound **18**), **kaempferol-3-*O*-(4-hydroxy-E-cinnamoyl)-(β)-glucopyranosyde** (compound **19**), **grandiamide B** (compound **21**)**, gigantamide A** (compound **25**) and **pyramidatine** (compound **26**) were obtained from the leaves of *Aglaia oligophylla*.

Preliminary experiments indicated that the crude extract obtained from *Aglaia oligophylla* caused significant insecticidal activity also under field conditions. The field experiments were conducted at the Tam Dao National Medicinal Garden, in Vietnam in July 2003. *Aglaia* formulations at five different concentrations (500 ppm, 1000 ppm, 2000 ppm, 4000 ppm and 6000 ppm) were prepared from the methanol extract of *Aglaia oligophylla* and proved effective against a newly occurring caterpillar in Vietnam (*Brithys crini*) seriously damaging the medicinal plant *Crinum asiaticum* (Amaryllidaceae). The effects of *Aglaia oligophylla* extract on *Brithys crini* did not consist in directly killing as compared to most of the very toxic chemical insecticides (e.g. Monitor ®), but it acts rather as a repellent in driving the insects away from the sprayed plants.

Aglaia oligophylla formulations were also effective against *Macrosinum phoniella* feeding on *Cynara scolymus* by apparently affecting the central nervous system of the insects. Twelve hours after spraying, aphids were observed to be affected at their central nervous system as shown by their uncontrolled movements. This was followed by 100% mortality after 7 days at concentration of 4000 ppm.

A second experiment was done on the *Aglaia* formulation which was conducted in a cabbage field at Dong Anh, Hanoi October 2003. The *Aglaia oligophylla* extract was also shown to be effective against *Spodotera litura* encountered in the vegetable field. The effect of *Aglaia* formulation on *S. litura* was not as efficient as the chemical product (Regent®) at the beginning of the experiment. However the efficiency of the *Aglaia* formulation lasted longer.

In a Petri dish experiment which was conducted on *Brassica rapa* leaves, *Aglaia* formulations exhibited efficiency to kill larvae of *S. litura* up to 60% at a concentration of 5 000 ppm and 40% at concentration of 2500 ppm in comparison to 30 % of the commercially available insecticide Regent ®.

The toxicity levels (LD_{50}) of the *Aglaia* extract were calculated as 4500 mg/kg, which could be considered to be in the range of a "very low toxicity" when tested with mice by administering the extract orally and showed a medium toxicity level at 2000 mg/kg by injecting the *Aglaia* extract directly into the gullet of the mouse.

The stability of *Aglaia* formulation was also tested under field condition by analyzing the residue of dasyclamide (a cinnamoyl bisamide which was found in high amounts in the leaves of *Aglaia gigantea*), which is a biogenetic building block for the rocaglamides. After 3 days, no trace of dasyclamide was found in the leaves of plants sprayed with the *Aglaia* formulation.

Table.5.1: List of isolated compounds from *Aglaia* sp. collected from Vietnam

Name	Structure	MW	Plant resourves	
Rocaglamide A (1)	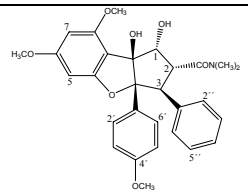	505	*A.duppereana (bark)*	known
Rocaglamide I (2)	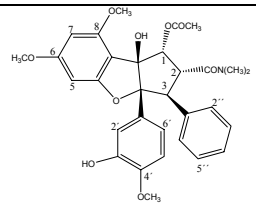	563	*A.duppereana (bark)*	known
Rocaglamide W (3)	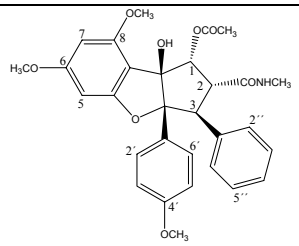	533	*A.duppereana (bark)*	known
Rocaglamide AB (4)	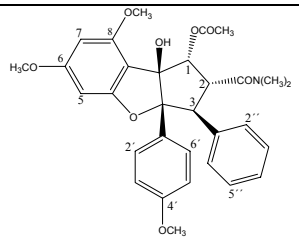	547	*A.duppereana (bark)*	known
Rocaglamide J (5)	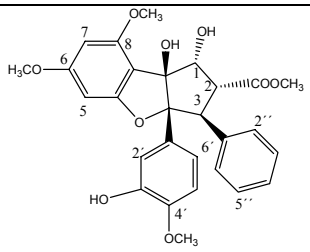	508	*A.duppereana (bark)*	known

Rocaglaol (6)	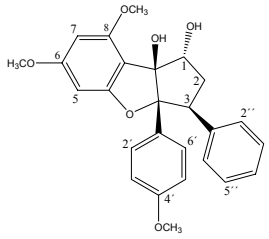	434	*A.duppereana (bark)*	known
Rocaglamide S (7)	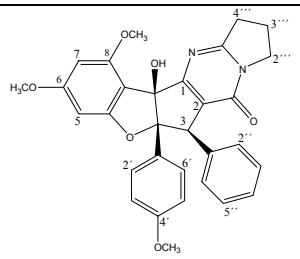	524	*A.duppereana (leaves)*	known
Rocaglamide AY (8)	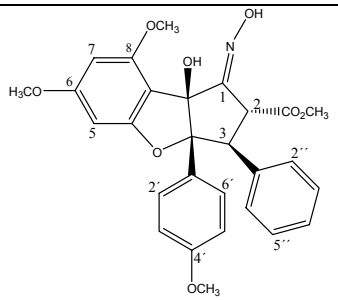	505	*A.oligophylla (leaves)*	new
Aglaixiflorin D (9)	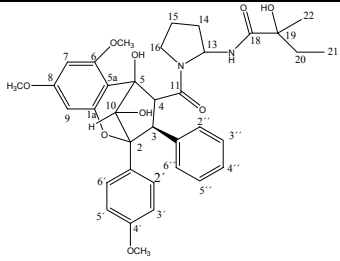	646	*A.abbriviata (leaves)* + *A.duppereana (leaves)*	known
Pinoresinol (10)	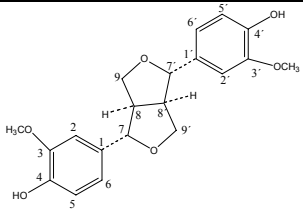	358	*A.oligophylla*	known
4´-O-Methyl-pinoresinol (11)	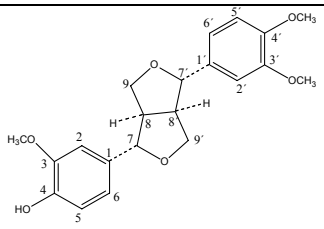	372	*A.oligophylla*	known

Eudesmin (12)	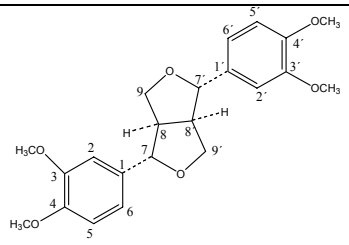	386	*A.oligophylla*	known
Epicatechin (13)	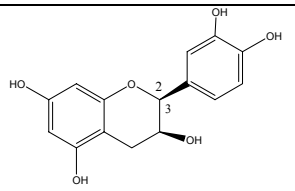	290	*A.duppereana (bark)*	known
4′,7-di-O-Methyl-naringenin (14)	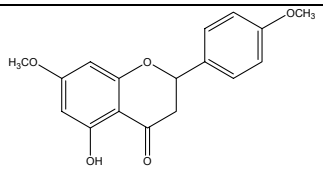	300	*A.duppereana (leaves)*	known
4′,5,7-Trimethoxydihydroflavonol (15)	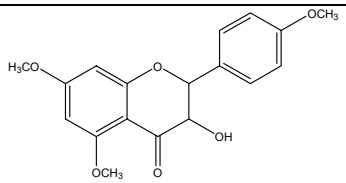	330	*A.oligophylla*	known
4′,5,7-tri-O-Methyl-kaempferol (16)	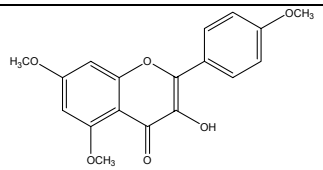	328	*A.oligophylla*	known
4′,5,7-Tri-O-Methyl-naringenin (17)	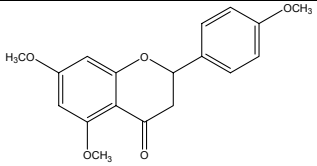	314	*A.oligophylla*	known
Kaempferol-3-rutinoside (18)	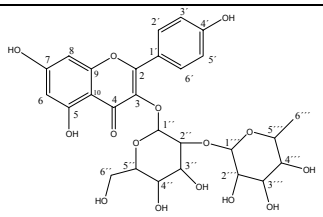	594	*A.oligophylla*	known

Kaempferol-3-*O*-(4-hydroxy-E-cinnamoyl)-(β)-glucopyranoside (19)	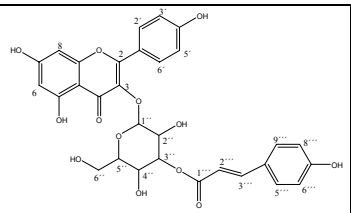	594	*A.oligophylla*	known
Dasyclamide (20)	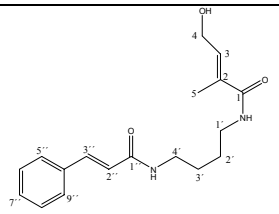	316	*A.gigantea (leaves)* + *A.oligophylla (leaves)*	known
Grandiamide B (21)	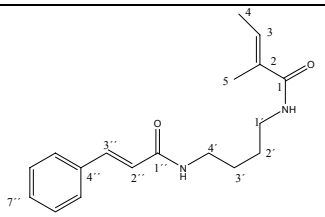	300	*A.oligophylla (leaves)*	known
Grandiamide D (22)	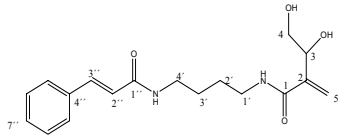	332	*A.gigantea (leaves)*	new
Odorine (23)	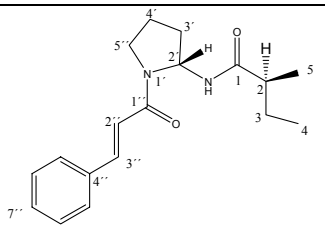	300	*A.duppereana+A. abbriviata*	known
Odorinol (24)	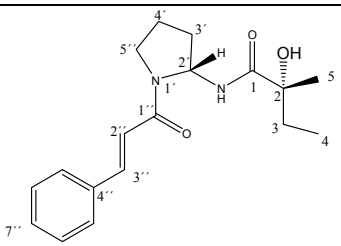	316	*A.duppereana+A. abbriviata*	known

Gigantamide A (25)	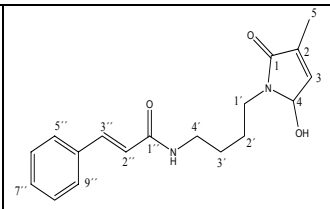	314	*A.gigantea +A.oligophylla (leaves)*	new
Pyramidatine (26)	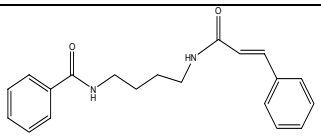	322	*A.oligophylla (leaves)*	known
Foveolin B (27)	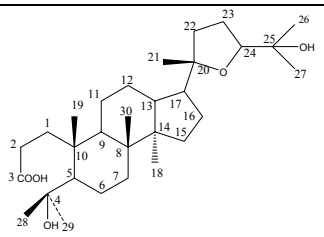	492	*A.giagantea (leaves)*	known
Niloticin (28)	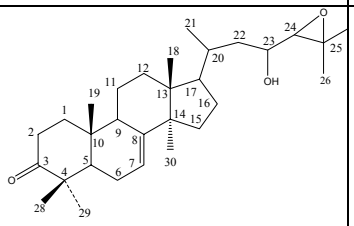	456	*A.dasyclada*	known
Lutein (29)	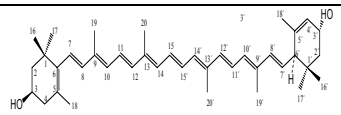	568	*A.oligophylla (leaves)*	known
Scopoletin (30)	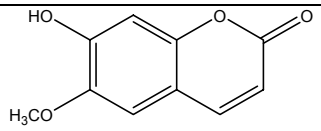	192	*A.elaeagnoidea*	known

VI. REFERENCES

Abott, W.S; A method of computing the effectiveness of an insecticide. *J. Econ. Entomol* 1925; **18**, pp 265-267

Baranyai, M., Molnar, P., Szabolcs, J., Radics, L., and Kajtar-Peredy, M.; ^{13}C NMR study of mono-cis capsanthins. *Tetrahedron* 1981; **37**, pp.203-207

Bohnenstengel, B.B., Siegmund, F. D., Wajant, H., Weber, C., Herr, I., Debatin, K.M., Proksch, P., Wirth, T.; *J. Biol. Chem* 2002; **47**, pp. 44791-44800

Brader, G., Vajrodaya, S., Greger, H., Bacger, H., Kalchhauser, H., and Hofer, O.; *J.Nat.Prod* 1998; **61**, 1482-1490

Buss, E.A., and Park-Brown, S.G.; Natural Products for Insect Pest Management, *ENY-350*, *Institute of Food and Agricultural Sciences, University of Florida*, Published 2002 by http://edid.ifas.ufl.edu

Casabuono, A.C and Pomilio, A.B; *Phytochemistry* 1994; **35**, No. 2, pp. 479-483

Chaidir, Lin, W.H., Ebel,R., Edrada Ebel, R.A., Wray, V., Manfred Nimtz, Wahono Sumryono, and Proksch, P.; *J.Nat.Prod* 2001; **64**, 1216-1220

Chaidir; Hiort, J.; Nugroho, B.W.; Bohnenstengel, F.I.; Wray, V.; Witte, L.; Hung, P.D.; Kiet, L.C.; Sumaryono, W.; Proksch, P; *Phytochemistry* 1999; **52**, pp.837

Chaidir; Lin, W.H.; Ebel, R.; Edrada, R.A.; Wray, V.; Nimtz, M.; Sumaryono, W.; Proksch, P; *J. Nat. Prod* 1999; **52**, pp. 837-842

Chang-Yih Duh, Shang-Kwei Wang, Rei-Sheu Hou, Yang-Chang Wu, Yu Wang, Ming-Chu Cheng, and Tai-Tsung Chang; *Phytochemistry* 1993; **34**, No. 3, pp. 857-858

Changzeng, W., and Zhongjian, J.; *Phytochemistry* 1997; **45**, No. 1, pp. 159-166

Chien-Chang Shen, Yuan-Shiun Chang and Li Kang Ho; *Phytochemistry* 1993; **34**, No. 3, pp. 843-845

Cloyd, R.A.; Natural Indeed: Are Natural Insecticides Safer and Better Than Conventional Insecticides. Pesticide review 2004; 17, No.3

Davis, A. L., Cai. Y., Davies, A.P., and Lewis, J.R.; *Magnetic Resonance in Chemistry* 1996; **34**, pp. 887-890

Deli, J., Molnar, P., Zoltan Matus, Gyula Toth, Andrea Steak, Urs A. niggli and Hanspeter Pfander; *Helvetica Chimica Acta* 1998; **81**

Detterbeck, R., and Hesse, M.; *Tetrahedron* 2002; **58**, pp. 6887-6893

Dewick, P.M.; A Biosynthetic Approach. *Medicinal Natural Products* 2003; Second Edition, Willey

Dhawan, B.N.; Dubey, M.P.; Mehrotra, B.N.; Rastogi, R.P.; Tandon, J.S; *Indian J. Exp. Biol* 1980; **18**, pp.594

Dreyer, M.; Nugroho, B.W.; Bohnenstengel, F.I.; Ebel, R.; Wray, V.; Witte, L.; Bringmann, G.; Mühlbacher, J.; Herold, M.; Hung, P.D.; Kiet, L.C.; Proksch; *J. Nat. Prod* 2001; ASAP article

Duke, S.O; *Natural pesticides from plants* 1990; p. 511-517

Dumontet, V.; Thoison, O.; Omobuwajo, O.R.; Martin, M.T.; Perromat, G.; Chiaroni, A.; Riche, C.; Pais, M.; Sevenet, T; *Tetrahedron* 1996; **52**, 6931

Estrada-Reyes, R., Ana Laura Alvarez C, Carolina Lopez-Rubalcava, Luisa Rocha, Gerardo Heinze, Julia Moreno and Mariano Martinez-Vazquez; *Zeitschrift für Naturforschung* 2002; **57**c, pp.29-32

Finney, D.J; Probit Analysis, *Cambridge University Press*, *Cambridge* 1971

Fonseca, S.F., Nielsen, L.T.,and Ruveda, E.A.; *Phytochemistry* 1979; **18**, pp. 1703-1708

Gray, A.I., Bhandari, P., and Waterman, P.G.; New protolimonoids from the fruits of Phellodendron chinense. *Phytotchemitry* 1988; **27**, N0. 6, pp.1805-1808

Guz, N.R., Stermitz, F.R.; *Phytochemistry* 2000; **54**, pp. 897-899

Hayashi, N., Lee, K.H.,Iris H. Hall, McPhail, A.T.; *Phytochemistry* 1982; **21**, No. 9, pp. 2371-2373

Hedin, P.A., and Phillips, V.A.; Electron impact Mass spectral Analysis of Flavonoids. *J. Agric.Food Chem* 1992; **40**, pp 607-611

Herz,W., Gibaja, S., Bhat, S.V., and Srinivasan, A.; *Phytochemistry* 1972; **11**, pp. 2859-2863

Hiort, J.; Chaidir; Bohnenstengel, F.I.; Nugroho, B.W.; Schneider, C.; Wray, V.; Witte, L.; Hung, P.D.; Kiet, L.C.; Proksch, P; *J. Nat. Prod* 1999; **62**, pp.1632

Inada, A., Nishino,H., Kuchide, M., Takayasu, J., Mukainaka, T., Nobukuni, Y., Okuda, M., and Tokuda, H.; *Biol. Pharm. Bull* 2001; **24**, No.11, pp. 1282-1285

Ishibashi, F., Satasook, C., Isman, M.B., Towers, G.H.N; *Phytochemistry* 1993; **32**, pp.307

Islam, M.T., Tahara, S.; *Phytochemistry* 2000; **54**, pp. 901-907

Itokawa, H., Kishi, E., Morita, H., and Takeya, K.; Cytotoxic quassinoids and tirucallane-type triterpenes from the woods of *Eurycoma longifolia*. *Chem.Pharm.Bull* 1991; **40**(4) 1053-1055

Jansen, J.F.G.A., and Feringa, B.L.; *Tetrahedron Letters* 1991; **32**, No. 27, pp. 3239-3242

King, M.L., Chiang, C.C., Ling, H.C., Fujita, E., Ochiai, M., McPhail, A.T.; *J. Chem. Soc., Chem. Commun* 1982*;*1150.

Kingston, D.G.I., and H.M.Fales, Methane chemical ionization mass spectrometry of flavonoids; *Tetrahedron* 1973; **29**, pp. 4083-4086

Lam, J., and Wrang, P.; *Phytochemistry* 1975; **14**, pp. 1621-1623

Le.V.T; Integrated Pest Management (IPM) and green farming in rural poverty alleviation on Vietnam. 2002; pp-110-114

Ley, S.V., Denholm. A.A., and Wood, A.; The chemistry of azadirachtin. *Nat Prod Rep* 1993; **10**, pp. 109-157

Luo, X.D., Wu, S.H., Ma, Y.B., Wu, D.G.; *Phytochemistry* 2000; **54**, pp. 801-805

Markham, K.R.; Techniques of flavonoid identification. *Academic Press* 1978

Mulholland, D.A., and Taylor, D. A. H.; Protolimonoids from Turraea nilotica. *Phytochemistry* 1988; **27**, No. 4, pp.1220-1221

Nakano, K., Kotaro Murakami, Toshihiro Nohara, Toshiaki Tomimmatsu and Toshio Kawasaki; *Chem. Pharm. Bull* 1981; **29** N0.5, pp. 1445-1451

Norbaek, R., Kondo, T.; *Phytochemistry* 1999; **51**, pp. 1113-1119

Nugroho, B.W.; Edrada, R.A.; Güssregen, B.; Wray, V.; Witte, L.; Proksch, P; *Phytochemistry* 1997; **44**, pp.1455

Nugroho, B.W.; Edrada, R.A.; Wray, V.; Witte, L.; Gehling, M.; Proksch, P; *Phytochemistry* 1999; **51**, pp.367

Nugroho, B.W.; Güssregen, B.; Wray, V.; Witte, L.; Bringmann, G.; Proksch, P; *Phytochemistry* 1997; **45**, pp.1579

Nugroho, B.W; *Ph. D. Dissertation, University of Würzburg*.1997

Oeveren, A.V., Jansen, J.F.G.A., and Feringa, B.L.,; *J. Org. Chem* 1994; **59**, pp. 5999-6007

Ohtani, I., Kusumi, T., Yoel Kashman, and Hiroshi Kakisawa; High-Field FT NMR application of Mosher´s method. The absolute configurations of Marine terpenoids. *J. Am. Chem. Soc* 1991; **112**, pp 4092-4096

Pelter, A., and Ward, R.S.; *Tetrahedron* 1976; **32**, pp. 2783-2788

Pelter, A., and Ward, R.S.; *Tetrahedron Letters* 1977; **47**, pp. 4137-4140

Pham, H.H.; An illustrated Flora of Vietnam. *Cay co Viet Nam* 1999;Volume II, pp. 398-405

Pouchert, C.J. and Behnke, J; *The Aldrich Library of 13C and 1H FT NMR* 1993; Spetra, Edition I ; **2**, 1214 B (7-hydroxy-6-methoxycumarin)

Proksch, P., Endrada, R.A., Ebel, R., Bohnenstengel, F.I., and Nugroho, B.W.; *Current Organic Chemistry* 2001; **5**, pp.923-938

Proksch, P., Giaisi, M., Treiber, M.K., Katalin Palfi, Anette Merling, Herbert Spring, Peter H. Krammer and Min Li-Weber; *The Journal of Immunology* 2005; **174**, pp. 7075-70-84

Rahman, M.M.A., Dewick, P.M., Jackson, D.E., and Lucas, J.A.; *Phytochemistry* 1990; **29**, No.6, pp 1971-1980

Rahman, M.M.A., Dewick, P.M., Jackson, D.J., and Lucas, J.A.; *Phytochemistry* 1990; **29**, No. 6, pp. 1971-1980

Roux, D. M.-T.Martin, M.-T.Adeline, T. Sevenet, A.H.Hadi and M.Pais; *Phytochemistry*, 1998; **49**, No.6, pp.1745-1748

Roy, S.C., Rana, K.K., and Guin, C.; *J. Org. Chem* 2002; **67**, pp. 3242-3248

Saifah, E., Puripattanavong, J., Kittisak Likhitwitaywuid, Geoffrey A. Cordell, Heebyung Chai, and John M. Pezzuto; *J Nat Prod* 1993; **56**, N0 4, pp 473-477

Satasook, C., Isman, M.B., Ishibashi, F., Medbury, S., Wiriyachitra, P., Towers, G.H.N; *Biochem. Syst. Ecol* 1994; **22**, pp.121

Schmidt, T.J.; Sesquiterpenlactone, Diterpene, Flavonoidaglyka und weitere Inhaltsstoffe der Blütenkörbchen von Arnica angustifolia Vahl und ihren Unterarten. *Inaugral-Dissertation zur Erlangung des Doktorgrades der Heinrich-Heine-Universität Düsseldorf* 1994

Schneider, C., Bohnenstengel, F.I., Nugroho, B.W., Wray, V., Witte, L.; Hung, P.D., Kiet, L.C., Proksch, P.; *Phytochemistry* 2000; **54**, pp.731

Sheldrick, G. M; SHELXL97 Program for the Refinement of Crystal Structures,

University of Göttingen, Germany 1997

Sheldrick, G. M; SHELXS86 Program for the Solution of Crystal Structures. *University of Göttingen, Germany* 1985

Shiengthong, D., and A. Ungphakorn; *Tetrahedron Letters* 1979; **24**, pp. 2247-2250

Su, R., Kim, M., Kawaguchi, H., Takehiko, Katsumi Goto, Tooru Taga, Yoshihi Miwa, Mutsuo Kozuka, and Shozo Takahashi; *Pharmaceutical Society of Janpan* 1990; **38**, pp. 1616-1619

Suginome, H., Kazuhiko Orito, Kaoru Yorita, Masataka Ishikawa, Noriaki, Shimoyama and Takahiro Sasaki; *J. Org. Chem* 1995; **60**, 3052-3064

Suginome, H., Kazuhiko Orito, Kaoru Yorita, Masataka Ishikawa, Noriaki Shimoyama and Takahiro Sasaki; *J.Org. Chem* 1995; **60**, pp. 3052-3064

Trost, B.M., Greenspan, P.D., Yang, B.V., Saulnier, M.G; *J. Am. Chem. Soc* 1990; **112**, 9022

Ware, G.W., and Whitacre, D.M.; an introduction to insecticides (4th edition) extracted from The Pesticide Book, 6th ed, Published by MeisterPro Information Resources A division of Meister Media Worldwide Willoughby, Willoughby, Ohio 2004

VII. ABBREVIATIONS

List of Abbreviations

[α]	: specific rotaion at the sodium D-line
br	: broad signal
COSY	: correlation spectroscopy
d	: doublet
dd	: double of doublets
DEPT	: distortionless enhancement by polarization transfer
EI	: electron impact
ESI	: electro spray ionisation
eV	: electrovolt
FAB	: fast atom bombardment
HMBC	: Hetero Multinuclear Bond Coherence
HMQC	: Hetero Multinuclear Quantum Coherence
HPLC	: high performance liquid chromatography
Hz	: hertz
LC	: lethal concentration
m	: multipliett
MeOD	: deuterated methanol
MeOH	: methanol
mg	: milligram
mL	: milliliter
MS	: Mass Spectrometry
m/z	: mass per charge
µg	: microgram
µL	: microliter
NADPH	: nicotinamide adenine dicucleotide phosphate (reduced)
nm	: nanometer
NMR	: Nuclear magnetic resonace spectroscopy
ppm	: part per million
Prep.HPLC	: high pressure liquid chromatography
q	: quartet
RP-18	: Reversed phase C-18
s	: singlet
SAM	: S-adenosyl methionine
t	: triplet
TFA	: trifluoroacetic acid
TLC	: thin layer chromatography
UV	: ultra-violet
VLC	: vacuum liquid chromatography

BIOGRAPHIC DATA

Personal Data

Full name	DUONG NGOC TU
Born	18th September 1975
Nationality	Vietnamese
Sex	Male
Status	Married
Place of Birth	Baoson, Bacgiang, Vietnam
Residential address	Max-Born-Straße 28, room 17, 40591 Duesseldorf
Home address	Institute of Chemistry (VAST), Hoang Quoc Viet 18, Nghia Do, Cau Giay, Hanoi, Vietnam

Educational Background

1992-1996	Bachelor degree in Chemistry at Hanoi National University-University of Natural Sciences
1997-1998	Post-graduate training course on natural products chemistry at University of Ghent, Belgium
1998-1999	Master degree in Chemistry at Hanoi National University-University of Natural Sciences
2000-2001	Training course on GMP (Good Manuafacturing Practice) Institute of Chemistry (VAST)
June-Sept. 2002	German language course at Goethe-Institute in Manheim, Germany
Oct. 2002 to present	PhD candidate, Institute of Pharmaceutical Biology and Biotechnology, Heinrich-Heine-Universität, Duesseldorf

Employment Record

1996-2002	Worked as a researcher at Department of Chemicals for Plants Protection, Institute of Chemistry (VAST)
1998-2001	Project on natural insecticide products from Vietnamese plants-Vietnamese Academy of Sciences and Technology (VAST)
1999-2001	Project on research and development in discovery of new drugs against cancer, AIDS, malaria, laishmaniasis and other tropical diseases from Vietnamese plants resources (Vietnam-Belgium)
2000-2001	GMP Project in production of new drugs to combat laishmaniasis from Vietnamese plants (Cooperation between WHO, TIBOTEC (Belgium) and Institute of Chemistry (VAST)

Awards & Hornors

October 2000	Medal Creative Young Scientist in Science and Technology

PUBLICATIONS

1. T. N. Duong, R. A. Edrada, R. Ebel, T. A. Duong, V. Wray, W. Frank, and P. Proksch; New derivatives of cinnamoyl bisamides from *Aglaia* sp. collected in Vietnam, *in preparation*, **2006**.

2. T. N. Duong, R. A. Edrada, R. Ebel, T. A. Duong, and P. Proksch; Configuration assignment of furofuran-lignans isolated from *Aglaia* sp. collected in Vietnam by employing NMR data, Advances in Natural Sciences, Vol. 6, No.3, **2005,** 289-297.

3. T. N. Duong, R. Ebel , R. A. Edrada, T. A. Duong, Nguyen.V.G and P. Proksch; Promising application of *Aglaia* extracts in plants protection in Vietnam. *Collection of Scientific reports* 2005; Institute of Chemistry (VAST)**.**

4. T. N. Duong, G. Eck, R. A. Edrada, R. Ebel, T. A. Duong, und P. Proksch; *Aglaia*-Arten aus Vietnam – Phytochemische Charakterisierung und Evaluierung der insektiziden Aktivität unter Feldbedingungen. **2004.**

5. T. N. Duong, G. Eck, R. Ebel, R. A. Edrada, M.T. Luu, T. A. Duong, and Peter Proksch; Insecticidal Rocaglamide compounds from *Aglaia* species collected in Vietnam.*10th Asian Chemical Congress 10 ACC 8th Eurosia Conference on Chemical Sciences* 2003; Hanoi, October 21-24**.**

6. R. Ebel, T.N. Duong, M.L. Luu, T.A. Duong, R.A. Edrada, and P. Proksch; Chemistry and Biological Activity of Insecticidal Active Rocaglamide derivatives and related compounds in Aglaia species.*10th Asian Chemical Congress 10 ACC 8th Eurosia Conference on Chemical Sciences* 2003; Hanoi, October 21-24**.**

7. T.A.Duong, T.N.Duong, M.T.Muu, A.K.Bui, D.M. Luu; High antifeedant activities against army worms (*Spodoptera litura*) of plumbagin, its halogen derivatives and natural limonoids compounds isolated from Vietnamese plants. *The 10th IUPAC International Congress on the Chemistry of Crop Protection* 2002; Basel-Switzerland, August 8-12**.**

8. T.A.Duong, T.N. Duong, M.T.Luu, L.H. Dong; Control of important pests of cabbage in suburb Hanoi by using natural insecticides (HBVTV1) containing principal antifeedant components isolated from Vietnamese plants. *The 10th IUPAC International Congress on the Chemistry of Crop Protection* 2002; Basel-Switzerland, August 8-12**.**

9. T.A. Duong,T.M Luu, B.D. Dai, Nguyen .M.P, T.N. Duong, G.V. Nguyen; Insecticidal activities of some Vietnamese plants. *Symposium on the Enviroment Protection and Substainable exploitation of natural resources* 2002; Hanoi, August 4-5**.**
10. T.A. Duong, A.K. Bui, T.N.Duong, Luu.T.M; Antifeedant activity against *S.litura* of plumbagin isolated from leaves of *Plumbago zeylanica* L. and its synthesized derivatives. *The4thVietnamese National Conference on Entomology* 2002; Hanoi, April, 519-524**.**

11. T.A.Duong, T.N.Duong , M.T. Luu, G.V. Nguyen, D.K. Nguyen, T.D. Nguyen; The promising results on the field experiments of new natural insecticide product from Vietnamese plants. *The 4th Vietnamese national Conference on Antomology* 2002; Hanoi, April, 498-494**.**

12. T.N.Duong , Duong .A.T, S.T. Phan; Isolation and structure elucidation of 7,7´´,4´-tri-O-methylementoflavone, a rare biflavone, from *Taxus wallichiana* Zucc. growing in Lam Dong, the South of Vietnam. *Journal of Chemistry of Vietnam* **2002.**

13. T.V. Mai, T.A.Duong ,T.N.Duong, S.T. Phan; Contribution on the study the chemical constituents of Yew tree (*Taxus wallichiana* Zucc.) growing in Lam Dong, South of Vietnam. *The 2nd Vietnam National Conference on Science and Technology of Organic Chemistry* 2001; Hanoi, December.

14. T.A. Duong, P.M. Nguyen, T.N. Duong , G.V. Nguyen, T.D. Nguyen; Isolation of Azadirachtin, a strong antifeedant activity against *Spodoptera litura*, from the seed of migrated neem tree in the South of Vietnam, *The 2nd Vietnam National Conference on Science and Technology of Organic Chemistry* 2001; Hanoi, December**.**

15. T.A. Duong, A.K. Bui, T.N. Duong, G.V. Nguyen; Insecticidal activity of some synthesied derivatives of plumbagin. *Collection of Scientific reports* 2001; Institute of Chemistry (VAST)**.**

16. T.N. Duong, T.A. Duong, S.V. Tran; Isolation, structure elucidation and isecticidal assay of 1,12-bis (3,3-dihydroxy-4,4´-dimethyl-5,5´-dimethoxyphenyl) dodecane from the leaves of *Maesa af.crassifolia* R.Br (Myrsynaceae) growing in Thai Nguyen-North of Vietnam. *Collection of Scientific reports* 2001; Institute of Chemistry (VAST)**.**

17. T.A. Duong, D.V. Nguyen, T.N. Duong, H.V. Nguyen; Study on the procedure for isolation of plumbagin from the leaves of *Plumbago zeylanica* Linn., and its determination by HPLC. *Collection of Scientific reports* 2000; Institute of Chemistry (VAST)**.**

18. T.A. Duong, A.K. Bui, T.N. Duong, C.D. Phan; Study on the limonoid constitutents from the seeds of *citrus* (Rutaceae) of Vietnam. *Collection of Scientific reports* 1999; Institute of Chemistry (VAST)**.**